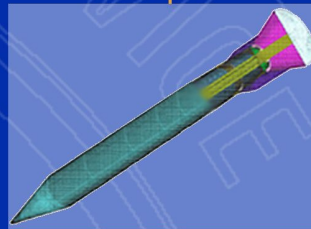
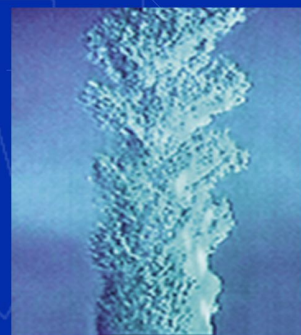
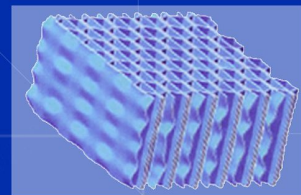
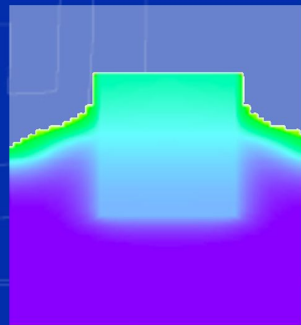


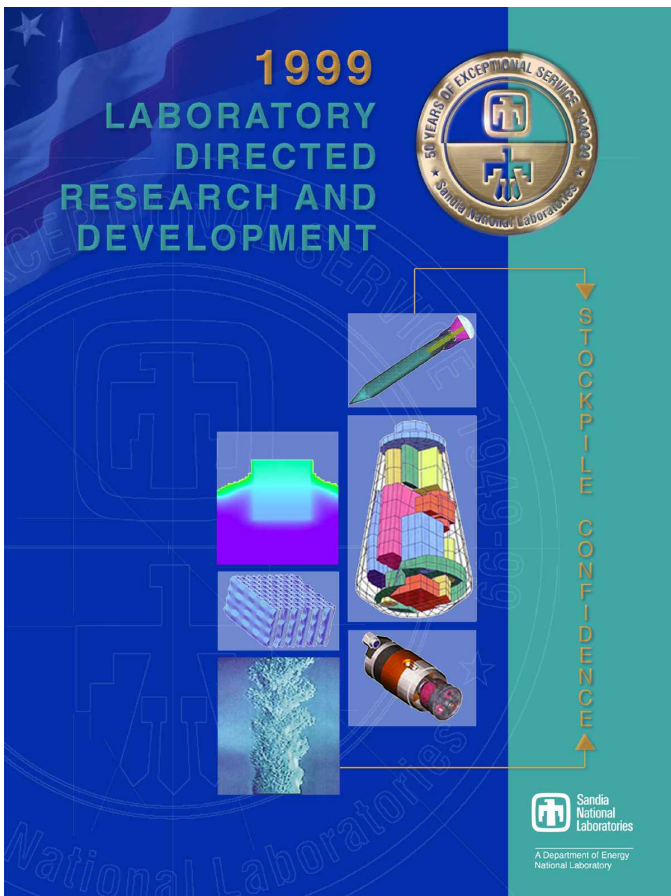
1999 LABORATORY DIRECTED RESEARCH AND DEVELOPMENT



STOCKPILE CONFIDENCE



A Department of Energy
National Laboratory



Cover (Above)

Over 90% of all Sandia National Laboratories LDRD projects provide both direct and indirect benefit to the national security and stockpile missions of the Laboratories and the DOE. LDRD is a key component of the weapons research effort that ensures Sandia's continuing ability to meet its commitments in surety, microsystems, performance, manufacturing, certification, radiation physics, and neutron-generators research and development.

LDRD projects span atomic, molecular, component, subsystem, and system-level research. At fundamental levels, research advances the capture and understanding of essential physical phenomena, including initial and boundary conditions. Such research is critical to develop confidence that computational tools (i.e., high-performance modeling and simulation tools) capture the interdependencies and interaction between coupled phenomena and the complexity invoked when dealing with complex engineered systems.

The LDRD program strategy is consistent with the critical Science and Technology (S&T) foundation of the Laboratories' missions. LDRD projects are invested in the range of the Laboratories' S&T research including Research Foundations, Roadmap Technologies, Grand Challenges, and Corporate Objectives investigations.

Abstract

This report summarizes progress from the Laboratory Directed Research and Development (LDRD) program during fiscal year 1999. In addition to a programmatic and financial overview, the report includes progress reports from 247 individual R&D projects in 12 categories.



This work was supported by the United States Department of Energy under Contract DE-AC04-94-AL85000.

Sandia is a multiprogram laboratory operated by Sandia Corporation, a Lockheed Martin Company, for the United States Department of Energy.

SAND 2000-0727
March 2000

LDRD Annual Report Staff:



Chuck Meyers
Cynthia Harvey
Donna Chavez
Bryon Cloer



Carol Whiddon
Joy Bemserfer
Donna Drayer
Douglas Prout

Table of Contents

12	“...exceptional service in the national interest.”	58	Atomic-Level Studies of Surfactant-Directed Materials Growth
13	Laboratory Directed Research and Development Program Review	62	Intelligent Polymers for Nanodevice Performance Control
<hr/>			
Materials Science & Technology			
24	Functional Materials for Microsystems: Smart Self-Assembled Photochromic Films	64	Freeforming of Ceramics and Composites from Colloidal Slurries
26	Innovative Experimental and Computational Diagnostics for Monitoring Corrosion in Weapons Environments	67	Quantum Dot Arrays
29	Self-Healing Molecular Assemblies for Control of Friction and Adhesion in MEMS	69	Laser-Assisted Arc Welding for Aluminum Alloys
31	Linking Atomistic Computations with Phase-Field Modeling	70	Reactivity of Metal-Oxide Surfaces
34	A Combinatorial Microlab Investigation of Critical Copper-Corrosion Mechanisms	73	Exploiting LENS™ Technology Through Novel Materials
37	Self-Assembled Templates for Fabricating Novel Nanoarrays and Controlling Materials Growth	76	Molecular Characterization of Energetic Material Initiation
39	Wetting and Spreading Dynamics of Solder and Braze Alloys	78	Nonvolatile Protonic Memory
42	Improved Materials Aging Diagnostics and Mechanisms Through 2-D Hyperspectral Imaging Methods and Algorithms	<hr/>	
45	Microscale Shock-Wave Physics Using Photonic Driver Techniques	Computer Sciences	
48	Molecular-to-Continuum Fracture Analysis of Thermoset Polymer/Solid Interfaces	81	Integration of Mesh Optimization with 3-D All-Hex Mesh Generation
52	Fundamental Aspects of Micromachine Reliability	83	Heterogeneous Simulation
55	Enabling Science and Technology for Cold-Spray Direct Fabrication	86	Volumetric Video Motion Sensing for Unobtrusive Human-Computer Interactions
		88	Hybrid Sparse-Dense Incomplete Factorization Preconditioners
		91	Big Eddy—Advanced Large-Eddy Simulation Algorithms for Complex Flow Physics and Complex Geometry
		93	Molecular Simulation of Reacting Systems
		95	Massively Parallel Global Climate Model for Paleoclimate Applications

Table of Contents

<p>97 Fast and Easy Parallel I/O for Efficient Scientific Computing</p> <p>99 Novel Load-Balancing for Scalable, Parallel Electromagnetic and Plasma Physics Simulation Software</p> <p>102 Massively Parallel <i>Ab Initio</i> Validation for ASCI Materials Modeling</p> <p>104 Computational Methods for Coupling Microstructural and Micromechanical Materials Response Simulations</p> <p>108 Integrated Quantum/Classical Modeling of Hydrogenic Materials</p> <p>110 The Next Generation of Teraflop Density-Functional Electronic Structure Codes</p> <p>112 Methodology for Characterizing Modeling and Discretization Uncertainties in Computational Simulation</p> <p>115 Global Optimization for Engineering Science Problems</p> <p>118 Dynamic Simulation of Mechanical Systems with Intermittent Contacts</p> <p>121 From Atom-Picoseconds to Centimeter-Years in Simulation and Experiment</p> <p>123 Emergent Behavior of Large Swarms of Intelligent Agents</p> <p>125 Parallel Combinatorial Optimization for Scheduling Problems</p> <p>128 Programming Paradigms for Massively Parallel Computers</p> <p>130 Multilevel Techniques for Unstructured Grid Problems on Massively Parallel Computers</p>	<p>132 Scalable Tools for Massively Parallel Distributed Computing</p> <p>134 Massively Parallel Methods for Simulating the Phase-Field Model</p> <p>137 Visual Explanation and Insight</p> <p>139 Computational Simulations of Self-Assembling Macrosystems by Direct Fabrication of Microscopic Structures</p> <p>141 Gamma-Ray Bursts and the Particle Mass Scale</p> <hr/> <p>Electronics & Photonics</p> <p>143 A Novel Nondestructive Silicon-on-Insulator Nonvolatile Memory</p> <p>146 Integration of Optoelectronics and MEMS by Free-Space Microoptics</p> <p>149 Advanced Laser Structures for Short-Pulsed Power in Active Optical Sensor Systems</p> <p>151 Integration of Microsensor Technology into a Miniature Robotic Vehicle</p> <p>153 Vacuum Encapsulation of MEMS Structures</p> <p>156 Massively Parallel Sensor Arrays for Volatile Organic Detection</p> <p>158 Agile Dry Etching of Compound Semiconductors for Science-Based Manufacturing Using In Situ Process Control</p> <p>161 Precision-Formed Micromagnets</p> <p>164 Time-Resolved Ion-Beam-Induced Charge-Collection (TRIBICC) Imaging</p> <p>167 Composite-Resonator Surface-Emitting Lasers</p>
--	--

Table of Contents

<p>169 Role of Defects in III-Nitride-Based Electronics</p> <p>172 Ultra-Low-Power Sensors for Microtelemetry Systems</p> <p>175 Double Quantum-Well Long-Wavelength Optoelectronic Devices</p> <p>179 The Development of Integrated Chemical Microsensors in GaAs</p> <p>182 Monolithic Integration of VCSELs and Detectors for Microsystems</p> <p>184 AlGaN Materials Engineering for Integrated Multifunction Systems</p> <p>187 Compliant Substrates for Epitaxial Integration of Dissimilar Materials</p> <p>188 Post-Processed Integrated Microsystems</p> <p>191 Development of Radiation-Hard Sensors for Space-Based Visible and Infrared Sensing Applications</p> <p>193 Silicon Three-Dimensional Photonic Crystal and Its Applications</p> <p>195 Monolithic Micromachined Variable Tuners for Rapid Prototyping and Optimization of Microwave Circuits</p> <p>198 Quantum Tunneling Transistors for Practical Application</p> <p>202 Development of Magnetically Excited Flexural Plate-Wave Devices for Implementation as Physical, Chemical, and Acoustic Sensors, and as Integrated Micropumps for Sensored Systems</p> <p>205 Novel Acoustically Driven Microoptoelectronic Devices</p> <p>207 Photonics Integration Devices and Technologies</p>	<p>210 Stress-Free Amorphous Diamond for High-Sensitivity Microsensors with Integrated Microstructures</p> <p>213 Semiconductor Current Filament Lasers</p> <p>215 Integration of Radiation-Hard Magnetic Random Access Memory with CMOS Integrated Circuits</p> <hr/> <p>Modeling & Engineering Simulation</p> <p>218 Development of <i>In Situ</i> Diagnostics for Simultaneous Measurement of Transient Gas Species and Soot in Large Fires</p> <p>221 Micromechanical Failure Analyses for Finite-Element Polymer Modeling</p> <p>224 Methodology for Optimal Selection of Test and Simulation Levels for Problems Involving Computational Simulation</p> <p>226 A Phenomenological Model for Multicomponent Transport with Electrochemical Reactions in Concentrated Solutions</p> <p>228 Structural Simulations Using Multiresolution Material Models</p> <p>230 Lightning-Induced Arcing</p> <p>232 Mechanisms of Adiabatic Shear Failure</p> <p>234 Evolvable Hardware</p> <p>236 Crack Nucleation and Growth: Combining Validated Atomistic and Continuum Modeling</p> <p>239 Applied Microfluidic Physics</p> <p>243 Transport and Fate Simulation of Chem/Bio Agents in Critical Infrastructures</p>
---	--

Table of Contents

245	Innovative Measurement Diagnostics for Fluid/Solid and Fluid/Fluid Interactions in Rotating Flowfields	281	Standard Cells for Microelectromechanical Systems (MEMS)
247	Capturing Recrystallization of Metals with a Multiscale Material Model	284	Laser Wire Deposition for Fully Dense Shapes
252	Nondeterministic Modeling in Engineering Science	287	High-Throughput Dry Processes for Large-Area Devices
255	Lagrangian Modeling of Radiative Transport	290	Assuring High Reliability and Production Readiness in Low-Volume Manufacturing
257	High-Resolution Modeling of Multiscale Transient Phenomena in Turbulent Boundary Layers	292	Scripting for Video Inspection
259	Dispersive Measurements of Velocity in Heterogeneous Materials	294	Advanced Machining Processes for Microfabrication
261	A Physically-Based Computational Method for Predicting Generalized Fracture	296	Fusion of Product and Process Data Using Real-Time Streaming Visualization
<hr/> Manufacturing & Process Sciences		298	Advanced Production Planning Models
265	Microdiagnostic MEMS Lab-on-a-Chip	<hr/> Information Systems & Technology	
267	Real-Time Error Correction Using Electromagnetic Bearing Spindles	301	Weighted-Nearest-Neighbor (WNN) Decision Making for Data Mining
268	Thin-Film Deposition Processes Incorporating <i>In Situ</i> Monitoring Capabilities	303	Varying QoS for Fixed and Mobile Networks
270	Optimization of Filled Polymer Materials	306	A Real-Time Decision-Support Framework to Guide Facility Response to Abnormal Events
272	Solid-State Neutron Generator for Use in Nuclear Weapons	308	Data Fusion for Chemical Sensing
274	Finite-Element Meshing Approached as a Global Minimization Process	310	Large-Scale Distributed Information System Modeling and Simulation
276	Application of Parallel Mechanism Technology to Manufacturing	313	High-Surety SCADA for the Critical Energy Infrastructures
278	Investigation of the Impact of Cleaning on Adhesive Bond and the Process Implications	316	Agent-Based Mediation and Cooperative Information Systems
		318	Dynamically Self-Configurable Network Protocol

Table of Contents

<p>321 Optical Backplane/Interconnect for Super-High-Speed Communication</p> <p>323 PUSH Technology Demonstration</p> <p>325 Controlling Information: Its Flow, Fusion, and Coordination</p> <p>327 Mission Surety for Large-Scale Real-Time Information Systems</p> <p>329 Low-Power, Reduced-Computation, Public-Key Protocols</p> <p>331 Ten-to-One-Hundred-Gigabit/Second Network Enabling R&D</p> <p>333 High-Performance Commodity Interconnects for Clustered Scientific and Engineering Computing</p> <p>336 AVATAR—Navigating and Mining in Massive Data</p> <p>338 Algorithm-Based Fault Tolerance on Heterogeneous Massively Parallel Computers</p>	<p>Sensing & Intelligent Controls</p> <p>350 Imaging of Moving Targets Using Simultaneous Synthetic Aperture Radar (SAR) and Moving Target Indicator (MTI) Radar</p> <p>352 Sparse Geophysical Networks for Monitoring Deep Targets</p> <p>354 Miniature Bioaerosol Concentrator</p> <p>356 Recognizing Partially Obscured Targets by Combining Multiple Data Sources Using Evidential Reasoning</p> <p>358 Computational Engineering of Sensor Materials and Integration with a Novel Biological Weapon Detection System</p> <p>361 Biological Weapon Detector Using Bioaffinity Array Impedance Analysis with Chemical Amplification Through Redox Recycling</p> <p>363 ATR/Exploitation Utilizing Ultra-High-Resolution, Complex SAR Imaging</p> <p>365 Thin-Skin Deployable Mirrors for Remote Sensing Systems</p> <p>368 Dispersible Granular Sensor (Smart Sand) for Landmine Detection Based on TNT Immunoassay</p> <p>371 Characterization of Underground Facilities in an Urban Environment</p> <p>373 Dexterous Robotic Manipulation of Hazardous Materials in Unstructured Environments</p> <p>376 Autonomous Dynamic Soaring Platform for Distributed Mobile Sensor Arrays</p> <p>378 Miniature UV Fluorescence-Based Biological Agent Sensor</p>
<p>Directed Energy</p>	
<p>341 Surface Decontamination of Bacterial Protein Toxins by RF Power</p> <p>343 Intense White-Light Pulse Propagation in Air Using Self-Guided Optical Filamentation: Applications to Remote Sensing and Countermeasures</p> <p>346 Improved Backscatter X-Ray Detection for Antiterrorist Applications</p> <p>348 HPM Vulnerability Assessment and Tests</p>	

Table of Contents

381	Automatic Planning of Life-Cycle Assembly Processes	420	Computer-Network Vulnerability-Analysis Method
384	Analysis of Very Large Assemblies	423	Approximate Public-Key Authentication with Information Hiding
386	Enabling Human Skills with Cooperative Automation	424	New Network Analysis Approaches to Evaluate Infrastructure Risk and Reliability
389	Cloud to CAD	426	Improved Tools for Identifying and Quantifying Potentially Dangerous Human Actions
392	Ergonomics in Life-Cycle Assembly Processes	428	Advanced Signal Processing for Thermal Flaw Detection
395	Feature Reduction of Geometric Solid Models for Analysis Tools	431	Production Surety and Disruption Vulnerability Analysis
397	Electrokinetic Immunoaffinity Chemical Sensors	433	An Optically Triggered Semiconductor Switch for Firing Systems
<hr/> Environmental Sciences		436	Source Code Assurance Tool
401	Designed Synthesis of Controlled Degradative Materials	438	System-Surety Life-Cycle Engineering
403	Mechanistic Models for Radionuclide Desorption from Soils	440	Integrated Approach to Develop Microelectromechanical System (MEMS) Reliability Tools
404	Adaptive 3-D Sensing	444	Simulation/Optimization Tools for System-Variability Analysis
406	Aqueous Organic Sensor	447	A Massively Parallel Microsimulation Model of Infrastructure Interdependency
409	Designed Ionophores for Liquid-Membrane Separation and Extraction of Metal Ions	450	Physical Models for Predicting the Effect of Atmospheric Corrosion on Microelectronic Reliability
412	An Electromagnetic Imaging System for Environmental Site Reconnaissance	453	Backside Localization of Open and Shorted IC (Integrated Circuit) Interconnections
414	Advanced Geosphere Transport Simulation	456	Reliability Predictions for Advanced Electronics in Smoke Environments
<hr/> Surety Sciences			
418	Hybrid Processing of Measurable and Subjective Information in Surety Analysis		

Table of Contents

458 Security of Bulk Power Systems

Grand Challenges

461 Science on the Microdomain

464 Autonomous MicroChem Laboratory
(μ ChemLab)

467 Cooperative, Distributed Sensing and Action
Using Microminiature, Intelligent Agents

469 Engineering Complex Distributed Systems

473 Laser Communication Nanosatellites

479 Information Collection (Acquisition of
Information from Denied Areas)

481 Accelerated Molecular Discovery Arrays—The
Next Revolution in Biotechnology

Corporate Objectives

485 Microcode Evaluation

486 Model-Based Design and Analysis of Remote
Access Monitoring Systems

489 Microwave Imaging Through Walls

490 Research of the Utility of Polarimetric Sensing

492 Real-Time Image Analysis Using Field-
Programmable Gate Arrays

494 Poco Switch Tubes

495 Chemiresistors Based on Metal-Loaded
Polymers for Solvent Spill Detection

497 Advance Neutron-Tube Design and
Producibility

498 Surface Hardening by Nanoparticle
Precipitation and Atomic Clustering in Ni(Al,O)

499 Dynamical Properties of Polymers;
Computational Modeling

501 Broadening Mechanism in 2-D Excitonic and
Electron Gases

503 Calculation and Interpretation of the Energies
that Underlie Transition-Metal Surface
Structure

505 Interfacial Reactions in Ceramic Systems

508 Direct Fabrication of Multifunctional
Nanocomposites Via Supramolecular Self-
Assembly

511 Raman Investigation of Phase Changes in PZT
Materials

513 Information Extraction from Hyperspectral
Images Obtained from Satellites

515 Expanding the Security Dimension of Surety

516 Overcoming Software Brittleness: A Swarm
Intelligence Approach

518 Synthesis and Applications of N-Type Diamond

521 A Molecular Theory of Gatekeeper Proteins

523 Development of Compact UV Laser Source for
Climate Studies and Chemical Sensing

525 Power Source Technologies for Autonomous
Microsystems

526 Advanced Radiation Sources: Rayleigh-Taylor
Mitigation Via Perturbation Reduction

528 Global Approaches to Infrastructural Analysis
(GAIA)

Table of Contents

<p>530 Capillary Elastohydrodynamics in Manufacturing Processes</p> <p>532 Real-Time Design of Improved Powder Pressing Dies Using Finite-Element Method Modeling</p> <p>535 Computational Methods for Predicting the Response of Critical As-Built Infrastructure to Dynamic Loads (Architectural Surety)</p> <p>537 Solar-Grade Silicon</p> <p>539 Low-Work-Function Thermionic Emission Materials</p> <p>541 Develop Mathematical Algorithms for the Integration of Disparate Information to Determine Critical Infrastructure Health and Status</p> <p>543 SERAPHIM Propulsion Technology Design for High-Speed Rail Applications</p> <p>545 Tomographically Measured Temporal Evolution of Hyperspectral Target Signatures</p> <p>547 Gas-to-Liquid Microabsorber</p> <p>550 High-Resolution Electromagnetic Imaging of Transport Pathways</p> <p>552 MPP Direct Numerical Simulation of Diesel Autoignition</p> <p>555 Electrokinetically Driven Mesoscale Actuators</p> <p>557 Pathogen Detection Using Microseparations for BW Nonproliferation</p> <p>560 Assessing the Emerging Threat of Limited WMD Use</p> <p>562 Z-Pinch Fusion for Energy Applications</p> <p>564 IFSAR Rapid Terrain Visualization and Real-Time Exploitation System</p>	<p>566 Technologies for System-Level Innovations in Ballistic Missile Defense</p> <p>567 Novel Collective Protection System for Decon of CBW Agents and Purification of Aircraft and Other Closed Environments</p> <p>568 Z-Backlighter Technologies</p> <p>570 Ultra-Intense Femtosecond Laser Interactions with Applications to High-Field Physics, Enhanced Electromagnetic Coupling in Materials, and X-Ray Generation</p> <p>572 Design of a Prototypical Snoopy Coprocessor for DynaMICs Software Fault Monitoring with Integrity Constraints</p> <p>574 Analytic Verification of Treaties, Protocols, and International Agreements</p> <p>575 Fabricating Microcomponents from Silicon-Carbonitride by a Novel Microcasting Process</p> <p>577 Magnetic Polysilicon MEMS Devices</p> <p>579 Living Tissue Engineering</p> <p>581 The Use of Active Fiber Composites for the Health Monitoring of Wind Turbine Blades</p> <p>583 Developing/Assessing Long-Term Impact of Design Innovations</p> <p>584 Composite Wire Plasma Formation and Evolution</p> <p>587 DNA Microarray Technology</p> <p>588 Research Issues in the System Engineering Aspects of High Assurance</p> <p>590 Investigation of Lateral Composition Modulation in GaAsSb Short-Period Superlattices</p>
--	---

Table of Contents

592	New Complexing Agent for Co(II) Analysis for CP
594	Enzyme-Mediated Electrochemical Redox Polymer Microelectronic Biosensor for V- and G-Type Chemical Weapons
596	Design and Optimization of VLSI Systems and Reconfigurable Hardware
598	Hydrodynamic Flow in Biosystems
600	IR Polarimetry and Lithographic Alignment
602	Shock Response of Diamond Crystals
603	Dynamic Computer-Aided Design Analysis of Containment Vessels for Z-Pinch Experiments
604	Investigation of Nanoscience Technologies
605	Surety Science
608	Stabilization of Enzymatic Molecular Recognition Materials Via Crystallization and Crosslinking
610	Novel Biosensor Fabrication Techniques
611	Appendix A Project Number/Title Index
622	Appendix B Awards/Recognition List
623	Appendix C Project Performance Measures
638	Appendix D DOE Critical Technologies
653	Appendix E Major National Programs
668	Appendix F Dual-Benefit Areas and Single-Area Categories
686	Author and Title Index

“...exceptional service in the national interest.”

Science and technology are at the heart of United States industrial competitiveness, national security, energy resources, environmental quality, and leadership in fundamental and applied science.

At Sandia, the Laboratory Directed Research and Development Program provides the knowledge that drives our future. We initiate research and development that spawn the knowledge that revolutionized technology. Areas of emphasis center on our core technical competencies and the major strategic thrusts of Sandia's Institutional Plan. Leading-edge experiments that validate our work are constructed and operated on schedule, within budget, and in a safe and environmentally responsible manner.

Our work continues to produce many scientific and technological breakthroughs that lead to new technologies, markets, and businesses for the nation.

To all those who have contributed so generously of their time and talent, thanks and congratulations for a job well done.

Laboratory Directed Research and Development (LDRD) Program Overview

B. K. Cloer

Sandia's LDRD Program is "... the lifeblood of the Laboratories."

*Ambassador C. Paul Robinson
President, Sandia National Laboratories
July 1999*

"LDRD is where the Labs fuels its 'technology engine.'"

*C. Paul Robinson
President, Sandia National Laboratories
October 1999*

Strategy

Sandia National Laboratories is a national resource that provides world-class science, technology, and engineering. Because the safety, security, and reliability of the U.S. nuclear weapons stockpile depends directly on them, the Laboratories' capabilities must remain on the cutting edge.

Sandia's LDRD Program supports the DOE's missions through Sandia's four primary strategic objectives: nuclear weapons, nonproliferation and materials control, energy and critical infrastructure, and emerging national security threats. To meet these objectives, LDRD promotes creative and innovative research and development that Labs' Director Ambassador C. Paul Robinson describes as "... the lifeblood of the Laboratories."

Sandia's LDRD Program provides the flexibility to invest in long-term, high-risk research activities that attract the best research talent from across the Laboratories. LDRD research provides an opportunity for this talent to explore innovative scientific and technological opportunities that hold high potential for payoff in future applications. As a result, LDRD advances significantly strengthen Sandia's science and technology base and provide considerable support to DOE and the Laboratories' mission needs.

FY 1999 Funding Levels (MIL\$)



FY 1999 Selected Statistics

Full-time Staff	277
Smallest Project (\$K)	7
Average Project (\$K)	321
Average Project (FTE)	1.12
Largest Project (\$M)	3.85
1st Year Projects	121
2nd Year Projects	73
3rd Year Projects	53

FY 1999 Performance

Refereed publications	342
Other communications	284
Patent disclosures	104
Patent applications	60
Patents	25
Copyrights	15

Authorized by federal law and implemented under DOE Order 413.2, LDRD is Sandia’s sole source of discretionary research funds. In FY 1999, the LDRD Program was funded by an assessment on all costed work at Sandia. Atomic energy defense activities were supported directly by 89 percent of LDRD projects, although weapons-related activities provided only 50 percent of FY 1999 LDRD funding. More than 99 percent of LDRD projects provided benefits in basic and applied research to national security needs.

In FY 1999, LDRD provided \$79.2 million to fund 247 projects (selected from 840 possibilities, including ideas and continuations). The program was divided into five major investment areas (including subdivisions):

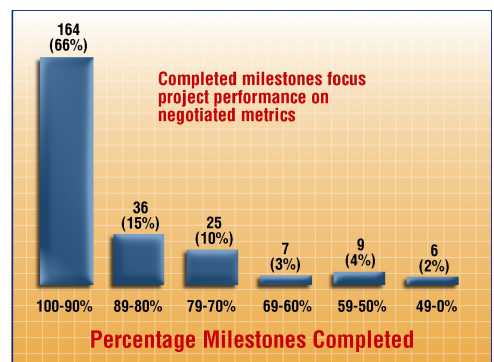
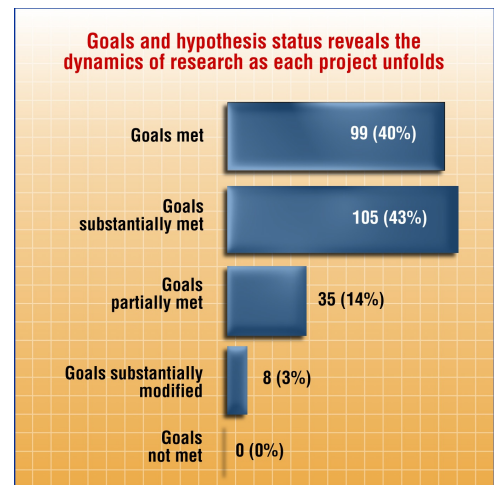
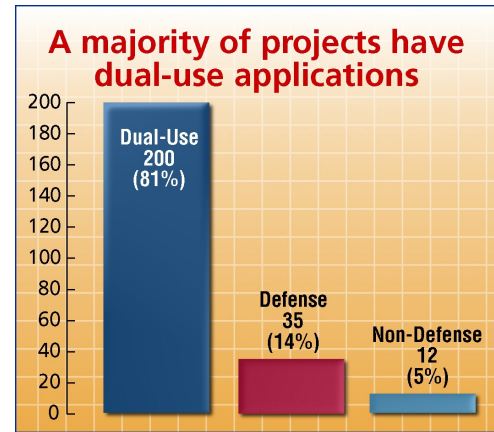
- **Research Foundations** (Materials Science and Technology, Computer Sciences, Electronics and Photonics, and Modeling and Engineering Simulation)
- **Roadmap Technologies** (Sensing and Intelligent Controls, Manufacturing and Process Sciences, Surety Sciences, Information Systems and Technology, Directed Energy, and Environmental Sciences)
- **Corporate Objectives** (Nuclear Weapons, Science and Technology, Partnerships, Energy and Critical Infrastructure, Nonproliferation and Materials Control, Emerging Threats, University Collaborations)
- **Grand Challenges** (Integrate multiple discipline explorations)
- **Development Reserve** (Partnerships)

Additional Reading

A comprehensive discussion of DOE and Sandia’s LDRD Program management and funding sources may be found in the “Sandia National Laboratories FY 1999–2004 Institutional Plan,” dated December 1998.

Achievements

The following sections provide an articulation of LDRD research achievements by the executive management of the Labs’ Nuclear Weapons, Science and Technology, and Neutron Generator Programs.



LDRD Impact on the Nuclear Weapons Program at Sandia

Thomas Hunter

Senior Vice President, Nuclear Weapons Program

The Nuclear Weapons Program at Sandia National Laboratories derives significant benefit from the Labs' LDRD Program. LDRD is a key driver for the fundamental research that will allow Sandia to meet its weapons and national security mission commitments.

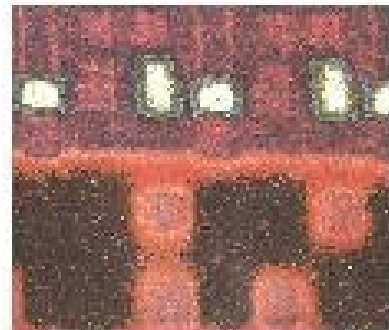
The entire Nuclear Weapons Stockpile will be revitalized in the next 15 years. In this timeframe, Sandia will incorporate new processes and will make investments in new, underlying technologies, including Surety Science, the Revolution in Engineering and Manufacturing (REM), and Integrated Microsystems. Surety Science focuses on safe, secure weapons and will also promote new applications across all of Sandia's business areas. The REM will establish a common information infrastructure for the Nuclear Weapons Complex (NWC) and will leverage modeling and simulation and advanced manufacturing technologies to reduce cost, defects, and cycle time for NWC products. Further, Sandia has developed and incorporated integrated microsystems into nuclear weapons as well as nonnuclear applications.

Reductions in the DOE Defense Programs (DP) budget have impacted the Labs' science and technology base over the last 10–15 years. LDRD funding has become a critical source for Directed Stockpile Work (DSW). Past LDRD research that has led to new technology for the stockpile includes automatic mesh generation (used for analysis of weapons safety, weapons design, manufacturing design), nonvolatile memories (circumvention memory for programmer, permissive action links, reprogrammable memory), and FastCast (housings for firesets and electronic assemblies). In addition, LDRD funding drove much of the initial research that helped develop the Labs' Accelerated Strategic Computing Initiative (ASCI) capability. LDRD research investments strengthen the science and technology foundation exploited by the Labs' stockpile mission.

Sandia is responsible for ensuring that DOE–DP electronics components are validated and certified against all specified radiation environments. Sandia LDRD research has improved our understanding of and our ability to protect microelectronics sensitivity to radiation effects. For example, LDRD research has supported the development of three forms of radiation effects microscopy (in conjunction with the Labs' modeling and simulation capabilities) to measure Single-Event Effects

The entire Nuclear Weapons Stockpile will be revitalized in the next 15 years.

LDRD funding has become a critical source for Directed Stockpile Work (DSW).



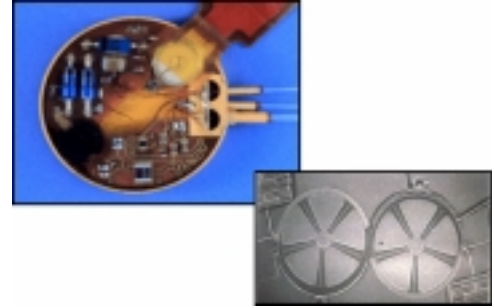
Ion-beam–induced charge collection

(SEE) *in situ*. SEEs are the result of high-energy nuclear particles (e.g., cosmic rays) impacting upon, and disrupting or disabling, a microelectronic device. As integrated circuit (IC) feature size decreases, SEE becomes increasingly probable, to the point that current 0.25-micron feature-size ICs sometimes fail in terrestrial applications.

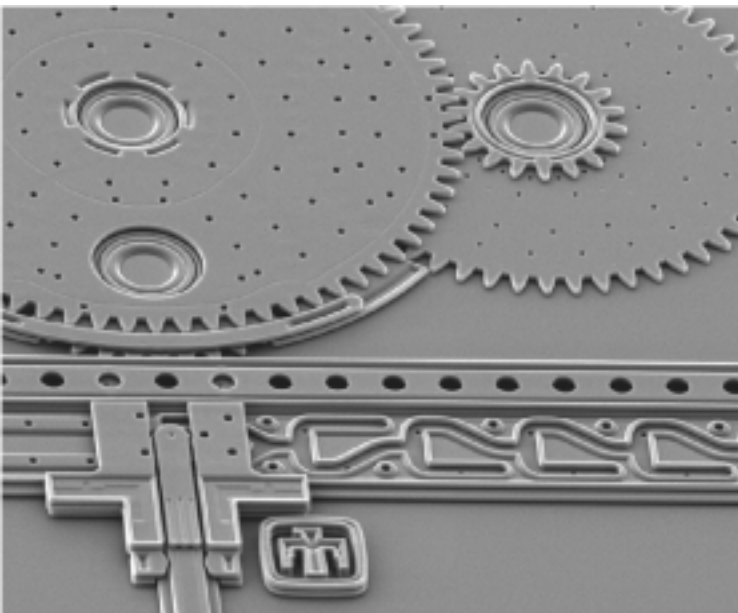
Sandia LDRD has funded approximately 20 projects that have developed the Labs' Asynchronous Transfer Mode (ATM) network technology security capability. This work contributed heavily to the ATM Forum Security Specification as well as to providing the standardizing techniques central to the current security of DOE's SECURENET. In addition, the LDRD high-speed networking research has led to the development of the world's fastest encryptor chip, which encrypts data at more than 6.7 billion bits per second.

The Trajectory Sensing System on a Chip (TSSC) is the most complex and ambitious microsystem that DOE-DP has attempted. It will add surety functions to the highly integrated fireset concepts now being developed by Sandia. This project consists of an environmental sensing discriminator that will include a Microelectromechanical Systems (MEMS)-based integrating accelerometer with a Photonic Integrated Circuit (PIC) readout head. Numerous LDRD projects have contributed to the main technology components upon which this system is based.

The W76 slapper stronglink is currently an option in the W76 SLEP plan and requires a miniaturized noncontact optical



Microsystems research



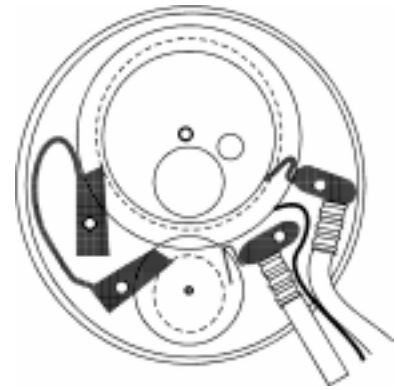
Surface-micromachined mechanical timer

monitor to determine the position of rotating parts in advanced stronglink designs. The monitors are based on a rotary shaft encoder system. The use of innovative packaging, VCSELs (Vertical-Cavity Surface-Emitting Lasers), and microoptics has allowed this system to be built in several cubic millimeters of volume. A long history of LDRD research advances in VCSELs and other areas has contributed to the development of key technologies supporting this system.

The Pantex Process Model (PPM), jointly researched and developed by Sandia, Pantex, Cornell University, and Rensselaer Polytechnic Institute, is having a major impact on the Weapons Complex by providing a capability to efficiently optimize Pantex activities from short- to long-term horizons. Long-term “what-if” planning capabilities have allowed DOE to extend its dismantlement planning from a 10-year horizon to 30 years.

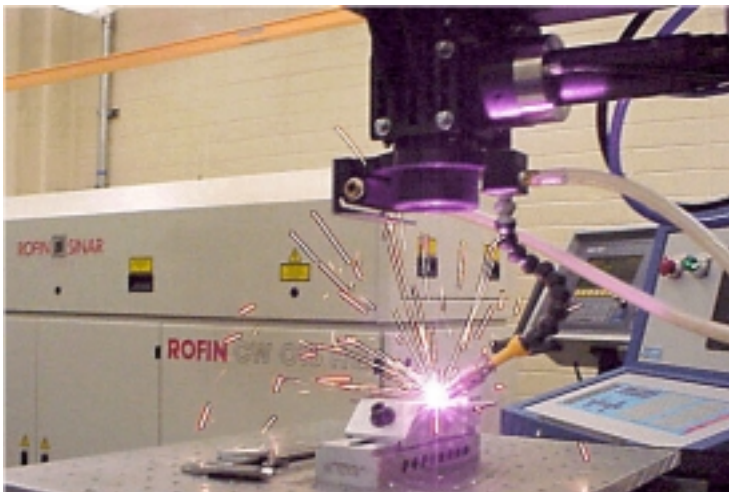
The PPM has made use of ASCI-developed capabilities (e.g., ASCI Red computation) to provide exact solutions to optimization problems as a benchmark for model-derived heuristic results. The model has expanded to encompass the Neutron Generator Capacity Planning Model, which is expected to have an impact at Sandia similar to that observed at Pantex. The model was honored as a finalist for the highly coveted 1999 Franz Edelman Award for Operations Research and Management Science.

Future LDRD research will explore enhancements to the safety and reliability of the stockpile. Miniaturized components will allow surety enhancement and placement ever deeper into complex weapons systems.



Electrokinetic pump for stronglink prime mover

Miniaturized components will allow surety enhancement and placement ever deeper into complex weapons systems.



Laser-assisted micro-gas metal arc welding

LDRD Impact on Sandia's Science and Technology Program

Al Romig

Vice President, Science, Technology and Components

Sandia's Science and Technology (S&T) portfolio focuses on building the Labs' long-term national security and stockpile mission capabilities. The S&T portfolio provides Sandia's essential base for success, including developing high-performance computing and modeling and simulation systems, creating risk-assessment tools, developing technology for enhanced surveillance and stockpile stewardship, studying the aging of systems, and building integrated microsystems (e.g., integrated circuit technology, the MicroChemLab, microoptics, etc.).

Sandia's Research Foundations are discipline-focused centers of excellence and comprise the following areas:

- *Computational and Information Sciences* — includes the development of the Teraflop machine
- *Materials and Processes* — develops new materials for advanced manufacturing; researches the aging of materials
- *Microelectronics and Photonics* — integrates critical microsystems and technologies; advances compound semiconductors
- *Engineering Sciences* — develops advanced computational and experimental tools enabling the continuing certification and assessment of weapons systems in the enduring stockpile

The Research Foundations provide the S&T focus areas with a distinctive set of competencies and growth potential. The surety revolution (i.e., the integration of safety, security, and reliability) has applications to the stockpile as well to the nation's power grid and air transportation systems. The Revolution in Engineering and Manufacturing (REM) improves the computational tools of desktop engineering systems and incorporates the power of the Teraflop machine to allow scientists and engineers to work more effectively. Integrated Microsystems will ultimately contain sensing, processing, mechanical actuators, and communications on a single chip. Because of their low cost and high functionality, Integrated Microsystems will enable entirely new systems and applications.

Technology is moving in the direction of increased functionality in ever-smaller packages, leading to the likelihood that entire systems functions will soon be available in integrated packages. This trend of rapidly changing technology tools

The S&T portfolio provides Sandia's essential base for success,....

Thanks to LDRD funding that began in 1992, Sandia's MEMS (Microelectromechanical Systems) technology has become the national standard for how microsystems are built.

makes it imperative that Sandia retain the core technologies necessary to create state-of-the-art engineering solutions. Correspondingly, it is essential that Sandia conduct research teaming system engineers and microtechnology providers to lead the creation of future integrated microsystems.

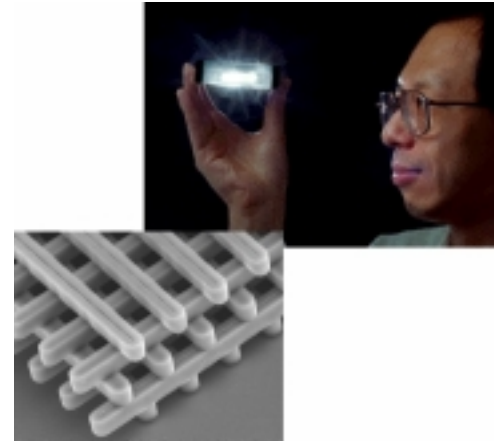
Thanks to LDRD funding that began in 1992, Sandia's MEMS (Microelectromechanical Systems) technology has become the national standard for how microsystems are built. This technology has matured and will have an impact on our weapons system, particularly the W80 and the W76.

Sandia's 3-D Photonics Lattice technology is LDRD-funding supported and a winner of a 1999 R&D 100 Award. The lattice of interlocking bars (i.e., photonic lattice) acts like a mirror to enable light to be "turned on a dime" and requires only one-tenth to one-fifth the space required by conventional light-bending waveguides. This capability will be useful in advanced spectroscopy for military applications, thermal emissivity control (thermal stealth), and military and commercial optical communications.

One of the biggest problems Sandia faces with systems reliability is broken solder joints, which are caused by thermal-induced stress cycling. LDRD materials modeling research is improving our understanding of material properties in order to prevent stockpile surprises and preclude future reliability problems.

Sandia is currently developing three integrated microsystems: the MicroChemLab-on-a-Chip, the Micronavigator, and a microsurity device. MicroChemLab technology, formed by miniaturizing and integrating sensing capabilities onto a chip, is a fully self-contained chemistry lab for gas and liquid chemical identification. The MicroChemLab was the first Sandia "Grand Challenge" LDRD project (FY97-FY00). The project required refining the basic building blocks of previous LDRD research to meet the specific goals for an integrated ChemLab system. The project also required the integration of a lab-wide, multidisciplinary team. Similar integration of technologies and multidisciplinary teams will be conducted in the new Microsystems and Engineering Sciences Application (MESA) facility.

Over the next five years, Sandia and DOE will commit \$300M for the design and construction of the MESA facility. MESA provides essential facilities and capabilities to integrate three key components of Sandia's mission to rebuild the stockpile: microsystems technology development, computational and engineering sciences and analysis, and weapon design, system



3-D photonics lattice



MicroChemLab-on-a-Chip

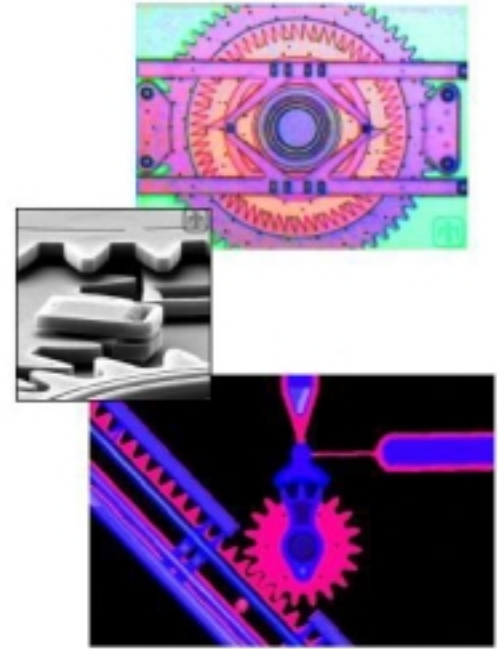
integration, and certification. MESA will support Sandia's responsibilities for stockpile upgrades with full-scale development of the W80 in 2002 and the W76 in 2005. The early work can be done in existing facilities, and the technical development and modeling simulation work can be started before the MESA facility is complete.

MESA integrates much of what Sandia excels in, from robotics to microsystems to information systems—to develop systems that can sense, “think,” act, and communicate. The MESA concept is based on LDRD investments made over the last 15 years—MESA would not exist without LDRD.

Where will we be in 2020? Sandia will utilize microsystem technologies in the stockpile, which means that we will utilize LDRD research-derived capabilities. Emergent behavior deals with new technologies derived from distributed and collective intelligence. Collective intelligence will raise surety science to new levels of performance for software protection, self-aware/self-correcting weapon systems, and distributed intelligence for sensing and monitoring. In addition, life sciences will play a bigger role as we explore a new direction for the Labs: biosciences.

Biotechnology advances have the potential to lead to new approaches and new options for future stockpile upgrades. Sandia cannot recreate an entire biotechnology portfolio, so we must partner to share knowledge and collaborate with the strengths of other organizations. For example, Sandia is strong in engineering, less so in traditional biological areas. Potential collaborators may include the National Institutes of Health (NIH) and medical schools. Biotechnology will be an emphasis for Sandia's LDRD Grand Challenge projects next year.

In addition, biotechnology is an important attraction for recruiting the best and brightest universities' graduates. This young talent will be essential for advancing new weapons components and systems designs. Migration to biologically driven systems will gradually be realized over the next couple of decades.



Microsystems research

The MESA concept is based on LDRD investments made over the last 15 years.

LDRD Impact on Sandia's Neutron Generator Program

J. Leonard Martinez

Vice President, Defense Programs, Products and Services

Neutron generators (NGs) are linear accelerators composed of numerous small parts that utilize high voltages. Due to their composition, stringent requirements present unique challenges to their manufacturing. For example, they have to be compact, exhibit long life, function reliably, provide high voltage, and operate in severe environments. Further, NGs are made of complex materials using high-vacuum technology, require dimensional precision, are built in low-volume production, and require a wide variety of processes.

Each NG has 60–80 very small parts that must be inspected with a microscope. As a result, it is difficult to consistently uncover defects. For example, brazing defects have a significant impact on generator quality by driving material, labor, and overhead costs. Sandia applies brazing process-based quality (PBQ) measures to improve the process and eventually eliminate the need for inspection. To approach inspectionless processes, Sandia is conducting diagnostic research to improve our understanding of process outputs and ultimately the manufacturing process itself.

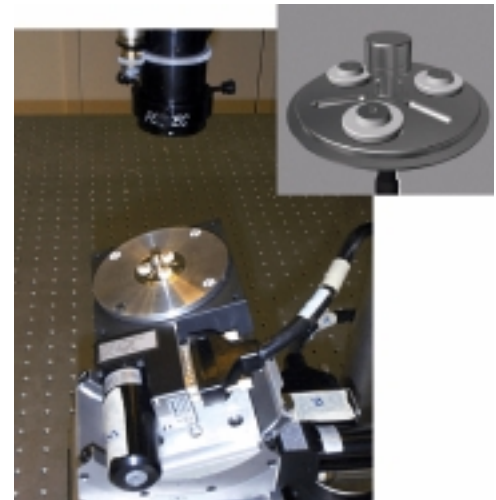
LDRD research (“Scripting for Video Inspection”) is currently being conducted to enhance process diagnostic capabilities via computer vision technology. This research will enhance our understanding of critical braze joints and will create visual records of these interfaces. The research combines lighting, optics, and decision-making processing expertise. In addition, the diagnostic inspection system must be insensitive to geometric tolerances, yet sensitive to cracks, blemishes, and missing components. This technology has the potential to save many hours of labor time and will develop a visual record archive much improved over currently collected records. This technology also has broad potential applications for other manufacturing processes involving polishing, grinding, and joining.

Traditional NGs used in nuclear weapons systems employ a portable ion accelerator with a tritium target. Such neutron tubes work well, but they are difficult to make in small sizes, require high-voltage power systems, and have a limited shelf life. Current Sandia LDRD research (“Solid-State Neutron Generator for Use in Nuclear Weapons”) is evaluating a novel approach to neutron generation involving the use of an alpha-emitting radioisotope mixed with beryllium. The traditional disadvantage of such an alpha-Be source is that they are always on—they emit

LDRD research is instrumental to Sandia's Neutron Generator Program....

....by discovernig solutions to a number of difficult challenges.

Visual diagnostics



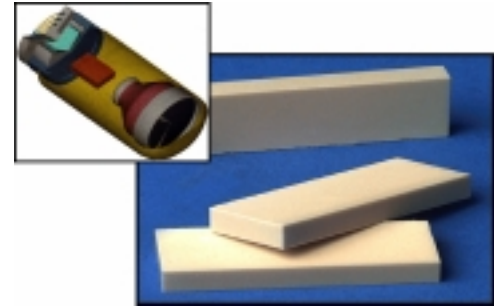
neutrons at a steady rate, even when stored, and require shielding to prevent exposure to personnel and sensitive electronics. However, with the advent of modern micromachining techniques (in particular, the LIGA [Lithography Galvanofarming Abforming] process), it may be possible to build a switchable, all solid-state neutron source that will emit negligible dose when in the off state.

Applications of thin films are found in many Defense Programs (DP) and industry applications. It is known that ion bombardment during vapor deposition modifies film properties and performance, including microstructure, residual stress, and adhesion. A current Sandia LDRD project (“Thin-Film Deposition Processes Incorporating In Situ Monitoring Capabilities”) has great potential to help solve a nagging ion source problem. New laser techniques are being investigated for measuring film stress and thin-film deposition methods via sputtering as opposed to evaporation techniques. This research has the potential to improve long-term film reliability by providing a method to manipulate and monitor film properties during deposition. In addition, this research is expected to lead to new, robust production processes and parts having reduced numbers of defects.

Additional LDRD projects are currently being conducted with potentially significant impact on the Sandia Neutron Generator Program. Examples of other research impacting the NG Program include (but are not limited to):

- Improving process capability for applying thermal spray coatings on NGs and reducing the need for costly and time-consuming inspections
- Developing advanced production planning models capable of optimizing capacity needs and production schedule performance
- Researching fundamental microscopic properties that control liquid-solid interfacial reactions to improve joining processes and meet production requirements, particularly for active brazing alloys
- Developing accurate and validated modeling tools for predicting braze microstructures, optimizing joining processes, and meeting production requirements.

In summary, LDRD research is instrumental to Sandia’s Neutron Generator Program for discovering solutions to a number of difficult challenges. Sandia LDRD research is helping to ensure predictable NG deliveries through process-based quality, to supply critical generator materials, to meet increased capacity requirements, and to achieve a “half-cost, half-time, and zero-defect” goal for new products.



Future materials

Sandia LDRD research is helping to ensure predictable neutron generator deliveries....

MATERIALS SCIENCE & TECHNOLOGY

Materials Science and Technology is one of Sandia National Laboratories' four LDRD Research Foundations investment areas. Research Foundations extend the core scientific and technical knowledge base of the Laboratories. In addition, Research Foundations focus on innovative, high-risk research that supports the long-term needs of the DOE's and Sandia's national security mission.

Sandia National Laboratories' National Security (NS) and the Stockpile Stewardship Program (SSP) missions are heavily dependent on the development of advanced materials and processes. The Materials Science and Technology (MS&T) investment area researches materials that behave in a predictable manner during all phases of their lifecycle. These investigations advance the research and development of products ranging from "smart devices" to mechanical, electronic, optic, chemical, and magnetic components and microsystems.

MS&T conducts materials and processing research in three areas: (1) aging and reliability studies to enable predictive stewardship of the nuclear stockpile, (2) novel materials-processing investigations that develop affordable, high-performance materials that behave and age predictably, and (3) scientifically tailored materials research that explores microelectronic, optical, electro-mechanical, magnetic, and chemical functions to enable microsystems to function and communicate.

The "Combinatorial Microlab Investigation of Critical Copper-Corrosion Mechanisms" project is

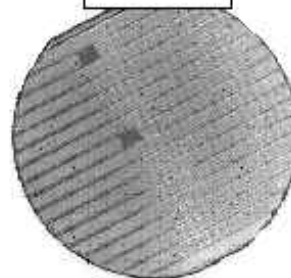
researching a capability to predict stockpile reliability based on a physics-based understanding of atmospheric corrosion. Corrosion presents one of the most pervasive and high-consequence problems in nuclear stockpile stewardship. The project is exploring corrosion effects on materials aging and electrical-device reliability by combining parallel miniature experimentation with ultra-sensitive microanalytical techniques in a microdomain "laboratory." Combinatorial experiments rapidly quantify variables that improve physical models for complex chemical processes of key importance to DOE Defense Programs.



From This

First step to creating massively parallel experimentation on microscopic scale

To This



3502330000

Functional Materials for Microsystems: Smart Self-Assembled Photochromic Films

A. R. Burns, C. J. Brinker, D. Y. Sasaki, M. H. Crawford, R. W. Carpick, F. B. Van Swol

Sandia will scientifically tailor smart interfacial films and 3-D composite nanostructures to exhibit photochromic responses to specific, highly localized chemical and/or mechanical stimuli, and to integrate them into optical microsystems. The project will involve the design of functionalized chromophoric self-assembled materials that possess intense and environmentally sensitive optical properties (absorbance, fluorescence), enabling their use as detectors of specific stimuli and transducers when interfaced with optical probes. Particularly strong candidates for initial studies are the conjugated polydiacetylenes (PDAs). We will immobilize the organic functional material in an ordered, mesostructured, inorganic host matrix that will serve as a perm-selective barrier to chemical and biological agents and provide structural support for improved material durability. We will facilitate construction of these hybrid organic/inorganic layers by advanced self-assembly techniques. Multitask scanning probe techniques (AFM [atomic force microscopy], NSOM [near-field scanning optical microscopy]) offering simultaneous optical and interfacial force capabilities will drive the chromophoric materials with localized and specific interactions for detailed characterization of physical mechanisms and parameters. We will directly interface the composite films with microscale devices as optical elements (e.g., intracavity mirrors, diffraction gratings), taking advantage of the very high sensitivity of device performance to real-time dielectric changes in the films.

We examined the mechanical transformation of the PDA from the nonfluorescent blue phase to the fluorescent red phase that is induced by local interaction of AFM or NSOM scanning probe tips. The nanomechanical transformation was the first-ever phase change induced by a probe tip. This achievement was made possible by the preparation of highly ordered, uniform Langmuir-Blodgett trilayers of PDA on mica and silica substrates. Extensive characterization of trilayer films via AFM, NSOM, and polarization fluorescence microscopy indicated huge (> 250 nm), atomically flat domains of conjugated backbone orientation. We successfully demonstra-

The project will involve the design of functionalized chromophoric self-assembled materials that possess intense and environmentally sensitive optical properties (absorbance, fluorescence), enabling their use as detectors of specific stimuli and transducers when interfaced with optical probes.

demonstrated that the monomer precursor can direct silica self-assembly into laminate mesostructures. Furthermore, the monomer can be polymerized within the laminate into the PDA blue form and then be thermally or chemically converted into the red form. The successful laminate was in large part due to modification of the diacetylene monomer to achieve the proper amphiphilic character. Other synthetic modifications include attachment of a glucose receptor site to the tail group for chemical sensing, and an amido alcohol head group for stabilizing monolayer films. Finally, we demonstrated micron-level selective-area PDA polymerization (blue or red form) on glass substrates. We should now be able to create responsive, mode-selective, optical components for microscale systems.

Refereed

Carpick, R. W., D. Y. Sasaki, and A. R. Burns. 1999.
“First Observation of Mechanochromism at the
Nanometer Scale.” *Langmuir*, in press.

Carpick, R. W., D. Y. Sasaki, and A. R. Burns. 1999.
“Large Friction Anisotropy of a Polydiacetylene
Monolayer.” *Tribology Letters*, in press.

3502340000

Innovative Experimental and Computational Diagnostics for Monitoring Corrosion in Weapons Environments

F. D. Wall, R. W. Cernosek, J. C. Barbour, C. C. Battaile, N. A. Missert

Sandia is advancing capabilities to detect and quantify aluminum (Al) alloy degradation in atmospheric environments by leveraging our expertise in nanofabrication technology to produce electrode microstructures and microelectrochemical test platforms amenable to testing in thin adsorbed water layers. We use planar arrays of individually addressable microelectrodes to perform both passive and perturbing electrochemical testing under conditions in which conventional electrochemical techniques are not applicable. Precisely engineered sample microstructures make it possible to systematically vary material characteristics and derive causal relationships with atmospheric degradation. Secondary phases in Al alloys can polarize surrounding material due to galvanic interactions, and many proposed degradation mechanisms include galvanic driving force as a critical component. To understand how secondary phases affect corrosion, it is necessary to describe the potential and current distributions on a sample surface. We are developing a mesoscale electrical model to incorporate arbitrary second-phase distributions and variable adsorbed electrolyte morphology in order to predict combinations of environment and microstructure that enhance the propensity for galvanic degradation. We take particle-particle interactions as well as particle-matrix interactions into account. To predict material performance in atmosphere it is also necessary to describe the adsorbed environment. Surface acoustic-wave (SAW) technology provides a means of detecting a fraction of a monolayer change in adsorbed species. By nanofabricating electrodes on a SAW platform, we can determine how microstructure and geometry impact water adsorption. SAW devices can also be used to sense changes in the acoustic properties of material oxides due to damage accumulation and may operate as early-warning sensors for atmospheric degradation. We will also make efforts to spatially resolve SAW signals to determine where as well as when damage initiates. The focusing of specimen design, electrochemical measurements, modeling, and environmental characterization to the mesoscale level is critical to lifetime predictions in stockpile environments.

The focusing of specimen design, electrochemical measurements, modeling, and environmental characterization to the mesoscale level is critical to lifetime predictions in stockpile environments.

We focused our efforts on the fabrication and validation of thin-film structures necessary to perform electrochemical testing and SAW measurements in thin, adsorbed water layers. We validated the performance of several types of individually addressable electrode structures and showed sensitivity to electrochemical signals under atmospheric exposure conditions. We developed a 3-D model to better understand the potential and current fields that arise due to differences between substrate material and secondary phases. We are expanding this model to accommodate electrochemical as well as electrical effects.

We fabricated two types of microelectrochemical cells. The first consists of pairs of interdigitated platinum (Pt) fingers that maximize electrode surface area while minimizing inter-electrode spacing. This configuration is desirable for making atmospheric electrochemical impedance spectroscopy (EIS) measurements. Measurements in a bulk aqueous environment indicate that the interdigitated electrodes yield similar data to standard thin-film electrodes with shifts in impedance due to differences in electrode area and no discernible artifacts from the high edge length to surface area ratio. We found EIS data from atmospheric exposures to be a function of relative humidity (RH) and temperature, indicating acceleration of reaction rates when the temperature was changed from 40°C to 60°C at 80% RH. The interdigitated electrode configuration appears to be a viable candidate for assessing *in situ* corrosion rate data. We fabricated second-generation interdigitated electrodes consisting of pairs of Al-Al, Al-Cu, and Cu-Cu fingers. These electrodes will be instrumental in deriving the galvanic corrosion component in atmospheric systems.

We fabricated a second type of microelectrochemical cell that consists of 19 electrically isolated, individually addressable Al, gold (Au), and Cu microelectrodes. We collected EIS data on the Al pads using the Au as a reference electrode and Cu as the counter electrode. The results were in agreement with data collected using external, macroscopic counter and reference electrodes. Furthermore, the free corrosion behavior (as reflected by open circuit potential measurement) of the Al pads in 50 mMol NaCl were in agreement with testing on standard electrodes. We acquired a multichannel microelectrode analyzer (MMA). The unit at Sandia is the first of its kind and is capable of simultaneously resolving signals from 100 segments of a multisegment electrode. This device will provide spatially resolved current and/or potential information from an electrochemical system. Besides providing direct inputs for

The unit at Sandia is the first of its kind and is capable of simultaneously resolving signals from 100 segments of a multisegment electrode. This device will provide spatially resolved current and/or potential information from an electrochemical system.

model validation, this system will allow interaction effects between material phases to be studied as a function of RH and contaminant level.

We developed a 3-D electric field model that calculates potential distributions on Al samples containing noble secondary-phase particles (Cu) and predicts the critical particle spacing required for corrosion initiation based on particle geometry. The model is in agreement with data from exposure of nanoengineered specimens to a chloride environment. We also used the model to predict the maximum anodic current available to an initiating site. These data will lend insight into whether or not specific microstructures can sustain localized corrosion once it has been initiated.

We used e-beam evaporation to deposit Al thin films onto quartz substrates that had been functionalized with Au transducers for generating and monitoring SAWs. These samples are the foundation for performing SAW experiments to sense water adsorption and initiation of atmospheric degradation. We are designing additional SAW devices to incorporate secondary features (such as analogues to noble strengthening phases) for impact studies on acceleration of atmospheric corrosion.

Other Communications

Wall, F. D., C. C. Battaile, J. C. Barbour, N. A. Missert, K. A. Son, M. M. Martinez, and R. G. Copeland. 1999. "Small Length Scale Electrodes Generated Using Microfabrication Techniques." Paper presented to the NACE '99, San Antonio, TX, April.

3502350000

Self-Healing Molecular Assemblies for Control of Friction and Adhesion in MEMS

M. T. Dugger, R. W. Carpick, M. J. Stevens, D. Y. Sasaki, T. M. Mayer

Major barriers to implementing microelectromechanical systems (MEMS) technologies are the ability to chemically passivate and lubricate the surface of micromechanical structures to prevent adhesion and reduce friction and wear, and to prevent electrostatic charging of devices in radiation environments. Sandia is investigating a new class of molecular coatings that offer silicon (Si) surface passivation, elimination of surface oxide layers, self-healing lubrication properties, and a built-in mechanism to release shear energy through reversible chemical cleavage. We investigated two approaches. First, we investigated molecular assemblies that form liquid crystalline lamellar structures with robust mechanical properties. Second, we explored the feasibility of chemically modifying the polycrystalline Si surface directly, without an intermediary oxide layer, in a process that occurs simultaneously with the etching step used to remove the sacrificial oxide. We performed mechanical stress studies on these materials at the nanometer using atomic force microscopy (AFM). We used molecular dynamics (MD) simulation techniques to examine multilayer structure and phase separation as a function of molecular interaction potentials.

We designed and synthesized several fluorocarbon-hydrocarbon amphiphiles. The molecules contain an ether linkage and were prepared using fluorocarbon-based alcohols and alkyl bromides. We determined critical micelle concentration (CMC) for these new molecules and varied them between 10 and 2 μm in toluene, where longer alkyl chains yielded lower values. In dodecane the amphiphiles exhibited only aggregated structures at concentrations detectable by nuclear magnetic resonance (NMR). In dodecane, the CMC is estimated to be below 1 μm .

Attempts at direct passivation of the Si surface in high-frequency (HF) solutions were inconclusive. Infrared (IR) spectroscopic measurements confirmed formation of an H-terminated Si surface, but we did not observe evidence for photochemically induced reaction of alkenes with this surface.

We discovered that silane films exposed to high humidity can ball up into agglomerates on the surface, suggesting the need to evaluate the deposition conditions and high-humidity performance of the new coatings as well.

We successfully dissolved alkene in the aqueous medium using surfactants, but it is not clear that the alkene is available at the surface for reaction. Significant barriers remain for direct passivation of Si with alkenes.

We used scanning probe microscopy (SPM) to investigate the morphology and friction properties of silane-coated Si as a base for the multilayer films. Under appropriate conditions, they exhibit uniform topography and friction response. We discovered that silane films exposed to high humidity can ball up into agglomerates on the surface, suggesting the need to evaluate the deposition conditions and high-humidity performance of the new coatings as well.

Simulations focused on determining force-field parameters for the coarse-grained system, how readily the coarse-grained systems phase-separate, and under what force-field parameters lamellar phases occur. We were able to demonstrate formation of lamellar phases with appropriate choice of Leonard-Jones interaction parameters for all the particles in the system. We concluded that the coarse-grained model must include the Van der Waals and polarization contributions. We confirmed that the calculated Van der Waals terms will not produce phase separation, even for a mixture of fluorocarbon and hydrocarbon chains.

Refereed

Dugger, M. T., D. C. Senft, and B. Smith. 1998. "Friction and Wear in Lubricated MEMS." Paper presented to the ASME Symposium on Microscale Mechanics of Materials, Anaheim, CA, 16–20 November.

Dugger, M. T., D. C. Senft, and G. C. Nelson. 1998. "Friction and Durability of Chemisorbed Organic Lubricants for MEMS." *Microstructure and Tribology of Polymer Surfaces* 1 (15 March) (Meeting of the American Chemical Society, Boston, MA, 26 August): 50–60.

Dugger, M. T., G. C. Nelson, J. A. Ohlhausen, and G. A. Poulter. 1999. "Effects of O₂ and H₂O on the Friction and Wear of Silane-Treated Surface-Micromachined Structures." Paper presented to the Symposium on Micromachining and Microfabrication, Santa Clara, CA, 20–22 September.

Other Communications

Dugger, M. T. 1998. "Tribology at the Nanoscale: Surface Treatments for Micromachines." Presentation to seminar at the Georgia Institute of Technology and Clemson University, Atlanta, GA, 9–10 November.

3502360000

Linking Atomistic Computations with Phase-Field Modeling

J. J. Hoyt, D. Fan, F. M. Hosking, V. Tikare, M. D. Asta

In recent years the phase-field model (PFM) has emerged as the method of choice for simulating the complex solidification microstructures that form during brazing or soldering. Unfortunately the PFM requires input materials parameters that are difficult, if not impossible, to measure experimentally. We used molecular dynamics (MD) and Monte Carlo (MC) simulations to obtain the three quantities necessary for PFM: the diffusion coefficient in the liquid, the velocity of a planar solid-liquid interface as a function of undercooling, and the solid-liquid interfacial free energy. Using embedded atom potentials, we obtained the diffusion coefficient in pure nickel (Ni) and copper (Cu) from MD simulations. We observed a linear relation between the diffusivity and temperature in the vicinity of the melting point, and experimental data available for Cu were in good agreement with the computed results. The solid-liquid interface velocity for both Cu and Ni showed a pronounced anisotropy for three low-index crystallographic directions: 100, 110, and 111, and we found the velocity to be a factor of four to five less than the theoretical upper limit. Also, we developed a novel method for computing the solid-liquid interfacial free energy and its anisotropy.

In addition to the atomistic simulations, we developed PFMs that describe the evolution of dendrite-like grains and the effect of solute trapping on grain growth. We characterized dendritic grains by a fractal dimension and found that the initial decay of the total interface length is governed by a power law with an exponent that depends on the fractal dimension. In the case of solute trapping, we found that in the low-velocity/low-driving-force regime the velocity of grain boundary motion departs from a linear relation with curvature due to the effects of solute segregation.

• *Atomistic simulations.* Atomistic computations resulted in two papers and one invited talk at an international conference. The first paper describes MD simulations using embedded atom potentials for pure Cu and Ni, which computed the liquid diffusion coefficient as a function of temperature in the vicinity of the melting point. The results were in quite good agreement with experimental data that are available for Cu. In addition, we employed MD simulations to simulate the motion of a

The solid-liquid interface velocity for both Cu and Ni showed a pronounced anisotropy for three low-index crystallographic directions: 100, 110, and 111, and we found the velocity to be a factor of four to five less than the theoretical upper limit. Also, we developed a novel method for computing the solid-liquid interfacial free energy and its anisotropy.

solid-liquid interface as a function of undercooling for three low-index crystallographic directions 100, 110, and 111. We found that the interface velocity is a factor of four to five less than the theoretical upper limit and observed significant anisotropy.

In the PFM of precipitate growth in alloys, an important input parameter is the gradient energy coefficient, which defines the energy cost of creating a coherent interface between a solute-rich precipitate and the surrounding matrix. The second paper demonstrates how first-principles, total-energy calculations plus the cluster variation method description of configurational entropy can be utilized to compute the gradient energy coefficient. We chose the Ag-Al (silver-aluminum) binary system for study, and the results showed significant differences from the simple mean field prediction.

The final parameter necessary to complete the PFM description is the solid-liquid interfacial free energy. In the theory of dendritic solidification, a key parameter controlling the growth velocity is anisotropy of the interfacial free energy. In metals, the anisotropy is expected to be small, about 1%, and small changes in the anisotropy result in large changes in the velocity. Therefore, to accurately model dendrite formation one is faced with the very difficult problem of computing the interfacial energy for different crystallographic orientations to an accuracy of better than 1%. There are a number of possible approaches to the computation of surface energy, but we believe the most promising is the observation of time-averaged fluctuations in the position of the solid-liquid interface. In collaboration with Northeastern University, we showed that the interface fluctuations are extremely sensitive to the small anisotropy of interfacial energy, and a comparison of the fluctuation spectrum of a 100 and 110 interface will allow a very accurate determination of the surface energy.

• *Phase-field modeling.* Continuum modeling for the previous year resulted in three publications and three technical presentations.

The morphological properties of dendrite microstructures are very different from normal grain structures, as they are composed of serrated and rugged grain boundaries with very high curvatures. We adopted and developed PFM to simulate and study the evolution kinetics of these fractal grain structures.

Simulations showed that there are three distinctive kinetics for shrinkage of a fractal grain. At the initial stage, the power-law decay of the total interface length is characterized by a

nontrivial coarsening exponent that depends on the fractal dimension. In the middle stage, we found a novel exponential relation of total length and time, which has not been predicted theoretically for fractal grains. As time elapses, the relaxation kinetics is dominated by the shrinking process of the grain and is governed by the parabolic law of normal grain growth.

Solute trapping or solute drag is an important phenomenon during solidification. Solute trapping will change the kinetics of grain boundary motion. We studied the effects of solute trapping on grain growth kinetics in two-dimensional computer simulations by using a PFM. We showed that, in the low-velocity/low-driving-force regime, the velocity of a grain boundary motion departs from a linear relation with driving force (curvature) with solute drag. The nonlinear relation of migration velocity and driving force comes from the dependence of grain boundary energy and width on the curvature.

Refereed

Asta, M. D., and J. J. Hoyt. 1999. "Thermodynamic Properties of Coherent Interfaces in FCC-Based Ag-Al Alloys: A First-Principles Study." *Acta Materialia*, accepted.

Fan, D., S. P. Chen, and L. Q. Chen. 1999. "Computer Simulation of Grain Growth Kinetics with Solute-Drag." *J. Mater. Res.* **3**: 1113.

Fan, D., V. Tikare, and L. Q. Chen. 1999. "Simulations of Grain Growth Kinetics with Impurity and Anisotropy." Paper presented to the MRS Spring Meeting, San Francisco, CA, April.

Hoyt, J. J., and M. D. Asta. 1999. "Obtaining Parameters of the Phase-Field Model from Atomistic Simulations." Paper presented at the Workshop on Thermodynamic and Structural Properties of Alloy Materials, Oranjestad, Aruba, June.

Hoyt, J. J., B. Sadigh, M. D. Asta, and S. M. Foiles. 1999. "Kinetic Phase-Field Parameters for the Cu-Ni System Derived from Atomistic Computations." *Acta Materialia*, accepted.

Other Communications

Fan, D., S. P. Chen, L. Q. Chen, and P. W. Voorhees. 1999. "Numerical Simulation of 2-D Ostwald Ripening in the High-Volume Fraction Regime." *Acta Materialia*, submitted.

3502370000

A Combinatorial Microlab Investigation of Critical Copper-Corrosion Mechanisms

J. C. Barbour, K. R. Zavadil, J. P. Sullivan, J. S. Nelson, N. A. Missert, W. G. Breiland, J. W. Braithwaite

An important aspect in developing a capability to predict the reliability of electronic components is a physics-based understanding of atmospheric copper corrosion. This topic has been investigated over the last few decades, but debate continues concerning the mechanisms underlying even the initial stages of degradation. The difficulty being encountered is caused by the large number of coupled chemical reactions that depend on complex interactions of materials with the environment and the function of the copper-containing device. A solution to this multidimensional problem requires new experimental approaches that can quantitatively identify critical phenomena occurring in corrosion-phase space. An effort is currently under way to examine the usefulness of microcombinatorial techniques as the basis for developing these needed efficient experimental approaches. The initial phase of this work focuses on the specific topic of atmospheric copper (Cu) sulfidation using H₂S as the sulfidizing agent.

*We made a combinatorial (parallel experimentation) matrix in which we varied the Cu oxide growth (oxide type and thickness), surface impurity concentrations, and point defect levels systematically to test the mechanism of solid-state transport by vacancy-mediated diffusion. Solid-state diffusion of vacancies and di-vacancies in Cu, Cu₂O, CuO, and Cu₂S are thought to be key mechanisms in determining the kinetics of Cu sulfidation in one region of corrosion space. We developed a new experimental probe in the form of lithographically patterned Cu resistance lines. We used the change in resistance of these lines during exposure to an H₂S atmosphere as an *in situ* probe to determine the relative sulfidation rate of Cu with varying degrees of alloying and level of point defects.*

We made a combinatorial (parallel experimentation) matrix in which we varied the Cu oxide growth (oxide type and thickness), surface impurity concentrations, and point defect levels systematically to test the mechanism of solid-state transport by vacancy-mediated diffusion.

We electron beam-evaporated Cu films onto silicon dioxide (SiO₂)-coated Si wafers and then exposed them *in situ* to either a backfill of O₂ gas at 1 Torr pressure and 25°C, or an electron

We developed a new experimental probe in the form of lithographically patterned Cu resistance lines.

cyclotron resonance (ECR) O₂ plasma at temperatures varying from 35°C to 150°C. The O₂ backfill formed Cu₂O at the surface (simulating a native oxide), and the ECR O₂ plasma formed CuO at the surface that can be reduced to Cu₂O through ion irradiation. We varied the CuO thickness by increasing exposure time to the O₂ plasma. We then irradiated vertical strips (broad areas) with 200 keV Cu⁺ ions with ion fluences from 10¹² to 10¹⁵ Cu/cm². The range of these ions is such that doping of Cu in the oxide layer is negligible.

We lithographically patterned portions of the sample into meander-pattern resistance lines (R=80–100 Ω). We ion-implanted the samples with indium (In), aluminum (Al), oxygen (O), and deuterium (D) to form a concentration of 0.5 at. % up to a depth of 150 nm and implanted them with Cu to produce the same atomic displacement damage profile as the In implantation. The In and Al are thought to form vacancy traps. We measured sulfidation of broad area samples described above and meander-line samples for implantation-doped samples and control samples. We used resistance changes to determine absolute (and thereby relative) sulfidation rates as a function of exposure time to a 50 ppb H₂S, 80% RH, air environment at 35°C. We determined the increase in Cu₂S thickness from a decrease in Cu thickness (ΔH), the initial resistance (R₀), and the resistance at a later time (R_t): $\Delta H = ((1/R_0) - (1/R_t))R_0H_0$. We monitored control samples (unirradiated) to examine possible effects of current flowing through the resistance lines during sulfidation—one drawing current continuously and the other tested at infrequent intervals to minimize current flow. Finally, we measured the total sulfide thickness using ion beam analysis.

The sulfidation rate data fell into three distinctive groupings: (1) enhanced rates for D- and Cu-implanted samples yielding about 85 nm Cu₂S/hr; (2) control rates for the two control samples and the O-implanted sample yielding about 60 nm Cu₂S/hr; and (3) decreased rates for Al- and In-implanted samples yielding about 30 nm Cu₂S/hr.

The flow of current through the samples and the existence of implanted O had little effect on the sulfidation rate. However, implanted In and Al slowed the rate in agreement with *ab initio* calculations, which predicted that In and Al would trap vacancies and reduce solid-state diffusion. Surprisingly, the implantation of D, which produced the smallest level of point defects, had the greatest impact on enhancing the sulfidation rate. The hydrogenation and the behavior of trapped H on the Cu corrosion rate must be explored more fully. The relative

rates determined in these experiments suggest that the sulfidation rate correlates to vacancy permeability (vacancy concentration times vacancy diffusion). However, all of these meander-line sulfidation rates were greater than those observed for the broad-area samples made from the same films, but unpatterned. Some unknown effects produce a higher sulfidation rate in the narrow meander lines. Such a result cannot be simply explained by narrowing of the line due to sulfidation. Possible reasons for a higher sulfidation rate in the narrow lines are an increase in gas-phase mass transport (a possible rate-limiting process), stress induced in the lines from the patterning process, or an increased surface area or contamination due to prior chemical attack from the patterning process.

Refereed

Barbour, J. C., J. W. Braithwaite, N. A. Missert, and J. P. Sullivan. 1998. "Corrosion Behavior of Plasma-Passivated Cu and Al." Paper presented to the 11th International Conference on Ion Beam Modifications of Materials, Amsterdam, The Netherlands, 3 September.

Other Communications

Barbour, J. C. 1998. "New Approaches to Corrosion Studies at Sandia National Laboratories." (Invited) Paper presented to the University of Manchester, Institute of Science and Technology Center, Manchester, England, UK, 11 September.

Barbour, J. C., J. W. Braithwaite, J. P. Sullivan, W. G. Breiland, N. A. Missert, and J. S. Nelson. 1999. "Combinatorial Microlab Investigation of Copper-Corrosion Mechanisms." (Invited) Paper presented to Combinatorial Approaches, Knowledge Foundation, Inc., San Jose, CA, 21–22 January.

Barbour, J. C., J. W. Braithwaite, J. P. Sullivan, W. G. Breiland, N. A. Missert, and J. S. Nelson. 1999. "Combinatorial Microlab Investigation of Copper-Corrosion Mechanisms." Paper presented to the Materials Research Society Fall Meeting, Boston, MA, 30 November–3 December.

3502380000

Self-Assembled Templates for Fabricating Novel Nanoarrays and Controlling Materials Growth

R. Q. Hwang, N. A. Missert, C. J. Brinker, A. K. Schmid, K. R. Zavadil, N. C. Bartelt, P. J. Feibelman, M. E. Bartram

Novel and exciting phenomena that have the potential to revolutionize science, materials, and next-generation production methods are manifested as structural dimensions approach the nanometer level. However, advances in lithography are insufficient to achieve this feature scale. As a result, molecular self-assembly has attracted a great deal of interest, since this provides a possible spontaneous mechanism by which nanometer-sized arrays can be formed without mechanical intervention. Although these low-tech processes are highly dependent on system/material specifics, Sandia proposed that new techniques and the science that underlies them can be developed in a manner that allows us to extend the natural order of self-assembling systems. We based our approach on previous work in which we fabricated templates of unprecedented size and regularity. We will then apply these templates to form nanoarrays based on a wide range of materials with tunable properties and nanoscale selective-area over-growth patterns for improving the materials quality of thin films.

We determined the nature and origin of the forces stabilizing the S/Ag/Ru(0001) (sulfur/silver/ruthenium) self-organized nanostructure templates. They form because of the interaction between the strain fields at the edges of the holes, which is mediated by the underlying substrate. We assessed the thermal stability of the structure and found a limit of 500°K. In addition we attempted to fill the template by the deposition of another metal and found that it is limited by the presence of the residual S in the holes. From these results, we began developing strategies for the removal of the S at low temperatures, that is, under 500°K. We demonstrated thin films resulting from sol-gel processes to have a high degree of periodicity. This is particularly compelling in view of the fact that the resulting SiO₂ film can be used for selective-area growth strategies for the deposition of films such as nitrides. However, the periodicity having both sufficient transparency of the openings and orientation with respect to the underlying substrate necessary for this kind of application has yet to be demonstrated. Such is

...molecular self-assembly has attracted a great deal of interest, since this provides a possible spontaneous mechanism by which nanometer-sized arrays can be formed without mechanical intervention.

the goal of the initial investigation of this materials system. Finally, we began to investigate the chemical origin of the S etching process by performing first-principles calculations of the defects of copper (Cu) in preparation for calculating the interaction of S.

Refereed

de la Figuera, J., K. Pohl, A. K. Schmid, N. C. Bartelt, J. Hrbek, and R. Q. Hwang. 1999. "Multiplication of Threading Dislocations in Strained Metal Films Under Sulfur Exposure." *Surface Science* **435** (2 August): 93–98.

Pohl, K., J. de la Figuera, M. D. Bartelt, N. C. Bartelt, J. Hrbek, and R. Q. Hwang. 1999. "Thermal Vibrations of a Two-Dimensional Vacancy Island Crystal in a Strained Metal Film." *Surface Science* **435** (2 August): 506–511.

3502390000

Wetting and Spreading Dynamics of Solder and Braze Alloys

G. L. Kellogg, D. R. Jennison, N. D. Shinn, F. G. Yost, R. Q. Hwang, G. S. Grest, F. M. Hosking

The purpose of this project is to investigate the dynamics of liquid metal and alloy spreading at the length scales necessary to address fundamental issues in complex wetting phenomena. The approach exploits advances in both experimental surface science tools and atomistic modeling methods. In the experimental part of the project Sandia used low-energy electron microscopy (LEEM) and scanning-tunneling microscopy (STM) to investigate the properties of lead (Pb) and tin (Sn) overlayers on copper (Cu). We examined submonolayer growth of Pb and Sn to determine diffusion properties and intermixing conditions needed for atomistic simulations. We produced submicron-sized, three-dimensional (3-D) clusters of Pb on Cu surfaces in the LEEM and found that we could control the average cluster size and size distribution by varying the growth time and by subsequent thermal treatments. We examined the spreading behavior of Pb nanoclusters as they melted. In the atomistic modeling part of the program, we developed embedded atom method (EAM) potentials for molecular dynamics (MD) simulations. We modified a preexisting MD computer code that implements the EAM to perform the necessary simulations. In addition to our efforts to develop and test realistic models, we studied the spreading of large droplets using simpler, two-body Lennard-Jones (LJ) potential. We used these algorithms to follow the spreading of several large droplets (approximately 85,000 atoms) for long times. In the continuum modeling part of the project, we developed an approach to model the wetting kinetics of a small droplet of metal containing a constituent that diffuses on and chemically reacts with a flat, smooth substrate. We constructed the model in the circular cylinder coordinate system; it satisfies the diffusion equation and considers diffusion and reaction at the wetting line to be processes in series. When this modeling is complete we will compute the wetting rate versus time for a variety of diffusion and reaction conditions.

We used LEEM and STM to investigate the growth, wetting, and spreading behavior of Pb and Sn overlayers on Cu at length scales ranging from nanometers to microns. We developed EAM potentials for MD simulations and modified a

In the experimental part of the project Sandia used low-energy electron microscopy (LEEM) and scanning-tunneling microscopy (STM) to investigate the properties of lead (Pb) and tin (Sn) overlayers on copper (Cu).

preexisting MD computer code that implements the EAM to perform atomistic simulations of wetting and spreading. We also developed a continuum approach to model the wetting kinetics of a small liquid droplet of metal. Specific accomplishments are as follows:

(1) In LEEM and STM experiments, we examined submonolayer growth of Pb and Sn on Cu to determine diffusion properties and intermixing conditions needed for atomistic simulations. For the system of Pb on Cu(100), LEEM experiments showed that thin-film growth follows classical Stranski-Krastanov behavior, i.e., well-defined overlayer structures form at submonolayer coverages followed by 3-D island growth at higher coverages. We used the LEEM to investigate the structural properties and thermal stability of the various submonolayer phases. Combined LEEM and STM measurements of Sn growth on Cu(111) showed an entirely different behavior. Here, initial deposition produced highly mobile monolayer-high Sn islands distributed over the Cu surface. With time at room temperature, the Sn islands disappeared from the image. This is due to alloying with the Cu substrate as well as forming small islands that are below the resolution of the LEEM. From these results, it is clear that the wetting of Sn on Cu(111) is intimately linked to the alloying of the two materials. We will conduct further experiments to understand the difference in behavior between Pb and Sn, as well as look at the behavior of Pb/Sn alloys.

(2) We produced submicron-sized, 3-D clusters of Pb on Cu surfaces in the LEEM and found that we could control the average cluster size and size distribution by varying the growth time and by subsequent thermal treatments. We then observed, in real time, the spreading behavior of Pb nanoclusters as they melted.

(3) In the first phase of the atomistic modeling work, we developed and tested suitable interatomic potentials. Two different sets of EAM potential functions emerged as the most prevalent. We used these two sets of EAM functions to measure the surface tension of the liquid metals. We found that the surface tension of these EAM metals order properly according to experimental data, but that the magnitudes in all cases are 30%–50% below the experimental values. Since the wetting and spreading properties are clearly very sensitive to the surface tension, we are now working on including additional contributions to the EAM potential to more properly account for the interface properties.

(4) We studied the spreading of large droplets using simpler, two-body LJ potential. We used these algorithms to follow the spreading of several large droplets (approximately 85,000 atoms) for long times. The methodologies and analysis algorithms developed for this phase of the study are directly applicable to the upcoming runs using the more realistic EAM codes.

(5) We developed a continuum approach to model the wetting kinetics of a small droplet of metal containing a constituent that diffuses on and chemically reacts with a flat, smooth substrate. A significant amount of work suggests that processes collateral to wetting can moderate or retard the wetting rate. Even very small additions of a constituent, known to react with the substrate, cause pronounced improvement in wetting and are exploited in braze alloys, especially those used for joining to ceramics. We constructed our model in the circular cylinder coordinate system; it satisfies the diffusion equation and considers diffusion and reaction at the wetting line to be processes in series. When this modeling is complete, we will compute the wetting rate versus time for a variety of diffusion and reaction conditions.

Other Communications

Kellogg, G. L. 1999. "Low-Energy Electron Microscope Investigation of Pb Overlayers on Cu(100)." Paper presented to the 46th International Symposium of the American Vacuum Society, Seattle, WA, 25–29 October.

3502410000

Improved Materials Aging Diagnostics and Mechanisms Through 2-D Hyperspectral Imaging Methods and Algorithms

D. M. Haaland, L. E. Martin, E. V. Thomas, M. C. Celina, C. A. Drewien, D. K. Melgaard, F. W. Koehler, C. M. Wehlburg

Sandia successfully developed and programmed the new prediction-augmented classical least-squares/partial least-squares (PACLS/PLS) hybrid algorithm required as an integral step in our proposed quantitative analysis of hyperspectral image (HSI) data without the use of standards. We programmed this method for both single-processor and parallel-processor environments. We successfully applied the new algorithm to nonimage infrared (IR) spectra of dilute aqueous solutions to demonstrate their improved performance over traditional multivariate calibration methods. We demonstrated improvements in prediction ability by factors of two and four for two separate datasets. These improvements are dramatic and demonstrate the significance of the new algorithms. We will further demonstrate the full value of the new algorithms when we apply them to HSI data. In addition, we applied the application of multivariate curve resolution (MCR) methods that can form the basis for the extrapolation of the spectral data to the pure-component spectra to spectral data obtained from aged polymers as a function of time and temperature. The result is the clear identification of three separate oxidative degradation products. We also obtained relative concentrations of each of the three identified degradation products. We measured hyperspectral IR images of inkjet inks on aluminum foil and of aged neoprene polymers. These data will serve as the initial framework for testing the new methods for quantitative spectral analysis without standards. Finally, we developed statistical methods that employ the synergistic information in the spatial and spectral content of the HSIs to improve the estimates of the pure-component spectra required for quantitation and for improving the spatial concentration maps of the sample.

Our most significant milestone was developing and coding the CLS/PLS hybrid algorithm that incorporated our newest PACLS improvements into our chemometrics software. This new Sandia proprietary algorithm is an integral part of the overall goal of the project to develop methods to perform quantitative HSI analysis without the use of standards.

We demonstrated improvements in prediction ability by factors of two and four for two separate datasets. These improvements are dramatic and demonstrate the significance of the new algorithms.

We completed testing the new algorithms on nonimage solution IR transmission calibration data. We tested the new hybrid algorithm on aqueous solution near-infrared (NIR) spectra of samples containing low concentrations of urea, creatinine, and NaCl (sodium chloride) in water at both constant and variable temperatures. In this study, we found that the new algorithm significantly outperformed the conventional PLS method. The new CLS/PLS method can overcome the detrimental effects of temperature variations through a process by which the spectrum representing the change in the temperature of water is simply added in the development of the original hybrid model. The use of this procedure improves the urea standard error of prediction (SEP) from 152 to 22 mg/dL for prediction of the variable-temperature dataset.

We also tested the methods on data collected for determining IR spectral detection limits for isopropanol in water using a new surface-modified sol-gel IR sensor. Since spectrometer drift was more than 90% of the spectral variance of this latter dataset, it represents an excellent test of the ability of the new hybrid algorithm to maintain a multivariate calibration in the presence of dominant spectrometer drift. In this study, the hybrid algorithm yielded a true prediction SEP of 10 parts per million (ppm) for isopropanol while the SEP for the conventional PLS algorithm applied to the same data was 21 ppm.

Due to the rapid development, programming, and testing of the hybrid algorithm on the single processor PC platform, we accelerated the schedule of implementing the same algorithm on a parallel processor system. We completed this parallel processor program and tested it with the above aqueous sample spectral test set.

Another task involved applying these new multivariate calibration methods to the IR spectra of aged polymers from accelerated aging tests. We applied methods known as MCR to the spectral data of the polymers as a function of aging temperature and time in order to extract the pure-component spectra of carbonyl degradation products in the polymer samples. We identified three different carbonyl degradation products using these MCR methods, where only one degradation product had been detected by conventional methods using these same data. We determined the relative concentrations of three newly identified degradation products as a function of temperature and time.

We also generated quantitative microscopic samples for these IR HSIs using an inkjet printer with the complementary

dyes representing three pure-component samples and three 50:50 binary mixtures of the dyes representing known mixtures. This sample represents an ideal test case for evaluating the performance of our new algorithms and methods for analyzing HSIs. We analyzed the images from these samples using several techniques to extract the spectra of the pure inks. We observed artifacts due to chromatic aberrations and generated ideas to correct for their presence.

Finally, we formulated new methods to simultaneously combine spatial and spectral information from the HSIs. To date, all analyses of the spectra in the images have ignored the potentially systematic information in the spatial relationships between pixels. If there is a known or continuously varying pattern in the spatial relationship between pixels, and if the component spectra are linearly additive, we have formulated methods to combine this spectral information with the spatial information to improve both spectral estimates and spatial resolution.

Other Communications

Haaland, D. M. 1999. "Chemometrics: A Historical Perspective and New Opportunities with Improved Algorithms." Paper presented to the Pittsburgh Conference for Analytical Chemistry and Applied Spectroscopy, Orlando, FL, March.

Haaland, D. M. 1999. "Classical Least Squares Multivariate Spectral Analysis: Revival of an Early Chemometric Method." Paper presented to the Society of Applied Spectroscopy Chemometrics Workshop, Naperville, IL, 18 February.

Haaland, D. M., and D. K. Melgaard. 1999. "A New CLS/PLS Hybrid Algorithm for Improved Multivariate Calibration Capabilities." (Invited) Paper presented to the Federation of Analytical Chemistry and Spectroscopy Societies Meeting, Vancouver, BC, Canada, 24–29 October. SAND 99-2161.

Haaland, D. M., and D. K. Melgaard. 1999. "Prediction-Augmented Classical Least-Squares Methods for Maintaining Calibrations on a Rapidly Drifting Spectrometer." (Invited) Paper presented to the Federation of Analytical Chemistry and Spectroscopy Societies Meeting, Vancouver, BC, Canada, 24–29 October. SAND 99-2163A.

3502420000

Microscale Shock-Wave Physics Using Photonic Driver Techniques

R. E. Setchell, W. M. Trott, A. V. Farnsworth, Jr.

The goal of this project is to establish a new capability for conducting shock-wave physics experiments at low per-experiment costs through a significant reduction in experimental length and time scales. Based on the earlier development of laser-based optical detonator technology at Sandia, this new capability will utilize the rapid absorption of optical energy from large, Q-switched, solid-state lasers to accelerate small planar films (a launch process known as photonic driving). The films subsequently impact another material, generating shock waves in both materials having amplitudes and durations that depend on the impact velocity and film thickness, respectively. We previously developed subnanosecond interferometric diagnostics to examine the motion and impact of these films. To address a useful range of materials and stress states, photonic driving levels must be scaled up considerably from optical detonator levels. An order-of-magnitude increase permits the study of the dynamic mechanical behavior of materials having thicknesses up to tens of microns. Some important materials, such as polycrystalline silicon (Si) (the basic structural material in surface micro-machines), can be studied at this stage. An additional order-of-magnitude increase is a future goal. To enable practical studies of the shock-wave response of a broad range of materials, however, photonic driving levels at least three orders of magnitude above detonator levels are necessary. At these levels we can study the dynamic behavior of materials up to a fraction of a millimeter thick, including a number of materials of current interest such as materials in shock-activated components. However, significant increases in laser energies pose severe challenges to be overcome with respect to laser-induced damage in optics, beam shaping, thermally driven phase transitions in the laser-accelerated materials, and instabilities in these materials during acceleration.

Our goal was to demonstrate the ability to make shock physics measurements using photonic driving levels one order of magnitude higher than optical detonator conditions (that is, with laser pulse energies > 250 mJ). The first step was to achieve suitable beam characteristics at the intended driving levels using an existing laser. We modified a 2-Joule,

...we can study the dynamic behavior of materials up to a fraction of a millimeter thick, including a number of materials of current interest such as materials in shock-activated components.

oscillator-only, Nd:glass laser by reducing cavity dimensions and eliminating internal apertures to achieve a highly multi-mode output with three times the original divergence (necessary for the intended delivery system). The next steps were to assess beam smoothing and shaping options and to determine an optimum approach for beam delivery. For accelerating planar flyers with no instabilities during acceleration, a uniform laser fluence must be incident on a substrate/flyer interface. In optical detonators this is achieved by transmitting the laser beam through an optical fiber. With suitable injection optics and a sufficiently long fiber path, a nearly flat intensity profile can be produced at the fiber exit face. Either a flyer film is deposited directly on this fiber face or the light exiting this face is re-imaged through a transparent substrate having a deposited flyer film. Challenges in high-intensity fiber transmission include air breakdown at the focal point of a beam-focusing lens, laser-induced breakdown or damage at the fiber entrance face, and laser-induced internal damage along the fiber path. We studied these challenges extensively in the course of developing and applying optical detonator technology, and a fiber-based delivery system was our choice for the desired first-year driving levels. Peak fluence thresholds for breakdown or damage at the fiber entrance face dictated that the fiber core diameter be 800 microns or larger, and we obtained commercial fibers having pure fused-silica cores with diameters of 800 and 940 microns. The modifications to the Nd:glass laser enabled a simple plano-convex lens to be used to inject the beam successfully into either of these fibers at the desired pulse energies. However, to further reduce the risk of breakdown or damage, we designed and fabricated a custom diffractive optic that is used with the focusing lens for this project. We re-imaged the output from the fiber onto a substrate/flyer interface using two graded-index (aberration-free) lenses.

Another project activity was to utilize a CTH-based hydrocode developed earlier during the optical detonator project to assess design options for flyers and targets. Unfortunately, the original laser deposition and energy transport routines were not written to run on the parallel platforms utilized by the current configuration of CTH. We changed these routines, made improvements in the handling of spatial and temporal variations in laser intensity, and are currently testing the code against experimental data obtained earlier using a detonator-level photonic driver system. These data resulted from a study of flyer boundary issues that arise with

the thicker flyers that can be accelerated with higher photonic driving levels. The dynamic yielding of material at the flyer perimeter represents a loss mechanism in the acceleration process, but this material also inhibits a second loss mechanism associated with lateral plasma expansion.

Our final important step was to demonstrate the ability to make fundamental shock physics measurements on materials with known properties at the desired photonic driving levels. The most challenging aspect is the launching of a suitable flyer (having a diameter as small as possible) using at least 250 mJ of energy. We achieved a successful launch of an 800-micron-diameter flyer. We are in the process of transferring the launch system to a different laboratory containing the laser interferometry system needed for quantitative demonstration experiments.

Other Communications

Trott, W. M., R. E. Setchell, and A. V. Farnsworth, Jr. 1999. "Investigation of the Effects of Target Material Strength on the Efficiency of Acceleration of Thick Laser-Driven Flyers." *Proc. APS 11th Topical Conference on Shock Compression of Condensed Matter* (Snowbird, UT, 27 June–2 July), in press.

3502430000

Molecular-to-Continuum Fracture Analysis of Thermoset Polymer/Solid Interfaces

M. S. Kent, M. J. Stevens, E. D. Reedy, Jr.

Fractures between adhesives and solid surfaces are an important factor affecting component viability in an aging stockpile. This project focuses on understanding the factors that control fracture at polymer/solid interfaces and incorporating such information into increasingly complex predictive models. Sandia's goal is to determine the dependence of joint strength and fracture toughness on interfacial chemical bonding, stress field, and the presence of flaws of various sizes. This information will provide the basis for a fundamental understanding of failure criteria in such systems. The model focuses on the fracture toughness for an epoxy/silicon (Si) interface. The model begins with a continuum mechanics calculation of the stress/strain fields near the crack tip loaded in a double cantilevered beam (DCB) geometry. The calculation becomes increasingly difficult as the size scale decreases (as the crack tip is approached) because the effects of high-stress/-strain fields on the material are not known. In particular, nonlinear viscoelasticity and plasticity must be modeled for high-stress/-strain fields. Ultimately, the molecular details of the fracture process at the crack tip are beyond the continuum limit. Moreover, certain important crack-tip events appear to be beyond the reach of direct experimentation. Therefore, we are investigating the molecular-level fracture events using molecular simulations covering length scales up to $\sim 500 \text{ \AA}$. We achieved the connection between the two approaches by comparing the stress field at the interface ($\sim 50 \text{ \AA}$) from the continuum calculation with the fracture stresses determined from the molecular simulations. To guide the development of the model and for validation, we developed a model experimental system. The system comprises an epoxy bonded to polished Si. We used polished Si wafers as substrates in order to (1) remove the effects of roughness, and (2) allow the interfacial chemical bonding to be varied continuously via self-assembling monolayer (SAM) techniques. This model system covers a wide range of the independent variables and thus represents a range of engineering materials.

We obtained fracture data in two test geometries: a napkin-ring torsion geometry and the DCB geometry. Both have led to

Sandia's goal is to determine the dependence of joint strength and fracture toughness on interfacial chemical bonding, stress field, and the presence of flaws of various sizes.

important insights that improve predictive capability. However, the detailed modeling focuses on the DCB geometry.

In a torsion loading with no preexisting crack, the interface strength has little effect on the fracture stress over a large range because failure apparently initiates cohesively. Only a low level of interface bonding is sufficient to achieve cohesive crack initiation. The transition from cohesive (high critical stress) to adhesive (low critical stress) crack initiation occurs over a narrow range of interface strength. The transition apparently occurs when the interface strength is sufficient to support stresses high enough to cause deformation within the epoxy. When this occurs, a large increase in applied stress is required to achieve a small increase in stress at the interface (rate or T dependent). The reason for the sharpness of the transition is not understood. It seems to imply that large-scale deformation is triggered over a narrow range of stress. In any case, the observed catastrophic relationship indicates that one cannot use joint strength as a measure of aging since no change is observed until catastrophic failure occurs. The fracture data involving substrates with patterned domains of SAMs give insight into the importance of flaws or defects. The fracture stress is greatly reduced when the SAM is deposited into 50- and 5-micron domains relative to when the monolayer is uniformly distributed. All the data taken together provide much insight into the importance of various types of contamination on joint strength.

In the DCB test (a nearly pure tensile loading), the fracture toughness increases strongly over a narrow range of interface strength.

Molecular simulations of crack-tip processes revealed several important phenomena. First, there is a distribution of bond breakage in time, even on a nanometer-length scale. We quantified this effect for the model molecular dynamics (MD) system to determine the decrease in total stress from the ideal stress value. The magnitude of the effect is likely to be rate sensitive. Second, the local strain at break is due to the minimal path through the network. Third, the strain tends to be localized at the interfaces due to the lower number of bonds per area. Fourth, the temperature (relative to the glass transition temperature) has a strong effect on the minimal paths and thus the fracture strains. Finally, we found the fracture stress to be nearly linear with interface bonding in either shear or tensile loading.

Continuum mechanics calculations determined the stress state down to tens of nanometers (DCB geometry) within

certain simplifying assumptions. These calculations begin with a linear elastic fracture mechanics analysis to determine the specimen's energy-release rate and mode mixity. Next we considered the effect of epoxy yielding. We analyzed the sandwiched DCB using a pressure-dependent Drucker-Prager epoxy yield model. We resolved stresses on the millimeter scale and quantified plastic zone size and crack-tip blunting. Since this analysis indicates that the yield zone is small compared to the region dominated by the elastic stress singularity, we next performed an asymptotic small-scale yielding analysis. This analysis considers the crack to be semi-infinite with the remote boundary loads specified by the elastic singularity solution. We used highly refined finite-element (FE) mesh to investigate the stress state on a nanometer scale. This pushed the continuum analysis beyond its rigorous limits of applicability. Nevertheless these results, which include the effect of rapid work hardening at large strain, should provide useful insights into the fundamental failure process.

By combining this information with the fracture stress results from the simulations, we arrived at a model that spans the length scales from the continuum to the molecular. This first-order model predicts a strong dependence of fracture toughness on interface bonding, which is qualitatively similar to that observed in the experiments.

Refereed

Yim, H., M. S. Kent, W. F. McNamara, R. Ivkov, S. Satija, and J. Majewski. 1999. "Structure Within Thin Epoxy Films Revealed by Solvent Swelling: A Neutron Reflectivity Study." *Macromolecules*, accepted.

Other Communications

Kent, M. S., H. Yim, A. Matheson, and E. D. Reedy, Jr. 1999. "Use of Self-Assembling Monolayers to Control Interface Bonding in a Model Study of Interfacial Fracture." *Proc. 22nd Annual Meeting of the Adhesion Society* 1 (Panama City Beach, FL, 21–24 February): 134–136.

Kent, M. S., H. Yim, A. Matheson, C. Cogdill, and E. D. Reedy, Jr. 1999. "Use of Self-Assembling Monolayers to Control Interface Bonding in a Model

Study of Interfacial Fracture." *Proc. 218th American Chemical Society National Meeting* 1 (New Orleans, LA, 22–26 August).

Kent, M. S., H. Yim, A. Matheson, C. Cogdill, D. Fein, and E. D. Reedy, Jr. 1999. "Use of Self-Assembled Monolayers to Control Interface Bonding in a Model Study of Interfacial Fracture." Paper presented to the Microelectronics Packaging Workshop, Albuquerque, NM, 2 March.

Kent, M. S., H. Yim, A. Matheson, C. Cogdill, D. Fein, and E. D. Reedy, Jr. 1999. "Use of Self-Assembling Monolayers to Control Interface Bonding in a Model Study of Interfacial Fracture." Paper presented to the Workshop of JOWOG/Organic Materials Working Group, Livermore, CA, 11–12 January.

Kent, M. S., H. Yim, A. Matheson, D. Fein, and E. D. Reedy, Jr. 1999. "Use of Self-Assembled Monolayers to Control Interface Bonding in a Model Study of Interfacial Fracture." Paper presented to the Annual Meeting of the American Physical Society, Atlanta, GA, 20–26 March.

Reedy, E. D., Jr. 1999. "Connection Between Interface Corner and Interfacial Fracture Analyses of an Adhesively Bonded Butt Joint." *Proc. 22nd Annual Meeting of the Adhesion Society 1* (Panama City, FL, 21–24 February): 394.

3502440000

Fundamental Aspects of Micromachine Reliability

M. P. de Boer, J. A. Knapp, T. M. Mayer, J. J. Sniegowski, J. M. Redmond

A fundamental basis for designing micromechanical devices with high-yield, reliable performance and long life is lacking. Mechanical design tools for macroscale machines relate reliability to inertial forces. However, the performance of micron-scale structures of high-aspect ratio is dominated by surface forces. The technical goal of this project is to use experimental reliability results obtained directly from micromachined test structures to develop and verify mechanics models containing interaction terms appropriate to the micron scale (e.g., capillarity, van der Waals forces, electrostatics, etc.). Issues to be addressed include autoadhesion (stiction), friction, and wear. Beginning with autoadhesion, Sandia will design and build microbridge structures with varying geometry and surface properties (roughness, chemical coatings, etc.). We will monitor deformations by interferometry in an environmental chamber. We will develop, verify, and refine finite-element (FE) models incorporating new surface elements by comparing against experimental results. Next we will investigate friction and wear using smart micromachined structures that enable self-diagnosis by electrical monitoring of capacitance and Q-factor changes. We will also explore optical detection techniques. We will verify dynamical response models incorporating internal friction terms as well as damping and refine them using experimental results. We will then extract friction due to energy loss at rubbing surfaces.

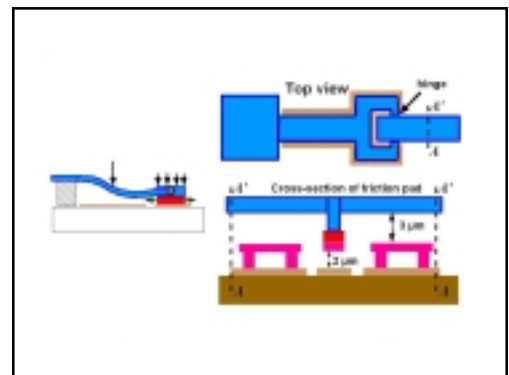
This project will develop a new toolset based on an experimental and theoretical foundation. We will use the toolset to calculate and characterize reliability of micromachines for integrated microsystem applications.

We accomplished the following:

- (1) We refined our methodology to obtain adhesion hysteresis measurements by incorporating non-idealities into the modeling. This greatly extended the usefulness of the technique.
- (2) We investigated a new design of the friction test structure. It shows greatly increased slip.

This project will develop a new toolset based on an experimental and theoretical foundation...to calculate and characterize reliability of micromachines for integrated microsystem applications.

A new friction test structure with a very large dynamic range.



(3) We demonstrated a new microelectromechanical system (MEMS) actuator based on the improved friction test structure. It has millinewton force capability (compared to micronewtons for most actuators) and large stroke (60 microns or more), requires much less area than a comb drive (about 10 times less), and can attain high speeds (mm/sec). It may prove very useful for future MEMS devices. Its reliability is related to the adhesion and friction work in this project.

(4) Our vacuum deposition process for hydrophobic perfluorinated coatings yielded films that show very little adhesion degradation up to 97% relative humidity (RH). Previous solution-deposited coatings degraded significantly above 90% RH.

(5) We found an important mechanism for degradation of our solution-deposited hydrophobic silane coupling agents that is a reconfiguration of the surface phase to a bulk phase at high humidity. We believe that the reconfiguration leaves behind hydrophilic areas that give rise to the adhesion increase.

(6) Investigation of repeatable/uniform surfaces (hydrophilic) has proven difficult. We are affected by contamination, and obtaining clean surfaces for fundamental studies is not trivial. We will continue to work on this, as important results will be achieved once we have clean surfaces.

Refereed

de Boer, M. P., and T. A. Michalske. 1999. "Accurate Method for Determining Adhesion of Cantilever Beams." *J. Appl. Phys.* **86** (15 July): 2.

de Boer, M. P., and T. A. Michalske. 1997. "Improved Autoadhesion Measurement for Micromachined Polysilicon Beams." *Proc. MRS 444* (May) (Boston, MA, December): 87–92.

de Boer, M. P., J. A. Knapp, J. M. Redmond, and T. A. Michalske. 1998. "Adhesion, Adhesion Hysteresis and Friction in MEMS Under Controlled Humidity Ambients." *Mechanical Behavior of Advanced Materials MD-84* (ASME International Mechanical Engineering Congress and Exposition, Anaheim, CA, November): 127–129.

de Boer, M. P., J. A. Knapp, T. M. Mayer, and T. A. Michalske. 1999. "The Role of Interfacial Properties on MEMS Performance and Reliability." (Invited) *SPIE Europto Proc.* **3825** (Microsystems Metrology and Inspection, Munich, Bavaria, Germany, June): 2–15.

de Boer, M. P., J. M. Redmond, and T. A. Michalske. 1998. "A Hinged-Pad Test Structure for Sliding Friction Measurement in Micromachining." *Proc. SPIE, Materials and Device Characterization in Micromachining 3512* (Santa Clara, CA, 21–22 September): 241–250.

de Boer, M. P., M. R. Tabbara, M. T. Dugger, P. J. Clews, and T. A. Michalske. 1997. "Measuring and Modeling Electrostatic Adhesion in Micromachines." *Transducers '97 1* (International Conference on Solid-State Sensors and Actuators, Chicago, IL, 16–19 June): 229–232.

de Boer, M. P., P. J. Clews, B. K. Smith, and T. A. Michalske. 1998. "Adhesion of Polysilicon Microbeams in Controlled Humidity Ambients." *Proc. MRS* **518** (December) (San Francisco, CA, April): 131–136.

Pelt, J. S., M. E. Ramsey, R. Magana, Jr., E. Poindexter, Jr., S. M. Durbin, Florida A&M and Florida State University; M. P. de Boer, D. A. LaVan, M. T. Dugger, and J. H. Smith, Sandia. 1999. "Pulsed Laser Deposited Coatings for Stiction and Wear Reduction in MEMS Devices." *Proc. SPIE* **3874** (Micromachining and Microfabrication Process Technology, Santa Clara, CA, 20–21 September).

Redmond, J. M., M. P. de Boer, and T. A. Michalske. 1998. "Integrated Modeling and Measurement of a Microhinged Test Structure for Sliding Friction Measurement." *Microelectromechanical Systems (MEMS) DSC-6* (ASME International Mechanical Engineering Congress and Exposition, Anaheim, CA, November): 305–311.

Rye, R. R. 1997. "Transition Temperatures for n-alkyltrichlorosilane Monolayers." *Langmuir* **13**(9) (30 April): 2588–2590.

Rye, R. R., G. C. Nelson, and M. T. Dugger. 1997. "Mechanistic Aspects of Alkylchlorosilane Coupling Reactions." *Langmuir* **13**(11) (28 May): 2965–2972.

Other Communications

Crozier, B. T., and D. F. Bahr, Washington State University; M. P. de Boer, J. M. Redmond, and T. A. Michalske, Sandia. 1999. "Friction Measurement in MEMS Using a New Test Structure." *Proc. MRS* (Boston, MA, December).

de Boer, M. P., J. A. Knapp, and T. A. Michalske, Sandia; R. Maboudian and U. Srinivasan, University of California, Berkeley. 1999. "Adhesion Hysteresis of Silane-Coated Microcantilevers." *Acta Materialia*, submitted.

de Boer, M. P., T. M. Mayer, R. W. Carpick, and T. A. Michalske, Sandia; U. Srinivasan and R. Maboudian, University of California, Berkeley. 1999. "Humidity Dependence of Adhesion for Silane-Coated Microcantilevers." *Langmuir*, submitted.

Mayer, T. M., M. P. de Boer, N. Shinn, P. J. Clews, and T. A. Michalske. 1998. "Vacuum-Deposited Fluorocarbon Coatings for Adhesion Control in MEMS." Paper presented to the Materials Research Society Fall Conference, Boston, MA, December.

Michalske, T. A. 1998. "Integrated Chemical and Mechanical Microsystems: Challenges and Opportunities." Microstructuring Science and Technology Workshop, Helsinki, Finland, 5 August.

3502450000

Enabling Science and Technology for Cold-Spray Direct Fabrication

M. F. Smith, D. L. Gilmore, J. E. Brockmann, R. C. Dykhuizen, R. A. Neiser, Jr.

Cold-spray processing (CSP) is an exciting material fabrication technology that can be used to deposit thick layers (tens of microns to millimeters) of ductile metals and composites at temperatures < 200°C. Some of the key features of cold-spray deposits include fine grain sizes, minimal oxidation, compressive residual stresses, high density, and excellent thermal and electrical conductivities. Since this process eliminates particle melting, the phase content and chemical composition of the coating closely match that of the feedstock material. The well-defined nature of the spray stream substantially reduces the need for expensive masking procedures. Interest in near net-shape forming using CSP is high, and development of an aerodynamic lens (ALS) to further focus the powder stream is of considerable interest. We made substantial progress toward understanding fundamental features of the cold-spray process and the deposits produced by it.

The well-defined nature of the spray stream substantially reduces the need for expensive masking procedures.

Key areas for research included process characterization studies and experimental validation of a computation model; an experimental and computational study of the particle impact and deformation process; materials characterization studies; and testing of two ALSs. We also organized and held a major workshop on CSP. Industrial interest in cold-spray technology is very high, and the purpose of the workshop was to present a technical overview and a business case for developing CSP into a commercially viable technology to potential industrial users. Sandia is currently in the process of organizing a Cooperative Research and Development Agreement (CRADA) between Sandia and approximately ten industrial partners to perform precompetitive cold-spray R&D.

We performed a wide variety of experimental and computational studies and demonstrated that numerous materials can be successfully cold sprayed. In order of increasing difficulty these include copper (Cu), austenitic, and martensitic stainless steels, aluminum (Al), Al bronze, various nickel (Ni) alloys, titanium (Ti), molybdenum (Mo), and several cermets (WC-Co and NiCr-Cr₃C₂). We also examined the properties and microstructures of cold-sprayed materials.

The microstructures are typical of heavily cold-worked metals, as expected. Typical grain sizes are in the 40 nm range. The deposits have a residual compressive stress measured in the tens of MPa. These residual stresses improve the bond strength and increase the fatigue life of the deposits. The density of cold-sprayed deposits is very high, especially when compared to most thermally sprayed materials. We measured cold-sprayed Cu's density as 99.6% of theoretical and Al's as 98.6%. We measured the thermal conductivity of cold-sprayed Cu as 80% of that of oxygen-free high-conductivity copper (Cu). This conductivity is exceptionally high for a sprayed material; typical values are frequently well below 30%. We made tensile test measurements on cold-sprayed Al specimens. Annealed specimens exhibited a distinct necking phenomenon and reasonably good yield strength. These experiments demonstrate that cold-sprayed materials can behave much more like bulk materials than traditional thermally sprayed materials.

We performed experimental and computational studies of coating formation mechanisms. The fundamental event is the impact of an individual metal particle onto the substrate at high velocity. Computational examination of a Cu particle striking a stainless-steel surface using the CTH penetrator code predicted the formation of a lip of highly sheared material at velocities in the 600–700 m/s range. We experimentally observed the presence of a lip in single-particle impact studies at these velocities. The critical velocity (i.e., the point at which a deposit starts to form) for Cu on stainless steel is 650 m/s. Successful bonding between the particle and substrate is thought to occur when the thin oxide layers on their surfaces are broken apart and swept aside, allowing nascent metal surfaces to come in contact and join. The presence of a sheared lip of heavily deformed material may be an indication that the oxide layers have been swept away.

Finally, we performed a large number of process characterization experiments. We aimed these experiments at quantifying the effect of various parameters on particle velocities and trajectories and comparing them to the predictions of models developed earlier in the project. Particle velocity predictions for several materials at various conditions gave good agreement with computational models: typically the calculated values were within ~ 5% of the measured values. This result makes use of the computational codes for such tasks as nozzle design very attractive. We designed and fabricated an ALS system that can be attached to the cold-spray nozzle. We

successfully performed focusing tests at the end of the year using 15-micron Al powder at low pressures.

Refereed

Dykhuizen, R. C., M. F. Smith, D. L. Gilmore, R. A. Neiser, Jr., X. Jiang, and S. Sampath. 1999. "Impact of High-Velocity Cold-Spray Particles." *J. Thermal Spray Technology*, accepted.

Gilmore, D. L., R. C. Dykhuizen, R. A. Neiser, Jr., T. J. Roemer, and M. F. Smith. 1999. "Particle Velocity and Deposition Efficiency in the Cold-Spray Process." *J. Thermal Spray Technology*, accepted.

Other Communications

Gilmore, D. L., R. A. Neiser, Jr., and R. C. Dykhuizen. 1999. "Modeling the Critical Velocity for Deposition in the Cold-Spray Process." Paper presented to the Materials Research Society Fall Meeting, Boston, MA, 29 November–3 December.

Gilmore, D. L., R. C. Dykhuizen, R. A. Neiser, Jr., and M. F. Smith. 1999. "Analysis of the Critical Velocity for Deposition in the Cold-Spray Process." Paper presented to the ASM International Materials Solution, Cincinnati, OH, 1–4 November.

Smith, M. F., A. Papyrin, and J. Karthikeyan. 1999. "An Overview of Cold-Spray Research in the U.S." Paper presented to the ASM International Materials Solutions, Cincinnati, OH, 1–4 November.

Smith, M. F., J. E. Brockmann, R. C. Dykhuizen, D. L. Gilmore, R. A. Neiser, Jr., and T. J. Roemer. 1998. "Cold-Spray Direct Fabrication—High-Rate, Solid-State, Material Consolidation." *Proc. MRS Symp.* **542** (Boston, MA, November): 65–76.

Smith, M. F., R. A. Neiser, Jr., D. L. Gilmore, R. C. Dykhuizen, and J. E. Brockmann. 1999. "Cold-Spray—High-Rate Deposition of Thick Metal Coatings Without Melting." Paper presented to the Materials Research Society Fall Meeting, Boston, MA, 29 November–3 December.

3502460000

Atomic-Level Studies of Surfactant-Directed Materials Growth

P. J. Feibelman, B. S. Swartzentruber, G. L. Kellogg, J. A. Floro, N. C. Bartelt, J. C. Hamilton

Sandia will convert surface impurities from a nuisance to a systematically applicable nanofabrication tool. Combining Sandia's special facilities, including the atom-tracker scanning-tunneling microscope (AT-STM), low-energy electron microscopy (LEEM), and massively parallel computation (MPC), we will learn how common adsorbed atoms (surfactants) can be used to manipulate and direct thin-film growth. Thus, we will develop a surfactant toolkit that enables us to produce either atomically flat or 3-D nanostructured surfaces. We will start with model systems, where we have experience in the absence of surfactants, studying surfactant-modified diffusion on and near metal and semiconductor surfaces, and integrating our real-time experimental and advanced computational modeling capabilities. We will use the AT-STM to study hydrogen (H)-assisted silicon (Si) adatom diffusion on Si(001), and LEEM to investigate both H-assisted step fluctuations on the same surface and oxygen (O)-assisted island growth on Pt(111) (platinum). Via novel surface stress measurements, we will study germanium (Ge) segregation versus adsorbate overlayer coverage in Si-Ge alloys. We will closely couple theoretical efforts to our experiments; MPC will be indispensable in developing reliable, atomic-scale, mechanistic models.

Attempting to make contact with STM experiments, we found that bond-counting arguments, supported by *ab initio* calculations, predict a lower barrier for "leapfrog" diffusion of Pt addimers on Pt(110)-1x2 than for adatom diffusion or addimer dissociation. This conflicts with experiment, possibly signaling effects of unwanted surfactants, i.e., contaminants. We explored potential contributions of adsorbed CO in this system, but cannot yet explain the discrepancy.

We computed step- and kink-formation energies on Cu(111), preliminary to efforts to understand why sulfur (S) contamination dramatically quickens island decay on this surface. Results for clean Cu(111) agree well with recent measurements. Calculations involving S contamination show that barrier rather than thermodynamic energies are at the heart of the speedup.

...we will learn how common adsorbed atoms (surfactants) can be used to manipulate and direct thin-film growth [and]... will develop a surfactant toolkit that enables us to produce either atomically flat or 3-D nanostructured surfaces.

We compiled extensive LEEM data on Pt-island decay on Pt(111) after developing algorithms to digitize images, mark positions, and measure island area versus time. From decay rates versus temperature, we determined that the detachment-barrier for Pt atoms from Pt islands is 1.64 eV, in excellent agreement with our calculations. Experiments with potassium (K)-precovered surfaces showed that K slows island decay. However, measurements over a sufficient temperature range to determine the modified energy barrier proved impossible.

We also studied how a metallic surfactant, Pt, induces faceting of W(111) (tungsten). LEEM reveals that (atomically rough) W(111), covered with a complete monolayer of Pt and annealed to temperatures higher than $\sim 750^\circ\text{K}$, significantly restructures the initially planar surface facets, forming an array of three-sided pyramids with $\{211\}$ faces. LEEM shows that when Pt is dosed onto the heated surface, the planar-to-faceted transition proceeds via nucleation and growth of spatially separated faceted regions, starting at $2/3$ monolayer coverage. Alternately, if a planar sample is first covered with a physical monolayer of Pt and gradually heated, there is no spatial separation in the faceting transition. This was explained by subsequent observations at Rutgers University, showing a continuous, uniform roughening of the surface toward the faceted phase.

We used a first-principles-based Frenkel-Kontorova model to understand silver (Ag) film growth on Pt(111). Ag/Pt(111) is very close to the transition between a commensurate (no dislocations) and an incommensurate film (dislocated film). Consequently it has an unusual incommensurate structure with very wide hcp and very narrow fcc domains. Our model also predicts dislocation structures for islands in excellent agreement with experiment over a wide range of island sizes.

Adsorbed atoms usually change surface and thin-film strain states. To accommodate such changes, surface dislocations are often created or destroyed. We modeled adsorbate-formed surface dislocations using the 2-D Frenkel-Kontorova model. We found that the formation is highly cooperative, involving a complicated sequence of dislocation reactions. We applied our model to dislocations in thin Cu films exposed to S. Here, step one in dislocation generation is vacancy-line creation, as S extracts individual Cu atoms from the film. Our model predicts the subsequent dislocation reactions, which remove the high-energy vacancy structures.

We showed that the critical-island volume for a first-order morphological phase-transition in SiGe coherent islands scales

Our model predicts the subsequent dislocation reactions, which remove the high-energy vacancy structures.

simply with lattice mismatch strain over five decades of volume. The scaling exponent implies that surface energy and elastic strain energy dominate the coherent-island total energy, while surface stress effects are negligible. We refined our mean-field model for coarsening when there is elastic repulsion. We calculated the repulsion energy directly from finite elements (FEs), incorporated it into our model, and ultimately reproduced all essential aspects of our data on accelerating coarsening during deposition.

Providing insight into surface-alloy formation's initial stages in Ge/Si systems, we performed kinetic measurements of Ge dimer diffusion on Si(001). Ge dimers diffuse faster than Si dimers along the dimer rows of Si(001) and show a "buckling" behavior at single lattice sites instead of the orthogonal rotation of pure Si dimers. Because Ge atoms intermix in the Si surface at low-T and are normally indistinguishable from Si, we developed low-bias-imaging techniques allowing Ge to be distinguished from Si.

Refereed

de la Figuera, J., K. Pohl, A. K. Schmid, N. C. Bartelt, J. Hrbek, and R. Q. Hwang. 1999. "Multiplication of Threading Dislocations in Strained Metal Films Under Sulfur Exposure." *Surface Science* **435** (2 August): 93–98.

Feibelman, P. J. 1999. "First-Principles Step- and Kink-Formation Energies on Cu(111)." *Phys. Rev.* **60** (15 October): 1118.

Feibelman, P. J. 1999. "Ordering of Self-Diffusion Barrier Energies on Pt(110)-(1x2)." *Phys. Rev. B, Rapid Communications*, submitted.

Floro, J. A., E. Chason, L. B. Freund, R. D. Twisten, R. Q. Hwang, and G. A. Lucadamo. 1999. "Evolution of Coherent Islands in Si_{1-x}Ge_x/Si (001)." *Phys. Rev.* **B59**: 1990.

Hamilton, J. C., R. Stumpf, K. Bromann, M. Giovannini, K. Kern, and H. Brune. 1999. "Dislocation Structures of Submonolayer Films Near the Commensurate-Incommensurate Phase Transition: Ag on Pt(111)." *Phys. Rev. Lett.* **82** (31 May): 4488–4491.

Pelhos, K., J. B. Hannon, G. L. Kellogg, and T. E. Madey. 1999. "LEEM Investigation of the Faceting of the Pt-Covered W(111) Surface." *Surface Science* **432**: 115.

Pelhos, K., J. B. Hannon, G. L. Kellogg, and T. E. Madey. 1999. "Nucleation and Growth During Faceting of the Platinum-Covered W(111) Surface." *Proc. ICSOS-6*, in press.

Pelhos, K., J. B. Hannon, G. L. Kellogg, and T. E. Madey. 1999. "Nucleation and Growth of Faceted Features on the Platinum-Covered W(111) Surface." Paper presented to the 46th International Symposium of the American Vacuum Society, Seattle, WA, 25–29 October.

Other Communications

Bartelt, N. C. 1999. "Dislocations at Surfaces." Paper presented to the Physics Department Seminar, Carnegie Mellon University, Pittsburgh, PA, 22 April.

Bartelt, N. C. 1999. "How Predictable Is Surface Morphology?" Paper presented to the AVS 45th International Symposium, Baltimore, MD, 5 November.

Bartelt, N. C. 1999. "Predicting the Future of Atoms on Surfaces." Presentation to the Physics Department Colloquium, Arizona State University, Phoenix, AZ, 16 September.

Feibelman, P. J. 1999. "*Ab Initio* Surface Diffusion Barriers vs. Experiment." Paper presented to the CECAM Workshop on Diffusion on Surfaces, Lyon, France, 26–28 May.

Feibelman, P. J. 1998. "The Forces that Control Surface Processes." Presentation to the Chemistry Colloquium, Brown University, Providence, RI, 30 October.

Feibelman, P. J. 1999. "The Forces that Control Surface Processes." Presentation to the Chemistry Seminar, UC–San Diego, La Jolla, CA, 16 February.

Feibelman, P. J. 1999. "The Forces that Control Surface Processes." Presentation to the Physical Chemistry Seminar, Lawrence Berkeley Laboratory, Berkeley, CA, 11 February.

Floro, J. A. 1999. "Adventures in Epitaxy: The Dynamic Evolution of Coherent Island Ensembles." Presentation to the University of Texas Physics Colloquium, Austin, TX, 3 February.

Floro, J. A. 1999. "Kinetic Constraints in Coherent Island Formation." Presentation to the Lawrence Symposium on Critical Issues in Epitaxy, Tempe, AZ, 6–9 January.

Floro, J. A. 1999. "Length Scales in Coherent Island Formation: What They Tell Us About the Physics." Paper presented to the Gordon Conference on Thin-Film and Crystal Growth Mechanisms, Plymouth, NH, 20–25 June.

Hamilton, J. C., R. Stumpf, K. Bromann, M. Giovannini, K. Kern, and H. Brune. 1999. "Dislocation Structures of Submonolayer Films Near the Commensurate-Incommensurate Phase Transition: Ag on Pt(111)." Paper presented to the Meeting of the American Vacuum Society, Seattle, WA, 28 October.

3502470000

Intelligent Polymers for Nanodevice Performance Control

G. M. Jamison, M. J. Carr, J. A. Shelnut, R. S. Saunders, D. R. Wheeler, D. A. Loy

Sandia continued to examine both chemically and thermally responsive materials. The chemically responsive systems included thermally unstable polyacetals with and without depolymerization catalysts. Part of this effort also focused on developing and testing photobase generators. We based the thermally responsive materials on a thermally labile weak link that we built into the polymer's architecture, using Diels-Alder adducts as the weak links.

Computational investigations focused on the blue-to-red color change in polydiacetylene (PDA)-linked detergent molecules as well as the properties of some directly linked porphyrin oligomers.

We focused computational efforts on the blue-to-red color change in PDA-linked detergent molecules as well as the properties of some directly linked porphyrin oligomers. Molecular dynamics (MD) calculations of PDA oligomers indicate the importance of hydrogen (H)-bonding of detergent head groups in maintaining the characteristic conjugation length along the PDA backbone of the linked detergent molecules. H-bonding is influenced by interfacial regions, such as that between hydrophobic and hydrophilic solvents. Initial indications suggest that the transition between the blue (ordered) and red (disordered) is irreversible because the ordered phase cannot be easily regenerated.

Studies of chemically responsive polyacetals with low ceiling temperatures (temperatures below which the equilibrium for the polymerization reaction favors monomeric species) included work on a variety of polyacetals. Results suggest that catalytic amounts of strong acids are insufficient to affect bulk depolymerization of polyacetal; likewise, photo-generated and thermally generated amines will not catalytically depolymerize poly(trichloroacetal). We attempted to employ stronger photobases by utilizing hydroxide-liberating N-methyl nifedipine, again with no degradation of the base-sensitive polyacetal. The heterogeneous nature of these systems is providing an effective kinetic barrier to depolymerization. A low ceiling temperature is clearly not the most critical factor in

Results suggest that catalytic amounts of strong acids are insufficient to affect bulk depolymerization of polyacetal; likewise, photo-generated and thermally generated amines will not catalytically depolymerize poly(trichloroacetal).

selecting a polymer as a thermally and/or chemically responsive material.

We investigated materials systems whose activation barrier to thermal depolymerization would be much less, making the thermal response more of a thermodynamic issue rather than one controlled predominantly by the system's kinetics. Employing a Diels-Alder cycloaddition/cycloreversion strategy, we prepared materials whose thermal behavior is such that at lower temperatures the equilibrium of the Diels-Alder reaction lies toward the polymeric product. This means that the polymerization proceeds as expected at room or slightly elevated temperature. At higher temperature, the equilibrium shifts back to the left and the polymer depolymerizes to give soluble or liquid monomers again. This class of materials acts as a thermoplastic-thermoset. After polymerization or curing, the materials have many of the properties of thermosets such as epoxies. Unlike classical thermosets, these thermal cycloreversions will render these polymers processible again. This chemical strategy has also been applied to organically modified polysilsesquioxanes, providing a new route to filled organic polymer systems.

This chemical strategy has also been applied to organically modified polysilsesquioxanes, providing a new route to filled organic polymer systems.

Other Communications

Shaltout, R. M., and D. A. Loy. 1999. "Maleimide Functionalized Siloxane Resins." *Polymeric Materials Science and Engineering* **80** (217th American Chemical Society National Meeting, Anaheim, CA, 21–25 March): 195–196.

3502480000

Freeforming of Ceramics and Composites from Colloidal Slurries

J. Cesarano, III, J. E. Smay, H. B. Denham, B. H. King, T. A. Baer, J. N. Stuecker, S. L. Morissette, M. T. Ensz

The objective of this project is to develop a model-based direct freeform fabrication technique for ceramic, metal, or graded composite components. Sandia fabricated these components by computer-controlled dispensing of colloidal suspensions through an orifice. Any conceivable 2-D pattern may be written layer by layer into a 3-D shape. We developed model-based processing rules that aid in the development of slurries with the appropriate rheology, density, and drying kinetics to ensure process success for a variety of ceramics and composites. We also developed software and equipment for precise control of layer thickness and feature resolution.

Development of this technique into a manufacturing process required computer simulations of the relevant physical phenomena; materials expertise for tailoring colloidal slurry properties and processing dissimilar materials; software and equipment expertise for computer-aided design (CAD) model conversion; and robotics expertise for process optimization.

We developed a new technique for the direct fabrication of ceramics and composites. The technique is model-based and dependent on knowledge and control of fundamental material phenomena. However, to date we have been unsuccessful in achieving the goal of incorporating closed-loop sensor control of fabrication and incorporating knowledge-based software based on material modeling.

This work will directly impact the production of neutron tubes, cermets, voltage bars, and ceramic fixtures for switch tubes.

During the past fiscal year, we made significant progress in the development of techniques for multimaterial deposition and the fabrication of composite structures. We designed, built, and demonstrated apparatuses for the simultaneous deposition of one to four materials. This advance resulted in a Technical Advance for fabrication with gel-casting formulations, demonstrations of parts that are compositionally and functionally graded, and unique mullite/zirconia composites for structural applications. Also, we made progress in fabricating Defense Programs (DP) prototype components and demonstrating utility for more reliable cermet fabrication. In

We developed a new technique for the direct fabrication of ceramics and composites.... [that] is model-based and dependent on knowledge and control of fundamental material phenomena.

addition, we fabricated unique structures with corrugation in all three dimensions that may have utility for filtration or catalyst supports. We also completed direct fabrication of silicon nitride (SiN) and completed studies related to the optimization of build parameters for improved surface roughness and tolerance. Our original patent was accepted; we disclosed our second patent related to direct fabrication with gel-casting formulations and are preparing an application. We demonstrated the utility of this manufacturing technique to many customers and secured a Cooperative Research and Development Agreement (CRADA) and funding for more development in the areas of cermet production, PZT (lead zirconate titanate) fabrication, and ZnO (zinc oxide) fabrication.

In general, the accomplishments mentioned above tended to be geared toward demonstration of the fabrication of unique structures and multimaterial structures in an effort to prove the vast versatility and utility of our direct fabrication technique for future manufacturing methods for both DP and commercial applications. However, we also accomplished fundamental understanding and modeling of the crucial material properties with very interesting results. We made a concerted effort to understand and model all aspects of our slurry deposition process: (1) the shape of beads that are extruded from the nozzle, (2) the development and effect of drying stresses on microstructure, and (3) the drying time necessary to induce a liquid-to-solid transition. We studied and modeled these phenomena with the goal of developing knowledge-based software that could be used to optimize build parameters depending on the slurry properties and ambient conditions. However, we finally concluded that the equilibrium bead shape and drying stresses have a negligible effect on the properties and quality of the final part. The estimation of drying time is indeed critical, and knowledge-based software based on drying would be valuable. So, even though we focused substantial effort on understanding phenomena that are not crucial to successful direct fabrication, the problem of developing knowledge-based control is drastically simplified. The utilization of sensors for closed-loop control has not been as forthcoming, and much more work needs to be accomplished for future implementation.

...we also accomplished fundamental understanding and modeling of the crucial material properties with very interesting results....the problem of developing knowledge-based control is drastically simplified.

Refereed

Cesarano, J., III. 1999. "A Review of Robocasting Technology." *Proc. MRS Symp.* **542** (January) (Boston, MA, December 1998): 133–139.

Morissette, S. L., J. Lewis, J. Cesarano, III, and D. Dimos. 1999. "Solid Freeform Fabrication of Alumina-Poly(vinyl Alcohol) Gelcasting Suspensions." *Proc. MRS Symp.* **542** (January) (Boston, MA, December 1998): 125–130.

Tuttle, B. A., J. A. Voigt, and J. Cesarano, III. 1998. "PZT95/5 Voltage Bars Phase Transformation Kinetics: Hopkinson Bar Tests." *DP-10 Newsnote* (July).

Other Communications

Cesarano, J., III, H. B. Denham, and B. H. King. 1999. "Overview of Robocasting Technology: Current Capabilities and Future Directions." Paper presented to the 10th Solid Freeform Fabrication Symposium, Austin, TX, August.

Cesarano, J., III, H. B. Denham, B. H. King, S. L. Morissette, and B. A. Tuttle. 1998. "Freeform Fabrication of Ceramics and Composites from Slurries." Presentation to the New Mexico Tech Materials Science Seminar, Socorro, NM, December.

Denham, H. B., J. Cesarano, III, and M. R. Baer. 1999. "Microstructure of Robocast Ceramics and the Effects of Drying Kinetics." Paper presented to the 10th Solid Freeform Fabrication Symposium, Austin, TX, August.

Stuecker, J. N., H. B. Denham, J. Cesarano, III, and R. E. Loehman. 1999. "Merging Robocasting with Other Processes for the Development of Unique Materials." Paper presented to the 10th Solid Freeform Fabrication

3502490000

Quantum Dot Arrays

J. E. Martin, R. A. Anderson, D. R. Jennison, P. P. Provencio, J. P. Wilcoxon

The goals of Sandia's research are to investigate methods of synthesizing quantum dot arrays (QDAs)—superlattices of nanoclusters—and to characterize and understand the properties of these novel materials. It is well known that nanoclusters have many unusual properties, including anomalous optical properties, size-dependent bandgaps, high catalytic activity, low melting temperature, anomalous magnetic properties, etc. However, the formation of cluster-based materials requires that these nanoclusters be isolated in a matrix to prevent the spontaneous sintering of clusters to form a bulk material. This can be accomplished by forming these clusters into periodic arrays where clusters are separated by an isolating matrix. These periodic arrays may exhibit coherent effects, or may simply be efficiently close-packed materials.

We developed synthetic strategies that for the first time enable the formation of 3-D QDA crystals from nanoclusters coated with very short chain-length thiols consisting of only six carbons. Previously we could obtain such structures only with alkane chains as short as twelve carbons. This significantly decreases the gaps between nanoclusters, and since tunneling currents are an exponential function of the gap, this has important implications for increasing these currents. To accomplish this required significant advances in our nanocluster synthesis strategy, to produce clusters with unprecedented size control. We measured the complex dielectric constant of solutions of gold (Au) nanoclusters in collaboration with NIST (National Institute of Standards and Technology). We are using these solutions to test the predictions of a new theory of the intrinsic and effective conductivity of particle dispersions. Accomplishing this required the development of new extraction strategies for the removal of ions from the reacted inverse micellar solutions, because trace ions contribute unwanted conductivity to the measurements. We investigated the properties of QDAs of magnetic materials in the limit where the particles are small enough to consist of a single domain and thus exhibit superparamagnetism. We synthesized iron (Fe) nanoclusters in very small sizes (as low as 2 nm) and studied their magnetic properties. In a parallel effort, we wrote

We developed synthetic strategies that for the first time enable the formation of 3-D QDA crystals from nanoclusters coated with very short chain-length thiols consisting of only six carbons.

simulated annealing simulations to understand the magnetic properties of superparamagnetic QDAs. In these simulations we allowed the fixed dipole moment of each nanocluster to rotate to align with the local field, which was the sum of the applied field and the field due to the dipole moment of every other nanocluster. We did not include quantum mechanical exchange coupling because it should be very small in nanoclusters separated by alkane chains. We determined the ground state by a simulated annealing method. We considered the full magnetization behavior of both perfect QDAs and QDA structures taken from transmission electron microscopes (TEMs). We discovered that the long-range dipolar interactions create a kind of superferromagnetic behavior that is strongly dependent on the presence of structural defects. Surprising to us was the appearance of magnetic domains and domain walls without the effect of quantum mechanical exchange coupling. In the presence of a field, these structures magnetize by domain wall motion and domain rotation, and thus seem to be a fully classical analog of atomic spin systems.

3502510000

Laser-Assisted Arc Welding for Aluminum Alloys

P. W. Fuerschbach

Sandia performed experiments using a coaxial end-effector to combine a focused laser beam and a plasma arc. The device employs a hollow tungsten (W) electrode, a focusing lens, and conventional plasma arc torch nozzles to co-locate the focused beam and arc on the workpiece. We selected plasma arc nozzles to protect the electrode from laser-generated metal vapor. The project goal is to develop an improved fusion welding process that exhibits both absorption robustness and deep penetration for small-scale (< 1.5 mm thickness) applications. On aluminum (Al) alloys 6061 and 6111, we showed the hybrid process to eliminate hot cracking in the fusion zone. We found fusion zone dimensions for both stainless-steel and Al to be wider than characteristic laser welds and deeper than characteristic plasma arc welds.

We made combined laser/arc welds on AISI 1008 steel samples. We have made only preliminary welds to date and did not anticipate or achieve full weld penetration. The goal of these initial tests was to test the latest end-effector design with the new continuous-wave Nd:YAG laser. We deliberately kept laser power low—between 300 and 500 watts. We observed a synergy of the two heat sources since we increased weld penetration substantially for welds made with the combined process. We also varied arc current through the end-effector from 20–40 A. The laser parameters did not result in the onset of keyhole penetration in the material, either with or without the addition of plasma arc current. The resulting weld pools were hemispherical in shape. Higher laser power will likely be needed to see the penetrating benefits of the combined process.

The goal of these initial tests was to test the latest end-effector design with the new continuous-wave Nd:YAG laser.

Other Communications

Fuerschbach, P. W. 1999. "Laser-Assisted Plasma Arc Welding." *ICALEO '99* **86** (San Diego, CA, 15–18 November).

3502520000

Reactivity of Metal-Oxide Surfaces

A. G. Sault, R. Q. Hwang, J. A. Ruffner, D. R. Jennison, B. S. Swartzentruber

Sandia is using a combination of experimental and theoretical techniques to explore atomic-scale defect chemistry on technologically important surfaces, with the goal of determining the salient factors that control defect chemistry. The formation, mobility, reactivity, and dissolution of atomic-scale surface defects play important roles in materials areas such as catalysis, corrosion, thin-film growth, semiconductor processing, sensors, and magnetic devices. Important defects include single adatoms, surface steps and kinks, dislocations, and vacancies. It is generally believed that a small number of localized surface defects may be particularly reactive and thereby dominate the surface chemistry of many materials. While past studies of this important problem were limited by an absence of appropriate experimental probes for imaging atomic-scale defects, the recent advent of specialized scanning probe microscopies (SPM) largely overcomes this problem and now allows more detailed studies of defect chemistry than previously possible. The unique atom-tracking scanning-tunneling microscope (AT-STM) recently developed at Sandia is a particularly powerful new technique that allows measurement of atomic-scale kinetic processes on a time scale that is more than three orders of magnitude faster than previous techniques. Similarly, a lack of sufficient computing power severely limited previous theoretical studies of defect properties. The recent development of massively parallel (MP) computational techniques at Sandia, which now allows calculations on systems containing hundreds of atoms per unit cell, will enable studies of surface defects with a level of detail and sophistication far greater than previously possible. By studying well-defined, well-ordered surfaces, we can greatly simplify the study of defect chemistry and obtain detailed fundamental information on defect formation and reactivity. Coupling experimental results with theoretical studies will allow the development of models that explain, predict, and ultimately help to control surface defect reactivity.

We learned how to prepare a single-crystal Pt(111) (platinum) substrate and initiated studies of adsorbate diffusion. A common defect on the terraces appears as a very slight protrusion surrounded by a ring of lower apparent height

The unique atom-tracking scanning-tunneling microscope (AT-STM) recently developed at Sandia is a particularly powerful new technique that allows measurement of atomic-scale kinetic processes on a time scale that is more than three orders of magnitude faster than previous techniques....The recent development of massively parallel (MP) computational techniques at Sandia, which now allows calculations on systems containing hundreds of atoms per unit cell, will enable studies of surface defects with a level of detail and sophistication far greater than previously possible.

with a diameter of $\sim 40 \text{ \AA}$. This ring may be due to a change in the local electronic structure or substrate strain induced by the contaminant.

We observed residual gas adsorbates on the surface—both those that appear as protrusions (light) and those that appear as depressions (dark). The dark adsorbates diffuse very rapidly over the surface at room temperature and are most likely oxygen (O) atoms. The light adsorbates diffuse more slowly on a time scale of between 10 and 0.05 Hz. By atom tracking the light adsorbates, we can image the Pt(111) lattice sites that they visit. These adsorbates do not strongly interact with the ring defects and appear to visit all of the defect lattice sites.

We continued our investigations of the reactivity of strained copper (Cu) films on Ru(0001) (ruthenium). In particular, we tested and verified our model as to the relationship between reactivity and film structure. The studies we conducted were to extend our work from last year, in which we investigated the reaction of O with two monolayers of Cu on Ru(0001). Since then, we have studied the reaction of carbon monoxide (CO), sulfur (S), and thiol with the same strained film.

The results of CO were consistent with the lower reactivity of CO with the Cu film. Previous work showed that the sticking coefficient of CO drops tremendously as the thickness of the Cu film reaches 2 ML. Our studies at room temperature indicated that no CO was adsorbing on the dislocated Cu film. The structure of the film remained intact.

S, on the other hand, showed high reactivity with the Cu film. In an identical manner, the S reacts first with existing threading dislocations in the film. In general, the sequence indicates that reaction is dominated by the existence and creation of threading dislocations.

We optimized deposition procedures for growing oriented $\text{Mg}_3(\text{VO}_4)_2$ films. By depositing a 50 nm layer of gold (Au) on oxidized silicon (Si) wafers followed by sputter deposition of magnesium (Mg) vanadate, we are able to achieve thermally and chemically stable stoichiometric films oriented with the (042) plane parallel to the surface. We deposited films ranging in thickness from 1.0 to 200 nm. Atomic force microscope (AFM) measurements show crystallite sizes ranging from 40 to 100 nm. Initial STM measurements on an 8.5 nm film show similar crystallite sizes, but difficulties in obtaining stable tunneling currents limited resolution. We plan STM measurements on thinner films to see if the resolution problems can be overcome. These films behave chemically in a manner

very similar to bulk $\text{Mg}_3(\text{VO}_4)_2$, indicating that they are excellent model catalysts.

We completed the first accurate theoretical study of the effects of common surface defects on metal island nucleation. Surprisingly, we found that O vacancies on Mg(100) do *not* nucleate Pt metal islands, in spite of several suggestions to the contrary in the literature. Similarly, neither the cation vacancy nor homogeneous divacancies promote island formation, but the mixed divacancy does significantly increase metal dimer stability. In addition, we examined water dissociation products, as these are also common oxide surface defects, and found that the ad-OH species strongly promotes dimer formation. In a separate study, we found that heavy (1/3 monolayer) hydroxylation of an alumina surface not only increases Cu metal adhesion by a factor of 2.5, but also changes the growth mode from 3-D islands to one of wetting. These results led to a patent disclosure on controlling adhesion and film growth using atomic-scale manipulation of oxide surfaces.

Refereed

Bogicevic, A., and D. R. Jennison. 1999. "Role of Surface Vacancies and Water Products for Metal Nucleation: Pt/MgO(100)." *Surface Science Lett.* **437**: L741–L747.

Bogicevic, A., and D. R. Jennison. 1999. "Variations in the Nature of Metal Adsorption on Ultrathin Al₂O₃ Films." *Phys. Rev. Lett.* **82**: 4050–4053.

de la Figuera, J., K. Pohl, A. K. Schmid, N. C. Bartelt, and R. Q. Hwang. 1998. "Linking Dislocation Dynamics and Chemical Reactivity on Strained-Metal Films." *Surface Science* **415** (30 September): L993–L999.

Jennison, D. R., and A. Bogicevic. 1999. "Ultrathin Alumina Film Al-Sublattice Structure, Metal Island Nucleation at Terrace Point Defects, and How Hydroxylation Affects Wetting." *Faraday Discussion No. 114: The Surface Science of Metal Oxides*, accepted.

Kelber, J. A., C. Niu, K. Shepherd, D. R. Jennison, and A. Bogicevic. 1999. "Copper Wetting of Alpha-Al₂O₃(0001): Theory and Experiment." *Surface Science*, accepted.

Li, M., W. Hebenstreit, U. Diebold, M. A. Henderson, and D. R. Jennison. 1999. "Oxygen-Induced Restructuring of Rutile TiO₂(110): Formation Mechanism, Atomic Models, and Influence on Surface Chemistry." *Faraday Discussion No. 114: The Surface Science of Metal Oxides*, accepted.

Li, M., W. Hebenstreit, U. Diebold, M. A. Henderson, D. R. Jennison, P. A. Schultz, and M. P. Sears. 1999. "Oxygen-Induced Restructuring of the TiO₂(110) Surface: A Comprehensive Study." *Surface Science* **437**:173–190.

Ruffner, J. A., A. G. Sault, M. M. Rodriguez, and R. G. Tissot, Jr. 1999. "Deposition and Characterization of Highly Oriented Mg₃(VO₄)₂ Thin-Film Catalysts." *J. Vacuum Science and Technology*, submitted.

3502530000

Exploiting LENS™ Technology Through Novel Materials

J. A. Brooks, T. J. Headley, J. D. Puskar, M. L. Griffith, C. V. Robino

Laser-Engineered Net Shaping (LENS™) is a direct fabrication process in which metal powders are deposited into a laser-melted pool, with succeeding layers deposited to build up complex engineering shapes. This process is a rapid, low-cost, low-footprint direct-fabrication technique that lends itself to the concept for advanced manufacturing. However, previous work developed LENS™ as an advanced manufacturing tool rather than exploiting its potentially unique attributes. These attributes include real-time control of microstructure, tailored material properties at different locations in the same part, the production of graded thermal expansion parts, etc. This project seeks to develop a science-based approach to utilize LENS™ to process for properties in a controlled fashion, or for the production of components that cannot be made using other methods. Sandia is investigating three materials—a tool steel with an optimized structure/property mix, a graded structure based on stainless-steel compositions, and a ceramic-to-metal transition—as novel material systems through which we will investigate and exploit LENS™.

We are achieving this goal by first developing a thorough understanding of the process in terms of how it impacts solidification and solid-state microstructure development and the nature of residual stresses in the layer-by-layer-fabricated structures. Additionally, we are studying and understanding the unique attributes and capabilities of the LENS™ process. From this knowledge base, we are designing and producing a suite of experimental materials and structures to optimally exploit the LENS™ process and demonstrate its unique potential. We are developing an understanding of the residual stresses in LENS™ parts and what mitigation techniques may be available.

A critical aspect of this project is to demonstrate that microstructure and process models can be developed to predict and tailor properties of LENS™-deposited components that will greatly enhance this direct-fabrication technology. In this endeavor we are using tool steels as one of the model alloy systems. We determined hardness, tensile properties, and microstructures over the acceptable processing window to

This project seeks to develop a science-based approach to utilize LENS™ to process for properties in a controlled fashion, or for the production of components that cannot be made using other methods.

assess the range of properties achievable with H13 alloy tool steel. We completed isothermal aging studies of single-pass LENS™ deposits over a range of times and temperatures, and developed carbide coarsening models to predict hardness and tensile strength. Using additivity rules that incorporate the LENS™ thermal cycles with the kinetics of carbide coarsening, we developed the tools to predict properties for different processing conditions. We showed that the top layers consist of a hard, untempered martensite where the lower layers sharply transition to a soft, overaged structure. This phase of the work was highly successful and informative and is the first application of material/process model-based predictions applied to the LENS™ process. Applying similar rationale to precipitation-strengthened martensitic stainless steels, we showed that, unlike the tool steels, the precipitation kinetics are too sluggish to respond to the rapid thermal cycles.

To fully utilize the rapid solidification and cooling rates of the LENS™ process, alloys should be designed specifically for LENS™. With that intent we designed and obtained three austenitic stainless-steel alloys considering solidification modes based on thermodynamic calculations of phase stability, dendrite tip undercooling, and solid-state transformations behavior. Early evaluation of LENS™ samples found a variety of microstructures that we are comparing to model predictions. We will use one of these alloys to demonstrate the ability to transition from a high-toughness austenitic stainless steel to the high-strength martensitic stainless steel.

The ability to produce graded microstructures and increase flexibility in alloy design largely depends on the capability to feed multiple powders at controlled, variable rates. This year, we improved powder feeders and delivery systems to minimize clogging and better control feed rates. However, our biggest advancement was the development of the capability to feed multiple powders at desired ratios to achieve specific compositions, and to transition through different ratios of individual powers. We accomplished this by using mass-flow-rate meters that can accurately deliver the desired mass of individual powders to the power delivery nozzles feeding the laser-melted pool. We demonstrated the functionality of this newly developed capability using a number of powder combinations. We achieved very good agreement between the target composition and that measured in LENS™ deposits.

Residual stresses can play a major role in build distortion and engineering performance of laser-fabricated structures. We

...our biggest advancement was the development of the capability to feed multiple powders at desired ratios to achieve specific compositions, and to transition through different ratios of individual powers.

obtained residual stress measurements using holographic hole-drilling techniques in collaboration with Stanford University. Results on LENSTM-processed 316 stainless-steel bars showed that the residual stresses were close to the measured yield strength. However, we found that using auxiliary heating of the base platen greatly reduced distortion of fabricated structures of steel alloys. This is a very important finding since in these alloys, distortion and residual stresses can be sufficient to result in severe cracking. Work continues to further investigate the role of preheat and process parameters on distortion and measured residual stresses. Accurate measurement of temperature fields using newly developed high-resolution thermal imaging and thermal couple techniques combined with the residual stress measurements will provide validation for future finite-element modeling (FEM) of residual stresses.

Our initial work on processing ceramic materials, Al₂O₃, looks promising in that we achieved power delivery and melting; however, as expected we observed cracking. Successful processing of these materials will prove to be the most difficult challenge of this project.

Refereed

Griffith, M. L., M. E. Schlienger, L. D. Harwell, M. S. Oliver, M. D. Baldwin, M. T. Ensz, J. E. Smugeresky, M. Essien, J. Brooks, C. V. Robino, W. H. Hofmeister, M. J. Wert, and D. V. Nelson. 1999. "Understanding Thermal Behavior in the LENSTM Process." *J. Materials Design* **20**(2/3) (June): 107–114.

Other Communications

Beuth, J., A. Vasinonta, and M. L. Griffith. 1999. "Process Maps for Laser Deposition of Thin-Walled Structures." *Proc. 10th Solid Freeform Fabrication Symp.* **10** (Austin, TX, 9–11 August).

Brooks, J. A., C. V. Robino, T. Headley, S. Goods, R. C. Dykhuizen, and M. L. Griffith. 1999. "Microstructure and Property Optimization of LENSTM-Deposited H13 Tool Steel." *Proc. Solid Freeform Fabrication Symp.* (Austin, TX, 10 August), in press.

Griffith, M. L., M. E. Schlienger, L. D. Harwell, M. T. Ensz, D. L. Greene, J. E. Smugeresky, C. V. Robino, W. H. Hofmeister, M. J. Wert, and D. V. Nelson. 1999. "Understanding Thermal Behavior in LENSTM Processing of Structural Material." *Proc. Mineral, Metals, and Materials Soc. Conf.* (San Diego, CA, 3 March), in press.

3502540000

Molecular Characterization of Energetic Material Initiation

A. M. Renlund, A. S. Tappan, J. C. Miller

Sandia has responsibility for a diverse mix of energetic materials (EMs) and components. Determining the microscale chemical and physical responses of EMs to abnormal thermal environments is fundamental to understanding the safety of these EMs. The high explosive HMX (1,3,5,7-tetranitro-1,3,5,7-tetraazacyclooctane) is an EM used in many applications and Sandia-responsible components. The high-temperature polymorph (designated d-HMX) is of special concern due to our recent discovery that it appears to control reaction progress for thermal initiation. The solid-solid phase transition of HMX is dependent on pressure and temperature, with high pressures favoring the less-sensitive b-HMX and high temperatures favoring the sensitive d-HMX. We believe we have established a clear link between the HMX b-d phase transition and increased reactivity, sensitivity to initiation, and subsequent burning. However, sampling techniques used in our preliminary tests are not amenable to most component configurations. We are developing an in situ probe to monitor the phase transition using Raman spectroscopy and second harmonic generation (SHG) detection, both of which distinguish the two phases. Probe development and incorporation of SHG detection into the probe are the main focus of the project. Following development of the experimental probe, we will study the phase behavior of HMX and HMX-containing plastic bonded explosives (PBXs) at elevated temperatures and pressures relevant to component and system cookoff environments. Understanding the rate and extent of the solid-solid phase transition as functions of confinement, pressure, temperature, particle size, and density at time of cookoff is vital to improving our safety analyses of the material. We will apply this experimental development to monitor the kinetics of the phase transition and how the phase transition affects subsequent decomposition and cookoff.

We completed the major hurdle of developing and selecting a Raman probe for this project. We solved problems inherent to the Raman phenomenon by customizing a spectrograph and adapting a filtered fiber-optic probe specifically designed for Raman spectroscopy. The fiber-optic Raman probe allows delivery of the laser light and collection of the Raman scattered

Understanding the rate and extent of the solid-solid phase transition as functions of confinement, pressure, temperature, particle size, and density at time of cookoff is vital to improving our safety analyses of the material.

light in our heated and confined fixture that, during the experiment, is housed within an evacuated explosives chamber.

We are on schedule for this project with the exception of integration of SHG detection into the experiment. We obtained samples of pure HMX at two densities and particle sizes representative of HMX in components. We completed the optimization of the useful Raman signal and are satisfied with the results. The initial completion of system integration resulted in nonuniform heating of the explosive pellet. We continued the project in this less-than-perfect condition and, although the experiments worked, the results were somewhat inconclusive. These results indicate that there is improvement to be made on the system integration task, and for this reason it can only be deemed mostly complete. Initial tests of heated, unconfined HMX using the probe and spectrograph demonstrate that this technique can dynamically monitor the phase transition. Initial tests on heated, confined HMX provided very interesting results that indicate that the phase transition is extremely sensitive to confinement geometry and directional heat flux. Because of the system integration improvements that we need to make, integration of SHG detection has been deemed less important and not completed. Collaboration with Los Alamos National Laboratory continues, and their results in SHG studies on HMX raise the question as to whether the SHG is due to the phase transition, or to microstructural defects resulting from the phase transition. Raman spectroscopy, coupled with SHG detection, will answer this question. Additionally, we observed anomalous behavior of thermally degraded HMX, where months after heating, the more-sensitive d-HMX remained in the sample, contrary to published kinetic data, but in HMX-containing PBXs the sample had completely reverted to b-HMX. Recently, we also observed the existence of a-HMX in samples of previously heated HMX and HMX-containing PBXs. a-HMX has a sensitivity that lies between that of b- and d-HMX and forms upon cooling of d-HMX. These interesting results further emphasize the necessity of continued studies to improve our safety analyses of this material.

Refereed

Tappan, A. S., A. M. Renlund, J. H. Gieske, and J. C. Miller. 1999. "Raman Spectroscopic and Ultrasonic Measurements to Monitor the HMX b-d Phase

Transition." *Proc. 1999 JANNAF Propulsion Systems Hazards Subcommittee Meeting* (Cocoa Beach, FL, 18–22 October).

3502550000

Nonvolatile Protonic Memory

R. A. Anderson, B. L. Draper, M. R. Shaneyfelt, D. M. Fleetwood, A. G. Sault, J. A. Shelnett, C. H. Seager

Sandia recently discovered a new principle for nonvolatile memory devices in which the space charge in the oxide layer of silicon (Si)/Si dioxide (SiO₂)/Si structures can be rapidly changed by applied electric fields. Because of their simplicity, process-compatibility, and apparent radiation hardness, these structures may have great potential in low-power nonvolatile memory applications. We are investigating two issues that stand between this technology and its incorporation into microelectronics fabrication: (1) formation of the memory state and (2) memory-retention stability. At present we create the memory state in the oxide by immersion in either forming gas (5% hydrogen [H] in nitrogen [N]), or rarefied H, at approximately 600°C, but this process is neither optimized nor physically well understood. Furthermore, a central assumption that mobile protons are primarily responsible for the memory remains controversial. Our studies included H-plasma treatment, and we will attempt to implant protons directly into the oxide using an H-ion beam. We will apply surface-sensitive techniques to the elucidation of the H anneal process and to determining its spatial uniformity, and will exploit deuterium (D) loading to advantage whenever appropriate. A variety of voltage-response measurements are currently under way to characterize not only memory retention, but also the transport kinetics of these devices in general. Transport modeling is also in progress as an aid in understanding the complex behavior that we are observing. The complementary goal of this investigation is to understand the chemistry of proton-induced memory activation via quantum molecular modeling.

Experimental work focused on employing voltage-dependent capacitance (CV) measurements to deduce internal charge distributions in the SiO₂ layer of capacitor-dot specimens. These had approximately 700 Å oxides on n-Si substrates, with polysilicon capping electrodes. We H- or D-treated them at 600°C in rarefied gas and achieved strong memory states. We also tested unibond buried-oxide structures H-/D-treated by USAF Phillips Lab and samples that we exposed to H plasmas (which did not produce useful memory effects).

Sandia recently discovered a new principle for nonvolatile memory devices in which the space charge in the oxide layer of silicon (Si)/Si dioxide (SiO₂)/Si structures can be rapidly changed by applied electric fields. Because of their simplicity, process-compatibility, and apparent radiation hardness, these structures may have great potential in low-power nonvolatile memory applications.

We developed a novel method that tracks time-dependent shifts in CV characteristics after a change in applied bias. This method allows us to observe internal charge rearrangement with the electric field at the interface between the oxide layer and Si substrate held fixed, and thereby avoid interference from device nonlinearities. These measurements show asymmetrical shifts in the CV characteristics that are consistent with several hypotheses of the polarization mechanism, including the motion of mobile protons. We also observed displaced charge directly in some low-leakage capacitor dots, with encouragingly consistent results.

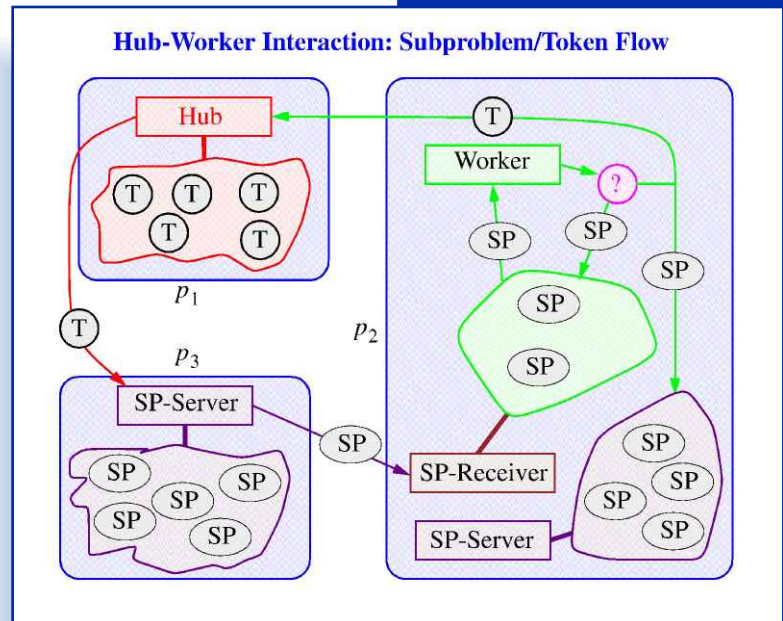
Our measurements probed the uniformity of the memory effect within the area of individual capacitor dots as well as the wider issues of the macroscopic uniformity over the area of a Si wafer and the reproducibility of memory activity. We found no obvious trends with position on the wafer, but the magnitude of the memory effect shows substantial dot-to-dot variation and a lack of reproducibility.

We found the temporal response to bias changes to be complex and sample-history dependent, but a common characteristic is an approximately first-order (decaying exponential) initial response, suggesting trap-release-rate dominance, followed by a persistent log-time dependency. Data from tens of samples that we either H- or D-treated showed no discernible isotopic shift in kinetic rates. We are investigating memory-retention stability, and we find that it is greatly influenced by the holding bias applied after a state is written. True long-term stability appears not to be realized in these initial samples.

We undertook transport modeling to assist in understanding the above-mentioned results. We are developing two numerical simulations that address (1) drift and diffusion of confined mobile ions, and (2) electronic capture and release from a distribution of H-generated traps, which are positive when vacant. Both models yield results that resemble some aspects of our data. In particular, the first of these models verified that electrostatic confinement alone, after mobile ions are forced near one of the electrodes by an applied bias, is not capable of retaining a memory state for greatly extended periods of time. If we had observed true stability, localized trapping or a shallow energy barrier would have been indicated.

COMPUTER SCIENCES

Computer Sciences is one of Sandia National Laboratories' four LDRD Research Foundations investment areas. Research Foundations extend the core scientific and technical knowledge base of the Laboratories. In addition, Research Foundations focus on innovative, high-risk research that supports the long-term needs of the DOE's and Sandia's national security mission.



The Computer Sciences (CS) investment area invests in research that is revolutionizing high-performance and simulation technologies in computing. These investments support the Stockpile Stewardship Program's (SSP) move toward computing-based methods of assuring nuclear reliability. CS LDRD projects include explorations in two research areas. Sandia is investigating distributed computing prototypes to enable computing over greater lengths of time and distance than ever before. We are conducting research in system software, software tools, load-balancing techniques, fault-tolerance, and Web-based tools in support of heterogeneous, distributed systems. In addition, large-scale computing investigations are focused on technologies that enable large-scale applications at the teraflops (one trillion floating-operations per second) scale. Research in advanced algorithms, virtual environments, multilevel methods involving multiple length

scales and/or multiple time scales, system-level simulations, and massively parallel (MP) geometry models for system analysis and control are being explored.

The "Parallel Combinatorial Optimization for Scheduling Problems" project responds to the SSP requirement that fielded weapons be taken apart, analyzed, and reassembled in a specific order. This research addresses difficult, resource-constrained scheduling problems where numerous tasks have deadlines, earliest start times, and precedence and resource constraints. The project is investigating new methods to create an MP combinatorial optimization engine that enables exact and approximate algorithm synergy. This will be the first mixed-integer programming (MIP) code that may be scalable to thousands of processors.



3504340000

Integration of Mesh Optimization with 3-D All-Hex Mesh Generation

P. M. Knupp, S. A. Mitchell

Sandia discovered and implemented a full set of hexahedral local-reconnection primitives. We conducted experiments on THEX (tet mesh, then subdivide tets into hexes) and whisker weaving (WW) meshes in an effort to improve quality: we generated a real-world mesh, manually examined and classified poor-quality areas, tried various reconnection strategies and smoothing, and evaluated the final mesh quality. Removing poor quality in one area often resulted in generating poor quality nearby, so we often applied many dependent levels of reconnection. We implemented a simple control loop that automatically applies reconnection and smoothing.

We developed advanced smoothing algorithms: untangle smoothing, with boundary terms, and optimize condition number smoothing. Untangle smoothing was mathematically sophisticated and successfully untangled a number of real-world meshes. Condition number smoothing successfully improved the quality of THEX meshes.

We developed a fairly full set of hexahedral local-reconnection primitives. All known, large-scale changes can be built up from them. We believe that this set is sufficient for our research, and finding additional primitives would not be helpful.

We conducted experiments on meshes generated by the THEX and WW algorithms in an effort to improve quality. We visually inspected and categorized areas of poor quality. The most common problems are nodes with too many hexes attached and hexes that are flat (small dihedral angles between some adjacent faces, and large dihedrals between others). Applying the rotate three hexes primitive was successful at removing some flat hexes in both THEX and WW meshes. We tried several strategies based on pillowing, inserting a layer of hexes, for nodes with too many hexes attached. Pillowing was not very successful. To get good quality, the set of hexes around which the layer is to be inserted must be nearly convex; such sets appear to be rare. Most other primitives produced many more quality problems than they solved.

Analyzing and applying primitives by hand was tedious, and we thought that perhaps we were overlooking some possible improvements. So we implemented a simple control

Sandia discovered and implemented a full set of hexahedral local-reconnection primitives....We developed advanced smoothing algorithms: untangle smoothing, with boundary terms, and optimize condition number smoothing.

loop that would categorize poor-quality hexes and automatically apply some connectivity swaps and smoothing. We achieved marginal mesh-quality improvements in some cases, but not as much as needed.

The most successful tet mesh improvement algorithms that we found in the literature rely on a strategy similar to the above, categorizing quality problems and applying known connectivity swaps. Such algorithms run very slowly and have difficulty improving the mesh near the boundary, as does our hex-improvement approach.

We made significant progress on our smoothing algorithms. We developed an untangle-based smoother that maximizes a global objective function based on getting all positive jacobians. This algorithm includes the unique feature of incorporating the jacobians on the fixed boundary of the smoothing region. We verified this algorithm in theory and in practice on meshes for which a positive jacobian mesh was known to exist. When applied to WW meshes, many problems could not be smoothed to have positive jacobians; we suspect that these meshes have connectivity and boundary constraints that prevent the existence of nodal positions that give a positive jacobian mesh. We also developed an algorithm that optimizes the condition number of the hexes, once all jacobians are positive, with the guarantee not to make any jacobians nonpositive. The condition number smoother proved successful in improving the quality of THEX meshes.

In most examples, poor-quality regions appeared near the boundary of the region. Most real-world examples have relatively coarse meshes through the thickness. Our conclusion is that using local rules and respecting a fixed-surface quadrilateral mesh, our approach is unlikely to produce high-quality meshes. In some limited cases, mesh quality can be improved marginally. It has been suspected for some years that certain small configurations of surface meshes admit no high-quality mesh. Perhaps this is also true of many—or most—larger, nonstructured surface meshes.

Other Communications

Knupp, P. M. 1999. "Achieving Finite Element Mesh Quality Via Optimization of the Jacobian Matrix Norm and Associated Quantities, Part III: Mesh Untangling." *Int. J. Num. Meth. Engr.*, accepted.

3504350000

Heterogeneous Simulation

F. J. Oppel, III, E. J. Gottlieb, P. G. Xavier

No generalized simulation framework exists to enable modeling behaviors of intelligent machines that depend on physical environments. This requires a heterogeneous simulation environment to model these intelligent machines operating in a real world containing different environments.

This effort will develop a framework for building and testing heterogeneous simulations. This research enables the integration of several models residing on different platforms that often contain varying model fidelity. It will interface with existing simulation packages through either on-line access or off-line data access. The framework will incorporate diverse simulation environments ranging from continuous simulations (modeling physics such as dynamics, thermodynamics, material deformation, radiation, plumes, etc.) to event-based simulations (modeling agent behaviors, state machines, etc.).

This effort will develop a framework for building and testing heterogeneous simulations.

(1) We evaluated the required hardware and software resources for a heterogeneous simulation of intelligent machines behaviors in diverse environments and made the following conclusions:

- The framework must be suitable for system engineers to rapidly study the collective behavior of intelligent agents/machines in heterogeneous environments. The framework implementation should reflect the modular aspects of the real system functionality through a graph flow diagram to reduce the cognitive load in system development.
- It should be efficient in that the cost of the framework abstraction should not significantly impact simulation performance.
- The framework also must allow the user to interact and rapidly develop the system modules to understand the characteristics of the behavior through “on-the-fly” module construction/deletion, queries, and parameterized instances for directing computational flow.
- The hardware platforms need to range from Windows NT on the PC and UNIX on the SGI to Linux on Cplant to rapidly obtain results with varying fidelity.
- The software resources across all platforms include the following: (a) C++ compiler (Visual C++ on PC and GNU G++ elsewhere), (b) GNU Make Development Tools, (c) CVS software configuration management, (d) MPI (message-passing

interface) parallel communication between groups of modules executing on different CPUs (central processing units), (e) CORBA (Common Object Request Broker Architecture) communication for remote visualization and online simulators, (f) 3-D real-time graphics (Optimizer for PC and SGI; OpenGL for Linux), and (g) a scripting language using Tcl/Tk (Tool Command Language/Tool Kit).

(2) The selected test problem consists of studying the collective behaviors of three different intelligent machines (ground vehicle, unmanned air vehicle (UAV), and a hopping vehicle) operating on a synthetic aperture radar (SAR)–generated terrain. These vehicles collectively detect and locate the source of a chemical plume. Several simulation worlds coexist—a communication world, a chemical plume world, a terrain world, and a visualization world.

(3) We developed the design of the basic heterogeneous framework and the multimodel design scheme and call this framework Umbra. Umbra modules written in C++ are instantiated with Tcl scripts. We can dynamically construct/destroy and connect/destroy these modules during initialization or runtime. Module parameters are accessible as Tcl parameters, which enables parameter query and modification during runtime. The framework utilizes the Tcl event-loop for creating and detecting events. The simulation event-loop may contain dynamic modules that get updated every event-loop or modules that get updated only when a state change occurs. The 3-D graphic visualization is an asynchronous event within the main Umbra simulation event-loop. The multimodel scheme developed within the Umbra framework models a universe (a heterogeneous simulation) as a collection of worlds (communication, plumes, radiation, terrain, visualization, etc.) that contain intelligent agents/machines. These worlds are loosely coupled to each other, such that the exchange of information between worlds occurs only once per timestep, which is one cycle through the event-loop. We model an intelligent machine as a collection of modules that relate to the actual components of the real device. We classify these modules as behavior, controls, vehicle physics, geometry, and sensors. The behavior module obtains information from worlds through sensor modules. The behavior module is the central module of the intelligent agent.

(4) This task implemented and demonstrated the new Umbra framework with the multimodel scheme. We successfully created and tested modules from the test problem. These include modules for three different intelligent devices

(UAV, ground vehicle, and hopping device) interacting with a terrain world, communication world, plume world, and a visualization world.

Other Communications

Oppel, F. J., and E. J. Gottlieb. 1999. "Disclosure of Technical Advance." *Umbra: A Modular Object-Oriented Framework for Building Intelligent Machine Simulations* (24 February).

3504360000

Volumetric Video Motion Sensing for Unobtrusive Human-Computer Interactions

J. J. Carlson, D. E. Small, C. F. Diegert

This project will develop sensing, parallel processing, and geometric reasoning algorithms to enable unobtrusive human-computer interactions. Our approach is to leverage two unique Sandia capabilities: volumetric video motion detection (VVMD) and large-scale computing. We will demonstrate unprecedented human-machine interactions through dramatic advances to the VVMD. By developing new parallel processing algorithms and a new PC cluster deployment architecture, we will extend the resolution of the current VVMD platform to its attainable limits. We will move from platforms that make video-rate constructions of several hundred volume elements (voxels) to platforms that update millions of voxels in real time. We will also develop robust geometric reasoning algorithms to interpret the constructions.

We will demonstrate two scales of human-computer interaction. On a small scale, the VVMD will monitor a small volume (several cubic feet) directly in front of a computer monitor. A person will interact with the computer through a combination of hand gestures and voice commands. This system could replace or augment a keyboard and mouse. On a larger scale, the VVMD will monitor the position and orientation of one or more humans in a room-sized volume. Differentiating itself from other position/orientation sensors, the VVMD allows participants to maneuver untethered, allowing more-natural human-machine interactions. By combining a VVMD at this scale with a state-of-the-art video wall and visualization platform, participants could use simple gestures to browse through high-fidelity simulation results and to collaborate with remote participants. Another application at this scale is a robotic work cell, where an operator can point at an object and gesture to cause the robot to move the object to a new position.

We operated the VVMD system as a distributed application on a cluster of industry-standard PCs, demonstrating successful completion of two tasks. The effort yielded parallel implementations to allow two types of scalability. First, the architecture scales from applications requiring only a few cameras (like four cameras used in a small security-monitoring system) to applications requiring dozens of cameras (installing 32

By developing new parallel processing algorithms and a new PC cluster deployment architecture, we will extend the resolution of the current VVMD platform to its attainable limits. We will move from platforms that make video-rate constructions of several hundred volume elements (voxels) to platforms that update millions of voxels in real time.

inexpensive cameras in a 3-D room for virtual reality [VR] training would not be excessive). Second, the architecture scales in resolution from hundreds to millions of voxels under surveillance. This groundwork is the basis for additional scaling in resolution with an implementation on track for year-end completion that should deliver real-time updates to over 10 million voxels. Using a CORBA (Common Object Request Broker Architecture)-based distributed computing architecture, we were able to update a 350,000-voxel volume at 18 Hz. We used the same platform to update a 2.6-million-voxel volume at 8.5 Hz. These data were visualized in real time over the network in an open-GL application.

In the course of our work, we discovered an unanticipated need to realize separate implementations of the VVMD back-projection algorithm: one for online deployment and a second for offline simulation. The offline simulation code (called PVOX) is also a parallel application. It uses message-passing interface (MPI) middleware that enables us to perform batch runs of PVOX on Sandia's Computational Plant (Cplant) to explore design decisions on alternative compression, domain decomposition, and load-balancing strategies. The PVOX code can use synthetic data or can simulate against actual data captured by running our online VVMD code. We completed runs of the PVOX code to study the load balance achieved with a modulation decomposition of the VVMD back-projection algorithm to a field of n-processors.

In the course of our work, we discovered an unanticipated need to realize separate implementations of the VVMD back-projection algorithm: one for online deployment and a second for offline simulation.

Other Communications

Carlson, J. J. 1999. "Volumetric Video Motion Sensing for Unobtrusive Human-Computer Interactions." Special Presentation to the United States Air Force, Force Protection Battle Laboratory, Albuquerque, NM, July.

3504370000

Hybrid Sparse-Dense Incomplete Factorization Preconditioners

M. A. Heroux, J. N. Shadid, R. R. Rao, P. R. Schunk

Sandia is developing a new class of preconditioners for large, complex, multiphysics applications on state-of-the-art parallel computers. The primary targets of this work are the codes GOMA and MPSalsa running on Cplant using new preconditioners delivered via Sandia's solver package AZTEC. We worked on the set of test problems collected from GOMA and MPSalsa. Approximately 10 difficult to previously unsolvable problems provided the target test suite for our work. We made improvements to GOMA that allow better integration of new solver technology. Specifically, we installed the latest version of AZTEC (Version 2.0) into GOMA as part of this project and completed changes to GOMA that allow us to install the next release of AZTEC.

The upcoming release of AZTEC 2.1 includes the sparse-dense preconditioners developed for this project. This package of preconditioners, called IFPACK, is integrated into AZTEC and runs in both serial and parallel modes. It is also, in principal, a stand-alone preconditioner package that can be integrated into any other compatible solver package.

We completed the initial port in our effort to port GOMA to Cplant, including changes in GOMA's underlying code design and the port of supporting packages.

- *Collection of test problems.* Our first task was to build a collection of test problems that would be the target for our algorithm development. We collected a variety of test problems, primarily from GOMA, but also from MPSalsa. Some of the most notable test problems were:

- *2-D laser spot-weld problem:* A critical problem within our neutron-generator manufacturing applications.

- *3-D braze joint:* A model for the joining of a neutron-tube base made out of alumina ceramic and a triclad alloy.

- *3-D bead-laydown problem:* A model being considered for neutron-tube production that is similar to a neutron-tube feed-through insulator process.

- *Algorithms and solver work*

- *Integration of AZTEC 2.0.* Prior to developing new methods for GOMA, we first wanted to incorporate and tune AZTEC Version 2.0 into the code. The results of this effort were very good. AZTEC 2.0 has the ability to apply Reverse

Sandia is developing a new class of preconditioners for large, complex, multiphysics applications on state-of-the-art parallel computers. The primary targets of this work are the codes GOMA and MPSalsa running on Cplant using new preconditioners delivered via Sandia's solver package AZTEC.

Cuthill-McKee (RCM) reordering to the preconditioner. This feature alone made a big improvement in AZTEC's ability to solve a broader set of problems. ILUT, a robust form of Incomplete Laser Ultrasonics (ILU) factorization, has also been helpful. These features made three problems solvable; however, inflation in iteration count due to parallel execution will likely be a problem.

– *IFPACK Block ILU preconditioner with local pivoting and block diagonal perturbation.* We fully integrated Version 1.0 of IFPACK into AZTEC. This code can take an existing matrix partitioning and apply Block ILU with level fill control, local pivoting, and, if necessary, perturb diagonal blocks to improve the global condition number. We can compute the condition number estimate after computing the ILU factors. This turned out to be an excellent indicator of how effective the preconditioner will be, especially in situations where the Block ILU factors are very ill-conditioned. By monitoring the condition number estimate and perturbing the block diagonal entries if the factors are ill-conditioned, we can strike a balance between accuracy and computability of the forward-back solve in the iteration phase. IFPACK runs in both serial and parallel modes in AZTEC.

– *Prototype sparse pivoting ILU.* In addition to local pivoting (within a block), we developed a capability to do row pivoting across the sparsity pattern of the matrix. Currently it works only for point entry sparse matrices, but we are extending it to block entry matrices. This preconditioner guards against the situation where an arbitrary ordering of equations is prohibiting solution.

– *Block generalized minimum residual method (GMRES).* Another additional piece of work is the formulation and implementation of a new Block GMRES algorithm. We have a prototype code that, in our initial tests, is very promising. It has excellent performance characteristics and is very efficient for systems with multiple right-hand sides, and we are seeing more of these types of systems as engineers start to do parameter optimizations.

• *GOMA port to Cplant.* Along with excellent progress in algorithm development, we built a serial and parallel version of GOMA for Cplant and thoroughly tested it. It is worth noting that in order to build GOMA on Cplant we also needed to port Netcdf 3.4, Sparse, Umfpack, Exodus II, and AZTEC 2.0. Also, as a part of this project, we are redesigning the data structures in GOMA to efficiently support the new solvers and, at the same time, have more flexible and efficient data

We have a prototype code that...is very promising.

structures for GOMA in general. This work is necessary to support block sparse matrices.

Other Communications

Schunk, P. R., R. R. Rao, and T. A. Baer. 1999.

“Current Progress Toward Fully-Coupled 2-D and 3-D Simulations of Rheologically Complex Coating and Related Manufacturing Flows.” Paper presented to the 3rd European Coating Symposium, Erlangen-Nürnberg, Germany, 7–9 September.

3504380000

Big Eddy—Advanced Large-Eddy Simulation Algorithms for Complex Flow Physics and Complex Geometry

R. C. Schmidt, T. M. Smith, A. R. Kerstein, T. E. Voth

The objective for this work is to advance the algorithms and methods for large-eddy simulation (LES) for unstructured grids, irregular geometry, and coupled physics. The emphasis for the effort is on developing the tools, the knowledge, and the experience needed to perform accurate and computationally affordable LES calculations of engineering problems with coupled physics in complex geometries.

LES is a promising alternative to traditional turbulence models because little empiricism is required for a broad spectrum of flow regimes, and transitional and time-dependent flows can be treated. However, although LES has been demonstrated for simple geometries, the treatment of complex geometries with unstructured grids is just beginning to be explored. The interaction between dispersive and diffusive errors, grid anisotropy, filters and filter scales, and subgrid scale (SGS) models has not been quantified in a rigorous way, resulting in uncertainty for many LES computations. These issues are compounded by Sandia applications that demand unstructured grids and accurate treatment of coupled physical processes. This research seeks to advance LES models and methods, reduce the uncertainty, and improve the reliability of LES by quantifying the effects of filters and filter scales, under-resolved flowfields, diffusive and dispersive errors, and stochastic SGS models on unstructured grid turbulence simulations. This effort will rely on Sandia's large-scale computational capability, advanced numerical analysis techniques, and controlled numerical experiments to develop an LES toolkit with models, algorithms, standard libraries for filters and derived flow statistics, and a suite of validation and verification (V&V) problems. The LES toolkit will directly impact multiple Sandia applications codes (ALEGRA, CTH, MPSalsa, GILA, and FUEGO) and will enhance Sandia's leadership in large-scale computing and turbulent simulation.

We created a comprehensive working document that documents the LES theory, model formulations, numerical experiments, and important conclusions of this research. We formulated the dynamic and k-transport subgrid LES models and documented them in the working document. Implementa-

The LES toolkit will directly impact multiple Sandia applications codes (ALEGRA, CTH, MPSalsa, GILA, and FUEGO) and will enhance Sandia's leadership in large-scale computing and turbulent simulation.

tion of the k-transport model into MPSalsa is complete, and the implementation of the dynamic model is in progress.

We wrote and documented Version 1 of a post-processing code called LESTATS, for deriving turbulence statistics from unstructured-grid LES. LESTATS provides a simple, flexible means for deriving turbulence quantities such as the mean and fluctuating velocity, Reynolds stresses, turbulent kinetic energy, velocity-temperature and velocity-pressure correlations, and higher-order statistics such as velocity skewness and flatness. We produced and distributed a draft user's manual.

We formulated, analytically evaluated, and implemented a promising class of explicit filters based on the Reproducing Kernel Particle Method (RKPM) into the LESTATS statistics package. *A priori* testing of these filters using direct numerical simulation (DNS) data is in progress.

We formulated and documented a significantly revised version of the one-dimensional-turbulence (ODT) model for use as a near-wall LES subgrid model. Implementation and testing of the new model in an LES code is in progress.

We modified the Sandia plotting code HISPLT so that we can perform Fourier transform signal processing. HISPLT will now generate power spectral densities (PSD) from point history data and plot the PSD with the same functionality of the other plotting commands.

We defined a suite of preliminary V&V problems and began model assessment by performing calculations on the first of these problems—the 3-D lid-driven cavity problem.

Other Communications

Voth, T. E., and M. A. Christon. 1999. "The Use of Reproducing Kernel Functions for Discrete Filtering in Large-Eddy Simulation." Paper presented to the 5th U.S. National Congress on Computational Mechanics, Boulder, CO, 4–6 August.

3504390000

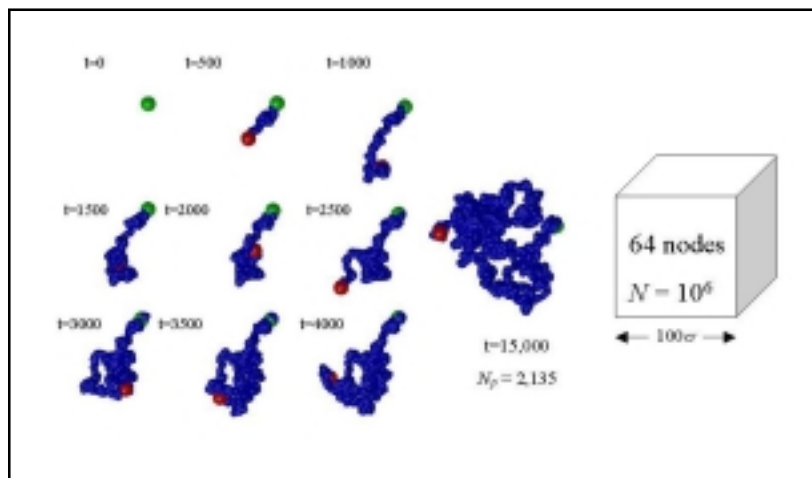
Molecular Simulation of Reacting Systems

A. P. Thompson, F. B. Van Swol

Reacting systems are critical in a wide variety of materials problems central to Sandia's missions, including polymer oxidation, epoxy curing (encapsulation), corrosion, reactive spreading and wetting (solder), and reactive equilibria in hazardous waste. In many cases, significant resources have been focused on molecular simulation of equilibrium and transport properties of materials in which chemical reactions play an important role, but the reaction events have been either completely ignored or greatly simplified. For example, in polymer aging it is likely that on some short length scale the oxygen reaction and diffusion processes are linked. Any truly predictive model of the chemical and physical processes underlying aging must include this reactive/diffusive linkage.

Sandia initiated two major efforts to incorporate reaction models into existing molecular simulation codes. For continuous forcefield molecular dynamics (MD), we added a Monte Carlo (MC) bond-making capability to the LAMMPS (Large-Scale Atomic/Molecular Massively Parallel Simulator) MD code, enabling us to simulate the irreversible polymerization in systems containing on the order of 10^6 particles. We used this code to examine how the impact of diffusion on the polymer dimensions scales with molecular weight (~ 1000 segments). We intend to extend the code to handle chemical reactions of arbitrary stoichiometry. This will require the implementation of a more general data structure for reactions. It will also require that we solve the problem of conflicting reactions occurring at processor domain boundaries.

Reacting systems are critical in a wide variety of materials problems central to Sandia's missions, including polymer oxidation, epoxy curing (encapsulation), corrosion, reactive spreading and wetting (solder), and reactive equilibria in hazardous waste.



Molecular dynamic simulation of polymer growth.

For hard-sphere MD, we extended the existing Hard-Sphere MC/MD code to handle so-called “tethered chains.” We tested this code against literature data for linear polymers. In the coming year we will use the code to simulate reaction and diffusion of a hard-sphere gas with cross-linked polymer structures.

The primary focus of this project is to introduce chemical reaction models into existing materials simulation models. We targeted three different classes of model: (1) hard-sphere MD, (2) continuous force-field MD, and (3) classical density-functional theory (DFT).

We extended the hard-sphere MD code to include bonds between atoms. This allows us to simulate polymeric systems of arbitrary functionality (e.g., linear chains, tetrafunctional networks, etc.). We tested the bond feature by comparing the pressure data obtained for linear hard-sphere tetramers with published equations of state (EOS), yielding good agreement.

We added the chemical structure change infrastructure to the LAMMPS code and developed a parallel MC bond-forming capability. This latter accomplishment provides half of the reaction ensemble capability. We will implement the reaction ensemble method. We are using the existing code to perform large-scale simulations (106 particles) examining the effect of diffusion limitation on linear polymer growth.

We dropped (3) above from the project and will concentrate on the hard-sphere and continuous force-field codes.

We added the chemical structure change infrastructure to the LAMMPS code and developed a parallel MC bond-forming capability.

3504410000

Massively Parallel Global Climate Model for Paleoclimate Applications

M. B. Boslough, B. D. Zak, T. R. Guilinger

Global climate was recently recognized as a national security issue. The potential economic costs associated with climate change are enormous, but so are the costs to avoid or minimize climate change. Predictive climate models must be developed, but the time scales of global climate change preclude validation before the damage is done. Thus, there will always be an element of uncertainty as to how good the models are and whether or not they should be trusted. One of the most notable successes in recent years was the ability of climate modelers to accurately hindcast the time dependence of global temperature changes in the twentieth century. This breakthrough resulted from the addition to the radiative transport model of the opacity of sulfate aerosol pollution and boosted the credibility of climate modeling in general. Another validation strategy is to take advantage of the Earth's geologic history to test the predictability of climate models in hindcast mode using paleoclimatic data. Sandia believes that successful paleoclimate models will lead to further gains in climate-modeling credibility, so we plan to parallelize a widely used paleoclimate code to take advantage of the massively parallel (MP) environments that are becoming available.

We carried out a detailed parallel performance analysis and scalability studies of the paleoclimate model GENESIS. We investigated autoparallelism as a means to achieve performance enhancements using the utility offered by shared-memory architectures and determined the feasibility of converting the code from shared-memory to message-passing parallelism. We carried out our timing analysis using the Timex central processing unit (CPU) timer, with performance analysis using a Silicon Graphics analyzer. We also examined the effect of DO loop partitioning by altering the code to accept MP_SCHEDTYPE at runtime, with a speedup gain of over 40% on eight processors, relative to the original code, which showed no significant gain above four processors.

We extracted individual routines from the GENESIS code and translated them to message-passing interface (MPI) using MPI_BROADCAST to share the data. Because nearly all of the pertinent variables in GENESIS are shared among program elements using common blocks, the MPI model is difficult to

...we plan to parallelize a widely used paleoclimate code to take advantage of the massively parallel (MP) environments that are becoming available.

implement without significant reconstruction of the semi-Lagrangian transport, fast Fourier transform, and Legendre transform. These can all be parallelized by decomposing the surface domain and keeping data local to a given processor for the physics and dynamics. This keeps communication to a minimum and requires only minor changes to much of the original GENESIS source code. We installed and compiled the source code for PCCM2 and are becoming familiar with it so we can use it as a model for modifying the parallelization of GENESIS.

Presently, 15 loops in GENESIS are parallelized for SGI or Cray shared-memory model. We experimented with DO loop partitioning using five different methods: (1) simple-contiguous pieces, (2) guided self-scheduling (GSS), which varies piece size depending on the number of iterations remaining, (3) dynamic-piece size set by chunk, which gives good load-balancing offset by higher overhead, (4) interleave-piece size set by chunk and interleave among processors, and (5) runtime-use environment variable in UNIX to select partitioning. By simply changing the DO loop partitioning in GENESIS, we achieved a speedup of 15% on four processors and over 40% on eight processors.

Refereed

Fawcett, P. J., M. B. Boslough, and D. A. Crawford. 1998. "Effects of an Impact-Induced Ring System on Earth's Climate." Paper presented to the AGU 1998 Fall Meeting, San Francisco, CA, 14–18 December.

3504420000

Fast and Easy Parallel I/O for Efficient Scientific Computing

J. E. Sturtevant, P. C. Chen, D. N. Sands, R. A. Haynes

The performance of input/output (I/O) subsystems on massively parallel (MP) computers lags the computational power of these machines. I/O includes data transfer to and from disks, archival storage, and networks. New algorithms and approaches to I/O are necessary to compensate for the imbalance between I/O and computational performance. In this project, Sandia will develop new tools and algorithms that allow applications programmers to use I/O resources easily and efficiently and will work with the ALEGRA and PRONTO programs to test these ideas in important applications on the Teraflop machine. Deliverables will include (1) an I/O research platform on which new application interfaces, libraries, and algorithms for I/O can be incorporated and tested, (2) an I/O library with a simple, general-purpose interface for application programmers, (3) a higher-level I/O library for finite-element (FE) applications, and (4) optimal data layouts for efficient data retrieval based on common or user-specified access patterns.

We will focus on collective I/O, i.e., coordinated requests from many processors, because of the increased potential for efficient use of disk and tape systems. Programs that require out-of-core computation or frequent checkpointing should see significant performance improvement due to lower I/O overhead. Moreover, new I/O capabilities developed in this project will allow larger simulations to be run, reduce the computer time required for these simulations, eliminate the long file-recombination process prior to visualization, and reduce the programming time to develop new applications. In sum, the Accelerated Strategic Computing Initiative (ASCI) and nuclear weapons complex (NWC) codes will be able to solve bigger problems than would otherwise be possible, and they will run faster while doing so.

We progressed toward the ultimate goal of having a scalable parallel I/O (PIO) library that simulation and visualization applications can use to transfer massive amounts of data among memory, disks, and tape archive. The research done by this project has affected both ASCI problem-solving environment (PSE) and DisCom plans.

...the Accelerated Strategic Computing Initiative (ASCI) and nuclear weapons complex (NWC) codes will be able to solve bigger problems than would otherwise be possible, and they will run faster while doing so.

Our accomplishments built upon the solid software infrastructure established previously, delivering usable, high-performance PIO libraries for Sandia's unstructured-grid FE applications. We continue to improve the low-level collective disk I/O library (PIO) that supports efficient transfers of locally permutable data arrays with minimal buffering requirements, the mid-level parallel data set (PDS) management library that supports collective, random access of primitive FE data arrays, and the Parallel eXodus Interface (PXI) library that provides a higher level of abstraction for both simulation and visualization applications.

Specifically, we accomplished the following:

(1) Continued the integration of the I/O libraries, PXI/PDS/PIO into ALEGRA and PRONTO. Observations from ALEGRA using the current parallel file system (PFS) on the Teraflop indicate an order-of-magnitude increase in I/O performance.

(2) Presented a technical paper at SC '98 PDS/PIO: Lightweight Libraries for Collective Parallel I/O.

(3) Provided Nemesis I functionality to support mesh-generation tools for FE modeling (FEM) simulation.

(4) Enabled the successful execution of PRONTO 3D on multiple shared-memory processors (SMPs) of an SGI Origin 2000 system.

(5) Improved the large data visualization interface by separating metadata from other data.

(6) Enabled file sizes > 2 GB for the Intel Teraflop system and SGI Origin 2000 system.

(7) Added support for adaptive meshing.

(8) PDS V2.0 enabled the successful demonstration of run-time visualization and remote navigation capability of ALEGRA simulation results.

(9) Provided rudimentary PIO capability for Cplant.

(10) Ported the I/O libraries, PIO, PDS, and PXI to the Cplant cluster.

Our accomplishments built upon the solid software infrastructure established previously, delivering usable, high-performance PIO libraries for Sandia's unstructured-grid FE applications.

Refereed

Sturtevant, J. E., M. Christon, P. D. Heermann, and P. C. Chen. 1998. "PDS/PIO: Lightweight Libraries for Collective Parallel I/O." *Proc. SC '98* 1 (Orlando, FL, 7–13 November): 1–11.

3504430000

Novel Load-Balancing for Scalable, Parallel Electromagnetic and Plasma Physics Simulation Software

D. B. Seidel, G. Montry, L. P. Mix, Jr., M. F. Pasik, D. J. Riley, S. J. Plimpton, R. S. Coats

Electromagnetic particle-in-cell (EM-PIC) simulation techniques are used to address many national security (NS) applications. These include simulation of neutron generators (NGs), weapon response to hostile x-ray environments, Z-pinch (x-ray) accelerators, radiography systems for weapon primaries, and high-power microwave devices. EM-PIC simulates the time response of EM fields and low-density plasmas in a self-consistent manner (the fields push the plasma and the plasma self-current modifies the fields). The Sandia QUICKSILVER/VOLMAX code suite is currently used for these applications, but it does not yet have the scalability required to perform full system-level simulations on thousands of nodes. The chief obstacles are load-balancing the computations due to the nonuniform, time-dependent density of particles on the grid and the use of different numerical algorithms and cell types in various grid regions. Sandia is testing and implementing novel methods to achieve a fully parallelized, scalable code and devised two potential candidates. The first is a static method that divides the grid into many more subdomains than nodes and assigns them to nodes so that, on the average, each node has nearly equal amounts of computation per timestep. The second is a dynamic method where weighted subdomains will migrate as needed between nodes to address the changing workload due to particle motion. We will also automate setup for parallel execution as well as parallelize diagnostics.

We modified the 3-D EM-PIC code QUICKSILVER to perform parallel simulations on teraflop-scale machines. Ongoing work continued to restore the remaining models and diagnostics of the original serial QUICKSILVER to the massively parallel (MP) version; to explore, understand, and successfully deal with a new numerical instability associated with the parallel implementation; and for validation/benchmarking. However, the bulk of the effort focused on one of the largest issues of efficiently implementing the code—dynamic load-balancing of the particle processing.

Extensive tests revealed subtle algorithmic sensitivities to parallel connection schemes that cause the simulation to

Sandia is testing and implementing novel methods to achieve a fully parallelized, scalable code and devised two potential candidates.

become unstable. We explored and gained understanding of the cause of this instability. The instability grows from slight differences (due to finite precision arithmetic) in the operands of the field-update equations that are nominally equivalent on more than one processor. By slightly changing the way current density is communicated between processors, by making small adjustments in the treatment of dielectrics, and by modifying the way differencing coefficients for the update equations are computed, we eliminated the three identified seed mechanisms for the instability and hence the instability itself.

We parallelized most of QUICKSILVER's extensive diagnostic capabilities. This includes time histories, field and particle snapshots, killed-particle fluxes, and killed-particle snapshots. We implemented field and particle snapshots using Sandia's parallel dataset/parallel input/output (PDS/PIO), producing PDS format files. We also wrote post-processing tools that convert PDS files to the portable file format (PFF) recognized by our array of post-processing analysis tools. Models that we implemented in parallel during this period include applied external magnetic fields and periodic boundary conditions.

We implemented a novel load-balancing technique and tested it in QUICKSILVER. In this new approach, we continue to use a static, balanced decomposition for the field grids, but dynamically migrate particles from overworked processors to underworked ones via contiguous subregions of grid cells (windows) within the overworked processor's grid. This method has significant advantages over other potential approaches, not the least of which is that it requires only slight modification to QUICKSILVER's existing structure to implement. Our first implementation demonstrated that this technique can significantly improve load balance and that the extra communication overhead required is acceptable. However, some details of the initial implementation ultimately limited its scalability. We subsequently refined the algorithm to address these problems and are testing it.

The new parallel version of QUICKSILVER is now routinely run on multimillion-cell, 10–100-thousand timestep problems (fields-only) on hundreds of processors for projects. It has also been used to a lesser extent in PIC mode for simulations of high-power microwave sources and will be used in the near future to simulate details of magnetically insulated electron flow. Other important applications on the horizon include the study of ion optics and of cavity SGEMP (system-generated electromagnetic pulse). The code has been ported to

By slightly changing the way current density is communicated between processors, by making small adjustments in the treatment of dielectrics, and by modifying the way differencing coefficients for the update equations are computed, we eliminated the three identified seed mechanisms for the instability and hence the instability itself.

Sandia's DEC 8400 and Cplant. At the end of this project, the new parallel version of QUICKSILVER implements nearly all the features of the original serial QUICKSILVER and can be run on any platform that supports the message-passing interface (MPI) standard as well as single-processor workstations.

Other Communications

Kotulski, J. D., C. D. Turner, D. J. Riley, M. F. Pasik, D. B. Seidel, and S. J. Plimpton. 1999. "Massively Parallel Implementations of Time-Domain Electromagnetic Solvers on Teraflop Platforms: Descriptions, Problems, and Results." *USNC/URSI Radio Science Meeting URSI Digest 1* (IEEE AP-S/URSI International Symposium, Orlando, FL, 11–16 July): 103.

3504440000

Massively Parallel *Ab Initio* Validation for ASCI Materials Modeling

C. F. Melius, C. L. Janssen, C. H. Tong, I. M. Nielsen, M. L. Leininger

Sandia is undergoing a revolutionary transition from being a lab based on experimental testing to a lab based on predictive computational modeling. A central part of the Accelerated Strategic Computing Initiative (ASCI) program is a detailed model-based understanding of the aging of weapon components. Such an understanding will require the simulation of molecular systems larger than have ever been studied at accuracies beyond the state-of-the-art, even for small chemicals. Currently, large-scale ab initio quantum chemistry (QC) simulations are possible using the massively parallel (MP) Hartree-Fock (HF) and density-functional methods developed at Sandia. Unfortunately, these workhorse QC techniques do not have predictive accuracy for many of the chemical species formed in the aging of polymers and energetic materials (e.g., the peroxy radicals formed in the aging of PETN). Chemically accurate predictions are possible with these methods if they are calibrated and if systematic corrections are developed that depend on the chemical system being modeled. Historically, these computer simulations were accurate QC methods, such as coupled-cluster theory, which approach the exact result with increased computational effort. The goal of the project is to provide methods for calibrating the workhorse simulation methods by developing MP versions of more accurate, highly electron-correlated QC methods.

We continued developing new diagnostics for judging the accuracy of wavefunctions computed with the second-order Möller-Plesset (MP2) and the coupled-cluster singles and doubles method. Our previously developed singles diagnostic did not utilize all the available information in the wavefunction. We found that we could develop a diagnostic with all of the desirable properties of our previous diagnostic utilizing the doubles amplitudes with an insignificant additional computational expense. These desirable properties include size-intensivity, invariance to orbital rotations that leave the energy unchanged, and the properties of a norm. Most importantly, the size of the diagnostic is a useful predictor for the accuracy of computed properties. We also found that the new diagnostic

Sandia is undergoing a revolutionary transition from being a lab based on experimental testing to a lab based on predictive computational modeling.

can reveal problems where the singles amplitude-based diagnostic fails, and vice versa.

Our work on message-passing interface (MPI) coupled cluster progressed greatly. We found that node pair synchronization issues in our first algorithm greatly limited the parallel efficiency of the code, so we undertook the development of a multithreaded communication scheme to remove latencies. We first implemented this in a second-order MP2 program, where it enabled us to do the largest MP2 calculation that had ever been performed. We then applied the technique to the coupled-cluster program. Now we can obtain reasonable scalability up to 64 nodes, the maximum number tested.

Refereed

Nielsen, I. B., and C. L. Janssen. 1999. "Double-Substitution-Based Diagnostics for Coupled-Cluster and Möller-Plesset Perturbation Theory." *Chem. Phys. Lett.* **310** (10 September): 568–576.

Nielsen, I. B., E. T. Seidl, and C. L. Janssen. 1999. "Accurate Structures and Binding Energies for Small Water Clusters: The Water Trimer." *J. Chem. Phys.* **110** (15 May): 9435–9442.

We found that node pair synchronization issues in our first algorithm greatly limited the parallel efficiency of the code, so we undertook the development of a multithreaded communication scheme to remove latencies. We first implemented this in a second-order MP2 program, where it enabled us to do the largest MP2 calculation that had ever been performed.

3504450000

Computational Methods for Coupling Microstructural and Micromechanical Materials Response Simulations

E. A. Holm, V. R. Vedula, C. C. Battaile, M. D. Rintoul, G. A. Knorovsky, T. E. Buchheit, D. A. LaVan, G. W. Wellman, M. K. Neilsen, S. J. Glass, H. E. Fang

Computational materials simulations have traditionally focused on individual phenomena: grain growth, crack propagation, plastic flow, etc. However, real materials behavior results from a complex interplay between phenomena. In this project, Sandia explored methods for coupling meso-scale simulations of microstructural evolution and micromechanical response. In one case, we dynamically coupled massively parallel (MP) simulations for grain evolution and microcracking in brittle materials. In the other, we iteratively linked MP codes for domain coarsening and plastic deformation. This project provided the first comparison of two promising ways to integrate mesoscale computer codes. To couple microstructure and mechanics codes, we developed time synchronization, mesh matching, and information-passing algorithms. In addition, since microstructural effects on materials response are length-scale dependent, a physically realistic coupled simulation will also require new mechanisms for incorporating an absolute length scale in micromechanics calculations. We investigated an approach to this problem. We experimentally validated the computer simulations on stockpile materials. We studied microcracking in brittle materials in the context of alumina used in stronglinks. We studied plastic deformation response in a silver-copper (Ag-Cu) eutectic braze alloy used in weapon components. This project provided the first full spatial and dynamic integration of computational models for coupled materials response phenomena. The mesh linkage and timestep synchronization techniques developed here will have applications in various simulation methods and will support Sandia's stockpile stewardship mission.

- *Coupling microstructural evolution with mechanical response*

- We demonstrated code coupling via information passing in two dimensions for JAS3D finite-element model (FEM) plasticity simulations with a continuum front tracking (CFT) microstructural evolution model. The CFT approach contains a dynamic mesh-based continuum treatment of boundary

This project provided the first full spatial and dynamic integration of computational models for coupled materials response phenomena. The mesh linkage and timestep synchronization techniques developed here will have applications in various simulation methods and will support Sandia's stockpile stewardship mission.

migration and is well suited to coupling with FEM, but its extension into three dimensions is cumbersome.

- We demonstrated code coupling via information passing in three dimensions for JAS3D FEM plasticity simulations with Monte Carlo Potts Model (MCPM) microstructural evolution model. The MCPM approach provides a convenient and efficient thermodynamic description of strain-induced coarsening in three dimensions, but the discrete nature of the MCPM lattice complicates the exchange of data between the codes. We used both plasticity and microstructure coupling strategies to ascertain the effects of plastic deformation on microstructure coarsening kinetics. In both cases, we found the rate of coarsening to increase with deformation.

- We developed an MP version of 3-D Material Point Method (MPM) code on IBM SP2 and Intel Tflops supercomputers and achieved scaling.

- We developed and implemented a preliminary phase-field-based physics model of coupled microstructural evolution and mechanical deformation and tested it in a 2-D version of the MPM code. We observed correct coarsening behavior.

- We performed a series of MPM calculations to exercise the code and models and to study the effects of microstructure on mechanics behaviors. We observed both geometry and scale dependencies.

- We completed 3-D PARGRAIN/GLAD dynamic coupling and partially examined the coupling between microstructural evolution and fracture.

- We developed a code (OIM2OOF) to allow crystallographic orientations from Orientation Imaging Microscopy (OIM) to be directly imported into Object-Oriented Finite Element (OOF).

- We performed the first simulations of microstructure-level stresses and cracking in polycrystalline ceramic materials using measured crystallographic orientations and grain boundary energies. We estimated residual stresses in large alumina microstructures using OOF. The maximum stresses were fairly high and localized at the grain boundaries and triple junctions. Cracks initiate at triple junctions and propagate along the grain boundaries. The increase in damage with increasing temperature difference occurred by both formation of new cracks and propagation of existing cracks.

- *Experimental validation*

- We directly compared tensile deformation experiments on Cu polycrystals with the micromechanics model for the first time. A scanning electron microscope/electron backscattering

We performed the first simulations of microstructure-level stresses and cracking in polycrystalline ceramic materials using measured crystallographic orientations and grain boundary energies.

pattern (SEM/EBSP) technique provides subgrain-scale data that can serve as input or validation for the model.

- The microstructural mechanics model successfully simulated fatigue, including capturing the essential back stress during deformation. The results showed that geometric constraints between grains, not the choice of work-hardening model, dominates a simulated polycrystal's response.

- We compared grain boundary energies and orientations of boundaries that fracture to the general population of grain boundaries in alumina. We found no apparent correlation between misorientation and cracking.

- We identified optical fluorescence imaging as a suitable technique to measure strains in alumina and compared them to the predicted values from an OOF code. We used atomic force microscopy (AFM) of grain boundary grooves to measure grain boundary energies.

- *Other accomplishments*

- We held a focused workshop to address the means for incorporating explicit physical length scales into FEM/MPM-based polycrystal simulations.

- We enhanced a continuum decohesion model for inter- and intragranular cracking simulations.

- We implemented MCPM on a random spatial tiling. We noted some important lattice effects that limit the MCPM utility on such lattices.

- We developed code for visualization of random spatial tilings to effectively convey results for the 3-D systems of interest.

Refereed

Battaile, C. C., E. A. Holm, T. E. Buchheit, G. W. Wellman, and M. K. Neilsen. 1999. "Coupled Simulations of Mechanical Deformation and Microstructural Evolution Using Polycrystal Plasticity and Monte Carlo Potts Models." *Proc. MRS Symp.* **538** (Boston, MA, December): 269–273.

Battaile, C. C., T. E. Buchheit, E. A. Holm, G. W. Wellman, and M. K. Neilsen. 1999. "Simulations of Microstructural Evolution in Deformed Polycrystals." (Invited) Presentation to the Argonne Theory Institute, Argonne, IL, August.

Buchheit, T. E., and G. W. Wellman. 1999. "Evolution of a Flow Surface As-Predicted by a Polycrystal Plasticity Deformation Model." Paper presented to the Materials Research Society Fall Meeting, Boston, MA, December.

Buchheit, T. E., D. A. LaVan, G. W. Wellman, and M. K. Neilsen. 1999. "Comparison Between Simulation and Experiment of a Polycrystal Plasticity Deformation Model." Paper presented to the TMS Fall Meeting, Cincinnati, OH, November.

Fang, H. E. 1999. "Multi-Level Modeling of Thermomechanical Fatigue in Solder Joints." (Invited) Paper presented to a seminar at the University of Missouri, Columbia, MO, March.

Fang, H. E., and E. A. Holm. 1999. "A Focused Workshop on Computational Approaches to Linking Microstructure and Mechanical Response." Paper presented to the Focused Workshop on Computational Approaches to Linking Microstructure and Mechanical Response, Albuquerque, NM, April.

Glass, S. J., V. R. Vedula, D. M. Saylor, and G. S. Rohrer. 1999. "Application of Electron Backscattered Diffraction (EBSD) and Atomic Force Microscopy (AFM) to Determine Texture, Microtexture, and Grain Boundary Energies in Ceramics." *Proc. 12th Internat. Conf. on Textures of Mater.* **2** (Montreal, Quebec, Canada): 1489–1494.

Holm, E. A. 1999. "Modeling Microstructure-Property Relationships." (Invited) Paper presented to the Michigan State University Physics Department Colloquium, Lansing, MI, May.

Holm, E. A. 1999. "Modeling of Microstructure-Property Relationships." (Invited) Paper presented to the Spring Meeting of the Ohio Section of the APS, Flint, MI, May.

Shen, Y. L., W. Li, and H. E. Fang. 1999. "Phase Structure and Cyclic Deformation in Eutectic Tin-Lead Alloy: A Numerical Analysis." *J. Electronic Packaging*, accepted.

Shen, Y. L., W. Li, D. L. Sulsky, and H. L. Schreyer. 1999. "Localization of Plastic Deformation Along Grain Boundaries in a Hardening Material." *Internat. J. Mechanical Sciences*, accepted.

Vedula, V. R., and S. J. Glass. 1999. "Residual Stresses and Cracking in Alumina." Paper presented to the Materials Research Society Fall Meeting, Boston, MA, December.

Vedula, V. R., and S. J. Glass. 1999. "Residual Stress Predictions in Alumina." (Invited) Paper presented to the CRC/NIST Workshop: Microstructure-Based

Computational Methods for Reliability Prediction in Ceramics, Gaithersburg, MD, 30 August–1 September.

Vedula, V. R., S. J. Glass, D. M. Saylor, G. S. Rohrer, and W. C. Carter. 1999. "Predicting Microstructural-Level Residual Stresses and Crack Paths in Ceramics." (Invited poster) Presentation to the Gordon Research Conference, Solid-State Studies in Ceramics, Holderness, NH, June.

Vedula, V. R., S. J. Glass, D. M. Saylor, G. S. Rohrer, and W. C. Carter. 1999. "Predicting Microstructural-Level Residual Stresses and Crack Paths in Ceramics." *Proc. 12th Internat. Conf. on Textures of Mater.* **2** (Montreal, Quebec, Canada, 9–13 August): 1507–1512.

Vedula, V. R., S. J. Glass, W. C. Carter, and S. A. Langer. 1999. "Predicting Microstructural-Level Residual Stresses in Ceramics Using Object-Oriented Finite Element Analysis (OOF)." Paper presented to the 101st American Ceramic Society Annual Meeting, Indianapolis, IN, April.

Other Communications

Fang, H. E., and E. A. Holm. 1998. "Multi-Level Modeling of Thermomechanical Fatigue in Solder Joints." Paper presented to the Tri-Laboratory Engineering Conference on Modeling and Simulation, Los Alamos, NM, November.

Shen, Y. L., W. Li, D. L. Sulsky, and H. L. Schreyer. 1999. "Localization of Plastic Deformation Along Grain Boundaries in a Hardening Material." Paper presented to the ASME Mechanics and Materials Conference, Blacksburg, VA, June.

Vedula, V. R., S. J. Glass, and E. A. Holm. 1998. "Modeling Microstructure-Level Elastic Stresses in Alumina Using NIST's OOF and Sandia's JAS-3D Codes." Paper presented to the NMACerS/ASM Annual Meeting, Albuquerque, NM, October.

3504460000

Integrated Quantum/Classical Modeling of Hydrogenic Materials

J. G. Curro, R. M. Fye, F. B. Van Swol

Sandia performed path integral (PI) Monte Carlo (MC) simulations and calculations on molecular hydrogen (H) liquids. We found the equation-of-state (EOS), internal energies, and vapor liquid-phase diagrams from simulation to be in quantitative agreement with experiments. We performed analytical calculations on H₂ liquids using integral equation methods to study the degree of localization of the H molecules. We found very little self-trapping or localization as a function of temperature and density. We found good qualitative agreement between the integral equation calculations and the quantum MC simulations for the radius of gyration of the H molecules. We also performed PI simulations on molecular H on graphite surfaces, slit pores, and in carbon (C) nanotubes and observed significant quantum effects on the adsorption of H.

(1) We performed quantum PI simulations on molecular hydrodynamics (MHD) at a graphite interface. We found good agreement between the simulation and experimental measurements of the adsorption isotherms at 13.28°K. We observed a first-order transition at a pressure of 0.13 Torr that coincides with the completion of the second layer of HD molecules on the graphite surface.

(2) We also performed quantum simulations on molecular H in porous graphite at low temperatures. We observed significant quantum effects in the adsorption isotherm at about 15°K. Quantum effects due to the lightness of the molecules shifts the adsorption isotherms to higher pressures, leading to the suppression of capillary condensation.

(3) We performed self-consistent Polymer Reference Interaction Site Model (PRISM) calculations on molecular H. In these calculations one takes advantage of the isomorphism between the quantum and the classical polymer ring problems. The radius of gyration of the ring, calculated by PRISM theory, is a measure of the delocalization of the molecular H due to quantum uncertainty effects. We found good agreement between the PRISM calculations and the results from quantum PI simulations.

We...performed PI simulations on molecular H on graphite surfaces, slit pores, and in carbon (C) nanotubes and observed significant quantum effects on the adsorption of H.

Refereed

Wang, Q., and J. K. Johnson. 1998. "Adsorption of Hydrogen in Graphite Slit Pores." *Internat. J. Thermophys.* **19**: 835.

Wang, Q., and J. K. Johnson. 1998. "Hydrogen Adsorption on Graphite in Carbon Slit Pores from Path Integral Simulations." *Molecular Phys.* **95**: 299.

3504470000

The Next Generation of Teraflop Density-Functional Electronic Structure Codes

M. P. Sears, R. A. Lippert, S. J. Plimpton, E. B. Stechel, K. Leung, N. A. Modine, A. F. Wright

The purpose of this project is to develop a next-generation electronic structure code. Such a code should utilize massively parallel (MP) computer technology and should embody the latest developments in linear scaling algorithms for DFT (density-functional theory).

Sandia developed a solid understanding of linear scaling algorithms for DFT as well as new linear scaling algorithms for calculation of linear response (LR) properties of materials. LR properties include important experimental measurables as phonon spectra, dielectric properties, and elastic moduli. We also worked on the development of quasi-particle methods to go beyond DFT to capture excited state-dependent properties (e.g., optical properties).

The results of this work are embodied in three computer codes. We implemented linear scaling for DFT using a real-space formalism in a high-performance FORTRAN (HPF) code (ACRES). This code is parallel and shows good scaling and efficiency on up to 32 processors for problems as large as 64 atoms.

We parallelized a second serial plane-wave code, written in FORTRAN 90 (F90) using message-passing interface (MPI) for parallel communications. We are currently restructuring this code to utilize object-oriented features of F90 and to develop the code as a basis for future work.

Last, we developed a nonparallel code to test the new LR algorithms. We used this code to compute phonon spectra for novel carbon (C) ring structures as well as phonon softening around certain defects in silicon (Si).

(1) We developed algorithms for linear-scaling LR (second-order response) and linear-scaling third-order response. These algorithms use a non-orthonormal localized basis. We used a computer code based on this work to compute phonon spectra for several complex materials.

(2) We developed a theory of linear-scaling algorithms for DFT. This theory shows that all linear-scaling algorithms have similar asymptotic behavior determined by the ratio of the bandgap to the range of energy eigenvalues.

The purpose of this project is to develop a next-generation electronic structure code. Such a code should utilize massively parallel (MP) computer technology and should embody the latest developments in linear scaling algorithms for DFT (density-functional theory).

(3) We developed a parallel computer program that utilizes a linear-scaling DFT algorithm. This algorithm uses non-orthonormal localized basis represented on a real-space grid together with a Grassman conjugate gradient acceleration method proposed by Lippert.

(4) We developed a quasi-particle code that corrects for bandgap errors in standard DFT codes. We are combining this code with the LR scheme derived above to compute bandgap corrections for semiconductor alloys.

(5) We modernized a dual-space electronic structure code. We parallelized this code using MPI and restructured it to use F90 allocation/deallocation and object-oriented features.

Refereed

Leung, K., and E. B. Stechel. 1999. "Occupied Subspace Invariant Linear Response Algorithm with Application to Dynamical Matrices." *Phys. Rev. B.*, submitted.

Lippert, R. A., and M. P. Sears. 1999. "Asymptotic Convergence for Iterative Optimization in Electronic Structure." *Phys. Rev. B*, submitted. SAND99-2986.

3504480000

Methodology for Characterizing Modeling and Discretization Uncertainties in Computational Simulation

K. F. Alvin, K. V. Diegert, W. L. Oberkampf, B. M. Rutherford

To meet the goals of the scientifically-based stockpile stewardship program, significantly improved confidence must be built into a wide variety of numerical simulations. The goal of these simulations is to accurately characterize the response of the complete system with high-fidelity, three-dimensional, unsteady, coupled physics together with uncertainty bounds on the response predictions. Quantifying the uncertainties in computational physics-based simulations is also critical to the verification and validation of these simulations; without uncertainty quantification, validation is highly subjective and arbitrary. Nondeterministic methods seek to quantify response uncertainties by propagating the uncertainties due to stochastic inputs and variability or uncertainty in the geometric, constitutive, and manufacturing parameters through the computational simulation. There remains a pressing need, however, to address the question of whether the proper physics have been modeled, both mathematically and numerically. The objective of the present research is to develop methods to quantitatively estimate the errors or uncertainties due to the mathematical form of the partial differential equations (PDEs) and the errors due to the discretization of the equations. Thus, this work complements, but is distinct from, nondeterministic methods for numerical simulations.

Sandia is developing a general methodology for characterizing the effects of modeling on computational simulation. This methodology is intended to apply in numerical simulations of continuum mechanics and heat transfer, assuming that the mathematical formulation of the physical model is given by a system of differential equations that are solved by discretization methods. The present research effort focuses on three strategies for characterizing computational simulation errors and uncertainties: identification of error sources and interactions, parameterization and survey of the model structure, and methods for evaluating model uncertainty and its contribution to global uncertainty. We will study two application areas, evolving from linear problems dominated by physical modeling considerations to nonlinear problems dominated by numerical discretization errors. The resultant methodology will be applicable to applications being

To meet the goals of the scientifically-based stockpile stewardship program, significantly improved confidence must be built into a wide variety of numerical simulations.

developed for the Accelerated Strategic Computing Initiative (ASCI), as well as for other computational mechanics disciplines.

We continued developing a methodology for combining discretization error estimation with propagation of continuous parameter variabilities (i.e., nondeterministic analysis). This technique involves estimating the parameters of a response surface that predicts the analysis output over a range of parameter values. We extended this response surface to include mesh spacing as a parameter. We performed code analyses with variations in both the uncertain continuous parameters of the model and the characteristic mesh length. We could then use the resulting response surface to propagate parameter uncertainties while also identifying the discretization error. An extension of previous work was to use a rational function representation of discretization error to improve the sphere of convergence of the error estimator. We collaborated with the University of Wisconsin to explore the use of Bayesian model averaging to combine multiple local response surfaces into a global metamodel. This also enables the combining of model forms with inconsistent parameter sets. We also identified a nonprobabilistic representation of model uncertainty in the form of a parameterized convex set that we can use to study the sensitivity of nondeterministic results to higher-order model uncertainty. Finally, we completed an extensive uncertainty analysis study in flight dynamics that combined input variabilities, discretization, and model structural uncertainty. We made additional progress on a structural dynamics example problem, but it is not yet in a completed form.

Refereed

Alvin, K. F. 1999. "A Method for Treating Discretization Error in Non-Deterministic Analysis." *AIAA Journal*, accepted.

Alvin, K. F. 1999. "Methodology for Treating Modeling Uncertainty and Discretization Error in Modeling and Simulation of Physical Systems." Paper presented to the IMA Workshop on Decision Making Under Uncertainty: Assessment of the Reliability of Mathematical Models, Minneapolis, MN, 16–17 September.

Kammer, D. C., K. F. Alvin, and D. S. Malkus. 1999. "Combining Metamodels and Rational Function Representations of Discretization Error for Assessment and Propagation of Model Errors, Uncertainty, and Variability." *Internat. J. Numer. Meth. in Engin.*, submitted.

Other Communications

Alvin, K. F. 1999. "A Method for Treating Discretization Error in Non-Deterministic Analysis." *Proc. 1999 AIAA Non-Deterministic Approaches Forum* (St. Louis, MO, April).

Oberkampf, W. L., S. M. DeLand, B. M. Rutherford, K. V. Diegert, and K. F. Alvin. 1999. "A New Methodology for the Estimation of Total Uncertainty in Computational Simulation." *Proc. 1999 AIAA Forum on Non-Deterministic Approaches* (St. Louis, MO, April).

Oberkampf, W. L., S. M. DeLand, B. M. Rutherford, K. V. Diegert, and K. F. Alvin. 1999. "Estimation of Total Uncertainty in Modeling and Simulation." Sandia Technical Report, in progress.

3504490000

Global Optimization for Engineering Science Problems

W. E. Hart, M. W. Trahan, K. O. Hunter, P. C. Gray, B. D. Schimel, J. S. Wagner

A wide variety of scientific and engineering problems can be posed as optimization problems for which the desired solution corresponds to an optimal set of parameters of an objective function, which measures a solution's quality. Sandia is developing a library of robust and efficient optimization algorithms that can be used to find globally optimal solutions to complex optimization problems. This library includes standard methods as well as new global optimization methods that we are developing to address weaknesses in standard techniques. Our algorithmic development focuses on several algorithmic factors: (1) the combination of global sampling and local optimization, (2) termination rules that provide practical confidence guarantees, (3) the design of constrained optimization methods, (4) methods for optimizing stochastic objective functions, and (5) the role of parallelism (for large-scale optimization problems). We are developing general-purpose optimization tools that can be applied to a wide variety of applications at Sandia. This research has an immediate impact on three application domains: neural network optimization for remote sensing, drug docking, and production planning for Pantex. This effort will develop new expertise in global optimization techniques as well as build on Sandia's current expertise in parallel algorithms.

Our work this year focused on (1) combinatorial global optimization methods, (2) extending the functionality of clustering global optimization methods, (3) further evaluating the statistical mechanical genetic algorithm (GA), and (4) developing GAs for constrained optimization problems.

Combinatorial global optimization methods can be qualitatively different from continuous methods because the optimizer does not need to worry about a step scale for search. However, these methods need to exploit problem-specific combinatorial structure. We focused on the development of two search methods: TABU search and GRASP. TABU search performs a local optimization process that records previous steps. We use this history to allow the searcher to move to a worse point, but only if it is not similar to a previously taken move. In this manner, TABU search can get out of local

Sandia is developing a library of robust and efficient optimization algorithms that can be used to find globally optimal solutions to complex optimization problems....This effort will develop new expertise in global optimization techniques as well as build on Sandia's current expertise in parallel algorithms.

minima to perform a global search. GRASP is a biased multistart local search algorithm that uses a greedy randomized process to construct the initial starting points. Given basic assumptions about the construction process, this method is asymptotically guaranteed to converge to the global optimum. We integrated both methods into SGOPT (stochastic global optimization), and we successfully applied the TABU search method to the Pantex production planning problem. Additionally, we extended the framework of SGOPT to enable the optimization of mixed-integer problems.

Our previous work with clustering global optimization methods used freely available implementations of these methods. Unfortunately, we found that these methods were limited in their ability to scale to large problems, and we found that it was difficult to specify different local optimizers for these methods. We reimplemented a cluster-based global optimization method to circumvent these difficulties. Additionally, we designed (but not tested) a cluster-based algorithm that uses local derivative statistics within clusters to bias the definition of clusters.

We further developed and evaluated statistical mechanical GAs. These GAs adapt the step scale for mutation using population statistics in a manner that is analogous to the statistical mechanics. We applied and evaluated these methods on a variety of standard global optimization test problems.

Our analysis of constrained global optimization methods focused on GAs. We surveyed methods used to solve various constrained optimization problems and focused on bound-constrained optimization. This is perhaps the simplest form of constrained optimization, but it has received surprisingly little attention. We analyzed several types of mutation operators to better understand how they affect the probability of finding improvements, and we began to empirically evaluate the utility of these operators. We extended the convergence analysis for evolutionary pattern search methods to include provable convergence for bound-constrained problems. Finally, we developed a method for solving problems with linear inequality constraints using these bound-constrained mutation operators, although we have not begun empirical tests of this methodology.

Finally, we investigated additional applications to which these methods can be applied. We began working with members of the Pantex Process Model (PPM) team on vehicle routing applications, which have been successfully solved by

...we developed a method for solving problems with linear inequality constraints using these bound-constrained mutation operators....

other researchers using GAs and TABU search methods. We also worked to formulate problems that can be used to find transition states in physical systems. Further, we are developing GAs that can be applied to sensor placement problems.

Most of these applications are in the early stages of development. One application that we successfully solved with global optimization techniques is the Pantex production planning problem. We developed a continuous formulation of this problem that we successfully solved with GAs. The GAs that we applied found solutions that were on average 5% better than the existing v-variable formulation used by the PPM. Further, refinements of these solutions with a local optimizer found improvements as great as 17%.

Refereed

Hart, W. E. 1999. "Comparing Evolutionary Programs and Evolutionary Pattern Search Algorithms: A Drug Docking Application." *Proc. Genetic and Evolutionary Computation Conf.* **1** (Orlando, FL, 13–17 July): 855–862.

Hart, W. E., and K. O. Hunter. 1999. "A Performance Analysis of Evolutionary Pattern Search with Generalized Mutation Steps." *Proc. Conf. Evolutionary Computation* (Washington, DC, 5–9 June).

Hart, W. E., C. R. Rosin, R. K. Belew, and G. M. Morris. 1999. "Improved Evolutionary Hybrids for Flexible Ligand Docking in AutoDock." *Proc. Internat. Conf. on Optimization in Comp. Chem. and Molecular Biology* (Princeton, NJ, 7–9 May).

Morris, G. M., D. S. Goodsell, R. S. Halliday, R. Huey, W. E. Hart, R. K. Belew, and A. J. Olson. 1998. "Automated Docking Using a Lamarckian Genetic Algorithm and an Empirical Binding Free Energy Function." *J. Comp. Chem.* **19**: 1639–1662.

Other Communications

Schimmel, B. D., and W. E. Hart. 1999. "An Analysis of Evolutionary Algorithms for Bound-Constrained Optimization." Sandia Technical Report, in preparation.

3504510000

Dynamic Simulation of Mechanical Systems with Intermittent Contacts

C. L. Lewis, R. A. LaFarge

We developed the ability to accurately predict motions of bodies of arbitrary shapes experiencing applied forces and intermittent contacts by combining Sandia-developed collision-detection software with a new contact force model. We found that while commercial software was very versatile in modeling an arbitrary scenario, their contact modeling capabilities were inadequate. We discovered that ADAMS best fit our needs for a simulation package in which to implement our contact model. For collision detection, we used the Configuration Space (C-Space) Toolkit (CS-Tk), a distance computation engine previously developed at Sandia. In collaboration with Ohio State University, we developed a contact force model based on a nonlinear damper. To provide users with a mature graphical user interface (GUI) for modeling jointed mechanisms, we incorporated our model and its interface to the CS-Tk into ADAMS.

We developed the ability to accurately predict motions of bodies of arbitrary shapes experiencing applied forces and intermittent contacts by combining Sandia-developed collision-detection software with a new contact force model. Our work provides a unique simulation capability in the areas of robotics, parts feeding, manipulation, the statistical robustness of mechanisms, and weapons simulation. Although commercial simulation software is quite adept at allowing users to easily model jointed mechanisms, its contact modeling capabilities are inadequate. They employ either weak or computationally expensive contact models. Some cannot handle contact between complex shapes. By implementing a contact model in commercial software, we are able to model arbitrary scenarios in our areas of interest. Our goal was to develop a contact model that is reasonably efficient yet captures a wide range of physical phenomena from simple impact to elastic wedging and viscous effects.

Toward this goal, we resolved two key technical issues: collision detection and contact analysis. For collision detection we integrated software developed at Sandia for efficiently determining the distances and the witness features between bodies of arbitrary shape. This software implemented, in

We developed the ability to accurately predict motions of bodies of arbitrary shapes experiencing applied forces and intermittent contacts by combining Sandia-developed collision-detection software with a new contact force model.

C-Space, a hierarchical geometric representation combined with an algorithm for fast distance computation, collision detection, and C-Space point-classification.

The second technical issue was the development of a computationally efficient contact model with friction for rapid simulation of impact, sustained contact under load, and transition between contact conditions. Our initial research revealed that there are two approaches for estimating contact forces. One is the hard contact approach in which the bodies are assumed to be rigid. Although appealing from an efficiency standpoint, modeling bodies as strictly rigid and persistent contacts as algebraic constraints sometimes fails to yield sufficient physical fidelity. We know that under the assumption of Coulomb friction, the rigid-body model can result in nonexistent or multiple governing equations. To avoid this fundamental limitation with the rigid-body formulation of contact dynamics, our approach relaxes the rigid-body assumption and models the contact with multiple nonlinear lumped elements (like having a thin elastic shell surrounding each body). Because forces of impact have high frequencies, the natural frequencies of the lumped elements used to model contact forces introduce stiffness into the governing differential equations; however, there are a number of advantages to the nonrigid formulation. First, it is straightforward to implement. Second, it can capture some phenomena like wedging or press fits, which greatly increases the types of automatic assembly processes that can be modeled. Because a unified approach applies to both impacts and persistent contacts, this method does not require reformulation of the governing equations with changes in contact states.

Using this model and the geometry engine, we wrote a test-bed code in C++. The test-bed allows for more than one body experiencing multiple contacts between faceted but not necessarily convex bodies. The test-bed required both a force model and a numerical methodology. We used it to verify the validity of the contact model and its interaction with the geometry engine.

Once the contact model was fully evaluated we added this same capability to the ADAMS software. With our contact analysis and the capabilities of ADAMS, we are now able to simulate articulated bodies experiencing intermittent contacts.

We wrote another software module in Visual Basic to facilitate design of experiments (DOE) analysis on mechanism designs. This module implements a Latin Hypercube Sampling (LHS) for the generation of random numbers that is

With our contact analysis and the capabilities of ADAMS, we are now able to simulate articulated bodies experiencing intermittent contacts.

significantly faster than that currently available. This stand-alone package uses the standard ADAMS file and creates multiple files with variations in the random parameters. We then execute ADAMS/Solver with our contact model on the individual files to generate statistical confidence intervals and to ascertain the effects of the variations.

Refereed

LaFarge, R. A., and C. L. Lewis. 1998. "Contact Force Modeling Between Non Convex Objects Using a Nonlinear Damping Model." *Proc. Internat. ADAMS Users Conf.* **1** (Ann Arbor, MI, June): 145–152.

LaFarge, R. A., and C. L. Lewis. 1998. "Contact Modeling for Robotics Applications." *Proc. IASTED Internat. Conf. on Controls and Applications* **1** (Honolulu, HI, 12–14 August): 254–260.

Tenaglia, C. A., D. E. Orin, R. A. LaFarge, and C. L. Lewis. 1999. "Toward Development of a Generalized Contact Algorithm for Polyhedral Objects." *Proc. IEEE Internat. Conf. on Robotics and Automation* **1** (Detroit, MI, 10–15 May): 511–517.

3504520000

From Atom-Picoseconds to Centimeter-Years in Simulation and Experiment

J. C. Hamilton, N. A. Modine, M. F. Horstemeyer, A. P. Thompson

Stockpile stewardship is Sandia's most important mission in the coming millennium. Understanding aging phenomena is critical to this mission. Accelerated aging and examinations of stockpile components play an important role but have their limitations. Accelerated tests at elevated temperatures skew the relative probabilities of various reactions. Examination of components provides a limited database and puts us in a reactive rather than proactive position; we may learn about a problem only when it is almost too late to do anything about it. Consequently it is a vital part of stockpile stewardship to develop simulation techniques that are accurate and valid over much greater time and length scales than those presently available. Most importantly the simulation techniques should be tested by experiment at various length and time scales so they can be validated and improved.

(1) Tested new accelerated molecular dynamics (MD) method. We tested a new method, temperature accelerated dynamics, to model diffusion of iridium (Ir) clusters on the iridium(111) surface. For certain problems, we can simulate a time scale of hours.

(2) Verified transition-state finding code. The massively parallel (MP) first-principles code for transition-state finding implemented last year was tested on experimental data for Ir island diffusion on Ir. We calculated diffusion mechanisms and activation energies in excellent agreement with experiment.

(3) Identified key problem in advanced transition-state finding. Efficient methods exist when the reactants and the products can be described exactly. It is much more difficult to find transition states if the reaction products are not known. The goal is to replace random searches with intelligent search techniques for transition-state finding.

(4) Used MP code to calculate diffusion constants for gases in zeolites. We refined the code for 3-D cavity transition-state analysis to give excellent agreement against MD simulations of gas penetration in zeolite ZK4. We then applied the same code to calculate cavities and transition rates in large polymer structures.

(5) Developed efficient technique for evaluating diffusion barriers in multiply-occupied zeolite pores. We used

*Stockpile stewardship is
Sandia's most important mission
in the coming millennium.
Understanding aging
phenomena is critical to this
mission.*

importance sampling to evaluate escape rates as a function of loading at high loads where multiple occupancy of pores is an issue.

(6) *Wrote code to calculate with 100 million atoms.* We wrote a new MP embedded atom method (EAM) code to handle simulations with up to 100 million atoms. This code also calculates local and average values of stress and strain.

(7) *Calculated yield under simple shear.* We used this code to model yield under simple shear of single-crystal nickel with dimensions as large as 1.6 microns.

(8) Determined kinematic variables such as strain, misorientation, deformation gradient, plastic spin, etc., and showed them within a post-processing scheme for MD simulations.

Refereed

Hamilton, J. C. 1998. "Applications of Transition-State Finding Techniques to Island Diffusion on Surfaces." (Invited) Paper presented to the MRS Meeting, Boston, MA, 30 November.

Hamilton, J. C., M. R. Sorenson, and A. F. Voter. 1999. "Compact Surface Cluster Diffusion by Concerted Rotation and Translation." *Phys. Rev. Lett.*, submitted.

Horstemeyer, M. F., and M. I. Baskes. 1998. "Atomistic Finite-Deformation Simulations: A Discussion on Length Scale Effects in Relation to Mechanical Stresses." *J. Eng. Mater. Tech. Trans. ASME* **111** (April): 114–119.

Horstemeyer, M. F., and M. I. Baskes. 1998. "Atomistic Simulations: A Parametric Study on Influences on Thermodynamic Stress State." Paper presented to the ASME Meeting, Chicago, IL, June.

Horstemeyer, M. F., and M. I. Baskes. 1999. "High Strain Rate Single-Crystal Atomistic Simulations." *Proc. Internat. Conf. Plasticity* **1** (Cancun, Mexico, January): 1005–1007.

Horstemeyer, M. F., and M. I. Baskes. 1998. "Yield Stress Effects and Size Scales." Paper presented to the MRS Meeting, Boston, MA, December.

Horstemeyer, M. F., J. Philliber, and M. I. Baskes. 1999. "Large-Strain Molecular Dynamics and Finite Element Simulations of Fixed-End Simple Shear." *Internat. J. Plasticity*, accepted.

Horstemeyer, M. F., M. I. Baskes, D. A. Hughes, and A. Godfrey. 1999. "Orientation Effects on the Stress State of Molecular Dynamics Large-Deformation Simulations." *Internat. J. Plasticity*, accepted.

Horstemeyer, M. F., S. J. Plimpton, and M. I. Baskes. 1999. "Size Scale and Strain Rate Effects on Yield and Plasticity of Metals." *Acta Materialia*, accepted.

Tunca, C., and D. M. Ford. 1999. "A Transition-State Theory Approach to Adsorbate Dynamics at Arbitrary Loadings." *J. Chemical Phys.* **111** (8 August): 2751–2760.

Other Communications

Horstemeyer, M. F., and M. I. Baskes. 1999. "Size/Time Scales in Large-Deformation Plasticity." Paper presented to the BES Meetings, Argonne, IL, March.

3504530000

Emergent Behavior of Large Swarms of Intelligent Agents

R. J. Pryor, B. L. Spletzer, J. E. Hurtado

Sandia's strategies for controlling large swarms of agents are all based on decentralized control methods. This is key because this philosophy allows each agent to determine its own control update, rather than having a centralized processing unit determine the update for each robot. We are developing methods to analyze, predict, and manipulate the emergent behavior of large swarms of cooperating agents. We used genetic algorithms (GAs) to construct tracking behaviors for large teams of agents. We also developed a distributed sensing and cooperative control (DSCC) approach for controlling a large team of agents.

We are developing methods to analyze, predict, and manipulate the emergent behavior of large swarms of cooperating agents.

We accomplished the following:

- Used particle physics concepts to generate models of large agent systems and to help understand their behavior.
- Continued developing our co-evolutionary concepts and the use of GAs to construct tracking behaviors for large teams of agents. The model runs on parallel computers due to the intensive tasks involved in generating best behaviors over a large number of simulations.
 - Modified the code to use the message-passing interface (MPI) protocol and to run on Sandia's Computational Plant (Cplant) cluster.
 - Improved the efficiency of the code.
 - Added time-varying signal sources to the code.
 - Used Mathematica to aid in visualization of signals and robotic behavior.
 - Established a Web site to present results to the community.
- Continued to investigate the potential of our DSCC ideas.
 - Solved time-dependent problems.
 - Obtained solutions involving fewer than six agents equipped with memory.
 - Obtained solutions to the problem of having a plume source behind a fence. This problem is especially interesting because a plume source can pass through a fence, but the agents can not.
 - Performed actual hardware demonstrations of our DSCC ideas.

- Extended our analysis methods to study the behavior of a swarm of agents that are locating a time-dependent source.
 - Compared the performance of our DSCC approach to a GA approach.

Refereed

Hurtado, J. E., R. D. Robinett, III, C. R. Dohrmann, and S. Y. Goldsmith. 1998. "Distributed Sensing and Cooperative Control for Swarms of Robotic Vehicles." *Proc. IASTED Internat. Conf. (IASTED International Conference Control and Applications, Honolulu, HI, 12–14 August)*: 175–178.

3504540000

Parallel Combinatorial Optimization for Scheduling Problems

C. A. Phillips, R. D. Carr, E. A. Kjeldgaard, W. E. Hart, D. A. Jones

Sandia will develop a state-of-the-art massively parallel (MP) combinatorial optimization engine that will be the first fully general mixed-integer programming (MIP) code scalable to thousands of processors. We will develop two general search strategies for MIP: branch-and-bound and branch-and-cut. We will study the feasibility of an MP version of a third strategy: branch-and-price. The engine will be able to adaptively incorporate application-specific methods (combinatorial approximation algorithms and genetic algorithms [GAs]), for both lower and upper bounds, to limit the search space explored by the MIP engine. We will use this exact method in a statistically rigorous performance analysis of sequential heuristics.

We will use the MIP engine to solve scheduling of stockpile activities throughout the DOE complex. MIP is a core optimization technology, and we can also apply this capability in other areas consistent with Sandia's mission: nonproliferation, transportation, infrastructure analysis and design, manufacturing, energy, environment, and tools for MP computation such as meshing and scheduling heterogeneous supercomputers.

Management of multiple, loosely coupled threads, each distributed and largely asynchronous, may require the development of new systems-level tools. Implementation of the search engine alone will require solution of novel global and semiglobal distributed resource-management problems.

We added considerable functionality to the basic Parallel Integer and Combinatorial Optimization (PICO) branch-and-bound engine, both to improve the efficiency of the optimization process and to improve our ability to monitor, evaluate, and verify the code.

We extended the parallel branching model within PICO to include a more scalable parallel formulation. Specifically, we developed parallel branching with multiple hubs (or worker/hubs) that coordinate the branching search across all processors. This required the development of several load-balancing strategies to evenly distribute both the quantity and the quality of unsolved subproblems in the search. We implemented code to allow the hubs to pull back work from

Sandia will develop a state-of-the-art massively parallel (MP) combinatorial optimization engine that will be the first fully general mixed-integer programming (MIP) code scalable to thousands of processors.... We will use the MIP engine to solve scheduling of stockpile activities throughout the DOE complex.

their workers. This allows more flexible task-pool management and load balancing.

The total amount of work needed to solve an integer program can be significantly reduced in practice by suitable preprocessing. We implemented basic variable-fixing techniques, and we are incorporating more advanced preprocessing techniques to fix variables and eliminate redundant constraints.

We implemented a process for initializing variable gradients used to intelligently generate subproblems. This significantly reduced search-tree sizes on many problems in the standard dataset mixed-integer programming library (MIPLIB).

We ported PICO to the ASCI (Accelerated Strategic Computing Initiative)-Red machine (Janus), and we collaborated with ILOG, Inc., to get a license for the CPLEX linear programming library on Janus. CPLEX is the premier commercial linear programming (LP) product. We began scalability studies of parallel branch-and-bound.

We developed mixed-integer nonlinear programming classes for PICO that perform branch-and-prune, with heuristic lower bounding (therefore no optimality guarantee). We linked PICO with SGOPT (Stochastic Global Optimization) DAKOTA (engineering design code), so PICO can use the local optimizers from these packages. We added communicator groups (under MPI). This allows PICO to run on a subset of processors in a DAKOTA run and to use parallel (upper and lower) bounding codes in the future (e.g., parallel LP solvers).

To facilitate debugging and increase confidence in PICO's solutions, we added a number of tools. We added scripts for a quality-assessment suite that runs a core test set and uses our new log analyzer to verify correctness of the solution and search. We now monitor timing and performance-critical parameters (such as load balancing). We also added hooks to visualize thread activations on each node.

We reimplemented our LP class to use CPLEX Version 6.0. Significant for branch-and-cut, which adds constraints, this version has fundamentally better memory management, including easy problem growth.

The Pantex resource-constrained scheduling problem is used to plan resource requirements for evaluation and maintenance of the stockpile. Benchmarking the PPM (in progress) will increase confidence in the quality of the solutions provided and will allow more informed decisions.

To apply PICO to this problem, we can now generate the standard MIP representation from PPM data files. We refined

Benchmarking the PPM will increase confidence in the quality of the solutions provided and will allow more informed decisions.

the MIP formulation to more closely model the PPM problem on short jobs. We designed customized C++ classes derived from the PICO MIP classes to allow new branching strategies and problem-specific lower- and upper-bounding operations. We are now collaborating with Polytechnic University to develop these problem-specific bounding methods. We started theoretical work that could lead to a new group of heuristic techniques. Also, we identified two lower-bound techniques that are potentially faster than LP: one based on network flows and the other on Lagrangian relaxation. We also designed a problem generator.

We developed a resource-constrained, capacity-planning model for neutron generators, though to date we have not required integer variables. We acquired complete datasets including product flow information and resource availability.

We developed new branch-and-cut techniques for scheduling and traveling salesman problems.

Refereed

Phillips, C. A., R. N. Uma, and J. Wein. 1999. "Off-Line Admission Control for General Scheduling Problems." *Proc. 11th Annual ACM-SIAM Symp. on Discrete Algorithms*, accepted.

3504550000

Programming Paradigms for Massively Parallel Computers

R. B. Brightwell, M. P. Sears, R. E. Riesen, S. J. Plimpton, T. B. Hudson

The goal of this project is to enable applications to take full advantage of the hardware available on Sandia's current and future supercomputers. Currently, nearly all Sandia codes on existing massively parallel processing (MPP) systems use only a single thread of execution. On the commodity-based machines, this approach will not allow us to achieve maximal performance. More generally, the future of high-end computing appears to be clusters of shared-memory processors (SMPs); i.e., a mixture of distributed and shared-memory hierarchies is exposed to the user. Learning how to program such machines effectively to achieve maximum impact, both inside and outside Sandia, with simulations is a must. We will discover the best model for each of the different types of applications through implementation and exploration of several programming models from both the system and the application perspectives.

- *Development of a thread-aware MPI implementation.*

This task required more effort than we anticipated. Few implementations of message-passing interface (MPI) exist that have been specifically designed to work in a threaded environment. Our initial intention was to simply modify the public domain version of MPICH to be thread-safe. However, it became clear that this approach would significantly hinder the overall goals of this project. To fully understand the implications and impacts of combining message passing, shared memory, and threads, an MPI implementation that is fully integrated into a thread environment is required. It is not enough to have an MPI implementation that does coarse-grain locking, or only allows a single thread to perform message passing. Ideally, the MPI library needs to be aware of the threaded environment so that it can take advantage of it. For example, the asynchronous message-passing operations in MPI should not waste central processing unit (CPU) cycles polling for completion, but rather should allow for descheduling of the calling thread based on completion of the message-passing event. This tight integration between threads and MPI is lacking in not only MPICH, but also in most vendor-supplied MPI implementations.

...the future of high-end computing appears to be clusters of shared-memory processors (SMPs)...Learning how to program such machines effectively to achieve maximum impact, both inside and outside Sandia, with simulations is a must.

In order to facilitate such an MPI implementation, the underlying message-passing layer upon which MPI is built needs to be integrated with threads. We designed a message-passing application programming interface (API), Portals 3.0, to provide this layer. Because Portals are designed to work in a threaded environment, they are ideal not only for supporting MPI, but also for supporting the types of one-sided data movement that may be needed to support a shared-memory style of message passing. In addition to completing the API, we completed a reference implementation on top of transmission control protocol/Internet protocol (TCP/IP). This implementation is currently thread-safe and will be fully integrated into a multithreaded environment in Linux. Portals soon will be fully functional on Computational Plant (Cplant) on Myrinet networking hardware.

We completed the design of an MPI implementation for Portals. This design allows for the MPI library to take advantage of the integration of message passing with threads that Portals provides. Because MPICH has yet to be designed to support threads, we collaborated with MPI Software Technology, Inc. (MSTI) to provide a thread-aware MPI for Portals. MSTI has a thread-aware MPI implementation for several virtual interface architecture (VIA)-based networks using Windows NT.

- *API extensions to MPI for SMP clusters.* We began to consider the design of this approach. We hope to complete an initial study of the constructs that MPI currently provides that can be leveraged to work in a clustered SMP environment.

SMP Linux made great strides. Any attempt at evaluating thread schedulers in Linux before the current release of Version 2.2 would not have been representative of the capabilities of the operating system. We have been waiting for a stable SMP version of Linux to fully test and plan to upgrade the Cplant environment to take advantage of the latest Linux kernels.

We also modified the run-time environment tools for Cplant to allow for investigation of the various programming models outlined in the original proposal. For example, we modified the application launcher (yod) and the compute node process manager (PCT) so that implementing a virtual node mode (VNM) capability on Cplant will be easier.

Other Communications

Brightwell, R. B., T. B. Hudson, R. E. Riesen, and A. B. Maccabe. 1999. "The Portals 3.0 Message Passing Interface." Sandia Technical Report, in review.

3504560000

Multilevel Techniques for Unstructured Grid Problems on Massively Parallel Computers

R. S. Tuminaro, A. B. Williams, P. R. Schunk, A. C. Robinson, C. D. Moen, J. N. Shadid

Robust and efficient linear system solution techniques are critical to Sandia's leading-edge scientific simulation capabilities. Current parallel iterative techniques suffer deteriorating performance and even failure as mesh sizes increase and geometric complexity grows (a significant problem for ALEGRA, GOMA, FUEGO, and MPSalsa). These difficulties are even more pronounced on larger, massively parallel (MP) systems such as Sandia's Computational Plant (Cplant). Without significant advances, convergence limitations will hinder next-generation simulations. This project will make a fundamental change in linear system solution strategy at Sandia by providing tools that facilitate the use of multilevel (ML) techniques. ML methods offer the best promise for overcoming convergence difficulties with iterative solvers. Unfortunately, ML methods are rarely used at Sandia due in part to MP implementation difficulties for unstructured grids. In this project, we will focus on two distinct tasks to address these difficulties and facilitate the use of ML preconditioners. The first corresponds to the development and analysis of automatic coarsening techniques (e.g., agglomeration) to construct mesh hierarchies. The second task is to define multigrid operators and ML preconditioners that utilize a given sequence of grids. In this second case we will specifically consider mesh hierarchies coming from adaptive meshes (important for MPSalsa and ALEGRA), as well as those arising from automatic coarse grid-generation techniques (important for MPSalsa, FUEGO, and GOMA). We will develop these techniques and integrate them in Sandia's award-winning parallel iterative solver library AZTEC and incorporate them into Sandia applications MPSalsa, ALEGRA, FUEGO, and GOMA.

We implemented a 3-D parallel algebraic multigrid scheme. We based the new scheme on Vanek's smoothed aggregation method; it requires only that the user supply the matrix being solved. A major obstacle in implementing this method is that the aggregation algorithm underlying the multigrid method given by Vanek is inherently serial and was thus not suitable for parallel computers. We designed and implemented a variety

This project will make a fundamental change in linear system solution strategy at Sandia by providing tools that facilitate the use of multilevel (ML) techniques.

of parallel aggregation schemes. For the most part, the new schemes yield aggregates that are almost as good (from the point of view of multigrid convergence) as the serial scheme. At this point, we are still evaluating which options among these aggregation methods are the best for overall use. We implemented a multigrid scheme based on interpolation operators supplied by an application. In particular, applications that are capable of adaptive grid refinement can often produce interpolation operators for a hierarchy of grids. We can now import this information into ML to create a multigrid iterative solver. We integrated ML with the ALEGRA application code. Currently, ALEGRA can use either the Vanek scheme or the refinement-based multigrid method. We obtained some very encouraging numbers on a limited set of test problems. In one case the number of iterations required for convergence was reduced by a factor of 20 on a 2.5 million degree-of-freedom (DOF) problem. We tightened the integration of ML and AZTEC. In particular, any AZTEC method or preconditioner can now be used as a smoother within a multigrid method. Additionally, we can use a multigrid method as a preconditioner within AZTEC. We performed an initial installation of ML into a prototype code used by the FUEGO team. Currently, we can carry out a pressure Poisson-type calculation using a multigrid solver.

Refereed

Tong, C., and R. S. Tuminaro. 1999. "Parallel Multilevel Methods for Scientific Applications." Paper presented to the SIAM Parallel Meeting, San Antonio, TX, 20 March.

Tong, C., and R. S. Tuminaro. 1998. "Some Results Using MLpack, a Parallel Multilevel Solver Package." Paper presented to the ASCI Tri-Lab Linear Solver Meeting, Albuquerque, NM, 6 October.

Other Communications

Tong, C., and R. S. Tuminaro. 1999. "A Multilevel Framework for Solving Parallel Finite Element Applications." Paper presented to the Copper Mountain Multigrid Conference, Copper Mountain, CO, 1 April.

3504570000

Scalable Tools for Massively Parallel Distributed Computing

R. C. Armstrong

Platforms for parallel computing that harness thousands of independent commodity machines, such as Sandia's Computational Plant (Cplant), will require robust, efficient, scalable, secure, and easy-to-use tools for system and user management. Sandia will identify and develop tools, via the Lilith framework, for the rapid development of distributed tools, which enhance the ability to use and maintain large platforms (e.g., controlling user processes, monitoring system status). We will design and develop a prototype for flexible security into the Lilith framework; such security is important when multiple users share a machine. We will define an easy-to-use application programming interface (API) for easy development of tools.

Work this year centers on developing new tools and providing tool security.

(1) We identified and developed two tools for large distributed clusters. The tools provide visual information on the system status, processes, and network traffic. They can be used for maintaining and monitoring the cluster and for debugging applications with network traffic. We installed these tools and used them on Cplant.

(2) We designed and developed the prototype security infrastructure for the Lilith framework. This infrastructure provides flexible security for hosts running the Lilith-based tools on a per-user, per-method invocation basis.

(3) We developed a well-defined user API for easier tool building. In designing the API support, we designed the user interactive classes to enable easy definition of security constraints on a per-user basis.

(4) We updated the Lilith-based tools developed previously to work with the new security infrastructure.

(5) We designed and developed enhancements to the Lilith framework, providing greater robustness and multi-user support.

Sandia will identify and develop tools, via the Lilith framework, for the rapid development of distributed tools, which enhance the ability to use and maintain large platforms (e.g., controlling user processes, monitoring system status).

Refereed

Evensky, D. A., A. C. Gentile, P. Wyckoff, and R. C. Armstrong. 1999. "The Lilith Framework for the Rapid Development of Secure, Scalable Tools for Distributed Computing." *Distributed Applications and Interoperable Systems* **1** (2nd IFIP WG 6.1 International Working Conference on Distributed Applications and Interoperable Systems, Helsinki, Finland, June): 163–168.

Evensky, D. A., A. C. Gentile, and P. Wyckoff. 1999. "Lilith Lights: A Network Traffic Visualization Tool for High-Performance Clusters." *Lecture Notes in Computer Science* **1593** (7th International Conference on High-Performance Computing and Networking [HPCN Europe '99], Amsterdam, The Netherlands, April): 1183–1186.

3504580000

Massively Parallel Methods for Simulating the Phase-Field Model

R. M. Fye, S. J. Plimpton, D. Fan, V. Tikare, M. D. Rintoul

Prediction of the evolution of microstructures in weapons systems is critical for meeting the objectives of stockpile stewardship. For example, accurate simulation of microstructural evolution in solder joints, cermets, lead zirconate titanate (PZT) power generators, etc., is necessary for predicting the performance, aging, and reliability both of individual components and of entire weapons systems. A recently developed but promising approach called the phase-field model (PFM) has the potential of allowing the accurate quantitative prediction of microstructural evolution, with all the spatial and thermodynamic complexity of a real microstructure. Simulating the PFM requires solving a set of coupled nonlinear differential equations, one for each material variable (e.g., grain orientation, phase, composition, stresses, anisotropy, etc.). While the PFM is versatile and can incorporate the necessary complexity for modeling real material systems, it is very computationally intensive, and it has been a difficult and major challenge to formulate an efficient algorithmic implementation of the approach.

The drawbacks of PFM simulations are that they (1) are very computationally intensive and become increasingly so with more complex materials behaviors, and (2) require the difficult task of formulating a set of differential equations that describes the materials phenomena and is numerically stable and efficient. We explored several discretization methods for improving efficiency and stability. Second order in space algorithm was most stable and most accurate. However, the computational demand still remains high. To reduce the calculations, we explored two algorithms to improve numerical efficiency. The first was only to consider updating the microstructural evolution calculation for active sites along the grain boundary where structural changes occur. We must identify and update the sites and will ignore all other sites at that timestep. The second algorithm to reduce computation was to reduce the number of fields considered by replacing the multiple fields that describe Q possible grain orientation (where Q is typically 50 to 100) with two fields. Thus we will reduce the number of differential equations that must be solved for each site at each timestep from 100 to 2.

Prediction of the evolution of microstructures in weapons systems is critical for meeting the objectives of stockpile stewardship...A recently developed but promising approach called the phase-field model (PFM) has the potential of allowing the accurate quantitative prediction of microstructural evolution, with all the spatial and thermodynamic complexity of a real microstructure.

We created a 3-D parallel version of the basic PFM. Computationally, the PF equations require local stencil operations on a regular 3-D grid to update the field variables in a coupled fashion for a single timestep. Using a spatial decomposition of the grid across processors, only subdomain boundary information need be communicated between processors for each field variable. Although the computation per grid point per field variable is relatively modest (in the basic PFM), we found this strategy to scale reasonably well to large numbers of processors.

We performed the following benchmark calculations with the new parallel PF code on the Intel Paragon. For a small problem (50x50x50 grid with 10 PF variables), the fixed-size parallel efficiencies are roughly 65% and 50% on 64 and 256 processors. A more typical production-scale problem (100x100x100 grid with 36 PF variables) has a fixed-size parallel efficiency of 92% and 75% on 64 and 256 processors. Scaled-size speedups would undoubtedly be even better. These preliminary numbers indicate that we will be able to run very large problems effectively with the new parallel code.

We also studied several materials simulation issues. The first was solute drag. Several important components that Sandia manufactures and maintains, such as the PZT voltage bars, solder joints, and cermet source feedthroughs, have compositional gradients at the grain boundaries. The grain boundary compositional changes can change the microstructural evolution of the components both during processing and during service by a process commonly known as *solute drag*. We successfully simulated this phenomenon in a variable composition system. No other mesoscale microstructural model has the ability to treat solute drag at the grain boundaries.

Many materials have high-curvature, fractal structures such as dendrites in braze joints or eutectic colonies in solder joints. Microstructural evolution in these structures is very different from that in equi-axed structures in both their kinetics and their morphology. We used the PFM to study the evolution of such high-curvature structures. We found two distinct kinetic regions in such a system. At high curvature, the time law of grain boundary length depends on the initial fractal dimension D_s of the grain boundaries with exponent $(1-D_s)/2$. At low curvature the behavior approaches the normal grain-growth behavior seen in the more equi-axed microstructures with a grain growth exponent $n = 1/2$. We compared this behavior to the results of a Potts Model simulation and found very good agreement between the two systems.

No other mesoscale microstructural model has the ability to treat solute drag at the grain boundaries.

We also developed the capability to treat microstructural evolution with internal strains in 2-D. We explored microstructural evolution of precipitates with lattice mismatch with matrix. Results showed that elastic anisotropies play a very important role in microstructural evolution.

Refereed

Chen, L. Q., D. Fan, and V. Tikare. 1998. "A Phase-Field Model for Grain Growth." *Grain Growth in Polycrystalline Materials* 3 (Pittsburgh, PA, August): 137–143.

Fan, D. 1999. "Microstructure Modeling: Connections Between Modeling, Theories and Experiments." Presentation to the Seminar Series of Materials Science and Engineering, Colorado School of Mines, Boulder, CO, October.

Tikare, V., E. A. Holm, D. Fan, and L. Q. Chen. 1999. "Comparison of Phase-Field and Potts Models for Coarsening Processes." *Acta Materialia* 47 (January): 363–371.

Other Communications

Fan, D., V. Tikare, E. A. Holm, and C. C. Battaile. 1999. "Modeling of Microstructural Evolution and Linkage Between Models and Length Scales." (Invited) Paper presented to ACERS 101st Annual Meeting and Exposition, Indianapolis, IN, April.

3504590000

Visual Explanation and Insight

B. N. Wylie, D. K. Johnson, K. W. Boyack, B. A. Hendrickson, M. H. Koller

For information visualization tools such as VxInsight™ to lead us from the information age into the knowledge age, Sandia must continue research in several areas.

- *Advancements need to be made in the current paradigms used for data gathering and management to allow viewing of heterogeneous data from different sources.*

- *Scalable algorithms for both visualization and data retrieval need to be developed for analysts to visualize the ever-increasing information base.*

- *Feature “enhancement” techniques should be investigated to accelerate and increase the knowledge gained during the exploration of data.*

- *Continued validation/development of ordination techniques used by VxInsight™.* Quantitative measures of cluster quality can be difficult to define. Currently we are using the two fundamental measures: normalized Euclidean distance for both similar and dissimilar objects. By using these two quantitative measures, we can measure the performance of adjustment parameters in the ordination algorithm.

Using normalized distance captures the quality of graph clustering in a mathematical form but does not represent how humans cluster objects visually. One technique under investigation that does measure the human factor is our “template matching” work. A combination of this and Euclidean distance techniques may prove to be the best measure of ordination quality.

- *Explored real problem domains*
- *Intelligence applications*

Collaborative work at Sandia has led to the use of VxInsight™ for intelligence uses, such as financial transaction analysis and weapon parts appropriations by various countries.

- *Medical applications*

We are using VxInsight™ to determine causal factors for diseases affecting both local and national populations.

- *Incorporated standardized database interface solution.*

As part of the project’s effort to tap into disparate data sources, the VxInsight™ data monitors now use the ODBC (Open Data Base Connectivity) protocol to communicate to a wide variety of data applications. The use of this powerful standard allows

One technique under investigation that does measure the human factor is our “template matching” work. A combination of this and Euclidean distance techniques may prove to be the best measure of ordination quality.

us to exchange data with Oracle, SQL (Structured Query Language) Server, Sybase, and even applications like Excel. In addition to using ODBC, we are also using the Java variant (JDBC [Java Data Base Connectivity]), which also has a broad range of support. The use of these two protocols gives VxInsight™ the ability to gather and query data from just about any data application.

- *Continued research in regular grid techniques for multiresolution viewing.* To enable the visualization of extremely large datasets, we developed new viewing techniques. We wanted the users to be able to interactively explore a multiresolution environment without the computational and storage costs of having the entire dataset in memory. Our solution involved the construction of a quad-tree data structure using the density of the objects as a virtual height field. By abstracting the density into a height field, we can now apply familiar terrain visualization techniques. The quad-tree data structure allows us to traverse only the sections of the tree currently being visualized and, in combination with lazy-evaluation, will allow the data to remain in the data source until requested.

The use of these two protocols gives VxInsight™ the ability to gather and query data from just about any data application.

Refereed

Beck, D. F., K. W. Boyack, O. H. Bray, and W. D. Siemens. 1999. "Landscapes, Games and Maps for Technology Planning." *Chemtech* **29**(6) (June): 8–16.

Davidson, G. S. 1999. "Visualizing Genome Expression Data with VxInsight™." Paper presented to the Nature-Genetics Annual Microarray Meeting, Scottsdale, AZ, 22–25 September.

Davidson, G. S., B. A. Hendrickson, D. K. Johnson, C. E. Meyers, and B. N. Wylie. 1999. "Knowledge Mining with VxInsight™: Discovery Through Interaction." *J. Intel. Info. Sys.* **11**(3) (November–December): 259–285.

Other Communications

Wylie, B. N. 1999. "VxInsight™: Visual Data Mining and Knowledge Discovery." Paper presented to the Siam Annual Conference, Atlanta, GA, 14 May.

3504610000

Computational Simulations of Self-Assembling Macrosystems by Direct Fabrication of Microscopic Structures

S. C. Istrail, A. J. Hurd, J. Cesarano, V. Tikare

Sandia is modeling and testing the processes that direct self-assembly of macroscopic components in an effort to understand and establish control over spontaneous structure formation of small Janus bricks. (The simplest Janus particle has one side hydrophobic, the other hydrophilic.) Janus bricks can be programmed with varying affinities for each other on their faces and edges so that red surfaces (e.g., hydrophobic) stick to red but not to blue (e.g., hydrophilic). With unlimited colors, any macroshape could be self-assembled if the bricks had sufficient mobility and time to find their proper neighbors by low-temperature, direct fabrication in a parallel self-assembling mode. Disparate materials could be accommodated in neighboring bricks, and near net-shape structures could be formed out of fully dense bricks with minimal shrinking from sintering. It is an open question what shapes are possible with just two colors and only one or two brick shapes. Moreover, since it is not clear what process is required to sinter a Janus assembly, we are developing a phase-field sintering model to predict the end-state structures. Small, experimental systems are being used to discover the phenomenology of simple Janus tiles, which have the attractive possibility of self-assembling very simple virus-like capsules from only six triangular tiles.

We developed the mathematical analysis of the Janus nanobricks that gives a complete classification and accurate prediction of the lowest-energy self-assemblies for arbitrary energy interaction matrices having nonpositive interaction values. These are the first such algorithms in the literature.

We developed algorithms for the prediction of optimal self-assembly of hydrophobic-polar bipoles on the Faced-Centered Cubic lattice. Our results provide support to our biplane conjecture as well as a proof of close to optimality for the biplane, showing that it has better than 99 % of the optimal energy when the number of bipoles is greater than 25. These are the first such methods for rigorous prediction of bipole self-assembly in the literature.

This research also impacted our work on prediction of protein folding on lattice models. Our best algorithms to date

We developed the mathematical analysis of the Janus nanobricks that gives a complete classification and accurate prediction of the lowest-energy self-assemblies for arbitrary energy interaction matrices having nonpositive interaction values....the first such algorithms in the literature.

are based on self-assembly of the hydrophobic side-chains, disconnected from the backbone, and then threading back the backbone and the hydrophilic side-chains. To our knowledge, the above algorithm is the best algorithm in the literature that accurately folds lattice model proteins in close to linear time.

Other Communications

Istrail, S. C., S. Batzoglou, J. Conway, R. Lippert, and A. J. Hurd. 1999. "Prediction of Protein Folding Through Self-Assembly." Paper presented to the Princeton University Conference on Optimization in Molecular Biology, Princeton, NJ, 25 May.

3504620000

Gamma-Ray Bursts and the Particle Mass Scale

P. C. Gray

A mode of detonation for neutron stars is derived based on a physically defined power residue counting system used to construct a particle mass scale that reflects supersymmetric fermion/boson pairing. The joint action of the supersymmetric classification and a new arithmetic selection rule designated as congruence conservation governs the condition of stability, and the dynamic participation of the magnetic monopole obviates baryon number conservation; these interpretations and techniques support the conclusion that the observations of gamma-ray bursts signal the existence of a radically new organizing principle of physical interactions that define a general condition of stability for massive particles and expresses the unstable case with the copious production of energetic emissions.

We made the first calculations on a high-speed computer. These calculations support the theory that the scale invariant system of enumeration represents the particle mass spectrum in a way that explicitly respects supersymmetric fermion/boson pairing. The manifest scale invariance of the counting procedure confers on it the capacity to represent a particle with an arbitrarily large mass, thereby enabling a description of neutron stars or even more massive objects. A specific result of the analysis of mass scale was the prospective identification of a fundamental supersymmetric pair composed of a light fermion, presumably representing the electron neutrino and its supersymmetric partner.

These calculations support the theory that the scale invariant system of enumeration represents the particle mass spectrum in a way that explicitly respects supersymmetric fermion/boson pairing.

ELECTRONICS & PHOTONICS

Electronics and Photonics is one of Sandia National Laboratories' four LDRD Research Foundations investment areas. Research Foundations extend the core scientific and technical knowledge base of the Laboratories. In addition, Research Foundations focus on innovative, high-risk research that supports the long-term needs of the DOE's and Sandia's national security mission.



The Electronics and Photonics investment area conducts research to ensure the availability of reliable components in support of the DOE Stockpile Stewardship Program (SSP). Advances in Electronics and Photonics are expected to enhance computing, satellites, telecommunications, and many other technology platforms. Electronics and Photonics LDRD investments strengthen Sandia's leadership in the research and development of advanced, integrated microsystems.

LDRD research emphasizes advanced microdevice concepts and integration solutions. Microdevice concepts include research leading to advances in microelectronics, photonics, microelectromechanical systems (MEMS), and sensors. Integration solutions seek innovative approaches to achieve greater levels of integration for high-yield, highly reliable microsystems, including integrated

packages capable of communication, self-authentication, and encryption.

The "Silicon Three-Dimensional Photonic Crystal and Its Applications" project has researched novel silicon technology to create lattice structures that are able to control radiation at microwave, infrared, and optical frequencies. This advance in technology will dramatically impact optical communications and computing as an inexpensive, yet efficient means for containing and bending light. This project's findings were recognized as a 1999 R&D 100 Award winner and were also awarded a 1999 Lockheed Martin Corporation NOVA Award for research, the Corporation's highest honor.



3506450000

A Novel Nondestructive Silicon-on-Insulator Nonvolatile Memory

J. R. Schwank, P. M. Smith, W. L. Warren, B. L. Draper, J. R. Murray, D. M. Fleetwood, M. R. Shaneyfelt

This project takes advantage of as-processed defects in silicon-on-insulator (SOI) buried oxides and moderate-temperature hydrogen (H) anneals to generate mobile protons in the buried oxide to form the basis of a nonvolatile memory. Sandia previously demonstrated the proof-of-concept of such a device using capacitors. We will focus on developing a nonvolatile field-effect transistor (NVFET) using the back-gate transistor of an SOI device.

NVFETs were fabricated in Sandia's Microelectronics Development Laboratory using a specially designed seven-layer mask set and Sandia's CMOS6rs (complementary metalorganic semiconductor) (SOI) radiation-hardened technology. The gate length of the transistors was 0.6 micron, and the gate width varied from 0.75 to 20 microns. Transistors had gate widths from 0.75 to 20 microns. We generated mobile protons in the SOI buried oxide by subjecting transistors to a 600°C, 30-minute anneal in forming gas (5% H). Each SOI transistor inherently includes two transistors—a top-gate transistor with a thin thermal-oxide and a buried-oxide transistor. We use the build-up of mobile protons in the buried oxide to control the leakage current characteristics of the top-gate transistor.

I-V measurements taken before and after the forming gas anneal showed that the forming gas anneal generated a large increase in leakage current and large amounts of fixed charge in both the buried-oxide transistors and the top-gate transistors. We characterized transistors for their memory properties by measuring the hysteresis voltage shift in the buried-oxide transistor obtained after poling the protons near either the top or the bottom buried-oxide/silicon (Si) interface. We observed hysteresis voltage shifts large enough to fabricate a nonvolatile memory. However, the magnitude of the hysteresis voltage shift varied nonuniformly across a test die. The largest hysteresis voltage shift (13.5 V) observed was for a transistor with a gate length of 20 microns.

This year's work focused on fabricating nonvolatile memory transistors. The previous year's work focused on fabricating capacitors to demonstrate the feasibility of a

NVFETs were fabricated in Sandia's Microelectronics Development Laboratory using a specially designed seven-layer mask set and Sandia's CMOS6rs (complementary metalorganic semiconductor) (SOI) radiation-hardened technology.

nonvolatile memory transistor. We designed a seven-layer mask set for fabricating fully processed nonvolatile memory transistors. We then designed and fabricated two types of transistors. One type of transistor (standard) included a top-gate transistor fabricated with a thermally grown oxide on an SOI substrate. The second type of transistor had the polysilicon gate of the top-gate transistor replaced with a silicon nitride (SiN) layer. We used this transistor to investigate whether proton transport in the SOI buried oxide could be controlled by the source and drain contacts of the top-gate transistor. Both types of transistors inherently include a back-gate transistor formed with the bottom Si substrate (gate), the SOI buried oxide, and the source and drain of the top-gate transistor. We fabricated transistors using Sandia's radiation-hardened CMOS6rs (SOI) technology. The gate length of the transistors was 0.6 micron, and the gate width of the transistors varied from 0.75 to 20 microns. We introduced mobile protons into the SOI buried oxide by annealing transistors in forming gas (5% H).

I-V measurements taken before and after the forming gas anneal showed that the forming gas anneal generated large amounts of fixed positive charge in the SOI buried oxide and the top-gate thermal oxide. The fixed charge causes a negative threshold voltage shift of the top-gate transistor. In some cases, the fixed charge was sufficient to prevent the top-gate transistors from being turned off. To overcome the effects of this fixed charge, we have to increase the transistor threshold voltage during processing to ensure that transistors can be turned to the off state. In addition to the fixed charge, the forming gas anneal also caused a large increase in parasitic leakage current (different from the desired leakage current discussed below). This leakage current is large enough to cause circuit degradation. Although the effects of fixed charge in the top-gate oxide can be circumvented through process changes, we must develop techniques to reduce the leakage current caused by the forming gas anneal.

We characterized the memory properties of the top-gate transistor by measuring the hysteresis voltage shift of the back-gate transistor. A shift in threshold voltage of the back-gate transistor can cause a change (high or low) in the leakage current of the top-gate transistor. A high leakage current indicates that the top-gate transistor is in the on state, and a low leakage current indicates that the top-gate transistor is in the off state. We measured hysteresis voltage shifts on all transistors characterized. The largest hysteresis voltage shift was 13.5 V and was measured on a 20-micron gate length transistor. This

hysteresis voltage shift is well above that required to fabricate a nonvolatile memory. Unfortunately, the magnitude of the hysteresis voltage shift varied considerably across a wafer die (from 1.5 to 13.5 V). The cause of this variation is unknown.

These results demonstrate the proof-of-concept of a protonic transport nonvolatile memory. We generated hysteresis voltage shifts large enough to fabricate a full memory; however, we must overcome some problems before a protonic memory can be a viable commercial product. One major problem is that of the nonuniform voltage shifts across a wafer. The variation across a wafer is large enough to prevent a protonic memory from being realized. We must also solve other problems with the large leakage currents generated by the forming gas anneal.

Other Communications

Schwank, J. R., K. Vanheusden, M. R. Shaneyfelt, B. L. Draper, D. M. Fleetwood, J. R. Murray, and P. M. Smith. 1999. "A Novel Nondestructive Silicon-on-Insulator Nonvolatile Memory." Sandia Technical Report SAND99-0750, Sandia National Laboratories, Albuquerque, NM.

3506460000

Integration of Optoelectronics and MEMS by Free-Space Microoptics

M. E. Warren, R. E. Asbill, O. B. Spahn, J. R. Wendt, A. A. Allerman, F. M. Hosking, M. S. Rodgers, D. J. Rieger

Combining microelectromechanical systems (MEMS) with optoelectronic components is a means of realizing compact optomechanical subsystems. Some examples are laser beam scanning, switching and routing and active focusing, and spectral filtering or shuttering of optical sources. A major obstacle to realizing these types of systems is the difficulty of integrating the two technologies. The devices use dissimilar materials with significant problems for a common process line. Another major difficulty with direct integration is providing the optical path for the MEMS components to interact with the light source. Simply stacking one device on top of another is not compatible with many optical wavelengths. Sandia will use folded optical paths in a transparent substrate to provide the interconnection route between the components of the system. The components will be surface-mounted by flip-chip bonding the substrate. Microoptics can be fabricated into the substrate to reflect and refocus the light at precise angles so that it can propagate from one device to another and be directed out of the substrate into free space. The MEMS components do not require the development of transparent optics and can be completely compatible with the current three-level polysilicon process. The optoelectronics devices will be vertical-cavity surface-emitting laser (VCSEL) arrays that are ideally suited for surface-mounting. This technology will enable the combination of two very successful activities (silicon [Si] MEMS and III–V optoelectronics) to address applications in weapons systems, sensor systems, and other areas. Optical systems that can be miniaturized include beam scanning for sensing, communications, or displays, active focusing for motion sensing or tracking, and 2-D arrays of phase shifters for real-time reconfiguration of optical systems or miniature displays.

Our final task is a MEMS-based scanner that is a hybrid assembly of a VCSEL array, a fused-silica microoptical system, and a MEMS component that provides a moving optical surface for the scanner. The optical system is composed of two diffractive optical elements (DOEs) etched into a fused-

This technology will enable the combination of two very successful activities (silicon [Si] MEMS and III–V optoelectronics) to address applications in weapons systems, sensor systems, and other areas.

silica substrate and a third DOE etched into the shuttle of the MEMS scanner. The first two elements relay the beam to the scanner and size it appropriately. The first element collimates the 690 nm VCSEL output beam and tilts it about 20° . The second element retilts the beam slightly and focuses it in front of the third element. The third element, located on the scanner, produces a collimated output beam that is perpendicular to the substrate at the center of the scanner travel.

The scanner consists of a large $500 \times 1000 \text{ mm}^2$ polysilicon shuttle that moves inplane by a linear rack attached to a rotary actuator. The rotary actuator is a microengine consisting of two orthogonal electrostatic comb drives operating 90° out of phase to convert the linear movement of the comb drive to rotational motion. We designed the bondpads and electrical leads to the comb drives with overhanging ridges in the uppermost layer of polysilicon to prevent shorting the electrical lines during the final blanket evaporation of 80 \AA of Ti followed by 500 \AA of Au (used to increase the reflectivity of the scanner surface). We fabricated the 2 mm-wide by 1100 mm-long springs on the sides of the shuttle using three mechanical layers of polysilicon, with a total thickness of 4.75 mm, providing out-of-plane rigidity but high in-plane compliance during operation. A conservative estimate for the resonant frequency of the microengine loaded by the mass-spring system of the shuttle is 314 Hz, which is above the intended operating frequency of 100 Hz. During operation the scanner performed as intended, providing smooth operation over the 100 mm scan range at scan frequencies ranging from 1–100 Hz.

We designed the system such that the beam is about 500 mm in diameter on all three diffractive elements. Thus the first two elements can be about 600 mm in diameter, and the third can be 600 mm by 700 mm. We chose to make these binary DOEs with only four phase levels to minimize processing steps and the possibility of damaging the parts.

The diffractive element on the scanner has a focal length of 700 mm, and the total travel of the shuttle is 100 mm; therefore, the total scan angle is 0.14 radian, which is 8 degrees, or ± 4 degrees. The optical system is diffraction-limited on axis, and the resulting 0.5 mm spot size is roughly 2x-diffraction limited at the limits of its $\theta = \pm 4^\circ$ scan range. Lenses are etched directly into the fused-silica substrate and the polysilicon scanner shuttle using reactive ion beam etching (RIBE), with aluminum (Al) as the metal mask. The Al mask is first

defined using direct-write e-beam lithography. We successfully completed the MEMS component with the high-efficiency DOE fabricated into the surface of the MEMS mirror and assembled the integrated unit.

Other Communications

Krygowski, T. W., D. Reyes, M. S. Rodgers, J. H. Smith, M. E. Warren, W. C. Sweatt, O. Blum-Spahn, J. R. Wendt, and R. E. Asbill. 1999. "Development of a Compact Optical MEMS Scanner with Integrated VCSEL Light Source and Diffractive Optics." *Proc. SPIE* **3878** (Miniaturized Systems with Micro-Optics and MEMS, Santa Clara, CA, 20–22 September): 20–28.

3506470000

Advanced Laser Structures for Short-Pulsed Power in Active Optical Sensor Systems

G. A. Vawter, A. Mar, G. R. Hadley, W. W. Chow, F. J. Zutavern, A. A. Allerman

To address Sandia's mission-related technological needs for high-power, low-cost, reliable pulsed lasers in the 0.01–100.0 ns regime, we will develop diode lasers for short-pulse duration and high-peak pulse power. Our goal is up to 10 W, while maintaining good far-field beam quality and ease of manufacturability for low cost. We will achieve high-peak-power picosecond pulses by gain switching flared-geometry waveguide lasers and amplifiers. In the longer-pulse-length regime, we will obtain 1 to 100 ns pulses using conventionally pumped ridge waveguide lasers of unique design. We will use novel very large optical cavity (VLOC) lasers to achieve high-saturated-output power.

A second, far-reaching aspect of pulsed diode lasers is their unique ability to generate very high repetition rate optical pulses in the microwave and millimeter-wave regime. We will explore experimentally all-optical monolithic integrated microsystems for direct generation of radio frequency (RF) and millimeter-wave frequencies. Based on our successful demonstration of 90 GHz power generation from mode-locked ring diode lasers, we will explore new techniques to reduce noise in the output signal and actually tune the output frequency by adjusting bias currents within the laser.

We made substantial progress toward our ultimate goal of 1 nJ laser pulse energy. Refinement of the flared-waveguide process for the gain-switched lasers improved performance considerably. These newer devices yielded record peak power levels of 18 W from a gain-switched flared waveguide. Considering the 35 ps pulsewidth, this is a total energy per pulse of 0.63 nJ. This value is well over half the originally stated goal of 1 nJ. In collaboration with the University of Arizona, we performed numerical simulations based on a microscopic laser model. These simulations verified the effectiveness of the saturable absorber in the generation of high-peak-power, single-pulse output. We obtained excellent qualitative and quantitative agreement between the measurements and simulations. Insight from the model suggests that the quantum-confined Stark effect is primarily responsible for saturable absorber operation.

To address Sandia's mission-related technological needs for high-power, low-cost, reliable pulsed lasers in the 0.01–100.0 ns regime, we will develop diode lasers for short-pulse duration and high-peak pulse power. Our goal is up to 10 W, while maintaining good far-field beam quality and ease of manufacturability for low cost.

Using information gleaned from the model, we determined that slight modifications to the length of the saturable absorber could potentially double the laser output to as much as 1.2 nJ. We completed new designs for the gain-switched flares to realize this improved performance. These devices are nearing completion and will be tested.

We fabricated mode-locked ring lasers; initial screening for non-mode-locked operation is under way.

Refereed

Mar, A., G. A. Vawter, S. W. Kock, W. W. Chow, R. Indik, and J. Maloney. 1999. "High Peak Power Gain-Switched Flared Waveguide Lasers." *Technical Digest of CLEO '99* (Baltimore, MD, 23–28 May): 487–488.

Vawter, G. A., and C. T. Sullivan. 1999. "RF and mm-Wave Photonics at Sandia National Laboratories." (Invited) *Proc. SPIE 3795* (International Symposium on Optical Science, Engineering, and Instrumentation, Denver, CO, 16–23 July).

3506480000

Integration of Microsensor Technology into a Miniature Robotic Vehicle

R. H. Byrne, K. O. Wessendorf, E. J. Heller, J. R. Bryan, D. R. Hayward

The goal of this project was to develop a 0.25-cubic-inch vehicle that incorporates a Sandia-developed sensor. We successfully developed a custom application-specific integrated circuit (ASIC) that interfaces to a chemical resistor. The chemical resistor is a carbon-laced polymer that changes resistance when exposed to different chemical reagents. We integrated the ASIC and chemical sensor into a prototype miniature robot that is 1 inch by 1 inch. The robot also incorporates wafer-scale integration to further reduce the size of the electronics. The robot consists of the chemical sensor, custom ASIC, a processor in bare die form, a temperature sensor, miniature brushless dc motors, and a battery. The overall vehicle volume is governed by the size of the battery, which in turn limits the total operating time of the robot. We also developed larger prototype robots that we used to evaluate different sensors and algorithms. These larger robots are still relatively small, on the order of 1 cubic inch in volume. These robots use optical sensors to detect obstacles and to communicate with each other.

One of the main limitations in employing wafer-scale integration was the availability of electronics in bare die form. The processor chosen (PIC 16C77) is adequate, but was the only processor that was available in a reasonable quantity. In this case, the minimum order was 1000 units. The PIC processor is in-circuit programmable, but uses ultraviolet (UV)-erasable programmable read-only memory (EPROM) for code storage. This results in a 45-minute turnaround time to erase and reburn new code. For the most part, commercial ICs are available only in bare die form in very large quantities, which makes it very difficult to develop small numbers of prototypes that employ wafer-scale integration.

We also developed larger prototype robots that we used to evaluate different sensors and algorithms. These larger robots are still relatively small, on the order of 1 cubic inch in volume. These robots use optical sensors to detect obstacles and communicate with each other. The robots employ traditional printed circuit boards (PCBs) with surface-mount electronics,

The goal of this project was to develop a 0.25-cubic-inch vehicle that incorporates a Sandia-developed sensor. We successfully developed a custom application-specific integrated circuit (ASIC) that interfaces to a chemical resistor.

and the PCB serves as the body of the robot. These robots use an Atmel 89LS8252 processor that is in-circuit programmable and code-compatible with the 8051 processor.

Refereed

Byrne, R. H., C. Anderson, and R. D. Robinett, III.
1999. "Design of a Miniature Robotic Vehicle." *Proc. 18th IASTED Internat. Conf. Modeling, Identification, and Control 1* (Innsbruck, Austria, 15–18 February): 428–430.

3506490000

Vacuum Encapsulation of MEMS Structures

S. Montague, B. D. Staple, J. G. Fleming, A. J. Farino, J. J. Sniowski

Although the interest in microelectromechanical system (MEMS) sensors is extremely high, except for a few cases, commercialization on a large scale has not yet materialized. This is due in part to packaging constraints. For example, most MEMS packaging today involves sawing the wafers into individual die, then releasing and packaging the individual die. There are several problems with this approach. First, releasing individual die is very time-consuming and uneconomical for large-scale production. Wafer-scale release and packaging would be more economical. Second, the fragile nature of MEMS structures renders them vulnerable to damage during post-release handling (e.g., during packaging). This may result in low device yield.

Sandia explored the design, manufacture, and evaluation of a new wafer-level, in situ vacuum encapsulation technology for MEMS. The technology uses a 4-micron-thick polysilicon lid, hermetically sealed with aluminum (Al) sputtered at 10 mTorr, to encapsulate MEMS devices inside a microcavity. With the lids encapsulated during the normal complementary metallic oxide semiconductor (CMOS) processing of the MEMS, detrimental factors associated with post-release handling of the MEMS devices are reduced. Preliminary characterizations of the technology indicate that the maximum spacing between supporting pillars of the lid to prevent it from deflecting excessively and interfering with the encapsulated MEMS devices was approximately 150 microns. For this and smaller lid support geometries, visual inspections revealed that the lid was not susceptible to damage from the sealing, wafer sawing, die separation, and packaging processes. Furthermore, the cavity was free of foreign particles, and there was no measured degradation in the performances of the encapsulated devices. Finally, characterization of the vacuum level inside the cavity using thermal MEMS microbridges indicated that vacuum pressure was approximately 10 mTorr.

These results indicate that the in situ vacuum encapsulation technology developed in this research holds tremendous promise as a tool for the realization of economical, wafer-scale packaging of MEMS.

...the in situ vacuum encapsulation technology developed in this research holds tremendous promise as a tool for the realization of economical, wafer-scale packaging of MEMS.

First, we designed a 4-micron-thick polysilicon lid, hermetically sealed with Al sputtered at 10 mTorr, to encapsulate MEMS devices inside a microcavity. This lid encapsulation technology met three major design requirements. First, the lid was sufficiently rigid to prevent it from excessively deflecting under internal vacuum and making physical contact with the encapsulated MEMS structures. Second, the lid had sufficient porosity to allow for easy release of the underlying MEMS structure. Third, the lid design provided sufficient protection from contamination from either the sealing material or the typical wafer sawing, die separation, or packaging processes.

Following the lid design, we designed practical MEMS devices serving as test structures in the cavity to evaluate the integrity of the encapsulation (i.e., the robustness of the encapsulating lid and quality of the seal) and the level of vacuum after encapsulation. The first test structures designed were electrostatically driven, laterally comb-drive resonators. We designed these devices to determine the integrity of the encapsulation technology and the level of vacuum in the cavity after encapsulation. Their operation is based on the pressure dependence of the quality factor (Q) of the resonator. The second set of test structures designed were thermal polysilicon microbridges, which we also designed to determine the level of vacuum in the cavity after encapsulation. We based their operation on the pressure dependence of the heat transfer through a gas across a gap between the microbridge, the substrate, and the encapsulating lid.

Next, we fabricated three wafer lots using the lid and test structure mask-level designs and a newly developed technology process flow. This flow process places the MEMS devices in a shallow trench, planarizes the wafer, and seals the micromechanical devices in the trench. This is followed by a four-mask-level process that encapsulates the MEMS device in a 4-micron-thick lid. We then used the resulting wafers with the completed, planarized micromechanical devices as starting material for depositing Al for electrical interconnect.

Following fabrication, we released the encapsulated devices using a 73% hydrofluoric acid (HF) solution. Release time for the encapsulated devices was approximately 43 minutes. The release provided fully functional structures inside the cavities.

Following the release, we encapsulated the devices with Al, sputtered at 10 mTorr over a custom stainless-steel shadow-mask. We needed a shadow-mask to prevent the sputtered Al from shorting exposed bond pads and Al interconnect lines.

After sealing the lid, we evaluated the technology for seal integrity and vacuum quality evaluations. Preliminary characterizations of the technology indicated that the maximum spacing between supporting pillars of the lid to prevent it from deflecting excessively and interfering with the encapsulated MEMS devices was approximately 150 microns.

For this and smaller lid support geometries, visual inspections revealed that the lid was not susceptible to damage for the sealing, wafer sawing, die separation, and packaging processes. Furthermore, the cavity was free of foreign particles, and there was no measured degradation in the performances of the encapsulated devices.

Finally, we attempted characterizations of vacuum level inside the cavity based on the pressure dependence of the Q of comb-drive resonators and on the heat-transfer characteristics of suspended thermal polysilicon microbridges. Because of the unavailability of closely integrated on-chip electronics for the resonators, vacuum-level evaluations proved to be more difficult than anticipated and produced nonreproducible results. This was mainly due to parasitic feedthrough currents that masked the extremely small currents produced by the resonator. However, characterization of the vacuum level using the thermal microbridges I-V data indicates that vacuum pressure was approximately 10 mTorr.

These results indicate that the *in situ* vacuum encapsulation technology developed in this research holds tremendous promise as a tool for the realization of economical, wafer-scale packaging of MEMS.

3506510000

Massively Parallel Sensor Arrays for Volatile Organic Detection

A. J. Ricco, W. G. Yelton, J. W. Bartholomew

Sandia will develop a flexible chemical sensor microlab (μ lab) for detecting volatile organic compounds (VOCs) with high chemical selectivity based on large (~ 30 sensors) arrays of sorption-based resistors and surface acoustic-wave (SAW) devices. This μ lab will comprise a massively parallel (MP) microsensor array using inexpensive, easily fabricated, polymer-coated, planar interdigitated resistors/polymers that are rendered conductive through admixture of conductive colloidal particles. Using chip-based electronics, we can monitor sensor-array resistance changes due to VOC exposure inexpensively in real time. The response of each sensor is rapid, reversible, and repeatable; hundreds of polymers with distinct sorptive characteristics are commercially available. Limits of detection (LODs) can reach ppb (parts-per-billion) levels; for high-volatility species, this is likely to require adding a preconcentrator as a front end for this μ lab. In contrast to separations-based μ lab concepts, this approach is analogous to spectroscopy. The rich spectrum of resistor responses enables high chemical selectivity through multivariate analyses without separations; sensor redundancy provides improved system robustness. Our goal is to determine the numbers and identities of sensor coatings needed to distinguish sets of VOCs. The most effective coatings can become part of a large library of potential sensor coatings for general-purpose applications. We are using the visually empirical region of influence (VERI) algorithm to evaluate the chemical discrimination capability of various sensor combinations.

The detection of VOCs is a key national security concern—detection of the proliferation of weapons of mass destruction (WMD). Particular combinations of chemical precursors, solvents, and by-products signal the production of nuclear, chemical, and biological WMD. We will determine system performance for WMD compounds. In addition, DOE environmental monitoring and remediation applications, as well as industrial waste minimization, require the development of effective, inexpensive VOC μ labs; we will address key species, as well, many of which are potential interferants for WMD detection and must therefore be included in any case.

The detection of VOCs is a key national security concern—detection of the proliferation of weapons of mass destruction (WMD).

The primary thrust of this project was to evaluate the effectiveness of very large arrays of partially selective chemical microsensors to distinguish chemicals of interest. We obtained results for a variety of sensor coatings on a relevant set of VOCs. We used the VERI algorithm to evaluate the chemical discrimination effectiveness of array sizes ranging from 2 sensors up to 29 sensors (for a set of 18 individual VOC analytes) as a function of (modeled) sensor response variability.

It was necessary to develop a new optimization approach, called the *upper band technique*, to identify the best performing arrays from among the 500 million combinations of sensors. It was also necessary to develop a variety of sensor coatings to achieve a good candidate set of sensors from which to build large arrays.

The key results showed that modest-sized arrays actually give the best performance on the limited sets of individual analytes that we examined with these sensors. In particular, we found that modest-sized arrays (8–15 sensors) provide the best separation of chemical classes and thus the most robust discrimination in the presence of variable sensor response sensitivities. The best choices of partially selective sensors tended to include the most chemically diverse sets of sensor coatings. We also found that the discrimination of similar chemicals within the same classes of VOCs (e.g., chlorinated hydrocarbons) breaks down first as either sensor noise or array size increases. These results suggest that a hierarchical analysis might provide a way to include large numbers of sensors in the analysis of huge sets of distinct chemicals. The hierarchical approach would allow general classes of chemical analytes to be distinguished first (with small arrays); then more specific chemical identification would follow with sensor combinations specialized to distinguish the individual analytes in the (already identified) general chemical classes.

Refereed

Osbourn, G. C., R. F. Martinez, J. W. Bartholomew, W. G. Yelton, and A. J. Ricco. 1999. "Optimizing Chemical Sensor Array Sizes." *Chemical Sensors IV 99-23* (Electrochemical Society Conference, Honolulu, HI, 19 October): 127.

Yelton, W. G., A. J. Ricco, and A. Stanton. 1999. "Mass-Transport-Limited Electrodeposition of High-Surface-Area Coatings for Surface Acoustic-Wave Sensor Technology." *Chemical Sensors IV 99-23* (Electrochemical Society Conference, Honolulu, HI, 18 October): 301.

3506520000

Agile Dry Etching of Compound Semiconductors for Science-Based Manufacturing Using *In Situ* Process Control

C. I. H. Ashby, L. A. Bruskas, G. A. Vawter, J. R. Woodworth, W. G. Breiland

Sandia developed and implemented in situ optical diagnostics and ion-beam diagnostics for plasma-etch and reactive ion-beam etch (RIBE) tools. The optical diagnostics provide real-time endpoint detection during plasma etching of complex thin-film layered structures that require precision etching to stop on a particular layer in the structure. The Monoetch real-time display and analysis program developed with this project displays raw and filtered reflectance signals that enable an etch system operator to stop an etch at the desired depth within the desired layer. The ion-beam diagnostics developed with this project will permit routine analysis of critical ion-beam profile characteristics that determine etch uniformity and reproducibility on the RIBE tool.

• *In situ optical diagnostics.* We developed a data collection program (Monoetch) that records a single-wavelength reflectance signal during plasma etching. Because substrates are usually patterned with photoresist (PR), the ADVISOR (Analysis of Deposition Using Virtual Interfaces and Spectroscopic Optical Reflectance) methods that use deposition rates in molecular beam epitaxy (MBE) and metalorganic chemical vapor deposition (MOCVD) applications are not useful in etching. Thus, we used more empirical methods for determining endpoints during the etch process.

The reflectance signal includes the plasma emission background, a long-period oscillation due to slow etching of PR, higher-frequency oscillations from the thin-film structure being etched, and noise. The Monoetch program disentangles these patterns using digital filtering methods. It displays the raw reflectance signal along with three waveforms that we filtered with the following constraints:

– A PR bandpass filter removes high-frequency (HF) noise and interference oscillations from the thin-film structure, leaving an oscillation that largely represents the interferogram that would result from etching PR alone. Given the PR

The ion-beam diagnostics developed with this project will permit routine analysis of critical ion-beam profile characteristics that determine etch uniformity and reproducibility on the RIBE tool.

refractive index, the PR etch rate may be determined from this waveform.

– A thin-film bandpass filter removes background, drifts, PR oscillations, and HF noise. The resultant waveform represents the interferogram that would result from etching an unpatterned thin-film structure. Layers may be identified by their characteristic oscillations, and interfaces are often seen as kinks in the waveform due to instantaneous phase shifts that occur at interfaces.

– An interface detector-smoothing second-derivative filter helps identify interface kinks by displaying singularities in the second derivative of the waveform that occur whenever there is a discontinuous change in slope.

These filters may be adjusted interactively to see their effect on the waveform. We are exploring two digital filtering methods. A finite impulse response (FIR) method presents an updated data point that is centered in a filter window. This method presents stable, filtered waveforms, but can only display filtered data information that occurred at times prior to half the data window. A fast Fourier transform (FFT) method presents a filtered waveform over the entire data range, including the most recently acquired data, but the recent data are distorted by Gibbs oscillation artifacts.

A playback feature allows filtering of a stored data file to optimize an endpoint detection scheme. It can also display the time-reversed interferogram from a deposition experiment that used the Monogrow program to record an *in situ* reflectance signal during growth of the thin-film structure.

To accommodate the unavoidable uncertainty in obtaining an unphase-shifted filtered waveform in real time, we are experimenting with a simple predictor method. By detecting two easily identified reflectance features in the structure, it determines the etch rate in real time and forecasts when the endpoint will occur.

• *Ion-beam diagnostics.* We measured spatially resolved beam divergence in the RIBE system. These were the first ever for a broad ion-beam source. We gained a better understanding of grid form factor issues and accelerator grid bias selection. We determined that the beam energy spectrum follows the setpoints well. These data determined the type of tool that would give the best benefit/cost ratio if installed permanently in our RIBE system. We concluded that we could build a linear Faraday-cup array using the same technology as the spectrum analyzer and that such an array could be made to fit in existing ports with the sample stage in place. We built the Faraday-cup

We measured spatially resolved beam divergence in the RIBE system. These were the first ever for a broad ion-beam source.

array and wrote the control software. The final tool will allow real-time display of the ion-beam uniformity across the sample diameter. We will use this display to optimize the ion-beam uniformity or divergence without resorting to time-consuming wafer-etch trials. We also expect to be able to monitor the etch system for grid wear, as manifested by long-term drift of the ion-beam profile. Such *in situ* measurements of beam quality will allow us to improve diagnosis and prediction of needed repairs before they are evident as out-of-spec etches.

Refereed

Vawter, G. A., J. R. Woodworth, and W. J. Zubrzycki.
1999. "Spatially-Resolved Ion Trajectory
Measurements During Cl₂ Reactive Ion Beam
Etching and Ar Ion Beam Etching." *J. Vac. Sci. and
Technol.*, submitted.

Vawter, G. A., J. R. Woodworth, and W. J. Zubrzycki.
1999. "Spatially-Resolved Ion Trajectory
Measurements During Cl₂ RIBE and Ar IBE."
(Invited) Paper presented to the 43rd International
Conference on Electron, Ion, and Photon Beam
Technology and Nanofabrication, Marco Island, FL,
1–4 June.

Zubrzycki, W. J., G. A. Vawter, and J. R. Wendt.
1999. "Influence of Ion Beam Divergence and
Chamber Pressure on High-Aspect Ratio
Nanophotonic Components by Cl₂ RIBE." *J. Vac. Sci.
and Technol.*, accepted.

Zubrzycki, W. J., G. A. Vawter, and J. R. Wendt.
1999. "Influence of Ion Beam Divergence and
Chamber Pressure on High-Aspect Ratio
Nanophotonic Components by Cl₂ RIBE." Paper
presented to the 43rd International Conference on
Electron, Ion, and Photon Beam Technology and
Nanofabrication, Marco Island, FL, 1–4 June.

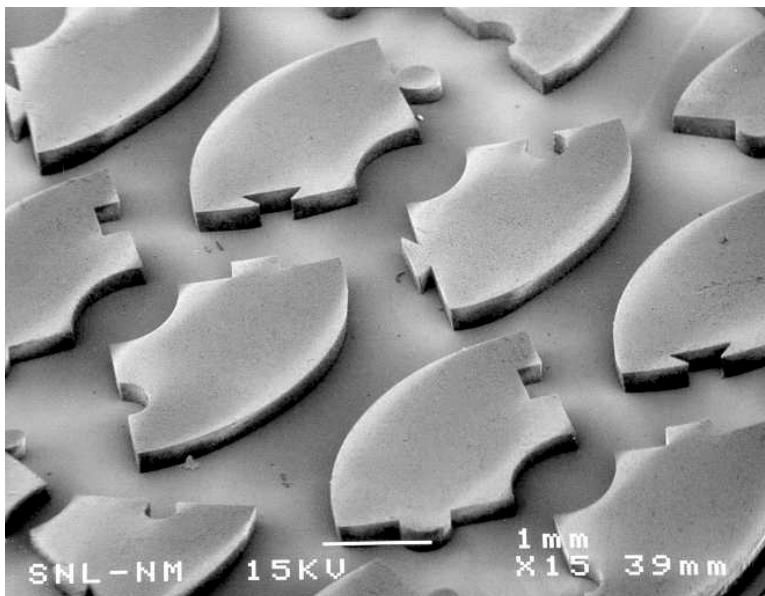
3506530000

Precision-Formed Micromagnets

T. R. Christenson, E. L. Venturini, T. J. Garino

An area in microelectromechanical systems (MEMS) research requiring substantial effort pertains to expanding the materials available to integrate into MEMS-based fabrication approaches where it is recognized that these approaches are based on planar batch (multiple devices/substrate) techniques. Magnetic microsystems have been handicapped precisely for that reason, which is also governed by scaling phenomena. The scaling result suggests that miniature magnetic devices profit the most if permanent magnets are incorporated. The permanent magnet figure of merit that is most pertinent to microactuators and static field production is maximum energy product for which by far the superior performance is possessed by rare-earth (RE)-based permanent magnet (PM) materials such as the SmCo (samarium cobalt) and NdFeB (neodymium iron boron) families. This project incorporated these permanent magnet (PM) materials into a batch-forming process that uses deep x-ray lithography-fabricated precision micromolds. We obtained bonded forms of REPM directly from an x-ray photoresist (PMMA [polymethylmethacrylate]) with dimensions as small as 5 microns, dimensional control less than 1 micron, and energy products up to 8 MGOe (Mega Gauss Oersted). We formed fully dense REPMs using an intermediate alumina mold that is cast from a PMMA mold. These magnets yielded energy products in submillimeter shapes of 23 MGOe. We subsequently fabricated miniature

The permanent magnet figure of merit that is most pertinent to microactuators and static field production is maximum energy product for which by far the superior performance is possessed by rare-earth (RE)-based permanent magnet (PM) materials such as the SmCo (samarium cobalt) and NdFeB (neodymium iron boron) families.



Bonded $\text{Nd}_2\text{Fe}_{14}\text{B}$ permanent magnets fabricated with the use of deep x-ray lithography rotor. Some distortion is present in the electron microscope image due to the local magnetic field present from the magnets.

brushless dc motors using these formed REPMs that have multipole PM rotors that would not be possible to realize using a multipole magnetizing fixture. We also realized other miniature multipole static PM configurations that are unique due to their size and precision at small scale.

We demonstrated micromolded bonded REPMs fabricated directly from PMMA molds that exhibited maximum energy products of up to 8 MGOe. These prismatically shaped magnets can be patterned to have nearly arbitrary geometry in the plane of the fabrication substrate with dimensions down to 5 microns and dimensional tolerance below 1 micron. Integrating these magnets into useful multipole arrangements follows as an additional issue as well as the possibility of increasing the maximum energy product by implementing higher-density anisotropic REPM material.

We demonstrated the integration of miniature multipole PM structures by constructing an 8 mm-diameter brushless dc motor. We chose a low-profile design with a 1.5 mm-thickness and 5 mm-diameter rotor in a slotless (air slot) nine-slot, four-pole, inner rotor configuration. Because of the precision that is possible at small dimensions with this REPM-forming process, a radial-anisotropic PM rotor configuration is possible with submillimeter dimensions as opposed to pole-anisotropic forms. We attached the four-pole PM rotor to a 320-micron-diameter shaft supported by a 1.6 mm-diameter ball bearing and surrounded it by nine coils with 120 turns of 47-gauge magnet wire connected in a three-phase delta configuration. This motor is capable of operating with an excitation as low as 1 mA of current per phase and rotates up to 20,000 rpm without closed-loop control.

The most promising approach found to achieving higher-energy-density microfabricated REPMs uses an intermediate mold compatible with higher processing temperatures combined with a hot forging scheme. In this approach, we obtain a precision alumina micromold by slurry casting in a PMMA mold and pressing in a uniaxial press. The excess alumina is removed by lapping, and the PMMA is burned out during an intermediate temperature step. We then heat the substrate with alumina structures to 1250°C in air for 2 hours, thereby yielding a partial sintering to minimize densification, and partially leave binder silica to avoid significant geometric distortion. We then coat the alumina mold with a copper layer to provide eventual mold release. We studied two techniques to fill the resulting mold with REPM material. Hot pressing is one

We subsequently fabricated miniature brushless dc motors using these formed REPMs that have multipole PM rotors that would not be possible to realize using a multipole magnetizing fixture. We also realized other miniature multipole static PM configurations that are unique due to their size and precision at small scale.

approach and is more readily suited to isotropic REPM powder since anisotropic powder must be aligned during pressing via a die-upset-like technique. An alternative, however, avoids the alignment issue by the use of pre-aligned bulk anisotropic REPM material and hot forging. In this approach, a bulk sheet is simply placed over the mold and pressed at a temperature yielding a reasonable strain rate. This avoids handling powder that is more susceptible to being affected by oxidation as well as avoiding a more difficult alignment procedure. We performed strain-rate experiments for a variety of bulk NdFeB material. We found the best material in this respect to be Magnequench MQ2-F and MQ3-F die upset $\text{Nd}_2\text{Fe}_{14}\text{B}$ material with strain rates of up to 22% at 2000 psi and 700°C for 500 seconds, which is well suited to the magnet thicknesses of interest (up to 1 mm). The largest energy product achieved was with MQ3-F material measured directly on a submillimeter molded test specimen at 23 MGOe using a squid magnetometer instrument. This energy product resides well within the family of REPM qualities.

Other Communications

Christenson, T. R., T. J. Garino, and E. L. Venturini. 1999. "Deep X-Ray Lithography-Based Fabrication of Rare-Earth-Based Permanent Magnets and their Application to Microactuators." (Invited) *Proc. 5th Internat. Symp. on Magnetic Mater., Processes, and Devices V* **98-20** (Electrochemical Society Meeting, Boston, MA, November 1998): 312–323.

Christenson, T. R., T. J. Garino, and E. L. Venturini. 1999. "Microfabrication of Fully-Dense Rare-Earth Permanent Magnets Via Deep X-Ray Lithography and Hot Forging." *Book of Abstracts, HARMST '99* **1** (Kisarazu, Japan, 13–15 June): 82–83.

Christenson, T. R., T. J. Garino, E. L. Venturini, and D. M. Berry. 1999. "Application of Deep X-Ray Lithography Fabricated Rare-Earth Permanent Magnets to Multipole Magnetic Microactuators." *Digest of Technical Papers, Transducers '99* **1** (Sendai, Japan, 7–10 June): 98–101.

Garino, T. J., T. R. Christenson, and E. L. Venturini. 1998. "Fabrication of MEMS Devices by Powder-Filling into DXRL-Formed Molds." *Proc. MRS Symp., Mater. Sci. Microelectromechanical Systems (MEMS) Devices* **546** (Boston, MA, 1–2 December).

Garino, T. J., T. R. Christenson, and E. L. Venturini. 1999. "The Development of a Ceramic Mold for Hot Forging Micromagnets." *Proc. Ceramics Soc. Meeting* **1** (Indianapolis, IN, 26–28 April).

3506540000

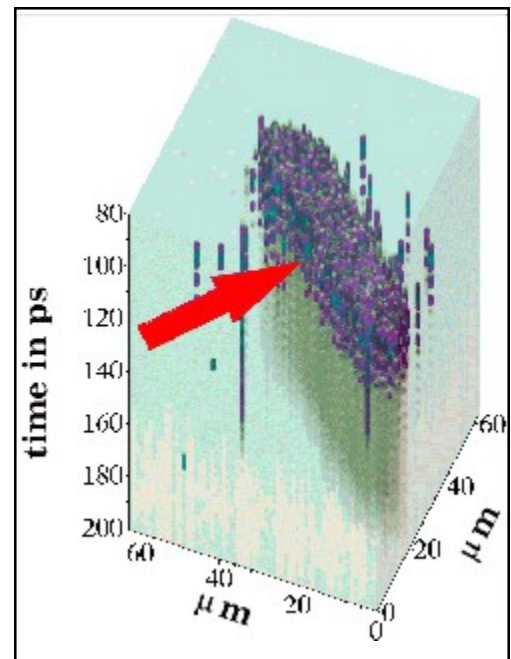
Time-Resolved Ion-Beam-Induced Charge-Collection (TRIBICC) Imaging

F. W. Sexton, D. S. Walsh, P. E. Dodd, R. S. Flores, J. F. Aurand

In this project, Sandia developed and demonstrated a new method for studying single-event upset (SEU) in microelectronics. This technique, called Time-Resolved Ion-Beam-Induced Charge Collection (TRIBICC), measures the transient charge-collection waveform from a single heavy-ion strike with a -3 dB bandwidth of 5 GHz. Bandwidth can be expanded up to 15 GHz (with 5 ps sampling windows) by using a fast Fourier transform (FFT)-based off-line waveform renormalization technique developed at Sandia. To preserve the high bandwidth from integrated circuit (IC) to the digitizing oscilloscope, we assemble individual test structures in custom high-frequency (HF) packages. A leading-edge digitized waveform is stored with the corresponding ion-beam position at each point in a two-dimensional (2-D) raster scan. The resulting data cube contains up to 1024 spatial charge distribution maps of 2-D- $Q(t)$, each representing a time slice as short as 5 ps of the charge collected. This tool overcomes limitations observed in previous techniques due to displacement damage effects that degrade the signal of interest during measurement. This system is the first demonstration of a single-ion transient measurement capability coupled with spatial mapping of fast transients.

We applied the system to the study of fast transients in ICs and devices. We measured single-event transients on CMOS6r (complementary metallic oxide semiconductor) n-channel transistors using three heavy ions: 5 MeV He (helium), 12 MeV C (carbon), and 28 MeV Si (silicon). The magnitude and shape of single-event transients varied with location on test devices. We measured fast transients from the center of drain regions, while slower transients were measured at the edge of the drain. We compared the measurements to predictions from a 3-D transport code that simulates charge transport and collection in semiconductor devices and discussed differences between measurement and prediction. Attempts to measure TRIBICC signals in more complex circuits are limited by noise in the device through control lines and test equipment. We are looking at approaches to minimize noise and to further improve the technique.

Sandia developed and demonstrated a new method for studying single-event upset (SEU) in microelectronics.



A representation of four-dimensional charge-collection data. The magnitude of the measured current is represented through the gray-scale intensity.

The TRIBICC configuration allows measurement of current transients on a device under test (DUT) to a maximum analog bandwidth of at least 20 GHz. At present, overall system response is limited by the 5 GHz digitizer and is not further reduced by other system components. The system captures each charge transient with peak amplitude above 50 mV threshold, and a high-speed (~ 100 ns) beam deflector rapidly sweeps the beam off the DUT to minimize further heavy-ion damage.

Sandia measured spatially dependent current transients after single strikes on $0.5 \mu\text{m}$ n -channel transistors manufactured at Sandia using 5 MeV He, 12 MeV C, and 28 MeV Si ions. Two-dimensional (2-D) scans resulted in up to 1024 spatial charge-collection maps, each representing a time slice as short as 5 ps of the charge collected. These single-ion transient measurements, as well as the spatial mapping of fast transients, have never before been achieved.

Measurements using 12 MeV C ions clearly show the dependence of current transients on spatial location. Strikes hitting up to $2 \mu\text{m}$ from the edge of the drain have a risetime of ~ 750 ps and a decay time of about 100 ns, consistent with a purely diffusion-dominated charge collection. In contrast, ions traversing the drain region induce large (about $-275 \mu\text{A}$) signals and exhibit a bandwidth-limited 70–75 ps risetime and 100 ps FWHM (full width, half maximum)-wide peak with a tail of about 10 ns decay time. The fast peak is evidence of drift charge collection within the pn-junction depletion region and the funnel region that extends below the original junction, while the slowly decaying component in this transient is consistent with diffusive charge collection from below the drain's n^+ -region. Some ringing is evident in the measurements and has a delay time of ~ 350 ps and probably originates from the gate, source, and bulk connections to ground. The risetime of the fast-drain center signals are limited only by the experimental bandwidth, indicating that the drift/funnel signal is appreciably faster than the experimental resolution.

We compared the measured current transients to the corresponding simulations using the DAVINCI 3-D code. In general, the calculations reproduce the experimental data. The distinct risetime and peak height differences between drift and diffusion are well reproduced. The ratio of drift to diffusion charge collection at late times, however, is not accurately reproduced. For off-drain ion strikes, the diffusive charge collection is underestimated by about 50%. This difference can arise in part through an incorrect estimate of the diffusion

This system is the first demonstration of a single-ion transient measurement capability coupled with spatial mapping of fast transients.

length and lifetime of injected minority carriers. Furthermore, small variations in the ion-strike distance to the drain area will result in significant changes in the amount of diffusive charge collection.

We also applied the TRIBICC technique to the study of SEU mechanisms in memory devices. Single-event transients may provide useful insights into the dynamics of upset and have never been directly measured. We mounted a specialized memory test structure on a HF fixture and measured transient signals in the power supply line to detect current transients resulting from upset in the memory cells. This measurement was limited by noise that was picked up in control lines into the device. We fabricated a modified test configuration using optocoupler isolation to reduce noise but have not completed full tests.

We did not meet our goal to perform a detailed comparison between TRIBICC measurements and 3-D simulations over a full memory cell because we did not complete a massively parallel (MP) version of DAVINCI.

Refereed

Schone, H., D. S. Walsh, F. W. Sexton, B. L. Doyle, P. E. Dodd, J. F. Aurand, and N. Wing. 1999. "Time-Resolved Ion-Beam Charge Collection (TRIBICC): A New Microbeam Technique." *Nucl. Instruments & Meth. Vol. B* (International Conference on Nuclear Microprobe Technology and Applications, Cape Town, South Africa, 13–16 October 1998).

Schone, H., D. S. Walsh, F. W. Sexton, B. L. Doyle, P. E. Dodd, J. F. Aurand, R. S. Flores, and N. Wing. 1998. "Time-Resolved Ion-Beam-Induced Charge Collection (TRIBICC) in Microelectronics." *IEEE Transactions on Nucl. Sci.* **45** (December) (IEEE Nuclear and Space Radiation Effects Conference, Newport Beach, CA, 20–24 July): 2544–2549.

3506550000

Composite-Resonator Surface-Emitting Lasers

K. D. Choquette, A. J. Fischer, A. A. Allerman, W. W. Chow, K. M. Geib

Applications of vertical-cavity surface-emitting lasers (VCSELs) have requirements ranging from amplitude modulation, frequency tunability, and amplitude or frequency stability to high output power. The present single-resonator VCSEL lacks the agility to readily perform many of the above functions. Sandia will use composite resonators to control spectral and temporal properties of VCSELs. This structure in effect is a coupled-resonator vertical-cavity laser (CRVCL). Using composite resonators opens up new possibilities because of their unique ability to (1) tailor the coupling between the monolithic cavities, (2) dynamically modify the cavity interaction, and (3) incorporate passive or active resonators that are spectrally degenerate or detuned. Composite resonators can be utilized to influence the spectral and temporal properties within a VCL.

The composite resonator will consist of a primary resonator containing the gain section and an active or passive secondary resonator. Separate contacts provide independent current injection into the resonators. The coupling between the resonators is controlled by the transmission of the shared distributed Bragg reflector (DBR). We will use different configurations of a monolithic composite-resonator surface-emitting laser structure to demonstrate (1) amplitude modulation, (2) gain-switching, and (3) frequency-tuning. The latter will allow fine-tuning of the mode/gain alignment after growth to compensate for temperature and injection-current fluctuations. Successful demonstration of these functions will be a major step toward making VCSEL technology viable for many defense and commercial applications.

(1) We demonstrated high-speed amplitude modulation with both forward and reverse bias in the passive cavity while operating the active cavity in a continuous wave (CW) mode. We limited the large signal modulation using a forward bias to 150 MHz due to the long carrier lifetime in the passive cavity. Using reverse bias allowed modulation speeds of 2–3 GHz.

(2) We successfully demonstrated Q-switching from the active/passive composite-resonator VCSELs and obtained pulses with 150 ps width at rates up to 3 GHz.

Successful demonstration of these functions ((1) amplitude modulation, (2) gain-switching, and (3) frequency-tuning) will be a major step toward making VCSEL technology viable for many defense and commercial applications.

(3) We developed an optical model of the active/passive and active/active cavities to compare with experimental results. The model accounts for optical coupling between the cavities as well as gain saturation in the active region(s).

(4) We successfully designed, fabricated, and tested active/active composite-resonator VCSELs with both cavities containing quantum wells (QWs). These new devices operate at 850 nm rather than 980 nm.

(5) We observed and characterized optical bistability from an active/active composite-resonator VCSEL.

(6) We observed dual-wavelength operation from an active/active composite-resonator VCSEL.

Refereed

Choquette, K. D., W. W. Chow, A. J. Fischer, A. A. Allerman, H. Q. Hou, and K. M. Geib. 1999. "Coupled-Resonator Vertical-Cavity Laser Diodes." (Invited) Paper presented to the Vertical-Cavity Surface-Emitting Lasers II, IEEE Summer Topical, San Diego, CA, August.

Fischer, A. J. , K. D. Choquette, W. W. Chow, H. Q. Hou, and K. M. Geib. 1999. "Coupled-Resonator Vertical-Cavity Laser Diode." *Appl. Phys. Lett.* **75** (November): 999.

3506560000

Role of Defects in III-Nitride-Based Electronics

J. Han, S. R. Lee, T. J. Drummond, D. M. Follstaedt, A. F. Wright, R. J. Shul, C. H. Seager, S. M. Myers, Jr., M. H. Crawford, A. G. Baca

Wide-bandgap III-nitride semiconductors are extremely promising materials for compact, high-power, high-frequency (HF) amplifiers required for future satellite cross- and up-/downlinks, and for the robust microelectronics required for future severe environment national security (NS) applications. Defects, including point, line, and planar defects, are recognized to exist abundantly in gallium nitride (GaN), frequently interfere with the intrinsic material properties of GaN, and ultimately limit the performance of electronic and optoelectronic devices. In the midst of application-orientated GaN efforts, this project is intended to provide a scientific base for understanding the roles of defects in GaN. Sandia's approach can be categorized into three subfields: (1) establishing a strong metalorganic chemical vapor deposition (MOCVD) growth capability for III-nitride, (2) applying various microscopic probes (some unique only at Sandia) to characterizing defects in GaN, and (3) performing state-of-the-art first-principles calculation of energetics of defects in GaN. Ultimately we expect that the computational effort will produce insight into defects and be coupled to the experimental findings.

- *Demonstrated III-nitride-based heterojunction bipolar transistor.* We grew a gallium nitride/aluminum gallium nitride (GaN/AlGaN) heterojunction bipolar transistor structure with magnesium (Mg) doping in the base and silicon (Si) doping in the emitter and collector regions on c-axis Al₂O₃. Secondary ion mass spectrometry (SIMS) measurements showed no increase in the oxygen (O) concentration in the AlGaN emitter and fairly low levels of carbon (C) throughout the structure. Due to the non-ohmic behavior of the base contact at room temperature, the current gain was < 3. Increasing the device operating temperature led to higher ionization fractions of the Mg acceptors in the base, and we obtained current gains of ~ 10 at 300°C.

- *Studied the electronic states of defects in Mg-doped GaN.* Hydrogen (H) is the most consequential impurity defect in GaN because of its inevitable introduction during MOCVD growth

Ultimately we expect that the computational effort will produce insight into defects and be coupled to the experimental findings.

and subsequent processing, its electrical activity as both a donor and an acceptor, and its passivation of dopants such as Mg. To this end, we formulated and numerically solved equations describing the H-related physical processes (uptake, release, transport, and reactions) for which there is either theoretical or direct experimental evidence. We evaluated parameters within the formalism from density-functional theory (DFT) together with our measurements of H solubility and H uptake rate in *p*-type GaN. We used this theoretical model without adjustable parameters to predict the release of H from GaN:Mg and the resultant increase in room-temperature hole concentration during activation annealing. Results agree quantitatively with our measurements of H release and observations of hole concentration during an isochronal heating sequence.

- *Performed modeling of defect complexes (Mg acceptor–nitrogen [N] vacancy) in GaN.* We performed calculations based on DFT to study the behavior of H at solution sites in GaN and near defects. Comparison of solution sites in zinc-blende and wurtzite GaN shows that H exhibits similar energetics in the two crystal structures, although H molecules are more stable in wurtzite because of the existence of extended trigonal channels in this phase. Furthermore, H is predicted to be equally stable at bond-centered and N antibonding sites in *p*-type wurtzite GaN. The stable site for H near a substitutional Mg atom has been determined for wurtzite GaN and, contrary to expectations, H is most stable at a N antibonding site adjacent to the Mg atom instead of at a bond-centered site as is the case in most semiconductor systems. The instability of the bond-centered site results from compression of the Mg–N bonds—this compression reduces the energy that can be gained by relaxing back bonds when the Mg–N bond is broken and H is inserted.

- *Studied strain relaxation in (Al,Ga)N heteroepitaxial structures.* We investigated strain relaxation of AlGa_xN_{1-x}/GaN heterostructures by transmission electron microscopy (TEM), x-ray diffraction, and *in situ* stress monitor. Relaxation is now thought to occur by a combined mechanism of cracking followed by misfit propagation on the interfacial plane, since the hexagonal nitride crystals do not have a slip system that can provide strain relaxation by glide of dislocations between the interface and the free surface. Instead, tension builds until cracks initiate at the surface and propagate to the interface, and then dislocations propagate from the cracks laterally along the interface.

- *Developed low-O content AlGaN MOCVD process.* O

behaves as a shallow donor in (Al,Ga)N and is often incorporated inadvertently during sample loading. We enclosed our MOCVD reactor with a N loadlock with an O content at the ppm level. We reduced the O concentration in AlGaN from mid- 10^{18} cm⁻³ to low- 10^{17} cm⁻³ (measured by SIMS).

- *Demonstrated high (> 20%) Al content AlGaN MOCVD-grown layers.* We demonstrated the growth of AlGaN with an Al fraction up to 44%. While the gas-phase parasitic reactions between trimethyl aluminum (TMA), trimethyl gallium (TMG), and ammonia still complicate the control of incorporation rates, the employment of an O-free load-lock has greatly reduced the tendency of Al reaction with O adsorbates inside the growth chamber.

Refereed

Donovan, S., J. Han, J. J. Figiel, M. H. Crawford, M. A. Banas, and M. E. Bartram. 1999. "Comparative Studies of AlGaN Grown by Trimethylaluminum (TMAI) and Tri-tertiarybutylaluminum (t-Bu3Al)." Paper presented to the 9th Biennial Workshop on OMVPE, Ponte Vedra Beach, FL, 23 May.

Han, J., A. G. Baca, C. G. Willison, R. J. Shul, L. Zhang, F. Ren, A. P. Zhang, G. T. Dang, S. M. Donovan, X. A. Cao, H. Cho, K. B. Jung, C. R. Abernathy, S. J. Pearton, and R. G. Wilson. 1999. "Growth and Fabrication of GaN/AlGaN Heterojunction Bipolar Transistors." *Appl. Phys. Lett.* **74** (3 May): 2702.

Myers, S. M., T. J. Headley, C. R. Hills, J. Han, G. A. Petersen, C. H. Seager, and W. R. Wampler. 1999. "The Behavior of Ion-Implanted Hydrogen in Gallium Nitride." *MRS J. Nitride Semicond. Res.* **4S1** (1 April): G5.8.

Wright, A. F. 1999. "Influence of Crystal Structure on the Lattice Sites and Formation Energies of Hydrogen in Wurtzite and Zinc-Blende GaN." *Phys. Rev. B* **60** (15 August): R5101.

Wright, A. F. 1999. "Theoretical Investigation of Hydrogen in Wurtzite GaN." Paper presented to the 1999 APS March Meeting, Atlanta, GA, 20-26 March.

3506570000

Ultra-Low-Power Sensors for Microtelemetry Systems

R. C. Hughes, J. R. Wendt, D. D. Chu

Sandia will design, fabricate, and test ultra-low-power sensors that are capable of being powered and read out by analog circuits that are in turn capable of coupling the sensor information to radio frequency (RF) telemetry. The microelectrochemical cell (MEC) is a key enabling technology for a wide variety of chemical sensors in the sensor/tag combination and opens the door to new applications in sensing for counterproliferation, weapon monitoring, and many other areas. The current state of electronic tagging circuits is effective for grain-of-rice–to jelly-bean–sized chips that can be remotely powered, programmed, and read out. The first new sensors proposed for this project are polymer film composites with metal powders. They conduct by percolation, and swelling of the polymer causes an increase in film resistance. A second kind of chemiresistor film involves the conductivity of ions and how that is affected by various analytes. Considerable literature on electroactive chemically sensitive films has developed over the last few years, and Sandia has the technology to combine the tagging electronics with these low-power electrochemical sensors. Issues to be resolved include the quality and type of data to be transmitted, how to handle analog data from the sensor as well as ultra-low-power management, and the range of operation. Other technical issues would involve the levels of voltage and charge required to obtain a reliable readout.

We developed the fabrication technology to deposit several different kinds of chemiresistors on very small electrode patterns using a computer-controlled liquid-dispensing system. We fabricated arrays of four different kinds of chemiresistor covering most of solvent space along with on-chip temperature sensors and heaters. We think that all solvents will give a signal on at least one of the sensors in the array and that individual solvents can be detected using pattern recognition (PR) software developed at Sandia. We demonstrated one of these square-centimeter-size arrays in a prototype, battery-operated, hand-held sensor unit with telemetry by transmitting chemical signals from a parking lot about 100 yards to a laptop inside a building. We did this demonstration for future possible customers of the technology. We designed an integrated circuit

The microelectrochemical cell (MEC) is a key enabling technology for a wide variety of chemical sensors in the sensor/tag combination and opens the door to new applications in sensing for counterproliferation, weapon monitoring, and many other areas.

(IC) chemiresistor array where the electronics to read out the chemiresistors are on the same chip with the electrodes for the chemiresistors. We designed the circuit to perform several functions to make the sensor data more useful. We implemented a new electronic temperature compensation circuit that can accommodate both positive and negative temperature coefficients of resistance by the adjustment of circuit resistance; the chemiresistor resistance is measured in a four-terminal configuration, and to accommodate the wide dynamic range of resistance to chemical signals, a linear-to-logarithmic circuit encompasses several decades of resistance change in a 0- to 4-volt output. A separate high-gain output allows observation of small changes in chemiresistor resistance, and the signal voltage outputs are buffered so that many kinds of analog/digital (A/D) and signal telemetry can be used to transfer the chemical signal to the user. We fabricated the circuit with aluminum (Al) electrodes, and in a post-processing step, we covered the Al with a platinum/titanium (Pt/Ti) layer and deposited the chemiresistor materials with a computer-controlled liquid-dispensing system.

We discovered a new mechanism for chemiresistor chemical sensing. In the course of examining the sensing properties of the solid polymer electrolyte, polyethyleneoxide (PEO), we found a vast difference in the sensing of semicrystalline films and purely amorphous films. It had previously been thought that volatile organic analytes were affecting the polymer chain flexibility and thus causing increased ion conductivity with increasing analyte partial pressure. However, the very large signals from the semicrystalline films led us to believe that the predominant mechanism in those films is the melting of crystalline regions along the necks or grain boundaries of the crystals. We observed good signals from sub-ppm concentrations of the chemical weapon (CW) simulant DIMP with these sensors, by far the most sensitive of the chemiresistors.

Refereed

Butler, M. A., G. Frye-Mason, R. C. Hughes, and G. C. Osbourn. 1999. "Chemical Microsensor and Micro-Instrument Technology at Sandia National Laboratories." *Proc. 2nd Internat. Conf. on Integrated Micro-/Nanotechnology for Space Applications* (Pasadena, CA, 11–15 April).

Eastman, M. P., R. C. Hughes, W. G. Yelton, A. J. Ricco, S. V. Patel, and M. W. Jenkins. 1999. "Application of the Solubility Parameter Concept to the Design of Chemiresistor Arrays." *J. Electrochem. Soc.* (October).

*We discovered a new mechanism
for chemiresistor chemical
sensing.*

Hughes, R. C., W. G. Yelton, S. V. Patel, and K. B. Pfeifer. 1999. "Ion-Conducting Polymer Films as Chemical Sensors." *Proc. Chemical Sensor Symp., 196th ECS Meeting* (Honolulu, HI, 17–22 October).

Patel, S. V., M. W. Jenkins, R. C. Hughes, W. G. Yelton, and A. J. Ricco. 1999. "Differentiation of Chemical Components in a Binary Solvent Vapor Mixture Using Carbon/Polymer Composite–Based Chemiresistors." *Anal. Chem.*, submitted.

Patel, S. V., R. C. Hughes, and W. G. Yelton. 1999. "Effect of Hydroxyl Concentration on Chemical Sensitivity of Polyvinylalcohol/Carbon Black Composite Chemiresistors." *Proc. Chemical Sensor Symp., 196th ECS Meeting* (Honolulu, HI, 17–22 October).

3506580000

Double Quantum-Well Long-Wavelength Optoelectronic Devices

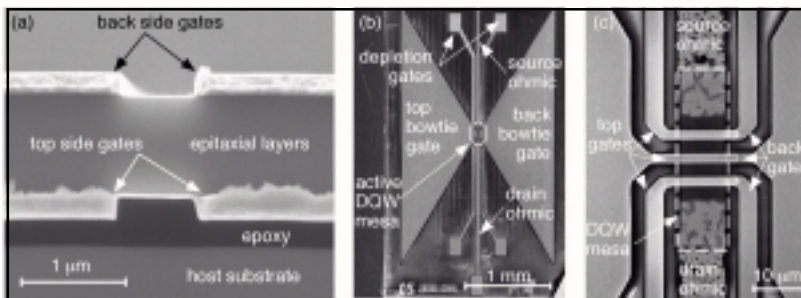
J. A. Simmons, J. R. Wendt, S. K. Lyo, J. L. Reno, S. R. Kurtz, S. Lin

Sandia will research and develop long-wavelength emitters and detectors based on intrasubband transitions in semiconductor-coupled quantum wells (QWs). Present work on long-wavelength optoelectronics is largely based on optical transitions across the intrinsic bandgap in the more exotic semiconductors. In contrast, the unipolar quantum structures on which we will work can be fabricated in the mature aluminum gallium arsenide (AlGaAs) system. Transition energies and thus wavelength and other properties can be tailored across a wide range by appropriately engineering the QWs and intervening barriers. The structures can also be electronically tuned.

Our approach leverages Sandia's innovative processing technology, initially developed for fundamental quantum transport experiments, to realize similar light emitters but with certain features that should enable superior performance. In addition to the application of novel processing technology, we will explore alternative intrasubband transitions.

Because the nature of light emission and detection in the proposed devices is substantially different from that in conventional lasers and detectors, this research provides rich opportunities for investigating fundamental phenomena, including tunneling, phonon-mediated relaxation processes, and electronic states in artificially structured materials. The knowledge gained will be valuable for both quantum and classical microelectronics and photonics. The work also exercises existing compound semiconductor fabrication techniques as well as driving the development of new capabilities for processing long-wavelength waveguide geometry devices.

...this research provides rich opportunities for investigating fundamental phenomena, including tunneling, phonon-mediated relaxation processes, and electronic states in artificially structured materials. The knowledge gained will be valuable for both quantum and classical microelectronics and photonics.



Scanning electron microscope images of a bow-tie antenna-coupled detector. (a) Image of the cleaved cross-section of a test structure, showing front and back gates placed on a semiconductor layer only 1 micron in thickness. (b) Image of the surface of a bow-tie detector. The bow-tie lobes comprise the front and back control gates. (c) Zoomed-in view, showing the active central region of the detector.

The primary goal of this project is to develop room-temperature long-wavelength semiconductor emitters and/or detectors that will be directly relevant to requirements for sensing and other applications. Semiconductor lasers should offer a variety of benefits for systems in terms of functionality. Mid-infrared lasers and detectors can be used for chemical analysis and thermal detection. Electronic tunability and narrowband operation are particularly attractive for spectroscopic systems.

- *Photoresponse of large energy offset detectors in THz (Terahertz) radiation.* We measured the photoresponse of large energy offset double quantum-well (DQW) detectors. The photoresponse appeared to be strongest when one of the electron layers was nearly depleted, indicating that the signal was primarily due to heating. We determined that further improvements in the coupling of the radiation to the structure were needed so that more of the power would go into photon-assisted tunneling (PAT).

- *Design, growth, fabrication, and direct current (dc) testing of bow-tie antenna-coupled detectors.* We designed a new detector geometry, in which a large bow-tie antenna is attached to the structure. Each lobe of the bow-tie forms either the top or back control gate, so that for radiation incident normal to the detector the electric field is steered by the bow-tie to be along the growth direction, appropriate for PAT.

We fabricated several dozen bow-tie antenna-coupled structures, using molecular beam epitaxy (MBE) material grown in collaboration with Bell Laboratories/Lucent Technologies. We placed an oxide/nitride gate insulation layer beneath front and back gates to reduce gate leakage currents.

These structures underwent extensive testing at dc (i.e., dark) to characterize the depletion voltages, I–V curves, position of the tunneling resonances, and effect of control gate bias. Most detectors worked well, exhibiting narrow (a few meV) resonances that could be shifted by gate bias over a wide range.

- *Observation of bolometric THz photoresponse in bow-tie antenna-coupled detectors.* After dc characterization, we measured the photoresponse of these bow-tie structures in collaboration with the University of California–Santa Barbara under a variety of conditions. Parameters varied included frequency, incident power, and gate and source-drain bias conditions. Typically we took source-drain I–V curves at

Because the nature of light emission and detection in the proposed devices is substantially different from that in conventional lasers and detectors, this research provides rich opportunities for investigating fundamental phenomena, including tunneling, phonon-mediated relaxation processes, and electronic states in artificially structured materials. The knowledge gained will be valuable for both quantum and classical microelectronics and photonics.

stepped control gate voltages under various illumination powers and frequencies.

Initial photoresponse measurements exhibited a broad photoresponse, rather than the narrowband response predicted by the Tien-Gordon theory of PAT. (Tien-Gordon theory predicts several additional resonant peaks corresponding to both the absorption and stimulated emission of one or more photons in a tunneling event.)

Because there remained a fairly strong noise background in the measurement system, we made a new measurement system incorporating improved grounding and shielding and performed a new series of measurements. Frequencies investigated included 2.0, 1.5, 1.0, and 0.3 THz.

Again, we observed a strong broadband photoresponse, rather than the narrowband photoresponse peaks predicted by Tien-Gordon. The response was clearly stronger for lower frequencies. In fact, at 300 GHz sample LP03 exhibited a strong response even when the beam from the free electron laser was entirely blocked, so that only stray reflected radiation was present. Such a strong response at such low illumination intensities is highly promising.

At present, we believe that the photoresponse can likely be separated into (1) electron heating and (2) resonant PAT, and that our present structures have sufficient heating that any PAT response is obscured. Two flaws in the structures are probably responsible for the heating. First, the in-plane resistance of the individual QWs is much lower than the inter-QW tunneling resistance, causing most of the power to be absorbed away from the tunneling region. A reduction in the thickness of the tunneling barriers to lower the tunneling resistance should alleviate this problem as well as increase the oscillator strength. Second, the in-plane electric fields are shielded for those regions that lie beneath the surface gates. Hence, most of the heating occurs in the ungated regions of the sample. A new bow-tie geometry could easily be designed in which the ungated areas of the sample are minimized. Such a structure should exhibit substantially reduced heating.

Our approach leverages Sandia's innovative processing technology, initially developed for fundamental quantum transport experiments, to realize similar light emitters but with certain features that should enable superior performance.

Refereed

Lyo, S. K., J. A. Simmons, and N. E. Harff. 1999. "Magnetic Modulations of Optical and Transport Properties of N-Doped Coupled Quantum Wells." *CD-ROM Proc. 24th Internat. Conf. on the Physics of Semiconductors* **1** (January) (Jerusalem, Israel, 2–7 August 1998).

Simmons, J. A., J. S. Moon, M. A. Blount, S. K. Lyo, V. M. Hietala, J. L. Reno, X. G. Peralta, S. J. Allen, P. J. Burke, and J. P. Eisenstein. 1998. "The Double Electron Layer Tunneling Transistor and Optical Applications." (Invited) Presentation made to the Army Research Office—MURI Symposium on Single Electron and Coherent Semiconductor Devices, Princeton, NJ, 19–20 November.

Simmons, J. A., J. S. Moon, M. A. Blount, S. K. Lyo, V. M. Hietala, J. L. Reno, X. G. Peralta, S. J. Allen, P. J. Burke, and J. P. Eisenstein. 1999. "The Double Electron Layer Tunneling Transistor and Optical Applications." Paper presented to the Advanced Heterostructure Workshop, Kona, HI, 29 November–4 December.

Wendt, J. R., J. A. Simmons, J. S. Moon, M. A. Blount, W. E. Baca, and J. L. Reno. 1998. "Double Electron Layer Tunneling Transistors by Dual-Side Electron Beam Lithography." *J. Vac. Sci. and Technol. B* **16** (November–December) (42nd International Conference on Electron, Ion, and Photon Beam Technology and Nanofabrication, Chicago, IL, 26–29 May): 3808–3811.

Other Communications

Burke, P. J., I. Spielman, J. P. Eisenstein, X. G. Peralta, S. J. Allen, J. A. Simmons, L. N. Pfeiffer, and K. W. West. 1999. "Terahertz Photon-Assisted Tunneling in Mesoscopic Double Well Systems." Paper presented to the Meeting of the American Physical Society, Atlanta, GA, 20–26 March.

Peralta, X. G., S. J. Allen, P. J. Burke, J. P. Eisenstein, J. A. Simmons, and J. L. Reno. 1999. "Terahertz Photoconductivity of Double Quantum Wells." Paper presented to the Meeting of the American Physical Society, Atlanta, GA, 20–26 March.

Simmons, J. A. 1999. "Tunable Narrowband FIR Detectors Under Investigation at Sandia." Presentation to the Department of Defense, DDRE, Jaspers Lupo's Division, Arlington, VA, 23 March.

Simmons, J. A., J. S. Moon, M. A. Blount, S. K. Lyo, V. M. Hietala, J. L. Reno, R. Lake, G. Frazier, X. G. Peralta, S. J. Allen, P. J. Burke, and J. P. Eisenstein. 1998. "Development of the Double Electron Layer Tunneling Transistor (DELTT) for Electronics and Optical Applications." (Invited) Presentation to the DARPA Ultra Electronics Program Review, Estes Park, CO, 18–21 October.

3506590000

The Development of Integrated Chemical Microsensors in GaAs

S. A. Casalnuovo, A. G. Baca, A. W. Flounders, S. L. Hietala, J. L. Reno, V. M. Hietala, G. C. Frye-Mason, E. J. Heller

By taking advantage of both the piezoelectric and semiconducting properties of gallium arsenide (GaAs), Sandia will fabricate arrays of acoustic-wave chemical microsensors integrated with microelectronic drive and output circuitry on a single GaAs substrate, resulting in a compact, extremely low-power, highly sensitive, chemical-detection system capable of discriminating among large numbers of liquid and gaseous chemicals. GaAs has several advantages in this application. Its piezoelectric coefficient is comparable to that of quartz, the standard material for acoustic resonator chemical sensors. High-frequency (HF) (nominally 1 GHz) resonator microelectronics are easily fabricated in GaAs using existing GaAs microfabrication technology and are process-compatible with GaAs acoustic devices. Selective etching of GaAs and aluminum gallium arsenide (AlGaAs) epitaxial films makes possible the fabrication of thin (typically 1 to 10 microns) piezoelectric membranes, nominally 100 microns in diameter, capable of high-sensitivity (1 femtogram) detection. No other piezoelectric material can support the integrated microelectronics nor produce the thin-film resonators. No other semiconductor, particularly silicon (Si), is piezoelectric, and fabrication process incompatibilities make the integration of Si and piezoelectrics difficult.

Our goal was to produce miniature arrays of chemical sensors by applying microfabrication technology to integrate, onto the same substrate, acoustic-wave chemical sensors with the microelectronics required to operate them. We expected that these devices would be significantly smaller, require less power, be easier to assemble, and potentially be more sensitive than existing systems. We have substantially achieved this goal and demonstrated improved performance over conventional systems.

Because acoustic-wave sensors require piezoelectric substrates for operation, we focused our research on GaAs. GaAs is piezoelectric and has a commercially available microelectronics technology that performs well at the high frequencies required for effective sensor operation. The sensors' requirement for high-frequency (HF) electronics was

...Sandia will fabricate arrays of acoustic-wave chemical microsensors integrated with microelectronic drive and output circuitry on a single GaAs substrate, resulting in a compact, extremely low-power, highly sensitive, chemical-detection system capable of discriminating among large numbers of liquid and gaseous chemicals.

the principal motivation for integrating the sensors with the electronics. Sensor performance is significantly improved while system packaging and assembly are dramatically simplified if all HF components (sensors and electronics) are fabricated on a single substrate. In addition, there are GaAs micromachining techniques that can produce novel acoustic-wave devices that can operate in liquids and gases with enhanced sensitivity.

As a first step toward the monolithic device, we produced a hybrid sensor array. This comprises a 1-cm-by-1-cm quartz substrate containing three surface acoustic-wave (SAW) chemical sensors and three GaAs integrated circuits (ICs) to drive and read out the sensors. Sandia designed the ICs, which are then commercially fabricated. They are attached to the quartz substrate and wire-bonded to metal traces leading to the SAW sensors. This approach allows us to test the IC design and the system performance without having to work out the complete monolithic fabrication scheme. We successfully produced a three-element chemical sensor array that requires only dc power to operate (120 mW at 3V dc) and provides 3 dc signals as sensor output, all in only one square centimeter. The sensors have sub-part-per-million sensitivities and can distinguish between a large number of volatile organic compounds (VOCs).

The fully integrated version is also designed and fabrication is nearly complete. The same circuits used in the hybrid device were commercially produced on a 4-mm-by-4-mm GaAs die. Within this die, we are also fabricating the three SAW sensors using a post-processing approach. We developed the etch processes to remove the dielectric films deposited during IC fabrication in order to expose the GaAs substrate. We also developed the lithography processes required to produce the SAW sensors on the exposed substrate.

The third phase of this project is to produce improved acoustic-wave chemical sensors by employing GaAs micromachining techniques. Using sacrificial etch processes similar to those used in Si surface micromachining, we produced GaAs membranes as thin as 0.5 micron. These membranes support flexural plate-wave (FPW) modes and thickness shear modes (TSM) that are potentially more sensitive than SAW sensors to adsorbed chemicals and can operate in liquids as well as gases. The FPW device behavior is in excellent agreement with theoretical predictions. The TSM device behavior is in good agreement with predictions, although reliability issues must still be resolved. We produced

We successfully produced a three-element chemical sensor array that requires only dc power to operate (120 mW at 3V dc) and provides 3 dc signals as sensor output, all in only one square centimeter.

TSM devices operating at 3.3 GHz that may ultimately result in monolithically integrated HF oscillators and filters for communications and signal-processing applications.

Refereed

Baca, A. G., E. J. Heller, V. M. Hietala, S. A. Casalnuovo, G. C. Frye-Mason, J. F. Klem, and T. J. Drummond. 1998. "Development of a GaAs Monolithic Surface Acoustic-Wave Integrated Chemical Microsensor." *Proc. 1998 IEEE GaAs IC Symp.* (Atlanta, GA, 1–4 November).

Baca, A. G., E. J. Heller, V. M. Hietala, S. A. Casalnuovo, G. C. Frye-Mason, J. F. Klem, and T. J. Drummond. 1999. "Development of a GaAs Monolithic Surface Acoustic-Wave Integrated Circuit." *IEEE J. Solid-State Circuits* **34** (September): 1254–1258.

Casalnuovo, S. A., G. C. Frye-Mason, R. J. Kottenstette, E. J. Heller, C. M. Matzke, P. R. Lewis, R. P. Manginell, A. G. Baca, S. L. Hietala, W. K. Schubert, V. M. Hietala, D. Y. Sasali, and J. L. Reno. 1999. "Gas-Phase Chemical Detection with an Integrated Chemical Analysis System." *Proc. IEEE Internat. Freq. Control Symp.* (Besancon, France, 13–16 April).

Heller, E. J., C. M. Matzke, V. M. Hietala, R. J. Kottenstette, R. P. Manginell, P. R. Lewis, S. A. Casalnuovo, and G. C. Frye-Mason. 1999. "An Integrated Surface Acoustic Wave–Based Chemical Microsensor Array for Gas-Phase Chemical Analysis Microsystems." *Proc. 196th Electrochemical Society Mtg., Chemical Sensors IV*, (Honolulu, HI, 17–20 October).

3506610000

Monolithic Integration of VCSELs and Detectors for Microsystems

K. D. Choquette, C. T. Sullivan, R. D. Briggs, J. A. Nevers, K. M. Geib, A. A. Allerman

Vertical-cavity surface-emitting lasers (VCSELs) are high-efficiency light sources appropriate for microsystem applications that will benefit from monolithic integration with compatible photodetectors. Such an integration of functions has applications ranging from near-term use in monitors for surety devices to longer-term enabling of on-chip photonic interconnects and advanced microsystems for sensing, surety, data storage, data routing, communication, and image manipulation, processing, and transmission. Moreover, 2-D arrays are an important extension of VCSEL technology, and intermeshed VCSEL/detector arrays will enable numerous advanced applications. Approaches for VCSEL/photodetector integration include the application of metal-semiconductor-metal (MSM) detectors on the laser substrate and the creation of resonant-cavity photodetectors (RCPDs) using the VCSEL epitaxial layers. Note that the detectors could be the same as the VCSEL wavelength, or be designed at different wavelengths using wafer-bonded detector material. This project will address the basic enabling technologies for these approaches and will use combinations of these approaches to create example prototypes that are designed to demonstrate the ability to enable new applications. In addition, this project will include environmental testing (radiation and high temperature) of these devices under conditions appropriate for DOE applications as well as external applications.

(1) We characterized RCPDs and MSM detectors from 100° to 400°K. The RCPD temperature dependence is nearly identical to the behavior of the VCSELs.

(2) We characterized the RCPD responsivity with differing mirror reflectivity (mirror periods). We found a tradeoff between maximum responsivity and bandwidth. Decreasing the number of periods decreases the maximum responsivity while increasing the bandwidth of the light absorption.

(3) We designed and fabricated intermeshed arrays of RCPDs next to or surrounding VCSELs.

(4) We characterized the uniformity of integrated VCSELs/RCPDs. We found the RCPDs have better uniformity than the adjacent VCSELs. This is because the RCPDs are reverse-

Such an integration of functions has applications ranging from near-term use in monitors for surety devices to longer-term enabling of on-chip photonic interconnects and advanced microsystems for sensing, surety, data storage, data routing, communication, and image manipulation, processing, and transmission. Moreover, 2-D arrays are an important extension of VCSEL technology, and intermeshed VCSEL/detector arrays will enable numerous advanced applications.

biased during operation, so no large currents are present to increase the local parasitic heating.

(5) We characterized the performance of VCSELs and MSMs or RCPDs separately and integrated them together (to form an optocoupler) in the presence of high-energy protons. VCSEL/MSM and VCSEL/RCPD optocouplers subjected to high-energy proton irradiation show some degradation of performance, but within specifications appropriate for spacecraft systems.

(6) We characterized selectively oxidized VCSELs biased to produce 1 mW at 80°C. Examining a population of eight devices, we observed one failure (at 1 year), while the remaining devices have operated for > 2 years. We believe that with proper prescreening, selectively oxidized VCSELs exhibit essentially the same reliability characteristics as implanted VCSELs.

Refereed

Briggs, R. D., M. G. Armendariz, K. M. Geib, K. D. Choquette, and D. K. Serkland. 1999. "Fabrication, Packaging, and Performance of VCSELs and Photodetectors for Space Applications." *Proc. SPIE 3627* (VCSELs III, San Jose, CA, January): 40. K. D. Choquette and S. Lei, editors.

Choquette, K. D., A. A. Allerman, H. Q. Hou, K. M. Geib, and B. E. Hammons. 1998. "Applications and Performance of VCSELs." (Invited plenary) Paper presented to the 1998 GaAs IC Symposium, Atlanta, GA, November.

Choquette, K. D., A. A. Allerman, M. J. Hafich, D. K. Serkland, and K. M. Geib. 1999. "Selectively Oxidized VCSELs for Advanced Applications." (Invited) Paper presented to the 1999 Micro-Optical Conference (MOC '99), Tokyo, Japan, July.

Choquette, K. D., and R. Bryan. 1999. "Vertical-Cavity Lasers: New Light for the Information Age." (Invited) Presentation made to the Science and Technology Policy Institute, Washington, DC, March.

Choquette, K. D., K. M. Geib, A. A. Allerman, D. K. Serkland, J. A. Nevers, and J. J. Hindi. 1999. "Integrated VCSEL/Detector Arrays for 2-Dimensional Microsystems." (Invited) Paper presented to the Spatial Light Modulators and Integrated Optoelectronic Arrays Meeting, Snowmass, CO, March.

3506620000

AlGaN Materials Engineering for Integrated Multifunction Systems

J. Han, N. A. Missert, M. H. Crawford, S. J. Martin, D. M. Follstaedt, R. J. Shul, S. A. Casalnuovo, J. G. Fleming, S. R. Lee

Sandia optimized various growth and device processing techniques toward the demonstration of high-brightness (1 mW) ultraviolet (UV) light emitters. We achieved p-type doping of (Al,Ga)N (aluminum gallium nitride) that is among the highest reported. We investigated dry etching of AlGaN for improved anisotropy and smoothness for optoelectronic applications. We demonstrated AlGaN multiquantum-well light-emitting diodes (LEDs) emitting at 338 nm, possibly the shortest-wavelength emitter from a semiconductor light-emitting diode. Our work revealed a potential tradeoff between short-emission wavelength and high-emission power output. By optimizing the growth conditions and using indium (In) to enhance the radiative recombination efficiency of the active layer, we increased the photoluminescence (PL) efficiency by more than two orders of magnitude. We successfully demonstrated surface acoustic-wave (SAW) in GaN, which enabled the evaluation of the piezoelectric properties of GaN. We also investigated the compatibility of GaN with the Sandia silicon (Si) processing facility using silicon nitride (SiN) as a diffusion barrier.

- *Evaluated and optimized the p-type doping of AlGaN alloys.* We closely investigated the physical transport and incorporation of the magnesium (Mg) precursor (Cp2Mg). We found that Cp2Mg tends to condense and adsorb easily on the cold surface upstream to the susceptor during gas delivery. Such premature condensation could lead to (1) a loss of Mg dopant efficiency, (2) inability to precisely control the Mg incorporation, and (3) very slow turn-on and turn-off transient leading to broadened doping profile. The gas-injection inlet configuration was henceforth modified and the inlet temperature was increased to avoid condensation. We have since optimized the Mg-doping; we demonstrated free-hole concentrations of $1 \times 10^{18} \text{ cm}^{-3}$ for GaN and $1 \times 10^{17} \text{ cm}^{-3}$ for AlGaN (15% Al), which are among the highest reported.

- *Evaluated electrical and optical properties of AlGaN UV (< 350 nm) LEDs.* We incorporated approximately 5% Al in the GaN quantum wells to form an Al_{0.05}Ga_{0.95}N alloy. We

We achieved p-type doping of (Al,Ga)N (aluminum gallium nitride) that is among the highest reported....By optimizing the growth conditions and using indium (In) to enhance the radiative recombination efficiency of the active layer, we increased the photoluminescence (PL) efficiency by more than two orders of magnitude.

believe this is the first time that an AlGaN QW LED has been demonstrated.

- *Demonstrated processing techniques for making AlGaN LEDs and laser diodes.* Compared to their more mature arsenide and phosphide counterparts, the III–V nitride-based LEDs suffer from higher-threshold current density and lower quantum efficiency. The reason for this is partly due to the lack of vertical profiles and sidewall roughness of the dry-etched laser facets in the III–V nitride structures, resulting in low mode reflectivity and high optical scattering loss. Therefore, it is essential to develop dry-etch processes that yield anisotropic, smooth sidewalls. We studied GaN sidewall profiles as a function of inductively coupled plasma (ICP) etch parameters and obtained sidewall angles ranging from less than 70° to greater than 85° for $\text{BCl}_3/\text{Cl}_2/\text{Ar}$ -based ICP chemistries.

- *Demonstrated optically pumped lasing from GaN (or AlGaN) structures.* We have not yet completed this task. We determined that our planned efforts in optically pumped lasing were premature, given the efficiencies of the GaN QW structures, and that a more constructive effort was to postpone optical pumping studies until we had developed more efficient active regions and LEDs. There are reports in the literature that the addition of small amounts of indium (In) to GaN to form InGaN for the active region could substantially increase the efficiency of the active regions while remaining at near-UV wavelengths. Our effort involved extensive materials growth and characterization to enable the growth of InGaN alloys with very small In concentrations (0.3–3%). PL measurements of InGaN epilayers showed increased output efficiency with In addition and increased emission wavelength from 365–380 nm. Optical emission efficiency was enhanced by more than two orders of magnitude.

- *Demonstrated AlGaN-based SAW devices.* As a first step, we designed, fabricated, and tested SAW delay lines in 10 μm -thick GaN epitaxial layers on sapphire substrates. We observed repeatable SAW propagation in these samples.

- *Demonstrated the growth of device-quality AlGaN on (111)Si or silicon-on-insulator (SOI) wafers.* We used an AlN buffer to nucleate hexagonal nitride material on (111) Si, whose surface atomic structure also shows hexagonal symmetry. Epitaxial GaN was grown on the AlN buffer. We observed cracking due to the differing thermal expansions of GaN and Si; we examined the material between the cracks with transmission electron microscopy (TEM) and found it to have a microstructure very similar to that of $\text{GaN}/\text{Al}_2\text{O}_3$.

...this is the first time that an AlGaN QW LED has been demonstrated....Optical emission efficiency was enhanced by more than two orders of magnitude.

heterostructure. Thus the material appears structurally suitable for devices.

- *Demonstrated the compatibility of GaN with SiN deposition.* From secondary ion mass spectroscopy (SIMS) measurements, we determined that SiN is a good barrier to Ga diffusion. Good-quality SiN deposited by low-pressure chemical vapor deposition (LPCVD) appears to be a good Ga barrier (as determined by the sharp SIMS profile); however, poorer quality films deposited by plasma-enhanced CVD (PECVD) or sputtering do not appear to be effective.

Refereed

Bartram, M. E., J. Han, M. H. Crawford, M. E. Coltrin, and N. A. Missert. 1998. "Manipulation of Growth Modes in GaN CVD for Defect Reduction and Luminescence Uniformity." *Proc. Fall '98 MRS Meeting* (Boston, MA, 30 November–4 December).

Cho, H., Y. B. Hahn, D. C. Hays, C. R. Abernathy, S. M. Donovan, J. D. Mackenzie, S. J. Pearton, J. Han, R. J. Shul, and J. R. Lothian. 1999. "III-Nitride Dry Etching: Comparison of Inductively Coupled Plasma Chemistries." *J. Vac. Sci. Technol.* **A17**: 2202.

Follstaedt, D. M., J. Han, P. P. Provencio, and J. G. Fleming. 1999. "Microstructure of GaN Grown on (111) Si by MOCVD." *MRS Internet J. Nitride Semiconductor Research* **4S1**: G3.72.

Han, J., and M. H. Crawford. 1999. "OMVPE Growth of AlGaInN for UV Light Emitters." Paper presented to the SSDM '99, Tokyo, Japan, 21–24 September.

Han, J., M. H. Crawford, E. Shul, S. Hearne, E. Chason, J. Figiel, and M. Banas. 1999. "Monitoring and Controlling of Strain During MOCVD of AlGaIn for UV Optoelectronics." *MRS Internet J. Nitride Semiconductors* **4S1**: G7.7.

Shul, R. J., C. J. Willison, M. M. Bridges, J. Han, J. W. Lee, S. J. Pearton, C. R. Abernathy, J. D. MacKenzie, and S. M. Donovan. 1998. "High-Density Plasma Etch Selectivity for the III–V Nitrides." *Solid-State Electronics* **42**: 2269.

Shul, R. J., J. Han, and A. G. Baca. 1999. "Fabrication and Performance of GaN/AlGaIn Heterojunction Bipolar Transistors." *Proc. Spring '99 MRS Meeting* (San Francisco, CA, 5–9 April).

Shul, R. J., J. Han, and A. G. Baca. 1999. "High-Density Plasma-Induced Etched Damage of GaN." *Proc. Spring '99 MRS Meeting* (San Francisco, CA, 5–9 April).

Shul, R. J., L. Zhang, A. G. Baca, C. Willison, J. Han, and M. H. Crawford. 1999. "High-Density Plasma Etching of Group-III Nitride Films for Device Applications." Paper presented to the SOTAPOCS, Electrochemical Society, Seattle, WA, 3–7 May.

Willan, C. C., M. E. Bartram, J. Han, J. G. Fleming, M. H. Crawford, N. A. Missert, A. G. Baca, J. Figiel, and M. Banas. 1999. "Selective Area Growth of $\text{Al}_x\text{Ga}(1-x)$ Using Patterned Substrates." *Proc. MRS Spring '99 Meeting* (San Francisco, CA, 5–9 April).

Other Communications

Crawford, M. H., W. W. Chow, A. F. Wright, S. R. Lee, E. D. Jones, J. Han, and R. J. Shul. 1999. "Wide-Bandgap Compound Semiconductors to Enable Novel Semiconductor Devices." Sandia Technical Report SAND99-0817, Sandia National Laboratories, Albuquerque, NM.

3506630000

Compliant Substrates for Epitaxial Integration of Dissimilar Materials

J. A. Floro, J. Y. Tsao, D. M. Follstaedt, S. R. Lee, J. F. Klem

This project will explore a promising approach to a substrate with a continuously variable lattice constant, the so-called compliant substrate. In collaboration with Cornell University, Sandia is focused on demonstrating and understanding the nature of compliancy effects in novel twist bicrystal compliant substrates. These substrates differ from the bulk only in the presence of a twist homointerface (created by wafer fusion) located just below the growth interface. Sandia's capabilities combining novel in situ diagnostics with advanced growth reactors and our expertise in heterostructure processing and properties uniquely position us for success in this area.

We performed several experiments to characterize the relaxation of strain at high Ge (germanium) fraction (greater than 0.5) in SiGe alloys on Si, using standard monolithic Si substrates. These films exhibited some interesting differences in behavior relative to low Ge fraction films in terms of the hierarchy of strain-relieving morphological transitions. We also got our stress sensor fully operational on the molecular beam epitaxy (MBE) system for antimonide compound semiconductor growth. But, again, the complete lack of twist-bonded substrates frustrated our efforts to gain further insight into compliancy behavior.

Refereed

Floro, J. A. 1999. "Length Scales in Quantum Dot Arrays: What They Tell Us About the Physics." Paper presented to the Gordon Conference on Thin Films and Crystal Growth, Plymouth, NH, 20–25 June.

Sandia is focused on demonstrating and understanding the nature of compliancy effects in novel twist bicrystal compliant substrates.

3506640000

Post-Processed Integrated Microsystems

R. J. Shul, T. R. Christenson, K. O. Wessendorf, W. K. Schubert, S. A. Casalnuovo, S. H. Kravitz

Sandia will develop a low-cost platform for integrated microsystems that is easily configured to meet a wide variety of specific applications-driven needs. Once developed, this platform, which incorporates many of the elements that are common to numerous microsystems, will provide integrated microsystem users access to this technology without paying the high upfront development costs that are now required. The process starts with the fabrication or acquisition of wafers of sparsely placed device or circuit components fabricated in any foundried technology (silicon [Si] complementary metallic oxide semiconductor [CMOS] or bipolar technologies, high-frequency (HF) gallium-arsenide [GaAs] technologies, microelectromechanical systems [MEMS], etc.). We call these smart substrates. Using Sandia's diverse processing capabilities, we will then post-process high-value components in open areas on the front or the back of the wafers, and microelectronically integrate the added components with the preplaced circuitry. Examples of post-processed components include sensors, antennas, surface acoustic-wave (SAW) devices, passive elements, microoptics, and surface-mounted hybrids. The combination of preplaced electronics and post-processed components will enable the development of many new types of integrated microsystems. Targeted applications include integrated sensed systems, tags, and electro-mechanical systems.

(1) We demonstrated a robust electroplated via technology for > 400-micron-thick Si structures. Even using steam oxidation, 100- and 300-micron-wide vias showed no contact.

(2) A single-chip SAW chemical sensor system with the sensor array, drive electronics, and readout electronics monolithically integrated on a GaAs substrate was fabricated by a commercial GaAs foundry and is currently being post-processed to add the SAW sensor array. We developed the etch process required to remove the dielectric layers that result from the integrated circuit (IC) fabrication in order to expose the GaAs substrate. This process selectively removes silicon dioxide (SiO₂), silicon nitride (SiN), and polymers, but does not etch metal (Au) or GaAs. We also demonstrated that we can pattern the SAW electrodes in the 7 μm-deep wells that

...this platform, which incorporates many of the elements that are common to numerous microsystems, will provide integrated microsystem users access to this technology without paying the high upfront development costs that are now required.

result from this etch, using an e-beam lithography lift-off process. The direct-write e-beam lithography system is critical in this project because it has adequate depth of focus to produce the electrode pattern in the etched wells. Conventional contact lithography could not produce the necessary electrodes. We successfully etched the first product wafer from the foundry and will add SAW sensor electrodes as soon as the e-beam is running again. These devices will then undergo electrical and chemical testing.

(3) We fabricated hybrid quartz SAW sensor arrays (1 cm by 1 cm) that comprise three SAW sensors and lithographically patterned wiring interconnects on the quartz substrate. We attached GaAs radio frequency (RF) ICs to drive and read out the sensors to the quartz substrate and wire-bonded them to provide electrical connection. We then attached a machined Pyrex lid to provide the gas-flow channel. This approach provides dc in/dc out operation at the quartz substrate; that is, all HF components are contained within the quartz substrate. These devices require 120 mW at 3 V dc to operate. They demonstrated sub-ppm sensitivity to a number of volatile organic compounds (VOCs).

(4) We developed a chemiresistor application-specific integrated circuit (ASIC) microsystem that will measure chemiresistor elements post-processed onto the IC substrate. We will then post-process the chemiresistor array on top of the ASIC die to yield a single-chip chemical-sensing system. We plan to demonstrate chemical plume detection by the chemiresistor ASIC mounted on a miniature robot at the end of the fiscal year.

(5) We fabricated an integrated magnetic flexural plate-wave (FPW)–sensored device using an amorphous-diamond (a-D) film as the membrane and deep reactive ion etch (DRIE) to form the Si via. The a-D films have significant advantages over more conventional low-stress SiN films for DRIE-processed mag-FPW devices because they offer significantly higher etch selectivity with respect to Si. The improved selectivity gives more flexibility in achieving the desired membrane edge profile. We processed diamond films ranging from 0.2 to almost 2 microns thick into mag-FPW two-port resonators. Film tension is controlled with post-deposition annealing. Early efforts produced devices with reasonable electrical characteristics for many sensor applications, although uniformity across the 100 mm wafer was poor. Subsequent efforts concentrated on achieving uniform, repeatable film properties over most of the wafer.

The direct-write e-beam lithography system is critical in this project because it has adequate depth of focus to produce the electrode pattern in the etched wells.

Refereed

Baca, A. G., E. J. Heller, V. M. Hietala, S. A. Casalnuovo, G. C. Frye-Mason, J. F. Klem, and T. J. Drummond. 1999. "Development of a GaAs Monolithic Surface Acoustic-Wave Integrated Circuit." *IEEE J. Solid-State Circuits* **34** (September): 1254–1258.

Shul, R. J. 1998. "Selective, Deep Si Trench Etching with Dimensional Control." *Proc. SPIE, Micromachining and Microfabrication Process Technology IV* **3511** (Santa Clara, CA, 21–22 September): 252–261.

Other Communications

Baca, A. G., E. J. Heller, V. M. Hietala, S. A. Casalnuovo, G. C. Frye-Mason, J. F. Klem, and T. J. Drummond. 1998. "Development of a GaAs Monolithic Surface Acoustic-Wave Integrated Chemical Microsensor." *Proc. 1998 IEEE GaAs IC Symp.* (Atlanta, GA, 1–4 November).

Casalnuovo, S. A., G. C. Frye-Mason, R. J. Kottenstette, E. J. Heller, C. M. Matzke, P. R. Lewis, R. P. Manginell, A. G. Baca, S. L. Hietala, W. K. Schubert, V. M. Hietala, D. Y. Sasaki, and J. L. Reno. 1999. "Gas-Phase Chemical Detection with an Integrated Chemical Analysis System." *Proc. IEEE Internat. Freq. Control Symp.* (Besancon, France, 13–16 April).

Heller, E. J., C. M. Matzke, V. M. Hietala, R. J. Kottenstette, R. P. Manginell, P. R. Lewis, S. A. Casalnuovo, and G. C. Frye-Mason. 1999. "An Integrated Surface Acoustic-Wave-Based Chemical Microsensor Array for Gas-Phase Chemical Analysis Microsystems." *Proc. 196th Electrochemical Society Mtg., Chemical Sensors IV*, accepted.

3506660000

Development of Radiation-Hard Sensors for Space-Based Visible and Infrared Sensing Applications

R. R. Kay, J. L. Rienstra, S. K. Dunlap, D. V. Campbell, M. K. Hinckley

A growing demand for radiation-hardened visible and infrared (IR) image sensors exists in the military space applications community. Custom image sensor design and manufacture capability exists in private industry, but little attention is given to the need for radiation-hardened products.

This project targets image sensor and IR readout integrated circuit (IC) design and fabrication using the radiation-hardened fabrication process (CMOS6R [complementary metallic oxide semiconductor] process).

Sandia designed a test device to assess the performance of image sensors fabricated using this process. The device contains structures for evaluating photodiode optical performance, unit cell amplifier characteristics, row and column amplifier performance, and digital circuitry needed to perform multiplexing functions.

We implemented several topologies for both photodiode and unit cell structures. Photodiode structures include N+ to P epitaxial layer, N+ to P well, and N well to P epitaxial layer. Unit cell amplifier structures include capacitive transimpedance, direct injection, and source follower configurations.

We designed a test device, referred to as DART (Detector Array Test), to investigate the performance of the building blocks of a visible imager or IR readout device in Sandia's CMOS6R process. A design goal of DART was to allow testing of the component blocks individually, as well as to provide an operational device in which all components work together. Thus, DART contains two primary sections: a 128 x 16-pixel focal plane array, and a device characterization block.

We designed the unit cell amplifier to convert the charge generated by the silicon photodiode (or by an external IR photodiode) to a voltage. Some of the more important parameters of the unit cell amplifier are noise level, conversion gain, saturation level, input impedance, linearity, and physical size. We designed the three amplifier topologies to optimize one or more of the above parameters.

This project targets image sensor and IR readout integrated circuit (IC) design and fabrication using the radiation-hardened fabrication process (CMOS6R [complementary metallic oxide semiconductor] process).

- The source follower (SF) topology uses the least area for the amplifier components and thus allows for most of the pixel area to be used for the photodiode. The diode capacitance converts the photo charge generated to voltage. Modeling indicates a noise level of 145 electrons, with a saturation level of 3.4 million electrons. It is not a good choice for use with IR diodes because of its high input impedance.

- The capacitive transimpedance amplifier (CTIA) topology uses much more area than the SF. The photocharge generated is converted to voltage by a polysilicon-to-polysilicon capacitor and is thereby very linear. Modeling indicates a noise level of 60 electrons with a saturation level of 125,000 electrons. It is a good choice for use with IR diodes because of its low input impedance.

- The direct injection (DI) topology uses slightly less area than the CTIA. Its input impedance and noise level are somewhat higher.

The device characterization block allows for testing individual transistors (primarily for noise characterizations), column and video buffer amplifiers, and photodiodes. The photodiode test structures include various diode formations with a variety of surface structures (with and without silicide removal, with and without passivation glass removal). Also included are structures to test various methods for photodiode-to-photodiode isolation, including trench and P+ guard rings.

The design of the DART device is complete and fabrication has begun.

The source follower (SF) topology uses the least area for the amplifier components and thus allows for most of the pixel area to be used for the photodiode.

3506680000

Silicon Three-Dimensional Photonic Crystal and Its Applications

S. Y. Lin, S. K. Lyo, J. G. Fleming

With an innovative silicon (Si) processing technique, Sandia made a historical breakthrough three-dimensional (3-D) photonic crystal. For the first time, a 3-D crystal was created at a wavelength of $\lambda=1.55 \mu\text{m}$, opening up tremendous opportunity for optical communication applications. This is the smallest 3-D crystal ever made with the shortest operating wavelength, about a factor of 10 improvement over our previous 3-D crystal.

A less well-known and yet equally important application of a 3-D photonic crystal is thermal emissivity engineering. The ability to control, suppress, and manipulate thermal emission of an object in the infrared (IR) $\lambda=3-6$ and $8-12 \mu\text{m}$ wavelengths will enable many important military applications. Examples are thermal sensing, IR countermeasure, and thermal image control. Our experimental data support the fact that our 3-D crystal has a complete bandgap and is an efficient material for emissivity engineering. Our observation is the first-ever evidence for modification of thermal emission by a 3-D photonic crystal.

(1) With an innovative Si processing technique, we made a historical breakthrough 3-D photonic crystal. For the first time, a 3-D crystal was created at a wavelength of $\lambda=1.55 \mu\text{m}$, opening up tremendous opportunity for optical communication applications. This is the smallest 3-D crystal ever made with the shortest operating wavelength, about a factor of 10 improvement over our previous 3-D crystal.

The photonic bandgap extends over a range of $\Delta\lambda=800 \text{ nm}$, from $\lambda=1.35$ to $2.15 \mu\text{m}$. Such a clean and wide gap would allow for the processing of optical signal with more than 100 THz (Terahertz) bandwidth. At this operating wavelength, the modification of spontaneous emission becomes a realistic possibility. For example, by introducing a gain medium into the optical 3-D photonic crystal, it is now possible to achieve enhanced light emission from a Si microcavity. We carried out a preliminary study using erbium (Er) atom as the gain medium, introduced into the lattice by a high-energy ion implantation.

(2) Localization of light to less than a cubic wavelength, λ^3 , has important quantum consequences. The creation of single-

With an innovative silicon (Si) processing technique, Sandia made a historical breakthrough three-dimensional (3-D) photonic crystal. For the first time, a 3-D crystal was created at a wavelength of $\lambda=1.55 \mu\text{m}$, opening up tremendous opportunity for optical communication applications. This is the smallest 3-D crystal ever made with the shortest operating wavelength, about a factor of 10 improvement over our previous 3-D crystal.

mode cavities and the modification of spontaneous emission are two important examples. A defect formed inside 3-D photonic crystal provides a unique optical environment for light localization. We built single-mode defect cavities for the first time from an IR 3-D photonic crystal. We observed a cavity state with modal volume of less than one λ^3 .

(3) A less-well-known and yet equally important application of a 3-D photonic crystal is thermal emissivity engineering. The ability to control, suppress, and manipulate thermal emission of an object in the IR $\lambda=3-6$ and $8-12 \mu\text{m}$ wavelengths will enable many important military applications. Examples are thermal sensing, IR countermeasure, and thermal image control.

Despite its importance, emissivity modification presents great challenges for the following two reasons. First, it is an intrinsic material property and thus is hard to change. Second, the radiation expands over all 4π solid-angle, with an arbitrary polarization. A 3-D photonic crystal suppresses radiation from all angles with all polarization and is an ideal candidate for the task. For small-area applications, 3-D crystals from a 6-inch wafer may be used to patch and suppress thermal emission. For large-area applications, a thermal paint must be created. We fabricated 3-D photonic crystals for both applications and also carried out preliminary testing for the former.

Our data support the fact that our 3-D crystal has a complete bandgap and is an efficient material for emissivity engineering. Our observation is the first-ever evidence for modification of thermal emission by a 3-D photonic crystal.

Our data support the fact that our 3-D crystal has a complete bandgap and is an efficient material for emissivity engineering. Our observation is the first-ever evidence for modification of thermal emission by a 3-D photonic crystal.

Refereed

Lin, S. Y., and J. G. Fleming. 1998. "A Three-Dimensional Photonic Crystal Operating at Infrared Wavelengths." *Nature* **391** (July): 251.

Lin, S. Y., and J. G. Fleming. 1999. "A Three-Dimensional Photonic Crystal with a Stop Band from 1.35 to 1.95 μm ." *Optics Lett.* **24** (January): 49.

Lin, S. Y., E. Chow, and V. M. Hietala. 1998. "Experimental Demonstration of Guiding and Bending of Electromagnetic Waves in a Photonic Crystal." *Science* **282** (October): 274.

3506690000

Monolithic Micromachined Variable Tuners for Rapid Prototyping and Optimization of Microwave Circuits

L. R. Sloan, S. L. Hietala, G. R. Schuster, C. P. Tigges, A. G. Baca

Microwave tuners are used to measure and optimize the performance of microwave devices by varying the impedance presented to the device. Once the optimal impedance for a performance parameter (noise, power, efficiency, gain, etc.) is known, a circuit is synthesized to present the proper impedance to the device to translate that impedance to the system environment (usually 50 ohms).

Present tuners are greater than 20 cubic inches with coaxial connectors as the interface. Loss incurred in the interface between the tuner and device diminishes the impedance range of the tuner. This project will develop miniature integratable tuners on substrates compatible with microwave devices (mainly gallium arsenide [GaAs] substrates).

This project will develop miniature integratable tuners on substrates compatible with microwave devices (mainly gallium arsenide [GaAs] substrates).

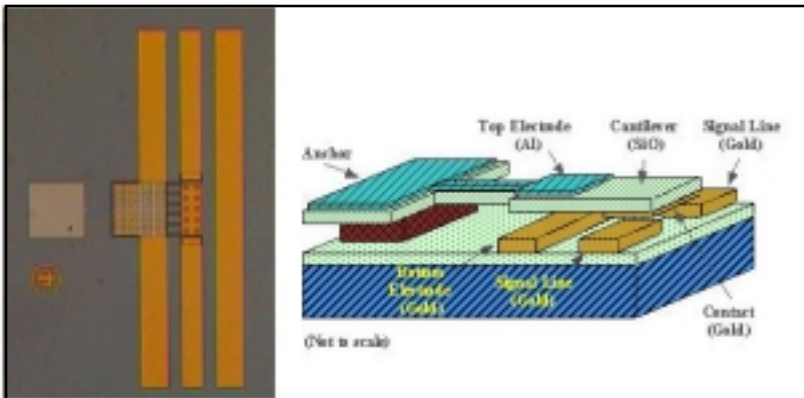


Photo and 3-D diagram of an electro-mechanical switch.

A key element in building an integratable microwave tuner is a small, low-loss, microwave switch. The switch can be used to connect and disconnect distributed and lumped components along a transmission line to present a large array of impedances.

Sandia developed surface microelectromechanical system (MEMS) processing techniques on GaAs substrates to fabricate a microwave MEMS switch. The size of the switch is 0.46 x 0.46 inch. On-state loss is less than 0.3 dB with a return loss of 25 dB from 0.1–20 GHz. Off-state isolation is greater than 25 dB. Switching times were in the range of 22 microseconds with actuation voltages of 27 volts.

Additionally, we developed an analog tuning element that uses a comb drive to move a radial arm. We can use these devices as a tuning element by processing them over a transmission line or to make a variable plate capacitor. Although the devices are functional, we are presently testing the tuning parameters.

We made a 3-D electromagnetic (EM) simulator with optimizer functional to model and simulate the microwave structures. We also developed complex mechanical analysis techniques and employed them to design the mechanical structures.

This year's effort included identifying potential miniature integratable precision-machined (MIPM) structures that could be developed to provide tunable microwave circuits. Initial analysis showed that the MIPM element with the most significant impact in providing microwave tunability would be an electromechanical switch. Successful development of the electromechanical switch would also provide a good starting point for implementing the design tools and developing processing techniques applicable to most of the MIPM structures. The electromechanical switch can also be used to provide a low-loss connection or to isolate lumped and distributed elements along a transmission line to realize a wide range of tunable impedances.

We used a full 3-D EM simulator for the microwave design of the electromechanical switch. We integrated an optimizer with software to allow the analysis of performance tradeoffs for various switch layouts. This enabled the identification of the key geometries of the switch to parameterize.

We modeled the switch parametrically to generate a mask set with 15 different switch designs. Characterization of the different designs would allow verification of the EM modeling and identification of the key geometries of the switch.

We also completed basic mechanical analysis on the switch designs to identify key structures of the switch that would affect actuation voltages, switching speed, stiction, damping, and mechanical stresses.

Several processing techniques had to be developed in order to fabricate the electromechanical switches. The adaptable processing capabilities within the compound semiconductor research labs enabled rapid evaluation of the processes. We performed all processes developed for this effort on GaAs to enable integration with microwave devices and to provide a low-loss substrate for microwave frequencies. Process

We performed all processes developed for this effort on GaAs to enable integration with microwave devices and to provide a low-loss substrate for microwave frequencies.

development included trilevel lift off, anisotropic etching, depositions, and isotropic release of polyimide.

We demonstrated an electromechanical switch. Actuation voltages are between 23 and 28 volts for the various designs. The switches are very low loss in the on state with adequate isolation in the off state. The return loss in the on state shows that electrically the layout of the switch is very close to 50 ohms, which is the characteristic impedance of most microwave environments.

We also completed processing a comb drive and radial arm. The radial arm can be processed over a microstrip line or capacitor bottom plate to make an impedance tuner or variable capacitor. Devices are functional, and quantitative testing is in process.

3506720000

Quantum Tunneling Transistors for Practical Application

J. A. Simmons, N. E. Harff, J. R. Wendt, S. K. Lyo, V. M. Hietala, J. L. Reno

The most significant advance in this project is the demonstration of the three-layer modification of the double electron layer tunneling transistor (DELTT) structure. This new structure provides substantial improvements, including (1) increase of the source-drain operating voltage into the volt range, (2) capability of achieving voltage gain, and (3) additional improvement in the operating temperature. Using an early three-layer structure that did not contain any indium gallium arsenide (InGaAs), Sandia demonstrated gate-controlled negative differential resistance at 0°C, just a hair under our goal of room temperature. We also performed speed measurements on early three-layer DELTTs with short, low-capacitance gates in a ground-signal-ground configuration and proposed a partial circuit model. The measured operating speeds were limited by resonance capacitance (RC) effects and were at a low 100 MHz due to the large tunneling resistances. It should be possible to lower the tunneling resistances by at least two orders of magnitude by decreasing the widths of the tunneling barriers, a goal for next year. Finally, we also developed a theory of nonlinear, nonequilibrium tunneling that included electron-impurity, electron-phonon, and electron-electron interactions, which agreed well with the data below ~ 125°K. (At higher temperatures, lateral effects and thermal activation of DX centers complicate the samples' behavior.)

We accomplished the following:

(1) Growth, fabrication, and temperature measurements of high-temperature DELTTs with InGaAs notches. We simulated, grew, fabricated, and measured a series of two-layer DELTT structures. We tested various structure changes on the operating temperature: (a) narrowing the quantum-well (QW) widths, (b) introducing InGaAs notches in the wells, and (c) adding pure AlAs cladding layers adjacent to the wells. Changes (a) and (b) improved the operating temperature significantly, although the addition of InGaAs lowered the mobility and hence the peak-to-valley ratio. Change (c) showed little improvement, probably because it also lowers the carrier density.

Unfortunately, around 190°K the gate setpoints begin to drift slowly, probably due to thermal excitation of DX centers.

The most significant advance in this project is the demonstration of the three-layer modification of the double electron layer tunneling transistor (DELTT) structure. This new structure provides substantial improvements,....

We are currently investigating ways to remove this problem, such as changing the Al composition near the doping layers.

(2) Demonstration of a three-layer version of the DELTT.

The original two-layer DELTT exhibited two drawbacks. (1) The resonant source-drain voltage is limited to a few tens of mV, incompatible with existing electronics and susceptible to noise. (2) Because the control gate must be biased ~ 100 mV to shift the QW Fermi energy by 10 meV, the two-layer DELTT has a voltage gain much less than unity.

We demonstrated a modified, three-layer DELTT structure that overcomes these difficulties. In this device, after an electron tunnels from the first QW to the second, it continues onward tunneling through a second barrier and into a wide collector layer. The tunneling is thus still 2-D–2-D and very sharp, but the resonant source-drain voltages are on the order of a few volts. Three-layer DELTT EA339 exhibited a resonant current peak near 0.4 V, much larger than the few tens of meV observed in two-layer DELTTs. EA339's control gate was ~ 6500 Å from the emitter, and so greater-than-unity voltage gain was not found. With a 400 Å spacing, as is typically found in high-electron mobility transistors (HEMTs), a voltage gain greater than unity should be obtained.

An additional advantage of the three-layer structure is that the resonant layer need not be occupied, providing several advantages. First, operating voltage can be made even larger. Second, the source-drain capacitance is dramatically reduced, improving the speed of the device. Finally, the three-layer DELTT operates at a much higher temperature than comparable two-layer structures. EA338 demonstrated gate-controlled negative differential resistance at 0°C, or 273°K. It seems certain that $> 300^\circ\text{K}$ will be achieved shortly.

(3) Speed measurements and partial development of a circuit model. We fabricated three-layer DELTTs in a ground-signal-ground geometry for microwave probing and performed speed measurements. With the gates unbiased, the device behaved like a dual-channel HEMT, with a maximum oscillation frequency of ~ 7 GHz. With the gates biased so the device was in the DELTT mode, S-parameter measurements indicated that negative differential resistance survived to only 100 MHz. This is consistent with the very low current density of these early structures. Our model confirms that the DELTT speed is currently limited by the RC charging time of the emitter-collector capacitance. By reducing the thickness of the tunneling barriers, the speed should increase by at least two orders of magnitude.

Our model confirms that the DELTT speed is currently limited by the RC charging time of the emitter-collector capacitance. By reducing the thickness of the tunneling barriers, the speed should increase by at least two orders of magnitude.

(4) *Development of a nonlinear response theory of nonequilibrium 2-D–2-D tunneling.* We developed a theory for nonequilibrium 2-D–2-D tunneling that takes into account electron-impurity, electron-electron, and electron-phonon interactions, and is based on a rigorous second-order perturbative approach. Using it, we numerically evaluated the source-drain I–V curves of a previously measured two-layer DELTT structure (G1881). The theory showed good agreement with 77°K data for source-drain biases below ~ 60 meV, where electrons begin to pass over the depletion gate barriers. Numerical evaluations at 300°K still show a strong peak in the I–V curve, although the data do not. This is likely due to problems with gate stability due to the thermal activation of DX centers, discussed earlier.

Refereed

Blount, M. A., J. A. Simmons, J. S. Moon, W. E. Baca, J. L. Reno, and M. J. Hafich. 1998. “Double Electron Layer Tunneling Transistor (DELTT).” *Semiconductor Sci. and Technol.* **13** (August): A180–A183.

Lyo, S. K., D. Huang, J. A. Simmons, and N. E. Harff. 1999. “Magnetic Modulations of Optical and Transport Properties of N-Doped Coupled Quantum Wells.” *CD ROM Proc. 24th Internat. Conf. on the Physics of Semiconductors* **1** (January) (Jerusalem, Israel, 2–7 August 1998): 0926.

Moon, J. S., J. A. Simmons, M. A. Blount, J. L. Reno, and M. J. Hafich. 1999. “Unipolar Complementary Circuits Using Double Electron Layer Tunneling Transistors.” *Appl. Phys. Lett.* **74** (11 January): 314–316.

Simmons, J. A., M. A. Blount, J. S. Moon, S. K. Lyo, W. E. Baca, J. R. Wendt, J. L. Reno, and M. J. Hafich. 1998. “Planar Quantum Transistor Based on 2D–2D Tunneling in Double Quantum-Well Heterostructures.” *J. Appl. Phys.* **84** (15 November): 5626–5634.

Wendt, J. R., J. A. Simmons, J. S. Moon, M. A. Blount, W. E. Baca, and J. L. Reno. 1998. “Double Electron Layer Tunneling Transistors by Dual-Side Electron Beam Lithography.” *J. Vac. Sci. and Technology B* **16** (November–December): 3808–3811.

Wendt, J. R., J. A. Simmons, J. S. Moon, W. E. Baca, M. A. Blount, and J. L. Reno. 1998. “Dual-Side Electron-Beam Lithography for Independent Submicron Gating of Double Quantum Well Devices.” *Semiconductor Sci. and Technol.* **13** (August) (Surfaces and Interfaces of Mesoscopic Devices '97, Kaanapali, Maui, HI, 8–13 December 1997): A86–A89.

Other Communications

Moon, J. S., J. A. Simmons, M. A. Blount, W. E. Baca, and J. L. Reno. 1999. “Three-Layer Modification of the Double Electron Layer Tunneling Transistor Operating at 0.4 V.” Paper presented to the 1999 March Meeting of the American Physical Society, Atlanta, GA, 20–26 March.

Moon, J. S., J. A. Simmons, V. M. Hietala, W. E. Baca, and J. L. Reno. 1999. “Cryogenic Probing of Double Electron Layer Tunneling Transistors.” Paper presented to the 1999 March Meeting of the American Physical Society, Atlanta, GA, 20–26 March.

Reno, J. L., J. A. Simmons, J. S. Moon, M. A. Blount, and W. E. Baca. 1999. "Double Electron Layer Tunneling Transistors Fabricated in InGaAs/AlAs for Higher Operating Temperatures." Paper presented to the 1999 March Meeting of the American Physical Society, Atlanta, GA, 20–26 March.

Simmons, J. A. 1998. "The Double Electron Layer Tunneling Transistor." Paper presented to the 1998 Advanced Heterostructure Workshop, Kona, HI, 29 November–2 December.

Simmons, J. A. 1998. "The Double Electron Layer Tunneling Transistor." Paper presented to the ARO-MURI Symposium on Single Electron and Coherent Semiconductor Devices, Princeton, NJ, 19–20 November.

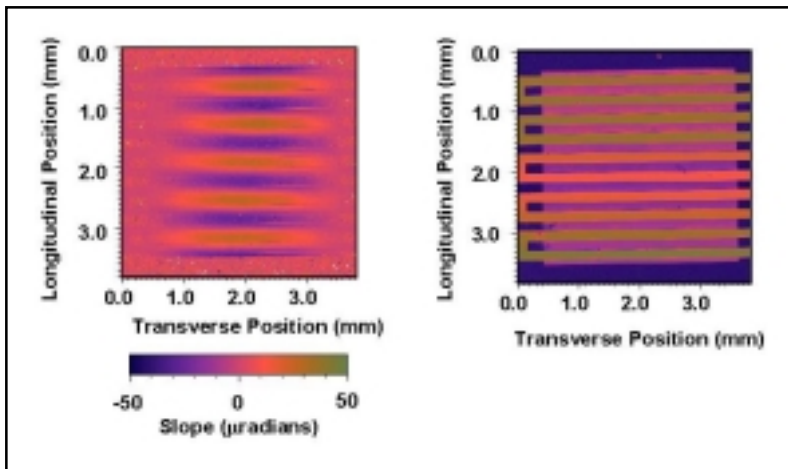
Simmons, J. A., J. S. Moon, M. A. Blount, S. K. Lyo, V. M. Hietala, J. L. Reno, R. Lake, G. Frazier, X. G. Peralta, S. J. Allen, P. J. Burke, and J. P. Eisenstein. 1998. "Development of the Double Electron Layer Tunneling Transistor (DELTT) for Electronics and Optical Applications." Paper presented to the DARPA Ultra Electronics Program Review, Estes Park, CO, 18–21 October.

3506730000

Development of Magnetically Excited Flexural Plate-Wave Devices for Implementation as Physical, Chemical, and Acoustic Sensors, and as Integrated Micropumps for Sensored Systems

W. K. Schubert, P. B. Herrington, R. Chanchani, J. L. Dohner, M. R. Daily, C. P. Tigges, R. J. Shul, D. R. Adkins

Sandia developed the magnetically excited flexural plate-wave (mag-FPW) device as a sensor platform. Work focused on gaining better fundamental understanding of the device through improved fabrication, characterization, and modeling. Preliminary work focused on specific applications, such as physical and chemical sensors, acoustic transceivers, and acoustic streaming micropumps.



The measured mode structure of a 10-leg magnetically excited flexural plate-wave (FPW) device with all legs driven. The left image shows the measured slope of the surface of the FPW membrane when the transducer lines are driven at the 10 x 1 mode resonant frequency. On the right is a false color image of the FPW device, showing the metal lines centered upon square membrane.

Our major goal was to get a more complete understanding of the critical design issues for mag-FPW resonator devices. One key element in reaching this goal was the refinement of our wet-etch-based bulk silicon (Si) micromachining process. This process can now reliably produce devices with critical dimensional control of ± 1 micron. We also made excellent progress in characterization and modeling capabilities. We established a mode imaging capability that allows us to measure membrane displacement amplitudes as small as one nanometer. We can image any mode excitable with the FPW meander-line transducer (MLT). We built up a finite-element modeling (FEM) capability that allows us to calculate mode

This process can now reliably produce devices with critical dimensional control of ± 1 micron.

shapes of driven membranes and to look at the effects of dimensional errors. We designed, fabricated, and imaged special test devices for explicit comparison with the FEM results. This combination of refined fabrication, new measurement, and new modeling capabilities has contributed significantly to our detailed understanding of the FPW resonator device. We verified both empirically and through modeling that the resonant mode structure of our two-port resonators is much more complicated than assumed in our earlier modeling efforts. Multiple resonances in two-port resonators previously ascribed to structural imperfections actually arise from the normal two-port operation where only a subset of the MLT legs is driven; the rest are used as the output port. This means that we can stop pursuing more precise dimensional control and concentrate on working with the expected characteristics. Furthermore, FEM results indicate that membranes oversized by five to ten percent of the wavelength cost very little in performance while providing a more robust fabrication process.

Although we have made great progress in developing the Bosch Si etch for Si micromachining, the dimensional requirements of the FPW resonator membrane are more stringent than any other Bosch application pursued so far. It has proven extremely difficult to define a straight-edged nitride membrane of the proper size after etching clear through a 400-micron-thick wafer. Part of the difficulty lies in the inadequate nitride-to-silicon etch selectivity of the Bosch process. We investigated amorphous, diamond-like carbon membranes for this purpose and found at least an order-of-magnitude-lower Bosch etch rate than the nitride. This may provide the added flexibility needed to define a sufficiently accurate membrane perimeter.

We developed preliminary designs for acoustic streaming test structures and vibration sensors. We also began fabrication of a batch of acoustic-streaming test structures. The vibration sensor development was delayed by the slower-than-expected development of an adequate Bosch etch process. These sensors require accurate membrane dimensions within a multidepth Bosch process, placing even greater demands on the Bosch process.

We investigated amorphous, diamond-like carbon membranes for this purpose and found at least an order-of-magnitude-lower Bosch etch rate than the nitride. This may provide the added flexibility needed to define a sufficiently accurate membrane perimeter.

Refereed

Shul, R. J. 1998. "Selective, Deep Si Trench Etching with Dimensional Control." *Proc. SPIE, Micromachining and Microfabrication Process Technology IV* **3511** (Santa Clara, CA, 21–22 September): 252–261.

Other Communications

Adkins, D. R., W. K. Schubert, M. A. Butler, and A. S. Chu. 1999. "Modeling and Imaging Flexural Plate-Wave Devices." *Proc. 1999 Internat. Mech. Eng. Congress and Expo.*, accepted.

Franco, R. J., C. O. Landron, J. C. Moser, III, D. R. Adkins, W. K. Schubert, and K. O. Wessendorf. 1999. "Nuclear Explosives Package (NEP) Magnetically-Coupled Instrumentation Development." Sandia Technical Report SAND99-0680 (ECI), Sandia National Laboratories, Albuquerque, NM, April.

Schubert, W. K., D. R. Adkins, M. A. Butler, S. J. Martin, M. A. Mitchell, R. Kottenstette, and K. O. Wessendorf. 1999. "Chemical Sensing with a Magnetically-Excited Flexural Plate-Wave Resonator." *Proc. 1999 Joint Internat. Meeting of the ECS and JECS, Chem. Sensors IV*, accepted.

3506740000

Novel Acoustically Driven Microoptoelectronic Devices

E. D. Jones, V. M. Hietala, S. A. Casalnuovo, R. L. White, B. L. Wampler

This project is investigating a novel, new approach for combining optical and surface acoustic-wave (SAW) techniques. In direct bandgap semiconductors, when a photon is absorbed, an exciton is formed in the focused spot region. If there are no interactions that disturb the exciton, it will emit a photon equal to the semiconductor bandgap energy minus the binding energy of the exciton. However, the presence of a short-pulse-duration SAW can transport the exciton from the original focused spot to another spatial location, and the photon is re-emitted. Because of the ability to control the input and output (I/O) locations, such a device could strongly impact several Sandia programs, most notably mass sensors and weapon security devices. Because electron-phonon and exciton-phonon interactions are required for carrier movement leading to spatial relocation, there are basic physics issues that need to be understood, specifically the electron-phonon interaction between the SAW, the exciton, and free carriers. Also, knowledge of exciton ionization processes by the SAW is important. Room-temperature operation is also an issue that must be resolved. In the beginning, this project emphasized the physics of the interaction between an exciton or electron-hole pair (ionized exciton) and the phonons of the SAW. We will pursue temperature effects, theory, and experiment.

Because this project relies on excitons that are being transported large distances (1000 μm), we need stringent sample requirements. Photoluminescence (PL) measurements for the exciton linewidth and lineshape are excellent indicators for sample quality. Initial measurements on molecular beam epitaxy (MBE)-grown gallium arsenide/aluminum gallium arsenide (GaAs/AlGaAs) structures showed poor PL, and subsequently, we tested a series of structures to identify the source of the problems resulting during growth. At this point, we feel that the growth problems are under control and are currently processing a GaAs/AlGaAs 80 \AA -wide single-quantum-well sample, complete with SAW devices.

- *Quantum-well (QW) growth and SAW device fabrication of a test device.* We grew and tested a number of undoped 80 \AA -wide single-QW GaAs/AlGaAs QW structures using PL

Because of the ability to control the input and output (I/O) locations, such a device could strongly impact several Sandia programs, most notably mass sensors and weapon security devices.

characterization techniques. We deemed the first few structures to be unacceptable because of poor PL lineshape and linewidths. Currently, a suitable sample complete with SAW devices is undergoing processing. We designed and partially fabricated a test probe and sample mount for operation at 4°K. The probe consists of two coaxial cables for RF I/O, and two fiber-optic cables for laser input and exciton luminescence detection. To minimize liquid helium (He) loss, low thermal conductivity coaxial cables are required for the SAW I/O signals. We purchased and evaluated several commercial stainless-steel-clad coaxial cable assemblies. We gained experience in soldering these cables for assembling the necessary coaxial fittings for the RF I/O during this period. We tested the cable assemblies at liquid nitrogen (N) temperatures for continuity checks. After we selected and purchased the stainless-steel coaxial cables, we designed and fabricated the sample mount from G10, a commercially available fiberglass material that is suitable for low-temperature operation.

- *Measurement of the frequency dependence of the acoustic attenuation factor.* We acquired and tested all equipment required for the experimental setup with a SAW device built on bulk GaAs. We tested the SAW attenuation characteristics as a function of the SAW frequency between 200 and 1500 MHz using two SAW devices (transmitter and a separate receiver). We found by adjusting either the amplitude and/or the RF pulsewidth that the SAW receiver signal was detectable down to – 40 dbm excitation, thus determining the dynamic range of the experiment. We overcame various problems associated with spurious RF pickup by the receiver by judicious placing of ground shields. We also plan these kinds of RF shields for the new probe.

- *Incorporation of optical fiber I/O mounts and testing of the basic photon transport system.* We designed the complete probe assembly for low-temperature operation and currently are fabricating it in the shops. We can make preliminary measurements using a single fiber by adapting an existing probe used for low-temperature PL studies.

We found by adjusting either the amplitude and/or the RF pulsewidth that the SAW receiver signal was detectable down to – 40 dbm excitation, thus determining the dynamic range of the experiment.

3506750000

Photonics Integration Devices and Technologies

G. A. Vawter, K. J. Kasunic, S. Y. Lin, W. W. Chow, J. R. Wendt, A. A. Allerman, O. B. Spahn, C. T. Sullivan

Sandia is using their world-class expertise in selective aluminum gallium arsenide (AlGaAs) oxidation, dry-etching, high-gain semiconductor laser simulation, and their recent progress in selective-area regrowth of AlGaAs to create new in-plane lasers with interconnecting passive waveguides for use in high-density photonic circuits and future integration of photonics with electronics. Selective oxidation and doping of semiconductor heterostructures have made vertical-cavity surface-emitting lasers (VCSELs) into the world's most efficient low-power lasers. We will use technologies developed for VCSELs to improve etched-facet lasers, making them suitable for monolithic integrated microsystems. We are investigating three types of lasers: (1) a ridge laser with resonant coupling to an output waveguide, (2) a selectively oxidized laser with a low active volume and potentially submilli-Amp threshold current, and (3) a one-dimensional (1-D) photonic lattice laser with the potential to exhibit submicro-Amp threshold current.

We will investigate a variety of methods for enhancing laser reflective feedback and laser-to-waveguide coupling both theoretically and experimentally. In addition to resonant couplers, we will evaluate such novel structures as in-plane refractive lenses formed by selective oxidation, subwavelength diffractive optic lenses, and photonic lattices as laser-to-waveguide couplers. Laser reflective feedback concepts include metal or dielectric-coated facets, single or multiple airgaps, photonic lattice mirrors, and total-internal-reflectance triangular ring cavities. Finally, we will fabricate integrated passive waveguides by selective area regrowth, selective oxidation, or high-temperature diffusion of Al, Ga, and In within adjoining layers.

The result of this project will be a high-performance active/passive photonic integrated circuit (PIC) technology enabling solutions appropriate for future monolithic integrated microsystems. The new technology will comprise highly efficient integrated waveguide-coupled lasers and the combined laser optics and time-dependent gain models that will enable future systems to be developed more efficiently.

Selective oxidation and doping of semiconductor heterostructures have made vertical-cavity surface-emitting lasers (VCSELs) into the world's most efficient low-power lasers.

- We designed and fabricated resonant-enhanced dual-etched-facet lasers and tested them to validate our approach for active-passive waveguide integration using selective-area regrowth. This multiple quantum-well (MQW) GRINSCH laser design shows the predicted improvement trends and specific values of pulsed threshold current of about 20 mA over doubly-etched and of about 10 mA over doubly-cleaved edge emitters.

- We started development of the comprehensive laser model. In its present form the model includes injected current and reflective feedback effects on threshold and efficiency. We benchmarked power output and efficiency against buried-oxide waveguide (BOW) laser data and calculated reflectivity of a resonant reflector.

- We assembled a time-independent microscopic laser-gain model for band-structure engineering and threshold current calculation and used this model to predict threshold gain of specific QW designs.

- We fabricated selectively oxidized nonlinear-optic waveguides and measured optical loss.

- We designed a low-threshold BOW laser. We developed the required process technology and completed fabrication and test of the BOW laser. Finished lasers have quite remarkable ~ 6 mA threshold current and 40% overall efficiency.

- We began selective-area regrowth on GaAs using dry- and wet-etched base epitaxial material with the key discovery that wet etching and mask overhang are beneficial to selective growth. Further work is needed to create smooth surfaces suitable for use in devices.

- We designed and began fabrication of a sub- μ A 1-D laser and demonstrated a photonic bandgap using a 2-D etched hole array. We designed and developed the process sequence and fabricated a 1-D photonic crystal microcavity. We calculated its resonant wavelength to be 1.17 micrometers to match the optical gain of our material, InGaAsN. Using a similar fabrication process, we also fabricated a 2-D photonic crystal waveguide with a stopband at 1.32 micrometers. Using fewer than 10 lattice periods, we reduced light transmission to less than 2% of transmission outside the stopband. This demonstration shows that we can use photonic crystals as very compact and efficient reflectors for microcavity laser applications.

This multiple quantum-well (MQW) GRINSCH laser design shows the predicted improvement trends and specific values of pulsed threshold current of about 20 mA over doubly-etched and of about 10 mA over doubly-cleaved edge emitters.

Refereed

Chow, E., S. Y. Lin, W. Zubrzycki, J. R. Wendt, and G. A. Vawter. 1999. "Experimental Study of Two-Dimensional Photonic Crystal in Optical Regime." Paper presented to the APS Centennial Meeting, Atlanta, GA, 20–26 March.

Vawter, G. A., O. Blum, A. A. Allerman, and Y. Gao. 1999. "Highly Efficient Laser with Self-Aligned Waveguide and Current Confinement by Selective Oxidation." *Proc. IEEE LEOS '99 12th Annual Meeting, Paper WQ4* (San Francisco, CA, 8–11 November).

3506760000

Stress-Free Amorphous Diamond for High-Sensitivity Microsensors with Integrated Microstructures

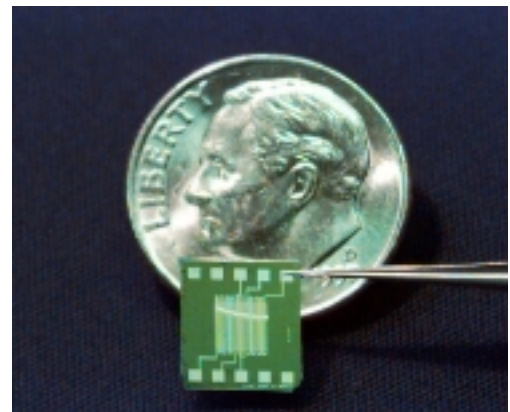
J. P. Sullivan, D. A. LaVan, C. I. H. Ashby, R. J. Shul, M. P. de Boer, W. K. Schubert, T. A. Friedmann

The objective of this project is to develop the science and technology to create high-sensitivity microsensors and rugged microelectromechanical systems (MEMS) using Sandia's recently discovered stress-free amorphous diamond (a-D) films. Work was targeted at demonstrating flexural plate-wave (FPW) devices and single-layer MEMS that use a-D as the working or structural layer. We will develop the FPW devices into chemical sensors by incorporating a polymeric layer that is chemically sensitive. Also, we will develop two-level MEMS structures that will permit direct demonstration of several advantages to the use of a-D compared to other MEMS materials (e.g., poly-Si), including the ability to easily tailor film stress from compressive through zero to slightly tensile, hardness and stiffness 90% that of diamond, very high wear resistance, surfaces that are intrinsically hydrophobic and thus require no stiction-reducing treatment, and extreme chemical inertness.

We demonstrated a-D sensor devices (FPW devices) and MEMS. To our knowledge, these represent the first membrane-based sensors and MEMS fabricated from a-D. To fabricate these devices, we developed a process to reliably create free-standing a-D membranes using a Bosch etch tool. The resulting FPW devices show strong, sharp resonances, making these devices suitable for high-sensitivity FPW-based chemical sensors. We also developed a new process to create the a-D MEMS. This process employs high-density plasma etching of the thick a-D layer and a timed wet-chemical release etch of an underlying sacrificial silicon dioxide (SiO₂) layer. We demonstrated a large variety of structures, including simple micromechanical structures for determining fundamental materials and thin-film properties as well as microelectromechanical structures, e.g., comb drives, to demonstrate electrostatic actuation. We successfully created and tested all structures. We found that we could control the film stress state from slightly compressive to slightly tensile; we could control the film strain gradient from positive to negative; stiction was low (structures could be released without supercritical drying

We demonstrated a-D sensor devices (FPW devices) and MEMS. To our knowledge, these represent the first membrane-based sensors and MEMS fabricated from a-D.

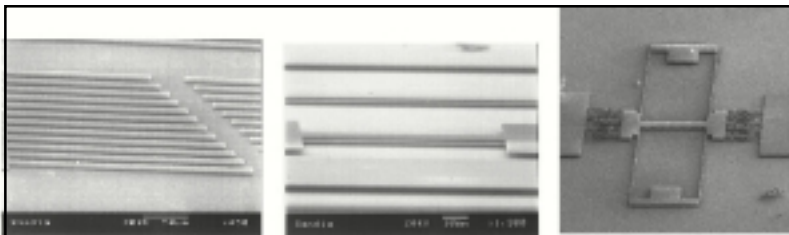
This image shows a flexural plate-wave device that is based on an amorphous diamond freestanding membrane. The pattern metal meander lines on the surface of the membrane permit membrane actuation.



or [self-assembled monolayers] SAMS coatings); and the film elastic modulus was quite high, approaching 750 GPa. We also demonstrated dc actuation of an electrostatic comb drive, yielding a static displacement of several microns and a resonance frequency of 5500 Hz. Currently a-D mechanical structures show great promise for achieving extremely wear-resistant MEMS devices.

In addition to demonstrating working FPW devices and MEMS that are based on a-D, we made several other discoveries regarding the use of a-D for sensors and MEMS. First, we found that the etch selectivity between a-D and Si using the Bosch process is 1 to 1000, meaning that in the time required to etch 1000 units into Si, only one unit of a-D would be etched. The significance of this finding is that it is easier to create ultra-thin free-standing membranes of a-D using a Bosch etch tool than it is to create membranes in other materials, such as silicon nitride (SiN), which has an etch selectivity of 1 to 75. This creates new opportunities for the use of a-D membranes for x-ray or electron detector windows, electron lithography, etc. The ability to fully release a-D MEMS structures without using a stiction-reducing treatment was another important discovery. Since the surface of a-D is hydrophobic, we expected that two a-D surfaces in contact would show little tendency for auto-adhesion due to the capillary action of water trapped between layers (i.e., stiction). Surprisingly, we found that even if only one surface is a-D and the other surface is hydrophilic (e.g., Si), stiction was not a significant issue, and a simple dehydration bake was sufficient to release parts. This is an important result, as issues with stiction can greatly affect the processing requirements and influence the yield and storage lifetime of poly-Si MEMS. Last, we found our theory of the stress-relaxation process in a-D, which is based on a first-order chemical kinetic process involving conversion of some fourfold coordinated carbon to threefold coordinated carbon, to be very successful at enabling a high degree of control of the stress state of the a-D films. This control is critical for achieving the FPW and MEMS devices, and work is advancing at using this

The objective of this project is to develop the science and technology to create high-sensitivity microsensors and rugged microelectromechanical systems (MEMS) using Sandia's recently discovered stress-free amorphous diamond (a-D) films.



Images of three different micromechanical structures fabricated out of a one-micron-thick film of amorphous diamond. The image on the left shows released singly clamped beams. The center image shows released double clamped beams that are in a state of tension. The image on the right shows a comb-drive structure that can be electrostatically actuated.

modeling to control and tune the strain gradient within the a-D film. This would enable the ability to control out-of-plane deflection of released a-D structures and is important for future-generation devices.

Refereed

Friedmann, T. A., J. P. Sullivan, M. P. de Boer, B. P. Jensen, D. A. Lavan, C. I. H. Ashby, J. A. Knapp, D. M. Follstaedt, M. A. Mitchell, and R. G. Dunn. 1999. "Amorphous Diamond MEMS." Paper presented to the 1999 Fall Meeting of the Materials Research Society, Boston, MA, 29 November–3 December.

Friedmann, T. A., J. P. Sullivan, N. A. Missert, D. R. Tallant, J. A. Knapp, D. M. Follstaedt, A. J. Magerkurth, and D. L. Medlin. 1998. "Residual Stress and Hardness in Amorphous Carbon Films Grown by Pulsed Laser Ablation." Paper presented to the 1998 Fall Meeting of the Materials Research Society, Boston, MA, 30 November–4 December.

LaVan, D. A., J. P. Sullivan, T. A. Friedmann, and C. I. H. Ashby. 1999. "Tensile Properties of Amorphous Diamond Films." Paper presented to the 1999 Fall Meeting of the Materials Research Society, Boston, MA, 29 November–3 December.

Sullivan, J. P., T. A. Friedmann, A. J. Magerkurth, M. P. de Boer, M. M. Bridges, and C. I. H. Ashby. 1998. "Amorphous Diamond Micromechanical Structures." Paper presented to the 1998 Fall Meeting of the Materials Research Society, Boston, MA, 30 November–4 December.

Sullivan, J. P., T. A. Friedmann, W. K. Schubert, D. R. Adkins, C. H. Seager, M. A. Mitchell, R. G. Dunn, and R. J. Shul. 1999. "An Amorphous Diamond-Like Carbon Sensor Device." Paper presented to the 1999 Fall Meeting of the Materials Research Society, Boston, MA, 29 November–3 December.

3506770000

Semiconductor Current Filament Lasers

F. J. Zutavern, M. W. O'Malley, G. A. Vawter, A. Mar, H. P. Hjalmarson, W. W. Chow, A. G. Baca

Sandia is developing miniature, short-pulse lasers for at least three general applications that are very important to their missions: (1) active optical sensors weapons systems in limited-visibility environments (optical fuzing, LADAR [laser radar], 3-D imaging, and secure communications), (2) nonlinear crystal pumping for frequency conversion, time-gating, and gain to process signals, (3) direct optical ignition (DOI) of fuels and explosives for military and commercial applications, and (4) micromachining micron-size features patterned over large areas of metals and alloys. At present, the highest-energy short-pulse semiconductor lasers deliver only a few nano-Joules in subnanosecond pulses.

We are making a new, high-beam-quality, semiconductor current filament laser (SCFL) that can produce several orders-of-magnitude more peak-power or short-pulse energy than conventional semiconductor lasers (CSL). These new lasers are created from the current filaments that form in high-gain photoconductive semiconductor switches (PCSS). Low-field, avalanche-carrier generation is the mechanism by which lightning-bolt-like channels of high-density, charge-neutral plasma are formed across the semi-insulating gap of the switch. Unlike CSLs, which inject current across p-n junctions, SCFLs use carriers in the electron-hole plasma of the filaments. The filaments are cylindrical and can be much larger (400 microns in diameter by several centimeters long) than p-n junctions, which are confined in one dimension by the diffusion length, 1–2 microns.

We designed and fabricated three generic types of devices: (1) lateral current flow with surface contacts and edge emission, (2) lateral current flow with transparent edge contacts and edge emission, and (3) vertical current flow with surface contacts and surface emission (quasi-vertical [QV]). The first type was easiest to fabricate but suffered from dead regions where the filaments curved away from the cavity to the contacts. The second type proved to be very difficult to fabricate because the devices had to be cleaved before we could process the transparent edge contacts. The third type allows conventional surface processing of the contacts before cleaving into bars that hold many devices. The epitaxial contacts grown

We are making a new, high-beam-quality, semiconductor current filament laser (SCFL) that can produce several orders-of-magnitude more peak-power or short-pulse energy than conventional semiconductor lasers (CSL).

for this type of device also showed increased longevity at high currents with no evidence of damage after 10,000 pulses at 55 A.

Using these structures, we demonstrated five properties of stimulated emission: spectral narrowing (50 nm spectral width from emission perpendicular to the filament versus 0.1–5 nm parallel to the current filament), a current threshold to optical emission, high intensity (70 nJ in 1 ns), < 3-degree beam divergence, and optical pulse compression (1 ns current pulse with a 10 ns current pulse). We measured optical properties for some of these devices versus temperature, device length, current pulse length, and amplitude. We are presently testing devices with different types of reflective coatings. We observed a high sensitivity to carrier-density uniformity and improved uniformity with tighter line triggering and the QV device structure. We improved electrical contacts on the QV, which demonstrated higher current capability than previous structures.

We calculated the carrier density at the gamma point and threshold to lasing from our collective ionization model for the initiation of current filaments. Although this calculation predicted that the filaments were within the theoretical uncertainty of lasing, a more accurate calculation of the carrier density is required because the present model for filament initiation is insensitive to the region of the distribution that is responsible for lasing (the gamma point).

Refereed

Loubriel, G. M., F. J. Zutavern, A. Mar, H. P. Hjalmarson, A. G. Baca, M. W. O'Malley, W. D. Helgeson, D. J. Brown, and R. A. Falk. 1998. "Longevity of Optically Activated, High-Gain GaAs Photoconductive Semiconductor Switches." *IEEE Transactions on Plasma Sci.* **26** (October) (IEEE Power Modulator Symposium, Rancho Mirage, CA, June): 1393–1402.

Other Communications

Hjalmarson, H. P., K. Kambour, and C. W. Myles. 1999. "Collective Impact Ionization Theory of Lock-On." *Proc. 12th IEEE Pulsed Power Conference* (Monterey, CA, June).

Kambour, K. K., C. W. Myles, and H. P. Hjalmarson. 1999. "Monte-Carlo Modeling of High-Gain PCSS." *Proc. 12th IEEE Pulsed Power Conference* (Monterey, CA, June).

Mar, A., A. G. Baca, D. J. Brown, G. J. Denison, W. D. Helgeson, H. P. Hjalmarson, G. M. Loubriel, M. W. O'Malley, and F. J. Zutavern. 1999. "Improved Longevity of Optically Activated, High-Gain GaAs Photoconductive Semiconductor Switches." *Proc. 12th IEEE Pulsed Power Conference* (Monterey, CA, June).

Zutavern, F. J., A. G. Baca, D. J. Brown, G. J. Denison, W. D. Helgeson, H. P. Hjalmarson, G. M. Loubriel, A. Mar, and M. W. O'Malley. 1999. "PCSS Technology for Short Pulse Lasers." *Proc. 12th IEEE Pulsed Power Conference* (Monterey, CA, June).

3506780000

Integration of Radiation-Hard Magnetic Random Access Memory with CMOS Integrated Circuits

D. R. Myers, O. B. Spahn, J. R. Jessing, R. S. Bennett

This goal of this project is to investigate the feasibility of developing radiation-hardened magnetic nonvolatile memories using giant-magneto-resistance (GMR) materials. We will investigate whether GMR materials are compatible with functioning complementary metallic oxide semiconductor (CMOS) circuits.

(1) We provided a concrete demonstration that GMR films could be deposited on functioning CMOS circuits without unacceptable degradation in circuit performance. The ability to insert GMR films onto functioning circuits enables the development of embedded nonvolatile memory for system-on-a-chip applications with development of an appropriate integration technology. A proof-of-principle integration technology is feasible using work on laser recrystallization of silicon (Si) in collaboration with Lawrence Livermore National Laboratory (LLNL).

(2) We demonstrated that GMR films can be deposited on radiation-hardened CMOS circuits without degrading the radiation hardness of the as-fabricated circuit. This key result overcomes a major obstacle to the development of fast-write, low-voltage, nonvolatile memory for radiation-hardened circumvention memories for DOE applications. When combined with the radiation testing of the GMR films described in the next result, this result indicates the viability of a GMR nonvolatile, rad-hard memory for DOE systems applications.

(3) We demonstrated that GMR films deposited on radiation-hardened CMOS circuits can absorb megarad (Si) doses of ionizing radiation with negligible degradation of their initial (unirradiated) magnetic properties. This key result overcomes a major obstacle to the development of fast-write, low-voltage, nonvolatile memory for radiation-hardened circumvention memories for DOE applications. When combined with the radiation testing of the CMOS circuits described in the previous result, this result indicates the viability of a GMR nonvolatile, rad-hard memory for DOE systems applications.

When combined with the radiation testing of the CMOS circuits..., this result indicates the viability of a GMR nonvolatile, rad-hard memory for DOE systems applications.

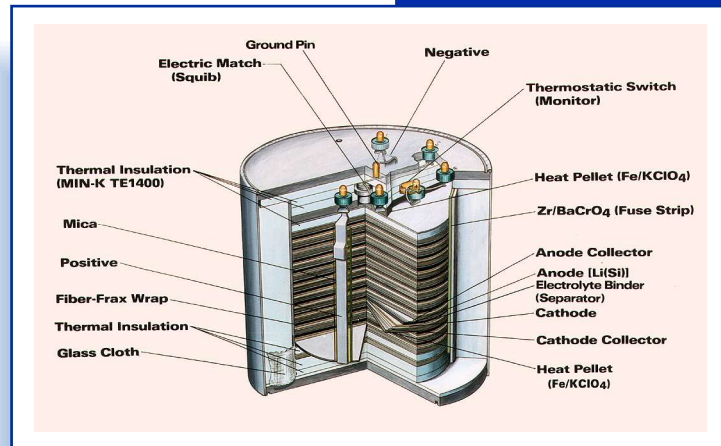
(4) We developed an approach to patterning GMR films deposited on functioning CMOS circuits without degrading the as-fabricated properties of the CMOS circuit. This result is necessary to pattern the deposited films into individual memory elements, as would be required for GMR-based memories.

Other Communications

Myers, D. R., J. R. Jessing, O. Blum-Spahn, and M. R. Shaneyfelt. 1999. "Process Integration of Giant-Magneto-Resistance Films with Rad-Hard CMOS Circuits." Sandia Technical Report, in preparation.

MODELING & ENGINEERING SIMULATION

Phenomenological Modeling and Engineering Simulation is one of Sandia National Laboratories' four LDRD Research Foundations investment areas. Research Foundations extend the core scientific and technical knowledge base of the Laboratories. In addition, Research Foundations focus on innovative, high-risk research that supports the long-term needs of the DOE's and Sandia's national security mission.



The Modeling and Engineering Simulation investment area is researching technology that uses teraflops-class (one trillion floating-operations per second), massively parallel computers to support engineering decisions based primarily on experimentally validated computational simulations. This capability will greatly reduce the need for testing to certify that the nation's nuclear stockpile is safe, secure, and reliable. Validation is an important focus of Modeling and Engineering Simulation research. Validation means that a code or algorithm exactly replicates the physics underlying the real-world situation that is being computer-simulated.

Modeling and Engineering Simulation LDRD projects support research in six areas: (1) development of high-fidelity physics models for mechanical and electrical simulations, (2) improved numerical solutions for high-performance computing platforms, (3) uncertainty quantification for modeling and simulation codes, (4) experimental discoveries that lead to

high-fidelity physics models, (5) experimental validation of algorithms and codes, and (6) advanced experimental diagnostics.

The "Phenomenological Model for Multicomponent Transport with Electrochemical Reactions in Concentrated Solutions" project has researched the development of unique predictive capability for modeling electrochemical processes such as thermal batteries. Such processes play an important role in support of technologies critical to Sandia's mission including thermal batteries, stockpile metal corrosion, fuel cells, and electrolytic plating. This project has developed and verified a thermal-battery computer model; developed software that allows the user to handle many aspects of liquid-phase kinetics, thermodynamics, and transport; and developed a capability to model microscale phenomena.



3508250000

Development of *In Situ* Diagnostics for Simultaneous Measurement of Transient Gas Species and Soot in Large Fires

C. R. Shaddix, G. L. Hubbard, P. D. Ludowise, J. R. Ross, H. A. Johnsen, P. J. Santangelo, L. A. Gritz, S. W. Allendorf, D. K. Ottesen

The thermal hazard that a fire poses to a weapon or other engineered system is a consequence of combined radiation and convection from high-temperature soot and gases. The development of advanced, predictive models of this hazard requires detailed knowledge of the transient chemical structure and soot distributions within real-scale fires. At present, there are no measurements, and hence no understanding, of transient gaseous species generation and transport in large, fully turbulent fires.

In this project Sandia is applying tunable diode laser absorption spectroscopy (TDLAS) to perform in situ, temporally and spatially resolved measurements of gas species in discovery and validation experiments in real-scale fires. We are combining the TDL measurements with absorption/emission measurements of soot concentration and temperature. We identified chemical species that are most likely to be detected and that are characteristic of the hydrocarbon fuel, combustion intermediates, and combustion products. We developed and employed a buoyant flame facility to evaluate multipass techniques for improving the system sensitivity and to evaluate the influence of flame transients on the species measurements. In addition, we designed custom electronics that allow us to simultaneously use (i.e., multiplex) several lasers while collecting data at kHz rates. We performed experiments in a low-pressure, flat-flame, Fourier transform infrared (FTIR) facility to identify and quantify the strongest absorption lines for the target species and have acquired two TDLs to measure H_2O and C_2H_2 in flames. We developed a fiber-based optical platform for performing the TDL and soot measurements in fires and will soon install it in a water-cooled probe for measurements in large pool fires.

We made substantial progress in developing a fast, robust, and sensitive electrooptical system for performing TDL gas-species measurements in fires. We made advances in the areas of TDL specification and acquisition, TDL temperature control

We made substantial progress in developing a fast, robust, and sensitive electrooptical system for performing TDL gas-species measurements in fires.

and high-speed current control, multipass optics for improved measurement sensitivity, development and demonstration of a suitable laser multiplexing approach, and probe design for TDL and soot measurements in fires.

Analysis of spectral considerations, expected species concentrations, and measured and predicted absorption linestrengths at high temperatures resulted in tentative identification of methane, carbon monoxide, acetylene, and water as good candidates for TDL detection in fires. We extensively analyzed the HiTran96 and HiTemp spectral databases and performed measurements of CO, CO₂, H₂O, CH₄, and C₂H₂ spectra, using a low-pressure, flat-flame, high-resolution FTIR spectroscopy facility and using relatively broadly tunable external-cavity TDLs in a high-temperature furnace flow. The detection of oxygen, while of substantial value in deducing fire structure, is not being pursued, due to the difficulty in acquiring an appropriate laser source and the complication of a separate detector required for the short wavelength (760 nm) of these transitions. We acquired TDLs suitable for detection of H₂O and C₂H₂ in flames. Acquisition of CO and CH₄ lasers is awaiting further analysis and furnace measurements of H₂O interferences.

To achieve the rapid response (> 100 Hz) and short measurement length (2–5 cm) desired for grid-level fire measurements, we must improve the sensitivity of the TDL system. We designed and tested open-cell Herriott mirror arrangements for multipassing the laser beam many times (up to 36x) across a short physical sample volume. We developed a buoyant flame apparatus in which soot loadings could be varied in order to evaluate the effects of transient soot attenuation and beam steering on TDL measurements with this multipass design. For a limited number of passes, the multipass design appears to work well, with acceptable laser transmittance.

We constructed high-speed custom lock-in amplifiers to evaluate the suitability of high-frequency multiplexing as a means of performing simultaneous measurements of several gas species at kHz rates with TDLs. Experiments revealed that cross-talk between different laser signals is negligible for all but small-frequency separations, so we are implementing this technique.

We designed a fiber-based optical system with relatively small optical components (lenses, mirrors, and fibers) for performing the TDL species measurements and soot

Experiments revealed that cross-talk between different laser signals is negligible for all but small-frequency separations....

absorption/emission measurements in large fires. We also designed a water-cooled aluminum probe for housing the optics and maintaining them at relatively low temperatures in these fires.

Other Communications

Santangelo, P. J., P. D. Ludowise, C. R. Shaddix, S. W. Allendorf, D. K. Ottesen, J. R. Ross, H. A. Johnsen, and G. L. Hubbard. 1999. "Development of a Probe for *In Situ* Measurements of Major Species in a Pool Fire Using Multiplexed Near-IR TDLAS." *Proc. SPIE* **3758** (44th Annual Meeting, Denver, CO, 21 July): 3758-24.

Shaddix, C. R., P. J. Santangelo, P. D. Ludowise, S. W. Allendorf, and D. K. Ottesen. 1999. "Development of a Near-Infrared TDL Probe for Rapid Species Measurements in Large Fires." *1999 OSA Technical Digest* (Advanced Semiconductor Lasers and their Applications, Santa Barbara, CA, 21–23 July): 141–143.

3508260000

Micromechanical Failure Analyses for Finite-Element Polymer Modeling

R. S. Chambers, E. D. Reedy, Jr., C. S. Lo, D. B. Adolf, T. R. Guess

Accurate failure models are needed in analyses to predict margins of safety to determine whether encapsulated components meet life-cycle requirements. Using Sandia's new nonlinear viscoelastic (NLVE) models for epoxy encapsulants, we are analyzing the stress concentrations in fracture process zones near failure-prone corners and material interfaces. This technology enables us to consider novel approaches for developing an NLVE, micromechanics-based, cohesive failure criterion.

Linear elastic fracture mechanics adopts a macro approach ignoring the detailed material behavior at crack tips. Alternatively, we will model the detailed stress-strain behavior within the highly nonlinear, crack-tip process zone. Using validated NLVE epoxy models, we are analyzing crack-tip deformation histories as samples are loaded to failure. Our intent is to identify correlations between the local continuum state and new as well as traditional fracture parameters. This approach will permit scrutiny of failure criteria based on such things as finite extensibility of the polymer network, shear-banding, or cavitation. Furthermore, we hope to collect data and develop models to understand the paradoxical observation that the failure strains of epoxy encapsulants in the rubbery state are many times lower than the failure strains in the glassy state. This project also provides a means for studying the dependencies of macro-fracture parameters (e.g., K_{Ic}) on temperatures and degree of cure. If successful, we hope to be able to deduce a more general approach for predicting failure; that is, one that works in situations where traditional fracture mechanics does not.

...we hope to be able to deduce a more general approach for predicting failure; that is, one that works in situations where traditional fracture mechanics does not.

This project progressed along two paths, one seeking to validate novel fracture analyses that extend traditional linear elastic fracture mechanics to discontinuities besides cracks, and the second, a risky pursuit of an NLVE, material-based, cohesive failure criterion. Work on the former continues to demonstrate successfully that it is possible to use stress intensities, characterizing the corners in an encapsulated inclusion loaded by thermal cycling, to predict the effects of interfacial adhesion versus slip, and of inclusion shape, diamond versus square. The interface corner fracture analysis

assumes that failure occurs when the stress intensity factor characterizing the stress field at the inclusion corner, K_a , attains a critical value, K_{ac} . We determined the relationship connecting K_a to applied load, inclusion geometry, and material properties by matching asymptotic results with full field solutions. The analyses suggested that encapsulant cracking from a fully bonded inclusion is unlikely, while cracking from an unbonded inclusion appears possible. Furthermore, when the inclusion is unbonded, cracking is more likely with a diamond than a square inclusion. Cracks observed during thermal cooling tests on different shaped inclusions with different interface adhesion have been consistent with these expectations.

We selected a three-point bending test on a precracked beam to experimentally measure the plane strain fracture toughness (K_{Ic}) values collecting data on cohesive failure. We performed tests at three temperatures and three crosshead rates, and computed the fracture toughness, average, and standard deviation of each dataset. We also collected data from partially cured samples. We are using these data to look for a new cohesive failure criterion.

Before performing the NLVE analyses, we validated the constitutive formalism against a large suite of test data. This included compression, tension, and torsion tests at various temperatures as well as thermal cycling, aging, and multistep loadings. We found all predictions to be within 20% accuracy. This is a major accomplishment in itself, rising well beyond what has ever been accomplished

To perform detailed viscoelastic analyses, one must obtain accurate, converged solutions with finite-element (FE) meshes at submicron scales around crack tips. Severe convergence problems can arise due to the large gradation in element sizes, which must be accommodated to model the entire fracture specimen. Although one can substructure, care must be taken not to compromise the zones of nonlinearity at the crack tip and reaction/loading points. Moreover, one must model the thermal history, not just the mechanical loading, because viscoelastic materials are subject to physical aging, volume, and stress relaxation during annealing and thermal cycling. This state must be determined to define the initial conditions at the time of the loading. To overcome these difficulties and greatly shorten the compute time, we modeled the initial histories on a one-element mesh and then mapped the viscoelastic state histories and volume strains directly to the fracture specimen

...we validated the constitutive formalism against a large suite of test data.... We found all predictions to be within 20% accuracy. This is a major accomplishment in itself, rising well beyond what has ever been accomplished.

mesh. We used this approach to analyze various specimen geometries, rubbery modulus changes, and thermal effects.

Mechanistically, we found finite extensibility and cavitation to be the two most likely failure mechanisms.

To further elucidate failure mechanisms, we performed compression and torsion tests on polymers in both glassy and rubbery states, loading them to failure. The glassy samples endured strains in excess of 50% and failed with a few large cracks. However, the rubbery samples that were tested at temperatures 50°C above the glass transition temperature (T_g) exploded into a coarse powder at strains of only a few percent. This result was totally unexpected since both the strains and stresses at the time of failure are far smaller in the rubber than in the glass.

Other Communications

Reedy, E. D., Jr., and T. R. Guess. 1999. "Rigid Square Inclusion Embedded Within an Epoxy Disk: Asymptotic Stress Analysis." Paper presented to the 1999 ASME Mechanics and Materials Conference, Blacksburg, VA, 27–30 June.

3508270000

Methodology for Optimal Selection of Test and Simulation Levels for Problems Involving Computational Simulation

B. M. Rutherford, K. F. Alvin, V. J. Romero, T. G. Trucano

Investigation and evaluation of a complex system are often accomplished through the use of performance measures based on system response models. The response models are constructed using computer-generated responses supported where possible by physical test results. The general problem considered is one where resources and system complexity together restrict the number of simulations that can be performed. The levels of input variables used in defining environmental scenarios and initial and boundary conditions and for setting system parameters must be selected in an efficient way. Sandia chose a resampling-based approach for performing this selection.

The resampling-based approach to selecting computer experiments described and illustrated here can support a wide range of applications. It can address the selection of computer runs among discrete (alternative models or alternative sets of assumptions) as well as the more traditional continuous range inputs to a computer analysis. The approach requires initial response information that we use to make an assessment of what is known about the system. Given this information, we can determine a most informative set of subsequent computer runs to perform in order to increase the system knowledge in a meaningful (user-defined) way. The resampling-based approach will also provide an estimate of prediction uncertainty based on both the uncertainty in the inputs and the uncertainty resulting from performing only a limited set of computer runs.

We can illustrate the methodology through a number of examples. These include a simple two-input computer analysis with a known analytical solution as well as two larger applications involving computational simulation codes. The two-input example provides an easy means of assessing and illustrating the algorithm's performance. The larger applications demonstrate its generality.

(1) We completed the development of (rough) software that we used to demonstrate the approach for small- and medium-scale problems.

The resampling-based approach...can determine a most informative set of subsequent computer runs to perform in order to increase the system knowledge in a meaningful (user-defined) way...[and] will also provide an estimate of prediction uncertainty based on both the uncertainty in the inputs and the uncertainty resulting from performing only a limited set of computer runs.

(2) The project included several components that we considered tactical aspects of the approach, in that while they were integral parts of the strategic methodology, their perfection was not required to demonstrate the potential of the algorithm. We further investigated and tested these components to an extent where we could include them in the “capability” described in (1) above. They include (a) the methodology for ensuring that the representation of system knowledge is consistent with that knowledge; (b) specific parametric methods for constructing response surfaces that are useful in engineering applications; (c) metrics that can be used to measure the potential information provided by a candidate experimental design; and (d) a tuned evolutionary algorithm to be used for selecting candidate designs.

(3) We illustrated the approach on a small analytical problem and on two larger problems involving computational simulation codes. The examples provided a means of assessing the capabilities of the approach and demonstrated the general applicability of the approach.

Refereed

Rutherford, B. M. 1999. “A Methodology for Selecting an Optimal Experimental Design for the Computer Analysis of a Complex System.” *Technometrics* **98-035** (August) (Alexandria, VA).

Other Communications

Rutherford, B. M. 1999. “A Resampling-Based Approach to Optimal Experimental Design for Computer Analysis of a Complex System.” *Proc. Joint Statistical Meetings—Section on Phys. and Engin. Sci.* (Baltimore, MD, 8–12 August).

3508280000

A Phenomenological Model for Multicomponent Transport with Electrochemical Reactions in Concentrated Solutions

K. S. Chen, W. G. Houf, R. S. Larson, G. H. Evans, D. R. Noble

Liquid-phase electrochemical processes play important roles in Sandia's missions (e.g., thermal batteries, stockpile metal corrosion, fuel cells, and electroless and electrolytic plating as in LIGA [German for lithography, electroforming, molding] fabrication of microelectromechanical systems [MEMS] devices). In the case of thermal batteries, the focus of this project, the process involves multicomponent transport of charged species with simultaneous electrochemical reactions in a concentrated solution. More specifically, in a thermal battery cell, an interacting molten mixture of electrolytes is transported between electrode surfaces where electrochemical reactions take place. Accurate prediction of battery performance (e.g., discharge voltage versus time) requires proper descriptions of diffusion of charged species (driven by concentration and electrical-potential gradients), energy transport, electrochemical reactions, and thermodynamic potentials. Classical dilute-solution framework based on Fick's first law is generally valid only for noninteracting species diffusing in dilute solution and is not appropriate for describing multicomponent diffusion in concentrated solutions as in thermal batteries.

We formulated a general framework and implemented it in GOMA, a multidimensional, multiphysics FE computer code for modeling multicomponent transport of neutral and charged species in concentrated solutions. We verified the new GOMA capability for modeling multicomponent transport of neutral species and validated it using the classical model problem of ternary gaseous diffusion in a Stefan tube. We developed a GOMA-based computer model of thermal batteries (multidimensional, multicomponent transport of ions in molten salt with simultaneous electrochemical reactions). We wrote a software driver routine based on the secant method for computing total cell voltage as a function of time under constant current-density constraint. We verified the GOMA thermal-battery model using an idealized battery cell in which concentration gradients are absent, and partially validated it using limited battery-performance data available at Sandia.

We developed a new Liquid Chemkin Software Package that allows the user to handle many aspects of liquid-phase kinetics, thermodynamics, and transport (particularly properties)... [and] a Lattice-Boltzmann-based capability for modeling porescale or microscale phenomena involving convection, diffusion, and simplified chemistry.

Moreover, we conducted a systematic study for estimating Stefan-Maxwell diffusivities for liquid-phase processes. We developed a new Liquid Chemkin Software Package that allows the user to handle many aspects of liquid-phase kinetics, thermodynamics, and transport (particularly properties). Last, we developed a Lattice-Boltzmann-based capability for modeling porescale or microscale phenomena involving convection, diffusion, and simplified chemistry.

Other Communications

Chen, K. S., G. H. Evans, R. S. Larson, and W. G. Houf. 1999. "Modeling Thermal Batteries Using a Multidimensional Stefan-Maxwell Framework." Paper presented to the 3rd Biennial Tri-Laboratory Conference on Modeling and Simulation, Lawrence Livermore National Laboratory, Livermore, CA, 2–3 November.

Chen, K. S., G. H. Evans, R. S. Larson, M. E. Coltrin, and J. Newman. 1998. "Multidimensional Modeling of Thermal Batteries Using the Stefan-Maxwell Formulation and the Finite-Element Method." *Proc. 194th Electrochemical Society, Selected Battery Topics* **98-15** (Spring) (Boston, MA, 1–6 November): 138–149.

Noble, D. R., and K. S. Chen. 1999. "Simulation of Pore-Scale Processes in Thermal Batteries." Paper presented to the 195th Electrochemical Society Meeting, Seattle, WA, 2–6 May.

3508290000

Structural Simulations Using Multiresolution Material Models

S. W. Key, R. S. Chambers, D. B. Adolf

The broad goal of this project is to develop the theoretical foundation for a sophisticated collection of new simulation tools that will allow a more accurate and reliable prediction of aging and service life of engineering materials. The hope is that this goal will be met by adequately modeling the effects of micromechanical features on macromechanical response. This project, therefore, focuses on developing techniques for better characterization of the geometry and mechanical properties of microstructure and their effects on global behavior, on including in the modeling apparatus the quantification of uncertainty in data and material characterization, on hierarchical modeling in which modeling error is assessed and adaptively corrected, and on the incorporation of modern techniques of imaging, tomography, visualization, and mesh generation in the overall simulation process. The project includes an experimental and testing component in which we will fabricate and test two-phase elastomeric composites. These tests will provide a basis for verification of simulation methods, damage models, and other theoretical and computational approaches to be developed with particular application to nonlinear viscoelastic (NLVE) materials.

Critical weapon components such as neutron generators are encapsulated in filled epoxies to provide structural integrity, environmental protection, and voltage isolation during their service life. Although polymer systems may exhibit linear or grossly NLVE behavior under certain thermomechanical conditions, they likewise can respond elastically when lightly loaded well above or well below the glass transition temperature. The breadth of material physics exhibited by these encapsulants can thus vary enormously over time and position within a component. For these reasons, we selected one of Sandia's epoxy encapsulants (Epon 828/DEA with glass filler) for study.

Over the last few years Sandia developed and validated a NLVE material model for epoxy encapsulants. Starting from established principles of rational mechanics, we constructed a thermodynamically consistent constitutive formalism from a Helmholtz free energy. We implemented the model in a 3-D finite-element (FE) program and extensively validated it by

These tests will provide a basis for verification of simulation methods, damage models, and other theoretical and computational approaches to be developed with particular application to nonlinear viscoelastic (NLVE) materials.

comparing analysis predictions to experimental data collected from tests encompassing tension, compression and torsion yield, physical aging, stress, volume and enthalpy relaxation, and thermal expansion/contraction, all conducted under various thermal histories. The choice of an NLVE material model provides a natural hierarchy of underlying material behavior needed for this project. Through the behavior of the material clock, which is defined by a shift factor, elasticity and linear viscoelasticity are subsets of the model's behavior. In fact, we proposed a nesting of five degrees of increasingly complex material physics: (1) elasticity—no relaxations, (2) linear viscoelasticity, (3) NLVE—add temperature and volume relaxation effects, (4) NLVE—add stress effects to (3), and (5) NLVE—add thermodynamically consistent work for large strains. This provides ample degrees of complexity for exploring material adaptivity.

In collaboration with industry and the University of Texas—Austin, we made progress on (1) imaging algorithms that will take data from CT (computer tomography) scans and convert it iteratively into effective properties of heterogeneous materials, (2) a new class of *a posteriori* error estimates that give both upper and lower bounds for errors in local quantities of interest where these errors define the difference between a fine-scale solution (reflecting the effects of microstructure) and a homogenized solution determined using the effective properties. We tested the quality of these estimates on a number of simple cases for which exact solutions are known, and (3) a research code that employs hp-adaptive FE methods. We will use this code as a test-bed for determining the effectiveness of *a posteriori* error estimates and adaptive modeling of heterogeneous materials.

Refereed

Oden, J. T., and K. Vemaganti. 1999. "Adaptive Hierarchical Modeling of Heterogeneous Structures." *Physica D* **133**: 405–415.

Oden, J. T., and K. Vemaganti. 1999. "Adaptive Modeling of Composite Structures: Modeling Error Estimation." *Internat. J. Civil Structural Engineering*, accepted.

The choice of an NLVE material model provides a natural hierarchy of underlying material behavior needed for this project.

3508310000

Lightning-Induced Arcing

R. E. Jorgenson, R. A. Anderson, H. P. Hjalmarson, K. O. Merewether, L. K. Warne

The purpose of this research is to develop a science-based understanding of the early-time behavior of electric surface arcing in air. The results will be used in safety assessments of weapons in a lightning environment. Sandia wrote a Monte Carlo (MC) code that seems to be successful in simulating the breakdown process in the first tenth of a nanosecond. Our goal in this research is to understand the early-time (on the order of nanoseconds) behavior of electrical breakdown in air at atmospheric pressure across a dielectric surface. Safety assessments of weapons exposed to a lightning environment require many judgments as to the likelihood of the formation of electrical arcing paths. Arcing due to lightning in a weapon occurs at atmospheric pressure and frequently involves the presence of dielectric surfaces, such as defects in cable insulation, or the dielectric supports of the pins in a connector.

We constructed a three-dimensional MC code that begins with a distribution of charged particles in space and energy and simulates their time evolution.

We successfully implemented a tree algorithm to calculate the electric field due to the charged particles in the problem. The tree algorithm gives more efficiency ($N \log(N)$ operations, where N is the number of particles in the problem) and is better able to resolve large contrasts in charge density than more traditional grid methods. We anticipate large contrasts to occur at the streamer boundaries. For maximum efficiency we selected image methods to account for the dielectric surfaces and electrode boundaries.

At the onset of streamering, we expect to have to account for 10^8 to 10^{10} particles. This necessitated the use of particle renormalization. The particles are collapsed into super-particles in a manner that maintains the energy distribution. The energy distribution is critical since this influences the ionization rate and ultimately the breakdown. With the tree algorithm and renormalizing the charged particles, we are able to run the simulation to 0.1 nanosecond. We are attempting to run beyond 0.1 nanosecond, but this may require further optimization of the tree algorithm.

We assembled two sets of cross-sectional data to describe the various processes when electrons collide with a neutral

Safety assessments of weapons exposed to a lightning environment require many judgments as to the likelihood of the formation of electrical arcing paths.

background of nitrogen (N) and of oxygen (O). We checked the code against swarm data for N and got good agreement. We have yet to check the code against O and air swarm data.

Multicomponent gases involve a large number of collision processes to account for the different types of gas species that exist in the problem. At an early time, it is not yet clear if all of the processes are needed, but we constructed the code to handle them, provided that we can obtain the proper cross-section data.

We incorporated photoionization into the code.

Photoionization is an essential driving process to obtain the proper front thickness and velocity of the streamers that eventually form in the breakdown process. A one-dimensional calculation indicates that with photoionization, we can expect the streamer front thickness to be on the order of 100 micrometers, which agrees with published data and indicates that the algorithms used in the code have a chance to resolve the streamer front and properly model the process.

Historically, the surface has been thought to interact with the breakdown process in two ways. The field is modified by the presence of the surface, which was accounted for by images and was discussed previously. The second method of interaction is that as the electrons collide with the dielectric surface, the surface captures the electrons or releases secondary electrons, depending on the energy of the colliding electron. This effectively charges the surface (and can provide more electrons for the avalanche process). We incorporated these processes into the code and will use them to compare with surface breakdown experiments.

We identified a possible new enabling mechanism for dielectric breakdown as long-range photoinduced electron emission. In this process, low-energy photons released during the gas-collision process propagate to long-range release electrons from the dielectric surface, effectively seeding the breakdown process near the surface ahead of the streamer front.

We identified a possible new enabling mechanism for dielectric breakdown as long-range photoinduced electron emission.

3508320000

Mechanisms of Adiabatic Shear Failure

D. B. Dawson, D. A. Hughes, J. J. Dike, S. H. Goods

Adiabatic shear is an extreme and usually catastrophic low-energy form of localized deformation that is observed in many types of applications involving dynamic loading. The adiabatic shear process is complex, with competition between material deformation modes and inherently tight coupling of thermal and mechanical fields. Accurate computational and phenomenological models do not currently exist. Sandia is conducting a systematic, coupled experimental and analytical study to establish failure mechanism maps and innovative design criteria relating critical physical aspects to adiabatic shear failure susceptibility. Initially, we developed two high-rate experimental techniques for evaluating susceptibility to adiabatic shear failure and are conducting screening tests on different alloy types used in weapons applications. We also identified existing models and failure criteria for adiabatic shear and conducted preliminary analytical simulations of adiabatic shear localization using materials models incorporated in current Sandia analysis codes.

We initiated experimental and analytical investigations of adiabatic shear susceptibility criteria and failure characteristics. We examined a large body of existing literature to identify phenomenology, critical parameters, proposed analytical models, and experimental techniques for characterizing and predicting adiabatic shear in a range of alloys. For the development of design criteria for avoiding adiabatic shear failure, our focus is on prediction of shear band initiation, rather than on understanding details of the subsequent propagation of the band. We selected and procured Sandia-used materials from different alloy classes with a wide range of mechanical and thermophysical properties known to affect adiabatic shear behavior. We obtained thermophysical and mechanical property data for use in phenomenological and analytical modeling for these alloys from an extensive search of the literature.

To provide the type of quantitative experimental data needed to define criteria for adiabatic shear band initiation and to screen alloys for adiabatic shear susceptibility, we selected the torsional Kolsky bar technique and dynamic linear shear. Torsional Kolsky experiments are being conducted in collaboration with CalTech. We tested specimen designs for

Sandia is conducting a systematic, coupled experimental and analytical study to establish failure mechanism maps and innovative design criteria relating critical physical aspects to adiabatic shear failure susceptibility.

dynamic linear shear using a modified drop-tower apparatus and are developing a linear shear capability for the Split Hopkinson Bar apparatus. Modifications of experimental apparatus and techniques required for strain-limited shear band initiation studies are also under development.

Screening tests conducted on different alloy types clearly show the importance of key thermophysical properties and strain-hardening behavior in distinguishing alloys that are resistant to adiabatic shear failure (e.g., annealed low-alloy steel and high-toughness aluminums [Al]) from those that are susceptible (titanium alloys, cold-rolled steel, high-strength Al). We are using these experimental results to develop alloy-specific susceptibility criteria and failure model maps for engineering design, and to identify a small subset of the alloys on which to now concentrate for detailed studies of adiabatic shear mechanisms and models.

Analytical modeling efforts focused initially on existing failure criteria for adiabatic shear band initiation, including identification of process-relevant material parameters and evaluation of suitability for implementation in Sandia analysis codes. Simulations also supported experimental design of test configurations. We performed sample calculations reproducing literature analyses to establish confidence in use of Sandia codes for predicting adiabatic shear localization. We also evaluated constitutive material models currently implemented in applicable analysis codes to identify those suitable for modeling adiabatic shear.

Screening tests conducted on different alloy types clearly show the importance of key thermophysical properties and strain-hardening behavior in distinguishing alloys that are resistant to adiabatic shear failure....

3508330000

Evolvable Hardware

J. S. Jones, D. J. Zimmerer, G. S. Davidson

Sandia is researching the use of evolvable hardware (EHW) as a design tool with the potential to expand Sandia's capabilities in any area requiring dedicated complex circuitry. EHW refers to the innovative technique of using evolutionary algorithms (EAs) to design and synthesize circuits on field-programmable gate arrays (FPGAs), with the eventual goal of allowing these circuits to dynamically and autonomously reconfigure themselves to adapt to changing conditions. Because evolutionary design explores an unlimited design space, it can discover novel designs and create them without expert knowledge. EHW does not require exact specification and thus can design complex systems that cannot be handled by conventional specification-based design approaches. EHW can design circuits that might be too difficult or costly to design by human experts. EHW can evolve much simpler and more compact designs than traditional methods. The types of initiatives that could benefit from this new method of circuit and system design range from on-satellite data processing to chemical-sensor devices to weapon components. Continuing to expand this capability will improve the speed and efficiency of design and production, as well as make Sandia a leader in this next generation of design methodology.

We created the core system that allowed considerable strides in the evolution of logic circuits. Test circuits were evolved using a single-processor WinNT machine, 64-processor UNIX machines, and a 143 WinNT cluster (Sandia's Computational Plant [Cplant]). The largest test circuits contained 50 to 100 gates, had no preset limits on topology, and included adders and multipliers.

There was also progress in evolving digital signal-processing circuits (low-pass filters) and other time-dependent circuits. This area will require more research in the second year because the nature of the problem means there is much more involved in specifying input requirements for evolution. One such factor is the specification of the delay time for the circuit. Another is the fact that we are trying to evaluate a circuit in the time domain while what we really desire is frequency domain performance.

We installed a commercial FPGA programming system in a Windows 95 PC. We designed test circuits and exercised them

Continuing to expand this capability will improve the speed and efficiency of design and production, as well as make Sandia a leader in this next generation of design methodology.

on the FPGA using traditional methods. We shifted the remainder of the hardware schedule, as it became apparent that we would need to take a higher-level approach to hardware circuit design in order to achieve our goals. This realization came from several factors: the changing technology of available FPGAs, the discontinuation of our first selected FPGA, the advantages of having the parallel software evolution operate at the same level as the hardware evolution, and the unnecessary calculation load incurred by evolving at a lower level. The new approach increases the power of the algorithms by removing device-dependent routing questions and allowing the parallel software to directly complement the hardware. It also insulates the system from changing FPGA technology.

Keeping with the new philosophy, we designed a multiplexer network and routed it on the selected FPGA. This initial multiplexer network allows an arbitrary feedforward logic circuit of 24 gates or less to be implemented on the chip simply by writing to registers. This evades the cost of routing each abstract logic circuit before it can be evaluated. We linked the software system to the hardware and implemented a basic version of the hardware evolution system. This system evolves logic circuit designs by implementing and evaluating the circuits directly in hardware. We ran initial tests to gauge the effectiveness of evolution in hardware compared to evolution in software.

The new approach increases the power of the algorithms by removing device-dependent routing questions and allowing the parallel software to directly complement the hardware. It also insulates the system from changing FPGA technology.

3508340000

Crack Nucleation and Growth: Combining Validated Atomistic and Continuum Modeling

J. E. Houston, P. A. Klein, S. M. Foiles, M. C. Bartelt, A. K. Schmid, R. Q. Hwang, J. C. Hamilton

Fracture and de-adhesion are critical material failure modes and impact areas ranging from advanced component development to the aging of stockpile components. Consequently, computational models of these processes are essential to Sandia's programmatic interest and to specific programs such as ASCI (Accelerated Strategic Computing Initiative). The wide range of length scales involved has dramatically hampered the computer modeling of fracture. For example, corrosion (i.e., molecular reactions at the crack tip) and stress (i.e., long-range elastic forces at a macroscopic scale) are the two fundamental processes involved in stress-corrosion cracking, a common failure mode for materials. Thus it is imperative to couple the atomistic understanding provided by solid-state physics with the stress analysis provided by theoretical mechanics. Sandia is coordinating this project in which experimental investigation of prototypical fracture events will guide modeling using atomistic and continuum techniques. Our goals are to achieve a common working vocabulary that merges the ideas of atomistic and continuum analysis, to develop codes that combine the two methods, and to validate these codes by comparing them with the experimental investigations of fracture situations.

We began by investigating the relationship between atomic-level processes and the longer-range behavior of the stress field through the use of a simple model of a crack, i.e., steps on a metal surface. In effect, a surface step represents half of a crack, and the crack surface in this model is exposed for detailed study. The stress concentration at the step, or crack tip, is by its nature an atomic-level property while the behavior of the stress field away from the step is better characterized by a continuum approach. How the plastic yield of the metal is affected by a stress applied by a neighboring indenter will help us understand the interplay between the atomic- and continuum-level effects. Work will then proceed to a similar configuration involving the surface of a brittle material.

We obtained nanoindentation results with the interfacial force microscope (IFM) exploring the plastic yield threshold for Au(111) (gold) single-crystal surfaces as a function of the

Our goals are to achieve a common working vocabulary that merges the ideas of atomistic and continuum analysis, to develop codes that combine the two methods, and to validate these codes by comparing them with the experimental investigations of fracture situations.

distance to neighboring surface steps. These studies involved obtaining constant-force images of the surface in order to establish the location and properties of steps on the Au surface. We performed loading curves, i.e., force versus relative displacement, with a parabolic probe and identified the onset of plastic yield by the deviation of the loading curve from the classic Hertzian behavior. We then tabulated the values for the yield stress and the contact area at yield, along with the height of the step, as a function of the distance from the tip center to the step edge. We found that on broad terraces the average yield stress is quite high (~ 7 Gpa), approaching the theoretical strength of the Au lattice. However, when we placed the probe at the step edge, the stress was reduced by almost a factor of two. The surface step represents a very controllable type of defect. Surprisingly, we found that the lowering of the yield stress by the neighboring step extends over a range of approximately three times the contact radius at yield. Contact mechanics would suggest that at such distances there is a negligible effect due to the step.

To be more specific about the expected effect of steps on mechanical properties, we also performed continuum-level calculations of a parabolic indenter deforming a surface in the presence of a neighboring step 30 Å tall and located one contact radius from the step edge. The calculation showed, as expected, that the stress distribution beneath the probe is negligibly affected by the step's presence.

We also performed atomic-level calculations on a system very similar to that dealt with in the experiments, except for the use of probes with radii approximately an order of magnitude smaller. The reduction in size is a tribute to the difficulty of scaling these very detailed calculations to large numbers of atoms. However, if the results are scaled with respect to the contact radius at yield (i.e., according to the probe radius), the results show a striking similarity to the experiment. The reduction in yield stress is somewhat larger (approximately a factor of three), but the range of the step's influence is also found to be about three times the contact radius at yield.

The implication from these two calculations is that the step is apparently affecting the material yield at a point other than the high-stress region beneath the probe, for example, by nucleating dislocations at the step itself, where the stress imposed by the neighboring probe is concentrated. The continuum-level method, including a radius at the base of the step, will permit us to establish the stress pattern and range while the atomic-level results will show the dislocation

structure after yield. Preliminary results from the latter indicate that the dislocations are nucleated at the step.

We also obtained preliminary results from our recently developed STM/IFM (scanning-tunneling microscopy/IFM) system with its ability to controllably apply a uniform stress to a microscopic sample. We probed the surface of the uniformly stressed sample by a unique combination of an STM and an IFM head. We obtained preliminary data on this unique instrument that involves the observation of the role of the applied stress in determining the spatial structure of the Au(111) reconstruction pattern. The normal herringbone pattern due to the surface stress generated by the termination of the bulk crystal structure is converted to a linear striped pattern reflecting the uniaxial nature of the remaining surface stress.

Refereed

Hamilton, J. C. 1999. "Atomistic Calculations of Dislocation Structures During Film Growth and Indentation." (Invited) Paper presented to the 40th Annual Meeting of the Society for Natural Philosophy, Pittsburgh, PA, 11 October.

Hamilton, J. C. 1999. "Large-Scale Atomic Simulation of Indentation Plasticity." (Invited) Paper presented at the Workshop on the Mechanics of Indentation and Penetration, Los Alamos, NM, 19 July.

Kelchner, C. L., and J. C. Hamilton. 1998. "Dislocation Nucleation and Defect Structure During Surface Indentation." *Phys. Rev. B* **58** (1 November): 11085.

Kiely, J. D., K. F. Jarausch, J. E. Houston, and P. E. Russell. 1999. "Initial Stages of Yield in Nanoindentation." *J. Mater. Res.* **14** (June): 2219.

Kiely, J. D., R. Q. Hwang, and J. E. Houston. 1998. "Effect of Surface Steps on the Plastic Threshold in Nanoindentation." *Phys. Rev. Lett.* **81** (16 November): 4424.

3508350000

Applied Microfluidic Physics

E. B. Cummings, A. J. Antolak, D. W. Arnold, R. H. Nilson, S. K. Griffiths

Microfluidic MEMS (microelectromechanical systems) exploit surface phenomena favored in microscopic geometries. Although such devices are capable of outperforming their macroscopic relatives, design guidelines are presently nonexistent. The purpose of this project is to develop, verify, and apply mathematical models that accurately describe microfluidic processes. Both the direct mathematical results of the modeling and the accompanying physical understanding are a bridge to enlightened microfluidic design.

Sandia produced optimization techniques and optimal device geometries for minimum dispersion in 90-degree bends and wye-shaped junctions for which we filed a patent disclosure. These optimization techniques employ the concept of the irrotationality of ideal electroosmosis. The conditions for ideal electroosmosis are well approximated in many fluidic devices that employ electrokinetic (EK) transport. This result is significant because powerful mathematical tools and theorems and a wealth of analogous experimental data are available for irrotational flows. We developed software to permit designers to simulate electrokinesis within planar devices. The computational grid is produced directly from an experimental image or drawing of the device, allowing rapid evaluation of design concepts.

This tool also supports close coupling and detailed comparison of modeling and experiment. The primary experimental diagnostic technique is microscale particle-image velocimetry (PIV). We refined an advanced image-processing methodology for PIV and implemented it in software. This methodology permits measurement spatial resolution down to a single pixel and improved accuracy over conventional approaches. Microscale-PIV measurements confirmed flow-field predictions of ideal electroosmosis and illuminated aspects of non-ideal electroosmosis. The methodology represents a significant practical and conceptual development in PIV.

We completed an analytical study of dispersion in electroosmotic flow and developed a general numerical model of electroosmosis and a theory of ideal electroosmosis. We fabricated and made velocity measurements in a test circuit that

Both the direct mathematical results of the modeling and the accompanying physical understanding are a bridge to enlightened microfluidic design.

contains channels and packed beds that represent all classes of microflows targeted for analysis in this project. These measurements precisely confirm the predictions of ideal electroosmosis and employ a new PIV methodology that we developed during this project.

Pure electroosmosis in a uniform channel has a uniform velocity field everywhere except in the region within several Debye lengths from the channel boundary. In this boundary-layer, the flow hydrodynamically disperses convecting molecules. We derived an analytical expression for hydrodynamic dispersion of a neutral, noninteracting molecule as a function of the molecular diffusivity, channel radius, bulk electroosmotic flow velocity, and Debye-layer thickness analogous to Taylor's analysis of hydrodynamic dispersion of Poiseuille flow (Taylor flow). We used this analytical expression to identify the molecular Peclet number that minimizes dispersion for a given channel and Debye thickness. This expression can guide the design of microfabricated separation columns and operating voltages. In addition, we will use the analytical expression for dispersion to validate numerical codes that can treat more-general geometries.

We developed a model of general electroosmotic transport in junctions based on stream-function and vorticity formulations of the Navier-Stokes equations. We treated species transport by ion drift, diffusion, and convection using continuum or Monte Carlo methods. The agreement between the predictions of this numerical model and experimental images of scalar transport via uncaged-dye fluorescence is exceptionally good. We utilized this numerical model to simulate the process of injecting a sample into a separation column. This project has shown how to bias the electric fields in the channels to optimize the injected sample.

We derived the conditions necessary for electroosmosis to be irrotational. The conditions for this "ideal electroosmosis" are well approximated in many microfluidic systems that employ electroosmosis. The importance of this result is that powerful mathematical techniques and theorems and a wealth of analogous experimental data can be applied to understanding the flows. The concept and study of "ideal electroosmosis" represent an advance in the field.

We made detailed quantitative measurements of the velocity fields in crosses, tees, offset junctions, contractions, and corners under ideal electroosmotic conditions. The velocity fields measured in the simple geometries are well represented by analytical solutions for the flows based upon Schwarz-

These measurements precisely confirm the predictions of ideal electroosmosis and employ a new PIV methodology that we developed during this project....The concept and study of "ideal electroosmosis" represent an advance in the field.

Christoffel techniques. For comparing results in complicated geometries, we developed an ideal-electroosmosis simulation tool. This tool composes its computational mesh directly from an experimental image or drawing of the (quasi-two-dimensional) microfluidic device. Consequently, detailed comparisons between experiment and theory are possible, even for complicated device geometries. This tool also permits the simulation of scalar transport inside devices with time-varying applied electric fields. This software is intended for use by device designers to test device geometries and control concepts.

We measured the velocity fields using a microscopic variant of PIV. We developed and refined an adaptive gridding, image-processing, and optimal nonlinear filtering methodology for PIV. This methodology extracts measurements with spatial resolution down to 1 pixel (< 1 mm) with high measurement accuracy. This methodology represents a significant practical and conceptual advance for PIV.

This methodology represents a significant practical and conceptual advance for PIV.

Refereed

Cummings, E. B. 1999. "Image Processing and Optimal Nonlinear Filtering Techniques for Particle-Image Velocimetry." *Proc. 3rd Internat. Workshop on PIV '99* **1** (Santa Barbara, CA, 16–18 September): 379–384.

Cummings, E. B., S. K. Griffiths, and R. H. Nilson. 1999. "Irrotationality of Uniform Electroosmosis." *Proc. SPIE, 27th Congress, Microfluidic Devices and Systems II* **3877** (Micromachining and Microfabrication, Santa Clara, CA, 20–22 September).

Cummings, E. B., S. K. Griffiths, R. H. Nilson, and P. H. Paul. 1999. "Conditions for Similitude Between the Fluid Velocity and Electric Field in Electroosmotic Flow." *Anal. Chem.*, submitted.

Griffiths, S. K., and R. H. Nilson. 1999. "Hydrodynamic Dispersion of a Neutral Non-Reacting Solute in Electroosmotic Flow." *Anal. Chem.*, accepted.

Griffiths, S. K., and R. H. Nilson. 1999. "Hydrodynamic Dispersion of a Neutral Solute in Electroosmotic Flow." *Proc. 2nd Internat. Conf. on Modeling and Simulation of Microsystems* **1** (San Juan, Puerto Rico, 19–21 April): 558–561.

Other Communications

Cummings, E. B. 1999. "Electroosmotic Microflows." (Invited) Seminar presentation to the Graduate Aeronautical Laboratories, CalTech, Pasadena, CA, 30 April.

Cummings, E. B. 1999. "Image Processing, Adaptive Gridding, and Optimal Nonlinear Filtering Techniques for Particle Image Velocimetry." Sandia Technical Report SAND99-8263, Sandia National Laboratories, Livermore, CA (October).

Cummings, E. B., S. K. Griffiths, R. H. Nilson, and P. H. Paul. 1999. "Conditions for Similitude Between the Fluid Velocity and Electric Field in Electroosmotic Flow." Sandia Technical Report SAND99-8246, Sandia National Laboratories, Livermore, CA (April).

Griffiths, S. K., and R. H. Nilson. 1999. "Hydrodynamic Dispersion of a Neutral Non-Reacting Solute in Electroosmotic Flow." Sandia Technical Report SAND99-8249, Sandia National Laboratories, Livermore, CA (June).

Griffiths, S. K., and R. H. Nilson. 1998. "Method and Apparatus to Reduce Dispersion in Microfluidic Systems." Disclosure of Technical Advance SD-8209, Sandia National Laboratories, Livermore, CA (23 December).

Griffiths, S. K., and R. H. Nilson. 1999. "Method and Apparatus to Reduce Dispersion in Microfluidic Systems." USPTO patent application 09/299269 (26 April).

3508360000

Transport and Fate Simulation of Chem/Bio Agents in Critical Infrastructures

K. K. Murata, R. C. Schmidt, F. Gelbard, S. R. Subia, M. W. Glass, J. E. Brockmann

The ability to model the transport and fate of gas and aerosol with large, complex systems is critical in addressing the accidental or malicious release of hazardous agents within and around critical national infrastructures. Substances of interest include radiological materials, smoke and poisonous combustion products from fires, and chemical and biological (C/B) agents. Transport and fate refers to the movement of agents into, out of, and within a facility, as well as the physical state and viability of the materials of interest during and after the transport process. Transport and fate modeling is needed to perform risk assessments of release events. These modeling efforts could guide facility and personnel response during an event, support facility design modifications to mitigate both risk and consequences of a release, help evaluate the effectiveness of mitigation and response strategies for any given facility, and guide cleanup and reclamation activities. All of these activities rely on the capability to accurately predict the time-dependent transport of gas and material of interest, as well as the state of that material at any given time.

The proposed use of gridded vortex technology has not been attempted for three-dimensional (3-D) problems. Sandia will explore this technology with respect to its feasibility with respect to large (100 million computational degrees of freedom [DOFs] and higher) calculations of convective flow within critical infrastructures. Promising, highly scalable domain decomposition and multigrid methods have been under development for the last decade to facilitate large calculations utilizing finite elements (FEs). However, the development of similar methods that would apply to the boundary-element-based gridded vortex technology is still in its infancy. Consequently, there are significant challenges not only in extending the vortex technology to 3-D, but also in developing scalable methods that would allow the technology to be used for large problems.

(1) Evaluated the scalability of the multizone technique for large 3-D problems. The multizone technique for boundary-element methods (BEMs) is the analogue of domain decomposition methods for finite-element methods (FEMs). In

The proposed use of gridded vortex technology has not been attempted for three-dimensional (3-D) problems.

contrast to BEM, such methods for FEM are in an advanced state of development. An extension of such methods to BEM therefore would be a significant breakthrough and could save considerable development time. We overcame significant conceptual difficulties with respect to how one might adapt FEM techniques to BEM and, in particular, proposed a way to extend the finite-element tearing and interconnecting (FETI) technique to BEM. The scalability of this extension to BEM has not been demonstrated, but it should be possible to demonstrate the degree of scalability numerically through a straightforward application of existing FETI and BEM techniques.

(2) Extended the gridded vortex code boundary condition (BC) formulations from two dimensions (2-D) to 3-D and implemented 3-D singular adaptive numerical quadrature methods for evaluating coefficient matrices. We extracted a unit-testing version of the 2-D gridded vortex code from the ALEGRA-based framework to use as a development test-bed. We are proceeding with the development of 3-D BC formulations and numerical quadrature methods. A parallelized version of the code is also currently under development, and an evaluation of current methods for evaluating hypersingular coefficient matrices is under way.

(3) Completed a benchmark calculation, using a conventional FE code, of a large-scale experiment simulating agent dispersal in a convention center. We will use this benchmark to study the nature of turbulence produced in this class of problems, as well as illustrate the limitations of conventional methods. We completed the mesh for this problem through an external contract and initiated GILA code calculations. We will use the mesh from this benchmark for future calculations with the 3-D vortex code and will use the results for comparison purposes.

In contrast to BEM, such methods for FEM are in an advanced state of development. An extension of such methods to BEM therefore would be a significant breakthrough and could save considerable development time.

3508370000

Innovative Measurement Diagnostics for Fluid/Solid and Fluid/Fluid Interactions in Rotating Flowfields

V. A. Amatucci, S. J. Beresh, D. J. Armistead, J. L. Kalb, W. R. Escapule, J. F. Henfling

Sandia's goal in this project is to develop novel and advanced measurement diagnostics for acquiring data on a rotating subscale model in a wind tunnel. The motive for the research is to develop an ability to acquire benchmarking and eventually validation data for compressible flow simulations of the flowfield on the surface and in the vicinity of a rotating body in a transonic mean flow. We initially subdivided the project into four primary tasks: (1) an onboard jet capability simulating a spin rocket exhaust plume, (2) microelectro-mechanical systems (MEMS)-based microsensors for pressure data, (3) an onboard miniaturized data-acquisition, storage, and telemetry system, and (4) onboard optics for flow visualization.

We successfully identified problems associated with data measurements on a spinning model and laying out initial steps in achieving new capabilities. The objective is to develop and integrate Lagrangian sensors on models in compressible flows and to measure and visualize fluid interactions while telemetering the data. The spinning-body flowfield is an extremely complex problem, and the work to incorporate capabilities into a compressible flow solver to compute this problem requires extensive data for comparison with results. The need for data arises from incorporation of rotating grid capabilities into SACCARA.

We worked to develop capabilities for (1) onboard jet production and regulation to simulate the spin rocket exhaust plumes, (2) application of pressure microsensor hardware, (3) onboard flow visualization, and (4) miniaturization of a system for acquisition and telemetry of flowfield data. We eliminated all efforts in the visualization portion on the recommendation of a review panel. The technical direction of the project was to develop individual capabilities initially for a nonspinning model, then address the technical difficulties that arise from model rotation.

- *Onboard jet design.* Simulation of the plumes exhausting from the solid rocket motors using a cold gas and onboard tank supply poses four challenges: (1) determine hardware that

Sandia's goal in this project is to develop novel and advanced measurement diagnostics for acquiring data on a rotating subscale model in a wind tunnel.

could produce the required pressure, flowrate, and duration but remain in the volume consistent with subscale models; (2) determine a nozzle geometry and specific heat ratio matching in order for the cold flow to correctly match shape and impingement properties of the combustion exhaust plume; (3) control the rate and pressure of flow from the reservoir to the nozzle; and (4) investigate performance deviations of the system due to model rotation. We also began the initial work on schematics for the nonrotating case.

- *Pressure microsensors acquisition.* We identified vendors of flush-mounted pressure microsensors and contacted them to determine product technical specifications. Wide ranges of microscale sensors were available, although packaging of the flush-mounted devices was inconsistent with wind-tunnel scales, except on large-scale models. We gathered data on the sensors and acquired sensors for later testing. We plan experiments where we will vary the pressure and temperature environment for all sensors and will examine output data for range, sensitivity, dynamic response, and repeatability.

- *Visualization system based on microoptics.* We scoped out ideas for visualization of the interaction of the plume with the freestream. We acquired possible particulate sources for seeding the flows in a rotating model experiment.

- *Data system development.* We began developing a data package on the scale of a wind-tunnel model to acquire at least 16 channels of data. This would include surface and base pressure microsensors, visualization digital signal, shear stress sensors, and next-generation quantitative data such as velocity and density. The data package comprises multiplexers, signal conditioners, and the storage/telemetry hardware, as well as an onboard power source. The miniaturized data package is a hybrid of existing and new hardware.

The initial exploratory study to examine rotating model experiments with appropriate diagnostics is complete. Baseline design efforts continue, with a goal of acquiring validation data for computational tools while advancing miniaturized diagnostics.

Other Communications

Amatucci, V. A., and W. H. Rutledge. 1999. "Jet/Fin Interactions on a Rotating Body in Transonic Flight—Experiment Design." Presentation to the 92nd Supersonic Tunnel Association International (STAI) Meeting, Huntsville, AL, 3-5 October

3508380000

Capturing Recrystallization of Metals with a Multiscale Material Model

D. A. Hughes, E. A. Holm, S. M. Foiles, D. J. Bammann

The goal of this project is to develop a predictive continuum model that incorporates essential mechanisms from the atomic, dislocation substructure, and grain-size length scales. Sandia will accomplish this by developing a nonlinear, nonequilibrium, thermodynamic gradient theory that provides the mathematical framework to incorporate key microstructural processes. We will predict the physics at each length scale from experimental discovery and theoretical calculations, and the bridges between each length scale and the continuum level will be established by their contribution to the thermodynamic process. Although the framework we are developing is often more general, we chose to apply this formulation to the prediction of recrystallization processes in metals.

Recrystallization (or annealing) occurs when cold-worked metals are heated. Above approximately 60% of the melt temperature, new strain-free grains nucleate and grow to consume all the cold-worked metal. This drastically changes the dislocation density, grain size, hardness, and ductility of the material. Recrystallization often occurs during manufacturing, during high-rate deformation, and in high-temperature environments. The continuum-level material model will evolve macroscale material response based on models at lower-length scales incorporating dislocation structure evolution, grain nucleation, and grain changes due to recrystallization. Specifically, a mesoscale recrystallization model based on a Monte Carlo Potts (MCP) model will embody the local dislocation structure, grain orientation, and strain energy, which we will correlate with the variables in the continuum model.

Automated microstructural analyses in the transmission electron microscope (TEM) supplemented by atomic-scale simulations will provide experimental discovery of dislocation structure evolution and nucleation in selected bicrystals. Quantitative statistical data of dislocation and boundary properties combined with results of atomic-scale simulations and scaling theory will provide relevant parameters for models at the mesoscale. These parameters will enter new kinetic equations for dislocation structure evolution and a multigrain model of local orientation evolution.

The goal of this project is to develop a predictive continuum model that incorporates essential mechanisms from the atomic, dislocation substructure, and grain-size length scales.

Specific accomplishments at the continuum-level material constitutive law include the following. (1) At the macroscale, we added an additional state variable to the rate- and temperature-dependent BCJ (Bammann Chiesa Johnson) plasticity model (nongradient version) to simulate the stress change during dynamic recrystallization. We did this work in collaboration with Georgia Tech. The evolution of the variable depends on a critical function of the existing state variables, strain rate, and temperature. The model compares reasonably well with data on copper compression specimens. (2) We incorporated the kinematics of finite-deformation plasticity into the thermodynamic approach of Gurtin and Fried. We extended this formulation to endow the continuum with an extra rotational degree of freedom (DOF) by decomposing the deformation gradient into elastic, plastic, and rotational parts. The rotational aspects stem from the experimental observations of universal scaling for deformation microstructure evolution. We utilized this same approach of Gurtin and Fried to develop a phase-field theory for use in modeling grain growth and recrystallization from a continuum perspective.

At the mesoscale we incorporated 3-D dislocation substructures determined by experiment and MC modeling into the mesoscale recrystallization model. The mesoscale modeling effort focused on determining how strain-free nuclei form from the subgrain network. To convert the 2-D data to a 3-D subgrain structure, we developed a new MC algorithm that adjusts subgrain orientations to reflect the experimentally observed scaling laws for misorientation angles. Using this method, we generated realistic microstructures in 3-D that match all geometric and orientational parameters determined from experiments. We implemented the Read-Shockley model for grain boundary energy as a function of misorientation in the subgrain model. We incorporated grain boundary mobilities from molecular dynamics (MD) simulations into subgrain growth simulations. We performed the first 3-D simulations of grain growth with anisotropic grain boundary energy, and they showed behavior consistent with the thermodynamic analyses.

At the atomistic to grain scale, the deformation characteristics and resulting dislocation structure of the deformed and subsequently recrystallized bicrystals are important to the nucleation study. We grew, deformed, recrystallized, and quantitatively characterized bicrystals with Laue x-ray diffraction, TEM, and electron backscattered pattern analysis in the scanning electron microscope (SEM).

We performed the first 3-D simulations of grain growth with anisotropic grain boundary energy, and they showed behavior consistent with the thermodynamic analyses.

We observed the dislocation structure of compressed [421] bicrystals and measured them in the TEM and SEM. This characterization revealed a very heterogeneous microstructure with large rotations forming banded regions. Subsequently upon heat treating, we observed the banded regions that had the highest rotations to be nucleation sites for recrystallization. The relationship between the rotations and the nucleation sites provides criteria for the mesoscale recrystallization model.

Refereed

Campbell, G. H., S. M. Foiles, H. Huang, D. A. Hughes, W. E. King, D. H. Lassila, D. J. Nikkel, T. Diaz de la Rubia, J. Y. Shu, and V. P. Smyshlyaev. 1998. "Multiscale Modeling of Polycrystal Plasticity: A Workshop Report." *Mater. Sci. Eng. A* **251**: 1–22.

Doherty, R. D., D. A. Hughes, F. J. Humphreys, J. J. Jonas, D. J. Jensen, M. E. Kassner, W. E. King, T. R. McNelley, H. J. McQueen, and A. D. Rollet. 1998. "Aspects of Recrystallization." *Mater. Sci. Eng. A* **238**(2): 219–274.

Godfrey, A., and D. A. Hughes. 1999. "Scaling of Deformation-Induced Dislocation Boundaries." *Acta Materialia*, accepted.

Gurtin, M. E., and M. T. Lusk. 1999. "Sharp-Interface and Phase-Field Theories of Recrystallization in the Plane." *Physica D* **130**: 133–154.

Hansen, N., and D. A. Hughes. 1999. "Microstructural Evolution and Hardening Parameters." *Mater. Sci. and Eng.*, accepted.

Hughes, D. A., D. C. Chrzan, Q. Liu, and N. Hansen. 1998. "Scaling of Misorientation Angle Distributions." *Phys. Rev. Lett.* **81**: 4664–4667.

Lusk, M. T. 1999. "A Phase-Field Paradigm for Recrystallization and Grain Growth." *Proc. Royal Society of London* **A455**: 677–700.

Miodownik, M. A., A. W. Godfrey, E. A. Holm, and D. A. Hughes. 1999. "On Boundary Misorientation Distribution Functions and How to Incorporate Them into 3-D Models of Microstructural Evolution." *Acta Materialia* **47**: 2661–2668.

Other Communications

Bammann, D. J. 1999. "Introducing a Physical Length Scale into the Continuum." Presentation to the CalTech Colloquium, Pasadena, CA, February.

Bammann, D. J. 1999. "Introducing a Physical Length Scale into the Continuum." Presentation to the University of Illinois Colloquium, Urbana-Champaign, IL, January.

Battaile, C. C., and E. A. Holm. 1998. "Evolution of 2-D Potts Model Grain Microstructures from an Initial Hillert Size Distribution." *Grain Growth and Polycrystalline Materials III* (3rd International Conference on Grain Growth, Pittsburgh, PA, June): 119–124.

Chrzan, D. C. 1999. "Scaling of Misorientation Angle Distributions in FCC Metals." Presentation to the Theory Institute on Multiple Length-Scale Simulation of Materials Microstructure and Evolution, Argonne, IL, August.

Chrzan, D. C. 1999. "Universal Scaling of Misorientation Angle Distributions." Paper presented to Plasticity '99, Cancun, Mexico, January.

Godfrey, A., and D. A. Hughes. 1999. "Changes in the Dislocation Structure and Grain Subdivision Due to the Presence of a Grain Boundary." Paper presented to the Fall 1999 Meeting of the Materials Research Society, Boston, MA, December 1998.

Godfrey, A., and D. A. Hughes. 1998. "Characterization of Dislocation Wall Spacing Distributions." *Solidification 1998* (TMS/ASM 1997, Indianapolis, IN, September 1997): 191–199.

- Holm, E. A. 1999. "Modeling of Microstructure-Property Relationships." Paper presented to the Spring Meeting of the Ohio Section of the APS, Flint, MI, May.
- Holm, E. A., and M. Miodownik. 1999. "A Mesoscale Model for Strain-Free Grain Nucleation and Recrystallization." *Plasticity '99: Constitutive and Damage Modeling of Inelastic Deformation and Phase Transformation* (7th International Plasticity Symposium, Cancun, Mexico, January): 997–1000.
- Holm, E. A., J. W. Cahn, and M. Miodownik. 1998. "Boundary Motion by Discretized Mean Curvature in the Ferromagnetic Ising Model." Paper presented to the TMS Fall Meeting 1998, Evolving Paradigms in Microstructure Evolution Symposium, Rosemont, IL, October.
- Hughes, D. A. 1999. "Cold Deformation and the Nucleation Aspects of Recrystallization." Paper presented to Plasticity '99, Constitutive Modeling of Inelastic Deformation and Phase Transformation, Cancun, Mexico, January.
- Hughes, D. A. 1999. "Dislocation Cell and Boundary Formation." Paper presented to the Meeting of the American Physical Society, Atlanta, GA, March.
- Hughes, D. A. 1999. "Distributions of Low- and High-Angle Boundaries in Deformed Metals." *Recrystallization '99, The 4th International Conference on Recrystallization and Related Phenomena* (Tsukuba City, Japan, July): 111–118.
- Hughes, D. A. 1999. "Grain Subdivision and Microstructure Evolution During Deformation." Presentation to the Colloquium, Johns Hopkins University, Baltimore, MD, May.
- Hughes, D. A. 1999. "Grain Subdivision and Microstructure Evolution During Deformation." Presentation to the Colloquium, University of Michigan, Ann Arbor, MI, April.
- Hughes, D. A., and A. Godfrey. 1998. "Microstructure and Texture Development of Compressed [421] Single Crystals and [421]/[13 4-3] Bicrystals." *Plasticity '99, Constitutive Modeling of Inelastic Deformation and Phase Transformation* (Cancun, Mexico, January 1999): 153–156.
- Lusk, M. T. 1999. "An Alternative Phase-Field Paradigm for Modeling Grain Growth and Recrystallization." Presentation to the Colloquium, Albuquerque, NM, June.
- Lusk, M. T. 1998. "Modulated Energy Functions and Recrystallization." Paper presented to the Materials Research Society, Symposium L: Interaction of Phase and Defect Microstructures in Metallic Alloys, Boston, MA, 2–6 December.
- Lusk, M. T. 1999. "Phase-Field Modeling of Microstructural Evolution." Presentation to the Student Workshop Seminar, Livermore, CA, August.
- Lusk, M. T., and P. Liu. 1999. "Accounting for Grain Misorientation Via Energy Modulation." Paper presented to Plasticity '99: The 7th International Symposium on Plasticity and Its Current Application, Cancun, Mexico, January.
- Lusk, M. T., and P. Liu. 1998. "A Modulated Energy Model for Simulating Grain Boundary Kinetics: Solid-State and Granular Media." Paper presented to the Society for Engineering Science, Pullman, WA, October.
- Lusk, M. T., G. Grach, and D. Bammann. 1999. "Simulating Inelasticity Using a Modulated Energy Function." Presentation to the Student Workshop Seminar, Livermore, CA, August.
- Miodownik, M. 1998. "A Monte Carlo Model of Zener Pinning Which Shows f^{-1} Dependence." *Grain Growth in Polycrystalline Materials, III* (3rd International Conference on Grain Growth, Pittsburgh, PA, June): 283–288.
- Miodownik, M., A. D. Rollett, and E. A. Holm. 1998. "Boundary Motion by Curvature in the Ferromagnetic Potts Model with Triple Functions." Paper presented to the TMS Fall Meeting 1998, Evolving Paradigms in Microstructure Evolution Symposium, Rosemont, IL, October.

Miodownik, M. A., E. A. Holm, A. W. Godfrey, D. A. Hughes, and R. LeSar. 1999. "Multiscale Modeling of Recrystallization." *Proc. MRS* (Boston, MA, December 1998).

3508390000

Nondeterministic Modeling in Engineering Science

J. R. Red-Horse, D. G. Robinson, V. J. Romero, T. L. Paez, R. V. Field, Jr.

The focus of this project is the probabilistic evaluation of nondeterministic effects that are present in the response of an engineering system due to input parametric uncertainty. The functional relationship mapping the uncertain parameters to the possible response outcomes defines what is known as a response surface, and the joint space over which the parameters themselves are defined is the design space. Statements of probability for the response, which can be expressed in terms of the probability that a response surface is less than some threshold, are specified via complex integrals over subdomains of design space. Quantifying these statements at a number of thresholds provides an approximation to the cumulative distribution function (CDF) for the given response and thus provides a complete statistical description of the response.

The methods under consideration in this project have the following in common. Each exploits some assumed analytical characteristics, either in the probabilistic models of the input parameters or in the response surfaces, to reduce in large measure the number of finite-element (FE) code runs, function evaluations, required in evaluating the statistics of the response.

A key point to consider is that while all methods, whether sampling-based or analytical, utilize probabilistic features of the input parameters in assessing those of the corresponding response, analytical approaches are often particularly sensitive to the correct characterization. This fact makes a compelling case for seeking to develop methods to make such characterizations accurately.

With regard to reliability-based approaches to evaluating the so-called *uncertainty propagation problem*, there were numerous accomplishments. Among these were (1) the development of a new methodology for evaluating integrated quantities, such as those one would encounter when evaluating statistical moments; (2) the development of a new approach to building a transformation to standard normal space that lies at the heart of many fast probability integration methods; (3) the development of two new methods for including uncertainty in

...while all methods, whether sampling-based or analytical, utilize probabilistic features of the input parameters in assessing those of the corresponding response, analytical approaches are often particularly sensitive to the correct characterization. This fact makes a compelling case for seeking to develop methods to make such characterizations accurately.

complex problems that have been identified, implemented in a user-friendly software package, and used to assess the reliability impact of a number of stockpile issues: (a) quasi-Monte Carlo (MC), where deterministic sampling is accomplished in Halton space resulting in lower estimation error with approximately a 25% reduction in the number of function evaluations when compared to stratified MC methods such as Latin Hypercube Sampling (LHS), and (b) the Field Analysis Method, a hybrid method that combines the benefits of quasi-MC sampling, the max-likelihood method of Breitung, and spatial statistics. This latter method requires fewer function evaluations than some analytical methods and minimizes the number of function evaluations to account for the complexity of the system uncertainty. We published a technical advance on this method and will submit a patent application. In the area of stochastic FEs, we built a simplified framework around a well-understood and accessible applications code, SALINAS, a structural dynamics FE program currently under development at Sandia. We completed an example nonlinear application, the modal analysis of a thin-walled tube possessing a structural joint with stiffness properties modeled as a random field. (4) We applied the Finite-Element/Lattice-Sampling (FELS) method to the global phase of a firing-set worst-case heating optimization problem. This new method handily outperformed genetic algorithm (GA) and random searching approaches previously tried at Sandia. We devised a new noise-tolerant local optimization method based on FELS principles and applied the method to a noisy firing-set optimization problem. The new local optimization technique dramatically outperformed conjugate gradient, GA, and coordinate pattern-search local optimization techniques. We devised and tested a framework that separates and efficiently treats the different sources of uncertainty in optimization problems. We demonstrated these new capabilities through an example heat-transfer application, namely, the effect of an uncertain material property (emissivity), and examined uncertainty in the form of its probability density function (pdf) in the firing-set optimization problem. We compared the different optima determined with (a) mean emissivity values, (b) bonding emissivity values, and (c) full distribution information (probabilistic).

The new local optimization technique dramatically outperformed conjugate gradient, GA, and coordinate pattern-search local optimization techniques.

Refereed

Ghanem, R. G., and J. R. Red-Horse. 1999. "Propagation of Probabilistic Uncertainty in Complex Physical Systems Using a Stochastic Finite Element Approach." *Physica D* **133** (January): 137–144.

Mahadevan, S., D. G. Robinson, and Z. Guo. 1999. "Stress Voiding of Electronic Circuits." *IEEE Transactions on Reliability*, in review.

Robinson, D. G. 1999. "Comparison of Quasi-Monte Carlo and Latin Hypercube Sampling for Structural Reliability Analysis." *Reliability Engineering and System Safety*, in review.

Robinson, D. G., S. Mahadevan, and Z. Guo. 1999. "Time-Dependent Stress Voiding of Electronic Circuits." Paper published as a chapter in the book *Computational Stochastic Mechanics*, Spanos, ed. Rotterdam, The Netherlands.

Romero, V. J. 1999. "Treatment of Uncertain Emissivity in a Large Thermal-Optimization Problem." *Proc. 33rd National Heat Transfer Conf.* (Albuquerque, NM, August).

Other Communications

Field, Jr., R. V., T. L. Paez, and J. R. Red-Horse. 1999. "Numerical Techniques to Evaluate Moments of Dynamic System Response." *Proc. 13th ASCE Engineering Mechanics Division Conf.* (Baltimore, MD, June).

Field, Jr., R. V., T. L. Paez, and J. R. Red-Horse. 1999. "Utilizing Gauss-Hermite-S Quadrature to Evaluate Uncertainty in Dynamic System Response." *Proc. 17th Internat. Modal Analysis Conf. 1* (Kissimmee, FL, February): 1856–1861.

Robinson, D. G. 1999. "An Adaptive Sampling Method Utilizing Regionalized Random Variables." *Proc. Internat. Conf. on Applications of Statistics*, accepted.

Robinson, D. G. 1999. "CRAX/Cassandra Reliability Analysis Software." *Proc. AIAA Structures, Structural Dynamics, and Materials (SDM) Conf.* (St. Louis, MO, April).

Robinson, D. G., and C. Atcitty. 1999. "Comparison of Quasi- and Pseudo-Monte Carlo Sampling for Reliability and Uncertainty Analysis." *Proc. AIAA Structures, Structural Dynamics, and Materials (SDM) Conf.* (St. Louis, MO, April).

Romero, V. J. 1999. "Efficient Global Optimization under Conditions of Noise and Uncertainty—A Multi-Model Multi-Grid Windowing Approach." *Proc. 3rd World Congress of Structural and Multidisciplinary Optimization* (Buffalo, NY, May).

3508410000

Lagrangian Modeling of Radiative Transport

L. A. Gritz, P. E. Desjardin, J. H. Strickland

Many complex multiphysics, multiscaled, time-dependent processes include radiative heat transfer in turbulent flow. Conventional grid-based models are not well suited for such problems due to the complexity of gridding domains, which are very large relative to the scale required to resolve the important transport phenomena. A logical alternative is the gridless, Lagrangian-based approach employed in vortex methods that have been used successfully to simulate turbulence dynamics in internal and external flows, mixing flows, and buoyant jets and plumes. The same strategy was employed at MIT in formulating the transport element method (TEM), which is used with the vortex method, to solve the species transport equation and the energy equation in nonreacting and reacting flows. Sandia developed a compatible approach to simulate radiative transport, which exploits fast solvers developed at Sandia and massively parallel (MP) architectures. The technique is capable of addressing 3-D problems with nonuniform properties and yields solutions that are significantly more accurate than methods invoking simplifications of the governing equations.

We developed a gridless technique (compatible with numerical simulation of the flow and temperature field by gridless vortex and TEMs, respectively) for the solution of the integral form of the radiative transfer equation for an emitting and absorbing medium with nonuniform properties. We obtained the solution by representing the medium by Lagrangian elements whose strength is dependent on the absolute value and/or gradients of local temperature. We compared results to established and newly developed closed-form solutions for a planar medium. We illustrated significant errors in other techniques that include simplifications of the governing equations by direct comparison with the present solutions. We also developed a fast-solver algorithm, based on the expansion of the Green's function in terms of a convergent separable series, for radiative transfer in a planar medium. We investigated axisymmetric forms of the radiative transfer equation and showed them to not be conducive to the favorable form of equations obtained in planar or 3-D media. We developed an accurate, approximate solution strategy that includes near- and far-field formulations and can couple it to

Sandia developed a compatible approach to simulate radiative transport, which exploits fast solvers developed at Sandia and massively parallel (MP) architectures. The technique is capable of addressing 3-D problems with nonuniform properties and yields solutions that are significantly more accurate than methods invoking simplifications of the governing equations.

the TEM code to provide combined solutions of reacting flow and radiative transport. We developed a 3-D direct solver and verified the results using closed-form solutions for planar media. We completed development of a 3-D fast solver. Fast solvers for both planar and 3-D media show order-of-magnitude decreases in computational expense for reasonable numbers of elements and were employed in a parallelization framework recently developed at Sandia. We developed and implemented methods for treating nonuniform radiative properties and grey boundaries. The boundary term includes the same form of the kernel as the field integral equation, but also includes anisotropy associated with hemispherical surface emission centered about the surface unit normal. Grey boundaries also serve to couple the field and boundary terms since energy within the field can reflect from the surface and be absorbed elsewhere in the field. We performed limited verification and validation. As a consequence of the detailed investigation performed as part of this work, we deemed the TEM unsuitable for coupling with the gridless radiation techniques to provide fully coupled fire solutions. Additional development is being performed in collaboration with MIT on alternative techniques that model transport of the scalars as opposed to modeling gradients as conducted in the TEM. While gridless scalar transport simulation technology matures, the gridless radiation approach developed in this work will be immediately applicable to model radiation heat transfer in Lagrangian submodels of particle transport.

While gridless scalar transport simulation technology matures, the gridless radiation approach developed in this work will be immediately applicable to model radiation heat transfer in Lagrangian submodels of particle transport.

Refereed

Gritz, L. A., and J. H. Strickland. 1999. "A Gridless Solution of the Radiative Transfer Equation for Fire and Combustion Calculations." *Combustion Theory and Modeling* **3** (March): 159–175.

Gritz, L. A., and J. H. Strickland. 1998. "A Vortex and Transport Element Method Compatible Technique for Solving 1-D and 3-D Radiative Heat Transfer." Paper presented to the 3rd International Workshop on Vortex Flows and Related Numerical Method, Toulouse, France, 24–27 August.

Lakkis, I., and A. F. Ghoniem. 1999. "Grid-Free Simulation of Radiative Transport in a Participating Medium." *European Series in Applied and Industrial Mathematics, Proc. 3rd Internat. Workshop on Vortex Flows and Related Numerical Methods* **7** (January) (Toulouse, France, 24–27 August 1998): 234–246.

Strickland, J. H., L. A. Gritz, R. S. Baty, G. F. Homicz, and S. P. Burns. 1999. "Fast Multipole Solvers for Three-Dimensional Radiation and Fluid Flow Problems." *European Series in Applied and Industrial Mathematics, Proc. 3rd Internat. Workshop on Vortex Flows and Related Numerical Methods* **7** (January) (Toulouse, France, 24–27 August 1998): 408–417.

3508420000

High-Resolution Modeling of Multiscale Transient Phenomena in Turbulent Boundary Layers

A. R. Kerstein, V. Nilsen, S. E. Wunsch, T. Echehki, R. C. Schmidt

Modeling of transient multiphysics phenomena in turbulence is especially difficult near walls, where the enhanced role of molecular transport introduces length scales far smaller than scales resolvable by three-dimensional (3-D) computational models. Present-day empirical wall treatments are not applicable to strongly coupled multiphysics environments.

One-dimensional turbulence (ODT), the novel modeling approach adopted in this project, addresses this difficulty by capturing relevant length and time scales in an unsteady 1-D simulation. One goal of this project is to incorporate the coupled effects of transient applied shear, buoyancy, exothermic chemical reactions, and heat and mass transfer, with attendant property variations, into ODT. Sandia will use this formulation to perform parametric studies to support the development of improved wall treatments for steady-state flow solvers, with emphasis on the needs of the FUEGO fire-model development effort.

Another goal of this project is to develop, test, and implement an ODT-based wall submodel for large-eddy simulation (LES). This effort will provide a proof-of-principle demonstration of capabilities to simulate combustion, heat transfer, and related multiphysics phenomena in turbulent flows with wall geometries relevant to programmatic applications.

We simulated turbulent jet diffusion flames using a formulation of ODT that was integrated into Sandia's CHEMKIN gas-phase chemistry/transport/thermodynamics code package. Favorable comparisons to measured fluctuation statistics of chemical species and temperature confirmed the validity of the ODT representation of turbulence-chemistry interactions.

We computationally implemented reformulation of ODT that we developed last year and initiated validation tests. The reformulation generalizes the model so that all three velocity components are represented on the 1-D domain, a feature needed for the implementation of ODT as a subgrid model for LES. We showed this formulation to reproduce key features of

This effort will provide a proof-of-principle demonstration of capabilities to simulate combustion, heat transfer, and related multiphysics phenomena in turbulent flows with wall geometries relevant to programmatic applications.

the anisotropic structure of turbulent shear flow. We performed simulations involving an array of coupled ODT domains as a prototype of ODT implementation as a near-wall subgrid-scale model for LES. These simulations reproduced the measured scaling of the friction coefficient in the turbulent flat-plate boundary layer, a key test of the subgrid formulation.

We formulated the couplings among the ODT domains, and between these domains and an LES solver, in a manner that captures the physics governing complex near-wall flow phenomena. To implement this formulation, we collaborated with a Stanford University researcher who provided an LES code. We integrated the ODT near-wall formulation into this code. We resolved several performance issues encountered during initial tests by modifying the physical modeling and numerical implementation of the coupling between the LES flow solver and the ODT subgrid simulations.

Refereed

Dreeben, T. D., and A. R. Kerstein. 1999. "Simulation of Vertical Slot Convection Using 'One-Dimensional Turbulence.'" *Internat. J. Heat and Mass Transfer*, submitted.

3508430000

Dispersive Measurements of Velocity in Heterogeneous Materials

W. M. Trott, M. D. Knudson, L. C. Chhabildas, M. R. Baer

To develop a database for validation of 3-D numerical simulations of heterogeneous materials subjected to impact loading, Sandia continued to exploit its adaptation of an optically recording velocity interferometer system (ORVIS) to a line-imaging instrument capable of generating precise measurements of spatially resolved velocity variations during dynamic deformation. Combining independently variable target magnification and interferometer fringe spacing, this instrument can probe velocity variations along line segments up to 5–10 mm in length. In high-magnification operation, we can achieve spatial resolution better than 10 μm ; moreover, for events appropriate to short recording times, we can obtain temporal resolution better than 0.2 ns.

The principal focus of our research involved line-imaging ORVIS evaluation and validation in numerous tests involving well-characterized impact loading of several different materials at a gas-gun facility. Also, we implemented several improvements to the interferometer as well as to the optical interface to the gas-gun target chamber. In particular, we modified the optical system to permit measurements over an expanded field of view (line segments up to 5–10 mm in length).

Initial gas-gun experiments involved symmetric impact of fused silica with velocity measurements performed on the distal free surface of the fused silica acceptor. For a given geometry and impact velocity, this configuration generates a predictable response (a ramp wave of known risetime to a known terminal velocity, followed by rapid unloading) that we can use to verify the system performance. The velocity-time histories measured by the line-imaging ORVIS were completely consistent with the predicted response, demonstrating the high-resolution (spatial and temporal) response of this system.

We performed numerous experiments on a variety of heterogeneous materials including low-density pressings of sugar (an inert simulant for the pressed, granular high-explosive HMX), foam, and glass-reinforced polyester. In most cases, we obtained simultaneous line-imaging ORVIS and conventional VISAR (single-point velocity interferometry

The principal focus of our research involved line-imaging ORVIS evaluation and validation in numerous tests involving well-characterized impact loading of several different materials at a gas-gun facility.

system for any reflector) measurements to allow direct comparison of the two techniques. In the case of sugar, we determined measured response as a function of both impact velocity and changes in particle-size distribution. We obtained a consistent picture of the dispersive nature of the wave transmitted through these samples as a function of impact velocity. The line-imaging ORVIS records clearly revealed both transverse and longitudinal wave structure on mesoscopic scales; we can use the amplitude and frequency of these effects to test and refine the highly structured mesoscopic response typically generated by 3-D simulations. We also observed definite variations in the degree of dispersion in the transmitted wave as a function of average particle size.

Collaborative 3-D simulations of the detailed response of low-density, pressed sugar to impact loading (for comparison with the spatially resolved experimental results) are in progress. We also performed collaborative experimental and theoretical work on the response of impact-loaded glass-reinforced polyester. Micromechanical modeling predicts substantial oscillations (resonance-like effects) in the transmitted wave profiles due to the fine-scale, periodic geometric structure of these materials. We observed highly structured response of this type with the line-imaging ORVIS technique.

In concert with experimental progress, we developed and tested the first-generation integrated data analysis package that includes ORVIS image preprocessing, extraction of fringe intensity versus time, and export to an existing VISAR analysis platform (Sandia's VISAR96 program). We identified several needed improvements to the data analysis routine (to account for geometric distortions in the detector sweep, maximize velocity-time information per image, etc.). We are incorporating these changes into a more robust second-generation package. In addition, we demonstrated a practical method for extracting an areal velocity map (at one point) from full-frame charge-coupled device (CCD) images of the interferometer fringe field.

In concert with experimental progress, we developed and tested the first-generation integrated data analysis package that includes ORVIS image preprocessing, extraction of fringe intensity versus time, and export to an existing VISAR analysis platform (Sandia's VISAR96 program).

Refereed

Trott, W. M., M. D. Knudson, L. C. Chhabildas, and J. R. Asay. 1999. "Measurements of Spatially Resolved Velocity Variations in Shock Compressed Heterogeneous Materials Using a Line-Imaging Velocity Interferometer." (Invited) *Shock Compression of Condensed Matter 1999*, accepted.

3508440000

A Physically-Based Computational Method for Predicting Generalized Fracture

P. A. Klein, J. A. Crowell, J. W. Foulk, III, S. A. Wimmer

Fracture is an important mode of failure, and computational methods for its simulation are essential to failure prediction. Yet an efficient, exhaustive computational method for accurate fracture prediction does not exist at this time. Attempts at combining classical (or continuum) fracture mechanics with the standard finite-element method (FEM) or with meshless methods, such as the element-free Galerkin (EFG) method, offer a good first step; however, FEM has inherent difficulties in resolving arbitrary crack trajectories, and the current development of EFG is limited to the growth of predefined, existing cracks. Furthermore, both approaches are subject to the limitations of classical fracture mechanics, which deals with preexisting cracks and with crack-growth criteria that have not been validated under generalized conditions. This project will develop a new computational tool based on meshless computational methods in conjunction with embedded traction-separation (or cohesion) relations. Meshless methods provide automatic resolution of new surfaces as they develop during the solution process, avoiding the remeshing and remapping required with traditional FEM. Traction-separation relations provide a physically-based resistance to fracture. This tool is capable of solving the complete evolution of fracture that encompasses crack nucleation, crack growth, crack interaction, crack branching, and material fragmentation. This provides a high-fidelity capability for predicting generalized fracture with application to a wide range of problems, including polymer aging, thermally induced cracking of encapsulants, glass fragmentation, and weapon slap-down.

We extended and generalized the capabilities of the fracture simulation code based on the EFG method. We can now use the code with arbitrary point arrangements in both two and three dimensions. Arbitrary fracture surfaces are represented with cutting facets, line segments in two dimensions, and triangular facets in three dimensions, across which the displacement field exhibits a discontinuous jump. Crack growth occurs when the cohesive strength of the material is exceeded. Crack extension is followed by efficient, selective recalculation of the EFG shape functions for nodes in the

This tool is capable of solving the complete evolution of fracture that encompasses crack nucleation, crack growth, crack interaction, crack branching, and material fragmentation.

vicinity of the new crack front without changes to the initial discrete model. We embedded the EFG formulation in a general-purpose FE simulation framework. This allows simulation of larger, more realistic models since the more computationally intensive EFG formulation can be applied only to regions in which fracture is expected. The remainder of the domain may be treated with standard FE techniques. We implemented the consistent EFG/FE coupling formulation developed at Northwestern University in both two and three dimensions. Generation of the coupling layer is largely automatic, requiring minimal preprocessing or user input.

Incorporation of the meshless method into a more general simulation framework resulted in the additional capabilities of implicit and explicit quasi-statics and transient dynamics at infinitesimal strains and finite strains, using a total Lagrangian hyperelastic formulation. The fracture process itself is modeled with cohesive tractions applied across surfaces that become additional crack faces through the course of the simulation. Cohesive surface laws of arbitrary form may be used in both two and three dimensions, though history dependence has not been incorporated yet. We have used 2-D and 3-D cohesive relations based on the formulation done at Brown University for initial benchmarking calculations, as well as more simple, mode-independent cohesive relations. For Mode I fracture of a slender, double-cantilever beam, predicted crack length as a function of applied displacement agrees well with the analytical solution derived from linear elastic fracture mechanics. We also performed more qualitative examples of generalized crack propagation in both two and three dimensions for which there are no analytical solutions. In two dimensions, we present the calculation of crack growth in an asymmetric three-point bending geometry. In three dimensions, we simulate the growth of cracks in an encapsulant loaded by differential thermal expansion. We have been working in collaboration with Brown University to identify experimental results of generalized brittle fracture that we could use to verify the code. Likely candidates include cone fracture during indentation and fracture in glass plates driven by residual thermal strains.

Incorporation of the meshless method into a more general simulation framework resulted in the additional capabilities of implicit and explicit quasi-statics and transient dynamics at infinitesimal strains and finite strains, using a total Lagrangian hyperelastic formulation.

Refereed

Klein, P. A., and H. Gao (Stanford). 1999. "A Study of Multiscale Dynamics of Crack Tip Branching Via the Virtual Internal Bond Model." Paper presented to the ASME Mechanics and Materials Conference, Blacksburg, VA, 28 June.

Klein, P. A., and H. Gao (Stanford). 1999. "Dynamic Fracture Simulation Using a Virtual-Internal-Bond Approach." Presentation to the U.S. National Congress of Computational Mechanics, Boulder, CO, 5 August.

Tabbara, M. R., and C. M. Stone. 1998. "A Computational Method for Quasi-Static Fracture." *Computational Mechanics* **22** (August): 203–210.

MANUFACTURING & PROCESS SCIENCES

Manufacturing and Process Sciences is one of Sandia National Laboratories' six LDRD Roadmap Technologies investment areas. Roadmap Technologies derive their scientific basis from and extend the applications of Research Foundations investments into new areas. Roadmap Technologies create or accelerate scientific and technical expertise for future program areas that are strategic to Sandia and important to the DOE and the nation.



Time and cost are keys to success for manufacturing systems. The Manufacturing and Process Sciences investment area targets research that offers new processes to reduce product or service defects, thus reducing manufacturing time and cost. Investigations enable technology advances—such as software, sensors and actuators, modeling, simulation, visualization, fixturing, and handling—with the potential to reduce defects and costs. The research is evaluated for impact on existing and emerging technologies, nuclear weapon technologies, and project feasibility.

The overall goal of the “Advanced Production Planning Models” project is to explore the development of an effective suite of solvers that has application for advanced production planning at facilities in the Nuclear Weapons Complex (NWC). The focus of the investigation has been the development of an innovative modeling approach for improving production and

transportation surety by increasing efficiency and agility, minimizing vulnerability to disruption, and increasing the ability to meet schedules. The approach entails a fundamentally different way of interpreting and formulating problems of this type by depicting time periods that may consist of variable lengths. A formulation of this research was implemented at Pantex and was honored as a finalist for the 1999 Franz Edelman Award, sponsored by the Institute for Operations Research and Management Science (INFORMS).



3510710000

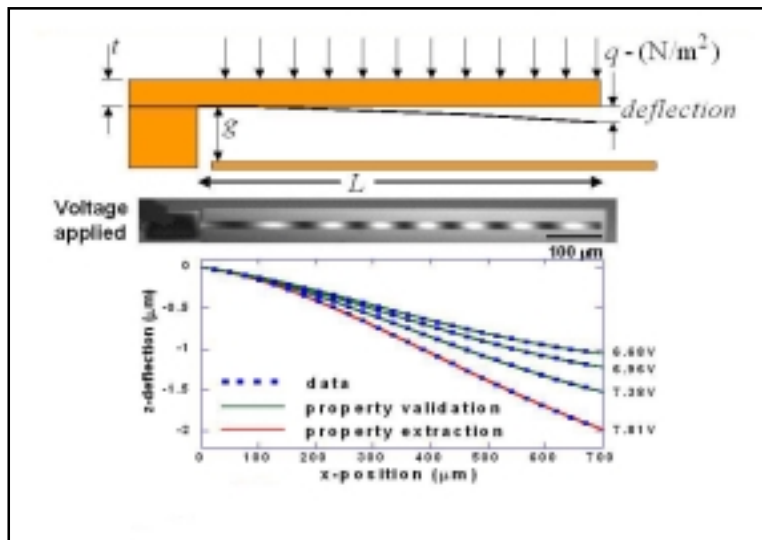
Microdiagnostic MEMS Lab-on-a-Chip

M. P. de Boer, M. B. Sinclair, N. Masters, N. F. Smith, F. Bitsie

Although mechanical properties of microelectromechanical systems (MEMS) structural materials are critical to product design and performance, there exists no infrastructure for their routine measurement. Furthermore, when measurements are presently made on an interferometric microprobing station, resolution is very high but accuracy is not well known. Sandia will overcome these deficiencies by developing a self-validating suite of small-area test structures for automated measurement. Statistical quality control can then become the basis for MEMS design, process improvement, and reliability. Because MEMS are radiation-hard and demonstrate promise for nuclear weapons surety, this work will directly benefit the nuclear weapons program.

We modeled our approach for developing microdiagnostic MEMS devices after parametric devices in microelectronics—we believe a similar avenue is feasible and is indeed the best approach for MEMS. Relevant mechanical properties include residual stress, stress gradient, adhesion, friction, and fracture strength. Our project will have two main thrusts. The first is to optimize test structures, in conjunction with a determination of the accuracy of the mechanical tests from optoelectrical probing techniques. To validate test results, we will use measured device parameters to predict performance of a composite test structure. We will then compare predictions to actual performance. The second thrust is to implement the

Sandia will...develop a self-validating suite of small-area test structures for automated measurement. Statistical quality control can then become the basis for MEMS design, process improvement, and reliability. Because MEMS are radiation-hard and demonstrate promise for nuclear weapons surety, this work will directly benefit the nuclear weapons program.



Interferometric measurements result in accurate, verifiable modeling as shown in this point-loaded cantilever beam test.

procedures on an automated prober by working in collaboration with an equipment vendor.

The development of a standard suite of diagnostic device designs with properly validated measurement and analysis specifications will enable first-run success of designs and facilitate the production and reliability of MEMS, both in Sandia nuclear weapons surety applications and in the commercial world.

We showed that our technique for measuring mechanical properties in MEMS is viable. Using interferometry data, we modeled and predicted MEMS deflections to high accuracy. We discovered unexpected non-idealities in the surface-micromachining process (SUMMiT), learned to model these, and are working with process engineers to minimize them. We are on track to build a prototype integrated instrument that will compare measured data to models in order to automatically extract MEMS mechanical properties to high accuracy. No such instrument exists. We presented a conference paper that drew high interest to our technique. We are working with ASTM (American Society for Testing and Materials), a standards committee, to urge that the method we are developing become an accepted standard. This instrument will significantly enhance Sandia's ability to make MEMS a reality in surety applications.

Refereed

de Boer, M. P., B. D. Jensen, and F. Bitsie. 1999. "A Small-Area *In Situ* MEMS Test Structure to Measure Fracture Strength by Electrostatic Probing." *Proc. SPIE, Mater. and Device Characterization II* **3875** (Micromachining and Microfabrication, Santa Clara, CA, 20–22 September): 97–103.

Jensen, B. D., F. Bitsie, and M. P. de Boer. 1999. "Interferometric Measurement for Improved Understanding of Boundary Effects in Micromachined Beams." *Proc. SPIE, Mater. and Device Characterization in Micromachining II* **3875** (Micromachining and Microfabrication, Santa Clara, CA, 20–21 September): 61–72.

Jensen, B. D., M. P. de Boer, and S. L. Miller. 1999. "IMaP: Interferometry for Materials Property Measurement in MEMS." *Modeling and Simulation of Microsystems*, ISBN 0-9666135-4-6 (San Juan, Puerto Rico, 19–21 April): 206–209.

Limary, S., H. Stewart, L. W. Irwin, J. McBrayer, S. Montague, J. H. Smith, J. J. Sniegowski, and M. P. de Boer. 1999. "Reproducibility Data on the SUMMiT Process." *Proc. SPIE* **3874** (Micromachining and Microfabrication Process Technology, Santa Clara, CA, 20–21 September): 102–112.

Other Communications

de Boer, M. P., and B. D. Jensen. 1999. "Analysis of MUMPS 28—Mechanical Properties of Beams." Paper presented to the ASTM Round Robin Committee Meeting, Seattle, WA, 18 May.

We are on track to build a prototype integrated instrument that will compare measured data to models in order to automatically extract MEMS mechanical properties to high accuracy. No such instrument exists....This instrument will significantly enhance Sandia's ability to make MEMS a reality in surety applications.

3510720000

Real-Time Error Correction Using Electromagnetic Bearing Spindles

J. P. Lauffer, P. S. Barney, J. M. Redmond

Electromagnetic (EM) bearing spindles have been identified as a critical component needed to revolutionize manufacturing in the next century. Ultra-high speeds are enabled by the noncontacting nature of the EM bearing, making it a candidate technology for machining very hard materials (such as ceramics) with reduced cutting forces, lower heating rates, and minimal coolant consumption as compared to conventional machining processes. Furthermore, high-bandwidth error correction can be achieved through manipulation of the magnetic fields in the bearing gaps, minimizing the potential for dimensional errors while producing superior surface finishes. As such, development of this technology is critical to the Defense Programs (DP) manufacturing infrastructure, which increasingly relies on rapid production of small-lot components.

Available research in this emerging technology has focused on simplistic control strategies for maintaining stable spindle levitation. Dynamic error compensation has not been rigorously examined due to the required controller complexity and concerns for robust stability margins. In this project, Sandia will develop nonlinear control strategies to improve the dynamic stiffness of an EM bearing spindle while providing real-time correction for rotational and translational spindle errors. We envision an integrated program of process modeling, controller development, and experimental evaluation of the EM bearing spindle in collaboration with Michigan Technological University (MTU) and the University of California–Santa Barbara.

We investigated high rpm (revolutions per minute) operations to evaluate a least mean squares (LMS) control algorithm and to measure bearing drag and wrote a symposium article.

The new LMS controller proved to be fairly stable and significantly reduced the imbalance error in the shaft. We used this algorithm to obtain rotational speeds well above 10,000 rpm.

...development of this technology is critical to the Defense Programs (DP) manufacturing infrastructure, which increasingly relies on rapid production of small-lot components.

3510730000

Thin-Film Deposition Processes Incorporating In Situ Monitoring Capabilities

D. P. Adams, J. A. Romero, R. S. Goeke, J. P. Brainard, J. A. Floro

This project explores thin-film deposition processes that combine flexible growth techniques and in situ, rapid-feedback diagnostics. This should impact components that require long-term, thin-film reliability by establishing new, robust processes with improved yield.

In particular, Sandia is investigating sputter deposition and reactive growth techniques for fabricating various two-component thin films, including metal hydrides. Applications of these films are found in defense programs and in many industrial applications. We are researching sputter deposition to modify film properties and performance, including microstructure, residual stress, and adhesion. Furthermore, reactive deposition should reduce the growth temperature required to form a stoichiometric compound, compared with processes that react on single-metal component films after deposition. Lower temperatures also prevent unpredictable, catastrophic changes in structure that affect performance.

We will also research the evolution of residual stress to understand its fundamental relationship(s) to process parameters. We incorporated a recently developed stress monitor onto a deposition system equipped for sputtering. The monitor allows accurate, real-time measurements of stress during different stages of film fabrication. We expect our studies will increase the general understanding of stress for two-component thin-film systems. We performed a few detailed in situ studies of stress evolution during reactive deposition for nitrides. However, no detailed studies address the stress evolution of hydride thin films.

We constructed a new ion-beam sputter-deposition system having multiple deposition sources, a sample holder/heater, and an *in situ* stress diagnostic tool. We designed this system for reactive deposition using an electron cyclotron resonance (ECR) source to generate a hydrogen (H) plasma and a Kaufmann source for sputtering metal. We used this ultra-high-vacuum system to grow stoichiometric erbium (Er) tri- and dihydride films. We completed a number of experiments to probe the phase-formation dependence on temperature and H partial pressure. Analysis of films included forward recoil

This should impact components that require long-term, thin-film reliability by establishing new, robust processes with improved yield....our studies will increase the general understanding of stress for two-component thin-film systems.

spectroscopy to determine metal/H ratios and x-ray diffraction for determining phase and stress.

In addition, we procured a Sandia-developed thin-film stress-monitoring technique and incorporated it onto the vacuum system. This multibeam optical sensor monitors thin-film residual stress in real time with high sensitivity. It is now calibrated and online. We conducted a few experiments with this sensor using a static sample geometry.

3510740000

Optimization of Filled Polymer Materials

J. A. Emerson, F. B. Van Swol, J. G. Curro

Filled polymers are the most common organic-based materials used throughout the world. However, the addition of fillers to polymer mixtures is an empirical procedure. The manufacture of neutron generators (NGs) and electronic packages are but two of a number of processes deemed crucial to Sandia's mission that require the careful tailoring of a mixture of filler and polymer fluids. Sandia will develop a powerful, novel approach designed to optimize the properties of this composite mixture. In particular, we seek to satisfy the need for the highest possible filler fraction with the lowest viscosity as dictated by the processing requirements.

Computational modeling is an ideal tool for this task, as it allows one to reliably determine the general trends needed to guide the mixture's design while minimizing the number of costly experiments. Our idea is based on the following step-wise approach involving validation experiments and modeling. From our polymer fluids theory Polymer Reference Interaction Site Model (PRISM) we will determine the effective solvation potential acting between two interacting filler particles. We will use these potentials as input to traditional molecular dynamics (MD) simulations of multiparticle systems to determine the viscosity, thermal expansion coefficient, conductivity, and other critical physical properties. To determine the filler-particle-size distribution that will optimize the composite's properties, we will build on our recent discovery that packing properties of polydisperse systems are almost entirely described by just three moments of the distribution. We will validate modeling predictions by measuring viscosity and thermal expansion coefficients as a function of particle-size distribution on well-characterized systems.

A useful but tractable model of a filled polymer is to consider it a collection of spherical particles of varying sizes in a polymer. The goal is to optimize the distribution of particle sizes such that we maximize the packing fraction of filler while minimizing the viscosity. At first sight this is a daunting task, as optimizing a size distribution represents solving a problem in a high-dimensional (or essentially infinite) parameter space consisting of size ratios and mole fractions. To solve this problem we use recent advances based on the statistical mechanics of liquid-state theory.

The manufacture of neutron generators (NGs) and electronic packages are but two of a number of processes deemed crucial to Sandia's mission that require the careful tailoring of a mixture of filler and polymer fluids. Sandia will develop a powerful, novel approach designed to optimize the properties of this composite mixture.

We found that the equation of state of a polydisperse mixture of hard spheres is fully described by the packing fraction and the second and third (scaled) moments of the size distribution. We used this fact to formulate a vast generalization of this observation, namely that at a given packing fraction the viscosity is also just a function of three variables. This then reduces the very large parameter space to just a three-dimensional (3-D) space.

We can use the two-moment approximation to predict the viscosity of a hard sphere mixture once the viscosity of a monodisperse system is known. There are two ways to do this. In the first method we make the ansatz that the viscosity is a function of the pressure and the two distribution moments. This allows the viscosity of a polydisperse mixture to be mapped onto that of an equivalent monodisperse system, namely that it is at the same pressure as the polydisperse mixture. In the second method we hypothesize that the viscosity can be written as a function of the random closed-packed density, f_{RCP} . This is a description that has been tested in the literature for colloidal systems. We then consider the latter a function of the two moments only. The two alternative methods do lead to different predictions for the viscosity as a function of the size distribution.

Simulation results tested the underlying assumption that f_{RCP} is a function of just two moments. We did this initially for symmetric distributions for which the second and third moments are linked and were left with just a single distribution parameter. We adapted the simulation code for this problem to run on a desktop computer.

A key step in simplifying the problem of simulation of filler particles in a polymer matrix is to replace the effect of the polymer chains by an equivalent solvation potential acting between filler particles. We studied the problem of semiflexible polymer chains between parallel surfaces. We calculated the distribution of polymer near the surfaces from Wall PRISM theory as a function of chain length N and chain stiffness, characterized through a persistence length. Typical results show that the molecular weight affects the polymer distribution in the immediate vicinity of the surface for distances between surfaces 100 times the statistical segment length of the polymer. We can use this information to extract the solvation forces by studying how the wall profile varies with the spacing between the surfaces.

Typical results show that the molecular weight affects the polymer distribution in the immediate vicinity of the surface for distances between surfaces 100 times the statistical segment length of the polymer. We can use this information to extract the solvation forces by studying how the wall profile varies with the spacing between the surfaces.

3510750000

Solid-State Neutron Generator for Use in Nuclear Weapons

J. C. Lund, K. L. Kurz, A. M. Romero, G. J. Miller, Jr., D. F. Clark, A. M. Morales, N. R. Hilton

Traditional neutron generators (NGs) used in nuclear weapons systems employ a portable ion accelerator with tritium (T) target. Such neutron tubes work well, but they are difficult to make in small sizes, require high-voltage power systems, and have a limited shelf life. Another approach to neutron generation involves the use of an alpha-emitting radioisotope mixed with beryllium (Be). The traditional disadvantage of such an alpha-Be source is that they are always on; that is, they emit neutrons at a steady rate even when stored. Thus, it is extremely awkward to use a conventional alpha-Be source in a weapon because of the neutron shielding required to prevent exposure to personnel and sensitive electronics. However, with the advent of modern micromachining techniques (in particular, the LIGA [German for lithography, electroforming, molding] process) it should be possible to build a switchable all-solid-state neutron source. The alpha particles from a typical radioisotope (e.g., ^{241}Am [americium]) have a very short range in dense materials (less than 50 microns). If an array of small isotopic sources is moved over an array of LIGA-fabricated wells, with Be at the bottom of the wells, a fully switchable solid-state neutron source would result. Such a device would be capable of rapid switching, provide suitable neutron flux for weapon applications, and be extremely portable (a few cm^2 and less than 3 mm thick), yet would emit a negligible dose when in the off state.

We made extensive progress in four general areas: (1) theory of operation of a solid-state NG and computer simulation of its performance, (2) selection of alpha-emitting radioisotopes for use in the solid-state neutron generator (SSNG), (3) design and construction of micromachined attenuator layers, and (4) design, construction, and testing of prototype SSNG units. Progress on the theory of operations and prediction of device performance actually exceeded our expectations. Most of this progress can be attributed to our use of the computer code Sources-3A written by Los Alamos National Laboratory. We anticipated having to write our own codes to solve the alpha-transport/NG problem, but access to

Progress on the theory of operations and prediction of device performance actually exceeded our expectations.

the code Sources-3A greatly enhanced our predictive capability. The search for alpha-emitting radioisotopes for SSNGs was also greatly accelerated by the use of modern software, in particular the Web-based Table of the Isotopes, with alpha-emission search capabilities, which allowed us to search a huge number of candidate isotopes in a relatively short period of time. The design and construction of the micromachined attenuator layers proceeded according to plan, with only minor delays invoked while we solved the problem of bonding the attenuator layer to an alpha source. Finally, we designed and constructed and are testing a prototype SSNG. The design goal of the initial unit was to test the efficacy of our predictive capabilities. Two other units—designed to improve the neutron output and switching time—are under construction.

The search for alpha-emitting radioisotopes for SSNGs was also greatly accelerated by the use of modern software, in particular the Web-based Table of the Isotopes, with alpha-emission search capabilities, which allowed us to search a huge number of candidate isotopes in a relatively short period of time.

3510760000

Finite-Element Meshing Approached as a Global Minimization Process

W. R. Witkowski, V. J. Leung, J. Jung, C. R. Dohrmann

The ability to generate a finite-element (FE) mesh in an automatic fashion is becoming the key to being able to automate the entire engineering analysis process. However, placing an all-hexahedron mesh on a general three-dimensional (3-D) body continues to be an elusive goal. The approach investigated here is fundamentally different from any other that we know of. Sandia started from the premise that the problem of placing an all-hexahedron mesh on an arbitrary 3-D geometry needs to be addressed from a global perspective. We will employ a physical analogy for the actual meshing problem that will allow us to construct a global mathematical description of the problem. The physical analogy that we are substituting for the meshing problem is that of minimizing the electrical potential of charged particles within a charged domain (the particles represent quad/hex elements).

We focused on extending the 2-D meshing technology into three dimensions and further developing the 2-D meshing process. To develop the 3-D technology, we used a path similar to the one we used for the 2-D meshing technology. Initially, we designed particles to represent the duals of hexahedron elements. We wrote a new functional for the 2-D and 3-D algorithms to describe particle movement and alignment and minimized this functional using the same solution scheme as in the 2-D work. We then investigated a new approach and incorporated it into solving the 3-D connectivity problem. We based this mathematical approach on using a combinatorics algorithm to find the optimal matching solution between the arms of each particle.

We prototyped the 3-D meshing algorithm within the CoMeT software package, which offered the flexibility to easily modify the algorithm and try new thoughts. Another advantage offered by working within CoMeT was 3-D stereograph viewing of meshes, which allowed for easy visual inspections of meshes.

Overall the state of the project is that 2-D and 3-D prototype meshing algorithms exist within CoMeT based on a global minimization approach. The 3-D algorithm is immature

The ability to generate a finite-element (FE) mesh in an automatic fashion is becoming the key to being able to automate the entire engineering analysis process. However, placing an all-hexahedron mesh on a general three-dimensional (3-D) body continues to be an elusive goal. The approach investigated here is fundamentally different from any other that we know of.

and needs to be tested more thoroughly. The state of the 2-D code is very good with very reasonable meshes being achieved almost all of the time for a complicated set of geometries.

Refereed

Dohrmann, C. R., M. W. Heinstein, J. Jung, S. W. Key, and W. R. Witkowski. 1999. "Node-Based Uniform Strain Elements for Three-Node Triangular and Four-Node Tetrahedral Meshes." *Internat. J. Numer. Meth. in Engin.* **1**: 29.

Other Communications

Wolfenbarger, P. R. 1998. "Exploration of a New Unstructured Quadrilateral Mesh-Generation Algorithm." MS Thesis at University of New Mexico, Albuquerque, NM (August).

3510770000

Application of Parallel Mechanism Technology to Manufacturing

L. F. Bieg, V. De Sapio, D. M. Kozłowski, D. L. Plymale, G. L. Benavides, D. J. Schmitt, C. King

The goal of this project was to apply human-like motion to the fabrication of Sandia components. Currently, Defense Program (DP) products are realized by processes and tools based on orthogonal motion. However, the constraints of orthogonal systems have become more apparent as component designs have increased in complexity. In an orthogonal world, the fabrication of complex parts requires multiple manufacturing processes and setups, resulting in numerous fixture transitions. Aside from cost, time, and quality disadvantages, orthogonal manufacturing processes also lead to orthogonal designs. Freeing designers from this bias will allow new and innovative designs to be developed based purely on component and assembly functionality.

The overall challenge remains to develop, control, and apply human-like motion to manufacturing. Sandia developed and evaluated nonorthogonal parallel motion (NOPM) devices. We defined the scalability and accessibility of NOPM devices for fabrication, microassembly, and micropackaging applications. The power of this paradigm cuts across the spectrum of Sandia's design and fabrication requirements and applies equally well to the micro and macro environments.

Because of this project, Sandia has become the U.S. leader in NOPM technology development, employing a number of mechanisms to evaluate future applications. In collaboration with Arizona State (ASU), Florida (UoF), and the University of Nottingham in the United Kingdom, we applied two hexapods to evaluate metal-removal applications for internal needs and private industry applications, a microdexterity system for automated assembly, a prototype Rotopod for research evaluation, and other NOPM-like devices for workpiece holding and alignment.

Because of this project, Sandia has become the U.S. leader in NOPM technology development, employing a number of mechanisms to evaluate future applications.

Additional accomplishments include the following:

(1) Demonstrated and quantified benefits of micro and macro applications. Based on test results, we compared the performance of Sandia NOPM prototypes to commercially available systems. We demonstrated on the existing NOPM hardware specific applications that established the benefits of this technology. This project resulted in five individual patent

applications. In support of quantifying benefits of NOPM devices over orthogonal systems, we actively interacted with NOPM builders, users, and researchers on a national and international level. This included hosting the 4th Hexapod Users' Group (HUG) meeting at Sandia.

(2) Implemented micro and macro NOPM applications into production. We applied the six-degree-of-freedom (6 DOF) capability of our hexapod machining center to metal-removal processes not possible by historical orthogonal processes. This resulted in a Cooperative Research and Development Agreement (CRADA) to fabricate complicated tire molds in one-fourth the time of conventional processes.

For applications in automated assembly, we sold a Sandia NOPM design to the Ford Motor Company for automatic transmission fabrication. In addition, we demonstrated both micro and macro prototypes to Sandia neutron-generator fabricators.

(3) Transferred technology to DOE-DP production agencies and industry. We provided process development guidance to DOE for AlliedSignal/Federal Manufacturing and Technologies (AS/FM&T).

Refereed

Jokiel, Jr., B., and L. F. Bieg. 1999. "Experimental Determination of Kinematic Parameters in Assembled Parallel Kinematic Mechanisms." Paper presented to the 1st European Advanced Manufacturing Conference, Nottingham, UK, 16–18 September.

Other Communications

Bieg, L. F., D. J. Schmitt, J. Ziegert, and B. Jokiel, Jr. 1999. "Hexapod Strut Bending and Radial Displacement—Analysis of the Rotopod: An all Revolute Joint PKM; Sandia Hexapod Machine Tool Calibration." Paper presented to the 4th Hexapod Users Group (HUG) Meeting, Albuquerque, NM, 18–19 June.

3510780000

Investigation of the Impact of Cleaning on Adhesive Bond and the Process Implications

J. A. Emerson, E. D. Reedy, Jr., J. G. Curro, E. P. Lopez

Surface cleaning is the most common process step in DOE manufacturing operations—approximately 75% of AlliedSignal/Federal Manufacturing and Technologies' (AS/FM&Ts') Kansas City plant's critical process steps for weapons manufacture involve surface cleaning or preparation. We do not understand the link between a successful adhesive bond and the surface clean performed prior to adhesion. When qualifying a new solvent for weapons manufacture, the cleaning engineer must rely on cumbersome laboratory tests, which are expensive, repetitious, and time-consuming. For many years, the cleaning community has called for an understanding of "how clean is clean?" Very little work has been done in this area since it requires a fundamental understanding of the process following the clean. This project will apply Sandia's computer-modeling expertise, fracture mechanics understanding, and cleaning experience in an innovative way to address the issue, "How do we achieve a good adhesive bond?" Modeling has not been commonly used to deal with cleaning processes in the past. Understanding the link between surface preparation and adhesion would result in reduced cleaning development time and testing, improved bonds, and improved manufacturability, and may also result in an understanding that leads to improved aging. This capability can ultimately be applied to agile manufacturing tools. This project helps advance product realization for encapsulated components. Developing a validated model for cleaning and surface preparation in adhesive bonding, coating, encapsulation, or painting processes would complete Sandia's capability for a process that ensures efficient, low-cost production of small lots.

We developed tools involving the convergence of several expert areas across Sandia that allow for the robust manufacture of bonded structures. These tools include models and test techniques that can be applied to adhesively bonded components (structural joints, weapon subassemblies) and also to encapsulated components (neutron generators, electronic packaging). Moreover, we established a fundamental understanding of the effect of known contaminants on the bond interface for both adhesives and encapsulants.

Developing a validated model for cleaning and surface preparation in adhesive bonding, coating, encapsulation, or painting processes would complete Sandia's capability for a process that ensures efficient, low-cost production of small lots.

A simulation modeling technique, Polymer Reference Interaction Site Model applied near wall (Wall PRISM), provided the capability to include contaminants on the surface. The process requires a molecular description of polymer and contaminant as input, and the results are critically dependent on its accuracy. We performed calculations on the effect of contamination for 1% by weight of ethanol contamination on the structure of a silicone adhesive near a surface. This change in the PDMS (polydimethylsiloxane) structure leads to approximately an 8% reduction in the work of adhesion.

We based the demonstration of repeatable coatings and quantitative analysis of the surface for deposition of controlled amounts of contamination on three deposition methods. We studied hexadecane and mineral oil contaminants, selecting hexadecane for study because it is less difficult to model, and mineral oil because it represents a typical contaminant used for machining.

We varied deposition times in the closed environment for different times and temperatures. We used time-of-flight SIMS (TOF-SIMS) to determine the uniformity and thickness of the contaminant deposited. We employed two other analytical methods, atomic force microscopy (AFM) and ellipsometry. AFM images for the 48-hour hexadecane exposure indicated that the contaminant deposition was in the form of islands or puddles. This discontinuous film was further supported through contact angle hysteresis measurements. The 70° hysteresis demonstrates that the coating was not continuous.

We determined the effect of the cleaning process used on interface toughness by measuring the toughness of an aluminum (Al)/epoxy interface for both Brulin- and TCE (trichloroethane)-cleaned Al surfaces. We determined the toughness using an asymmetric double cantilever beam (ADCB) specimen. The measured toughness of samples with a Brulin-cleaned Al surface is significantly greater (~ 50% greater) than that with a TCE-cleaned Al surface.

We determined the sensitivity of measured fracture toughness to various test conditions to ensure the reliability of the measurement. We found that interfacial toughness (measured using ADCB sample) is a strong function of surface roughness, increasing by about a factor of five as the surface roughness increases from 1 to 5 micron rms (root-mean-square). Interface corner toughness (measured using a butt-joint specimen) is also strongly dependent on surface roughness. It is interesting to note that surface roughening is a

common technique used by adhesion experts to improve the chances of achieving good adhesion.

We also investigated the effect of bond thickness on interfacial toughness (ADCB). There were relatively small variations in measured toughness when the bond thickness was varied from 0.5 mm to 1.5 mm. The dependence of butt-joint strength on bond thickness is predictable, and the interface corner toughness is independent of bond thickness.

We determined the work of adhesion value for silicone/silicone interface by a contact mechanics technique known as the JKR (Johnson, Kendall, Roberts) method. These values compare within experimental error with recent theory and other experimental techniques. The interaction between silicone and a clean stainless-steel surface shows a dependence on surface roughness and chemical interaction. We synthesized new silicones to study the effect in more detail. Contaminated surfaces with hexadecane could readily be measured by this technique. Correlation with fracture data has allowed a better understanding of the correlation between interfacial fracture parameters and surface energy.

*Correlation with fracture data
has allowed a better
understanding of the correlation
between interfacial fracture
parameters and surface energy.*

Refereed

Curro, J. G., J. D. Weinhold, J. D. McCoy, and A. Yethiraj. 1998. "The Structure of Amorphous Polymers Near Surfaces: Athermal Systems." *Computational and Theoretical Polymer Sci.* **8** (August): 159.

Emerson, J. A., G. V. Miller, C. R. Sorensen, and R. A. Pearson. 1999. "Self-Adhesion Hysteresis of a Model Siloxane Elastomer." *ACS Polymeric Mater.: Sci. and Engin.* **81** (American Chemical Society, PMSE Division, New Orleans, LA, August): 385.

Emerson, J. A., J. Benkoski, G. V. Miller, and R. A. Pearson. 1999. "Work of Adhesion Measurements of Silicone Networks Using Contact Mechanics." *Proc. 22nd Annual Meeting Adhesion Soc.* **22** (Panama City Beach, FL, February): 186.

Hooper, J. B., J. D. McCoy, and J. G. Curro. 1999. "Density-Functional Theory of Simple Polymer in a Slit Pore: 1. Theory and Efficient Algorithm." *J. Chem. Phys.*, accepted.

Hooper, J. B., J. D. McCoy, and J. G. Curro. 1999. "Density-Functional Theory of Simple Polymer in a Slit Pore: 2. The Role of Compressibility and Field Type." *J. Chem. Phys.*, accepted.

Reedy, E. D., Jr. 1999. "Connection Between Interface Corner and Interfacial Fracture Analyses of an Adhesively Bonded Butt Joint." *Internat. J. Solids and Structures*, accepted.

Reedy, E. D., Jr., and T. R. Guess. 1999. "Additional Interface Corner Toughness Data for an Adhesively-Bonded Butt Joint." *Internat. J. Fracture*, accepted.

Reedy, E. D., Jr., and T. R. Guess. 1997. "Interface Corner Failure Analysis of Joint Strength: Effect of Adherent Stiffness." *Internat. J. Fracture* **88**: 305–314.

Weinhold, J. D., J. G. Curro, A. Habenschuss, and D. Londono. 1999. "Self-Consistent Integral Equation Theory of Polyolefins and Comparison to X-Ray Scattering Experiments." *Macromolecules* **32**: 7276.

3510790000

Standard Cells for Microelectromechanical Systems (MEMS)

M. S. Rodgers, M. S. Burg, P. C. Galambos, D. N. Reyes, S. M. Barnes, M. P. de Boer, B. D. Jensen, V. R. Yarberr, J. J. Allen

Although polysilicon surface-micromachined microelectromechanical systems (MEMS) are fabricated using the same tools and techniques employed to fabricate an integrated circuit (IC), the design of these systems does not offer the same level of abstraction that exists in IC layout. A handful of core electrical components such as resistors, capacitors, and transistors can be designed and characterized, and can then be used over and over again to create very sophisticated electronic circuits without having to redesign these core elements each time. The focus of this project is to create a core set of verified microelectromechanical structures and assemblies that mechanical designers can confidently utilize in much the same way that a circuit designer pulls a transistor from a predefined library of components. This is to provide for standardization and compatibility in designs while eliminating the high costs in time and money associated with each designer developing core components from scratch. To fully support a low-overhead and rapid-turnaround prototyping environment, the library is also inclusive of all the structures required by the processing equipment and engineers during device fabrication. The final goal is to integrate the standard components into the mechanical layout environment, so designers will be able to utilize these cells as the foundation and building blocks for new MEMS designs with only minimal additional training.

We generated a number of technical advances in conjunction with the development of these components. We have already submitted several of the concepts as full patent applications and expect the patent office to file additional applications in the near future.

A complete standard cell library needs to contain not only the components required for designs, but also the structures that the processing equipment and engineers need to fabricate the devices. Therefore, we developed a standard frame that incorporates numerous alignment targets, diagnostic monitors, and the streets that define the size and shape boundaries. Designs are readily plugged into this standard frame, and we use the resulting drawing to generate the photolithographic

The focus of this project is to create a core set of verified microelectromechanical structures and assemblies that mechanical designers can confidently utilize in much the same way that a circuit designer pulls a transistor from a predefined library of components....to provide for standardization and compatibility in designs while eliminating the high costs in time and money associated with each designer developing core components from scratch.

masks required to define the structures during the fabrication process. We also developed a handy parametric text generator that provides for easy device labeling through the use of standard cells that define each of the letters in the alphabet.

A final task was to add three designs per specifications. We developed new torsional rotary actuators, advanced short-stroke electrostatic comb drives, and several ratcheting components in support of this goal. Given the universality of the requests for these types of components, the final set of standard cells that we submitted for fabrication contains more than 50 variations of similar devices that we designed to further enhance functionality and performance.

To fully verify the library, we needed to fabricate the components, confirm functionality, and then demonstrate that they can be successfully integrated into designs. The latter was successfully established through beta testing in collaboration with the University of California–Berkeley and the University of Wisconsin–Madison.

The library is being distributed on a compact disc (CD) rather than over the Web. This CD is a licensed product that also contains the other design tools required to design in Sandia’s MEMS technology.

The library is more extensive and more advanced than originally envisioned, and it contains many components based on Sandia’s latest five-level polysilicon fabrication process. This is a technology that did not even exist when this project was initiated. This project has served to greatly enhance the visibility of Sandia’s programs within the MEMS community while simultaneously serving as a development vehicle to improve and advance the state-of-the-art in surface micromachining.

This project has served to greatly enhance the visibility of Sandia’s programs within the MEMS community while simultaneously serving as a development vehicle to improve and advance the state-of-the-art in surface micromachining.

Refereed

Allen, J. J., and H. K. Schriener. 1998. “Micromachine Wedge-Stepping Motor.” *Microelectromechanical Systems (MEMS)—1998 DSC-6* (ASME International Mechanical Engineering Congress and Expositions—MEMS Symposia, Anaheim, CA, 15–20 November): 317–322.

Dyke, C. W., J. J. Allen, and R. J. Huber. 1999. “Parallel-Plate Electrostatic Dual-Mass Oscillator.” *Micromachined Devices and Components V 3876* (SPIE Micromachining and Microfabrication, Santa Clara, CA, 20–21 September): 198–209.

Rodgers, M. S., J. J. Allen, K. D. Meeks, B. D. Jensen, and S. L. Miller. 1999. “A Microelectromechanical High-Density Energy Storage/Rapid Release System.” *Micromachined Devices and Components V 3876* (SPIE Micromachining and Microfabrication, Santa Clara, CA, 20–21 September): 212–222.

Rodgers, M. S., J. J. Sniegowski, J. J. Allen, S. L. Miller, J. H. Smith, and P. J. McWhorter. 1999. "Intricate Mechanisms-on-a-Chip Enabled by 5-Level Surface Micromachining." *Transducers '99* Paper 3A3 2 (10th International Conference on Solid-State Sensors and Actuators, Sendai, Japan, 9 June).

Rodgers, M. S., T. W. Krygowski, J. H. Smith, J. J. Allen, J. J. Sniegowski, S. L. Miller, and S. Montague. 1998. "Multi-Level Micromachined Systems-on-a-Chip: Technology and Applications." Paper presented to the IMMM/ESARDA Workshop on Science and Modern Technology for Safeguards, Albuquerque, NM, 21–24 September.

Other Communications

Rodgers, M. S. 1999. "The Intelligent Micromachine Initiative at Sandia National Laboratories: An Overview." Presentation to a Seminar at Tohoku University, Sendai, Japan, 11 June.

3510810000

Laser Wire Deposition for Fully Dense Shapes

M. L. Griffith, T. E. Buchheit, V. Tikare, M. T. Ensz

The purpose of this project is to characterize the laser wire deposition process (WireFeed) and develop the technology to fabricate complex near-net shapes directly from a computer-aided design (CAD) solid model. This additive process will fabricate solid metal parts directly from the software representation, thereby saving numerous steps and time compared to current methods and technologies.

This year's intent was to further develop our understanding in three main areas: processing, materials, and shape fabrication. In the processing area, Sandia wants to further understand how the processing parameters (laser power, wire feed rate, traverse velocity) control the deposition of material. We will continue to expand our knowledge of the resulting material properties and model the grain evolution or solidification behavior of the process. By understanding the experimental and theoretical aspects for WireFeed deposition, it will be possible to fabricate metal parts with appropriate material properties.

The other goal is to develop a system that rapidly fabricates accurate, complex parts. We will develop software to translate CAD data into process commands for complex geometry fabrication and will determine procedures to selectively deposit material for controlled geometry fabrication. Development of this process will allow engineers to produce functional parts of their designs directly from CAD files. The turnaround time will be hours instead of days, and days instead of months. With reduced turnaround time, more time can be spent on the product design phase to ensure that the best component design is achieved. Maturation of this technology will revolutionize the way the world produces structural components.

The central task for this year was the full implementation and investigation of the new WireFeed system. We utilized diagnostic techniques to gain a better understanding of the process. In addition, we completed more materials characterization, metallography, and mechanical testing to obtain a better understanding of the process and the new system. We developed mechanical controls and interfaced them with the software for controlled deposition. We developed software to drive the WireFeed system from a computer model.

Development of this process will allow engineers to produce functional parts of their designs directly from CAD files. The turnaround time will be hours instead of days, and days instead of months....Maturation of this technology will revolutionize the way the world produces structural components.

We fabricated representative geometries to show the capability of the new WireFeed system for complex part fabrication. We used metallography results as input values to verify the development of the microstructural model.

- *Complex geometry fabrication.* The key issue to complex geometry fabrication was determining a method to reliably control the deposition of the wire. During fabrication of each cross-section, the wire must connect and disconnect repeatedly from the molten pool to draw the desired shape. We completed significant work to develop a means to reliably and repeatedly stop one deposition section, disconnect the wire, move to a new position, re-initialize the molten pool, and start the wire feed again. This was accomplished after significant effort and tests. We completed the post-processor software necessary to drive the WireFeed system from a CAD solid model. We developed scanning techniques to maximize material deposition rates and maintain desired material properties. We fabricated complex shapes to demonstrate this new capability.

- *Process understanding.* We utilized visible imaging techniques to investigate the wire deposition process. By using a high-speed imaging system, with the optics magnified to look directly at the molten pool area, it was possible to capture the nature of the process for insertion, deposition, and detachment of the wire during fabrication. With the ability to slow the process (on video), it was possible to “see” the critical aspects that required further understanding for robust part fabrication. Using a design-of-experiments methodology coupled with imaging, we easily monitored progress and overcame processing hurdles.

Second, imaging captured the basic behavior of the molten pool. We modified the fluctuations in the molten pool through changes in various processing parameters. With a more stable molten pool, the wire fed more consistently and complex part fabrication was possible.

- *Materials understanding.* We continued to investigate stainless-steel alloys (304L and 308L) in this process. With our new, improved system configuration, we fabricated many samples for mechanical testing. Testing in stainless-steel 304L revealed high-strength properties with retained ductility—a good structural combination. We investigated the effect of the raster pattern on resulting properties. Results showed that layers that are parallel to the test direction had the best properties, whereas properties were weaker in the perpendicular direction.

It is necessary to guarantee a level of cleanliness of the starting wire to fabricate fully dense components. If the initial wire is not appropriately cleaned after the drawing process, small glassy inclusions are processed into the part. This leads to premature failure in mechanical testing, because these sites act as porosity centers or high-stress concentration centers.

We compared our 3-D microstructural model to experimental microstructures and found the model could reasonably describe our stainless-steel grain evolution for a given set of parameters.

Refereed

Griffith, M. L., M. T. Ensz, D. L. Greene, D. E. Reckaway, J. T. Romero, T. B. Crenshaw, L. D. Harwell, T. E. Buchheit, and V. Tikare. 1999. "Solid Freeform Fabrication Using the WireFeed Process." *Proc. Solid Freeform Fabrication Symp.* **10** (Austin, TX, 9–11 August).

Other Communications

Griffith, M. L. 1999. "3D Wire Process Transforms Rapid Prototyping." *Advanced Manufacturing Technology Alert* (11 June), New York, NY.

Griffith, M. L. 1999. "WireFeed Laser-Engineered Net Shaping." *Rapid Prototyping Report Newsletter* (Solid Freeform Fabrication Conference, San Diego, September), Geoff Smith-Moritz, editor.

3510820000

High-Throughput Dry Processes for Large-Area Devices

D. S. Ruby, P. A. Miller, R. N. Stokes, C. I. H. Ashby, R. J. Buss, D. J. Rieger, P. Yang, G. A. Hebner

Sandia began this project to study the plasma processes of reactive ion etching (RIE) and plasma-enhanced chemical vapor deposition (PECVD) on large-area silicon (Si) devices. Our goal was to develop numerical models that could be used in a variety of applications for surface cleaning, selective etching, and thin-film deposition. We chose Si solar cells as the experimental vehicle for this project because we identified an innovative device design that would benefit from immediate performance improvement using a combination of plasma etching and deposition processes. These validated process models can be used in a variety of applications for surface cleaning, selective etching, and thin-film deposition. The models will provide guidance for development of the next generation of plasma reactors and of new device designs and applications.

We made four primary accomplishments:

- *Self-aligned selective emitter (SASE) cell processing.* We used the silicon nitride (SiN) deposition parameters that produced the minimum J_{oc} values obtained from the second year in the processing of 130 cm² Solarex cells. The cells were processed up through gridline firing on the Solarex production line and sent to Sandia for nitride deposition.

The SASE cells have consistently higher short-circuit current density (J_{sc}) than the controls, because with lower refractive index, the increased internal quantum efficiency (IQE) due to passivation is not lost due to excessive parasitic absorption. The cells that received 10 minutes of NH₃-hydrogenation performed the best, exceeding the controls by almost a full percentage point due to the large improvement in V_{oc} (open circuit voltage). However, improvement in V_{oc} is reduced for the cells that received a 20-minute NH₃-exposure. These cells also suffered a loss in fill factor due to an increase in diode ideality factor.

We found the use of an optimum-duration, NH₃-plasma hydrogenation treatment to be crucial to the increased performance. As the data show, the fill factor and V_{oc} increase for durations of up to 10 minutes, and then decrease due to higher non-ideal diode recombination, probably due to

These validated process models can be used in a variety of applications for surface cleaning, selective etching, and thin-film deposition...[and] will provide guidance for development of the next generation of plasma reactors and of new device designs and applications.

accumulated plasma-induced surface and gridline damage. This is consistent with the results of the emitter passivation studies because even though they predicted lower J_{oc} values for longer durations, they were performed on bare Si wafers and did not incorporate the effect of the plasma on the gridlines.

- *SiN refractive index model.* The refractive index of SiN can be varied with the Si-to-N ratio in the material. From a processing perspective, we achieved this goal by varying the composition of reaction gases in the thin-film deposition process. Since N can not be effectively dissociated under our operation conditions, the changes in the N content in the SiN film will primarily rely on N atoms dissociated from the ammonia source. By varying the flowrate of the silane mixture, with a total flowrate of N and silane up to 1200 sccm, the Si-to-N ratio in the reaction gases can be changed.

We observed a linear relationship between the refractive index of plasma-deposited SiN film and the Si-to-N ratio. Results indicate that the refractive index of the nitride film can be varied from 1.95 to 2.45 within this processing space. Since bonding between Si and N is also more covalent in nature (less than 22% ionic character), the difference in electronic polarizability between S-Si and Si-N will be negligible relative to the great changes in electron density as the composition of the film varies. Therefore, the observed linear relationship can be attributed to the increase in electron density in the nitride film as the composition in the film gets more Si rich. By extrapolation or interpolation technique, different refractive index layers of PECVD-nitride films can be sequentially deposited to form a multilayer antireflection coating (ARC).

- *Modeling a dry-etch process.* We studied a dry process for plasma-etchback of the emitter in full-size multicrystalline Si cells. The plasma is pure SF₆ in a capacitively coupled parallel plate commercial reactor. Plasma diagnostic measurements include etch rates, Langmuir probe measurements of ion-saturation currents, mass spectrometric probes of the plasma gas, and gas temperatures. We developed a plasma model and tested it against these data, obtaining reasonable agreement with the measurements. From an analysis of the model results for the fall-off in etch rate at high pressure, we conclude that the plasma is likely to become very sensitive to minor system perturbations at high pressure and low power. Operation in this regime is liable to result in reduced process stability and reproducibility. Further refinement of the model will be possible as more kinetic data and diagnostic

measurements become available; however, the current model should be reliable enough to guide process scale-up and optimization.

Other Communications

Buss, R. J., D. S. Ruby, G. A. Hebner, and P. Yang. 1999. "Modeling a Dry Etch Process for Large-Area Devices." *Extended Abstracts and Papers, 9th Workshop on Crystalline-Silicon Solar Cell Materials and Processes 1* (Breckenridge, CO, 9–11 August): 175.

Ruby, D. S., P. Yang, S. H. Zaidi, M. Roy, and S. Narayanan. 1999. "Plasma Texturing, Etching and Passivation of Multicrystalline Silicon Solar Cells." *Proc. Renewable and Advanced Energy Systems for the 21st Century CD* (Maui, HI, 11–15 April): RAES99-7684.

3510830000

Assuring High Reliability and Production Readiness in Low-Volume Manufacturing

S. V. Crowder, J. T. Spooner, E. W. Collins, M. F. Martin, A. J. Johnson

The manufacturing philosophy in the nuclear weapons complex (NWC) has shifted dramatically from the regular production and delivery of significant orders to less frequent small orders. New weapons components are produced less frequently and in smaller quantities. The challenge is to build much smaller lot sizes while maintaining the same high-reliability standards. For Sandia to meet this challenge, specific areas need more attention, including assuring and assessing reliability given few actual performance tests of the final product. Current Sandia reliability prediction/assessment methodology is based on final product tests in simulated or actual weapon-use environments. A large number of tests for each major component within the weapon over the weapon's life span is necessary to confirm and track the weapon reliability. In a small-lot production environment with a limited number of product tests, the current methodology is not viable. What is needed is a reliability assurance/assessment methodology that correlates information from the manufacturing processes and subcomponent testing to end-use reliability. This project presents a new approach to reliability assurance/assessment that relies on such manufacturing data and high-fidelity testing at the subcomponent level to assure and assess reliability with limited actual end-product testing.

The challenge is to build much smaller lot sizes while maintaining the same high-reliability standards.

Efforts focused on developing a reliability assurance and assessment methodology for small-lot production. Using the current reliability assessment methodology to demonstrate high reliability for a component requires a large number of tests (usually > 100) over the weapon's lifecycle with a large number of successful test results. Detection of a component failure in this process usually results in additional testing and/or analysis and simulation to fully understand the root cause and impact of the failure at the component and system level. In small-lot production of a component with a limited number of product tests, a single failure could result in an unfavorable component reliability assessment using the existing methodology. Additional information is necessary to accurately assess and demonstrate the true reliability of the component. A potential rich source of information to support component

reliability assessment is process and product measurements collected during the manufacturing process. A second potential source of information is available from high-fidelity testing of subcomponents that make up the component of interest. To use this information in a reliability assessment methodology, a correlation of these types of data to end-use reliability needs to be established. This research developed a methodology for small-lot reliability using such data. We applied the methodology to two different components, a complex electronic assembly and a complex mechanical assembly.

Refereed

Crowder, S. V. 1998. "Small Sample Properties of an Adaptive Filter with Application to Low-Volume Statistical Process Control." Paper presented to the Fall Technical Conference of the ASQ, Corning, NY, October. SAND98-1109.

Other Communications

Crowder, S., E. Collins, and M. F. Martin. 1999. "Assuring and Assessing High Reliability in Small-Lot Production." Sandia Technical Report, in review.

Johnson, A. J., C. DeCarli, and S. V. Crowder. 1999. "Small Sample Experimental Design Optimization and Repair." Sandia Technical Report SAND99-8236, Sandia National Laboratories, Albuquerque, NM (April).

3510840000

Scripting for Video Inspection

J. T. Feddema, D. J. Schmitt, C. W. Wilson, K. M. Jensen, J. J. Rivera, J. J. Carlson

Sandia's primary mission of ensuring a safe, secure, and reliable nuclear deterrent depends critically on the reliability of deployed components. Visual inspection of these components serves as the last chance to prevent a defective part from entering the stockpile. Most of these parts are subjected to manual visual inspection, which raises questions of consistency and accuracy. Even state-of-the-art commercial visual inspection systems are inadequate, because they require skilled engineers to artfully adjust camera parameters, lens settings, lighting, and processing, which is prohibitively expensive for small-lot manufacturing. In this project, Sandia fills this research gap in visual inspection by developing technology to automatically inspect parts with a video camera. Using a computer-aided design (CAD) model of the part, our system will automatically determine camera locations, lens settings, and illumination to make good images. We refer to this combination of imaging parameters as a script, and it will result in a movie of the part highlighting the sections that need to be inspected. These images will be compared automatically to CAD renderings of the part, with differences marked as defects. We will enhance the system with specialized inspection routines that cannot be accomplished with the CAD model. The



Sandia fills this research gap in visual inspection by developing technology to automatically inspect parts with a video camera. Using a computer-aided design (CAD) model of the part, our system will automatically determine camera locations, lens settings, and illumination to make good images.

Photo of a neutron-generator tube.

result of this work will be a system for automatically inspecting parts such as neutron generators (NGs), printed wiring boards, semiconductor wafers, and machined parts.

We created a CAD-based video scripting system that can make a movie or generate still pictures of a NG part at various stages of inspection. Currently, the operator selects the regions to be inspected, and the scripting system generates an MPEG movie or TIFF image file of the synthesized views. Texture and lighting models are used to generate photorealistic images. We developed the interface needed to download these path plans and lens controls to physical hardware that is being developed to inspect NG components.

In the process of developing the CAD interface, we evaluated three commercial packages for generating photorealistic images from CAD data. Two of the products are very nice optical design packages that would be useful for generating lighting models, but they do not provide photorealistic images in a usable format. We selected Kinetix's 3D Studio MAX as the product to generate the photorealistic images.

Using the third computer package, we are able to bring in Pro/Engineer CAD drawings of NG parts such as the header. The operator can position the camera and lighting relative to the parts and view a photorealistic image of the part as seen by the camera. In the simulation, linear and rotary stages are used to position the part underneath either a camera or a microscope. We use the kinematics of the stages to limit the possible camera or microscope views. The simulation is used to generate setpoints that are directly downloaded to the physical hardware. The same is true for automated camera/microscope settings such as focus and zoom.

We created a CAD-based video scripting system that can make a movie or generate still pictures of a NG part at various stages of inspection.



CAD-based video scripting of a neutron-generator tube.

3510850000

Advanced Machining Processes for Microfabrication

G. L. Benavides, P. Yang, D. P. Adams

An important product realization goal for Sandia is to reduce the volume of weapon components by 50%. Sandia is a national leader in microfabrication technologies such as silicon (Si)-based microelectromechanical systems (MEMS) and electroformable metal-based LIGA (German for lithography, electroforming, molding). However, there are micromachining technology voids that need to be filled to meet the volume reduction goal. Sandia must attain capabilities unavailable through LIGA, i.e., to fabricate subminiature parts from nonelectroformable metals or ceramics and to micromachine nonplanar features. We will augment our microfabrication technologies by researching novel applications of Sandia-owned excimer laser and focused ion beam (FIB). The process of micromachining by material removal is new to both Sandia and industry.

We will use the FIB to fabricate microsize features in desirable materials and to fabricate steel microtools for use in conventional processes such as drilling, milling, lathe turning, and sinker electrodischarge machining (EDM). The FIB beamwidth of 100 nanometers can create 0.5-micron-size features in high-strength/high-temperature metals and ceramics. We partnered with Louisiana Tech University (LTU) on FIB/micromachining research.

We will use the excimer laser to fabricate microsize features in materials including ceramics, magnetic materials, and polymers. This ultraviolet (UV) laser ablation process removes material without sample melting, providing the precision essential to fabricate high-aspect ratio microstructures. Thin sheet materials will be directly machined into three-dimensional (3-D) structures. Unlike LIGA, this process will not require a synchrotron, wet chemical process, or planarization. We also plan to partner with the University of New Mexico (UNM) to explore the micromachining capabilities of titanium-sapphire femtosecond lasers.

We accomplished the following:

- (1) Designed a parameter test for FIB-fabricated microtools.
- (2) FIB-machined various micro end mills in tool steel and C₂ micrograin tungsten (T) carbide.

Sandia is a national leader in microfabrication technologies such as silicon (Si)-based microelectromechanical systems (MEMS) and electroformable metal-based LIGA (German for lithography, electroforming, molding)...Sandia must attain capabilities unavailable through LIGA, i.e., to fabricate subminiature parts from nonelectroformable metals or ceramics and to micromachine nonplanar features.

(3) Micromilled aluminum (Al) and mild steel with T carbide end mill.

(4) Selected Archimedes screw as a 3-D part to micromachine using FIB tools (has potential application in a micropump).

(5) Used XeF₂ gas to increase material removal rate during FIB machining.

(6) Successfully raised the micromilling feedrate from 2 mm/minute to 5 cm/minute to vastly increase machining speed in Al 6061.

(7) Presented a paper in a collaborative work with LTU.

(8) Excimer laser-machined trenches and holes in alumina, aluminum nitride, and PZT (lead zirconate titanate).

(9) Improved beam quality of Sandia's excimer laser by installing an internal aperture.

(10) Successfully performed projection laser machining of a matrix of .002-inch-diameter holes in kovar and alumina.

(11) Installed microstage for laser machining.

(12) Initiated collaborative femtosecond laser machining with UNM. We are performing femtosecond laser machining in both air and vacuum.

(13) Collaborated with Exitech to laser machine a matrix of 5-micron holes in 50-micron kovar for the NT pellet screen.

(14) Electro-discharge-machined NT screens using LIGA-fabricated electrodes.

Refereed

Adams, D. P., G. L. Benavides, and M. J. Vasile.
1999. "Micrometer-Scale Machining of Polymers and Metals Enabled by Focused Ion-Beam Sputtering."
Proc. MRS Fall Meeting **546** (Fall) (Boston, MA, November 1998): 201–206.

3510860000

Fusion of Product and Process Data Using Real-Time Streaming Visualization

V. De Sapio, J. M. Baldwin, R. G. Hillaire, C. M. Leonard, Jr.

In today's Defense Programs (DP) product realization enterprise, it is imperative to reduce the design-to-fabrication cycle time and cost while improving the quality of DP parts (reducing defects). Much of this challenge resides in the inherent gap between the product and process worlds. The lack of seamless, bidirectional flow of information prevents true concurrency in the product realization process. The essence of this work is a framework for product-process data fusion to help achieve next-generation product realization. This will build extensively on past and current Sandia work in process-monitoring and characterization. The objective is to create an open environment for multichannel observation of process and inspection data, and subsequent mapping of those data onto product geometry. The result of meeting this objective will be a rich fusion of product and process data, facilitating the improvement and optimization of unit processes while advising the design community as to the manufacturability of a part. The entire enterprise can then have concurrent desktop access to visually fused media, both static and in-process, through the existing mechanism of an electronic traveler (a robust, Web-based information system for integrating and disseminating design, process, and inspection information related to a specific product). To the fabrication community such an environment would provide immediate feedback regarding the performance of a particular unit process in terms of the relevant process parameters. To the inspection community such an environment would accelerate the time to assimilate the metrological performance of a particular part, by directly and visually mapping probe point data to the nominal part geometry. Deviation of the part being inspected from the design specification would be visually apparent in real time without the labor-intensive review of inspection reports. Collectively, all disciplines within the product realization enterprise would have a centralized medium for the merging of product and process data. Ultimately, such a system would have potential implementation in the production environment.

We addressed the technical issues involved with batch-mode data capture and fusion using an incremental approach. We custom-created the applications for the first phase of work

The essence of this work is a framework for product-process data fusion to help achieve next-generation product realization....to create an open environment for multichannel observation of process and inspection data, and subsequent mapping of those data onto product geometry. The result of meeting this objective will be a rich fusion of product and process data, facilitating the improvement and optimization of unit processes while advising the design community as to the manufacturability of a part.

in AVS/Express, a high-level software development toolkit with a C/C++ library of visualization functions. We read the parsed process data files and inspection data files, along with the Pro/Engineer computer-aided design (CAD) geometry definition associated with the part, into the custom-created visualization applications. Both process and inspection data were then overlaid on the part model.

The resulting fused data are accessible in three forms. The first is the stand-alone visualization applications created in AVS/Express. For greater accessibility, especially through an electronic traveler, we addressed two browser-based solutions. The first of these involved creating browser-component versions of the stand-alone visualization applications. With these, standard copies of Netscape or Internet Explorer can be configured to employ graphical user interfaces (GUIs) and functionality similar to the stand-alone applications. The second solution involved exporting the product-process data as static VRML (virtual reality modeling language). We built a VRML export module into the stand-alone visualization applications, allowing automated delivery of the product-process data to an electronic traveler, in a Web-standard 3-D format. This is the most widespread means of information dissemination since it involves no special stand-alone applications or browser components installed on the user's desktop.

After we completed the static fusion of product-process data, the second phase of this incremental approach involved dynamic, real-time process data acquisition and streaming. We employed the same multichannel data acquisition described earlier. However, instead of writing to a file and then employing batch-mode processing of the data, we used socket input/output (I/O) to acquire the process data and stream it into a data and simulation server. We used the open architecture machine simulation packages Envision and Virtual NC to receive the multichannel socket input through serial connections and process it in real time. We created machine kinematic models in Envision. Tool position data sent from the machine controller to the data and simulation server drive the simulated virtual machine. The simulation environment simulates material removal on the workpiece while receiving real-time cutting parameter data from sensors at the tool. We noted that while the data and simulation server will act as a centralized node for collecting primarily sensor-based process data, this architecture will also have the capability to receive input from external model-based code (e.g., MT-AMRI-developed models for cutting-tool, physics-based simulation).

We built a VRML export module into the stand-alone visualization applications, allowing automated delivery of the product-process data to an electronic traveler, in a Web-standard 3-D format. This is the most widespread means of information dissemination since it involves no special stand-alone applications or browser components installed on the user's desktop.

3510870000

Advanced Production Planning Models

D. A. Jones, C. R. Lawton, M. A. Turnquist, G. F. List, W. E. Hart, C. A. Phillips

The overall goal of this project is to provide an effective suite of solvers for advanced production planning at facilities in the nuclear weapons complex (NWC). Although Sandia focused development activities to date on data related to Pantex operations, these types of scheduling problems appear in many contexts other than Pantex—both within the NWC (e.g., neutron generators [NGs]) and in other commercial manufacturing settings. It appears that an innovative and effective solution strategy approach to task-based production scheduling will be a major breakthrough for large-scale, realistic scheduling problems in a variety of production settings resulting in a new generation of advanced production planning models. The progress made thus far will allow the development of prototypical applications so that these innovative solution techniques can be tested on a wider variety of problems.

We focused our effort in two areas: the development of an innovative modeling approach for solving resource-constrained, multiproject planning/scheduling problems, and producing technical papers, SAND reports, and a peer-reviewed article documenting the formulation and a variety of solution techniques. The formulation developed and implemented at Pantex as part of the Pantex Process Model and a key component of this research was a finalist in the Edelman Award Competition. This type of formulation has direct application to the planning of stockpile-evaluation activities at Pantex, as well as stockpile life-extension program (SLEP) activities. Although we focused our development to date on Pantex-related operations, these types of project scheduling problems appear in many contexts other than Pantex—both within the NWC (e.g., NGs) and in other commercial manufacturing settings.

The essence of the resource-constrained, multiproject planning/scheduling problem is to determine when tasks should be scheduled during a given analysis period. The resulting solution must generate two types of outputs, the most important of which is the task schedule. A schedule of resource assignments must also be produced, resulting in output on how a set of resources is to be used in a given time period. Due to

...an innovative and effective solution strategy approach to task-based production scheduling will be a major breakthrough for large-scale, realistic scheduling problems in a variety of production settings resulting in a new generation of advanced production planning models.

their mathematical complexity, finding practical solutions to these large-scale task-scheduling problems is very difficult. We have developed an innovative and effective solution strategy for solving these types of problems.

One of the most innovative aspects of our approach is to represent the problem using a set of continuous variables rather than integer variables. In previous solution approaches, we used integer variables to decide whether or not a task begins in a given time period. This results in a mixed-integer programming (MIP) problem, which we have formulated and documented. Our approach formulates the problem differently using actual start times (as continuous variables) to represent task start times.

With this new formulation, we created a unique way of interpreting and formulating math programs for a class of resource-constrained scheduling problems, resulting in distinct advantages over existing techniques. First, its time periods can have variable lengths. This means that we can precisely match calendar boundaries, resolving a significant implementation barrier. Second, the principal choice variables are the starting times for each task, rather than using a period index for a start time, as is done in integer-programming approaches; we showed that this allows more efficient solution strategies. It appears that this approach to task-based production scheduling will be a major breakthrough for large-scale, realistic scheduling problems in a variety of production settings, resulting in a new generation of advanced production planning models.

We also began investigating the feasibility of applying these solution techniques to the NG production line. The first step in this investigation was to develop a resource-constrained, capacity-planning model for a group at Sandia. We also acquired complete datasets, including product flow information and resource availability.

Refereed

Kjeldgaard, E. A., D. A. Jones, G. F. List, M. A. Turnquist, J. W. Angelo, R. D. Hopson, J. Hudson, and T. Holeman. 1999. "Swords into Plowshares: Nuclear Weapon Dismantlement, Evaluation, and Maintenance at Pantex." *Interfaces*, accepted.

Kjeldgaard, E. A., D. A. Jones, G. F. List, M. A. Turnquist, J. W. Angelo, R. D. Hopson, J. Hudson, and T. Holeman. 1999. "Swords into Plowshares:

Nuclear Weapon Dismantlement, Evaluation, and Maintenance at Pantex." Paper presented to the INFORMS Spring National Meeting, Cincinnati, OH, 3 May.

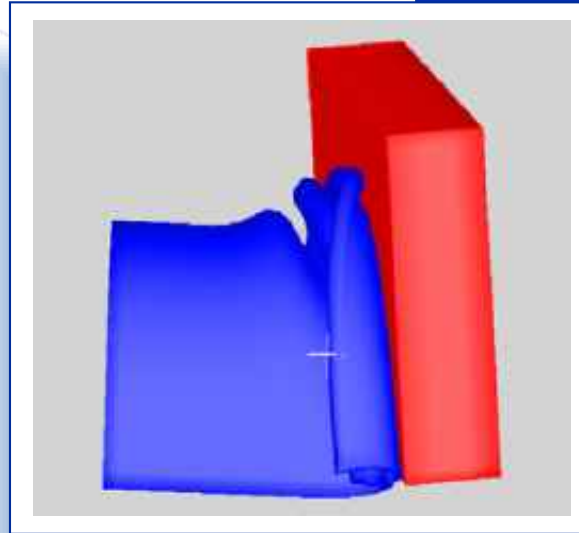
Other Communications

Jones, D. A., C. R. Lawton, M. A. Turnquist, and G. F. List. 1999. "Formulations of the Evaluation Planning Module." Sandia Technical Report, in review.

With this new formulation, we created a unique way of interpreting and formulating math programs for a class of resource-constrained scheduling problems, resulting in distinct advantages over existing techniques....this approach to task-based production scheduling will be a major breakthrough for large-scale, realistic scheduling problems in a variety of production settings, resulting in a new generation of advanced production planning models.

INFORMATION SYSTEMS & TECHNOLOGY

Information Systems and Technology is one of Sandia National Laboratories' six LDRD Roadmap Technologies investment areas. Roadmap Technologies derive their scientific basis from and extend the applications of Research Foundations investments into new areas. Roadmap Technologies create or accelerate scientific and technical expertise for future program areas that are strategic to Sandia and important to the DOE and the nation.



The Information Systems and Technology (IS&T) investment area invests in research that supports the Laboratories' Energy and Critical Infrastructures (E&CI) and Emerging Threats (ET) missions as well as the DOE's Stockpile Stewardship and Nuclear Nonproliferation and Materials Control Programs. IS&T research emphases include (1) high-speed, secure networks, (2) location-insensitive computing, and (3) conversion of data to information. High-speed, secure network investigations examine a wide range of technical innovations including optical networking and switching; reliability, architectures, and protocols; interconnect methods and scalable applications; multilevel access and need-to-know protective features; risk, threat, and vulnerability assessment; and intrusion detection and response. Location-insensitive computing examines novel solutions for distributed, heterogeneous software, intelligent agents, wireless networks, and collaboration tools. Conversion-of-data-to-information projects address data mining and automated data indexing;

data fusion and user-interface technology; network-based, sensor-driven information systems; and decision-support systems and automatic code generation from business rules and data models.

The "AVATAR: Navigating and Mining in Massive Data" project has researched and developed tools that help visualize vast amounts of data and make them understandable. The idea driving AVATARS (Adaptive Visualization Aid for Touring and Recovery) development was the exploitation of massive parallelism and robust pattern recognition to manipulate derived properties of datasets. The AVATAR approach produces avatars, which are sophisticated user profiles attached to data. The visualization tool exploits the avatars, permitting data to be understood in a fashion uniquely adapted to specific users. This research has potential applications in support of the vast information needs of the DOE's Stockpile Stewardship Program (SSP) and Accelerated Strategic Computing Initiative (ASCI).



3512290000

Weighted-Nearest-Neighbor (WNN) Decision Making for Data Mining

J. J. Carlson, J. A. Tauscher, C. L. Nelson

Data mining involves the discovery of information sources that are in some way related to observed phenomena, and determination of models that accurately define the relationships. For example, financial experts are interested in discovering what and how information (features) can be used to predict stock prices. Current efforts involve application of statistical techniques, fuzzy logic, neural networks, and expert systems. These efforts have generally been unsuccessful because there is no validated theory for adaptively discovering, selecting, and fusing distinguishing features in terms of uncertainties caused by measurement errors, randomness, ambiguities, and information warfare tactics. The result is the development of a large number of highly specialized algorithms that work only in very limited conditions.

A major thrust of this project involves the development of a theoretical and practical data-mining methodology. Sandia will develop a methodology for discovering and fusing features to achieve near-minimum probability of error (MPE) decision and estimation algorithms. Our approach combines a weighted-nearest-neighbor (WNN) decision model for classification and estimation with a genetic algorithm (GA) for feature discovery and model optimization. We will use the WNN model to provide the mathematical framework for adaptively discovering and fusing features into near-MPE algorithms. We will use the GA to discover and select inputs and to determine the weights in the WNN decision model that will optimize performance. A major advantage of the WNN model over other approaches is that the WNN model requires estimation of significantly fewer parameters (therefore, significantly fewer training samples) to accurately partition the feature space. This is of paramount importance as information sources are often incomplete or sparse in many dimensions. We expect to demonstrate that the WNN model will allow robust and practical application to a wide variety of data-mining problems.

Our accomplishments this year focused on (1) enhancements to the WNN algorithm, (2) parallel implementations of both the GA and the WNN algorithm, and (3) application of the methodology to diverse data-mining problems important to

Sandia will develop a methodology for discovering and fusing features to achieve near-minimum probability of error (MPE) decision and estimation algorithms.... We expect to demonstrate that the WNN model will allow robust and practical application to a wide variety of data-mining problems.

Sandia. We realized enhancements to the WNN algorithm by applying the GA to minimize the number of decision points required by the WNN algorithm to achieve a desired performance level. In many applications, we realized reductions by several orders of magnitude. We investigated parallel implementations of the WNN and GA for applications involving extremely large datasets. We gave attention to scalability, load balancing, and communication requirements between processors. We completed a timing analysis on each section of code to identify bottlenecks and to determine runtime characteristics. We found the GA process of selecting and weighting the features and establishing the decision points to be the most time-consuming. However, the application of the WNN using the optimized feature weights and decision points was very fast. We used the results of the analysis to identify sections of code that would benefit greatly from parallelization. The results also led to significant improvements in the serial coded version of the software. Finally, we applied the WNN model to two diverse problems. The first problem investigated the application of the WNN algorithm to security monitoring problems. The second problem investigated the application of the WNN algorithm to determine risk factors for contracting Hepatitis C. The results support the conclusion that the WNN model can be used to discover and fuse features from large databases to establish near-MPE decision and estimation models.

In many applications, we realized reductions by several orders of magnitude.

3512310000

Varying QoS for Fixed and Mobile Networks

R. L. Hutchinson, J. D. Dillinger, J. T. Michalski, J. P. Brenkosh, R. P. Tsang, T. D. Tarman

Sandia is building a prototype system that will provide applications with an application programming interface (API) to allow them to dynamically request bandwidth from the underlying network system. Currently an application with quality of service (QoS) requirements would require a network administrator to statically establish a channel.

The system we are building is essentially a bandwidth broker system that will provide signaling for distributed resource management applications that require Internet protocol (IP) network QoS. A bandwidth broker gathers and monitors the state of QoS resources. We will use this information, along with its corresponding policy information, to provide admission control to QoS flows to the network, as well as aid in route computation for connection-oriented flows.

Our bandwidth broker system is an essential component for allowing distributed applications to share network resources while receiving a predictable level of network QoS.

For networks with insufficient capacity to support requested QoS, we are developing methods of integrating hierarchical encoding of data. We are using multicast trees to transport base- and enhancement-layers of information. We encode the base-layer with minimum sufficient information while each enhancement-layer is encoded with an incremental improvement in information. Unsatisfied QoS requests will trigger incremental rejection of enhancement layers. This approach will ensure efficient use of available network resources.

We investigated several methods of hierarchical encoding of video signals, using the following criteria to evaluate these methods:

- efficiency (must be able to implement in software),
- simultaneous transmission of several different qualities of video in a channel capacity comparable to that of the highest quality alone,
- scalability in the number of receivers, and
- ability to dynamically change the quality at any receiver as the network QoS changes.

Sandia is building a prototype system that will provide applications with an application programming interface (API) to allow them to dynamically request bandwidth from the underlying network system.

We identified and evaluated a candidate hierarchical video-encoding tool, VIC (Video Conferencing), developed at Lawrence Berkeley Labs. The QoS team installed and evaluated this application in our lab. VIC assigns hierarchically encoded streams (layers) to different multicast trees. There is a single base-layer to which all receivers must subscribe. In addition, there are three enhancement layers, each of which provides improved video resolution. With this implementation, we can encrypt each multicast tree separately, providing a straightforward security solution for classified data. However, having one key per multicast tree may not be a desirable solution, and we will continue to investigate alternative methods of encryption. One remaining challenge is the unreliable transport of multicast services. Partial corruption of a critical video signal may require retransmission of the entire video signal (military applications). However, there is much ongoing work in the area of reliable multicast, so we will continue to use separate multicast trees to transport the base- and enhancement-layers.

...we can encrypt each multicast tree separately, providing a straightforward security solution for classified data.

We developed a model that will support requirements to a reasonable extent. The labs can demonstrate networks based on both IP and asynchronous transfer mode (ATM). ESNet will provide high-speed ATM links between Albuquerque and Livermore while the Sandia internal network will provide high-speed links between the Albuquerque labs. Analog modems and direct serial links will simulate low-speed satellite and wide-area communications.

The team investigated resource management packages, QoS specification languages, and operating system QoS mechanisms. The criteria we developed for selection of a resource management package include:

- availability of source code,
- flexibility of scheduling algorithms,
- good design-level documentation, and
- modularity to support future QoS enhancements.

We investigated products developed by Globus, Network Queuing System (NQS), and Portable Batch System (PBS), and compared them against our criteria. We selected PBS and are currently running it in the lab. We are developing mechanisms to integrate the PBS resource management package with network policy control. We selected common open policy service (COPS) as our network policy protocol. We have not identified available source code and are working on an implementation. This will allow policy communication among PBS, the policy server, and the Linux routers.

We attended an Internet Engineering Task Force (IETF) meeting focusing on QoS. QoS policy specification languages are being developed in the IETF. These languages are approaching request-for-comments (RFC) status and are already being implemented by a few companies. We will likely adopt these RFCs in our implementation.

The VIC application is running, and we have an ATM connection. We are currently using multicast trees for hierarchically encoded voice.

3512320000

A Real-Time Decision-Support Framework to Guide Facility Response to Abnormal Events

J. E. Brockmann, L. D. Brandt, F. Gelbard, D. M. Edwards, K. K. Murata

Adverse consequences to facilities that are subject to abnormal environments can be reduced dramatically if timely and appropriate mitigation actions are taken. Success in damage limitation requires the real-time fusion of data from diverse sources. An information and decision framework is required to evaluate these data, assess the probable impacts, and develop a decision and control strategy. The framework must develop graded facility responses appropriate to the quality of information available and the predicted consequences of the event and prospective mitigation options.

This project will provide the technical basis and prototype information tools for guiding facility response in threatening environments. Sandia will develop a decision framework that propagates prediction uncertainty, addresses decision risk measures, incorporates temporal updating, and links disparate information. We will develop robust predictive models able to utilize sparse sensor data to predict transport and consequences. We will construct and evaluate an integrated decision tool initially against a realistic reference facility. The initial prototype will provide a proof-of-concept and indication of the performance of the new technologies. We will refine the tools and evaluate them against more diverse facilities and more general environments as the final step in the research.

Successful completion of this project will provide key results supporting development of information and decision systems that improve safety and security of virtually all of the key facilities in the nation. The work will provide a technical foundation for several emerging areas of importance to Sandia, including a broad range of infrastructure protection programs. The work is particularly applicable to the development of protection systems for chem/bio (C/W) attacks on civilian infrastructure targets, a growing area of national interest. The research is structured specifically to provide the laboratory with a demonstrated technological base and fundamental tools to address these problems.

(1) We developed the Real-Time Decision Support System Functional Description, which specified the functional requirements of the system for a C/B event.

The work will provide a technical foundation for several emerging areas of importance to Sandia, including a broad range of infrastructure protection programs. The work is particularly applicable to the development of protection systems for chem/bio (C/W) attacks on civilian infrastructure targets, a growing area of national interest.

(2) We made a major advance in performing the inverse problem calculation for a multizone facility based on limited sensor data. We developed an algorithm that solves the problem of determining contaminant concentrations in a structure with interconnected volumes (such as rooms in a building), given time-dependent sensor readings at a limited number of locations, and the flow characteristics of the structure. Thus, the algorithm provides a method for inferring contaminant concentrations in volumes without sensors and does not require any adjustable parameters to make the inference. The algorithm can also be used to assess how to optimally locate sensors within a structure. We filed a Technical Advance (TA) that combines the flow characteristics of a structure with limited sensor data into a form that can be solved using a least-squares algorithm.

(3) We established a procedure for generating a complex building model from computer-aided design (CAD) drawings. This represents a significant step forward. We are completing a building model of the courthouse that we can use to perform flow and transport calculations, the results of which can be visualized in three dimensions. This capability is tied directly to our calculation-based predictive model and the ability to provide situational understanding through visual integration of extremely large datasets.

We developed an algorithm that solves the problem of determining contaminant concentrations in a structure with interconnected volumes, given time-dependent sensor readings at a limited number of locations, and the flow characteristics of the structure. Thus, the algorithm provides a method for inferring contaminant concentrations in volumes without sensors and does not require any adjustable parameters to make the inference.

Refereed

Gelbard, F., J. E. Brockmann, and K. K. Murata. 1999. "Sensor Analysis Software (SAS): An Algorithm for Determining Airborne Agent Concentrations Throughout a Large Multi-Room Building." Sandia Technical Report SAND99-1945 (OUO), Sandia National Laboratories, Albuquerque, NM (August).

Griffith, R. O., J. E. Brockmann, A. S. Geller, K. K. Murata, F. Gelbard, C. Lieshman, T. Wisely, S. McLain, R. Vantheempsche, D. Shawver, J. Zepper, and F. Dempsey. 1999. "Understanding and Mitigating the Chemical/Biological Threat to Facilities." Paper presented to the Emerging Technologies Meeting on Emerging Threats: Focus on WMD and Homeland Defense, Sandia National Laboratories, Albuquerque, NM, 2–3 June.

Other Communications

Griffith, R. O., *et al.* 1999. "Modeling and Simulation for Awareness in CBW Environments." (Invited) Paper presented to the WMD Emergency Responders Symposium, Honolulu, HI, 22–23 September.

3512330000

Data Fusion for Chemical Sensing

T. M. Berg, C. Springer, R. Shediac, R. G. Hillaire, N. M. Berry, D. S. Anex, D. C. Roe, I. R. Shokair

A wide range of weapons, from exotic biological and chemical (C/B) to conventional explosives, threatens military and civilian targets. Sandia wishes to produce sensors capable of sniffing out such weapons to detect their production, transportation, or placement. The problem is that obvious chemicals can be altered and improved or, worse yet—biological weapons (BW) can be engineered to unknown forms. The purpose of this project is to develop the means to interpret C/B sensor data so that known and unknown substances can be detected and their likely identity and potential harmfulness surmised.

Sandia is attempting to do this using molecular model-based data fusion of multisensor, parallel separation array data. We made multiple separations over several physical properties along a range of property values, including additional calibration channels. We performed initial data fusion based on models of the separation and detection processes to combine the outputs of the different simultaneous separation experiments at the highest confidence and resolution levels to compute a pool of physical properties. We used the property pool to estimate the number of sources contained in the sample and make likely identifications. We can base the identifications on existing separation data for known and available compounds and on simulated output from a molecular model. The idea was to take a pool of detected properties and construct the molecules that produced the signature, then determine what concerns the substances might present.

Our goals were to evaluate data fusion techniques for relevance to the biodetection domain and to validate the feasibility of identification using physical models. We achieved these by testing two data fusion techniques and the physical model using available data from peptides, amino acids, explosives, and other chemicals.

We assessed the data fusion problem from the perspectives of data properties, the sensing and detection process, and the information quality of multicolumn sensing. We can make some identifications by data matching alone, but this may ignore systematic errors or be confounded by an unknown

The purpose of this project is to develop the means to interpret C/B sensor data so that known and unknown substances can be detected and their likely identity and potential harmfulness surmised.

combination. The sensing and detection process model is also very useful, but methods must be developed to account for unmodeled nonlinear effects. From an information standpoint, the identification confidence level can be marred by measurements on a property that are improperly tuned for residence time. If measurements are fused using a traditional array algorithm, increasing the number of columns in the array could actually degrade the signal-to-noise ratio.

The data fusion assessments included implementing the algorithms and testing them on available data. For the data analysis-based algorithm, we used run-to-run and column-to-column variabilities with a data-filtering algorithm, implemented in the Java software language, to demonstrate identification based on matching outputs to a database of known sample signatures. We also demonstrated the calculation of analyte concentrations using an algorithm based on the modeled sensing and detection process physics. We implemented this second algorithm in FORTRAN and applied it to peptide separation data. The algorithm development addresses the problems of background subtraction, calibration, evaluation of noise characteristics, and the calculation of the certainty level of the identification. We will improve the algorithm to better account for overlap conditions of a chemical with an unknown when multiple columns are used.

We demonstrated the feasibility of performing identifications using correlations for the predictions of a physical, molecular model. We used a quantitative structure activity relationship (QSPR) to define a linear relationship between molecular descriptors and measured capillary electrochromatographic (CEC) separation retention times. We obtained the retention times using a peak detection algorithm based on the detection physics described above. We then examined 161 descriptors of four basic types. High correlations between the model and the preliminary experimental data indicate that it should be possible to predict retention times for molecules based on all types of descriptors.

Other Communications

Shokair, I. R., J. Wu, and T. M. Berg. 1999. "Implementation of a Detection Algorithm for μ ChemLab." Internal memo, Sandia National Laboratories (30 August).

Shokair, I. R., T. M. Berg, and J. Wu. 1999. "Preliminary Evaluation of Analysis Techniques for CEC Chemical Sensors." Internal memo, Sandia National Laboratories (15 April).

3512340000

Large-Scale Distributed Information System Modeling and Simulation

M. M. Johnson, M. E. Goldsby, A. S. Yoshimura, T. D. Plantenga

Large enterprises are evermore dependent on their large-scale information systems (LSIS), computer systems that are characterized by distributed components—data sources, networks, computing engines, simulations, man-in-the-loop control, and remote access stations. These systems provide such capabilities as workflow, data fusion, and distributed database access. The nuclear weapons complex (NWC) contains many examples of LSIS components, a fact that motivates the present research. However, most LSIS in use grew up from collections of separate subsystems that were not designed to be components of an integrated system. Consequently, they are often difficult to analyze and control. The problem is made worse by the size of a typical system, its diversity of input sources, and the institutional complexities associated with its distribution across the enterprise.

Sandia believes that simulation can be used to attain better understanding and control of LSIS. We are developing an integrated approach for the modeling and simulation of such systems. Our techniques allow the substitution of simulated components for actual components in the operation of the system; thus, we can explore questions relevant to the enterprise by interacting with the LSIS through simulated components designed with those questions in mind. We are also investigating the effect of using reduced-fidelity models on the speed of the simulations and accuracy of the results. The work involves enhancing Sandia's in-house simulation capability to allow interaction with external applications and legacy systems and includes the construction of interfaces to various commercial-off-the-shelf (COTS) simulation and database products.

The Infrastructure for Distributed Enterprise Simulation (IDES), a parallel discrete-event simulation engine developed at Sandia, plays a central role in our scheme of LSIS modeling, in that it is used to coordinate and sequence the actions of the various LSIS components. To make it capable of playing that role, we extended IDES to allow external programs to connect to it and to exchange messages with it. Special measures were required to convert between the external programs' real time and IDES' simulation time. IDES was also given a pause/

Sandia believes that simulation can be used to attain better understanding and control of LSIS. We are developing an integrated approach for the modeling and simulation of such systems.

resume capability, which pauses all nodes synchronized at the same simulation time, to allow human-in-the-loop control via externally connected submodels. We wrote a user manual and an internal manual for the extended IDES system and presented a course on IDES.

We used the extended IDES system as a fundamental component of the Confederation of Models to Perform Assessments in Stockpile Stewardship (CoMPASS), a geographically distributed simulation of the Department of Energy (DOE) NWC. We wrote interfaces between IDES and the COTS software packages Extend, iThink, Microsoft Access, and Microsoft Excel. We also wrote methods for converting data formats from each software package to Java. The Microsoft Access interface makes use of JDBC (Java Database Connectivity) and the JDBC-ODBC Bridge, which makes most ODBC (Open Database Connectivity) drivers available to JDBC calls.

We used CoMPASS as a platform for integrating LSIS components. We integrated reduced-fidelity models (RFMs) of the Pantex Planning Model (PPM) and the Y-12 Canned Secondary Assembly (CSA) planning model. We integrated both full-fidelity and reduced-fidelity models of the Transportation System Division's Transportation Planning Model (TPM), as well as the real Tritium Production Model and the Defense Program Requirements Planning Model (DPRPM). Use of the RFMs provides faster-than-real-time simulation; for instance, the real PPM can require eight hours to produce a schedule, whereas the RFM PPM produces one in seconds.

We demonstrated human-in-the-loop capability for the models in the CoMPASS system. The capability can be used to steer, modify, suspend, or terminate the operation of the LSIS and can be used with or without simulated components. Our work also demonstrated that reduced-fidelity and actual models can be combined in a coordinated simulation.

We undertook work in modeling information as a fluid in collaboration with Dartmouth College, which is developing advanced techniques for doing massive simulations. Companion simulations of a communication switch were written using a fluid model and a packet model and were used for purposes of comparison. The simulations were written using the new Scalable Simulation Framework (SSF). The comparisons revealed an interesting phenomenon. Although the fluid model showed substantial performance gains over the packet model for simulations of moderate size, they could

Our work also demonstrated that reduced-fidelity and actual models can be combined in a coordinated simulation.

actually run more slowly for massively large simulations. We identified the cause, a ripple effect in which a change in a single fluid flow causes redistribution of the switch capacity, and hence changes in all the fluid flows that propagate to downstream switches. We are currently investigating statistical smoothing techniques as a way of controlling the propagation of the changes in the individual flows. Addition of fluid constructs to IDES will be held back until this issue is resolved.

Refereed

Nicol, D. M., M. E. Goldsby, and M. M. Johnson.
1999. "Fluid-Based Simulation of Communication
Networks Using SSF." *Proc. 11th European
Simulation Symposium*, accepted.

3512350000

High-Surety SCADA for the Critical Energy Infrastructures

R. E. Carlson, R. J. Granfield, A. M. Johnston, A. E. Bentley, J. E. Stamp

The domestic critical energy infrastructures comprise a complex and interdependent network that is vital to the national security and social well-being of our nation. The control mechanisms for these infrastructures are often referred to as SCADA (Supervisory Control and Data Acquisition) systems. The President's Commission on Critical Infrastructure Protection identified that the widespread and increasing use of SCADA for control of energy systems provides an increasing ability for an adversary to cause serious damage to the energy infrastructures. This damage could arise through cyber infiltration of the SCADA networks, by physically tampering with the control networks, or through a combination of both means. The need exists for a secure SCADA that can quantify safety as a function of load, as well as allow greater loading of the infrastructure at a higher level of safety. Sandia will develop a new model for infrastructure monitoring and control: high-surety SCADA. To meet the new infrastructure threats and requirements, not only must contemporary SCADA systems be able to report the infrastructure state with confidence (security), but they need to measure the entire infrastructure, be robust in their communication, and be timely and optimal in their control (surety). In addition, the SCADA must be confident in the accurate delivery of that control and provide these services under adverse conditions. These are the qualities that a SCADA system needs to assume in order to enhance the surety (security, safety, and reliability) of the underlying infrastructure. In this sense, we call a SCADA system with these qualities a high-surety SCADA. Sandia is currently pioneering highly secure SCADA systems. The time is now to extend the development of high-security SCADA to that of high-surety SCADA systems.

- *Completed the plan for the Sandia SCADA test-bed and implemented the plan.* The primary use case for the test-bed is to identify and validate specific security hypothesis in SCADA. The development of the test-bed has generated wide interest from industry. We are currently in discussions with EPRI (Electric Power Research Institute), WEPEX, Cisco, and MCI

Sandia is currently pioneering highly secure SCADA systems. The time is now to extend the development of high-security SCADA to that of high-surety SCADA systems.

to leverage and augment the SCADA test-bed to investigate particular industry configurations. Such industry involvement will help strengthen the resulting high-surety SCADA specification by increasing the number of security case studies.

- *Developed a survey of public-key cryptographic methods and authentication strategies for SCADA networks.* We completed a survey of public-key cryptographic methods and authentication strategies and identified several methods that are applicable to SCADA networks. This survey is one of the foundations for the SCADA security model.

- *Produced a taxonomy of real-time control problems in SCADA.* The taxonomy is a collection of the control problems associated with delivering real-time control through a SCADA system to an electric power network. Since the term *load control* is restrictive, developing the real-time control taxonomy replaces the FY99 load control task as a better representation of what is needed to support the high-surety SCADA specification. In addition, the SCADA team created a preliminary model of a real-time controller for a SCADA system over an electric power grid. Such a model had not previously been considered.

- *Related to the problem of real-time control, developed a definition of surety for electric power networks.* By augmenting the NERC (North American Electric Reliability Council) definition of reliability with information security, physical security, and confidence metrics supplied by our research in real-time control, we were able to develop a new perspective for the electric power industry. This perspective will become important as deregulation forces the adoption of new operational standards. We also collaborated with Clemson University.

- *Secured the information necessary to develop a unifying and unambiguous representation of SCADA systems in the electric power industry.* This model is facilitating the development of the required information-security and -surety technologies. All other successes in the project followed from this detailed understanding, making it one of our most important accomplishments. We completed the conceptual SCADA model, developed 80% of the major architectural components of the logical model, and secured the data to complete the logical and physical models. In addition, we completed a conceptual framework for the information-security model and are 30% finished with the logical information-security model for SCADA systems.

- *Secured a wealth of information by leading the U.S. delegation to the IEC TC 57 AHWG06.* Pivotal in obtaining the information necessary to develop the SCADA model is Sandia's participation on the IEC TC 57 AHWG06 (International Electrotechnical Commission, Technical Committee 57, Ad Hoc Working Group 06). The IEC TC 57 develops international standards for electric power control systems, including SCADA and Energy Management System (EMS). Combining Sandia's security expertise with the detailed information available through the AHWG06 catapulted Sandia to the forefront of worldwide SCADA security research and ensured the successful development of the high-surety SCADA specification. We are in a unique position to drive the security requirements for the international standards in SCADA and, more generally, electric power automation.

Combining Sandia's security expertise with the detailed information available through the AHWG06 catapulted Sandia to the forefront of worldwide SCADA security research and ensured the successful development of the high-surety SCADA specification. We are in a unique position to drive the security requirements for the international standards in SCADA and, more generally, electric power automation.

3512360000

Agent-Based Mediation and Cooperative Information Systems

L. R. Phillips, R. A. Billington, S. V. Spires, S. Y. Goldsmith, H. E. Link, B. D. Murphy-Dye

Agent-mediated information management is currently the most promising solution to the problem of integrating and accessing large legacy data stores and for utilizing networked information sources such as the Internet. Collections of agents can assist human users and other agents with cooperative information processing and time-consuming search tasks. Sandia developed the Standard Agent Framework (SAF), a general-purpose development environment for constructing multiagent systems that assist a diverse set of users with knowledge-intensive tasks in a network environment. The RETSINA (Reusable Environment for Task Structured Intelligent Network Agents) framework under development at Carnegie-Mellon University (CMU) is being used to develop distributed collections of intelligent software agents that cooperate asynchronously to perform goal-directed information retrieval and information integration in support of performing a variety of decision-making tasks. A collection of RETSINA agents forms an open society of reusable agents that self-organize and cooperate in response to task requirements. Sandia will develop agent-based mediation functions that enable interoperation and cooperative problem-solving across both agent systems. By combining the two technologies, we will achieve a superior system capable of complex real-world information processing in an information environment such as the Internet. At this writing, we have not investigated interoperation of two large-scale multiagent systems. The technical challenges include the development of standards for knowledge and data sharing, ontological leveling of different knowledge bases, and cooperative problem-solving techniques that transparently utilize different agent systems. This project will significantly advance the state-of-the-art in cooperative information retrieval and will enable Sandia's development of advanced information systems for concurrent engineering, battlefield management, infrastructure modeling, and enterprise integration.

...we will achieve a superior system capable of complex real-world information processing in an information environment such as the Internet....This project will significantly advance the state-of-the-art in cooperative information retrieval and will enable Sandia's development of advanced information systems for concurrent engineering, battlefield management, infrastructure modeling, and enterprise integration.

We accomplished the following:

- Established interconnectivity and communications.
- Made contact with the CMU server.

- Acquired the CMU agent nameserver code (the “phonebook” service) and got it running at Sandia for testing. SAF agents interacted with the CMU nameserver code.
 - Established AF interface to RETSINA agents.
 - Established KQML (Knowledge Query and Manipulation Language) communication framework: tell/ask message objects built and sent to one another by SAF agents. These objects are serialized into ASCII (American Standard Code for Information Interchange) KQML for RETSINA agents.
 - Transmitted hand-built KQML messages to RETSINA agents as a test.
 - Designed respective mediation agents.
 - Established message framework for communicating in KQML: request for registration, registration success/failure, withdraw registration, withdrawal success /failure, request for service, commit/refuse request for service, and renege on service commitment.
 - Tested prototype agent system interfaces.
 - Preparing to send test KQML messages from the message framework containing preliminary ontological content.
 - Preparing to test initial interoperability features.
 - Started knowledge-sharing interfaces.
 - Developed preliminary automated domain ontology and service description code for SAF agents. Intent is to express SAF ontologies and services in CMU’s concept language and description logic.

Other Communications

Phillips, L. R., and H. E. Link. 1999. “The Role of Conversation Policy in Carrying Out Agent Conversations.” *Proc. Workshop on Conversation Policy 1* (Conference on Autonomous Agents, Seattle, WA, May): 11–17.

3512370000

Dynamically Self-Configurable Network Protocol

B. P. Van Leeuwen, L. B. Dean, W. F. Young, J. J. Harrington, J. Espinoza

This project is addressing the problem of adaptive message routing in a decentralized packet communication network with nodal mobility. Nodal mobility leads to frequent network topological changes, thus requiring routes to be reestablished. The communication medium is a radio channel shared by many contending users. These ad hoc networks are of importance in the context of tactical battlefield communications, antipersonnel landmine replacement communications, mobile robotic communications, and other distributed communication networks.

The objective of this research is to investigate current routing and media access algorithms and develop a network protocol that will permit networks to self-configure their communication topology dynamically. A major product of this research will be the development of a self-configuring ad hoc network protocol. Sandia will apply this network protocol to networks that have a random node distribution when created and to networks that have mobile nodes.

The project will take advantage of existing network protocols and components of protocols used in networking technologies, with a focus on minimizing the amount of control necessary since these nodes can be mobile and battery-operated. The research will develop a protocol that is applicable to the networks with the described attributes. Efforts will include simulating a model network by applying the developed protocol with network simulation tools such as University of California–Berkeley’s network simulation (NS) tool. Network performance, such as throughput and packet delay, will be characterized, evaluated, and optimized for the developed protocol. Finally, this project will present a demonstration simulation and possibly demonstrate the developed protocol on an actual communication network.

Our accomplishments focused on laying a foundation for the development and optimization of a dynamically self-configuring *ad hoc* network routing protocol. Initial efforts addressed the need to evaluate the performance of various approaches to *ad hoc* networks. There is a great deal of interest in the mobile communication community for the ability to

These ad hoc networks are of importance in the context of tactical battlefield communications, antipersonnel landmine replacement communications, mobile robotic communications, and other distributed communication networks.

accurately simulate mobile communications networks. We collaborated with Carnegie-Mellon University (CMU) in an effort to extend the NS-2 simulation tool to simulate mobile communication networks. These efforts resulted in Sandia's now having access to an open source code simulation tool that meets our needs. This simulation tool continues to be developed by university research groups as well as by Sandia.

In addition, our research investigated the recent *ad hoc* protocols proposed by other research groups. The Internet Engineering Task Force's Mobile Ad Hoc Network Group is responsible for establishing standards for these protocols. Our research took these proposed routing protocols and evaluated their attributes so as to utilize these attributes in developing *ad hoc* protocols for our specific types of applications. In addition, our efforts associated these specific routing protocol attributes with the specific performance attributes we desired. We identified many of the trade-off criteria associated with *ad hoc* protocols. We identified the protocols in lower layers of the OSI communication stack that must be evaluated with a routing protocol because of the direct coupling of the layers.

An additional completed objective of this research was to understand and evaluate proposed routing protocols for wireless *ad hoc* networks. We did this evaluation to understand the theoretical aspects of the proposed protocols as well as to understand their simulation results. Our research determined the candidate routing protocol approaches that are applicable to mobile *ad hoc* networks and their attributes. The approaches are link state, distance vector, source routing, and destination routing. These candidate routing algorithms are further classified into categories as follows:

- Centralized versus Distributed
- Static versus Adaptive
- Reactive versus Proactive

Preliminary simulations demonstrated a need for special *ad hoc* routing protocols when network topologies have mobility of the individual nodes. Conventional routing protocols like open shortest-path first (OSPF) undergo a dramatic decrease in performance when mobility is introduced. In addition, our research showed that a routing protocol should not depend only on messages at the network level but should also include support mechanisms at the lower levels of the OSI stack. Possible support mechanisms at the lower layers include link failure detection and neighbor discovery, as well as any of the media access techniques

...our research showed that a routing protocol should not depend only on messages at the network level but should also include support mechanisms at the lower levels of the OSI stack.

We also completed investigations of the channel access techniques for a wireless *ad hoc* network. We will incorporate the IEEE 802.11 standard into the simulation tool since this standard is an expected component in our implementation of mobile *ad hoc* networks.

We will perform our protocol testing with the Linux operating system. We considered issues of implementation of the protocols at the user level or in the operating system kernel and did preliminary investigations to determine the issues involved in this *ad hoc* routing protocol implementation.

3512380000

Optical Backplane/Interconnect for Super-High-Speed Communication

P. J. Robertson, H. Y. Chen, C. T. Sullivan, T. D. Tarman, E. L. Witzke, L. B. Dean, L. G. Pierson

Current copper backplane technology has reached the technical limits of clock speed and width for systems requiring multiple boards. Currently, bus technology such as VME (VersaModule Eurocard) and PCI (peripheral component interconnect) (types of buses) will face severe limitations as the bus speed approaches 100 MHz. At this speed, the physical limit of an unterminated bus is barely three inches.

Terminating the bus enables much higher clock rates but at drastically higher power cost. Sandia developed high-bandwidth parallel optical interconnects that can provide over 40 Gbps throughput between circuit boards in a system. Based on Sandia's unique vertical-cavity surface-emitting laser (VCSEL) technology, these devices are compatible with complementary metallic oxide semiconductor (CMOS) chips and have single-channel bandwidth in excess of 20 GHz.

In this project, we are researching the use of this interconnect scheme as the physical layer of a greater asynchronous transfer mode (ATM)-based backplane. Advantages to this technology include small board space, lower power, and noncontact communication. This technology is also easily expanded to meet future bandwidth requirements in excess of 160 Gbps, sometimes referred to as UTOPIA 6. ATM over optical backplane will enable automatic switching of wide, high-speed circuits between boards in a system.

Our work focused on the development of concepts and protocols needed to achieve 160 Gbps (1E9 bits per second) parallel optical interconnects for supercomputing and network switch applications. Our accomplishments include the following:

(1) Developed the optical ATM bus architecture. At the hardware level, we identified commercially available fiber-optic connectors that can hold parallel optical ribbon fibers in groups of twelve. We will use multiple connectors to implement the backplane.

(2) Developed a new generation of VCSELs and receivers and will fabricate initial devices that will be integrated as VCSEL/receiver pairs that we can either use over separate fibers or possibly operate bidirectionally over a single fiber.

Sandia developed high-bandwidth parallel optical interconnects that can provide over 40 Gbps throughput between circuit boards in a system. Based on Sandia's unique vertical-cavity surface-emitting laser (VCSEL) technology, these devices are compatible with complementary metallic oxide semiconductor (CMOS) chips and have single-channel bandwidth in excess of 20 GHz.

(3) Designed prototype hardware to fit in a computer that will have two optical connections. We plugged multiple cards into a host system and sent data over the optical bus to exercise the architectural concepts.

(4) Developed two broadcast-and-select architectures implemented as star networks that can utilize passive optical couplers and/or tunable transmitters/receivers to implement a shared-memory module of a supercomputer. A third approach avoids some disadvantages of the previous architectures such as their lack of multicast and collision avoidance by implementing a token-based control system.

3512390000

PUSH Technology Demonstration

W. E. Boebert, J. T. Gardner, T. E. Woods, T. Q. Thai, D. A. Rieb

Sandia will evaluate a sample “PUSH” technology for security problems and, if any are found, to demonstrate some of those vulnerabilities in a manner that might compel the appropriate care in deploying such systems. Planned milestones included the following: (1) evaluate and select a specific example of PUSH technology, (2) acquire, configure, and install this software on a sample network of modest complexity, (3) study the system for vulnerabilities related to the specific technology, and (4) develop a capability for demonstrating a subset of those vulnerabilities.

We selected BackWeb Server from BackWeb Technologies, Inc., to run on Microsoft Windows NT 4.0 using relatively standard Intel-based hardware for the sample technology. We chose this software because it is capable of handling multiple client hardware architectures and is expected to be expanded to handle several server architectures as well.

We identified and established baseline configurations for the following test scenarios:

- *Unsecured*: A scenario in which the client was configured to resemble a workstation on the Sandia External Operational Network.

- *Restricted*: A scenario in which the client was configured to resemble a workstation on the Internal Restricted Network with external BackWeb Server.

- *Distributed*: A scenario in which the client was configured to resemble a workstation on the Internal Restricted Network with internal BackWeb Server.

- *Protected*: A scenario in which the client was configured to resemble a workstation on the Internal Secure Network with internal BackWeb Server.

We acquired a test-bed network consisting of BackWeb server, several BackWeb clients, network firewall and associated routers, and a sniffer system to capture communication packets. This network contains Windows NT-based nodes with ancillary NT domain controllers and name servers for each side of the firewall. We configured the BackWeb Server in a manner described by the documentation in a form suitable for developing novel BackWeb packages and serving them to clients over the Internet.

Sandia will evaluate a sample “PUSH” technology for security problems and, if any are found, to demonstrate some of those vulnerabilities in a manner that might compel the appropriate care in deploying such systems.

Initially, we checked each test configuration for operational stability and exercised all features of the PUSH technology. We identified and characterized baseline network protocol traffic first with, then without, BackWeb services. We analyzed and documented the protocols utilized by the BackWeb systems, noted documented and undocumented features, and assigned them a priority of analysis.

We generated test scripts to allow repeated testing and analysis of areas that were of concern. Although some of these were in the area of operational and administrative implementations, it was apparent quite early that this technology posed a high security risk in most of the test scenarios.

Our findings and demonstrations exceeded expectations by finding modes, which allow these untoward effects even when protected by firewalls, routers, and C²-configured operating systems. The client could introduce intentionally at the server and without the possibility of repairing security-critical effects. Further, actual control of the PUSH clients could be assumed by a route or impersonating BackWeb Server.

We are writing a report that identifies all of the areas of security concern. We identified and are testing mitigation of security-critical functions and areas. Phase PUSH Technology is currently in beta. The next phase is to analyze this implementation, review previous areas of concern, and perform more indepth analysis of the final planned version of the technology.

We identified and are testing mitigation of security-critical functions and areas.

3512410000

Controlling Information: Its Flow, Fusion, and Coordination

T. M. Berg, I. R. Shokair, L. J. Lehoucq, R. G. Hillaire

Increasingly, robust networks of computer-based sensing stations must operate without central coordination in a wide range of applications from factory control to battlefield situation understanding. Exacerbating the difficult task of engineering decentralized hardware systems is the fact that they must operate on large amounts of distributed data. The data are often widespread, overlapping, redundant, delayed, of uncertain reliability or value, and obtained from different perspectives.

The goal of this project is to create an engineering theory of distributed information, particularly as applied to decentralized, sensor-based systems. The theory should provide a basis for the design of distributed system architecture, helping to account for the many complicated tradeoffs between communication, computation, memory, and setup effort.

Sandia's approach was to develop a measure of distributed information useful for representing the information content of distributed data. We can then also use this information to map the distributed data to an implementation via the constraints on the solution. In this way, we can engineer the complex interconnections of decentralized hardware and distributed software to meet system performance requirements.

Our first task was to find a measure of information useful for engineering distributed sensor-based information systems. This information measure must lend itself to the distributed information properties recognized from the human perspective as overlapping information, information from different perspectives, and information of a certain value or reliability. These properties were satisfied by the Fisher information concept possessing the mathematical notions of correlation, affine transforms, and variance. We found the Shannon information useful as it was intended as a channel capacity measure, but not useful as it was not intended by Shannon as a substantive information measure.

The Fisher information concept lends itself to the transfer of a useful data summary between distributed data-processing centers. It is a statistically derived measure, the successful product of Fisher's attempt to fill a need for a sufficient and

The goal of this project is to create an engineering theory of distributed information, particularly as applied to decentralized, sensor-based systems.

efficient data statistic. The measure is directly related to the covariance, so it leads directly to a measure of information value and reliability, even as compared to data from another node, as well as the degree to which data from another node overlaps with existing data at a processing node.

The Fisher information form is recognized as the basis for the information form of the ubiquitous Kalman filter sensor-processing algorithm. Because it is a sufficient statistic of an optimal, linear, or affine estimator, it can be easily transformed by matrix multiplication and made useful for sharing information between nodes, or agents, of a distributed processing system. In this way, the differences in sensor perspective between processing nodes are accounted for, and sensor information from other nodes may be effectively shared.

Our second task was to determine how we can use this information measure to map the properties of the distributed data into an implementable solution. We accomplished this using our internodal transformations. These provide a complete method of determining system topology by simply calculating the transfer matrix. If no communication link is necessary, the transfer matrix is the null matrix. We are currently looking into how to code this solution in a Java programming language simulation and demonstration of decentralized system design.

This task was aided by comparison of the internodal transformation with the blending matrices derived by UCLA for accomplishing communication between agents in a decentralized network. There are many similarities in the result, and we collaborated with UCLA to further develop this notion.

We modified the third task because completing the second task solved part of the problem. Instead of casting the problem as an optimization problem in control of information leading to design techniques, we will attempt to go after the systems-level design decisions directly using a carefully designed simulation.

Other Communications

Lehoucq, L. J. 1999. "Fisher Information: A Summary." Research working papers.

Speyer, J. 1999. "Summary of Research into Decentralized and Distributed Sensor Systems." Working papers.

3512420000

Mission Surety for Large-Scale Real-Time Information Systems

S. J. Bepalko, H. L. Dison

This project will develop a new capability termed mission surety that will enable the designers of large-scale real-time systems to guarantee the correctness of results. Complexity of a system, and thus the propensity for error, is best characterized by the number of states the systems can encounter. In general, the number of states grows exponentially as data sources are added. It is unlikely that current ad hoc methods of developing systems will be able to handle this increasing complexity.

Two technologies will provide the basis for establishing mission surety. Sandia analyzed the problematical modules in an operational defense system and then developed extensions to existing formal language techniques. These new methods provide a comprehensive and compact method for specifying and subsequently automatically generating error-free implementations.

We explored several applications of the theory developed in the two previous years. These included a potentially (and radical) new theory of the underlying mathematical foundation for the global positioning system (GPS), a proposal for a new multiplatform secure operating system that runs most common applications as well as has amazing ability to withstand unauthorized attack by insiders.

A component of the new GPS theory required a new, more accurate approximate solution. This, in turn, was dependent on placement of points on a sphere that were as far apart as possible, but also as nearly equidistant as possible. The novel algorithm developed for the project was a combination of a new result of Saff ('98) of the University of South Florida and the multiple lookahead parsing theory. The current algorithm places one point at a time and is already believed to be close to the limit of optimality.

[We] will develop a new capability termed mission surety that will enable the designers of large-scale real-time systems to guarantee the correctness of results.

Refereed

Bespalko, S. J., M. Wyman, D. Sulsky, and H. L. Dison. 1999. "A Nonlinear Correction of Spatial Data." Paper presented to the Arizona Geographic Information Conference '99, Tucson, AZ, 8–10 August.

Turner, K., and S. J. Bespalko. 1999. "The Future of Spatial Data Technologies—A Look into the New Millennium." *Transportation Research News*, accepted.

Other Communications

Sandia National Labs. 1999. "Navigating Computational Wrong Turns." *Sandia Technology Journal* (January).

3512430000

Low-Power, Reduced-Computation, Public-Key Protocols

V. A. Hamilton, E. V. Thomas, C. L. Beaver, R. A. Gonzales, T. J. Draelos, R. D. Miller

The goal of this project is to research and develop mechanisms that will enable the use of public-key cryptography in low-power and/or reduced computation environments. Sandia did a lot of work in researching and developing candidate algorithms and implementing primary algorithm choices in both software and hardware. We are constructing a decision table comparing the performance of various algorithms to easily illustrate the benefits and tradeoffs realized by using a given algorithm.

- *Reviewed, documented, and implemented any technical advances in candidate(s) for baseline public-key protocol(s)/algorithm(s) where appropriate.* We determined that there are three distinct classes of public-key algorithms/protocols that show promise: number-theoretic, one-time, and combinatorial. We are researching a new number-theoretic subclass based on modular polynomials. This class promises short signatures and relatively more-efficient algorithms. There appear to be efficiency tradeoffs between short signature lengths and computational requirements. We are currently researching the computational toolkit required to implement these schemes. We believe that one-time public-key schemes can be modified to provide very low resource schemes with development to address the associated key management issues. In particular, we are investigating an improvement that would allow chaining of the public keys. We believe this mechanism has some potential and are currently looking at attacks against this scheme. The combinatorial class of algorithms is our most difficult research area. We are not convinced, however, that the problems associated with this class (long authentication signatures, and therefore increased power requirements for communication) cannot be overcome and will continue research here.

- *Implemented in software primary choice(s) for public-key protocol(s)/algorithm(s).* We implemented several algorithms in software including Optimal El Gamal, ESIGN, and several one-time schemes. We are also implementing the underlying tools necessary for the modular polynomial algorithms as part of our research into those algorithms.

We are constructing a decision table comparing the performance of various algorithms to easily illustrate the benefits and tradeoffs realized by using a given algorithm.

We purchased several commercial low-power devices and are comparing the performance of algorithms on these devices.

- *Reviewed and documented technical advances (TAs) in candidate(s) for key management techniques.* We reviewed several of the key management issues associated with these algorithms. Of particular concern are the key management problems associated with one-time schemes. To that end, we implemented authentication trees for the efficient management of the public keys. We continue to conduct research into the structure of these trees and its impact on low-power applications.

- *Implemented in hardware primary choice(s) for public-key protocol(s)/algorithm(s) if hardware feasible.* We began implementing several of the common underlying functions. We completed the hardware design for an efficient implementation of the Secure Hash Algorithm (SHA-1). We are also reviewing the possibility using a very low power chip, developed at Sandia for an asynchronous transfer mode (ATM) application, which implements the Data Encryption Standard (DES). We plan to compare a DES-based hash and SHA-1 to determine which is more appropriate for the low-power environment. Additionally, we are implementing both a Montgomery modular multiple-precision multiply and a standard modular multiple-precision multiply function. These functions are required for many of the algorithms.

Finally, we are investigating modular reduction algorithms that exploit the fact that most reductions are always performed using the same modulus. We believe that this is an area for some real performance improvements in the number-theoretic schemes.

- *Created decision table (algorithm versus time of execution, exportability, storage requirements, etc.).* We incorporated this table (in an incomplete form) in the current draft of the final report from this project. The table includes the computational complexity of both the authentication and verification functions of each algorithm we investigated as well as storage requirements. We will augment the table as research continues.

3512440000

Ten-to-One-Hundred-Gigabit/Second Network Enabling R&D

L. G. Pierson, P. J. Robertson, T. D. Tarman, E. L. Witzke, L. B. Dean

The next major performance plateau for high-speed, long-haul networks is at 10 Gbps. Data visualization, high-performance network storage, and massively parallel distributed processing (MPP) all demand these (and higher) communication rates. MPP-to-MPP distributed processing applications and MPP-to-Network File Store applications already require single conversation communication rates in the range of 10 to 100 Gbps. And, MPP-to-Visualization Station applications can already utilize communication rates in the 1 to 10 Gbps range.

There are major research holes in the technical base required to develop secure, high-speed, low-cost communications systems in the 10 to 100 Gbps range. Critical gaps in standards and technology impede collaborative development and delivery of such information in a secure fashion. Some of these are (1) super-high-speed segmentation/fragmentation, reassembly, and framing of asynchronous transfer mode (ATM) cells or Internet Protocol (IP) datagrams into Synchronous Optical Network (SONET) payload envelopes, (2) streamlining of wavelength division multiplexing (WDM) media access methods, (3) inverse multiplexing of ATM for high-speed channels, (4) development of bit rate and format-independent signaling methods that can be optically regenerated for transmission over long distances, and (5) maturation of standards to these ends. Implementations of communication systems that carry 10 to 100 Gbps exist only as laboratory curiosities. Expensive 10 Gbps optical multiplexers are only now emerging on the market. To enable practical communications in the range of 10 to 100 Gbps, we must develop methods of efficiently processing communication protocol functions at extremely high speed and/or in parallel.

This project will develop an end-to-end architecture for 10 to 100 Gbps computer networking and address the gaps that it requires. We will examine the emerging technologies and components with which to streamline communication protocol processing and will develop prototypes as appropriate. We expect collaborations with academia and members of the telecommunications industry.

The next major performance plateau for high-speed, long-haul networks is at 10 Gbps....This project will develop an end-to-end architecture for 10 to 100 Gbps computer networking and address the gaps that it requires.

This project examined several emerging technologies for high-speed communication, including erbium (Er) and neodymium (Nd)-doped optical-fiber amplifiers for application to multiple transparency windows in long-haul optical fiber. We extended the PLD-11 flexible prototyping board with SONET OC-48 (2.4 Gb/s) interfaces for ATM/SONET framing and dense wave division multiplexing (DWDM) studies. We simulated Operating System Bypass and Virtual Interface Architecture (VIA) performance utilizing the OPNET Modeler tool set. We surveyed DWDM technology. We presented viable designs to the ATM Forum for scalable Universal Test and Operation Interface for ATM (UTOPIA) interfaces that reside between the ATM and the SONET layers of communications. We collaborated with partners on revised and innovative techniques for scaling UTOPIA interface functionality. We participated in the ATM Forum development of extensions to the means for Inverse Multiplexing over ATM (IMA), a major theme of our work in matching rates to processes and available circuits. A detailed study of the layers below ATM led to investigation of methods of achieving SONET functionality more efficiently. This research determined that three attributes are required for streamlined functionality. These involve the accommodation of both variable and fixed-length data transfers, extremely efficient framing and synchronization of ATM cells and/or variable length datagrams, and the minimum-required SONET-like diagnostic capabilities. We developed a set of techniques to accomplish these objectives that surpasses concepts proposed by industry research. These techniques incorporate the innovative modulation of framing signals on the clock signal, thus increasing efficiency.

This research determined that three attributes are required for streamlined functionality. These involve the accommodation of both variable and fixed-length data transfers, extremely efficient framing and synchronization of ATM cells and/or variable length datagrams, and the minimum-required SONET-like diagnostic capabilities.

Other Communications

Robertson, P. J., S. Merchant, and D. King. 1999. "Proposal for the Basic Structure for a 32-bit UTOPIA Level 4 Specification." *ATM Forum Contribution # 99-0166 to the Physical Layer Working Group of the ATM Forum Technical Committee* (25 April).

3512450000

High-Performance Commodity Interconnects for Clustered Scientific and Engineering Computing

L. Stans, M. M. Miller, J. P. Brenkosh, T. D. Tarman, T. C. Hu, R. C. Armstrong, P. S. Wyckoff, H. Y. Chen

The Computational Plant (Cplant) runs distributed parallel applications on a large cluster of commodity PCs. Because properly load-balanced distributed parallel applications tend to send messages synchronously, minimal blocking is as crucial a requirement as high bandwidth and low latency. Therefore, the following factors are important network design considerations: (1) the selection of an optimal commodity interconnect network technology and topology to provide both high bandwidth and congestion control, and (2) the development of an efficient local-area communication layer to minimize per-packet processing latency in compute and input/output (I/O) nodes.

The goal of this project is to develop and demonstrate a design methodology for constructing high-performance interconnects using high-bandwidth, low-latency, local-area network (LAN) technologies such as Myrinet, asynchronous transfer mode (ATM), switched Gigabit Ethernet, and the emerging operating system (OS) bypass Virtual Interface Architecture (VIA). An important element of the research has been the pursuit of an emerging communication model that decouples I/O support from the OS and allows individual applications to directly control their own I/O processing. This approach will eliminate the large delay introduced by the per-packet Transfer Control Protocol/Internet Protocol (TCP/IP) processing overhead.

Since Sandia's network design goal is to facilitate the performance of real applications, we have worked to evaluate the above LAN technologies in the context of working applications on a small test-bed. We scaled our results to larger networks with thousands of interconnections using modeling and simulation tools developed in this project. These modeling and simulation tools will be invaluable in designing the next-generation interconnect for a large Cplant system and its associated applications. In addition, we evaluated the ability of techniques such as priority queuing, enhanced message-passing algorithms, network-based multicast/broadcast, and cut-through routing to increase throughput and reduce latency and congestion.

The goal of this project is to develop and demonstrate a design methodology for constructing high-performance interconnects using high-bandwidth, low-latency, local-area network (LAN) technologies such as Myrinet, asynchronous transfer mode (ATM), switched Gigabit Ethernet, and the emerging operating system (OS) bypass Virtual Interface Architecture (VIA)...[Sandia] will eliminate the large delay introduced by the per-packet Transfer Control Protocol/Internet Protocol (TCP/IP) processing overhead.

We expanded the hardware test-bed and completed the 4-, 8-, 16-, and 32-node VIA fabric test for bandwidth and latency. We completed the numerical aerodynamic simulation (NAS) message-passing benchmarks for MPI (message-passing interface) on the test-bed and made comparison runs on the Teraflop and Cplant systems. In addition, we ran the same benchmarks with the TCP/IP stack over standard 100 BaseT Ethernet. We also examined the interface between the VIA cluster and legacy network. Based on the test results from the Netpipe signature graphs and Netperf over Gigabit Ethernet, we concluded that a custom gateway is needed to interconnect VIA to legacy networks and that VIA can provide excellent bandwidth performance with a low latency. The current commercial implementations of VIA hardware are still not stable enough to implement a 24x7 production service.

We completed the development of the simulation model components, which allow prediction of communication performance in large-scale, VIA-connected computing clusters. We developed the components to model VIA over ATM Adaptation Layer 5 (AAL5). In addition, we adapted the VIA simulation model to a commercial implementation of VIA from Giganet, Inc. We validated the latter model against various test-bed topologies and extended it to represent a 1024-node cluster. Simulation runs on this cluster model, with basic application traffic source models, show that VIA provides very low latency for 2-D torus topologies with moderate mesh loading.

We evaluated the performance of the Myrinet technology by extending the simulator developed at the University of Utah. We adapted the Myrinet part of the code from the original component-level simulator and added task- and event-handling capabilities to conduct a network-level study and developed a set of parsing and plotting tools to help analyze our simulation results. We developed four representative parallel algorithm models to drive the simulation.

We conducted the commodity Gigabit Ethernet study using the MIL 3 OPNET modeler. The four parallel models previously developed were run directly on top of the Ethernet layer. We developed an adaptation layer that handles the segmentation and reassembly of the application's messages to fit the Ethernet MTU (maximum transmission unit) and minimum size constraints. In addition, the model resolves source and destination MAC address for Ethernet framing at the Ethernet MAC layer.

We developed an adaptation layer that handles the segmentation and reassembly of the application's messages to fit the Ethernet MTU (maximum transmission unit) and minimum size constraints. In addition, the model resolves source and destination MAC address for Ethernet framing at the Ethernet MAC layer.

The Avici terabit switch router offers a low-latency, high-bandwidth, nonblocking switch that can connect ~ 20,000-gigabit Ethernet end hosts. The Avici switch achieves its scalability by allowing 1024 switching nodes to be interconnected in a 3-D torus configuration, with each switching node supporting up to 16-gigabit Ethernet ports. The switch simulator has the capability to generate random traffic at its line card interfaces to stress the switching fabric, but it lacks the ability to simulate the network beyond. We extended the Avici model by adding an Ethernet model to the Avici switch fabric model. We designed this interface such that the parallel algorithm models previously developed could be used with a minimum of modification. We used the same parsing and plotting tools previously developed to do our performance analysis.

Our results show that the Myrinet technology offers low latency in the absence of traffic congestion. However, with certain network topologies and under heavy load, blocking within the fabric can become a performance bottleneck, producing a performance comparable to a conventional store-and-forward Gigabit Ethernet switch. As a result of Avici's six-times speed-up to its internal links, diverse paths from its 3-D torus configuration, cut-through routing, and intelligent queue management, it can offer commodity Gigabit Ethernet hosts a means to achieve a much lower latency than Myrinet. The Avici switch has the potential of providing both low latency and the robustness and reliability of telephone company class hardware.

Refereed

Tarman, T. D., L. Stans, and T. C. Hu. 1999. "A Simulation Study of the Virtual Interface Architecture." *Proc. OPNETWORK '99 I* (September) (Washington, DC, 30 August).

As a result of Avici's six-times speed-up to its internal links, diverse paths from its 3-D torus configuration, cut-through routing, and intelligent queue management, it can offer commodity Gigabit Ethernet hosts a means to achieve a much lower latency than Myrinet.

3512460000

AVATAR—Navigating and Mining in Massive Data

W. P. Kegelmeyer

The sheer scale of modern datasets defeats attempts to understand that data. Even when coupled with advanced visualization systems, the volume is such that all data can no longer be available at a glance. Thorough inspection is impossible, yet inspection is necessary, especially when the phenomena of interest are easier to recognize than to describe.

This project will develop an advanced tool for data understanding, one that supports exploration, easy collaboration, and knowledge encapsulation. The core idea is to exploit massive parallelism and robust pattern recognition (PR) to manipulate derived properties of the datasets. This approach is called AVATAR (Adaptive Visualization Aid for Touring and Recovery) and will produce avatars, sophisticated user profiles that are attached to data. These, in turn, are exploited by the visualization tool, permitting the data to be understood in a fashion uniquely adapted to a particular user.

Sandia developed a powerful and robust PR method known as dense feature maps (DFM). We previously applied DFM methods to a similarly difficult problem, detection of cancer in mammograms, with noted success (two patents and a commercial software license). We will use DFM here, as well, to extract the avatars by invisibly watching how a user interacts with the data.

The end result will be prototype AVATAR software, integrated with a 3-D physics visualization application already in active use at Sandia with full documentation.

- *Pattern recognition.* We showed ScalParC, a popular and apparently pertinent parallel processing approach, to be a dead end.

We invented (or extended), implemented, and tested three specific methods for parallel learning on distributed datasets: conflict resolution, specialization, and weighted voting. We showed weighted voting to be both completely parallel and superior in performance. We also showed it to be mathematically equivalent to bagging (without replacement), a method known to optimize the performance of serial classifiers.

We implemented all parallel PR algorithms (both the serial versions and the code to operate them in parallel) and tested

Sandia developed a powerful and robust PR method known as dense feature maps (DFM)...The end result will be prototype AVATAR software, integrated with a 3-D physics visualization application already in active use at Sandia with full documentation.

them on the ASCI (Accelerated Strategic Computing Initiative) Red parallel machine.

- *Human factors and visualization tools.* We improved the AVATAR/MUSTAFA interface to move all AVATAR-related activities to a single optional panel so that AVATAR can be used in a pure MUSTAFA mode.

AVATAR can now compute record saliencies as physics variables in the Exodus II dataset, which means that AVATAR/MUSTAFA can visualize the saliency with the same range of tools and visualization methods as can be applied to any physics variable.

A full end-to-end prototype integration with the parallel PR means that an AVATAR/MUSTAFA session can read in an ASCI dataset, record interactive saliencies as it is examined, write training data, generate the classification rules, apply them to a new dataset, and display the highly salient regions.

AVATAR can now compute record saliencies as physics variables in the Exodus II dataset, which means that AVATAR/MUSTAFA can visualize the saliency with the same range of tools and visualization methods as can be applied to any physics variable.

Refereed

Hall, L. O., and P. Lande. 1998. "Generation of Fuzzy Rules from Decision Trees ." *J. Advanced Computational Intelligence* **2**: 128–133.

Hall, L. O., N. Chawla, K. W. Bowyer, and W. P. Kegelmeyer. 1999. "Large-Scale Parallel KDD Systems." Chapter in *Learning Rules from Distributed Data*, edited by M. J. Zaki and H. Ching-Tien; Series: *Lecture Notes in Computer Science* (New York, NY).

Hall, L. O., N. Chawla, K. W. Bowyer, and W. P. Kegelmeyer. 1999. "Learning Rules from Distributed Data." *Technical Report 99-8, Rensselaer Polytechnic Institute, CS Dept. 1* (Workshop on Large-Scale Parallel KDD Systems, San Diego, CA, August): 77–93.

Other Communications

Chawla, N., and L. O. Hall. 1999. "Modifying MUSTAFA to Capture Salient Data." **ISL-99-01**. Presentation to the University of South Florida, Computer Science and Engineering Department, Tampa, FL.

Hall, L. O., K. W. Bowyer, N. Chawla, T. Moore, and W. P. Kegelmeyer. 1999. "AVATAR—Adaptive Visualization Aid for Touring and Recovery." Sandia Technical Report, in preparation.

Kegelmeyer, W. P., L. O. Hall, K. W. Bowyer, N. Chawla, and T. Moore. 1999. "AVATAR—Terascale Pattern Recognition and Visualization." Presentation to the LDRD Program Review, Albuquerque, NM, 27 July.

3512470000

Algorithm-Based Fault Tolerance on Heterogeneous Massively Parallel Computers

P. D. Hough, M. E. Goldsby, E. J. Walsh

Sandia will perform research and development of fault-tolerance strategies (e.g., in redundancy design, fault detection, fault recovery) and the implementation of a fault-tolerant software environment for massively parallel (MP) heterogeneous systems such as Sandia's Computational Plant (Cplant). Such systems are more vulnerable to failures than homogeneous systems, like Sandia's Tflo (Teraflop) machine, due to the diverse subsystem and network architectures, the need for multiple operating system support, and the decentralized computing and storage platforms. These unique features mandate a fundamental change in fault-tolerance strategies. We will develop an algorithm-dependent fault-tolerance methodology based on a combination of disk-based and diskless checkpointing. This hybrid approach offers low overhead and allows fine-tuning for efficient performance of individual applications. We will encapsulate the techniques in a Java-based object-oriented framework and apply it to a number of Sandia applications, including linear system solvers in AZTEC, numerical optimization methods in OPT++, and enterprise simulations (IDES [Infrastructure for Distributed Enterprise Simulations]). In addition, we will develop failure models to assess the effectiveness of and to suggest refinements for the fault-tolerance strategies. The effort will enhance the robustness of Sandia's distributed computing applications, especially on heterogeneous platforms such as the Cplant. It will have an immediate impact on problems in enterprise modeling and optimal design. Moreover, the fault-recovery techniques to be developed for the software environment will include strategies for process migration, processor reconfiguration, and reclamation, thus contributing to the advancement of location-insensitive heterogeneous computing technology at Sandia.

In collaboration with the College of William and Mary, we completed the implementation and testing of an asynchronous and fault-tolerant parallel direct search (APDS) optimization algorithm. This was run on Cplant to successfully solve problems arising in the design of a chemical vapor deposition (CVD) furnace and in circuit simulations.

The effort will enhance the robustness of Sandia's distributed computing applications, especially on heterogeneous platforms such as the Cplant. It will have an immediate impact on problems in enterprise modeling and optimal design....[and] will include strategies for process migration, processor reconfiguration, and reclamation, thus contributing to the advancement of location-insensitive heterogeneous computing technology at Sandia.

We implemented a fault-tolerant version of the IDES and will complete thorough testing.

In collaboration with the High-Performance Computing and Simulation (HCS) Research Laboratory at the University of Florida, we developed and tested a number of hierarchical schemes for fault-detection and scalable consensus algorithms in a simulative environment. Software is now under development.

We designed and implemented a prototype of the middleware required for interaction between the fault-detection protocols and the applications.

We incorporated Lilith, a tool for developing scalable system tools, as a means of starting up our fault-tolerance services. In addition, we are investigating future uses of Lilith in our setting.

We developed a number of graphical user interfaces (GUIs) to assist in troubleshooting our algorithms and to use for demonstration purposes.

Refereed

Burns, M. W., A. D. George, and B. A. Wallace. 1999. "Simulative Performance Analysis of Gossip Failure Detection for Scalable Distributed Systems." *Cluster Computing*, accepted.

Hough, P. D., T. G. Kolda, and V. J. Torczon. 1999. "An Asynchronous Parallel Direct Search Algorithm for Nonlinear Optimization." Paper presented to the SIAM Optimization Conference, Atlanta, GA, May.

Other Communications

George, A. D., S. Ranganathan, R. El-Kadi, R. Todd, M. Chidester, and B. Nguyen. 1999. "Simulative and Experimental Performance Analysis of Gossip-Based Failure Detection with Consensus." *J. Cluster Computing*, submitted.

Hough, P. D., T. G. Kolda, and V. J. Torczon. 1999. "Asynchronous Parallel Direct Search Algorithms for Nonlinear Optimization." Sandia Technical Report, Sandia National Laboratories, Albuquerque, NM, SAND2000-8213.

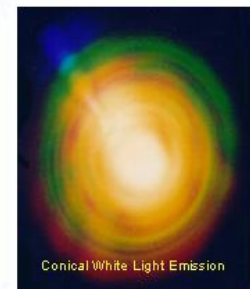
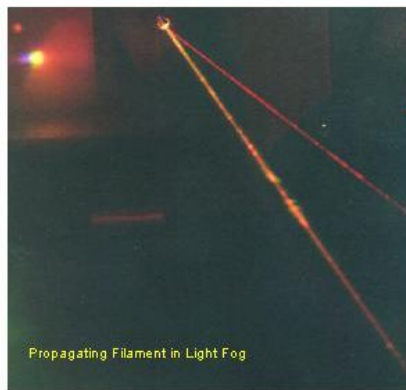
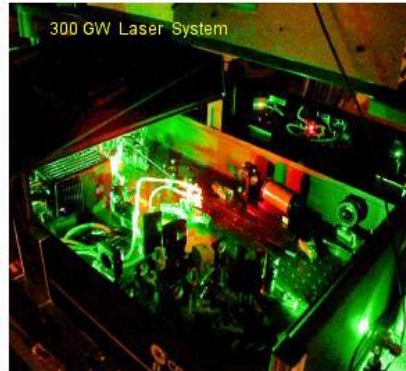
DIRECTED ENERGY

Directed Energy is one of Sandia National Laboratories' six LDRD Roadmap Technologies investment areas. Roadmap Technologies derive their scientific basis from and extend the applications of Research Foundations investments into new areas. Roadmap Technologies create or accelerate scientific and technical expertise for future program areas that are strategic to Sandia and important to the DOE and the nation.

The Directed Energy investment area researches concepts and technologies for advanced directed energy (DE) systems and applications. In the broadest sense, DE deals with the active projection of energy over a distance for weapons, sensors, and material processing applications. Research in this area addresses novel solutions for the (1) destruction, disruption, or defeat of adversary systems, (2) active imaging or other sensing applications, (3) processing methods such as chemical/biological decontamination or materials processing/inspection, and (4) technology for protection against adversarial use of DE against U.S. systems.

The "Intense White-Light Pulse Propagation in Air Using Self-Guided Optical Filamentation: Applications to Remote Sensing and Countermeasures" project is investigating the propagation of gigawatt peak power, femtosecond optical pulses through the atmosphere over long distances (~100 meters). The parameter space governing Kerr self-

focusing pulse propagation in the atmosphere is being explored in order to develop a basic physical model for stability analysis and adaptive control. In addition, remote sensing and countermeasure concepts are being explored in simple laboratory scenarios. The results of this research have important ramifications for laser beam transport, directed energy weapons, and optical remote sensing applications.



3514150000

Surface Decontamination of Bacterial Protein Toxins by RF Power

R. P. Toth

Sandia based this project on a radio frequency (RF) electromagnetic (EM) (nonionizing radiation) method of decontamination. This method requires no water, no cleanup, and no drying, and offers very fast inactivation of bacterial protein toxins. It inactivates biological products rather than merely diluting them. Further, it penetrates joints, bearings, and the like. The photon energy is so low that photocurrents are not produced. Neither water nor chemicals are used. In this way, sensitive electronic equipment is not affected.

The method operates by irreversible alteration of the tertiary (conformational) state of biomacromolecules. It is energy-efficient, leaves no toxic residue, and may be applied either by hand-held antenna (ca. 12 inches diameter and 10-pound weight) with a cart-mounted power source or by a transportable multimode cavity.

We developed the RF system necessary to test for decontamination effectiveness. The RF system has the following subtasks: (1) noncontacting applicator development and testing (the antenna and feed structure); (2) the RF power tube assembly and testing (extended interaction oscillator and high-voltage power supply); (3) rectilinear scanner to move the antenna/tube in order to cover a target zone 30 cm by 30 cm (stepper motor driver and linear position encoder); and (4) RF diagnostics (validate RF power production and beam maps for the applicator).

The first subtask represents a critical path. If we were unable to obtain focused fields within near-field distance from the feed structure, the project could not continue. The necessary antenna is one of elliptical geometry. That is, a feed structure is located at the first focal point, and the target is located at the second focal point. The main (elliptical) reflector was of "super alloy" suitable for vacuum forming. The feed structure is composed of dominant mode waveguide, an orthomode transducer to produce circularly polarized fields from the transverse electric (TE) guide, and a corrugated conical horn to illuminate a hyperbolic subreflector (Cassegrain configuration) at the calculated first focal point.

Tests for the applicator consisted of field maps at and near the calculated second focal point. Well-known relationships

This method requires no water, no cleanup, and no drying, and offers very fast inactivation of bacterial protein toxins.

exist between the beamwidth and gain of the antenna. Since we were able to determine a fullwidth half-power beam of 2 degrees in azimuth and elevation, the antenna gain is ca. 50 dB.

The second subtask was to fit the RF power package to the applicator and scanner. This involved mounting the extended interaction oscillator and high-voltage power supply umbilical to the antenna support on the scanner. Then we made full-power tests with photochromic film at the target zone (second focal point). We were able to confirm predicted power density given the gain and aperture efficiency of the applicator.

The third subtask, the scanner assembly and operation, involved development of software and drivers for the stepper motors in elevation and azimuth. Position control was closed-loop by virtue of linear position encoders on each axis.

The fourth subtask, development of RF diagnostics, involved a lossy (absorber-lined) "chamber" for the target, directional couplers, matched diode detectors, and standard gain horns to validate system performance by beam pattern and power density.

3514160000

Intense White-Light Pulse Propagation in Air Using Self-Guided Optical Filamentation: Applications to Remote Sensing and Countermeasures

S. M. Cameron, T. R. Lockner, T. S. Luk, D. E. Bliss

Recent experimental observations of stable, self-guided propagation of gigawatt peak power femtosecond optical pulses through the atmosphere over long distances (~ 100 meters) without diffractive divergence has important ramifications for laser-beam transport, directed energy applications, and optical remote sensing. Dynamic stabilization of the laser channel is attributed to a balance between the Kerr self-focusing nonlinearity in air and the combined effects of normal diffraction and refractive defocusing from the induced ionization column, which act synergistically to produce a longitudinal waveguide or swept moving focus structure for robust power transmission. This novel electromagnetic (EM) propagation regime eliminates previous fundamental limitations of thermal blooming, dielectric breakdown, and diffractive imaging on resolution and projected brightness in conventional active systems. By using adaptive pulse shaping and dispersion compensation to manipulate onset and stability of the self-focused beam-forming process, optical energy can be concentrated in a prescribed focal volume at a predetermined range for remote nonlinear spectroscopy and high-field short-pulse material interactions. Conical white-light emission generated in the propagating atmospheric filament can be used for multispectral characterization and hyperspectral imaging (HSI) over long coherence lengths, and transient inversion of the probed sample population resulting from the ultra-fast excitation is expected to cause preferential backward conductance of weak Raman and fluorescence signatures with amplified spontaneous gain for improved collection efficiency. The combination of peak intensity with short interaction time and abrupt temporal development profile in the laser channel will have profound consequences for enhanced rectification of secondary radiation impulses (FIR [far infrared], x-rays, EMP [electromagnetic pulse]) or shocks in intervening material systems, and for the evolution of nonsteady-state responses to penetrating fields. When the transmitted optical or rectified pulse shape is faster than the medium permittivity response

This novel electromagnetic (EM) propagation regime eliminates previous fundamental limitations of thermal blooming, dielectric breakdown, and diffractive imaging on resolution and projected brightness in conventional active systems.

time, kinematic properties of the associated radiation field may be altered to facilitate EM transparency through normally dispersive or absorptive layers for early-time signature discrimination analysis.

We used an unfocused 300 GW femtosecond Ti:sapphire CPA (chirped pulse amplification) laser to create stable, diffraction-free, 20-meter-long, atmospheric filaments with estimated beam-pointing variance of 300 microradians. The measured Kerr self-focused beam collapse diameter at the onset of filamentation (~ 550 microns) was consistent with multiphoton ionization dynamics, and the final on-axis termination length diameter (~ 900 microns) produced an estimated hundredfold enhancement in focal irradiance over normal diffractive propagation. In preliminary experiments, the effective focusing distance for producing a channel appeared to be consistent with standard self-focusing theory and was found to be sensitively dependent on initial parameters including critical power, spatial intensity profile, and chirp. Pronounced off-axis conical white-light continuum emission in the form of concentric color rings was observed as a function of incident laser pulse energy with a wavelength-ordering (normal diffraction or blue-shifted anti-Stokes parametric coupling) and divergence angle attributed to a self-phase-modulation dynamic involving the interplay of plasma nonlinearities and group velocity dispersion in the focusing region. We performed on-axis energy measurements using a calibrated piezoelectric transducer; it exhibited laser-filament coupling efficiencies of 10%–25%. We evaluated effects of Mie scattering, humidity, and stochastic atmospheric density fluctuations on whole-beam self-focusing using an artificial mist chamber inserted along the propagation path. We assembled frequency-resolved optical gating (FROG) and wavefront-sensing apparatus to longitudinally characterize the spectral phase, temporal profile, and evolving transverse intensity spatial distribution of the self-focused channel in anticipation of systematic mapping investigations of the parameter space to resolve conflicting theoretical models for moving focus and waveguide self-trapping, and to develop a unified predictive model for adaptive stability control. We identified new ultra-fast pulse material damage mechanisms and surface morphologies, including large-aspect-ratio microstructures without peripheral recast or thermal ablation damage, and the production of standing wave gratings.

Refereed

Bliss, D. E., T. S. Luk, D. Adams, and S. M. Cameron. 1999. "Laser Machining with Ultrashort Pulses." *MRS Proc.—American Physical Society* (Boston, MA, November 1998).

Diels, J. C., J. Schwarz, P. Rambo, S. M. Cameron, T. S. Luk, and A. Bernstein. 1999. "Measurements Toward Better Understanding about Filamentation in Air." *Internat. Conf. Electromagnetics in Advanced Applications—Litografia Geda* (Torino, Italy, September): 19.

3514170000

Improved Backscatter X-Ray Detection for Antiterrorist Applications

G. J. Lockwood, J. C. Wehlburg, M. M. Selph

Sandia successfully demonstrated the use of backscattered x-rays to image bombs in suitcases. We accomplished this using a scanning technique that is slow and requires large scintillating detectors. To improve speed and reduce size of the detection system, we developed a system using an x-ray pinhole camera that could use either intensified film or a charge-coupled device (CCD) camera coupled with a scintillating screen.

We designed and tested a pinhole camera. Using Polaroid film with an intensifier, we obtained images of test objects and demonstrated that the camera was functional and radiation-tight.

We obtained an inexpensive CCD camera designed for use with telescopes. Since this camera is not radiation-hard, we used a scintillator screen and coherent fiber-optic cable to keep the camera in a low-radiation environment.

We used the imaging technique utilizing a scanning source and scintillating detectors to image a section of wall typical of what is used in home construction, two-by-fours, insulation, and sheetrock. Wires, electrical outlets, a bag of sugar (to simulate drugs), and several metal objects could be imaged and identified in the wall.

We characterized an astronomical CCD camera for light-gathering efficiency and compared it to the Polaroid film used in our pinhole camera imaging. The CCD camera is about 5 to 10 times faster than the ASA 3000 speed film. We chose this camera since it was readily available, inexpensive, and came with its own imaging program.

Because this particular camera was not radiation-resistant, we moved it about 8 feet from the source and used a coherent fiber-optic cable and 35 mm lens mounted on the CCD camera to try to capture an image. We mounted a scintillating screen on the front of the fiber-optic cable and placed it in the pinhole. We were unable to resolve an image with this setup. We identified several reasons for this; in particular, there was a mismatch in the quantum efficiency of the camera and the scintillating screen that reduced the camera response a factor of five.

To improve speed and reduce size of the detection system, we developed a system using an x-ray pinhole camera that could use either intensified film or a charge-coupled device (CCD) camera coupled with a scintillating screen.

During this project we established a Web site for the imaging work we were doing that has drawn a lot of attention from the news media and potential customers. *Discovery* magazine published some of our work, and the Discovery News sent a crew to film our work.

3514180000

HPM Vulnerability Assessment and Tests

G. M. Loubriel, L. D. Bacon, L. F. Rinehart

High-power microwave (HPM) technology has matured to the point that practical devices are becoming technically feasible. One option for HPM systems is to use them against terrorists, drug lords, or rogue state communications centers. Sandia will investigate the use of HPM to upset a very simple system: hand-held radios. We will test effects on complete units, partially assembled units, and individual electronics, and will compare the results to those obtained with computer codes that perform circuit analysis.

Three major efforts met our objectives: (1) perform an analysis of possible targets, (2) develop a theoretical model of system performance to optimize the design of the test system (a hand-held radio), and (3) build a nonfrequency-tunable system to test the radios. We obtained the target list earlier than anticipated; the preferred target was a hand-held radio that operates in the so-called "Family Service Radio" band at about 462 MHz. We designed a frequency-tunable system for these tests but did not use it since the radios operate at fixed frequency; however, we did perform tests at various frequencies. We designed and built a nonfrequency-tunable system and used it. We obtained schematics for the electronics, which allowed us to understand the voltages in the system and to test individual electronics parts.

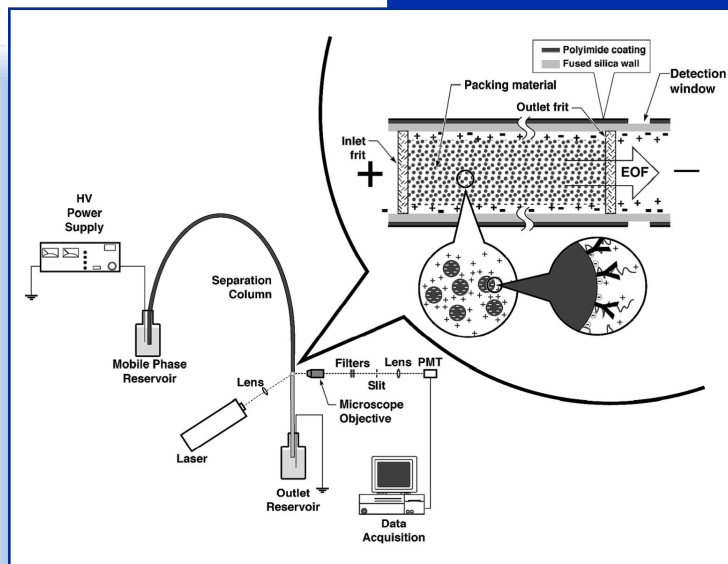
Other Communications

Rinehart, L. 1999. "HPM Vulnerability Assessment and Tests." Presentation at Sandia National Laboratories to visiting DOE officials, Albuquerque, NM, September.

One option for HPM systems is to use them against terrorists, drug lords, or rogue state communications centers. Sandia will investigate the use of HPM to upset a very simple system: hand-held radios.

SENSING & INTELLIGENT CONTROLS

Sensing and Intelligent Controls is one of Sandia National Laboratories' six LDRD Roadmap Technologies investment areas. Roadmap Technologies derive their scientific basis from and extend the applications of Research Foundations investments into new areas. Roadmap Technologies create or accelerate scientific and technical expertise for future program areas that are strategic to Sandia and important to the DOE and the nation.



The Sensing and Intelligent Controls investment area investigates advanced sensor and algorithm technologies to address a variety of national security problems with potential applications ranging from the battlefield to nonproliferation and to environmental cleanup activities. Advances in sensors and algorithms are key to realizing systems that can reason as well as navigate and manipulate complex environments.

Sensing and Intelligent Controls research responds to the Laboratories' needs in the following areas: (1) physical imaging, especially of partly or fully concealed targets and particularly related to buried targets and munitions, underground contaminants, and pipelines; (2) distributed sensor systems that can detect, characterize, locate, or monitor complex environments; (3) distributed command and control of distributed military assets; (4) algorithms and sensing for autonomous navigation in complex, unstructured environments; (5) dexterous manipulation, dexterous robotics to manipulate objects for which

no computer-automated design (CAD) models exist; (6) chemical and biochemical sensing to detect minute quantities of specific chemicals and biochemicals in complex mixtures; and (7) novel concepts, new applications, techniques, and/or skills with significant growth potential.

The "Electrokinetic Immunoaffinity Chemical Sensors" project is exploring the feasibility of capillary affinity electrochromatography (CAEC) with laser-induced fluorescence (LiF) detection as a portable means for the detection of trace quantities of toxins in liquid samples. The research focuses on the detection of analytes (e.g., biological warfare agents) for which there is currently no portable sensor capability with adequate sensitivity and specificity. A sensor based on CAEC has the potential to combine the versatility of capillary electrochromatography (CEC), the high sensitivity of LiF, and the exquisite selectivity of molecular recognition.



3516170000

Imaging of Moving Targets Using Simultaneous Synthetic Aperture Radar (SAR) and Moving Target Indicator (MTI) Radar

J. T. Cordaro, C. V. Jakowatz, Jr., J. A. Hollowell

Synthetic aperture radar (SAR) uses the relative motion between the radar and an object to form an image of the object. To image an object fixed on the earth, the relative motion can be sensed by an inertial measurement unit aided by the global positioning system (GPS). Targets moving over the earth will be shifted and defocused in the image. In this project Sandia will develop and test methods to detect, reposition, and focus moving targets in a SAR image.

Before a moving target can be repositioned or focused, it must be distinguished from stationary objects. This detection process can be accomplished in a number of ways. We tested a method that requires a two-phase center antenna operating in an azimuth interferometry mode. For stationary objects, the measured interferometric angle is equal to the angle predicted by Doppler frequency. However, for a moving target, these angles differ by an amount proportional to the target's radial velocity. The quality of the angle measurement depends on radar cross-section, so an angle comparison provides a way to identify bright targets. Weaker moving targets can still be detected by phase-correcting and subtracting complex images from the two-phase centers. This cancels stationary clutter and can enhance detection of moving targets.

The algorithm for focusing relies on a parametric model for the phase history of the detected target. For straight-line motion, the phase correction is a two-parameter function. A contrast optimization algorithm employs Fletcher's method to search for the two parameters, which turn out to be range and cross-range velocity components.

We concentrated on developing algorithms for detecting, repositioning, and focusing moving targets. We undertook no new data collections. The detection and azimuth-angle work showed that both are sensitive to channel-to-channel amplitude and phase errors. From measurements on the antenna range we found that the radome and its position relative to the antenna affected amplitude and phase differences. This was confirmed by a comparison with data from the second flight test. After this, we did an extensive study of channel variability using

Sandia will develop and test methods to detect, reposition, and focus moving targets in a SAR image.

flight data alone. The main result was to convince us that it will be necessary to compensate for channel errors by using clutter data directly from a pair of images. As a first try, we averaged clutter over range bins at far range and used this as a correction function at the center ranges. With this approach, magnitude differences are within .1 decibel near the beam center and 0.5 decibel at the edge. The corrected phase difference is about 1 degree at the center and as much as 10 degrees at the edge. This is sufficient to obtain worst-case cancellation of stationary targets of 30 decibels at the center and 15 decibels at the edge. In many examples, the errors and resulting cancellation are better than this at the edge.

We used the azimuth-angle measurements to identify bright stationary targets and to reposition moving targets. The two antenna phase centers function as an azimuth interferometer. The measured angle for stationary targets agrees with the angle predicted by Doppler frequency. However, for moving targets, the target image is shifted in Doppler. By comparing the interferometric and Doppler angles, it is possible to separate high cross-section, stationary targets from moving targets. This is not a new idea, but to our knowledge it has not been used at fine resolution. Taking a bright-target threshold of 10 square meters, we were able to separate stationary from moving targets at an angle shift of 0.1 to 0.2 degree, depending on conditions. Because the angle shift is the ratio of the target radial velocity to the radar-platform velocity, this result shows that we are able to detect rather low velocity targets. Some improvement would come from a better antenna or perhaps a better way of compensation antenna errors. Still, we completed this phase of the work with results better than we had expected.

The effort on focusing moving targets is going well. This phase of the work is fairly open-ended because whenever a test under one set of conditions is completed, we go on to a more complicated case. The focus algorithm can handle the situation where the moving target travels on a smooth road with straight-line motion. The situation where the vehicle is on a rougher gravel road gives good results. The approach offers another solution to target repositioning since it provides an estimate of target velocity.

By comparing the interferometric and Doppler angles, it is possible to separate high cross-section, stationary targets from moving targets. This is not a new idea, but to our knowledge it has not been used at fine resolution.

3516180000

Sparse Geophysical Networks for Monitoring Deep Targets

G. E. Sleepe, A. A. Yee, L. C. Bartel, C. W. Sicking, M. D. Ladd, H. D. Garbin, J. P. Claassen, G. J. Elbring

Facilities for the manufacture and storage of weapons of mass destruction (WMD) are often contained within deeply buried structures or tunnels. The ability to detect, characterize, and monitor these deep underground production and storage sites is critical to the defeat of these threats to our national defense. The use of a sparse seismic network is desirable for this application since it represents a practical field-deployable configuration. However, the application of sparse networks for accurately determining the 3-D location of underground activities has heretofore never been addressed. As such, the objective of this project is to design, develop, and test an advanced algorithm that exploits sparse seismic networks to accurately determine the 3-D location of underground activity. The proposed algorithm will incorporate several novel elements to address the sparse network problem: (1) the use of enhanced 3-D geophysical modeling to optimize sensor layout and distribution; (2) the isolation of local soil effects by using both velocity inversion and spectral ratio methods; (3) the use of modified array processing methods to handle the spatially aliased network dataset; (4) exploitation of advanced signal-processing techniques such as multisensor covariance and three-component polarization analysis; (5) and the incorporation of an active calibration source to remove geophysical biases. To validate these advanced geophysical and signal-processing methods, we will process data previously acquired at the Nevada Test Site (NTS) P-tunnel using the novel algorithms. Additionally, we will collect novel datasets at an NTS tunnel to confirm the optimized sparse network approach.

We made significant progress in developing and testing a novel algorithm for locating underground target activity using sparse seismic networks. Building on the algorithm blocks developed in the first year, we integrated the complete model-based algorithm into a MATLAB environment. The complete algorithm consists of signal preprocessing, adaptive parameter estimation (cross-correlations, covariance matrices, times-of-arrival, and three-component estimators), model-based coherent beam-forming, and model-based location estimation.

The ability to detect, characterize, and monitor these deep underground production and storage sites is critical to the defeat of these threats to our national defense. The use of a sparse seismic network is desirable for this application since it represents a practical field-deployable configuration.

We fully tested and validated the algorithm using both synthetic seismograms and data from the P-tunnel. The algorithm testing involved the study of phenomenological processes in the datasets as well as enhancing the algorithms to provide the required performance. Using the novel 3-D finite-difference seismic propagation model developed in this project, we successfully designed an optimized sensor layout to perform a novel sparse network data collection. Henceforth, we fielded a sparse seismic network at an NTS tunnel and collected a unique dataset on underground activity. We applied the novel algorithm to portions of the NTS dataset; localization performance on the underground activity is very promising.

Using the novel 3-D finite-difference seismic propagation model developed in this project, we successfully designed an optimized sensor layout to perform a novel sparse network data collection.

Refereed

Sleepe, G. E., M. D. Ladd, T. S. McDonald, and G. J. Elbring. 1999. "Acoustic and Seismic Modalities for Unattended Ground Sensors." *SPIE Aerosense Conference 1* (Orlando, FL, April): 1.

3516190000

Miniature Bioaerosol Concentrator

K. Wally, D. J. Rader, S. H. Kravitz, R. F. Renzi

In this project, Sandia hopes to develop a miniature bioaerosol concentrator capable of collecting biological warfare (BW) agent from bioaerosols as diffuse as one pathogen particle per liter of air. To be effective with microseparations-based detectors, a minimum of 10 to 20 of these pathogen particles must be concentrated into as little as one microliter of collection solvent. The concentrator device we are developing employs a two-stage geometry to achieve its goals. The first stage is a microseparator that uses geometry to collect and concentrate the bioaerosol (particles in the 1-to-5-micron-size range) via inertial separation principles. We discard articles smaller or larger than this size range, as well as the bulk of the collected air. The second stage is a microimpinger that collects a directed, concentrated stream of size-segregated particles into a tiny amount of fluid within collection microchannels. We use electrokinetic (EK) flow phenomena to move the aqueous collection solvent through the open microchannels in the microimpinger. The microseparator we are developing achieves inertial separation and concentration by employing the Opposed-Flow Virtual Cyclone (OFVC) geometry invented by Sandia, in part in response to the performance requirements of this project.

We developed a new method for particle concentration by inertial separation, called OFVC. Based on both analysis and numerical simulations, we filed a patent application for the OFVC with the U.S. patent office (SD-8192). The goal is to collect and concentrate into a microliter of fluid bioaerosol particles (1.5 to 5.0 microns) from a flow of 10 to 20 liters per minute of collected air. A miniature, low-pressure-drop, battery-powered device is desired. This range of particle sizes covers typical BW agents.

We completed numerical fluid/particle simulations (using the commercial flow solver FIDAP 7.60, Fluent International) of several 2-D OFVC designs. The simulations show that 2-D OFVC devices should provide significant particle concentration along the plane of symmetry for particle diameters in the range of 1 to 5 microns. We found particle behavior to be in very good agreement with analytic predictions. The simulation results have interesting implications for micromachined

Sandia hopes to develop a miniature bioaerosol concentrator capable of collecting biological warfare (BW) agent from bioaerosols as diffuse as one pathogen particle per liter of air....The microseparator we are developing achieves inertial separation and concentration by employing the Opposed-Flow Virtual Cyclone (OFVC) geometry invented by Sandia, in part in response to the performance requirements of this project.

devices; smaller devices concentrate particles at lower gas velocities and lower pressure drop.

We constructed an OFVC test device based on a 400-micron throat width. The test device is modular so various inlet widths can be tested. We are performing characterization experiments with monodisperse particles generated by a TSI Vibrating Orifice Aerosol Generator. We are measuring particle transport through the OFVC with an aerodynamic particle sizer, which allows independent verification of particle size and concentration.

We developed a preliminary engineering design for the microseparator portion of our miniature bioaerosol concentrator. The microseparator has a one-inch-square footprint and can pass a flow of 10 to 20 liters per minute of collected air.

The microseparator locates the fluid-filled collection microchannels of the microimpinger portion of our bioaerosol concentrator. Preliminary modeling suggests that microimpinger channel depth must be at least 100–150 microns. Tall, narrow channels minimize fluid volume and fluid evaporation. Because we propose to move fluids through the microimpinger via EK flow, glass is a preferred material, but high-aspect-ratio microchannels cannot be etched into ordinary glasses. Alternatively, silicon (Si) microchannels produced using the Bosch deep-etching process require very thick (1 to 5 microns) coatings of dielectric if they are to stand off the high voltages employed in EK flow. To date, all Si devices have proven inadequate. We are therefore investigating Foturan, a special photolithographically processable glass, as the microimpinger material. We demonstrated microchannel etching, through-via etching, and thermal diffusion bond sealing. Evaluation of EK performance remains to be investigated. We completed the preliminary design of several variants of an EK fluid-flow microimpinger.

We also ran tests to determine whether laser detection of particle scattering could be used for real-time characterization of collected particles in fluid microchannels. Excessive light scattering by microchannel walls seems to preclude this approach. Alternatively, we are investigating the use of the Coulter principle for particle characterization in fluid microchannels. This principle, also called the *electrical sensing zone method*, measures changes in overall resistivity as particles displace electrolyte in flow through short, tiny orifices. The technique appears potentially promising.

3516210000

Recognizing Partially Obscured Targets by Combining Multiple Data Sources Using Evidential Reasoning

M. W. Koch, J. S. Salazar, M. M. Moya, D. A. Yocky

Military commanders in the battlefield need accurate and reliable target information. Yet any single sensor has limited detection capability and inherent sensitivities to some false targets. Multiple sensors, particularly those with different sensing modalities, can provide complementary target information. However, even small increases in the amount of sensor data can quickly overwhelm a human analyst. Automating the target recognition process, by combining data from multiple sensors to produce a single likelihood for each target's existence/location, can assist analysts in identifying significant threats.

Sensor evidence is typically uncertain; it allows for multiple interpretations, which can be incomplete and/or conflicting. Because of these characteristics, we combine evidence from multiple sensors using an evidential reasoning engine. First, we extract evidence from the different sensors by applying image-processing and pattern recognition (PR) algorithms to identify target subparts or chunks. Each of these feature-level chunk detectors functions as a separate knowledge source that provides evidence to the reasoning engine. Since Sandia can tailor the algorithms to exploit each sensor's unique characteristics, we maximize the relevance of each sensor's information.

The reasoning engine represents its knowledge of the target as multiple-level frames of discernment, where each sensor target template consists of a spatially registered combination of chunks. It updates evidence for the presence of target templates based on information from individual chunks. Thus, the evidential reasoning engine provides a formalized methodology for combining incomplete and uncertain evidence from feature-level sensor chunks to allow recognition of partially obscured targets.

We developed an evidential reasoning engine that combines evidence from multiple synthetic aperture radar (SAR) template subparts (chunks). We extended Random Sample Consensus (RANSAC) to estimate the template parameters of attenuation-compensation and position. Probabilistic analysis of the RANSAC approach revealed that occlusions not only

Since Sandia can tailor the algorithms to exploit each sensor's unique characteristics, we maximize the relevance of each sensor's information.

reduce the amount of information, but also the uniqueness of the remaining information. This RANSAC analysis helped us to determine the optimal chunk size and conclude that improving obscuration performance requires multiple independent data sources and higher spatial resolutions. Using actual SAR target and clutter data, we determined the detection and false alarm rates for the chunky evidential reasoning algorithm. For partially obscured SCUDs, these results indicate slightly better performance than previous STARLOS (SAR [synthetic aperture radar] Target Recognition and Location System) work and are significant because they will combine directly with the multispectral (MS) results.

For the 12-channel MS datasets, we used the first ten channels, which span the visible to short-wave infrared (0.42–2.35 microns). We also removed atmospheric effects using calibration panels, corrected cross-track intensity gradients, and registered the data onto a Universal Transverse Mercator (UTM) grid for geometric distortion correction. We developed focus of attention (FOA) algorithms for both SAR and MS data. The FOA algorithms use thresholds and morphology to discriminate targets by size and intensity. The MS FOA first applies a matched filter to detect T62 tank material and to compress the data from 12 bands to 1 band. The SAR FOA detects partially obscured T62 and SCUD targets. We analyzed the SAR SCUD FOA to quantify the uncertainty in position and aspect angle estimates. We implemented constrained spectral unmixing algorithm for MS subpixel materials classification.

Other Communications

Koch, M. W., J. S. Salazar, M. M. Moya, and D. A. Yocky. 1999. "Recognizing Partially Obscured Targets by Combining Multiple Data Sources Using Evidential Reasoning." Presentation at meeting with Lt. Col. Susan Durham, National Reconnaissance Office, Albuquerque, NM, 18 August.

Koch, M. W., J. S. Salazar, M. M. Moya, and D. A. Yocky. 1999. "Recognizing Partially Obscured Targets by Combining Multiple Data Sources Using Evidential Reasoning." Presentation at meeting with Troy Hayes and Rodney Downie, Albuquerque, NM, 25 August.

Using actual SAR target and clutter data, we determined the detection and false alarm rates for the chunky evidential reasoning algorithm. For partially obscured SCUDs, these results indicate slightly better performance than previous STARLOS (SAR [synthetic aperture radar] Target Recognition and Location System) work and are significant because they will combine directly with the multispectral (MS) results.

3516220000

Computational Engineering of Sensor Materials and Integration with a Novel Biological Weapon Detection System

D. C. Roe, J. S. Schoeniger, S. Istrail

This project will develop the computational tools to efficiently design combinatorial peptides (CPs) for use as sensor materials in the detection of bioagents. A necessary step in sensor design is to discover a material that binds and molecularly recognizes a target biomolecule. CPs are a new class of molecular recognition materials (MRMs), based on small molecules that can be engineered to bind tightly and specifically to a target analyte. They have a significant advantage over antibodies and enzymes in that they are much more rugged, cheaper, and more versatile. However, identifying highly selective CPs can be time-consuming, since potentially 10^{12} CPs may be possible, but only 10^5 compounds can be tested at a time. Sandia will use computational modeling of molecular recognition to develop a unique software algorithm, shuffle-and-screen, that will greatly enhance the efficiency of the sorting process to discover highly select CPs. In our approach, CP MRMs will be generated in a simplified three-step process. First, we use bead synthesis to create and evaluate an initial set of CPs specific for a target analyte. Second, we will apply a novel CMR “shuffle-and-screen” algorithm to abstract the key interaction properties of the most promising candidates of the initial bead synthesis, and search a “virtual library” of all possible CPs, for ones containing those recognition features, and thus may have improved detection properties. Third, we will generate and test these designed CPs in a second bead assay. The final result will be CPs that are highly selective for a target analyte. The successful completion of this project will have several important impacts. The methodology developed will enable rapid generation for a broad range of other biological weapon (BW) targets. The computational methods developed will be generally useful tools for all areas of molecular recognition.

- *Improvements to the shuffle-and-screen algorithm.* The shuffle-and-screen algorithm examines a combinatorial set of compounds and analyzes the key molecular recognition features of the top binders from an initial bead assay. It searches through a virtual library of all possible CPs for ones that contain the same molecular binding features and therefore

Sandia will use computational modeling of molecular recognition to develop a unique software algorithm, shuffle-and-screen, that will greatly enhance the efficiency of the sorting process to discover highly select CPs...The methodology developed will enable rapid generation for a broad range of other biological weapon (BW) targets. The computational methods developed will be generally useful tools for all areas of molecular recognition.

have improved detection properties. The initial algorithm looked at a 2-D topological index called the *Wiener index*. Examining a test library of 1015 compounds, this algorithm can speed the calculation from approximately 37 years to exhaustively examine all compounds to less than one day. We made the following three improvements to the algorithm. First, we expanded our algorithm to look at any 2-D topological descriptor rather than only the Wiener index. Second, we expanded from atom-pair-based descriptors to triplets of atoms. Triplets add significantly to the calculation time, but by using our fast shuffle-and-screen to examine 2-D atom-pairs as a pre-filter, we can reduce the dataset to about 2% of the original before the time-consuming triplet calculation. Third, we developed an algorithm to examine compound scores from the shuffle-and-screen algorithm and choose the appropriate combinatorial subset, as opposed to maximum scoring compounds whose members may not make up a combinatorial set, for a second-generation library.

- *Secondary screen of ovalbumin CPs.* We collaborated with North Carolina State University to (1) complete secondary screen of CPs that bind to ovalbumin in primary assay; (2) complete a secondary screen of CPs that bind to alpha-1-protease, a structurally related protein, for structure/function analysis; (3) test a second-generation library of CPs for ovalbumin; and (4) test a primary library of CPs for SEB (*Staphylococcal enterotoxin B*).

We continued the primary testing of CPs in a bead assay for binding to ovalbumin. We performed the primary bead assay on a random library of CPs on a Tentagel resin and ran it in high-salt conditions to minimize discovery of nonspecific electrostatic binders. To test the binding specific to ovalbumin, we performed blocking tests with 1% casein, 1% casein plus *E. coli lysate*, and *E. coli lysate*. A full-scale screen resulted in 16 beads initially identified as binding to ovalbumin, which we sent for sequencing and then analyzed.

We performed a secondary screen on six of the CPs, based on cursory evaluation of possible consensus motifs and qualitative assessment of binding based on signal strength from the autoradiography films. We resynthesized these peptides on resin for confirmation of binding in a secondary screen. Of the six retested, four showed significant binding to ovalbumin. We determined complete binding isotherms for those sequences, and the resulting four sequences, along with their binding, are shown below:

Triplets add significantly to the calculation time, but by using our fast shuffle-and-screen to examine 2-D atom-pairs as a pre-filter, we can reduce the dataset to about 2% of the original before the time-consuming triplet calculation.

Combinatorial Peptide Density (mmol/g) on resin K (M-1)

Ile-Leu-Phe-His-Asn-Ala $160.01.35 \times 10^5$

Ile-Leu-Leu-Ala-Phe-His $192.09.43 \times 10^4$

Asn-His-Ala-His-Trp-Pro $177.11.85 \times 10^4$

Glu-His-His-Tyr-Tyr-Ala $120.62.74 \times 10^4$

We are now resynthesizing the remaining eight CPs identified in the primary bead assay and will perform secondary screening and binding isotherms on these compounds.

We ordered the four sequences verified by secondary screening and will use them as material for separation channels specific for ovalbumin (as a toxin surrogate). We are developing a second-generation library of improved peptides predicted by the shuffle-screen algorithm.

- *SEB binding*. We completed the primary assay and are continuing the secondary assay. We identified and sequenced fifteen peptides (many homologous) and are testing them for specific binding using blocking studies.

We are developing a second-generation library of improved peptides predicted by the shuffle-screen algorithm.

Other Communications

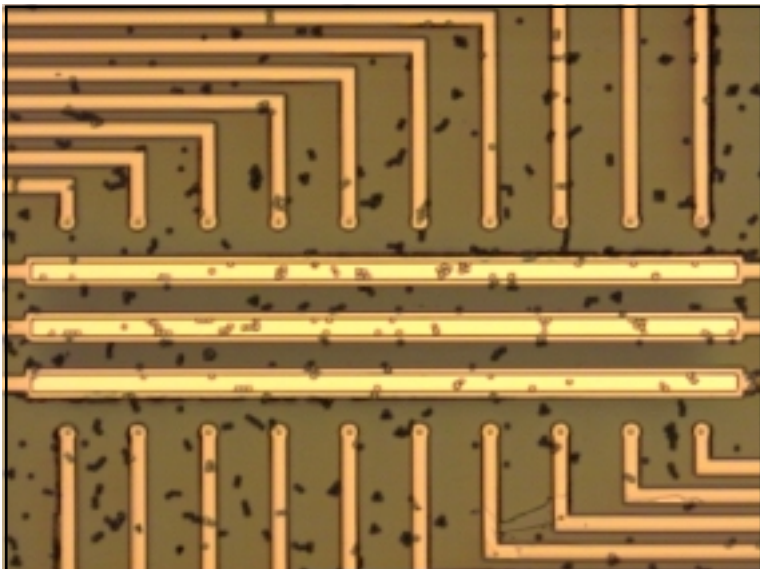
Istrail, S., D. Roe, and B. Walenz. 1999. "Algorithms for Molecular Recognition: Inverse Problems in Combinatorial Chemistry and Classification of Protein Folds." Presentation to Optimization in Computational Chemistry and Molecular Biology, Princeton, NJ, May.

3516230000

Biological Weapon Detector Using Bioaffinity Array Impedance Analysis with Chemical Amplification Through Redox Recycling

A. W. Flounders, S. M. Brozik, D. D. Chu, S. H. Kravitz, R. C. Hughes, K. Wally, J. S. Schoeniger, R. P. Janek

Sandia will develop a novel structure for ultra-sensitive detection (1 particle per liter of air) of biological warfare (BW) agents, e.g., anthrax, to the sensor prototype stage. Surface-attached specific affinity components (antibodies, combinatorial peptides [CPs], or glycolipids) will capture a particle on one element of a microelectrode array monitored via impedance analysis transduction, chemically amplified through disruption of redox recycling. We monitored Faradaic impedance using a reversible redox couple (e.g., $\text{Fe}[(\text{CN})_6]^{3-/4-}$) recycled between its oxidation states by each microelectrode and a shared counter electrode. Capture of a single pathogen blocked one microelectrode, disrupting the redox cycle at that electrode. An array of pathogen-sized, individually monitored, small-area ($2 \times 2 \mu\text{m}^2$) microelectrodes enables single-particle detection. Many identically coated array elements (100s–1000) covering one surface of the flow cell enhances the probability of single-particle capture and provides interferant discrimination by spatio-temporal tracking of the capture/release of each particle traversing the cell. Small capture area is key to single-particle detection; a multi-element array is key to rapid response, realistic sample volume, and improved discrimination.



Sandia will develop a novel structure for ultra-sensitive detection (1 particle per liter of air) of biological warfare (BW) agents, e.g., anthrax, to the sensor prototype stage.

A photograph of a completed electrode array installed in the flow cell and bathed with a solution of 4.6 micrometer latex spheres. Only those spheres in the focal plane of the image are in focus.

We developed a conceptual design for integration of a microelectrode structure with a CCD readout system. We designed and fabricated a liquid flow cell with a transparent window to enable visual confirmation of particle capture. We completed three fabrication runs of the microelectrode array process flow. We measured redox-controlled currents with these microelectrode arrays to characterize anticipated redox currents. Results indicate that the microelectrode currents are more than sufficient for CCD charge binning; initial currents are in the nanoamp range. We fabricated and tested a capacitor test system. We used redox-generated currents for capacitor charging, and as the capacitor charged, the collector electrode current decreased to zero as expected. The goal is to now read out the charge accrued at each microelectrode-linked capacitor during each sampling period.

We deleted evaluation of additional bioaffinity coatings on macroelectrodes. We modified our initially proposed structure from an affinity-coated electrode to a nonmodified electrode surrounded by affinity capture material immobilized to insulator. Therefore, additional testing with macroelectrode structures is no longer appropriate. We replaced this task with the much more critical demonstration of discriminatory particle capture with the microelectrode system and are still working to demonstrate discriminatory particle capture. This task is delayed because of the need to resolve preferred ionic concentration (micromolar) for electrophoretic particle movement with preferred redox species concentration (millimolar) for current measurement. We are setting up a dual solution flow cell system to resolve this issue.

3516240000

ATR/Exploitation Utilizing Ultra-High-Resolution, Complex SAR Imaging

D. W. Harmony, M. R. Nissen, W. J. Bow

The goal of this project is to develop novel automatic target recognition (ATR) and exploitation techniques utilizing ultra-high-resolution as well as complex (magnitude, phase) synthetic aperture radar (SAR) imagery. Current ATR techniques utilize classification metrics applied only to high-resolution magnitude images. Sandia will research and develop new classification metrics and algorithms designed to take advantage of the increased information content of the complex and ultra-high-resolution SAR imagery. Analyses show that significant increases in the number of resolved scatterers as well as improvements in the ability to localize them are necessary before the ATR can successfully handle the extended operating conditions of partial obscuration, articulation, camouflage, etc. This is particularly true for small tactical targets where the number of image resolution elements on target is limited. Our research will provide these needed improvements and then some. Not only will we take advantage of the enhanced information content coming from increased signature bandwidth, but this improved resolution also will now separate the underlying scatters enough to allow us to utilize the additional information carried in the phase of the complex image pixels. We believe, from a system perspective, that our combination of sensor resolution enhancements coupled with new complex-image ATR algorithms will significantly outperform other approaches.

We completed a large ultra-high-resolution SAR data collection in which we collected more than 3000 images, including approximately 70 km² of clutter. The five military vehicles in this year's data collection included two different models of T72 tanks, two SCUD missile launchers, and one T62 tank. In addition to baseline configurations, we performed vehicle articulations (e.g., turrets rotated, missiles raised) to provide data for testing the robustness of algorithms under development.

We considered several algorithms for exploiting phase. These include subaperture processing, unwrapped phase residues, phase curvature under peaks, and coherent change detection (CoCD)-based approaches. Presently, we are aggressively pursuing a CoCD technique since it shows the

Sandia will research and develop new classification metrics and algorithms designed to take advantage of the increased information content of the complex and ultra-high-resolution SAR imagery....our combination of sensor resolution enhancements coupled with new complex-image ATR algorithms will significantly outperform other approaches.

most promise. The method first creates a complex target template from the phase and magnitude data. We then compare unknown chips to the template using a CoCD match metric that identifies coherent points between the unknown chip and the template. The number of coherent points between the chip and template determines whether or not the chip contains the target. Preliminary testing shows that the algorithm is reasonably robust and can identify different vehicles of the same type while maintaining a low false-alarm rate (FAR).

Preliminary testing shows that the algorithm is reasonably robust and can identify different vehicles of the same type while maintaining a low false-alarm rate (FAR).

3516250000

Thin-Skin Deployable Mirrors for Remote Sensing Systems

T. D. Henson, J. W. Martin, J. C. Wehlburg, R. J. Blake, J. M. Redmond

In support of the DOE nonproliferation mission, Sandia is investigating the use of large ultra-lightweight deployable mirrors for remote sensing systems. The ultimate limitation in obtainable resolution and sensitivity for space-based imaging systems is the size of the optical collecting aperture. Large collecting apertures are at odds with maintaining low launch costs and with current launch vehicle configurations. Development of a deployable mirror is one approach being considered to satisfy these conflicting requirements.

The focus of this project is to develop fundamental technology toward the realization of deployable piezoelectric thin-film mirrors. A bimorph layer of film will bend in response to an applied electric field and can therefore be deformed into desirable shapes using a scanning electron gun. Surface curvature measurements govern the electron-gun scanning strategy, yielding distributed shape corrections.

We made significant progress toward the development of fundamental technology that will enable deployable thin-skin mirrors for remote sensing systems. The key areas of accomplishments are mirror concept development, mirror figure sensing methods, shape-control algorithm development, electron-gun excitation, experimental test-bed development, and space implementation assessments.

We completed an extensive literature search to study the various types of large, ultra-lightweight, deployable mirror systems and their shape-control methods. We determined that a deployable piezoelectric bimorph mirror whose shape is controlled remotely via electron-gun excitation holds the most promise for meeting the long-term aerial density goals of less than 1 kg/m².

The ability to accurately assess mirror figure on orbit is key to achieving an optical quality surface from a deployable mirror. We can obtain low-resolution measurements suitable for coarse shape corrections and laboratory-based electron-gun development by using Sandia's Multi-beam Optical Stress Sensor (MOSS) system and a Keyence LK-2500 Series CCD (charge-coupled device) Laser Displacement Sensor.

The focus of this project is to develop fundamental technology toward the realization of deployable piezoelectric thin-film mirrors.



A highly curved piezoelectric thin-film bimorph mirror inside a vacuum tank. This type of mirror has applications on space-based or other remote sensing systems.

However, we will ultimately require high-resolution mirror figure sensing systems. Traditional optical sensors such as interferometers lack the dynamic range needed for this application. We are therefore utilizing three nontraditional interferometric techniques to measure the mirror surface profile. The first is a differential measuring interferometer. The second is electronic speckle pattern interferometry. The third is multiwavelength heterodyne interferometry, which was developed in collaboration with the Air Force Research Laboratory (AFRL).

Progress in shape-control algorithms progressed through finite-element modeling (FEM) of the bimorph mirrors. We used measured surface curvature errors to produce a corrective excitation profile. We also developed a 2-D shape-control algorithm. The development of a bimorph whose layers exhibit preferential deformation, coupled with independent excitation of the two layers, provides the necessary control authority to correct arbitrary 2-D deformations. We implemented the algorithm on an FEM and showed it to achieve the desired profile. We filed a technical advance disclosure for 2-D shape correction of a bimorph mirror through electron-gun excitation, SD-6496/S-93,738.

Interactions between the electron gun and the piezoelectric bimorph mirror have been extensively studied. This knowledge aids us in producing direct curvature adjustments of the bimorph mirror with electron-gun excitation. The electron-gun approach, as opposed to the traditional electrode approach to controlling bimorph materials, gives us the ability to deliver minute charge packets to discreet areas on the bimorph mirror, greatly improving the spatial resolution of the curvature adjustment.

Sandia developed an electron-gun/vacuum chamber test-bed to validate the shape-control algorithms and the electron-gun excitation parameters as well as to aid in determining the achievable optical quality of an electron-gun-controlled bimorph mirror. The test-bed includes a vacuum system, electron gun, bimorph mirrors, electron-gun control system, shape-control algorithms, and a variety of optical sensors. We wrote lab view programs to control the electron-gun excitation of the piezoelectric bimorph mirrors. Beam size, energy, and beam position are all precisely controlled. We completed electron-gun calibrations. Realization of general mirror shape correction requires additional research in converting top and bottom surface excitation profiles into electron-gun control parameters such as beam power and dwell time.

Sandia developed an electron-gun/vacuum chamber test-bed to validate the shape-control algorithms and the electron-gun excitation parameters as well as to aid in determining the achievable optical quality of an electron-gun-controlled bimorph mirror.

We are studying critical implementation issues of deployable electron-gun-controlled mirrors in space-based remote sensing systems as part of an overall feasibility assessment. We chose the piezoelectric mirror material and examined mirror folding and deployment methods. We considered issues involving operation of the electron gun in space. We discovered no show-stoppers at this time.

Refereed

Martin, J. W., J. A. Main, and G. C. Nelson. 1999. "Development of a Test-Bed for Evaluating Electron Gun Shape Correction of Distributed Structures." *1999 AMSE Internat. Mechanical Engineering Congress and Exposition*, accepted.

Redmond, J. M., P. S. Barney, T. D. Henson, J. A. Main, and J. W. Martin. 1999. "Distributed Sensing and Shape Control of Piezoelectric Bimorph Mirrors." *1999 ASME Internat. Mechanical Engineering Congress and Exposition*, accepted.

Other Communications

Henson, T. D. 1999. "Thin-Skin Deployable Mirrors for Remote Sensing Systems." Presentation to a joint meeting between Sandia and AFRL, Albuquerque, NM, 19 May.

Henson, T. D. 1998. "Thin-Skin Deployable Mirrors for Remote Sensing Systems." Presentation to the DOE Annual LDRD Review, Albuquerque, NM, 26 August.

Main, J. A., J. W. Martin, and G. C. Nelson. 1999. "Noncontact Shape Control of Membrane Mirrors." Presentation to the NASA Ultra-Lightweight Space Optics Challenge Workshop, Napa, CA, 24–25 March.

3516260000

Dispersible Granular Sensor (Smart Sand) for Landmine Detection Based on TNT Immunoassay

C. J. Brinker, B. G. Hance, C. S. Ashley, J. S. Schoeniger, A. K. Singh

Approximately 100 million unexploded landmines currently exist worldwide. There exists a need for remote sensing technology capable of rapidly screening large areas for the presence of mines or other unexploded ordnance (UXO). Sandia continued efforts to develop enzyme-based granular sensors combining sample preconcentration, molecular recognition, amplification, and optical transduction all in a grain of sand. Our strategy is a sensor that is dispersed by air with each granule capable of performing a 2,4,6-trinitrotoluene (TNT) immunoassay of its local environment. A luminescent signature is included to allow remote imaging of UXO locations.

We directed work on our distributed granular sensor system toward the detection of TNT, since this compound is a major component of landmines and UXO. Briefly, the overall performance of the envisioned sensor system depends on the following components: (1) sufficient mass transfer of the analyte (TNT) from ambient environment into the pores of the silica host, (2) TNT molecular recognition via binding to TNT antibodies, and (3) chemical amplification of the recognition event through coupling of the immunoassay step to enzyme-catalyzed dye production. Accomplishments are summarized here.

(1) Our collaborators at UCLA demonstrated antibody-TNT-conjugate versus antibody-TNT competitive binding in gel host matrices. They showed TNT antibodies incorporated in silica sol-gel matrices to maintain molecular recognition capabilities, as demonstrated by a competitive immunoassay performed using antibodies prebound to TNT labeled with a fluorescent dye (fluorescein). As the sol-gel host materials were immersed in liquid containing unlabeled TNT, the fluorescence signal decreased as TNT-fluorescein was displaced by its unlabeled analogue.

(2) For the sensor particles to function effectively for trace detection of TNT in minefield environments, the particle matrix must absorb the signature compound from the ambient. Studies of the environmental fate and transport of TNT indicate

Sandia continued efforts to develop enzyme-based granular sensors combining sample preconcentration, molecular recognition, amplification, and optical transduction all in a grain of sand.

that the majority of the analyte is adsorbed on soil particles under minefield conditions, but that the principal mechanism for transport of nitroaromatic compounds through soils is through the aqueous phase following precipitation.

Accordingly, we measured the equilibrium distribution coefficient (K_d) for partitioning between the aqueous dissolved phase and the adsorbed phase, for TNT adsorbed on natural soils and on sol-gel-prepared porous silica host particles. We evaluated three sol-gel materials: an uncoated silica gel, a trichloromethylsiloxane (TCMS)-coated gel, and a hexamethyldisilazane (HMDS)-coated gel. We measured the dimensionless K_d values $[(g \text{ TNT}/g \text{ H}_2\text{O})/(g \text{ TNT}/g \text{ gel absorber})]$ by allowing a series of aqueous solutions of different concentrations to come to equilibrium with preweighed amounts of the solid absorbers. We measured the resulting solution concentrations by high-performance liquid chromatography (HPLC). The partition coefficients for the uncoated gel and the HMDS coated gel were approximately 8, while the coefficient for the TCMS coated gel was found to be approximately 16. As a comparison, the literature values for the partition coefficient of TNT in soils range from 4 to 10. This indicates that the TCMS gel should offer a modest preconcentration of TNT if mixed with typical soils under conditions where aqueous transport dominates the movement of TNT in the environment.

(3) We demonstrated the use of a conjugated enzyme in an antibody-modified enzyme activity immunoassay for TNT using an enzyme-amplified TNT homogeneous immunoassay. This assay depends on the use of an enzyme-analyte conjugate that is highly catalytically active in the unbound state; however, when an antibody against the analyte binds to the analyte-enzyme conjugate, the activity of the enzyme decreases due to steric hindrance of the active site in the enzyme by the presence of a bulky antibody molecule. This scheme requires that the analyte be bound very closely to the active site of the enzyme during the analyte-enzyme conjugation reaction. We conjugated trinitrobenzene (TNB), a molecule similar to TNT, with several candidate enzymes. We achieved the greatest success, i.e., the largest difference in catalytic activity between bound antibody-TNB-enzyme and unbound TNB-enzyme, using glucose-6-phosphate dehydrogenase (G6PDH). We detected TNB using this enzyme by measuring adsorbance of a reaction product from G6PDH catalysis: protonated nicotinamide adenine dinucleotide (NADH). NADH is a very inefficient fluorophore with an impractically short maximum

excitation wavelength (340 nm); thus we developed a new strategy to produce a fluorescent, rather than absorptive, dye in the enzyme-catalyzed TNT assay. Linkage of G6PDH catalysis with horseradish peroxidase will result in fluorescent dye production and allow enhanced detection.

Refereed

Bhatia, R. B., K. Butler, C. J. Brinker, and C. S. Ashley. 1999. "Bio-Inorganic Composites for Sensor Applications." Paper presented to the Materials Research Society Spring Meeting, San Francisco, CA, 5–9 April.

Singh, A. K., A. Gupta, A. Mulchandani, W. Chen, R. B. Bhatia, J. S. Schoeniger, C. S. Ashley, and C. J. Brinker. 1999. "Encapsulation of Enzymes and Cells in Sol-Gel Matrices for Biosensor Applications." *Proc. Internat. Society for Optical Engineering (SPIE)* **3858** (December) (SPIE Advanced Materials and Optical Systems for Chemical and Biological Detection, Boston, MA, 19–22 September).

Other

Brinker, C. J., and C. S. Ashley. 1999. "Aerogels for Enhanced Detection and Collection of BW/CW/UXO." Presentation to the DARPA Biological Detection Conference, Santa Fe, NM, 27–30 April.

Brinker, C. J., C. S. Ashley, R. B. Bhatia, K. Butler, and T. Harris. 1999. "Synthesis of Bio-Inorganic Composites Using an Aqueous Route for Sensor Applications." Paper presented to the 217th Annual Meeting of the American Chemical Society, Anaheim, CA, 21–25 March.

Simonson, R. J. 1999. "Distributed Chemical Sensor Particles for Remote Optical Detection of Landmines." Presentation to Dr. Jeff Marqusee, Technical Director, U.S. DoD Strategic Environmental Research and Development Program (SERDP), Albuquerque, NM, 2 February.

Simonson, R. J. 1999. "Distributed Chemical Sensor Particles for Remote Optical Detection of Landmines." Presentation to Norwegian Defense Research Establishment (FOA) representatives, Albuquerque, NM, 16 February.

Simonson, R. J. 1999. "Distributed Chemical Sensor Particles for Remote Optical Detection of Landmines." Presentation to Rafael Rodriguez, Defense Department Manager, GTD, Barcelona, Spain, Albuquerque, NM, 3 May.

Simonson, R. J. 1999. "Distributed Chemical Sensor Particles for Remote Optical Detection of Landmines." Presentation to the U.S. State Department Arms Control and Nonproliferation Advisory Board, Albuquerque, NM, 14 July.

Simonson, R. J. 1999. "Distributed Chemical Sensor Particles for Remote Optical Detection of Landmines." Presentation to U.S. Army Training and Doctrine Command (TRADOC) representatives, Albuquerque, NM, 2 March.

3516270000

Characterization of Underground Facilities in an Urban Environment

M. D. Ladd, C. W. Sicking, T. S. McDonald, H. D. Garbin, J. P. Claassen, G. J. Elbring, D. L. Faucett, G. E. Sleaf

It is well known that rogue nations are concealing facilities for the manufacture and storage of weapons of mass destruction (WMD) by placing them in urban areas. The ability to characterize and monitor these facilities is recognized as an important national concern. Because of the multisource and high-noise nature of urban environments, such sites pose special challenges for unattended sensors. The intent of this project is to develop and apply novel adaptive signal-processing methods and sensor deployment configurations to permit the characterization of concealed facilities in an urban environment. In particular, Sandia will explore seismic monitoring from adjacent building basements, subway tunnels, and sewer systems, and, to a lesser extent, monitor vibrations in plumbing, air-handling ducts, and windows of a suspect facility. Characterization of the source vibrations and the use of advanced signal-processing techniques such as the application of adaptive array techniques to cancel out noise signals based on source location will be required. In addition to algorithmic development, we will establish factors affecting sensor fidelity such as timing accuracy and separation tolerances in deployment layouts. We will study novel deployment strategies, including the use of 3-D seismic arrays, in neighboring buildings. To validate the algorithms, we will perform simulations and process recorder data collected at an urban site. While current programs address the non-urban, 2-D monitoring domain, the system being developed in this project provides a totally new capability for the urban environment. This project directly addresses the critical need for characterization in urban multisource environments.

We created a seismic model and synthetic dataset with multiple sources from a seismic model. We also assessed the characteristics of the earth's propagation environment in light of the urban environment and evaluated the impact of that environment on array design and processing. We designed a 3-D array to overcome the effect of limited spatial coherence, multipath, mode conversion, multipolarized emissions, and partially coherent simultaneous arrivals. These effects are significantly different from those encountered in typical array-

Sandia will explore seismic monitoring from adjacent building basements, subway tunnels, and sewer systems, and, to a lesser extent, monitor vibrations in plumbing, air-handling ducts, and windows of a suspect facility....While current programs address the non-urban, 2-D monitoring domain, the system being developed in this project provides a totally new capability for the urban environment. This project directly addresses the critical need for characterization in urban multisource environments.

processing applications. We developed a complex observational model that accounts for these effects and used it to evaluate the array design. We used a 3-D cube array design composed of multiple symmetric subarrays of three component sensors to effectively focus on a selected emitter while attenuating the emission of unwanted sources. We developed software to perform searches accounting for polarization using the 3-D array and completed the software to estimate the covariance matrix that forms the basis of the adaptive beam former. Single-source simulation results indicate that the design provides better angular resolution and improved discrimination against competing propagation modes. We identified high-resolution methods of mapping the field of coherent emitters and will combine them with an adaptive noise-canceling beam former method for continuously monitoring the source.

Other Communications

Claassen, J. P., M. D. Ladd, and G. J. Elbring. 1999. "The Feasibility of Monitoring Continuous Wave Sources with Seismic Arrays." *Proc. SPIE, Unattended Ground Sensor Technologies and Applications* **3713** (SPIE AeroSense, Orlando, FL, 5–9 April): 22–32.

3516280000

Dexterous Robotic Manipulation of Hazardous Materials in Unstructured Environments

S. G. Kaufman, C. S. Loucks, T. S. Gladwell, E. A. Mitchell, R. J. Anderson, D. M. Kozlowski

Sandia proposes to develop and demonstrate a mobile remote manipulation system capable of acquiring, examining, and manipulating explosive devices in unstructured environments. The technology need stems from the ever-increasing number of encounters with unexploded ordnance (UXO), such as munitions left on firing ranges, mines left on battlefields, and improvised explosive devices left by terrorists.

The two scientific motivations for constructing such a system are determining how useful laboratory-tested sensing and control technologies are when actually deployed into the field, and determining how they may best be integrated. The first advances the state-of-the-art in the component technologies by establishing limits on their practical use and flaws in accepted problem definitions. The second also establishes limits on the component technologies that allow them to successfully coexist with one another. This knowledge increases the chances of successful transition of the technologies to the field.

The system to be built will be teleoperated, but with some built-in autonomy to lessen the burden on the operator. This autonomy will be in the form of automatic planning of manipulator motions required to grasp an object or perform an operation at a location designated by the operator. Teleoperation will include high-bandwidth force feedback and control responses, which will be enabled by using parallel manipulation mechanisms. By mounting the manipulator on a simple, stiff gross positioning device, in turn mounted on a mobile vehicle, the system will be capable of performing tasks such as opening unlocked doors and going through them, drilling holes, inserting inspection devices, and unscrewing fuzes.

- *Problem and task identification.* We chose the general area of analyzing and manipulating improvised explosive devices. We made this choice for three reasons. First, the ability to robotically manipulate such devices is an unmet requirement of military and law enforcement agencies, as evidenced by FBI and Navy funding of projects with less ambitious goals than ours. Second, technologies developed to

Sandia proposes to develop and demonstrate a mobile remote manipulation system capable of acquiring, examining, and manipulating explosive devices in unstructured environments....The system to be built will be teleoperated, but with some built-in autonomy to lessen the burden on the operator.

meet these requirements can be readily applied to ARG needs for delicate manipulation of material at accident sites. Finally, this area is a rich source of unsolved technical problems.

Specifically, we chose the following tasks to be performed: open an unlocked car door and examine its interior; open a car trunk and examine its interior; attach a tow rope to a car; place, aim, and arm a disrupter; place an x-ray plate and source to examine suspicious packages; and pick up a suspicious object such as a briefcase or backpack. We will perform all of these tasks with the greatest amount of autonomy possible.

• *Automated planning and programming.* To perform the tasks listed above, the robot must be able to plan its motions to manipulate closed kinematic chains. These are mechanical systems with more than one fixed position, such as a fixed manipulator opening a door with a fixed-hinge axis. Motion-planning algorithms assume that kinematic chains are open. We implemented a planner for closed kinematic chains and demonstrated it with a robot opening a door. The planner allows six degrees of freedom in the manipulator.

• *Manipulator development.* The goal tasks require high-bandwidth force data so that their controllers may make appropriate responses to the changing task dynamics in real time. This requirement can be met with parallel manipulators—those that use a number of small, light actuators simultaneously in contact with the object being manipulated. We have three such manipulators and made the following progress on each:

(1) The Smartee (smart end effector) is a lightweight parallel device. Its original commercial controller is too large to deploy on a mobile vehicle, so we reverse-engineered it to implement on a much smaller controller. We have implemented all the control software for it in the new environment.

(2) The Paradex is a very high precision parallel mechanism. It demonstrated force control at 2.2 kHz bandwidth, well above our original goal of 1 kHz.

(3) The Barrett Hand is a lightweight, three-finger mechanical hand. We characterized its dynamics, which is required for planning and controlling its use in manipulation.

• *System integration.* The technologies described above must be combined into a single mobile system to meet our goals. After much searching, we identified the base system for initial integration. It is an omnidirectional vehicle equipped with a Mitsubishi PA-10 manipulator. This system is well suited because it saves us the effort to integrate a vehicle and manipulator so we may concentrate on the more difficult control issues. The Mitsubishi arm has sufficient payload

We implemented a planner for closed kinematic chains and demonstrated it with a robot opening a door. The planner allows six degrees of freedom in the manipulator.

capacity to carry the Smartee and the Barrett Hand. It also has sufficient on-board computing power to carry out the required motion planning discussed in the second section. In the coming year, we will assess deploying the same capabilities on the existing High-Mobility Multipurpose Wheeled Vehicle (HMMWV)-based Automated Reliability and Maintainability Measurement System (ARMMS) system, which has two hydraulic manipulators and was developed for ARG use. These hydraulic manipulators will be able to carry the Paradex mechanism.

Refereed

Milgram, R. J., and S. G. Kaufman. 1999.
“Topological Characterization of Safe Coordinated Vehicle Motions.” *Internat. Conf. on Robotics and Automation* (April 2000), submitted.

3516290000

Autonomous Dynamic Soaring Platform for Distributed Mobile Sensor Arrays

M. B. Boslough, L. C. Marron, R. J. Pryor, B. L. Spletzer

Among the greatest practical challenges to the realization of robotic swarms is the relative lack of rapid mobility and the limited power supply associated with currently available autonomous devices. Unmanned airborne vehicles (UAVs) are particularly constrained because they must consume significant power just to stay aloft. This limits the potential feasibility of UAV swarms for most applications unless the individual vehicles can derive energy of locomotion from their local environment. It is theoretically possible for a robotic glider to remain aloft and navigate by dynamic soaring in the shear boundary layer near the Earth's surface or in separation flow on the leeward side of a topographic high.

We made progress in the following areas: (1) development of a robust soaring algorithm for a glider in a neutrally buoyant boundary layer, (2) hardware design and procurement with testing, (3) study of relevant meteorology and assessment of conditions under which autonomous gliders could be expected to fly using both static and dynamic soaring, and (4) identification of an advanced concept to use collective behavior of autonomous glider swarms to use turbulence at the tropopause to stay aloft. Item (2) includes both design, construction, and test flight of our first prototype, and design and construction of an onboard data logger.

In the hardware part of the project, we need various sensing elements to accomplish control of the autonomous sailplane. Examples of the instrumentation needed include heading, attitude, altitude, air speed, vertical speed, position, and the relative wind vector. We purchased additional ground equipment for instrumented flight tests and data acquisition, including radio transmitters, meteorological equipment, and object position tracking equipment. We bought off-the-shelf models of small-scale angular rate sensors, accelerometers, magnetometers, and pressure transducers, and hired an experienced contractor to integrate them with the onboard data logging equipment.

To assess opportunities for dynamic soaring over the continental U.S., we downloaded and plotted hourly meteorological summaries, which include wind vectors fit to real-time data, for several months. This required installation of

Among the greatest practical challenges to the realization of robotic swarms is the relative lack of rapid mobility and the limited power supply associated with currently available autonomous devices.

Test of robust dynamic soaring algorithm with sail planes.



GRADS (Graphics Real-Time Applications Display Support System) software, a meteorological plotting package. We concluded that the variability and magnitude of continental winds—coupled with topographic variability, surface roughness (which deepens the boundary layer), and existence of obstacles—precludes us from making wide use of boundary layer dynamic soaring over land, with rare exceptions. However, there are very special conditions under which both static and dynamic soaring can, in principle, be used to keep a robotic sailplane aloft. Real-time–resolved meteorological data over the world’s oceans were difficult to come by, but we can extract average surface winds from general circulation models, demonstrating that many strategically important areas have conditions that are ideal for boundary layer dynamic soaring. We also identified a potential means of staying aloft near the tropopause under certain conditions. This method would require emergent behavior of soaring agents that communicate with one another.

We selected Parker Mountain, California, as our site for test flights, and successfully flew an uninstrumented flight with our prototype (dubbed the D.S. Beast).

We also identified a potential means of staying aloft near the tropopause under certain conditions. This method would require emergent behavior of soaring agents that communicate with one another.

3516310000

Miniature UV Fluorescence-Based Biological Agent Sensor

K. L. Schroder, A. M. Morales, P. J. Hargis, Jr., M. H. Crawford, K. S. Potter

Sandia will develop miniaturized sources and a spectrometer for ultraviolet (UV)-induced fluorescence detection of biological agents. The sources are UV light-emitting diodes (LEDs) based on the AlGaN (aluminum gallium nitride) family, which has direct optical bandgaps from 364 nm (GaN) to 200 nm (AlN). The wide wavelength range of these materials makes them attractive as compact UV light sources. The miniature spectrometer is based on producing wavelength-selective waveguide channels using photoinduced refractive index changes in photosensitive materials, in either a planar waveguide or an optical fiber geometry. A miniature LIGA (German for lithography, electroforming, molding)-micromachined spectrometer design is a possible backup to the waveguide design. We are fabricating, characterizing, and evaluating devices in biofluorescence measurements.

- **GaN/AlGaN UV LEDs.** Initially we fabricated and packaged 2x2 arrays of LEDs and characterized their optical and electrical properties. We were able to obtain peak emission at 354 nm and an optical output power of 32 mW with a voltage drop of 6.9 V at 40 mA of current. We delivered these devices and used them for biofluorescence measurements.

We then optimized the material growth and device design to improve the output power and electrical characteristics and to generate wavelengths closer to 360 nm. We increased the output power to 39 μ W with a voltage drop of 5.5 V at 40 mA of current and a peak emission wavelength of 357.5 nm. We also delivered these devices for biofluorescence measurements.

The nickel (Ni) top contacts of the above devices transmit only 35%–40% of the UV emission, resulting in significant loss. We developed a new top contact composed of a Ni/Au (gold) multilayer that is subjected to an oxygen (O) environment to convert Ni to NiO, which has a much higher transmission in the UV.

- **Miniature spectrometer.** Photosensitive materials demonstrate a photoinduced change in the base material refractive index, thus enabling optical patterning of refractive index structures in waveguide geometries. Two candidate

Sandia will develop miniaturized sources and a spectrometer for ultraviolet (UV)-induced fluorescence detection of biological agents....We are fabricating, characterizing, and evaluating devices in biofluorescence measurements.

geometries for these waveguides are planar thin films and optical fiber. It was our goal to test the viability of using photosensitive device technology to produce a visible, planar-waveguide miniature spectrometer. We fabricated a number of unique photosensitive planar (thin-film) waveguides using a Sandia-developed RF-sputtering process that produces films demonstrating large, optically induced refractive changes. We evaluated two film geometries: a single photosensitive thin film on a SiO₂ (silicon dioxide) substrate, and a similar sample with an additional low-index overlaid SiO₂ layer on top of the photosensitive layer to reduce optical scattering losses. Losses in the single-film samples ranged from 6 dB/cm to 9 dB/cm at visible wavelengths. By contrast, we greatly reduced optical losses in the overlaid samples, ranging from 1 dB/cm to 6 dB/cm. From the measurements it is clear that the losses in these films cannot be accounted for solely by such scattering loss; additional losses likely arise from optical absorption tails in the wavelength range investigated. The addition of the overlaid resulted in a significant reduction in optical losses but not enough to make the photosensitive thin films ideal candidates for the spectrometer application. We are now pursuing a comparable approach using an optical-fiber geometry. We showed optical fibers doped with germania to demonstrate a strong photosensitive response to UV optical radiation and to have the advantage of very low optical loss figures (1 dB per several kilometers). The device design will be identical to that proposed for the thin-film device and will require changes only in the method of coupling detected light into the spectrometer unit.

• *Biofluorescence measurements.* We made the first-ever biofluorescence measurements with UV LEDs. The broad spectral output of the LEDs made it necessary to filter the LED output with a spectrometer to keep the emission from interfering with biofluorescence signals. Even though the optical imaging arrangement made very poor use of the LED emission, throughput was sufficient to obtain very strong fluorescence signals from microorganisms in solution. We detected the fluorescence with an intensified charge-coupled device (CCD) camera coupled to an imaging spectrometer. We measured fluorescence signals from unwashed *Bacillus thuringiensis* (BT), contaminated with spent culture media, in phosphate-buffered saline solutions at concentrations ranging

We made the first-ever biofluorescence measurements with UV LEDs....We developed a more efficient optical scheme utilizing optical fiber to transport the LED output to the biosample. We expect an order-of-magnitude increase in the biofluorescence signal.

from about 10^7 to 10^9 cells per milliliter. Considering the poor collection efficiency, these initial measurements are very encouraging. We developed a more efficient optical scheme utilizing optical fiber to transport the LED output to the biosample and expect an order-of-magnitude increase in the biofluorescence signal.

We...expect an order-of-magnitude increase in the biofluorescence signal.

3516320000

Automatic Planning of Life-Cycle Assembly Processes

T. L. Calton, E. A. Mitchell, G. A. Laguna, R. R. Peters, R. G. Brown

More effort is expended on upgrade and disposal projects than on clean-slate design. However, commercial computer-aided design (CAD) tools are better suited to initial product design than to the product's full lifecycle. Computer-aided analysis, optimization, and visualization of life-cycle assembly processes based on the product CAD data can help ensure accuracy and reduce effort expended in planning these processes for existing products, as well as provide design-for-lifecycle analysis for new designs. To be effective, computer-aided assembly planning systems must allow users to express the plan selection criteria that apply to their companies and products as well as to the lifecycles of their products.

Designing products for easy assembly and disassembly during its entire lifecycle for purposes including service, field repair, upgrade, and disposal is a process that involves many disciplines. In addition, finding the best solution often involves considering the design as a whole and by considering its intended lifecycle. Different goals and constraints (compared to initial assembly) require revisiting significant fundamental assumptions and methods underlying current assembly planning techniques. Previous work in this area has been limited to either academic studies of issues in assembly planning or applied studies of lifecycle assembly processes, which give no attention to automatic planning. Sandia believes that merging these two areas will result in a much greater ability to design for, optimize, and analyze life-cycle assembly processes.

The original goals of this project emphasized disassembly planning and optimization. We added goals that would capitalize on the Archimedes planning algorithms. The need arose for a computerized planning tool to automate the design of small smart machines and to automate calculations of their manufacturing costs. We hoped that the underlying planning algorithms used in the Archimedes system could be leveraged to develop such a tool.

Our work focused primarily on destructive and nondestructive disassembly algorithmic issues; however, we completed the Design for Lifecycle (DFLC) module and fully integrated the optimizing search algorithm (shortening

Sandia believes that merging these two areas will result in a much greater ability to design for, optimize, and analyze life-cycle assembly processes.

algorithm) and service/upgrade constraint reconcile feature into Archimedes.

In the case of destructive and nondestructive disassembly, we implemented and propagated new actions to the load, save, animate, etc., routines that needed to use them.

We also revised the tools framework. The intent was that the tools, rather than being applied in an arbitrary fashion, be applied in a manner consistent with operations they support. Thus, by specifying that an operation is a weld operation, one specifies/restricts that if a construction tool is applied, it must be a welder, and that if a destruction tool is applied, it must be a cutting torch or similar tool. We prototyped a tentative framework for how tools interact with the various actions for assembly/disassembly and cost analysis, and the specific organization of the revised framework is as follows: Overrides were reduced to completely nonmanufacturing-related issues. That is, contact and collision analysis, faceting parameters, color, and mate overrides, which were once handled as manufacturing issues, are now handled separately. These types of overrides relate specifically to inconsistencies in data due in part to translation issues (as opposed to, e.g., mates requiring user intervention because of intentionally tight/nonexistent tolerances for pressfits). Constraints remained essentially unchanged, except that the REQ_TOOL constraint is now either rendered an anachronism or modified to check action types before allowing use of a particular type of tool. The "Manuf" constraint option picks up the threaded mate/unmate actions, as well as dismantlement operations and any other assembly/disassembly actions not currently listed, which might be added in the future. Specification of manufacturing operations now includes the optional specification of tool applications. A corollary effect of this framework was to make the framework easier to apply assembly/disassembly costs. Archimedes would apply generic assembly and disassembly costs based on the action type, if no other information were available. Now, if a tool selection is available, this framework will refine costs. For better estimates, the user would still be able to provide specific costs for a given operation on two parts.

We prototyped a tentative framework for how tools interact with the various actions for assembly/disassembly and cost analysis....

Refereed

Calton, T. L. 1999. "Advancing Design-for-Assembly: The Next Generation in Assembly Planning." *Proc. 1999 IEEE Internat. Symp. on Assembly and Task Planning 1* (Porto, Portugal, 21–24 July): 57–62.

Calton, T. L., and R. G. Brown. 1999. "An Optimizing Algorithm for Automating Lifecycle Assembly Processes." *J. Artificial Intelligence in Engineering Design and Manufacturing*, special issue sponsored by AAAI SIGMAN, Philadelphia, PA.

Calton, T. L., and R. R. Peters. 1999. "A Framework for Automating Cost Estimates in Assembly Planning." *Proc. 1999 IEEE Internat. Symp. on Assembly and Task Planning 1* (Porto, Portugal, 21–24 July): 100–105.

Calton, T. L., and R. R. Peters. 1999. "Automatic Planning of Life Cycle Assembly Processes." Sandia Technical Report SAND99-2808, Sandia National Laboratories, Albuquerque, NM, November.

Other Communications

Calton, T. L. 1999. "Assembly-Oriented Design Workshop." (Invited) *Proc. 1999 IEEE International Symposium on Assembly and Task Planning—Toward Flexible and Agile Assembly and Manufacturing* (Porto, Portugal, 21 July).

Calton, T. L. 1999. "Automated Assembly Analysis: The Archimedes Tool." (Invited) Presentation to the 1999 Robotics Industry Association International Conference on Robots and Vision, Detroit, MI, May.

Holder, D. A., R. D. Harrell, T. L. Calton, J. F. Atkinson, and B. M. Brasfield. 1999. "Integration of Newly Developed AI Assembly, Production, and Material Flow Virtual Tools." *Proc. 2nd Internat. Conf. on Intelligent Processing and Manufacturing of Materials 1* (Honolulu, HI, July).

3516330000

Analysis of Very Large Assemblies

T. L. Calton, E. A. Mitchell, G. A. Laguna, R. G. Brown

Sandia's automated assembly analysis software package, Archimedes, had been applied successfully to several large industrial and weapon assemblies. While Archimedes represents the state-of-the-art in automated assembly planning software, applications of the software to very large assemblies highlighted limitations of the system and the need for extensive modifications to support practical analysis of assemblies with several hundred to a few thousand parts. We believed that there was substantial potential for enhancing Archimedes to routinely handle much larger models and/or to handle more modestly sized assemblies much faster. For example, two areas that would benefit are those of automating shipboard maintenance tasks and battlefield-condition custom assembly of autonomous and teleoperated vehicular robots. In the case of automated shipboard maintenance tasks, Archimedes could be invaluable for evaluating the feasibility and efficiency of various designs for shipboard systems, relative to the cost and difficulty of automating maintenance and service tasks on those systems. In the case of battlefield robotic vehicles, the evaluation of designs and design strategies could be quite valuable, but so would the ability to generate multimedia training documentation. Since shipboard systems and vehicular robots tend to be quite complex, Archimedes needed to be able to handle large systems quickly and efficiently.

We addressed the three main resources identified earlier as barriers to the application of Archimedes to very large assemblies: memory utilization, contact analysis computation time, and planning time. We integrated into the system the assembly reconciliation facility enabling the migration of manufacturing constraints and component geometric overrides between different computer-aided design (CAD) representations of an assembly (developed last year). To further improve contact analysis capabilities, assembly sequence planning, and playback times, we incorporated automatic geometric model simplification methods. We tested these features, combined with the reconciliation facility, on previously archived very large assemblies as well as on newly acquired very large assemblies, and showed significant improvements in analysis capabilities, both in geometric manipulation and in planning time.

We tested these features, combined with the reconciliation facility, on previously archived very large assemblies as well as on newly acquired very large assemblies, and showed significant improvements in analysis capabilities, both in geometric manipulation and in planning time.

We developed a prototype software tool to design and estimate manufacturing costs of small smart machines. We wrote the system in C++ and implemented a Tcl/Tk graphical user interface (GUI). We designed the computer algorithms to read in customer-specified mission requirements, to generate a set of Sandia design requirements using a components database designed and developed using pre-existing small smart machines, and then to couple the datum to produce a cost-effective machine design based on user-defined optimization criteria. The system also provided an interactive display feature to allow a user to modify calculated design requirements. Mission requirements included several options: type, payload, computational, operation environment, travel range, communication range, duty cycle, duration, dimensional footprint, quantity, budget, schedule, and optimization criteria. The Sandia design requirements included chassis, motors, batteries, cameras, sensors, radios, pivot bearings, central processing units (CPUs), and actuators. Optimization rules and calculations that we implemented included cost of the machine, weight of the machine, size in volume, and power consumption.

We developed a prototype software tool to design and estimate manufacturing costs of small smart machines.

Refereed

Calton, T. L. 1999. "Advancing Design-for-Assembly: The Next Generation in Assembly Planning." *Proc. IEEE Internat. Symp. on Assembly and Task Planning 1* (Porto, Portugal, 21 July): 57–62.

Calton, T. L. 1999. "Analysis of Very Large Assemblies." Sandia Technical Report SAND2000-0210, Sandia National Laboratories, Albuquerque, NM, November.

Calton, T. L., and R. G. Brown. 1999. "An Optimizing Algorithm for Automating Lifecycle Assembly Processes." *J. Artificial Intel. in Engin. Design and Manuf.* (special issue sponsored by AAAI SIGMAN, Philadelphia, PA.), submitted.

3516340000

Enabling Human Skills with Cooperative Automation

D. J. Schmitt, T. S. Gladwell, R. J. Anderson

This project will produce, for the first time, the ability of humans and automated systems to cooperate to perform tasks within the same workspace. The intent is to enable efficient task execution by simultaneously utilizing the best skills of the human and machine to perform a task. Cooperative automation frees the human from mundane and hazardous tasks and allows the human to perform the more insightful operations such as task supervision. This technology will provide the potential for reducing personnel requirements in manufacturing and national security operations by providing cooperative automated assistants, and by allowing a single individual to direct multiple cooperative systems.

Sandia will create sensor systems capable of detecting both stationary and moving objects within a robotic work environment, and algorithms for utilizing this data for cooperation between humans and robots. The robotic systems are capable of safe, autonomous navigation in the presence of a human operator, while taking direction from that operator to cooperate to perform tasks. We also address issues of human/system interfaces, in this case, in direct interfaces between the human and machine. We also identified some candidate applications for the technology. For example, this project will produce the intelligent controls for creating cooperative automated assistants that can carry and deploy tools for mine and unexploded ordnance (UXO) detection and automated assistants for ordnance handling and loading on aircraft carriers. This will result in the extension of a human's logistical capabilities and safety in these hazardous operating environments.

- *Demonstrated real-time control necessary for cooperative task.* We continued to take advantage of the advances in microprocessor speeds to provide both increased data throughput and more sophisticated data. We upgraded from a 2-D video motion detection (VMD) system to a full 3-D system for human tracking. The 3-D system monitors the entire working volume with a three-cube (voxel) subdivision. We maintained real-time data rates and are now able to control the robot in 3-D space versus only 2-D (x-y plane) from the previous year. In addition, faster processing speeds allowed us

This project will produce, for the first time, the ability of humans and automated systems to cooperate to perform tasks within the same workspace....This technology will provide the potential for reducing personnel requirements in manufacturing and national security operations by providing cooperative automated assistants, and by allowing a single individual to direct multiple cooperative systems.

Demonstration of cooperative automation using a pedestal robot. The system includes real-time, vision-based tracking of the human operator, and structured light measurement of the location of static objects.



to also extract further data from the tracked human operator. We are able to analyze the voxel image in real time to detect human gestures that the supervisory control system utilizes to communicate human intent.

- *Reviewed safety aspects of human/robot interaction.* The demonstrations implemented in FY99 continue to be within the Robot Industry Association's (RIA) safety standards. We reviewed the developed technologies and demonstration with our internal robot safety organization and developed a wireless live-man safety switch. The RIA standard requires a live-man switch when in the vicinity of the moving robot, and we developed a wireless version (as opposed to the wired teach-pendant used in FY98), which is less cumbersome and provides additional switches for directing the cooperative behavior.

The supervisory control system now includes a zone-based monitoring scheme that determines allowable zones for the human operator. Without proper permission to be within the robot's workspace, the supervisor will E-stop the robot.

- *Demonstrated human/robot fully cooperative task.* We implemented a full-featured demonstration of human/robot cooperation on a pedestal robot platform. The critical sensor systems are 3-D Video Motion Detection (3DVMD) for human tracking, laser-based structured lighting for object detection, and a force sensor on the robot for direct guidance of the end-effector by the operator. We developed a voice-input system for the operator to command operations from the robot and an audio output system to communicate information back to the operator. We are also in the process of incorporating gesture recognition as a further means of nonverbal communication between human and robot. All these systems are coordinated by the supervisory control system.

In the demonstration task, the human and robot work together to process cylinders within the working environment. The human's task is to select the cylinders to be processed and hand them to the robot. During hand-off operations, we use 3DVMD location data in real time to allow the robot to move to the operator's current location. The robot inspects the cylinders and informs the operator of their status. The operator can command a variety of operations to control the robot's processing of these cylinders. This demonstration shows the concept of a human assessing the work environment and using the capabilities of an automated system to assist the human to cooperatively perform a task.

This will result in the extension of a human's logistical capabilities and safety in these hazardous operating environments.

- *Defined example target application with mobile robot.*

We defined a mobile robot-based demonstration to show that our results from the pedestal robot development are applicable and tailorable to other types of robotic systems. In this demonstration, we planned to show the three basic capabilities we believe are necessary for mobile cooperative platforms: the ability to summon the vehicle to the operator's location, the ability to have the vehicle follow the operator (heel like a dog), and the ability to send the mobile platform forward to an indicated destination. We will utilize the 3DVMD system developed for the pedestal application, as well as the voice input system.

3516350000

Cloud to CAD

A. L. Ames, P. G. Xavier, C. Q. Little

A fundamental requirement of sensing and intelligent controls is the ability to see unexpected objects and construct models of them to support reasoning. A typical mechanism for seeing objects is to perform range scanning with structured lighting techniques. Many of the interesting devices are engineered and exhibit significant regularity. Surfaces are parallel and perpendicular; surface equations are quadric rather than fractal. These regularities permit a variety of advantages in understanding and dealing with the unknown.

Sandia is developing algorithms that recognize engineering shapes from scanned data. The algorithms partition points into groups that represent engineering surfaces, trim and extend surfaces, and adjust representations to achieve model closure. The algorithms will integrate geometry from multiple views and suggest surfaces based on engineering expectations to account for occlusions. The result of this processing is a computer-aided design (CAD) solid model. This representation is suitable for a wider variety of applications than any other geometric representation.

The benefits of generating engineering representations of scanned objects include tremendous data compression and object reasoning. The shape of an object can be stored, transmitted, and reasoned about in an appropriate language (e.g., radius and height of a cylinder), rather than in the verbose terms of thousands of points. We can compare an object in the field to known designs in engineering terms. This reduces communication requirements for battlefield reconnaissance and surveillance.

We can directly apply all of our automatic engineering algorithms to the engineering representation of an acquired object in the following applications: identifying targets, analyzing a competitor's products, designing fixtures, planning operations for demilitarizing old ordinance, and archiving the as-built geometry of a stockpile component.

Our previous work in segmentation and surface-fitting assumed a human operator in the process to help select appropriate points for surface fitting. We extended the algorithms developed there toward developing a fully autonomous segmentation and fitting algorithm for use in applications such as fielding a mobile robot.

Sandia is developing algorithms that recognize engineering shapes from scanned data....The result of this processing is a computer-aided design (CAD) solid model. This representation is suitable for a wider variety of applications than any other geometric representation.

We extended the surface-fitting algorithms to support more general quadric fitting. Currently, all quadric surfaces can be correctly fit, including ellipsoid, hyperboloids of one and two sheets, quadric cone, elliptic and hyperbolic paraboloids, and elliptic, hyperbolic, and parabolic cylinders. We discovered degeneracies in the fitting process, in terms of the possibility for both degenerate data and degenerate functions being fit.

We began work in fitting higher-order surfaces. In cases where quadric functions are insufficient to follow the curvature of an object, we have the choice of fitting a smoothing surface (e.g., NURBS, a nonuniform rational b-spline surface), or using a triangulation of the surface. We have an operational triangular surface-fitting algorithm and are exploring a NURBS-fitting algorithm that obeys principal curvature (Gaussian and mean curvatures). Some of the quadric surfaces (e.g., hyperbolic paraboloid) have no specialized representation in CAD. For such surfaces, we fit a NURBS.

The surface-fitting algorithm forms the basis for a surface-based segmentation algorithm. Our segmentation algorithm proceeds by determining what surface fits a neighborhood of points, then moving outward in brush-fire fashion, adding points to the surface if they are sufficiently close to the surface previously defined. Tests with real scanned data have been encouraging. The surface-fitting algorithms are able to distinguish a wide spectrum of surfaces in the presence of sensor noise.

We developed an algorithm for constructing solid model faces from the surfaces recognized by the segmentation/fitting algorithms above. The algorithm determines one or more edge boundaries for the collection of points associated with a particular surface and produces a piecewise boundary associated with the points at the edges of the region. In this way we are able to see a ragged boundary to each surface. After we construct the basic faces, adjacent faces are located by topological and geometric proximity. We find the face/face intersection, which defines the equation for the edge shared by two adjacent faces.

We developed the essential solid-building algorithm. We are currently working on problems associated with model accuracy being significantly lower than typical solid modelers require. In such cases, we are considering an algorithm that tweaks surface definitions, within their statistical validity, to improve the likelihood of edge intersections working correctly.

To test the algorithms, we scanned a variety of real-world objects using the LAMA sensor. These objects included entry

The surface-fitting algorithm forms the basis for a surface-based segmentation algorithm.

doors, car locks, door knobs, laboratory spaces, and a glove box. The surface fits were quite robust, while the solid fitting algorithms require further development. Shiny and transparent surfaces left holes in the range data, and, as is typical of LAMA scans, occluded regions from both the laser and the camera leave shadows in the range image.

In cases where the camera sees no return from the surface, we developed an approach for computing limits on the possible spatial extent of the surface by finding boundaries at the edge of good points (as was done in computing ragged boundaries of faces) and using these boundaries, along with information on camera and laser location, to compute faceted cone frustums as limits on where surfaces might be. This result is useful in determining positions that a robot must assume in order to fully characterize a scene safely. We designed the algorithm and are ready to implement the prototype.

*We designed the algorithm and
are ready to implement the
prototype.*

Other Communications

Ames, A. L. 1998. "Cloud to CAD." Presentation to the Ford Expo, Dearborn, Michigan, October.

3516360000

Ergonomics in Life-Cycle Assembly Processes

T. L. Calton, J. J. Carlson, D. E. Small, C. Q. Little, D. J. Schmitt, T. S. Gladwell, J. C. Trinkle, R. J. Anderson, R. R. Peters

To meet the design-to-costs of Sandia's operation/sustainment, we need to develop the means to identify, develop, and integrate improved, affordable manufacturing technologies that allow for design and assembly at a lower cost with greater flexibility. Automatic assembly sequencing and visualization tools are valuable in determining the best assembly and disassembly sequences and plans for weapons and other military and industrial system components and subassemblies, but without Human Factors and Figure Models (HFFMs) it is difficult to evaluate or visualize human interaction. HFFMs allow engineers to verify that maintenance is possible and to see ways to make the design even better. The automated simulation and analysis tools resulting from this project could have significant impacts in the reduction of physical mock-ups required for training personnel in operations and maintenance by providing repair-on-demand services and analyzing the design for human interactions.

We will create a framework for integrating HFFMs with the automated assembly planning techniques used in maintenance operations and simulation. During the first year (and some this past year), we emphasized coupling HFFMs with Sandia's Automated Assembly Analysis Software Package, Archimedes. Since tools used for a manufacturing process include fixtures that may impose significant constraints on the manufacturing process, we added an additional goal to the project: to create a framework for integrating automatically designed fixtures with the automated assembly planning (with HFFMs). The need arose to more tightly couple the enabling of human skills in cooperative automation with automated assembly analysis. We hoped that such a coupling would provide improved intelligent controls for creating cooperative automated assistants for a human's logistical capabilities and safety in hazardous operating environments.

One goal of the project was to couple the Human Figure Modeling Software Package, Jack, by Transom, Inc., with the automated assembly analysis algorithms of Sandia's automated assembly analysis software package, Archimedes. To integrate Archimedes with the Jack software package, two basic steps

The automated simulation and analysis tools resulting from this project could have significant impacts in the reduction of physical mock-ups required for training personnel in operations and maintenance by providing repair-on-demand services and analyzing the design for human interactions.

were required. First, we used the Archimedes assembly planner to automatically analyze the feasibility of assembly and then to automatically generate an assembly sequence for selected assemblies requiring the use of handtools to put them together. We generated a textual script capturing this assembly sequence, part-mating trajectories, and tool-and-hand application trajectories. We added output routines to Archimedes to capture this information for Jack input. Second, we individually converted the ACIS (Applications of Collectively Intelligent Systems, a geometry modeling package from Parametric Technologies Corporation) geometry files used in Archimedes, including assembly components, tools, and respective use-volumes, and handgrips on those tools, with their respective tool-and-hand use-volumes to the IGRIP files. Jack accepts IGRIP format as input. What is lacking in this framework is the ability to quickly generate collision-free motion paths and hand-grasps for the human. Future work is aimed at integrating these two aspects.

We also worked on developing a framework for integrating automatically designed fixtures with automated assembly planning. This initiative focused on integrating Sandia's fixture design software package, HoldFast, with Archimedes. The integration resulted in a two-phased approach. In the first phase, we upgraded HoldFast to use ACIS 3-D objects. Specific tasks required for the ACIS upgrade included converting the HoldFast geometry from 2-1/2-D to 3-D and developing interface capabilities between HoldFast and ACIS. HoldFast previously used 2-1/2-D geometry to interrogate an object's geometry. We rewrote those functions in order to be compatible with the ACIS 3-D representation. Also, since HoldFast was initially written in LISP, and ACIS is written in C++, we had to develop interface routines to allow a seamless transition between HoldFast and ACIS. When the conversion was complete, we made the actual integration of the two software packages. The integration method starts with 3-D CAD descriptions of an assembly whose assembly tasks require a fixture to hold the base part. The fixture planning algorithms use CAD descriptions of that part to generate geometric representations of a fixture pallet to use in the assembly planning software. (The resulting fixture is designed to rigidly constrain and locate the part, obeys various task constraints, is robust to part shape variations, is easy to load, and is economical to produce.) The geometric descriptions generated by the fixture planner and additional assembly components are then loaded into the assembly system for

We also worked on developing a framework for integrating automatically designed fixtures with automated assembly planning.

analysis. Using the assembly analysis constraint framework, the fixture is first declared as a base component. The assembly analysis system then tests for feasibility of tool use during the pallet assembly and assembly of the components. The assembly planner not only generates assembly plans for the assembly, but can also be used to generate assembly plans for the fixture. The combined algorithms guarantee that the fixture will hold the base part without interfering with any of the assembly operations. What is lacking in this framework is the ability for the assembly planner to automatically provide feedback to the fixture planner. Future work should provide a more complete integration of the planners.

The combined algorithms guarantee that the fixture will hold the base part without interfering with any of the assembly operations.

Refereed

Calton, T. L. 1999. "Advancing Design-for-Assembly: The Next Generation in Assembly Planning." *Proc. IEEE Internat. Symp. on Assembly and Task Planning 1* (Porto, Portugal, 21–24 July): 57–62.

Calton, T. L., and R. R. Peters. 1999. "Ergonomics in Life Cycle Assembly Processes." Sandia Technical Report SAND99-2808, Sandia National Laboratories, Albuquerque, NM (November).

Other Communications

Calton, T. L. 1999. "A Framework for Geometric Reasoning about Human Figures and Factors in Assembly Operations." *Proc. ITS 3rd International Conf. on Engineering and Automation 1* (Vancouver, British Columbia, Canada, 3 August).

Calton, T. L., and R. R. Peters. 1999. "A Practical Approach for Integrating Automatically Designed Fixtures with Automated Assembly Planning." *Proc. ITS 3rd Internat. Conf. on Engineering and Automation 1* (Vancouver, British Columbia, Canada, 2 August).

3516370000

Feature Reduction of Geometric Solid Models for Analysis Tools

P. A. Watterberg

The goal of this project is to facilitate task-specific simplification of solid geometric models for interaction with sensing, design, analysis, planning, and execution tools. Sandia will design and implement algorithms that will streamline the design-to-analysis progression, thereby increasing the capabilities of Sandia's existing and analysis tools under development (e.g., Archimedes, CTH, and CUBIT applications, SANDROS applications) by eliminating complexity, which is unnecessary for specific applications. These algorithms will also provide support for the automatic creation of simplified geometric representations that would be appropriate for use with real-time planning and execution systems, such as might be used on autonomous insectoid or vehicular robots. Example simplifications include elimination of purely internal features from subassemblies in an assembly-planning scenario, eliminating small holes from an obstacle in a motion-planning scenario, and simplification or removal of complex fillets for fixturing analysis. We would also incorporate some ability to simplify and refine faceted models. Preliminary experiments indicate that these capabilities would enable our analysis tools to tackle problems an order-of-magnitude larger than they can currently handle and would greatly facilitate seamless integration of Sandia's many analysis tools with the variety of solid-modeling packages currently used both within the weapons complex and within U.S. industry. The ability to simplify geometric models is becoming vital, as it will become increasingly difficult for the tools used to plan manufacturing and service operations to handle the complexity of the modeling systems used to represent parts and assemblies. Thus, any design or execution code used to deal with large, complex geometries in either the manufacturing or the robotic vehicle realms would benefit from inclusion of this technology into its core.

- *Prototype interactive viewing/interaction tool.* We built a Motif- and GL-based, mouse-driven viewing/visualization tool that allows a user to view an ACIS (Applications of Collectively Intelligent Systems, a geometry modeling package from Parametric Technologies Corporation) object dynamically from multiple directions and magnitudes, and to interact with

Sandia will design and implement algorithms that will streamline the design-to-analysis progression, thereby increasing the capabilities of Sandia's existing and analysis tools under development (e.g., Archimedes, CTH, and CUBIT applications, SANDROS applications) by eliminating complexity, which is unnecessary for specific applications....The ability to simplify geometric models is becoming vital, as it will become increasingly difficult for the tools used to plan manufacturing and service operations to handle the complexity of the modeling systems used to represent parts and assemblies.

certain classes of geometric features using the mouse. We enhanced the viewing tool to highlight specific face types and allow the selection of a single face.

- *Faceted data.* We implemented stereolithography (STL) (faceted) to planar-ACIS-body conversion and cylindrical approximation detector. We can now replace many cylindrical surface approximations by an actual cylindrical surface. We implemented several different feature-removal heuristics. We removed holes less than a specified size, slots and voids in planar surfaces, and chamfers and fillets. We applied these heuristics to several sample objects, yielding mostly modest results, but some objects yielded dramatic results. Continued refinement of the algorithms should yield satisfactory results on most objects.

- *Removal of internal geometries.* Using available graphics hardware greatly speeded up our ability to remove internal geometries—removing 90% of the geometry on some models. We implemented the ability to select and remove specific holes and planar voids and added the ability to highlight a specific face so it could be tracked through the system and handled as a special case. We also added the ability to delete specific faces as a lowest-level, brute-force simplification technique when all else fails. In addition, we can now write out the simplified geometry in different formats, e.g., IGRIP part format. We used several of the models we simplified in other packages analyses and saw speedups of up to two orders of magnitude. We are now able to create arbitrary group faces and save them as a subset of the original body. We can also raise slightly offset shelves and benches such as O-ring grooves or countersunk slots, etc.

Using available graphics hardware greatly speeded up our ability to remove internal geometries—removing 90% of the geometry on some models.

Other Communications

Watterberg, P. A. 1999. "Feature Reduction Geometric Solids." Sandia Technical Report SAND99-3117, Sandia National Laboratories, Albuquerque, NM, November.

3516380000

Electrokinetic Immunoaffinity Chemical Sensors

J. S. Schoeniger, J. V. Volponi, V. A. Vandernoot, G. A. Hux, D. W. Neyer, D. S. Anex, A. K. Singh

The purpose of this project is to establish the feasibility of capillary affinity electrochromatography (CAEC) with laser-induced fluorescence (LiF) detection as a portable means for the detection of trace quantities of toxins in liquid samples. The project focuses on the detection of analytes for which there is currently no portable sensor capability with adequate sensitivity and specificity, e.g., potential biological warfare (BW) agents (bacterial toxins). In CAEC, the chromatographic matrix consists of immobilized molecular recognition materials (MRMs) (e.g., antibodies [Abs] or receptors) that bind selectively to the target analyte, surpassing the specificity of capillary electrochromatography (CEC). A sensor based on CAEC has the potential to combine the versatility of CEC, the high sensitivity of LiF, and the exquisite selectivity of molecular recognition.

- *Electrokinetic trapping (EKT) of proteins.* We more fully examined the phenomenon EKT to evaluate the potential of EKT for improving sensitivity. To quantitate the concentration behavior, we measured areas and heights of the peaks eluted by application of pressure. The amount of protein injected in a packed column is a function of three variables: injection voltage, duration of injection, and concentration of protein in the sample. We changed all three variables, one at a time, to quantitate the concentration factor achieved during trapping of proteins under the influence of an applied electric field and subsequent release by application of pressure. We observed that we can achieve a 170-fold concentration by injecting ovalbumin for almost three hours on a column packed with porous silica particles.

- *Synthesis and characterization of affinity phases for protein toxins*

- *Ricin/lactose.* We explored additional immobilization chemistries to enhance the overall performance of the lactose-based affinity phases. A modification of the binding protocol increased the yield of immobilized lactose on silica by approximately two orders of magnitude, resulting in a full monolayer coverage of lactose (fluorescein coupled to ethylene diamine as a tracer). Performance of these phases was much

The project focuses on the detection of analytes for which there is currently no portable sensor capability with adequate sensitivity and specificity, e.g., potential biological warfare (BW) agents (bacterial toxins).

improved, with a greater percentage of the injected peak binding to the column. Use of the portable detector, developed in FY98, led to a detection limit of 10 nM in pressure mode and 1 nM in EK mode.

– *Tetanus (botulinum)/ganglioside*. We explored the noncovalent attachment of the ganglioside GT1b to commercially available 1.5 μm C18 silica. While tetanus (Tet C) did appear to bind, it required the addition of organic solvents to the elution buffer to elute the toxin. We observed this to dissociate the ganglioside from the beads in control experiments, requiring the regeneration of the ganglioside surface prior to each run. We deemed this problematic with packed columns and did not pursue it further in favor of covalent attachment of GT1b.

We identified an enzyme, ceramide glycanase, to cleave the ceramide tail from the ganglioside after which we isolated and chemically modified the heptasaccharide head group of GT1b via reductive amination to incorporate a primary amine-containing tail, allowing covalent coupling to the beads. As with the noncovalently bound ganglioside, Tet C did bind to the column, with the size of the elution peak increasing with the amount of Tet C injected. Increasing the amount of ligand bound would undoubtedly improve performance further.

– *Ovalbumin/peptides*. We identified several peptides as ovalbumin binding using a combinatorial approach. We commercially synthesized peptides based on these sequences, incorporating a three-serine repeat as a spacer arm. The last sequence listed, very recently identified, is expected to have the tightest, most selective binding ($K_d \sim 1 \mu\text{M}$).

We developed binding chemistry to couple through the carboxy terminus of the peptide (i.e., the spacer arm). Fluorescently tagged peptides used as tracers indicated that affinity phases prepared in this way contained 10%–50% of a monolayer coverage of peptide.

Preliminary testing showed ovalbumin may be binding, but elution in 2% (and higher) acetic acid is minimal. We are exploring this further, along with additional elution conditions.

– *SEB/peptides*. Only very preliminary data have been collected regarding combinatorial peptides that display affinity for SEB. We identified two sequences that appear to bind SEB (over the control) and are not eluted in high salt conditions, suggesting that the interaction is not simply electrostatic in nature. In binding studies, however, the overall binding was quite low, possibly indicating poor affinity.

We identified two sequences that appear to bind SEB (over the control) and are not eluted in high salt conditions, suggesting that the interaction is not simply electrostatic in nature.

Refereed

Thomas, D. H., J. S. Schoeniger, D. L. Rakestraw, J. M. Van Emon, and V. Lopez-Avila. 1999. "Selective Trace Enrichment by Immunoaffinity Capillary Electrochromatography On-Line with Capillary Zone Electrophoresis-Laser-Induced Fluorescence."

Electrophoresis **20** (January): 57–66.

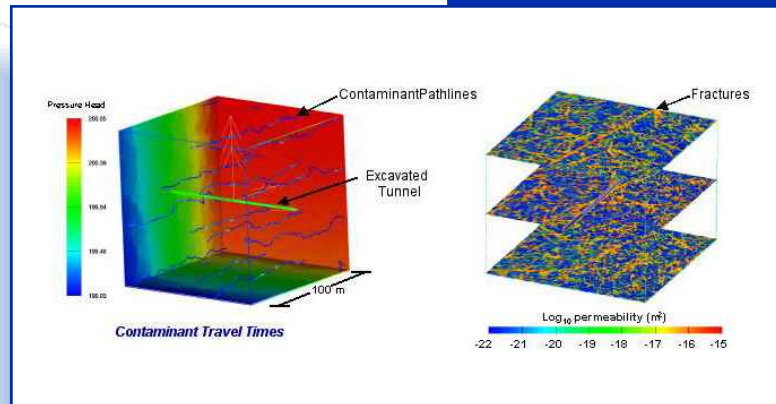
ENVIRONMENTAL SCIENCES

Environmental Sciences is one of Sandia National Laboratories' six LDRD Roadmap Technologies investment areas. Roadmap Technologies derive their scientific basis from and extend the applications of Research Foundations investments into new areas. Roadmap Technologies create or accelerate scientific and technical expertise for future program areas that are strategic to Sandia and important to the DOE and the nation.

The Environmental Sciences investment area investigates issues of environmental quality and sustainability, intelligent systems, and innovations that complement the Environmental Management Science Program. The goal of this research is to expand scientific knowledge and to explore innovative technologies with the potential to reduce future costs and risks and to improve scheduling. Environmental quality and sustainability research strives to reduce harmful by-products of manufacturing and production and to increase energy efficiency without sacrificing quality, reliability, or performance. Intelligent-systems research investigates intelligent robotics and advanced controls for hazardous-waste cleanup.

The "Advanced Geosphere Transport Simulation" project is researching a massively parallel code with the potential to significantly enhance performance assessment capabilities for understanding and

controlling geosphere transport—these are key capabilities with the potential to impact the Nuclear Waste Management Program (NWMP). This code addresses the limitations of other tools that have had significant negative effects on performance assessment: (1) simplifications have become regulatory points of contention, (2) critical details about fast-path transport have been lost, and (3) turnaround times for assessing uncertainty have been too long to drive project decisions. This code will also have the potential to enhance research and development in other technologies whose performance hinges on understanding and controlling geosphere transport, including system design and decision analysis for radioactive-waste disposal, subsurface environmental remediation, and petroleum reservoir management.



3518160000

Designed Synthesis of Controlled Degradative Materials

T. A. Ulibarri, D. A. Loy, M. J. Carr, S. H. Scott, R. S. Saunders, J. G. Curro, T. R. Guess, D. R. Wheeler

This year's effort focused on three areas: (1) modeling the superslick phenomena, (2) investigating the mechanism for loss of superslick properties in polyethylene oxide (PEO), and (3) developing new removable encapsulants. In the first area, Sandia successfully applied density-functional theory (DFT) to help understand superslick behavior with hydrated thin films of polymers. In the second area, we determined that ascorbic acid can oxidatively degrade the PEO through a radical mechanism. We performed viscosity studies with ascorbic acid, photosensitizers, and radical inhibitors. In the third area, we developed a new class of removable encapsulants based on Diels-Alder chemistry and polysiloxanes substrates. The monomers used to make these materials also have promise as new coupling agents between unsaturated polymers, such as rubber, and silica fillers.

Sandia successfully applied density-functional theory (DFT) to help understand superslick behavior with hydrated thin films of polymers.

- *Modeling of the superslick phenomena.* We showed that high-molecular-weight PEO becomes extremely slippery when wetted on the surface with water. This can be accomplished by spreading a thin film of the powdered polymer on a hard, flat surface and spraying a mist of water onto the polymer. We proposed the mechanism for this slipperiness to be the formation of a thin gel phase on the surface of the polymer. How this translates exactly into slipperiness was the subject of this project.

- *Degradation mechanisms for PEO.* A survey of the literature revealed that ascorbic acid would quickly degrade the slipperiness of PEO. We proposed that the ascorbic acid was generating radicals that would cause cleavage of the PEO into shorter lengths. We previously showed that the slipperiness of the hydrated PEO is directly dependent on molecular weight, with a critical threshold of around 1 million Daltons being necessary for a slippery surface. We proposed that this radical-induced cleavage could rapidly degrade high-molecular-weight PEO to lower-molecular-weight material with a parallel decrease in performance. There is considerable evidence that ascorbic acid degrades PEO through the generation of hydroxide radicals that then abstract an alpha hydrogen from the polymer. This leads to chain scission of the PEO lowering

the mean molecular weight. We confirmed this hypothesis with viscosity studies on aqueous solutions of high-molecular-weight (8 million Daltons) PEO with 25 wt.% ascorbic acid. Within 1000 seconds the molecular weight had decreased to 1 million Daltons. After two hours the weight was down to 250,000 Daltons. Interestingly, hydrogen peroxide or photoradical generators like benzophenone-triethyl amine did not result in any measurable degradation of the PEO. Nor were most organic (organic-soluble) radical generators sufficiently soluble in the aqueous solutions for any measurable degradation to be observed.

To attempt to prevent degradation of slipperiness with ascorbic acid, we synthesized alternative polymers based on lightly cross-linked polyacrylamides and evaluated them for slipperiness. We showed the polyacrylamide crosslinked with ethylene diacrylate (2–3 mol%) to have slipperiness comparable with high-molecular-weight PEO. Those based on bis(acrylamide) crosslinkers were not slippery. We did not perform degradation tests.

• *New removable encapsulants.* We developed a new class of removable encapsulants based on organosilane precursors functionalized with maleimide groups. These materials would thermally cure at room temperature without catalysts or reagents and would depolymerize to low molecular constituents at temperatures at or above 90°C. These new materials could be irreversibly cured by autopolymerization with or without a radical generating catalyst or through Alderene chemistry. The monomers are also very promising as a new class of coupling agents for coupling unsaturated polymers such as rubbers to silica fillers.

We developed a new class of removable encapsulants based on organosilane precursors functionalized with maleimide groups.

3518170000

Mechanistic Models for Radionuclide Desorption from Soils

P. V. Brady, M. D. Siegel, D. J. Borns, E. R. Lindgren

The object of this project is the development and implementation of a procedure for relying on natural processes (monitored natural attenuation [MNA]) to clean up contaminated soils and groundwaters in the DOE complex. Sandia believes that complex-wide implementation of the technical protocol will result in the savings of several billion dollars in cleanup costs. The first two years of the project involved development of the technical protocol. In this time we collaborated with the U.S.-EPA, the New Mexico Environmental Department (NMED), and several other national labs.

We accomplished the following:

- (1) Reviewed MNA-based site cleanups at Oak Ridge National Laboratory (ORNL), Lawrence-Livermore National Laboratory (LLNL), Weldon Springs, and Brookhaven National Laboratory (BNL).
- (2) Completed a SAND report describing the MNAToolbox—an MNA site-screening tool.
- (3) Published several papers in peer-reviewed technical journals.
- (4) Examined and subsequently developed techniques for establishing historical case analysis of metal-bearing contaminant plumes.
- (5) Began historical case analyses for ^{137}Cs , ^{90}Sr , and U.
- (6) Presented our technical results at several national meetings.
- (7) Sponsored two special sessions of the Association for the Environmental Health of Soils in the East and West Coast Meetings.
- (8) Sponsored a special issue of the *Journal of Soil Contamination* on MNA.

Sandia believes that complex-wide implementation of the technical protocol will result in the savings of several billion dollars in cleanup costs.

Refereed

Eick, M. J., J. D. Peak, P. V. Brady, and J. D. Pesek. 1998. "Kinetics of Lead Adsorption/Desorption on Goethite: Residence Time Effect." *Soil Science* **164**: 28–39.

Yeh, G., M. Li, and M. D. Siegel. 1999. "Numerical Modeling of Coupled Variably-Saturated Fluid Flow and Reactive Transport with Fast and Slow Chemical Reactions." *Radiochemica Acta*, in press.

3518180000

Adaptive 3-D Sensing

C. Q. Little, D. E. Small, D. J. Schmitt, J. J. Carlson

The purpose of this project is to create sensing, reasoning, and control technologies that will allow the safe and effective cooperation of humans and intelligent machines in a variety of operations. This will rely heavily on real-time three-dimensional (3-D) sensing and interpretation of the 3-D data. The results of this research will include a new adaptive 3-D sensing system as well as new research into dynamic object modeling, behavior recognition, and sensor-based control. The 3-D sensing system will combine two existing sensing technologies in a new way to create a site-monitoring system that can continuously maintain an accurate 3-D model of the site and real-time estimates of the shape, location, and motion of humans and machines. A key strength of this system will be its ability to monitor simultaneous activities, such as several robots and humans working independently, while also detecting unexpected entry into the workspace. We will use data from this sensing system to allow automated systems, such as robots, to not only safely co-exist with humans within the workspace but also to cooperate in performing tasks. This will improve the practicality and efficiency of many operations by simultaneously using the best skills of both humans and machines.

We demonstrated human-machine cooperation with technology-related applications. Work this year concentrated



We will use data from this sensing system to allow automated systems, such as robots, to not only safely co-exist with humans within the workspace but also to cooperate in performing tasks....[to] improve the practicality and efficiency of many operations by simultaneously using the best skills of both humans and machines.

Camera view of human interacting with robot adaptive 3-D model.

on using the framework created last year to test various algorithms and ideas. The addition of audio, both input and output, has opened communication options. The vision work concentrated on locating the human. We now have a fully operational 3-D motion detector.

A human operator can engage an active pedestal robot, which uses human location data to control its movement to track and hand off objects to and from its gripper. The operator can additionally give direction to the robot while in the workspace through voice and body gestures. This has opened a new area of research for human-machine interface work with an active test-bed. Incorporated technologies include voice input, audio feedback, first-generation gesture recognition, motion detection and tracking, 3-D scene construction, object recognition, and a wireless "live-man" switch for greater flexibility of human interaction while maintaining strict safety standards.

*We now have a fully operational
3-D motion detector.*

3518190000

Aqueous Organic Sensor

M. J. Kelly, K. J. Kasunic, S. A. Kemme, D. S. Blair, W. C. Sweatt

Current drinking-water standards specify that concentrations of certain aromatic hydrocarbons must be very low, e.g., below 100 parts per billion (ppb). However, quantitation of compounds in water at these concentrations is difficult and is typically performed using purge-and-trap analytical methods. These techniques have inherently long analysis times and, for field-deployable instrumentation, high device maintenance requirements and equipment failure rates. The goal of this research is to provide the technology base for eventual production of a field-deployable aqueous organic sensor that is compact, rugged, and simple to use, and that provides the ability to measure aromatic hydrocarbons in water at concentrations as low as 100 ppb. The technology developed at Sandia uses spectroelectrochemistry as its fundamental transduction mechanism. Here, the detection and quantitation of analytes in water rely on monitoring the electrochemical generation or consumption of an optically detectable compound. The spectroscopic method that we are combining with electrochemistry is known as grating light reflection spectroscopy (GLRS). A new, emerging technology, it noninvasively provides information about the dielectric function (i.e., both the real and imaginary parts of the refractive index) of the sample. This can then be translated into quantitative chemical information.

We designed and fabricated a spectroelectrochemical cell and optical spectroscopy system and used them to evaluate the prototype GLRS sensor concept. The cell's working electrode was a diffraction grating with chromium (Cr) metal lines (1.0 micron period) deposited onto fused silica. Since Cr is not a suitable working electrode for electrochemical measurements, we evaporated approximately 200 nm of semiconformal gold over the Cr lines. This gold (Au) layer slightly diminished the diffraction efficiency but did provide satisfactory optical transparency at the wavelength of interest.

The GLRS measurements summarized here were made at 52.5 degrees, which is at or near the spectral singularity, i.e., the angle at which the first transmitted diffraction order changes from propagating to evanescent. The light source was a green HeNe (helium neon) laser (543.5 nm). We directed the laser beam through a chopper wheel and steered it by two

The goal of this research is to provide the technology base for eventual production of a field-deployable aqueous organic sensor that is compact, rugged, and simple to use, and that provides the ability to measure aromatic hydrocarbons in water at concentrations as low as 100 ppb.

mirrors through a beam pickoff onto the grating. We directed the reference beam onto one silicon (Si) photodiode detector while directing the zero diffracted order (reflection, from the beam incident upon the grating) onto a second detector. We sent the outputs from the detectors to two transimpedance amplifiers, and the resulting voltage signals to two digital lock-in amplifiers. We used a custom LabView virtual instrument to acquire the data from the lock-in amplifiers.

We performed spectroelectrochemistry experiments either in high-purity water or in a supporting electrolyte of potassium nitrate in water. Although the absence of a supporting electrolyte in the former case resulted in extremely high-resolution resistivity, there was sufficient conductance to allow electrochemical modulation of the grating.

We scanned the working electrode between + 3 and - 3 volts at a scan rate of 500 mV/s. It should be noted that these potentials were not sufficient to electrolyze water (even though they are greater than the 1.2 V electrolysis potential) because of the large solution resistivity, which produced a large potential drop through the solution. These potentials were large enough, however, to produce measurable changes in the reduction (and subsequent oxidation) currents attributable to the analyte. Cyclic voltammetric (CV) modulation of the grating produces changes in the zero-order reflectance, which we fit to an expression of the following form:

$$R = m1 + m2 * [\sin(m3 * \text{time} + m4)]$$

Our approach to detection of the organic molecule in water has excellent lower limits of detection (LLDs) (less than 50 ppb). Similar experiments performed with 2,4,6-trinitrotoluene (TNT) demonstrated an LLD of approximately 50 ppm. The reason for this dramatic difference in detection limits is under investigation. Our current hypothesis is that a large decrease in optical absorbance (at 543.5 nm) accompanies the electrochemical reduction of Meldola's Blue and that this is reflected in a correspondingly large change in the measured complex dielectric function. We further hypothesize that no such change in optical absorbance at 543.5 nm accompanies the electrochemical reduction of TNT, resulting in a higher LLD.

Our current hypothesis is that a large decrease in optical absorbance (at 543.5 nm) accompanies the electrochemical reduction of Meldola's Blue and that this is reflected in a correspondingly large change in the measured complex dielectric function.

Refereed

Burgess, L., A. Brodsky, S. Smith, M. J. Kelly, W. C. Sweatt, D. S. Blair, S. A. Kemme, S. H. Zaidi, and J. McNeil. "Grating Light Reflection Spectroscopy." Presentation at the Center for Process Analytical Chemistry (CPAC) Semiannual Review, University of Washington, Seattle, WA, 1-4 November.

Other Communications

Kelly, M. J., W. C. Sweatt, D. S. Blair, S. H. Zaidi, S. A. Kemme, K. J. Kasunic, L. Burgess, and A. Brodsky. 1999. "Grating Light Reflection Spectroscopy (GLRS) Study of Meldola's Blue and 2,4,6-trinitrotoluene During Electrochemical Modulation of a Metal-Line Grating." Sandia Technical Report, in review.

3518210000

Designed Ionophores for Liquid-Membrane Separation and Extraction of Metal Ions

J. A. Shelnut, J. E. Miller

Sandia is developing new materials and processes for metal-ion separation and extraction, mostly based on selective transport of ions across membranes. Using molecular simulations, we designed a new group of porphyrin-based ionophores (molecular ion carriers) for selectivity in complexing and transporting metal ions. Design molecular parameters include controlling basicity, shape, and size of the ionophore active site. Using the initial design results, we designed ionophores specifically for extraction of heavy metals and radionuclides. We synthesized and tested promising ionophores for applications in two different membrane systems. The first is a supported liquid membrane that separates two liquid phases—one containing soluble-waste metal salts and the other a liquid to which the specified metal ions are extracted. The ionophores selectively transport a specified metal ion through the intervening liquid layer to give a pure solution of the metal ion that is easily concentrated. In a second, we are developing metal-ion transport and entrapment in surfactant vesicles or as zero-valent metal particles using the new materials. Separation of the vesicles or particles leaves a pure metal-ion solution or solid. These extraction technologies offer convenient new means of separation and extraction for processing Mo-99, decontamination and decommissioning (DAD), radioactive-waste remediation, and heavy-metal waste stream and in situ treatment. The initial focus area is high-level waste tank remediation of heat and gamma emitters (^{137}Cs and ^{90}Sr), long-lived radionuclides (^{99}Tc), and other heavy-metal ions (Hg, Pb, Cr, Ag, Cu, U) contained in high- and low-level waste. Ion-extraction technologies using designed ionophores and photoreducers led to increased sustainability and lower cost and complexity of manufacturing processes. We are also considering adaptation to pump/treat methods for use at sites such as the White Sands Experimental Test Station and Tuba City. The technology is differentiated from other efforts by the use of molecular simulation to engineer high-performance ionophores and photoreducers, the application of Sandia's recognized expertise in unexplored ionophore and photocycle types, and the use of new membrane systems.

The technology is differentiated from other efforts by the use of molecular simulation to engineer high-performance ionophores and photoreducers, the application of Sandia's recognized expertise in unexplored ionophore and photocycle types, and the use of new membrane systems.

We synthesized new porphyrin ionophores and evaluated them for their ion-transport properties, including ionophores that can act as the negative organic counter-ions. These ionophores represent a significant advance in the technology because they hold up the possibility of eliminating need for the addition of the organic counter-ion, a requirement of most existing ionophores. We used bulk-liquid membranes in the transport testing protocols. We identified ionic metal complexes of the new ionophores by spectroscopic methods and subjected single crystals of two ionic complexes to single-crystal x-ray crystallographic analysis. These crystals elucidated an undesired proton-leakage mechanism. We are currently growing other crystals for x-ray analysis. The new ionophores allow metal ions in the source to be exchanged for protons in the receiving phase. The possibility exists for extraction of very low-level contaminants by forced extraction by using a high pH gradient. We also computer-designed several new neutral ionophores of the older type and synthesized them, including some with improved abilities to solubilize metal ions, for example, by adding many ether groups in analogy with crown ethers. Most interesting is a novel tetrameric calix[4]arene-porphyrin ionophore. The ionophores tested so far exhibit a wide range of ion-transfer rates, varying from almost no transport to some that are comparable to or better than currently used ion carriers. Many of the designed ionophores have been structurally characterized with ultraviolet (UV)-visible absorption, nuclear magnetic resonance (NMR), x-ray crystallography, and resonance Raman spectroscopy. In particular, we used ^7Li NMR to investigate Li^+ ion-ionophore complexes, and also obtained two x-ray crystal structures of dodecaphenylporphyrin-picric acid complexes. Because of the successes with the bulk liquid-membrane extraction methods, we focused on these types of processes. However, we see that the ionophores developed using this method function in an analogous way in the supported liquid-membrane process. We also investigated the extraction of metal ions by reduction to the zero-valent metal or insoluble metal compounds using cytochrome c3 or tin (Sn) porphyrins as a reducing mediator. We found the hemoprotein, cytochrome c3, which contains four Fe (iron) porphyrins, to reduce copper (Cu), mercury (Hg), lead (Pb), chromium (Cr), silver (Ag), and uranium (U) soluble salts either to metal particles or to insoluble metal compounds, whereas the strong reducing agent, sodium (Na) dithionite, alone would not reduce the soluble metal salts. Subsequently, we found that the

We synthesized new porphyrin ionophores and evaluated them for their ion-transport properties, including ionophores that can act as the negative organic counter-ions. These ionophores represent a significant advance in the technology because they hold up the possibility of eliminating need for the addition of the organic counter-ion, a requirement of most existing ionophores.

cytochrome/dithionite system could be replaced with a light-driven photocatalyst system composed of a Sn-porphyrin photomediator and ethylenediaminetetraacetic acid (EDTA) or triethanolamine (TEA) as an electron donor. Some, but not all, of the metal salts that could be reduced to the metal by the cytochrome could also be reduced by the Sn porphyrin/TEA system. However, the properties of the metal precipitate are different in the two systems. Both of these systems can potentially be used for *in situ* cleanup of heavy-metal-waste sites.

Refereed

Franco, R., J. G. Ma, Y. Lu, G. C. Ferreira, and J. A. Shelnett. 1999. "Porphyrin Interactions with Wild Type and Mutant Mouse Ferrochelatase." *Biochemistry*, accepted.

Kadish, K. M., E. Van Caemelbecke, F. D'Souza, M. Lin, D. J. Nurco, C. J. Medforth, T. P. Forsyth, B. Krattinger, K. M. Smith, S. Fukuzumi, I. Nakanishi, and J. A. Shelnett. 1999. "Synthesis and Electrochemical Studies of a Series of Fluorinated Dodecaphenylporphyrins." *Inorg. Chem.* **38** (1 July): 2188–2198.

Muzzi, C. M., C. J. Medforth, M. Cancilla, C. Lebrilla, J. G. Ma, J. A. Shelnett, and K. M. Smith. 1999. "Novel Dodecaarylporphyrins: Synthesis and Dynamic Properties." *Tetrahedron Lett.* (1 September): 1–5.

Nelson, N. Y., C. J. Medforth, D. J. Nurco, S. L. Jia, J. A. Shelnett, and K. M. Smith. 1999. "Synthesis and Unusual Properties of the First 2,3,7,8,12,13,17,18-octabromo-5,10,15,20-tetraalkylporphyrin." *J. Chem. Soc., Chem. Commun.* (1 October): 2071–2072.

Shelnett, J. A. 2000. "Molecular Simulations and Normal-Coordinate Structural Analysis of Porphyrins and Heme Proteins." *The Porphyrin Handbook*, Chapter 50, Volume 7, New York, NY (January).

3518220000

An Electromagnetic Imaging System for Environmental Site Reconnaissance

G. M. Loubriel, A. G. Baca, G. L. Peace

The advantages of time-domain, ultra-wideband transmitters for ground-penetrating radar (GPR) are many and well known: GPR has the potential for high-resolution subsurface imaging unmatched by any other subsurface sensing method. With GPR there are large contrasts between contaminated and noncontaminated regions. Thus GPR may detect man-made buried objects and detect and define the extent of contaminated soil. This project seeks to develop a GPR system that can be utilized for environmental site reconnaissance and, in particular, for (1) detecting disrupted soil layers where there is a potential for buried waste, (2) finding buried metallic objects such as 55-gallon drums at depths of up to 10 m (and other man-made objects at various depths), and (3) detecting contaminated soil. Because of the simplicity of the time-domain technique, the system will be fast enough to evaluate extensive land areas that may be contaminated. The primary disadvantages of GPR have been low penetration depth and low signal-to-clutter. This project is designed to minimize both of these problems. Sandia will augment the penetration depth by using (1) high-peak-power, high-repetition-rate operation for high average power, (2) low center frequencies that better penetrate the ground, and (3) short-duration impulses. The latter allow for the use of low platforms that increase the power on target relative to a high flying platform (due to the R^4 term in the radar equation, where R is the range to the target). We minimize clutter by time-gating the surface clutter return and using low frequencies (since natural objects are smaller than the wavelengths used here, and their cross-section is smaller than for higher-frequency systems). The factor that makes this work unique is that we will utilize direct time-domain radar at low frequency and high average power.

We accomplished our major objectives: (1) to continue modeling the problem, (2) to build and test an impulse transmitter for GPR field tests, and (3) to improve the system's longevity and efficiency. Three major efforts were required to meet the FY99 objectives and to ensure success in the field tests in FY00. In collaboration with Duke University, we theoretically modeled ground penetration to guide the

Because of the simplicity of the time-domain technique, the system will be fast enough to evaluate extensive land areas that may be contaminated....The factor that makes this work unique is that we will utilize direct time-domain radar at low frequency and high average power.

transmitter development, performed pulser construction at fixed frequency, and designed a new pulser unit with longer-lived switches. The calculations were method-of-moments calculations of expected radar returns from 55-gallon drums buried in clay soils with 10% water content. The calculations predict that a suitable system can be built to detect 55-gallon drums at depths of up to 3 meters. To calibrate the calculations we performed tests of the system with the drums above ground. Finally, we developed and tested a new pulse unit with a totally redesigned pulse-forming line. The new pulser is more efficient than the old pulser. We also improved the efficiency of the optically triggered switches that are the enabling technology for this radar. We redesigned the antenna to make the system more compact and transportable.

Refereed

Loubriel, G. M., J. Aurand, G. Denison, L. Rinehart, D. Brown, F. J. Zutavern, A. Mar, M. O'Malley, W. Helgeson, and L. Carin. 1999. "Optically Activated GaAs Switches for Ground-Penetrating Radar and Firing Set Applications." *Proc. 12th IEEE Pulsed-Power Conference* **1** (Monterey, CA, 27–30 June).

Stanz, K., R. Asher, S. Cameron, G. M. Loubriel, R. D. Robinett, M. Trahan, and J. Wagner. 1998. "Adaptive Remote Sensing Techniques Implementing Swarms of Mobile Agents." *Proc. 4th Joint Workshop on Standoff Detection for Chemical and Biological Defense* **1** (Williamsburg, VA, 26–30 October).

3518230000

Advanced Geosphere Transport Simulation

M. J. Martinez, T. Hadgu, P. C. Reeves, P. L. Hopkins

During the past decade, the need for predictive tools in areas ranging from environmental remediation to oil and gas extraction has prompted the development of subsurface, multiphase-flow, and contaminant-transport simulators. Numerical simulation is a key technology in system design and decision analysis for radioactive-waste disposal, subsurface environmental remediation, and petroleum reservoir management. Present limitations in computational technology drive model simplifications in the range of physical processes simulated, site geometry, and geologic realism, with significant negative impacts: (1) simplifications become regulatory points of contention, (2) critical details about fast-path transport are lost, and (3) turnaround times for assessing uncertainty are too long to drive project decisions. A massively parallel (MP) geosphere transport model will overcome these limitations and place Sandia in an advanced position with respect to repository simulation capabilities. The waste legacy, weapon safety, and national energy security programs have a unique opportunity to leverage major Defense Program (DP) investments in computational simulation and to develop a fast, flexible geosphere transport simulation capability, running on MP computers and networked workstations.

One of our objectives this year was to transition the PorSalsa effort into the geoscience and weapon safety communities. This code has been the driver in a series of contracts to perform large-scale, high-resolution simulations of flow in heterogeneous fractured granite formations. We based calculations on 50 realizations of formation properties with flow simulations performed on a high-resolution mesh composed of over 1 million grid points. We performed the runs on 20 processors on Sandia's DEC8400 parallel machine, requiring a total time of about 17 hours for all 50 realizations. This rapid turnaround time allowed the entire suite of simulations to be run overnight. Another important product of this work is a new, powerful way to model flow in fractured media made possible by combining new geostatistical methods of representing spatially correlated heterogeneous formation properties and high-resolution numerical modeling. We used raw statistical data on the fractured geology to construct a fractured continuum model of permeability and porosity

A massively parallel (MP) geosphere transport model will overcome these limitations and place Sandia in an advanced position with respect to repository simulation capabilities.

distributions that we used directly in the flow simulation. The result is a realistic representation of a discretely fractured medium. We had several other accomplishments, as well.

- We implemented and verified an advective/dispersive, reactive, multispecies transport capability. The implementation allows the use of fully heterogeneous auxiliary data (including the advective Darcy fluxes from a previous flow simulation) in parallel processing.

- We completed and demonstrated the capability to fully utilize geostatistical data in flow simulations. The implementation is very general, allowing specification of common statistics such as random, normal, and log-normal distributions, and can also use correlated heterogeneity as generated with geostatistical simulation (GSLIB), the de facto standard used in the Sandia geoscience community.

- We implemented several thermodynamic equation-of-state (EOS) upgrades to facilitate the calculation of phase appearance/disappearance with our persistent variables thermodynamic formulation. These upgrades enabled the solution of several phase-transition problems, including complete dryout (two-phase to single-phase gas) in a heatpipe problem, flashing calculations (single-phase liquid to two-phase), and a fill-up, moving water table problem (two-phase to single-phase liquid). Even though these results are encouraging, the algorithm is not robust enough and needs further study.

- We implemented a general atmospheric boundary condition (BC). This is a generalization of a seepage boundary, usually applied in the context of isothermal unsaturated flow, to the general case of nonisothermal, two-component situations. We can use this capability to formulate other coupled BCs, such as for a study of fuel spills involving fire safety for the weapons program. It is also useful for nuclear repository and underground research laboratory applications where the exchange of fluids and heat between the drift and subsurface must be modeled. As well, specified hydraulic head and liquid pressures may be used as initial and BCs as surrogates for water density.

- We implemented the capability to compute gas- and liquid-phase Darcy fluxes and heat fluxes via a projection method, which results in a continuous field. These quantities can be output to an Exodus II file for visualization or use in advective solute transport. The capability is fully functional for execution on serial and parallel machines. We also added several useful output variables for visualization, including

liquid- and gas-phase mass fractions, hydraulic head, liquid- and gas-phase densities, and phase pressures.

- We formulated an implementation plan that enables a very general model for treating fractured and/or aggregated media by a dual continuum approach in the present code architecture.

Other Communications

Hopkins, P. L., and M. J. Martinez. 1999.
“Implementation of Species Transport.” Sandia internal memorandum to distribution (28 September).

Hopkins, P. L., M. J. Martinez, and P. C. Reeves. 1999. “Summary of Enhancements to PorSalsa.” Sandia internal memorandum to distribution (October).

Martinez, M. J., and P. L. Hopkins. 1999.
“Implementation of Flux Calculations.” Sandia internal memorandum (19 April).

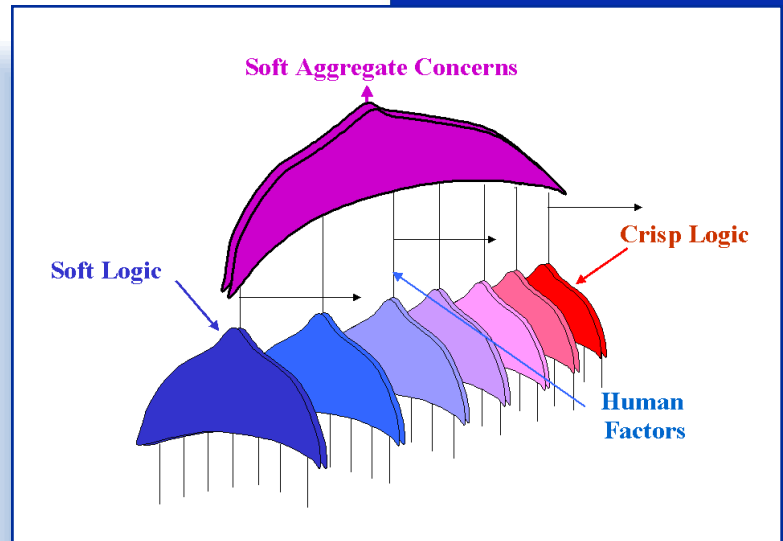
Reeves, P. C., S. A. McKenna, A. H. Treadway, E. K. Webb, M. J. Martinez, and P. L. Hopkins. 1999.
“Intercomparison of Flow Calculations for H-12 Reference Fractured Rock, Final Report on Stage 2 Calculations.” Report submitted to Japanese Nuclear Cycle Development Institute (June).

Reeves, P. C., S. A. McKenna, A. H. Treadway, E. K. Webb, M. J. Martinez, and P. L. Hopkins. 1999.
“Intercomparison of Flow Calculations for H-12 Reference Fractured Rock, Progress Report on Stage 1 Calculations.” Report submitted to Japanese Nuclear Cycle Development Institute (April).

Reeves, P. C., S. A. McKenna, A. H. Treadway, E. K. Webb, M. J. Martinez, and P. L. Hopkins. 1999.
“Intercomparison of Flow Calculations for H-12 Reference Fractured Rock.” Report submitted to Japanese Nuclear Cycle Development Institute (15 March).

SURETY SCIENCES

Surety Sciences is one of Sandia National Laboratories' six LDRD Roadmap Technologies investment areas. Roadmap Technologies derive their scientific basis from and extend the applications of Research Foundations investments into new areas. Roadmap Technologies create or accelerate scientific and technical expertise for future program areas that are strategic to Sandia and important to the DOE and the nation.



The new field of Surety Sciences focuses on researching and developing technologies that ensure reliable performance, safe environments, and security against malevolent attacks. Surety is defined as confidence that a system will perform in acceptable ways in both intended and unintended circumstances. The Surety Sciences investment area invests in research with the potential to impact National Security (NS) applications through (1) studies in integrated methodologies and technologies, (2) development of robust surety principles, (3) examinations of how systems fail, (4) creation of validation models for sure system designs, and (5) simulation capabilities that lead to predictive capabilities.

The "Hybrid Processing of Measurable and Subjective Information in Surety Analysis" project is investigating surety concepts in high-consequence decision making that, of necessity, combine both subjective (e.g., judgment calls) and objective (e.g., measurable, computational) inputs.

Traditional tools are best suited for assessing strictly objective information. This project is researching and developing a hybrid, mathematics-based process that allows precise tracking of the degree of subjective information in a decision output. The process has the potential to improve the information considered by decision makers responsible for high-consequence systems in abnormal environments.



3520340000

Hybrid Processing of Measurable and Subjective Information in Surety Analysis

J. A. Cooper

Conventional system-surety analysis is basically applicable only to measurable or physical-model-derived data. However, most analyses, including high-consequence system-surety analysis, must also utilize subjectivity. There has been considerable effort on analytically incorporating engineering judgment. For example, Dempster-Shafer theory establishes a framework in which frequentist probability and Bayesian incorporation of new data are subsets. Although Bayesian and Dempster-Shafer methodology both allow judgment, neither derives results that can indicate the relative amounts of subjective judgment and measurable data in the results. Sandia is deriving a hybrid-mathematics-based subjective process that allows precise tracking of the degree of subjective information in the output, thereby providing more informative and appropriate results.

Also, most high-consequence systems have difficult-to-analyze features under conventional approaches. For example, in our nuclear weapons program, we must determine the probability that a weapon responds safely when exposed to an abnormal environment. There are also nonprobabilistic DOE and DoD requirements (e.g., for determining the adequacy of positive measures). The type of processing required for these and similar situations transcends conventional probabilistic and human factors methodology.

We conducted literature, conference, and personal contact searches of methodologies applied by others to subjective processing and followed this by significant developments of our own origination. We emphasized four approaches with the aim of incorporating them into our tool set:

(1) We completed our development of contest methodology, which allows entities to compete for success (or failure). The mathematical result is the possibility of prevailing for each entity. We also found an externally developed solution to the probabilistic portion of contests, which we will incorporate into the objective portion of our tool set.

(2) We completed fuzzy anding (where the satisfaction of the AND logic has a degree, rather than a crisp yes or no) and fuzzy oring (where the satisfaction of the OR logic has a degree). These are important in serial and/or parallel arrays of

Sandia is deriving a hybrid-mathematics-based subjective process that allows precise tracking of the degree of subjective information in the output, thereby providing more informative and appropriate results.

similar but not identical components, which are difficult to treat with conventional methodology because they may not respond identically.

(3) Development of a new decision-based methodology, which we term *soft aggregation*, is well along in development. This involves the nonlinear combination of decision factors and comparison with a non-abrupt decision threshold.

(4) We developed the preliminary structure for a subjective processing addition to conventional Dempster-Shafer theory.

All of these can provide possibilistic information processing as well as probabilistic (multiple-value degree of membership as well as probability distributions). We completed these mathematical structures and improved our software methodology through Windows control features, incorporation of a Windows graphics package, and a clearer display of the involvement of subjectivity in determining output values and uncertainty.

We completed the constrained mathematics methodology and conducted a workshop on the status of our methodology for the International System Safety Society Conference. We also continued incorporating our newest methodologies (subjective modification to the Dempster-Shafer model and soft aggregation) into the existing software.

Refereed

Cooper, J. A., and S. Ferson. 1999. "New Mathematical Derivations Applicable to Safety and Reliability Analysis." *Safety and Reliability* 2 (European Safety and Reliability Conference, Munich, Bavaria, Germany, 13–17 September): 975–980.

3520350000

Computer-Network Vulnerability-Analysis Method

L. P. Swiler, B. P. Van Leeuwen, D. E. Ellis, S. Y. Chakerian, C. A. Phillips

Current network-security tools check a laundry list of potentially exploitable holes but do not consider the network configuration in conjunction with a set of attacks. Sandia has developed an approach to model vulnerabilities in computer networks and is implementing this approach in a prototype computer tool. The tool will systematically identify the set of most effective attacks on a network resource and identify the universe of possible negative consequences from a security breach.

Our method uses an attack graph to represent all possible attack paths. We automatically generated this graph by matching a database of known or hypothesized attacks with specific network configuration and topology information and an attacker profile. Graph nodes represent attack stages; arcs represent attack steps. Local overwrites to the configuration file or attacker profile represent malicious changes to network configurations and attacker learning/acquired capability respectively. Edges are weighted by estimated success probability or cost. Using shortest-path algorithms, we can represent all near-optimal attack paths (low cost or high probability). As a set, these paths represent the most vulnerable portions of the network.

We developed a PERL program that searches a network and automatically generates configuration information. We stored this information (including hardware types, operating systems, and vulnerabilities on machines) in a configuration file. We also created an initial library of attack templates. Each attack template contains a listing of requirements and a list of vulnerabilities and capabilities acquired by or deleted from the system state when the template is instantiated in the full attack graph. When the requirements are met, an edge is added to the attack graph along with a new node. This new node contains the extra vulnerabilities and capabilities gained as the result of the edge transition.

The graph-generation program matches the information in the configuration file to the templates in the template library, then generates an attack graph. The attack graph shows all of the potential attack steps that are allowable based on the

Sandia has developed an approach to model vulnerabilities in computer networks and is implementing this approach in a prototype computer tool. The tool will systematically identify the set of most effective attacks on a network resource and identify the universe of possible negative consequences from a security breach.

network configuration and the attack requirements. The network configuration is locally overwritten as the graph is generated, representing new vulnerabilities or configuration changes that take place as a result of the attacker actions. This dynamic updating of the graph is crucial to proper identification of attack paths.

The graph generator is a C++ program that creates the attack graph and populates the edges with edge weights representing a security metric of interest such as time or probability of success. Currently, our graph analysis program calculates a concise representation of all epsilon-optimal or near-optimal paths (all paths that have a distance less than or equal to $[1+\epsilon]$ times the shortest-path distance). We can generate specific paths from this representation (there are exponentially many, so in general we will not enumerate). The analysis code also computes the number of near-optimal paths that cross each edge. We linked the graph-generation and analysis program with a user interface developed in Tcl/Tk (Tool Command Language/Tool Kit). The user interface is a menu that allows the user to specify basic parameters for the graph generation, run the graph generator, analyze the graph, and view the output. We draw and display the attack graph with a program called *dot*, which is public release software for drawing general graphs.

One of the most challenging implementation issues has been determining how to curb the combinatorial explosion of the attack graph by eliminating redundant or non-interesting paths. We increased the efficiency of suppression of (directed) cycles by keeping a list of ancestor or antecedent attack templates in each node data structure and suppressing these templates when generating from these nodes. We identified more general ways to do this. We must also suppress the generation of multiple paths that differ only in the ordering of independent steps. We plan to do this by enforcing an ordering but we need to be very careful that we are not eliminating combinations that lead to a different set of vulnerabilities (or with different costs).

We made some major changes in our template and node definitions recently. These changes allow more powerful logic processing within the template; for example, the template may apply to all versions of an operating system before a particular release, and requirements can involve arbitrary logic operations such as AND, OR, and NOT. However, the changes require serious revisions to our data structures, template parser, and graph-generation code.

We increased the efficiency of suppression of (directed) cycles by keeping a list of ancestor or antecedent attack templates in each node data structure and suppressing these templates when generating from these nodes.

Refereed

Phillips, C. A., and L. P Swiler. 1999. "A Graph-Based System for Network-Vulnerability Analysis." *Proc. New Security Paradigms Workshop 1* (April) (Charlottesville, VA, 22–25 September 1998): 71–79.

3520360000

Approximate Public-Key Authentication with Information Hiding

T. J. Draelos, R. C. Schroepel, C. L. Beaver, E. V. Thomas, V. A. Hamilton, H. L. Scott

In many situations, it is desirable to authenticate data without revealing the data in detail. Encryption alone cannot solve this problem. Additionally, certain data are prone to statistical variation, thus creating difficulties for consistent authentication results using standard digital authentication techniques. Gamma spectra are also examples of statistically variant data. Finally, public-key cryptographic techniques are often useful in situations where one authenticating party seeks to convince multiple verifying parties or when the origination of data must be verifiable (nonrepudiation). In this project Sandia will investigate and develop digital public-key mechanisms that can be used to authenticate data prone to statistical variation and to investigate techniques for hiding data details while still proving the authenticity and integrity of the data.

We identified two approaches to the approximate authentication with information-hiding problem. We are investigating both of these approaches with respect to the weapon-monitoring application and the biometric application.

The first approach involves coalescing a statistically variant input signal into a consistent image that we can then authenticate using standard public-key techniques, and encrypt or hash to hide the image. This approach was realized by other researchers using error correction coding techniques and applied to biometric identification. We developed the second approach, which involves the retention of information in the original signal in a statistical sense while provably hiding the original data. This second approach is noninvasive in the sense of allowing users to utilize the same statistical authentication measures and evaluations on the measured signal that are used without any information hiding. The algorithm for hiding the original data involves permuting the original signal, applying a linear transformation, and then permuting the transformed signal. Through this process the output signal becomes independent and identically distributed. Under this condition, the individual elements of the output signal or vector are completely uncorrelated.

Sandia will investigate and develop digital public-key mechanisms that can be used to authenticate data prone to statistical variation and to investigate techniques for hiding data details while still proving the authenticity and integrity of the data.

3520370000

New Network Analysis Approaches to Evaluate Infrastructure Risk and Reliability

G. D. Wyss, D. G. Robinson, C. A. Phillips, R. G. Cox

Virtually all critical infrastructures deliver their goods and services through the use of a network. As the protection of critical infrastructures has recently become a national priority, it is increasingly important that means exist to assess the surety of these infrastructure networks in light of such factors as aging, new technology, emerging cyber and terrorist threats, increased competition, and a changing regulatory environment.

Sandia has extensive background in the area of network analysis. However, limitations in current network analysis techniques and the sheer size of typical infrastructure networks have combined to make it difficult or impossible to answer a number of questions that are important to network surety analysts. These questions relate to the performance of a network under conditions where capacity is limited, and supply and demand for services are uncertain. In addition, classical network analysis techniques become insufficient when characteristics of autonomous groups of consumers become complex, gaming behaviors become significant, uncertainties are large, or fixed costs dominate.

This project will develop mathematical methods to solve network design, equilibrium, and emergency response problems, and to adapt those solution techniques to parallel computer architectures. To accomplish this, we will extend existing classical techniques (including a method for which patent has been applied), and hybridize them with advanced techniques to develop an analytic toolkit for network surety issues. Advanced solution methods to be considered for hybridization include stochastic search techniques, simulated annealing, and evolutionary techniques (e.g., genetic algorithms, agent-based approaches). Since hybrid methods will require extreme computational power, the project will investigate methods to implement them on the Sandia parallel computer architectures.

The project will also qualitatively characterize the relative merits of different network architectures to provide guidance to network designers who do not have access to these sophisticated techniques and computational tools.

Sandia has extensive background in the area of network analysis....This project will develop mathematical methods to solve network design, equilibrium, and emergency response problems, and to adapt those solution techniques to parallel computer architectures.

We examined many available network analysis methodologies, including game theory and optimization theory, and identified a gap in the existing technology base. Current methods do not provide for probabilistic and systematic examination of the universe of infrastructure scenarios without computationally inefficient Monte Carlo simulation.

To fill this gap, we developed a new methodology called *object-based event sequence trees* (OBEST). An OBEST can probabilistically explore the universe of possible scenarios that might arise from a set of initial conditions much like a traditional event tree analysis. Yet, unlike an event tree, OBEST sequences support variable event ordering and are derived from an object-based system behavior model. Thus, many analyses can be derived from a single system model.

OBEST embodies each component or infrastructure element in an object model that describes its internal behavior and external interactions. Each object is capable of both immediate and delayed reactions (both deterministic and probabilistic) to internal and external stimuli. We connected component objects based on the influences they exert upon each other to form the system object model. We analyzed the system object model by following the sequence of events experienced dictated by the objects through a series of nonuniform time steps from an analyst-specified initial condition. Probabilistic branching is possible at each timestep, so a variation of the depth-first search algorithm determines branching behavior. When a scenario is completed, the algorithm recursively retrieves and completes another incomplete path in the same manner until the scenario space is exhausted (subject to truncation constraints). We computed the probability of each scenario deterministically by appropriate combination of the relevant branch probabilities. We will group scenarios with similar characteristics according to criteria supplied by the analyst.

We are developing a realistic validation problem set in collaboration with FEMA (the Federal Emergency Management Agency) and the city of Carlsbad.

Other Communications

Miller, L. A. 1999. "Aviation Safety Modeling and Simulation." Presentation to Team Coordination for Modeling and Simulation Subelement in Aviation Operations System Base for the Aviation Safety—NASA Ames Research Center, Moffett Field, CA, 9 April.

...we developed a new methodology called object-based event sequence trees (OBEST). An OBEST can probabilistically explore the universe of possible scenarios that might arise from a set of initial conditions much like a traditional event tree analysis.

3520380000

Improved Tools for Identifying and Quantifying Potentially Dangerous Human Actions

J. A. Forester, D. W. Whitehead, V. J. Dandini, D. P. Miller

Human reliability analysis (HRA) is a critical component of probabilistic risk assessment and is an important tool for understanding human errors in complex adaptive systems. HRA is needed to assess the potential for human error in high-consequence arenas such as medicine, military command and control, and aviation. Sandia is developing a new HRA method (a step-by-step process) that will allow us to identify and quantify certain dangerous human actions that have been observed in serious accidents and that are not treated by existing HRA tools. These errors include errors of commission. The result will be a product that we can use to reduce human error in many different high-consequence domains.

- We performed and documented detailed retrospective analysis of three human-caused aircraft accidents in terms of the HRA model perspective being developed. The three airplane accidents analyzed included the American Airlines controlled-flight-into-terrain (CFIT) accident near Cali, Colombia; the British Midland Airways Boeing 737 partial-loss-of-engine crash near Kegworth, England; and the China Airlines Airbus crash that occurred on approach for landing at Nagoya Airport, Japan. Analysis of these events helped in understanding the nature of cockpit performance and pointed out important differences between cockpit and nuclear power plant control-room human performance characteristics. The documented event analyses are essentially complete, but will probably be revised as the method development continues.

- We identified a set of critical functions required to keep an airplane from crashing and represented them in a set of event trees. We used the Kegworth crash as an example accident scenario and documented the critical functions related to the survivability of a generic commercial airplane in the event trees. Our current general approach for the overall search process involves identifying base case and deviant accident scenarios (for classes of airplanes) with a focus on those scenarios with a high potential for a strong error-forcing context. We expect the base case scenarios to be standard training scenarios in which an initiating event (e.g., an engine failure or a navigation error) occurs and will use it as the basis

Sandia is developing a new HRA method (a step-by-step process) that will allow us to identify and quantify certain dangerous human actions that have been observed in serious accidents and that are not treated by existing HRA tools....The result will be a product that we can use to reduce human error in many different high-consequence domains.

for deriving the deviant scenarios. The deviant scenarios are reasonably possible but do not progress in a predictable manner. We will examine the interaction between the unexpected behavior of the airplane and normal human information processing strategies to identify potential unsafe human actions. We will extend or develop models of human information processing as necessary to facilitate this process.

We developed a basic search process and quantification process and are performing a preliminary application/test of the process before completing initial documentation. Once we complete the preliminary test, we will complete the draft documentation for use in more rigorous tests.

3520390000

Advanced Signal Processing for Thermal Flaw Detection

M. T. Valley, A. Urbina, T. L. Paez, B. D. Hansche, D. M. Ashbaugh

Dynamic thermography is a promising technology for inspecting metallic and composite structures used in high-consequence applications. This technology has demonstrated the ability to detect, identify, and quantify hidden flaws at levels that in many applications dramatically exceed the capabilities of competing nondestructive inspection technologies such as radiography and ultrasound. However, the reliability of this emerging technology is limited by the need for extensive operational experience and the use of human judgment and visual acuity to detect flaws in the large volume of collected infrared (IR) image data. The inspection speed, reliability, and sensitivity, as well as cost-effectiveness of this promising technology, can be significantly improved with advanced physics-based signal-processing algorithms.

The objective of this project is to develop, characterize, and validate automated flaw-detection software for dynamic thermography. Sandia will tailor the underlying analysis algorithms—robust in the presence of realistic noise—to the physics of the inspection process. This report documents the progress made in the development of the data-analysis algorithms. Specifically addressed areas include thermal modeling, noise characterization, selected measurable metrics, and preliminary algorithm test results.

Preliminary finite-element modeling (FEM) results, corroborated by experimentation, demonstrated that thick paint affects inspection sensitivity. Therefore, we expanded the modeling effort to investigate paint influences on flaw detection. Accomplishments include the following:

- We developed software to convert 16-bit image data into an analyzable format. We compressed the acquired image data with a proprietary algorithm that precludes direct analysis with the developed software.
- We completed FE thermal modeling to support the development of automated data-analysis software. The modeled systems included metallic structures with material thinning and bonded metallic structures with disbonds. The model parameters studied included variations in paint thickness (including no paint) and flaw characteristics (e.g., size, shape, depth, etc.).

The objective of this project is to develop, characterize, and validate automated flaw-detection software for dynamic thermography. Sandia will tailor the underlying analysis algorithms—robust in the presence of realistic noise—to the physics of the inspection process.

- We wrote a program to convert the FE temperature results into equivalent thermal images. By integrating the expression for spectral photon flux exitance for a gray body over the camera spectral operating range, we can compute the total flux exitance from the modeled inspection surface. This exitance, together with the optical system transmission and F/#, defines the image plane irradiance (flux density) that would be produced by the simulated inspection surface. We can convert the computed image plane irradiance to grayscales using the known detector noise equivalent photon flux and sensitive flux range. We performed the integration using Gauss-Laguerre quadrature.

- We statistically characterized the noise found in real thermal images. The noise level varies based on the calibration method used to perform the detector nonuniformity correction. However, in the worst case the detector noise is approximately normally distributed with a fluctuation standard deviation/mean $< 0.1\%$ after the nonuniformity correction is performed. Without the correction, the standard deviation/mean is typically 1.5 to 2 %. The maximum noise fluctuation levels provide a noise-equivalent detectable temperature (NEDT) less than 0.025°K . However, practical considerations suggest the high-reliability NEDT is 0.1°K . For modeling purposes, we conservatively used a noise standard deviation level of 1% of the mean value.

- The thermal inspection system IR camera measures the signal emitted from the surface as a function of time. This signal is directly related to the surface temperature $T(x,y,t)$. From an evaluation of the heat diffusion equation and experimental results, we were able to identify two measurable metrics for highlighting the presence of internal structural defects. Both the time rate of change of the internal energy and the net lateral conduction heat flux along the surface highlight the presence of internal flaws. We are investigating methods for coupling these metrics to improve flaw-detection sensitivity.

- We developed preliminary data-analysis algorithms. The initial algorithm evaluations successfully demonstrated robust flaw-detection capabilities in metallic structures. Further, the results suggest that the algorithm may also be suitable for quantitatively characterizing the flaw (e.g., specifying flaw size and depth, per cent material loss, etc.). Though further work is needed, preliminary results for unpainted specimens indicate that the developed algorithm should reliably find 0.125-inch flaws in 12-inch x 12-inch inspection regions (camera images

The initial algorithm evaluations successfully demonstrated robust flaw-detection capabilities in metallic structures. Further, the results suggest that the algorithm may also be suitable for quantitatively characterizing the flaw....

12-inch-square region with each frame). The results for painted specimens vary with paint thickness.

- Analytical and experimental investigations of painted specimens identified a transition region in the time rate of change of the internal energy that provides information about the required camera frame rate. The presence of a sharp transition region highlights the need for faster acquisition rates. The focal plane array camera being used in the experimental work has adjustable frame-rate capabilities with a maximum achievable speed of about 1400 frames per second. Experimental results confirmed that the transition region becomes smooth when the appropriate frame rate is used.

3520410000

Production Surety and Disruption Vulnerability Analysis

D. A. Jones, C. R. Lawton, M. A. Turnquist, G. F. List, W. E. Hart, C. A. Phillips

The goal of this project is to develop new capabilities for improving production and transportation surety in the nuclear weapons complex (NWC). The benefits of the effort will include increased efficiency, reduced vulnerability to disruption, and increased ability to meet schedules with high confidence.

We produced a document describing the surety science tools and techniques applicable to system planning for manufacturing and transportation. Four main algorithmic threads emerged from the literature review: (1) stochastic programming, (2) decision analysis/statistical decision theory, (3) dynamic programming/Markov processes, and (4) stochastic optimal control. The main differences among them are the way in which the system is described (e.g., algebraic equations, probabilistic transition matrix, first-order differential equations), the objective function(s) applied (e.g., maximize output, minimize variance), and the process by which optimal solutions are found.

Stochastic optimization (SO) is arguably the most useful of these tools insofar as manufacturing and transportation planning are concerned. We designed an extension of linear programming (min cTx subject to $Ax = b$, $x, \geq 0$), SO to find robust optimal solutions to complex problems involving uncertainty. Uncertainty can be introduced into the c , A , b , or any combination thereof. The choice variables x are broken down into two *categories*: those that are deterministic (set X_d) and those that are stochastic (set X_s). In so-called *two-stage* problems, the X_d first-stage decision variables transcend all outcomes and are set to hedge against uncertainty. The X_s variables specify how the scenarios will be accommodated given the master (or first-stage) decisions.

Three methodological tools in the SO arsenal appear to have particular promise for the types of problems that need to be considered in the NWC. They are chance-constrained programming (CCP), stochastic decomposition (SD), and importance sampling (IS).

We formulated a production planning example as a stochastic optimization. We focused on the production capacity planning model of the NG facility. We highlighted uncertainty

The goal of this project is to develop new capabilities for improving production and transportation surety in the nuclear weapons complex (NWC).

in three principal parameters: workstation availability, process duration, and step-specific yields. The computational experiments illustrated the effects of those uncertainties and provided indications of how stochastic optimization might allow us to design robust systems.

The stochastic formulation—one of successively introducing uncertainty in key resource and process parameters—shows the very dramatic effects that uncertainty in a few key parameters can have on complex models used for production planning. It also indicates the importance of continued effort to better understand surety in production systems and to develop tools for making effective production plans under uncertainty.

Finally, we formulated a fleet-sizing model that addresses stochastic conditions. We used the model to explore both the tool (SO) and the insights gained from its use in the context of DOE's Transportation Safeguards. Implementation of the tool was a success, and the results demonstrated that future uncertainties do play a major role in affecting the optimal overarching decisions to select. Given four potential future demand scenarios, the overarching optimal fleet investment decisions were quite different from those that would pertain for any one of the scenarios individually, or for the conditions implied by taking the average of the four scenarios.

The stochastic formulation...shows the very dramatic effects that uncertainty in a few key parameters can have on complex models used for production planning.

3520420000

An Optically Triggered Semiconductor Switch for Firing Systems

G. M. Loubriel, A. Mar, S. C. Holswade, H. P. Hjalmarson, A. G. Baca

Conventional high-current firing sets are complicated, demanding systems that require special switches. For Defense Program (DP) applications we use a sprytron, an electrically triggered, hand-assembled vacuum switch (3 kV/3 kA). This project will develop an optically triggered gallium arsenide (GaAs) switch that performs as a sprytron with the added advantages of semiconductor batch manufacture, compactness, optical isolation, and low jitter. The main challenges in making this device a reality are switch longevity (> 100 pulses) and ease of use. Recently, these switches triggered sprytrons at 500 V and 80 A (meeting voltage, loss, off-resistance, radiation-hardness specs) for thousands of pulses. The results of this low-current study, and improvements in longevity at even lower currents (~ 10 A), show that it is feasible to meet the demanding requirements of the firing-set application. The techniques that Sandia will use to improve longevity at kiloamp currents all rely on spreading the current by using either state-of-the-art semiconductor processes such as epitaxial growth, regrowth, and diffusion, or using improved switch geometries. Such a switch would result in dramatically reduced size, reduced part count, and enhanced surety of firing sets for nuclear weapons (including stockpile retrofit). Surety is enhanced because it enables new architectures, has small size to increase its high-g tolerance and free volume for features such as joint test assemblies, is optically isolated, and allows for state-of-health monitoring. Other switch applications are direct optical ignition, Q-switching lasers for the X-1 accelerator, ground-penetrating radar (GPR) for environmental site reconnaissance, sensors in low-visibility environments, and high-power microwave generation.

The filamentary nature of the current produces very high current densities at the semiconductor-to-metal interface in high-gain photoconductive switches and causes switch degradation at high currents. Our standard p-i-n switches yield about 10,000 pulses with lots of damage on the *p* contact. To improve longevity we pursued metal contacts made with deep dopant diffusion. Diffused (*p*-side) switches have shown little degradation in 50 million pulses at 13 A per filament. A p-i-n

Such a switch would result in dramatically reduced size, reduced part count, and enhanced surety of firing sets for nuclear weapons (including stockpile retrofit).

switch with diffusion only in the p side was triggered 50 million pulses at 13 A, 3.5 ns duration pulse, 2.0 to 2.2 kV charge. We stopped the test because the switch was misfiring due to damage at the n contact. We also performed tests at 9 kV (forward bias), 80 A, and the switch survived for 2,000,000 pulses with similar n -side damage. For firing set applications, we require very high switch-off resistance prior to triggering and, thus, the switches must be reverse-biased. We stopped a test of a reverse-biased p-i-n switch with diffusion on the p side after 10,000 pulses at 30 A, 3.5 ns, 5.0 kV, because of p -contact damage. We also carried out tests at 1 kV in a firing set circuit, but the switches were too conducting, did not hold voltage, and were not tested for longevity.

We also developed multiple filament triggering configurations to improve longevity further at low currents and short pulse duration (100 A and 3 ns). The more normal trigger geometry produces a strong, sharp filament. We carried out longevity tests in both geometries at low and high currents. The diffused triggering geometry shows some improvement at low currents but not at 1 kV/1 kA. Other structures under investigation at low currents rely on epitaxially grown contacts such as metalorganic chemical vapor deposition (MOCVD) regrowth. Another mechanism that has shown improvements in longevity is neutron irradiation. The great advantage of the neutron irradiation is that it also improves radiation hardness. We used neutron-irradiated GaAs to a dose of 1 E14 rads to obtain well over 1,000 pulses in forward-biased switches at 80 A and over 300 pulses with reverse-biased switches. The neutron irradiation activated the metals in the switch; thus, we decided to irradiate the bare wafers and then process them into switches. We found that the switches did not hold voltage, a problem that we traced to the annealing of the irradiation damage. We reduced the resistance of the switch from 1 GOhm to 200 MOhm, and the voltage hold-off drops from 820 V to 600 V by reversing the irradiation and metallization steps.

- *Longevity and jitter results trigger a sprytron.* We tested whether the photoconductive semiconductor switch (PCSS) could trigger a sprytron—and tested the longevity of the PCSS and the sprytron jitter under these conditions. *Longevity:* We tested 400 pm gap switches forward- and reverse-biased with neutron doses of 1 E 14 and 3 E 14 rads and the 0.5 mm gap n-i-n switches, and they all triggered the sprytron for more than 1,000 pulses. At current levels of 80 A, we obtained excellent longevity for this application two different ways: (1) p-i-n forward-biased switch (400 pm gap) at 480 V and obtained

The great advantage of the neutron irradiation is that it also improves radiation hardness.

- 2,000 pulses, and (2) n-i-n switch, 500 pm gap, 540 V, > 10,000 shots (> 700 V hold-off). We also tested the system jitter in a variety of ways and obtained values that range from 1.55 ns to 2.71 ns. The peak current delivered to the sprytron is heavily dependent on inductance. We tested two circuits: a large strip line circuit with $C=2$ nF, $L=30$ nH that resulted in 80 A at 500 V and a small, low-inductance, capacitor discharge unit (CDU) tester circuit $C=1.4$ nF, $L=3.8$ nH that also gave 80 A but at 240 V.

Refereed

Loubriel, G. M., J. F. Aurand, G. J. Denison, L. Rinehart, D. J. Brown, F. J. Zutavern, A. Mar, M. W. O'Malley, W. D. Helgeson, and L. Carin. 1999. "Optically-Activated GaAs Switches for Ground Penetrating Radar and Firing Set Applications." *Proc. 12th IEEE Pulsed Power Conference* (Monterey, CA, 28 June).

Mar, A., G. M. Loubriel, F. J. Zutavern, M. W. O'Malley, W. D. Helgeson, D. J. Brown, H. P. Hjalmarson, and A. G. Baca. 1999. "Doped Contacts for High-Longevity Optically Activated, High-Gain GaAs Photoconductive Semiconductor Switches." *Proc. 12th IEEE Pulsed Power Conference* (Monterey, CA, 28 June).

Other Communications

Baca, A. G., *et al.* 1999. "Tailored Doping Profile for Photoconductive Semiconductor Switches." SD-6444, Albuquerque, NM (15 June).

3520430000

Source Code Assurance Tool

R. L. Craft, J. Espinoza, P. L. Campbell

While significant effort has gone into giving programmers the ability to develop software systems correctly from the start, human inspection and testing of code remains a key element in ensuring the code's correctness. Unfortunately, manual inspection methods are time-intensive, and existing tools do little to alleviate the problem. Given this, high-consequence software projects are often forced into one of two unacceptable outcomes—to slip delivery dates to finish manual inspections or to deliver code that has not been fully assessed. The quality of the assessment is also highly dependent on the analyst. Analyst biases and the sheer volume of things to be considered in an assessment can lead to critical problems being overlooked. For these reasons, a tool that increases the human analyst's level of performance in software assessment—in both terms of time invested and accuracy—would be of significant benefit.

Sandia will develop a software tool that assists the human analyst by automatically parsing a program's source code to map the causal relationships that exist between the source code elements. Using a browser developed as part of the tool, an analyst will rapidly discern how changes in one part of the software being assessed affect the rest of the software or the associated system, or how changes in the system affect the software. For the initial release of this tool, we will target the C++ language for the parser and will develop a browser that acts as a plug-in tool for the Microsoft Visual Studio. As time allows, we will add support for analysis of additional programming languages and different programming environments.

- *Research in current code slicing activities.* One of the primary goals for the year was the development of a slicer that parsed a subset of the C programming language. In a survey of the software tools market, we found a commercial-grade C slicer (CodeSurfer) that we could use to support our efforts. We believe that this represents the state-of-the-art in slicing capabilities.

- *Graphical front-end development.* We examined several different implementation platforms, including Visio Professional, Microsoft Visual Studio, and Platinum Paradigm Plus (an object-oriented [OO] CASE tool). We spoke with

Sandia will develop a software tool that assists the human analyst by automatically parsing a program's source code to map the causal relationships that exist between the source code elements.

Information Sciences Institute, which has built what they call a *design editor*. This is a research tool only. We also looked at Sun's Workshop Visual idraw, Xfig, Tfig, ivtools, graphdraw, Macao, FrameKit, EDGE, DiGraph, gnet, VGJ, Visual Thought, UCI Graph Editing Framework, Argo/UML (Unified Modeling Language), Rational Rose/RT, Visio, and Graph Layout Toolkit.

Each of these products had its various strengths and weaknesses. For our initial release, we settled on using a Visual Basic-based graphical user interface (GUI) and Visio as a reasonable implementation approach.

We published information about our work in the Information Assurance Technology Analysis Center's (IATAC) *IA Newsletter*. This led to an initial inquiry by Secure Computing Corporation which, in turn, led to very recent efforts to establish a collaborative research arrangement with them.

We were invited to participate in a DARPA (Defense Advanced Research Projects Agency) Information Assurance Security Engineering Tools workshop and were one of only three attendees invited to present our assurance methodology concepts. Based on the discussions held at this workshop, it appears that our system's approach to surety is well ahead of most other organizations.

- *Requirements and design*. We produced a document that describes the concept of operations for a source code analysis tool and the tool's functional requirements. We developed user-interface concepts and initial screen layouts. We identified the major building blocks that constitute the tool. We developed a plan segmenting the functional requirements into four major builds, along with a detailed plan for reaching all of the capabilities assigned to the first build.

...it appears that our system's approach to surety is well ahead of most other organizations.

Other Communications

Craft, R. 1998. "The Next Generation of Security Engineering Tools." *IA Newsletter* 2 (Winter): 1.

3520440000

System-Surety Life-Cycle Engineering

R. A. Sarfaty, S. Y. Goldsmith

System surety modeling currently lacks formalized overarching methods that scrutinize the engineering lifecycle commencing with abstraction and requirements-gathering. Object-oriented methodologies evolved to yield, inter alia, encapsulation, polymorphism, and inheritance. However, surety's security and availability balance are obviated by the Object-Oriented Unified Method (UM) modeling technique dynamic model, particularly user authentication, confidentiality, and nonrepudiation. UM also lacks cost/risk information, assessed through consequence modeling, thereby failing to address the system as a whole.

This project will expand each of UM's three models (object, dynamic, and functional) under systems engineering lifecycle, to include surety's components (reliability, user-authentication, data integrity, confidentiality, nonrepudiation), and incorporate the consequence model yielding bidirectional temporal cost analyses complemented with stochastic probabilistic risk assessment (PRA) or similar techniques.

The meta-modeling techniques (enhanced UM) would include object-based technology to ensure validation and cross-referencing among the four models. Surety objects would gain cognition through a dynamic knowledge base such as secure network segments, encryption algorithms, and vulnerability assessments resulting from natural and anthropogenic threats. Most knowledge-base repositories are static, requiring triggers for updates; conversely, surety objects would augment their knowledge dynamically (emergent behavior) based on empirical outcomes, hence serving as the filters to coalesce surety elements into the system's lifecycle.

Subsequently a tool development effort would deliver a modeling engine with graphical interfaces accessible to a systems/surety engineer. The engine that transparently performs system constraint validations to the user facilitates the modeling process. This allows for systems surety modeling without the UM expert knowledge while yielding robust and valid system designs throughout the lifecycle.

Using object role modeling (ORM) as the metamodel metalanguage, we validated two views for semantical robustness, namely the activity and the object views. We selected ORM due to its "natural language" accuracy and ease

This project will expand each of UM's three models (object, dynamic, and functional) under systems engineering lifecycle, to include surety's components..., and incorporate the consequence model yielding bidirectional temporal cost analyses complemented with stochastic probabilistic risk assessment (PRA) or similar techniques.

of interpretation. It should be noted that ORM is also used in certain professional circles to develop relational data repositories (i.e., databases); that is not the way we used ORM in this project. The activity view uses the IDEF0 technique, one that is proven and was developed for the U.S. Air Force in the late 1970s. The object view uses ORM itself to describe objects and their characteristics. We are incorporating the temporal (or dynamic) view and will perform a semantical robustness test. The last view, namely consequence, is also nearing completion and is mostly incorporated into the overall methodology. We conduct the semantical tests using CLOS; this code serves as a proof-of-concept for the project and provides the avenue for tool development in the future should additional research be funded on this topic.

Other Communications

Sarfaty, R. A. 1999. "Creating an Electronic Management System Architecture Using Object Role Modeling." *Cessi '99*, accepted.

3520450000

Integrated Approach to Develop Microelectromechanical System (MEMS) Reliability Tools

D. M. Tanner, D. L. Gregory, F. A. Brown, L. W. Irwin, M. T. Dugger, N. F. Smith, W. P. Eaton, J. A. Walraven

The burgeoning new technology of microelectromechanical systems (MEMS) shows great promise in the weapons arena. We can now conceive of microgyros, microsurity systems, and micronavigators that are extremely small and inexpensive. By solving MEMS reliability and failure issues, Sandia serves our primary defense program (DP) customer and provides applicable solutions to industry.

We integrated the individual research areas of failure and performance analysis, reliability characterization, and wafer-level reliability. This work has not been attempted before and will produce the knowledge that is essential for maintaining world-class MEMS status at Sandia. The overall goals of this work are (1) to perform statistical characterization, (2) to identify failure modes, (3) to develop reliability test structures, (4) to develop reliability models that account for temperature, humidity, cycles, operating speed, etc., and (5) to develop failure analysis tools for MEMS.

We focused successfully on MEMS reliability in weapons systems environments. We investigated humidity, shock, vibration, temperature, and storage life. We determined that storage life is the crucial issue to resolve before MEMS components can be used in weapons systems. We copyrighted and licensed computer software, Super μ Driver, to run MEMS devices and developed a method and apparatus to measure force on the microscale.

We showed humidity to be a strong factor in the wear of rubbing surfaces in polysilicon micromachines. We demonstrated that very low humidity can lead to very high wear without a significant change in reliability. We showed that the volume of wear debris generated was a function of the humidity in an air environment. As the humidity decreases, the wear debris generated increases. For the higher humidity levels, the formation of surface hydroxides may act as a lubricant.

We identified wear as the dominant failure mechanism in the humidity study. We also identified the wear debris as amorphous oxidized silicon (Si). Large slivers (approximately

By solving MEMS reliability and failure issues, Sandia serves our primary defense program (DP) customer and provide applicable solutions to industry....This work has not been attempted before and will produce the knowledge that is essential for maintaining world-class MEMS status at Sandia.

1 micron in length) of debris observed at the low humidity level were also amorphous oxidized Si.

To find an upper bound on susceptibility to vibration, the tests performed were four times the requirement for our typical system. The microengine performed quite well at these high levels, with 17 out of 22 functioning after the stress.

We performed tests using haversine shock pulses in the range from 500 g to 40 Kg (to up to twenty times the requirement for our typical system). The microengine performed quite well at these high levels with a majority functioning after the stress.

Some of our observations from the shock tests follow. Debris moved at levels greater than 4000 g, causing shorts in the actuators. Bond wire and packaging problems surfaced there also. The die-attach bond failed at 10 Kg, allowing the die to slam into the package lid. At 20 Kg we began to observe structural damage. Ceramic packages fractured at 40 Kg.

We analyzed potential effects on reliable MEMS operation due to thermal expansion of the polysilicon components. Modeling results indicate that this should not be a significant failure mechanism. While continuously observing a running microengine, we heated the wafer from room temperature (25°C) to 150°C in about 12 minutes. We saw nothing unusual in the microengine operation. At 150°C, we stopped and restarted the microengine several times without any problem. We probed several microengines, known to be functional at room temperature, and found them to be operational at 150°C, as well. We then cooled the wafer to 0°C in less than 14 minutes, again while continuously monitoring a running microengine. We stopped and restarted the microengine several times at 0°C. Again, the microengine operated flawlessly.

In storage tests, we have seen a dramatic improvement in microengine lifetime by using a newer die attach. Only one microengine has failed with the new die attach, and we predict a lifetime of six years. We identified storage life to be the crucial issue to solve before MEMS can be implemented in weapons systems.

Complex MEMS devices with multiple comb drives working together require function generators phase-locked together to operate. In addition, to improve lifetime, model-based drive signals are essential for smooth operation. Commercial software was not up to the task, which led to the development of flexible waveform-generation software and hardware. This system is referred to as *Super μ Driver*. The characterization of microactuators requires methods to

We identified storage life to be the crucial issue to solve before MEMS can be implemented in weapons systems.

measure force. We developed the Force Detector, which is a balanced microscale spring, and submitted a technical advance with a possible patent forthcoming.

Refereed

Tanner, D. M., W. M. Miller, K. A. Peterson, M. T. Dugger, W. P. Eaton, L. W. Irwin, D. C. Senft, N. F. Smith, P. Tangyunyong, and S. L. Miller. 1999. "Frequency Dependence of the Lifetime of a Surface-Micromachined Microengine Driving a Load." *J. Microelectronics Reliability* **39**(3) (March): 401–414.

Other Communications

Eaton, W. P., N. F. Smith, L. W. Irwin, D. M. Tanner, J. J. Allen, S. L. Miller, and W. M. Miller. 1999. "Characterization Techniques for Surface-Micromachined Microengines." *Proc. SPIE* **3514** (Micromachining and Microfabrication Symposium, Santa Clara, CA, September 1998): 171–178.

Miller, S. L., M. S. Rodgers, G. LaVigne, J. J. Sniogowski, P. Clews, D. M. Tanner, and K. A. Peterson. 1998. "Failure Modes in Surface-Micromachined Microelectromechanical Actuators." *Proc. IEEE Internat. Rel. Phys. Symp.* (Reno, NV, March): 17–25.

Peterson, K. A., P. Tangyunyong, and A. A. Pimentel. 1998. "Failure Analysis of a Surface-Micromachined Microengine." *Proc. SPIE* **3512** (Micromachining and Microfabrication Symposium, Santa Clara, CA, September): 190–200.

Peterson, K. A., P. Tangyunyong, and D. L. Barton. 1997. "Failure Analysis for MEMS." *Proc. 23rd Internat. Symp. for Testing and Failure Analysis* (Santa Clara, CA, November): 133–142.

Smith, N. F., W. P. Eaton, D. M. Tanner, and J. J. Allen. 1999. "Development of Characterization Tools for Reliability Testing of Microelectromechanical System Actuators." *Proc. SPIE* **3880** (MEMS Reliability for Critical and Space Applications, Santa Clara, CA, September): 156–164.

Tanner, D. M. 2000. "Reliability of Surface-Micromachined Microelectromechanical Actuators." (Invited keynote) *Proc. Internat. Conf. in Microelectronics* (Spring) (Nis, Yugoslavia, 14–17 May, 2000).

Tanner, D. M., J. A. Walraven, L. W. Irwin, M. T. Dugger, N. F. Smith, W. M. Miller, and S. L. Miller. 1999. "The Effect of Humidity on the Reliability of a Surface Micromachined Microengine." *Proc. IEEE Internat. Rel. Phys. Symp.* (International Reliability Physics Symposium, San Diego, CA, March): 189–197.

Tanner, D. M., K. S. Helgesen, J. A. Walraven, J. J. Clement, L. W. Irwin, F. A. Brown, and D. L. Gregory. 2000. "MEMS Reliability in Shock, Vibration, and Temperature Environments." *Proc. Internat. Rel. Phys. Symp.*, submitted.

Tanner, D. M., L. W. Irwin, W. P. Eaton, N. F. Smith, K. A. Peterson, and W. M. Miller. 1998. "Linkage Design Effect on the Reliability of Surface Micromachined Microengines Driving an Inertial Load." *Proc. SPIE* **3512** (Materials and Device Characterization in Micromachining, Santa Clara, CA, 21–22 September): 215–226.

Tanner, D. M., N. F. Smith, D. J. Bowman, W. P. Eaton, and K. A. Peterson. 1997. "First Reliability Test of a Surface-Micromachined Microengine Using SHiMMeR." *Proc. SPIE* **3224** (Micromachining and Microfabrication Symposium, Austin, TX, September): 14–23.

Tanner, D. M., S. L. Miller, and D. W. Plummer. 1999. "MEMS Actuators: Applications, Failure Modes, and Reliability." *Internat. Rel. Phys. Symp. Tutorial Notes* (San Diego, CA, 23–25 March): 3.1–3.54.

Tanner, D. M., W. M. Miller, W. P. Eaton, L. W. Irwin, K. A. Peterson, M. T. Dugger, D. C. Senft, N. F. Smith, P. Tangyunyong, and S. L. Miller. 1998. "The Effect of Frequency on the Lifetime of a Surface-Micromachined Microengine Driving a Load." *Proc. IEEE Internat. Rel. Phys. Symp.* (Reno, NV, March): 26–35.

Walraven, J. A., T. J. Headley, A. N. Campbell, and D. M. Tanner. 1999. "Failure Analysis of Worn Surface Micromachined Microengines." *Proc. SPIE* **3880** (MEMS Reliability for Critical and Space Applications, Santa Clara, CA, September): 30–39.

3520460000

Simulation/Optimization Tools for System-Variability Analysis

J. E. Campbell, E. W. Collins, K. D. Marx, S. D. Wix, R. J. Sikorski, R. F. Billau

Sandia has used electrical system simulation successfully over the past decade. Two common applications are (1) supporting the electrical system design process, and (2) analyzing anomalies detected in the fielded product. Simulation also has a future role in helping to predict failures when degradation precursors are identified. In short, electrical simulation is a tool that can be used during the entire product lifecycle to develop an understanding of the system over the range of expected conditions.

Electrical simulation typically treats a single data point in the very large input space of component properties. For electrical simulation to reach its full potential as a design tool, it must be able to address the unavoidable variability and uncertainty in component properties. Component variability is strongly related to reliability of the end product. This project addresses a set of problems that hinders effective use of simulation, especially in the context of understanding variability.

The first goal of this project was to create a novel linkage of disparate variability analysis approaches to greatly reduce the overall analysis time. There is an associated need for methodologies to effectively apply this toolset to a range of problem types. The second goal was to develop an approach to quantify the reliability impacts of variability, especially for time-dependent issues. We added variability analysis to the user interface, which is much easier to use by the design community.

I. Tool Linkage

We pursued two approaches to tool linkage.

- The first tool linkage used the following:

- Software for linked input vector generation and netlist formulation. First, the code converts an input vector file into a form that can be parsed and combined with a circuit file; this is a combination of SUNS (Sensitivity and Uncertainty Analysis Shell), which creates an input vector file of sample values, and some additional code that converts an input vector file into a form that can be parsed. Then the code actually parses the input vector and builds the circuit netlists.

Sandia has used electrical system simulation successfully over the past decade....electrical simulation is a tool that can be used during the entire product lifecycle to develop an understanding of the system over the range of expected conditions.

- The MPACTR (Massively Parallel Computer Resource) machine and Distributed Queuing System (DQS) to allow for program and input/output (I/O) management of multiple SPICE (Simulation Program with Integrated Circuit Emphasis) jobs.

- A set of custom software routines that automated the extraction of response variable values from output data.

- The second tool linkage approach capitalized on the graphical user interface (GUI). This interface effectively shields the user from the intricacies of the SPICE electrical simulation tool but provides enough control to the user to perform meaningful analyses. This provided an opportunity to enhance the project work to date in the following areas:

- It is a Web-based interface, which is much easier to use than SPICE

- It offers the potential for a more general interface solution, albeit at a cost of some user flexibility initially.

II. Tool Use Methodology

We identified and documented five tool applications and their methodologies:

- Design margin analysis

- Specification limits

- Anomaly investigation

- Lifetime prediction

- Probability quantification

III. W80 Firing Set Application

We applied the SPICE/SUNS tool to the W80 firing-set charging circuitry. We used SUNS and CHILISPACE for this application, with SUNS run on an NT machine and CHILISPACE run on the Computational Plant (Cplant). CHILISPACE is the parallelized version of SPICE developed by Sandia. Note that we executed the problem as a set of independent runs on the Cplant processors rather than as distributed runs.

The goals of the analysis were (1) to determine the major contributors to variability and (2) to actually model the variability of the firing set, given the assumptions on random part variability and behavior over temperature. We completed this analysis and documented the results. More importantly, we identified and resolved several issues (regarding both tools and approaches) during the course of this analysis.

IV. Other

We completed documentation for both SUNS and GO (the variability analysis software and optimization software, respectively) and obtained software copyrights on both.

Refereed

Bierbaum, R. L., R. F. Billau, J. E. Campbell, K. D. Marx, R. J. Sikorski, and S. D. Wix. 1999. "Final Report on LDRD Project: Simulation/Optimization Tools for System Variability Analysis." Sandia Technical Report SAND2000-8200, Sandia National Laboratories, Albuquerque, NM.

3520470000

A Massively Parallel Microsimulation Model of Infrastructure Interdependency

D. C. Barton, R. J. Pryor, K. L. Stamber, D. A. Schoenwald, D. L. Harris

The U.S. infrastructure is a complex system of interdependent elements whose continuous and stable operation is vital to national security. These interdependencies create tremendous vulnerabilities that must be understood and then managed to minimize the impact of deliberate disruptions, human error, or natural disasters to the surety of the infrastructure system.

To understand these interdependencies and the results of unexpected events, Sandia is developing a model of critical infrastructure interdependencies utilizing our unique microsimulation approach. This simulation technology capitalizes on recent technological advances in evolutionary learning algorithms and massively parallel (MP) computing. We model interactions among infrastructure elements individually by intelligent software agents representative of real-world decision makers. This modeling protocol can utilize thousands of agents to model very complex systems and offers several advantages over traditional modeling techniques for modeling infrastructure interdependencies. For example, unlike analytic models, functional forms of the model's endogenous relationships are not required. For problems where macroscale information is sparse or nonexistent, as is the case for infrastructure interdependencies, microsimulation models are differentiated in their capacity to utilize extensive sources of microlevel data to develop interaction forecasts.

Extending Sandia's existing microsimulation model Aspen to include rules and interactive agents for additional infrastructures will result in an improved simulation tool that can be used to study emergent behavior in extremely complex, interconnected infrastructure networks. We are developing agents representative of decision makers in the electric grid, communication, and fuel supply infrastructures, and retrofitting existing Aspen agents, i.e., industries, households, etc., with energy demand profiles. This expansion of Sandia's microsimulation framework will provide a credible model of the infrastructures most critical to the nation's economy and security. The final product will allow users to analyze implications of infrastructure system complexity on network

Extending Sandia's existing microsimulation model Aspen to include rules and interactive agents for additional infrastructures will result in an improved simulation tool that can be used to study emergent behavior in extremely complex, interconnected infrastructure networks....This expansion of Sandia's microsimulation framework will provide a credible model of the infrastructures most critical to the nation's economy and security.

stability and vulnerability and will provide a simulation tool for testing policy decisions, like deregulation, on infrastructure networks.

Development continued on a microanalytic simulation model, ASPEN-EE, that links telecommunication infrastructures (from Aspen) with the energy (electric, oil, and gas) infrastructure (from ENERGY 2020). We used Sandia's existing Aspen prototype model to define consumer demand for power and therefore energy. Power generation and energy supply agents took their general framework from the government agents of Aspen and were supplemented with logic processes based on market concepts that may result from restructuring and those already used in a regulated environment in ENERGY 2020.

The first concept developed from this analysis was agent aggregation. Developing a large-scale model of the electric grid utilizing Aspen's economic agents (in a modified form) as electric consumers clearly points toward a lack of data on the transmission and distribution system below certain thresholds required in federal data filings by utilities. This led to the conclusion that, at some point on the grid, consumer demand would be aggregated, with shares of that demand being met in a competitive environment by different generation companies.

The second concept was to define the structures and role of generation companies. Because we are designing the model to analyze fully regulated systems as well as systems in which the generation portion of the equation has been freed to competition, we defined the agent structures to allow for all combinations of potential electric utilities that might result from a restructuring of the marketplace. In addition, any competitive generation scenario will include some system operator agent(s) to control power reliability and help in the determination of electricity price.

The third concept is that of the timeliness of events. A number of events have already been analyzed by other models, both agent-based and non-agent-based. These primarily include the short-term dispatch of power and the bidding cycle. Our model aims to go several steps further than these to include:

- Incorporating capacity expansion and retirement;
- Including the process of utility corporation mergers and takeovers (from existing work in ENERGY 2020); and
- Including government determination of the timeliness of

restructuring as a function of the aversion toward or interest in restructuring by energy consumers and producers.

We derived agent concepts from an analysis of the regulated market, the different varieties of restructuring, and the energy consumption and forecasting decision-making processes of agents. We converted these concepts into code and used them to supplement both existing agents and new energy industry agents.

We implemented a basic energy-trading model and tested it with a small-scale version of ASPEN-EE. We tested it with two generation companies under regulated and competitive generation conditions to determine that the physical and economic conditions of the real world are accurately modeled.

We completed changes to the prototype model and analyzed calculations on disruptions of varying degrees. This year's work led to a pair of interrelated results:

- We now have confidence that ASPEN-EE can model infrastructure disruptions; and
- We identified the changes needed for the development model.

Developing the behavioral algorithms for individual agents in a multi-agent model is one of the challenges of producing useful models. One of the problems to be faced by power-generation agents in the ASPEN-EE model is determining the optimum operating schedule of a number of electric power production units to meet forecasted demand over a short-term period while minimizing total operating cost. Closed-form solutions for this problem are not feasible for large power systems, so we developed an optimization using a genetic algorithm for the power agents in the model. This algorithm can be used to evaluate the impacts of loss of particular power-generation units in terms of both cost and the capability of the system to continue to meet power demands.

This algorithm can be used to evaluate the impacts of loss of particular power-generation units in terms of both cost and the capability of the system to continue to meet power demands.

Other Communications

Stamber, K. L. 1999. "Developing a Simulation Toolkit to Analyze Electric Grid Reliability and Infrastructure Interdependencies." Presentation to the INFORMS Spring Meeting, Cincinnati, OH, May.

3520480000

Physical Models for Predicting the Effect of Atmospheric Corrosion on Microelectronic Reliability

J. W. Braithwaite, J. R. Michael, D. G. Robinson, J. N. Sweet, D. W. Peterson, N. R. Sorensen

Atmospheric corrosion is a stockpile age-related degradation mode that has a high likelihood of occurrence and the potential for significant consequence. As such, Sandia's science-based stockpile stewardship mission requires that we develop and use an analytical capability to predict any effect corrosion can have on weapon reliability. Presently, the stockpile contains numerous microelectronic devices contained in ceramic hermetic packages (CHP). In the near future, the unavailability of CHP devices and the desire to shrink their size will drive the insertion of plastic-encapsulated microelectronic (PEM) devices into stockpile electrical components. A significant concern with using PEM devices is an uncharacterized effect corrosion could have on performance and reliability during long-term dormant storage. Analytical tools that can be used to effectively assess microelectronic corrosion damage must be based on a physical understanding of the moisture-related phenomena relevant to metallization failure. The specific objective of this project is to provide this needed foundation for the principal feature of present concern: corrosion of aluminum (Al) metallization features. We can attain the desired toolset by combining associated process models with computational reliability techniques that are required to efficiently address uncertainties inherent in the corrosion processes and the storage environments. We are following a three-phase approach that will culminate with the integration, validation, and application of a new predictive capability. We will incorporate into the final product the ability to incorporate the existing PEM model to be adapted to include CHP concerns. The important outcomes of this work will include a quantitative assessment of the validity of the PEM storage concern, a validated tool to assess most microelectronic corrosion effects of interest, and finally, a demonstration of the attractiveness of using computational reliability to model materials-degradation processes.

- *Effect of plastic encapsulant on intrinsic kinetics.* An objective was to modify the intrinsic corrosion model to

The important outcomes of this work will include a quantitative assessment of the validity of the PEM storage concern, a validated tool to assess most microelectronic corrosion effects of interest, and finally, a demonstration of the attractiveness of using computational reliability to model materials-degradation processes.

include the effects of water and contaminant transport through the plastic encapsulant. This capability would allow us to determine the local bondpad environment. We initially pursued two efforts: a mathematical portion in which we identified the governing transport equations and relevant 3-D physical configuration and an experimental activity to measure unknown transport parameters and to provide validation data. We made a very significant discovery during the pursuit of the validation information—best-commercial-practice (BCP) parts are very robust and are practically impossible to fail using reasonable accelerated aging conditions that include external contamination and elevated humidity/temperature. Some ancillary work that we performed showed that physical defects (due to manufacturing or thermal cycling) in the plastic are necessary to provide a permeation path for externally available contamination. Thus, those defects that run from the surface to the interior of the die (e.g., along lead-frame metallization) are especially important. Based on measurements of the detrimental effect of defects and the extended storage period applicable to our systems, we now believe that bulk transport processes within the plastic are not rate controlling and will have minimal impact on the local environment. The contribution of real defects (involving their physical size and distribution) within devices and the possible existence of *in situ* contamination still must be characterized during the coming year.

- *Bondpad degradation kinetics and mechanisms.* We expended a significant effort to effectively refine the governing corrosion-rate equation. The needs included encompassing a larger range of environmental parameters (higher humidity, lower gas-phase contaminant concentration, more uniform solid-phase contaminant), addressing the effect of heat-treatment (performed during encapsulant curing), and assessing the phenomenological cause of the non-intrinsic variability in the measured surface reaction-rate constant. We made progress in all of these areas, but the most significant advancement involved identifying the role of the intermetallic compounds and an associated development of a novel technique to directly observe bondpad degradation. The technique consists of a noninvasive process to remove the die substructure from the backside of the bondpad. The corroded bondpad structure is then clearly visible. We then developed a complementary scanning electron microscopy (SEM)–based technique to characterize this area. By changing the beam energy, we can generate a 3-D image of the entire wirebond structure.

We made a very significant discovery during the pursuit of the validation information—best-commercial-practice (BCP) parts are very robust and are practically impossible to fail using reasonable accelerated aging conditions that include external contamination and elevated humidity/temperature.

Important physical insight already gained from these studies includes the following: (1) corrosion is concentrated under the wirebond and propagates along an Al/intermetallic interface, and (2) considerable variability exists in the distribution and structure of the intermetallic phases, even on adjacent wirebonds. This latter finding suggests that the observed stochastic nature of corrosion may actually be the result of manufacturing process variability, providing even further justification for using our selected computational reliability technique.

- *Corrosion-based reliability prediction.* We successfully applied the CRAX computational reliability techniques to the deterministic bondpad corrosion model and performed an aging simulation of a simple LM185 voltage reference device for a desert, Gulf Coast, and arctic environment. We integrated the corrosion degradation model directly with an electrical system model (Chile-Spice) to enable us to calculate corrosion effects on the reliability of an electrical component. We then performed a reliability simulation involving a three-transistor (12-bondpad) voltage comparator device. This simulation demonstrated that the end-product capability desired in this project is attainable.

Refereed

Braithwaite, J. W., and N. R. Sorensen. 1999. "Corrosion in Non-Hermetic Microelectronic Devices." *22nd Aging, Compatibility and Stockpile Stewardship Conf. I* (Oak Ridge, TN, April): 151–156.

Other Communications

Braithwaite, J. 1998. "Predicting the Effect of Corrosion on the Reliability of Microelectronic Components." Presentation to the NMIMT Materials Science Seminar, Socorro, NM, October.

Frankel, G., and J. Braithwaite. 1999. "Corrosion of Microelectronic and Mass-Storage Devices." *Corrosion Mechanisms in Theory and Practice*, Chapter 15; 2nd Edition, ed. P. Marcus and J. Oudar, New York, NY (June).

Sorensen, N. R., J. W. Braithwaite, D. W. Peterson, and J. N. Sweet. 1998. "Detecting Corrosion in Plastic-Encapsulated Microelectronic Packages." *Proc. 194th Electrochem. Soc. Meeting: Corrosion Sensors I* (Boston, MA, November): 3.

3520490000

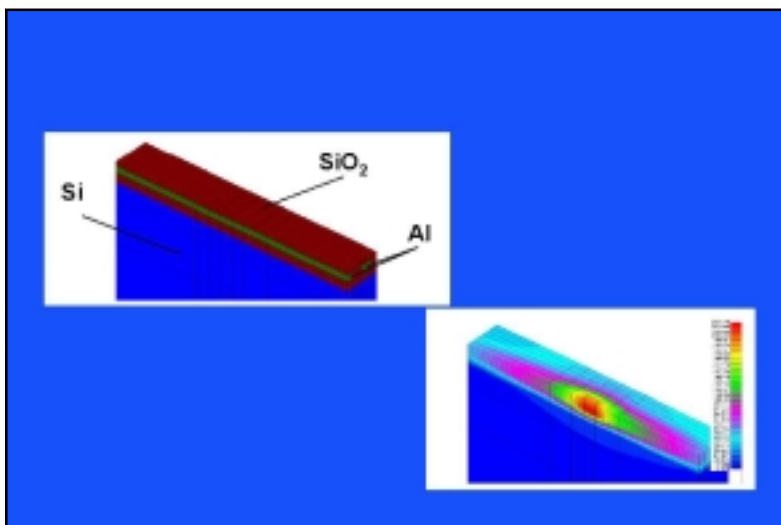
Backside Localization of Open and Shorted IC (Integrated Circuit) Interconnections

E. I. Cole, Jr., D. L. Barton, P. Tangyunyong, D. A. Benson

Integrated circuits (ICs) are critical components of virtually every Sandia system. Open and shorted internal IC interconnections are major reliability concerns and have been significant in stockpile systems. These failures occur as a result of processing defects and/or stress during operation and use. Both failure mechanisms have been significant in stockpile components. Localization of these defects has been extremely difficult due to decreasing feature sizes and increasing levels of interconnections. Concurrently, the implementation of flip-chip packaging has made backside analysis the only feasible examination method in many cases. Most active circuit elements in these ICs are accessible only from the backside and, to date, there are no effective backside techniques to directly localize open and shorted interconnections.

Sandia proposes to develop two new imaging techniques for IC backside open and short localization: Seebeck Effect Imaging (SEI) for localizing open interconnections and Short Localization (SL) for localizing short-circuited sites. The imaging modes use constant current biasing to make defect activation by an outside stimulus more readily detected. Our detection method uses thermal gradients produced by a scanned infrared (IR) laser. On open interconnections, thermal gradients induce voltage gradients (Seebeck effect). Thermal gradients change the resistivity of electrical shorts. Both effects are used to localize defects.

Sandia proposes to develop two new imaging techniques for IC backside open and short localization: Seebeck Effect Imaging (SEI) for localizing open interconnections and Short Localization (SL) for localizing short-circuited sites.



Modeling of temperature changes with laser illumination.

SEI and SL have the potential to revolutionize backside IC analysis in the same way Sandia's Charge-Induced Voltage Alternation (CIVA) technique has for frontside open interconnection localization. Backside SEI and SL, for which there are presently no alternatives, could have greater benefits by providing critically needed missing links in analysis capabilities.

We improved the SEI and TIVA techniques developed during the first year's work. Overall the technique development was very successful.

- *Sample thinning and applied coatings.* We received thinned samples from external customers interested in knowing if the SEI/TIVA analysis techniques would be useful for their advanced technologies from the backside of IC dice. Thinning the samples increases the amount of heat delivered to defects, and hence increases the SEI and TIVA signals highlighting the defects. This proved to be true for the samples examined. Additionally, the application of an antireflective, infrared coating to the backside of the sample increased the heat delivery by about two times.

- *Models.* Modeling analysis showed how the heat was distributed through various layers from the backside of the IC die and how quickly the heat would dissipate into the IC substrate. Our modeling work explained the increase in signal from conductors through thicker dielectric layers and through polysilicon conductors between the laser source and the conductors of interest. The heat dissipation with time analyses indicated that a pulsed laser at a 1 MHz pulse rate might provide increased signal sensitivity.

- *Pulsed laser.* We attempted increasing the TIVA/SEI system's sensitivity by using a pulsed laser and a lock-in amplifier on the TIVA/SEI signal synchronized to the pulse frequency. This did not yield an improved defect signal. We believe now that the minimum scan frequency of the scanning laser microscope is too fast to capture the TIVA/SEI signals. There are also unexpected limitations in the power supply to react at the 1 MHz pulsed frequency used.

- *Higher power.* We increased thermal power to the sample by two factors. First, we used an approximately 4X higher-power laser. Second, we inserted a 1/2 wave plate in the beam path of the laser. By rotating the 1/2 wave plate, the polarization of the laser rotated. The rotation of the wave plate could be set to minimize the reflection losses on the mirrors of the scanning laser microscope. Optimum placement of the 1/2

SEI and SL have the potential to revolutionize backside IC analysis in the same way Sandia's Charge-Induced Voltage Alternation (CIVA) technique has for frontside open interconnection localization. Backside SEI and SL, for which there are presently no alternatives, could have greater benefits by providing critically needed missing links in analysis capabilities.

wave plate increased the laser power delivered to the sample by about 50%. The net result was a little more than 5X increase in power delivered to the test samples.

• *Nonlinear effects.* An expected bonus of the increase laser power was a nonlinear, almost exponential increase in SEI and TIVA signals with power. The increase occurs because the transistors on the IC associated with the defects that are heated will respond as nonlinear amplifiers. The 5X increase in laser power produced an almost 100X increase in SEI/TIVA signals on some devices. The results of these increases are greatly reduced analysis times (45 minutes to 30 seconds or less) and the ability to detect defects in less than 1 minute that could not be observed in the first year of the project with 1 hour of signal averaging.

An expected bonus of the increase laser power was a nonlinear, almost exponential increase in SEI and TIVA signals with power.

Refereed

Cole, E. I., Jr., P. Tangyonyong, D. A. Benson, and D. L. Barton. 1999. "TIVA and SEI Developments for Enhanced Front and Backside Interconnection Failure Analysis." Paper presented to the European Symposium on Reliability and Failure Physics (ESREF), Arcachon, France, 5–8 October.

Tangyonyong, P., D. A. Benson, and E. I. Cole, Jr. 1999. "Thermal Modeling of TIVA Profiles of a Polysilicon-Metal Test Structure." *J. Appl. Phys.*, to be submitted.

Other Communications

Tangyonyong, P., E. I. Cole, Jr., D. A. Benson, and D. L. Barton. 1999. "Defect Localization Using Advanced Photon Probing Methods: LIVA, SEI, and TIV." (Invited) Presentation to the Hamamatsu Defect Localization Conference, Boston, MA, 1 October.

3520510000

Reliability Predictions for Advanced Electronics in Smoke Environments

T. J. Tanaka, L. A. Gritz, S. P. Nowlen, V. F. Nicolette, C. R. Shaddix, J. E. Brockmann, D. J. Anderson, C. W. Bogdan

Smoke is known to cause electrical equipment failure, but the likelihood of immediate failure during a fire is unknown. Traditional failure assessment techniques measure the density of ionic contaminants deposited on surfaces to determine the need for cleaning or replacing electronic equipment exposed to smoke. Such techniques focus on long-term effects of the fire. This research focused on the immediate effect of the smoke on electronic equipment. Sandia exposed various circuits and components to smoke from different fuels in a static smoke exposure chamber and monitored them throughout the exposure. Electrically, the loss of insulation resistance was the most significant change caused by smoke. For direct current (dc) circuits, smoke collected on high-voltage surfaces and tended to form semiconductive soot bridges that shorted the circuit. For high-voltage alternating current (ac) circuits, the smoke also tended to increase the likelihood of arcing, but did not accumulate on the surfaces. Static random-access memory (SRAM) chips failed for high levels of smoke, but hard disk drives and communications throughput connectors did not. High humidity increased the effects of the smoke and is suspected to be the cause of some memory chip failures after an hour of exposure. The conductivity between high-voltage surfaces increased with the amount of smoke produced, but was not proportional to smoke density as we first believed at the beginning of this project.

This project concentrated on measuring the immediate effects of smoke on electronics, in particular the increase in conductivity. We studied two cases in particular, the conductivity of air-borne particulates (using vertically suspended parallel plates) and the conductivity of the surface of a printed circuit board (PCB) printed with an interdigitated comb pattern. We studied these two cases because their simple geometric forms allow the data to be generalized to more complex problems.

We placed both dc and ac potentials on the parallel plates to determine the effect of polarization of smoke particles in the air. The dc potential attracted the smoke particles so that a soot bridge formed between the plates and shorted them together.

This project concentrated on measuring the immediate effects of smoke on electronics, in particular the increase in conductivity.

The conductivity at the height of the smoke density was similar for the 50- and 500-volt dc parallel plates; however, the 50-volt plates dropped back to pretest conditions earlier than the 500-volt plates. The ac potential on the parallel plates tended to arc when smoke was added, but no obvious smoke built up on the conductors.

As a result of the dc measurements, we modified the interdigitated comb pattern so that the smoke on the surface of a PCB with this pattern could be weighed and compared to the conductivity. Although the mass of the smoke deposited was proportional to the amount of fuel burned, the resulting conductivity could not be similarly modeled. The conductivity varies over several orders of magnitude during the smoke exposure, influenced both by having smoke in the air and by the changing relative humidity (RH). Because of the great variation in conductivity, we devised no satisfactory method of determining a value for the conductivity to compare with the soot mass on the circuit board. Since RH levels above 60% are known to increase conductivity, the last effort at solving this problem was to measure RH in the smoke chamber to determine how much the humidity was varying. The humidity seems to affect the conductivity of the 5-volt-biased comb pattern the most, while the 50- and 500-volt conductivities are more affected by the smoke in the air.

We burned cable insulation, wood, and jet fuel to determine how the different fuel types behaved. We also varied the amount of fuel to determine how the conductivity changes. We compared the optical density to the mass of smoke in the air by taking many filtered samples of the smoke and weighing the soot collected on the filters. The optical density was proportional to the mass density except when the smoke was so thick that very little light could penetrate the smoke chamber.

As a result of the dc measurements, we modified the interdigitated comb pattern so that the smoke on the surface of a PCB with this pattern could be weighed and compared to the conductivity.

Refereed

Tanaka, T. J. 1999. "Measurements on the Effects of Smoke on Active Circuits." *Fire and Materials* **23** (16 February): 103–108.

Tanaka, T. J. 1998. "Effects of Smoke on Equipment Reliability II." Paper presented to the Bell Atlantic/UL NEBS Conference, Lake Tahoe, CA, 20–22 October.

Other Communications

Tanaka, T. J., and J. T. Chapin. 1998. "The Effect of Smoke from Plastics on Digital Communications Equipment." *Plastics in Telecommunications VIII* (conference preprints) **1** (London, UK, 14–16 September): 213–222.

Tanaka, T. J. 1999. "Predicting Electronic Failure from Smoke." Presentation to the 44th International SAMPE Symposia and Exhibition, Long Beach, CA, 23–27 May.

3520520000

Security of Bulk Power Systems

D. G. Robinson, P. C. Butler

The electrical grids of North America are an extremely large and complex set of interconnected networks vital to the economic lifeblood and safety of over 380 million people. These networks are dynamic and constantly changing systems whose surety (safety, security, and reliability) is vulnerable to significant disruptions due to evolving energy policies as well as from natural and man-made sources. The President's Commission on Critical Infrastructure Protection has identified electric power as a critical infrastructure sector. The 1996 breakups of the western power system demonstrated the weaknesses of the current power-grid vulnerability analyses and highlighted the need for improved techniques to deal with the unexpected. An alternative approach involves probabilistic load flow characterization and is closely related to the analysis methods being developed as part of the nuclear weapons system stockpile surveillance program. Integration of the new probabilistic load flow analysis techniques and sensitivity analysis methods will provide the tools necessary to statistically characterize the voltage instability at each major bus in a very large bulk power system. Sensitivity of the network to voltage instability was the root of the 1996 outages, which in turn were the result of unexpected generation and loading situations. Traditional analysis could not account for these situations. By probabilistically characterizing the voltage stability at each network node and then relating this measure to the sensitivity of the grid to failure of this node, the vulnerability of the grid can be more thoroughly understood. A particular benefit of this approach is the ability to statistically characterize the dependency between generation and load. This capability will be an extremely important tool for network reliability analysis in a competitive, open-market environment.

We developed contingency-based reliability analysis capability and performed preliminary analyses on the IEEE Reliability Test System (RTS) and a 400-node model of the Arizona–New Mexico–Texas region within the WSCC (Western States Coordinating Council). This project provides the hierarchical capability to model networks involving both AC (accounting for both active and reactive power flow) and DC (an approximation involving only real or active power flow). We ported this software to the DEC 8400 computer

This project provides the hierarchical capability to model networks involving both AC (accounting for both active and reactive power flow) and DC (an approximation involving only real or active power flow).

network at Sandia and also implemented it on the 28-node computer network in collaboration with New Mexico State University.

We completed two significant literature reviews. The first emphasized the probabilistic characterization of power flow in a bulk power system, while the second concentrated on recent efforts to combine dynamic bifurcation (a branch of chaos theory) and probability theory to characterize voltage instability. We identified an analysis method that permits the combination of these two techniques and that will permit the static reliability model being developed to be used to statistically characterize dynamic voltage stability. Of significant interest in this research was the ability to model renewable energy components and assess their impact on power-grid reliability. We remodeled the behavior of rechargeable batteries and analyzed them using statistical and neural network methods to simulate the behavior of various components of the power system.

Refereed

Patton, A. D., C. Singh, and D. G. Robinson. 1999. "Impacts of Deregulation on the Reliability of a Multi-Area Power Pool." *Proc. 13th Power Systems Computing Conf.* (Trondheim, Norway, 28 June).

Robinson, D. G. 1998. "Impact of Deregulation on Power Grid Reliability: A Case Study." (Invited) Paper presented to the American Nuclear Society Special Workshop: Impact of Deregulation on Grid Reliability and Offsite Power Operability, Washington, DC, 15 November.

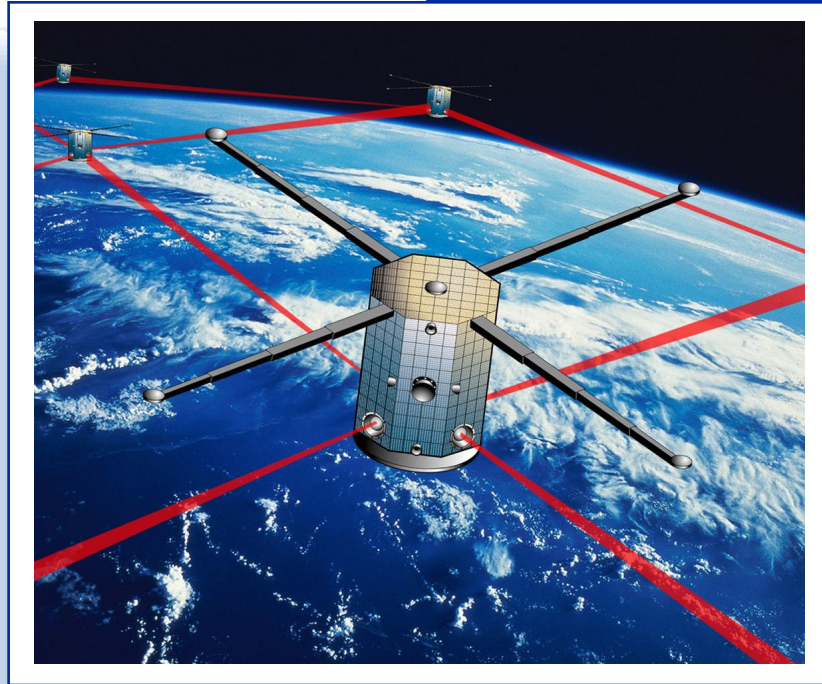
GRAND CHALLENGES

The Grand Challenge investment area supports research with the potential to significantly impact Sandia National Laboratories' and the nation's needs. High-risk, potentially outrageously successful ideas are considered for investigation.

Grand Challenge projects investigate innovative ideas with the potential for dramatically impacting national-level concerns—such as effectively counter-acting terrorism, developing sensors with advanced chemical/biological sensitivity and specificity capabilities, and creating solutions that significantly reduce energy prices, among others. The challenge threshold for Grand Challenge projects is an improvement in yield by at least a factor of two. In addition, all proposals must support achieving the business goals of Sandia National Laboratories.

The “Laser Communication Nanosatellites” project is researching and developing technologies that will advance the use of dozens or even hundreds of nanosatellites (i.e., small, inexpensive satellites weighing less than 10 Kg) to replace functions currently performed by large, heavy, and expensive satellites. Applications range from constellations of several hundred nanosats for seamless coverage of the globe to closely knit clusters that act cooperatively to execute imagery, surveillance, intelligence collection, and threat-detection missions to single nanosats that might be used for anomaly resolution. This research is focusing on advancing technologies with the potential to overcome challenges currently

surrounding highly distributed communication satellite networks. For example, this project is investigating satellite laser communications; advanced, highly efficient, and more radiation-tolerant solar cells; and novel methods for microsystems integration designed to reduce overall nanosatellite weight and size. Successful development of these systems on a nanosat platform will introduce the microsystem revolution into space applications.



3522010000

Science on the Microdomain

T. A. Michalske, D. J. Rakestraw, G. C. Osbourn, C. C. Wong, M. H. Crawford, M. E. Warren

This project is organized into four technical focus areas: (1) integrated optics, (2) on-board data analysis, (3) microscale transport, and (4) micromechanical actuators.

- *Integrated optics.* One of Sandia's key strengths is in the invention, design, and fabrication of miniaturized optical systems. Integration of these systems into the $\mu\text{ChemLab}^{\text{TM}}$ will provide a clear and differentiating strength for the Sandia effort in the lab-on-a-chip arena. Our work in this area addresses three programmatic needs: (1) providing optical components and design expertise for first-generation, fluorescence-based liquid chemical-sensor systems, (2) developing new compact optical sources that emit into the ultraviolet (UV) wavelengths, and (3) developing advanced concepts for miniaturized optical-sensor systems.

- *On-board data analysis.* A major difference between a sensor and a total chemical analysis system is the ability of the device to interpret sensor output and form conclusions about its chemical surroundings. This part of the project explores the application of vision science-based multivariate analysis to provide this function in the $\mu\text{ChemLab}^{\text{TM}}$. This approach is crucial to the $\mu\text{ChemLab}^{\text{TM}}$'s ability to achieve high sensitivity with low false-alarm rates.

- *Microscale transport.* The physical laws governing gas and fluid transport at the microscale differ greatly from those known to act at macroscopic dimensions. Our ability to design miniaturized gas- and liquid-chemical handling systems will depend on the development of new, validated models that are appropriate to the microscale. This project will develop the experimental and modeling tools needed to develop miniaturized chemical handling systems. In particular, this project will examine the feasibility of performing chemical separations in miniaturized chemical systems. Our efforts are divided into the areas of liquid- and gas-phase transport.

- *Micromechanical actuators.* We designed our gas-phase analysis around the use of acoustic resonator structures. We are using dynamic mechanical modeling to refine the design of miniaturized resonator structures with maximum efficiency.

- *First-generation optical fluorescence chip.* We demonstrated the first-generation, fluorescence-based, liquid-

One of Sandia's key strengths is in the invention, design, and fabrication of miniaturized optical systems. Integration of these systems into the $\mu\text{ChemLab}^{\text{TM}}$ will provide a clear and differentiating strength for the Sandia effort in the lab-on-a-chip arena.

chemical sensor system, which includes flip-chip–bonded vertical-cavity surface-emitting laser (VCSEL) and detector and microfabricated flow channels. We made a detailed evaluation of this system, which included determining chemical sensitivity and performing liquid-chemical flow and separation characteristics.

We fabricated and tested the second-generation optical fluorescence chip design. This design allowed for the use of flow channels that were etched into a separate silicon (Si) substrate. We made the interface between the optics chip and the Si flow chip with an index matching fluid.

- *Advanced optical sources.* We extended the current design for an optically pumped intracavity frequency-doubled VCSEL to an electrically injected VCSEL design. This design utilized the same nonlinear optical material but allows for direct mechanical coupling between the doubling crystal and the VCSEL emitter.

We explored packaging designs for the current optically pumped doubled VCSEL design. This design included a miniature pump laser and heat sinking in a small package that was suitable for hybrid integration with electrochromatographic separations chip design.

We explored other nonlinear optical materials to increase the range and efficiency of the doubled output source to 430 μm .

We explored direct integration of photochemically sensitive films with UV light-emitting diode (LED) sources. The first films explored were chosen to absorb in the UV and emit in the visible.

We implemented current design for microcavity flow cell with an electrically injected VCSEL.

We explored performance characteristics and sensitivity of newly designed chemically sensitive microcavity flow cell and characterized it for different chemical-sensing films.

We explored performance of chemically sensitive film-based microcavity sensors using spatially patterned film structures.

We used the analytical model for microflow and separations to evaluate and optimize on-chip separation column design and to define required injector performance.

We developed an overall gas-phase system performance simulator. Starting with the existing gas chromatography (GC) column design tool, we incorporated new analytical transport models for other components such as a sample preconcentrator

We developed an overall gas-phase system performance simulator.

and linked components through an overall simulator architecture.

We used a perturbation analysis on the equations of mass, momentum, and state to produce equations of motion for first- and second-order effects. Results indicate that within the assumptions of only first- and second-order effects, acoustic streaming can be harnessed as an effective micropumping strategy. However, we expect the pumping pressures to be rather modest and to need confirmation by direct experiment.

...within the assumptions of only first- and second-order effects, acoustic streaming can be harnessed as an effective micropumping strategy.

Refereed

Alford, W. J., T. D. Raymond, M. H. Crawford, and A. A. Allerman. 1999. "Intracavity Frequency Doubling of an Optically-Pumped External-Cavity Surface-Emitting Semiconductor Laser." *Proc. Advanced Solid-State Laser Conf.* **1** (Boston, MA, August): 1.

Alford, W. J., T. D. Raymond, M. H. Crawford, and A. A. Allerman. 1999. "Spectral Properties of External-Cavity Surface-Emitting Lasers Operating at 980 nm and 490 nm." *Proc. 1999 Conference on Lasers and Electro-optics* **1** (Baltimore, MD, May): 1.

Crawford, M. H., W. J. Alford, T. D. Raymond, and A. A. Allerman. 1998. "Intracavity Frequency Doubling of Vertical External-Cavity Surface-Emitting Lasers for Compact Milliwatt-Level Blue-Green Sources." *Proc. IEEE LEOS '98 Annual Meeting* **PD1.4** (Orlando, FL, May): 1.

Raymond, T. D., W. J. Alford, M. H. Crawford, and A. A. Allerman. 1999. "Intracavity Frequency Doubling of a Diode-Pumped External-Cavity Surface-Emitting Semiconductor Laser." *Optics Letters* **24** (May): 1127.

Other Communications

Allerman, A. A., M. H. Crawford, W. J. Alford, and T. D. Raymond. 1999. "The Growth and Design of Vertical External-Cavity Lasers for Intracavity Frequency Doubling." Paper presented to the 9th Biennial Workshop on Organometallic Vapor Phase Epitaxy, Ponte Vedra Beach, FL, 23–27 May.

Crawford, M. H., J. Han, R. J. Shul, M. Banas, J. J. Figiel, and L. Zhang. 1998. "Characterization of UV Light-Emitting Diodes with GaN and AlGa_N Quantum Well Active Regions." Paper presented to the 1998 Fall MRS Meeting, Boston, MA, November.

Han, J., and M. H. Crawford. 1999. "MOCVD Growth and Characterization of AlGa_N/Ga_N UV Emitters." (Invited) Paper presented to the SPIE International Symposium on Optoelectronics, San Jose, CA, 23 January.

3522020000

Autonomous MicroChem Laboratory (μ ChemLab™)

G. C. Frye-Mason, J. Wu, C. G. Bailey, D. W. Arnold, E. J. Heller, P. R. Lewis, W. B. Chambers, S. H. Kravitz, D. J. Rakestraw, G. N. Ryba, R. Kottenstette

This project is developing a new generation of field-ready and compact chemical analysis devices that have unprecedented capabilities for measuring and deciphering detailed chemical signatures. This project includes development of both gas- and liquid-phase analysis capabilities. The gas-phase module has demonstrated sensitive and selective detection of chemical warfare (CW) agent simulants using three cascaded components: (1) a microfabricated sample collector/concentrator, (2) a miniature gas chromatograph column, and (3) a sensitive and chemically discriminating detector based on an array of surface acoustic-wave (SAW) devices. The liquid-phase module has demonstrated effective separation and detection of explosives using electrokinetic (EK) separations with laser-induced fluorescence (LiF) and/or electrochemical detection. Sandia conducts the separations in complex microfabricated structures that are interfaced and integrated with miniaturized fluidic and electronic components. The project also involves developing the system architecture and supporting electronic hardware and software to produce complete autonomous systems. Prototype technology demonstrators for both the gas- and liquid-phase modules are completed.

We will demonstrate an optimized autonomous microscale chemical laboratory (μ ChemLab™) that will establish Sandia as a leader in this field. This project will position Sandia to support increasing demands for detailed chemical information by current national security customers and is essential for developing new industrial partnerships as well as new customers in nonproliferation, counterterrorism, energy, and critical infrastructures. The μ ChemLab™, formed by miniaturizing and integrating sensing capabilities, sampling and separation systems, and systems architecture, would meet the needs of applications in Defense Programs (DP) (nuclear material monitoring, material aging), and other national security issues.

We made dramatic progress on the development of μ ChemLab™. Selected accomplishments for the gas module

We will demonstrate an optimized autonomous microscale chemical laboratory (μ ChemLab™) that will establish Sandia as a leader in this field. This project will position Sandia to support increasing demands for detailed chemical information by current national security customers and is essential for developing new industrial partnerships as well as new customers in nonproliferation, counterterrorism, energy, and critical infrastructures.

include the following: (1) demonstrated microfabricated sample preconcentrators with concentration factors > 100, (2) demonstrated effective separation of sarin, soman, and mustard simulants using miniature gas chromatograph chips, (3) demonstrated sensitive and selective detection using an acoustic array with miniature GaAs (gallium arsenide) drive electronics, (4) demonstrated collection, separation, and detection of trace concentrations of CW simulants in two minutes using three components together, (5) designed, fabricated, and demonstrated a novel PC board that provides both electrical and fluidic interconnections for dual analysis channels, and (6) designed, fabricated, and demonstrated a PC board for supporting electronics, including temperature control and data-acquisition circuitry.

Selected accomplishments for the liquid module include the following: (1) demonstrated LiF detection in a microchannel separation using a microoptical detection system, (2) demonstrated on-chip separations of 10 explosives in one minute using micellar EK chromatography, (3) achieved detection limits of ~ 1 ppm in on-chip separations of explosives, (4) demonstrated ~ 1 ppm detection limits for explosives using electrochemical detection, (5) developed capability to fabricate complex fluidic architectures required for three independent on-chip separations, (6) developed compact, high-sensitivity, photodiode-based, optical detector, and (7) demonstrated EK pumping as a means to generate high pressures.

For the system and supporting electronics, we (1) designed and built an integrated programmable high-voltage supply to drive EK separations, (2) developed and fabricated a control system allowing manipulation of up to 80 input/output (I/O) lines for system operation, (3) designed and fabricated power supply and control electronics, (4) fabricated a robust fluidic system to interface the "macro outside world" with the liquid-phase microseparation chip, and (5) designed and fabricated a hand-held box with liquid crystal display (LCD) and simple four-key operation. We designed all the chemical analysis components and associated electronics to fit into the box, allowing complete gas- and liquid-phase analysis systems to be assembled into a single autonomous, battery-powered system measuring 2.75 x 4.25 x 9.2 inches (7.0 x 10.8 x 23.4 cm).

Refereed

Baca, A. G., E. J. Heller, V. M. Hietala, S. A. Casalnuovo, G. C. Frye-Mason, J. F. Klem, and T. J. Drummond. 1999. "Development of a GaAs-Based Monolithic Surface Acoustic Wave Integrated Chemical Microsensor." *IEEE J. Solid-State Circuits* **34**(9): 1254–1258.

Bailey, C. G., and C. Yan. 1998. "Separation of Explosives Using Capillary Electrochromatography." *Analytical Chemistry* **70**: 3275.

Other Communications

Arnold, D. W., C. G. Bailey, M. G. Garguillo, C. M. Matzke, J. R. Wendt, W. C. Sweatt, S. H. Kravitz, M. E. Warren, and D. J. Rakestraw. 1998. "Microseparations and Microfluidic Studies." *Proc. Micro Total Analysis Systems (MicroTAS) Workshop 1998* (Banff, Canada, 13–16 October): 435–438.

Casalnuovo, S. A., G. C. Frye-Mason, R. J. Kottenstette, E. J. Heller, C. M. Matzke, P. R. Lewis, R. P. Manginell, S. L. Hietala, W. K. Schubert, V. M. Hietala, D. Y. Sasaki, and J. L. Reno. 1998. "Gas-Phase Chemical Detection with an Integrated Chemical Analysis System." *Proc. IEEE Internat. Freq. Control Symp.* (Paris, France, July).

Frye-Mason, G. C., R. J. Kottenstette, E. J. Heller, C. M. Matzke, S. A. Casalnuovo, P. R. Lewis, R. P. Manginell, W. K. Schubert, V. M. Hietala, and R. J. Shul. 1998. "Integrated Chemical Analysis Systems for Gas-Phase CW Agent Detection." *Proc. Micro Total Analysis Systems '98* (Banff, Canada, 13–16 October): 477–481.

Frye-Mason, G. C., R. J. Kottenstette, P. R. Lewis, R. P. Manginell, S. A. Casalnuovo, E. J. Heller, C. M. Matzke, W. K. Schubert, V. M. Hietala, M. L. Hudson, C. C. Wong, C. J. Brinker, D. Y. Sasaki, and J. W. Grate. 1999. "Miniaturized Chemical Analysis Systems (μ ChemLab) for Selective and Sensitive Gas-Phase Detection." *Proc. 29th Internat. Conf. on Environmental Systems* (Denver, CO, 12–14 July).

Manginell, R. P., D. A. Rosato, D. A. Benson, and G. C. Frye-Mason. 1998. "Finite Element Modeling of a Microhotplate for Microfluidic Applications." *Proc. Modeling and Simulations of Microsystems 1999 (MSM'99)* (San Juan, Puerto Rico, April).

Manginell, R. P., G. C. Frye-Mason, W. K. Schubert, R. J. Shul, and C. G. Willison. 1998. "Microfabrication of Membrane-Based Devices by Deep-Reactive Ion Etching (DRIE) of Silicon." *Proc. Electrochemical Society Meeting* (Boston, MA, October 1999).

Paul, P. H., D. W. Arnold, and D. J. Rakestraw. 1998. "Electrokinetic Generation of High Pressures Using Porous Microstructures." *Proc. MicroTAS Workshop 1998* (Banff, Canada, 13–16 October): 49–53.

Paul, P. H., M. G. Garguillo, and D. J. Rakestraw. 1999. "Imaging of Pressure- and Electrokinetically-Driven Flows Through Open Capillaries." *Analytical Chemistry* **72**: 2459–2467.

Thomas, G. A., G. C. Frye-Mason, C. Bailey, M. E. Warren, J. A. Fruetel, K. Wally, J. Wu, R. J. Kottenstette, and E. J. Heller. 1999. "MicroChemLab—An Integrated Microanalytical System for Chemical Analysis Using Parallel Gas and Liquid-Phase Microseparations." *Proc. SPIE Unattended Ground Sensors* (Orlando, FL, April).

3522030000

Cooperative, Distributed Sensing and Action Using Microminiature, Intelligent Agents

B. L. Spletzer, E. Gottlieb, P. G. Xavier, J. E. Hurtado, T. K. Mayer, J. H. Buttz, G. Nagasubramanian, P. R. Klarer, T. M. Weber, J. T. Feddema, C. L. Lewis

This project developed a strong technical base for Sandia in modeling, simulating, designing, evaluating, developing, and deploying cooperative microminiature intelligent machines. The main thrust of the project is to build simulation tools and develop control systems for cooperating intelligent agents. We demonstrated this achievement by deploying multiple autonomous robotic vehicles in a cooperative sensing environment. Specifically, we produced the world's first mobile autonomous cooperative sensing system able to detect and localize a chemical source, and located both acoustic and simulated chemical emissions sources using cooperative distributed sensing.

This project has positioned Sandia as a leader in the community of researchers in computer science and mathematics regarding cooperative behavior and as a supplier of microminiature intelligent systems and technology.

We developed a number of algorithms providing the level of cooperation, communication, and behavior needed for autonomous agents to work as a single unit. We completed the work on algorithms and pursued numerous different approaches and tested them, showing that multiple useful behaviors can be implemented in cooperating agents.

We completed a simulation tool allowing for rapid design, development, and testing of new algorithms and behavior schemes. We ported the simulation to a Windows NT platform to make it widely available to researchers in cooperative behavior development. The simulation has the capability of handling real-world terrain and various chemical plume models to provide realistic and rapid testing of proposed behavior algorithms.

We upgraded required hardware for actual testing of algorithms from that produced in previous years. The completed hardware consists of eight Robotic All-Terrain Lunar Exploration Rover (RATLER)-based vehicles, each with onboard radio communication, GPS (global positioning system) navigation, data acquisition, and computing. We designed the vehicles to serve as a general-purpose test-bed for

...we produced the world's first mobile autonomous cooperative sensing system able to detect and localize a chemical source, and located both acoustic and simulated chemical emissions sources using cooperative distributed sensing....

This project has positioned Sandia as a leader in the community of researchers in computer science and mathematics regarding cooperative behavior and as a supplier of microminiature intelligent systems and technology.

developing control algorithms, sensors, and behavior for cooperative distributed sensing. Additionally, hardware development has proceeded in the production of a fixed sensor array designed to provide navigational beacons to the RATLER vehicles where GPS is not available. Initial tests with this hardware show promise.

Finally, we conducted demonstration testing of the behavior and control algorithms using the RATLER-tested vehicles. We used the completed hardware to demonstrate successful localization of both acoustic sources and simulated chemical sources.

...hardware development has proceeded in the production of a fixed sensor array designed to provide navigational beacons to the RATLER vehicles where GPS is not available.

Refereed

Driessen, B. J., J. T. Feddema, and K. S. Kwok. 1998. "Decentralized Fuzzy Control of Multiple Nonholonomic Vehicles." *Proc. 1998 American Control Conf.* (Philadelphia, PA, 24–26 June).

Feddema, J. T., and B. L. Spletzer. 1999. "Probability of Detection for Cooperative Sensor Systems." *Proc. SPIE 3713* (Unattended Ground Sensor Technologies and Application, Orlando, FL, 8–9 April).

Feddema, J. T., C. Lewis, P. Klarer, R. Eisler, and R. Caprihan. 1999. "Cooperative Robotic Sentry Vehicles." *Proc. SPIE Vol. 3839* (Sensor Fusion and Decentralized Control in Robotic Systems II, Boston, MA, 19–20 September).

Pryor, R. J. 1998. "Developing Robotic Behavior Using a Genetic Programming Model." Sandia Technical Report SAND98-0074, Sandia National Laboratories, Albuquerque, NM.

3522040000

Engineering Complex Distributed Systems

S. Y. Goldsmith, R. S. Tamashiro, R. C. Schroepel, T. J. Draelos, B. M. Nation, H. E. Link, R. A. Billington, B. D. Murphy-Dye, S. V. Spires, L. R. Phillips

In this project, Sandia will demonstrate a collective composed of intelligent software agents operating in an open (Internet-like environment) with a high degree of both security of operations and capability of operations. We will configure the Secure Agent Collective as a purely cyber collective (a cooperating team of software agents on computers) and, if time and resources allow, as a collective with one of the computers replaced by an agent-equipped robot participating in the collective via wireless communication. The principal focus of the demonstration will be to exhibit the enhanced level of reliability and integrity provided by the collective when under attack by malevolent or defective insiders. The insider threat constitutes one of the toughest challenges in information system security.

We based our selection of this proof-of-concept demonstration on a focus provided by examining two applications of significant direct importance to national security: the requirement to establish and operate within secure (i.e., need-to-know) enclaves in a less secure information environment, and the need to securely manage information provided by mobile and fixed sensors in the battlefield information environment. The Secure Agent Collective is a major task on the critical path for both these applications. The demonstration utilizes a number of the core technical capabilities developed in the first two years of the project, including invention of the secure agent architecture (SAA), development of agent components of that architecture, and the exploration of collective security concepts. Our metric of success will be to show a significant level of security against insiders during the course of the autonomous performance of a set of information-processing tasks.

- *Collective security infrastructure.* We developed models of network (software) agent collectives that exhibit self-protection through the use of proactive threshold cryptography. These agents collaborate to maintain group-level cryptographic security throughout an open network that is resistant to malicious defectors (including human actors) numbering not more than one-third of the total agent population. Loyal agents

Our metric of success will be to show a significant level of security against insiders during the course of the autonomous performance of a set of information-processing tasks.

that constitute at least two-thirds of the population maintain digital certificates for existing and new agents. New agents are produced by reproductive mechanisms that ensure that the dynamic threshold of loyal-to-malicious agents of 3:1 is maintained. Trust is ensured by inheritance of orthodox code genomes signed by a special group of human actors that commission the collective and maintain group-level control of its operations.

- *Secure agent architecture.* In collaboration with the University of New Mexico, we developed and implemented an integrated software agent architecture that combines the individual elements developed last year (e.g., sensory mechanism, deliberative mechanism, etc.) into a viable network agent. The new integrated architecture includes a comprehensive capability to securely handle any network information stream (Simple Mail Transfer Protocol [SMTP], HTML [Hypertext Markup Language], http, File Transfer Protocol [FTP], etc.), with the exception of Extensible Markup Language (XML). The new architecture supports agent cloning and reproduction, shared ontologies, and agent modeling based on reputation mechanisms, and has deeply embedded cryptographic protocols that provide a high level of intrinsic security. We will use elements of this architecture to build the above-mentioned Collective Security Infrastructure.

- *Detection probabilities of unattended ground sensors.* We completed an analysis of the probability of detection of multiple unattended ground sensors working as a self-organizing network. This analysis predicts the number of sensors that we need to achieve a specified probability of detection given the range of the sensing element and the communication range. In this distributed self-organizing network, each sensor learns of alarms from its neighbors and propagates this information out to the base station. Multiple vehicles will use information from neighboring vehicles to spread out in a specified formation state-space model that describes the equations of motion of a robotic perimeter detection application. Within this model, we describe the position of a vehicle around the perimeter in terms of the position of the neighboring vehicles. This state-space model also includes the communication architecture, in this case, a token ring.

- *Distributed neural networks.* In collaboration with Texas Tech, we performed initial analysis and simulations of a collaborative architecture for robot teams based on neural networks and adaptive critic designs. We demonstrated the

...we developed and implemented an integrated software agent architecture that combines the individual elements developed last year (e.g., sensory mechanism, deliberative mechanism, etc.) into a viable network agent.

concept of distributed collective reasoning and learning based on adaptive critics.

- *Network robots.* We initiated the development of network robots, Robotic All-Terrain Lunar Exploration Rover (RATLER) robots with increased processor and memory capacity that are inhabited by network software agents and are considered part of a network agent collective. We identified the new processor platform and investigated mobile Internet communications hardware.

- *Modeling robot swarm dynamics using LGA.* Lattice gas automata (LGA) reproduces both qualitatively and many times quantitatively the flow of fluids and gases and, in this case, robots. Such a model can be used to determine the minimum number of nearest-neighbor information necessary to maintain cohesion while tracking a moving target, to understand the swarm's flow around an obstacle, and to internally redistribute a heterogeneous (multisensor) swarm while maintaining its global integrity. This year we showed that LGAs provide both a mathematical and physical description of a multirobot system (dynamics). We achieved clear links between local interactions and macroscopic phenomena. To date, we have used genetically trained neuro-fuzzy networks to develop sensor fusion for the obstacle avoidance problem.

...we showed that LGAs provide both a mathematical and physical description of a multirobot system (dynamics). We achieved clear links between local interactions and macroscopic phenomena.

Refereed

Cameron, S. M., G. M. Loubriel, R. D. Robinett, III, K. M. Stantz, M. W. Trahan, and J. S. Wagner. 1999. "Adaptive Remote-Sensing Techniques Implementing Swarms of Mobile Agents." *Proc. SPIE 13th Annual Internat. Symp. on Aerospace/Defense Sensing, Simulation and Controls* **3713** (Orlando, FL, 8–9 April).

Feddema, J. T., C. Lewis, P. Klarer, and J. Orlando. 1999. "Control of Multiple Robotic Sentry Vehicles." *Proc. SPIE* **3693** (Unmanned Ground Vehicle Technology, Orlando, FL, 7–8 April).

Goldsmith, S. Y. 1998. "Object Filtering by Adaptive Default Hierarchies." Paper presented to OOPSLA '98, Vancouver, BC, Canada, October.

Goldsmith, S. Y., and S. V. Spires. 1999. "Agent Communications Using Distributed Metaobjects." *Proc. IJCAI '99 Workshop on Agent Communications Languages* (Stockholm, Sweden, 30 July).

Goldsmith, S. Y., J. T. Feddema, and R. D. Robinett, III. 1998. "Analysis of Decentralized Variable Structure Control for Collective Search by Mobile Robots." *Proc. Conf. on Decentralized Control, SPIE '98* (Boston, MA, November).

Kantz, K. M., S. M. Cameron, R. D. Robinett, III, M. W. Trahan, and J. S. Wagner. 1999. "Dynamical Behavior of Multi-Robot Systems Using Lattice Gas Automata." *Proc. SPIE 13th Annual Internat. Symp. on Aerospace/Defense Sensing, Simulation and Controls* **3693** (Orlando, FL, 7–8 April).

Orlando, J., J. T. Feddema, and B. L. Spletzer. 1999. "Probability of Detection for Cooperative Sensor Systems." *Proc. SPIE* **3713** (Unattended Ground Sensor Technologies and Applications, Orlando, FL, 8–9 April).

Phillips, L. R. 1999. "CHI: A General Agent Communication Framework." *Proc. Hawaii Internat. Conf. on System Sciences I* (Maui, HI, January).

Phillips, L. R. 1999. "The Role of Conversation Policy in Carrying Out Agent Conversations." *Proc. Workshop on Conversation Policy 1* (Seattle, WA, May): 11–17.

Phillips, L. R., S. Y. Goldsmith, and S. V. Spires. 1999. "A Multi-Agent System for Coordinating International Shipping." *Springer-Verlag Lecture Notes in Computer Science* (May).

Other Communications

Gilliom, L. R. 1999. "Assurance in Agent-Based Systems." (Invited keynote) Presentation to the Texas A&M 2nd Annual Computer Science Graduate Student Forum, College Station, TX, April.

Goldsmith, S. Y., and L. R. Gilliom. 1999. "Assurance in Agent-Based Systems." Paper presented to the ACM 1999 New Security Paradigms Workshop, Toronto, ON, 22–24 September.

Link, H. 1999. "Demonstration of MASMaS: A Multi-Agent Simulation Management System." *Technical Abstracts of the Software Demonstration Session on Autonomous Agents '99* (Seattle, WA, May).

Spires, S. V. 1999. "Engineering Collectives at Sandia National Laboratories." Paper presented to the Computational Science Division, NASA–Ames, Houston, TX, May.

3522050000

Laser Communication Nanosatellites

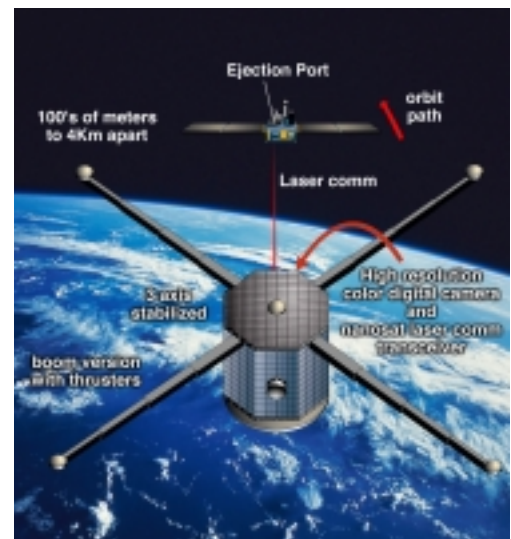
J. L. Schoeneman, B. C. Brock, G. B. Haschke, L. B. Dean, T. J. Kim, D. J. Johnson, W. C. Sweatt, C. T. Sullivan, P. J. Robertson, A. A. Allerman, D. Ingersoll

A paradigm shift in satellite systems is occurring based on the use of dozens or even hundreds of small, inexpensive satellites to replace functions currently performed by large, heavy, expensive satellites of today. These small satellites, which are referred to as nanosatellites or nanosats (under 10 Kg), would be used in a wide variety of applications. These applications range from constellations of several hundred nanosats covering the globe for seamless coverage, to closely knit clusters of nanosats flying in formation that think and act cooperatively to accomplish missions such as imagery, surveillance, intelligence collection, and threat detection, to single nanosats that might be used for satellite inspection for anomaly resolution.

Numerous government agencies have expressed and documented need for small-satellite technology to meet future requirements for material monitoring, surveillance of potential proliferants of chemical and biological weapons (CW/BW), threat/missile detection, and tracking and impact prediction, to name a few. These organizations include the U.S. Department of Energy, Central Intelligence Agency, National Reconnaissance Office, Defense Intelligence Agency, and the Air Force.

For nanosat systems to be affordable and reliable, satellite and launch cost must be drastically reduced (by an order of magnitude), and challenges in the control and exploitation of highly distributed communication satellite networks must be overcome. The development of the nanosat will require a wide range of enabling technologies and disciplines for miniaturization and multifunctional integration of satellite power, attitude determination and control, propulsion, communication, payload, and thermal control systems. Successful implementation of these systems on a nanosat platform will bring the microsystem revolution to space.

Sandia has more than 35 years of experience in developing space-based solutions to national security challenges. This experience directly supports the development of nanosat technology as a means to address the nation's future challenges. Sandia also has state-of-the-art silicon (Si) and compound semiconductor processing facilities for



Nanosat used for remote inspection.

Sandia has more than 35 years of experience in developing space-based solutions to national security challenges.

This experience directly supports the development of nanosat technology as a means to address the nation's future challenges.

microcircuits and photonics, state-of-the-art packaging, microelectromechanical systems (MEMS) devices, advanced batteries, and photovoltaic technologies needed in nanosat development.

- *Satellite laser communications.* The satellite laser communication task developed a gimballess acquisition and tracking concept with wide field-of-view telescope optics for short-range inter-nanosat laser communications. We developed and performed laser crosslink simulations that demonstrate the viability of efficient low-power VCSEL (vertical-cavity surface-emitting laser) emitters and advanced photodiodes (APDs) for 1 Gbps communications over a 4 km inter-satellite link with an extremely small 1 cm optical aperture. In the area of laser beam steering for transmission and reception, we designed and built a nonmechanical, 16-channel Optical Phased-Array Steering System (OPASS) and evaluated it utilizing photonic integrated circuits (PICs) for aberration/thermal corrections over the array aperture, thereby reducing stiffness/weight of a gimballed steering system that would be used for coarse laser pointing. In the area of MEMS, we designed and built a laser beam comm-link system using micromirror arrays that use polysilicon surface-micromachining (SMM) technology and are currently evaluating it. This system of micromirrors would be beneficial for correction of atmospheric distortions for possible lasercomm up-/downlink applications.

- *Advanced InGaAsN solar cells.* Advanced four-junction solar cells promise efficiencies 50% greater than today's three-junction cells. In this development effort, Sandia is at the forefront and recently set a new mark for the highest internal quantum efficiency (> 80%) reported to date for an InGaAsN (aluminum gallium arsenide nitride) solar cell. Improvement in cell efficiency is expected with optimization of material growth and cell design. Collaboration between experimentalist and theorist continues to yield insights to the fundamental properties and carrier transport of InGaAsN alloys that influence solar cell design. Other advancements include improvements in material growth and characterization, process control, and cell design.

- *Advanced silicon solar cells.* In advanced Si solar cell development, it is extremely desirable to produce a more radiation-tolerant, crystalline-Si solar cell using subwavelength optical structures (transmission gratings). The purpose of the grating on the surface is to couple the light into near-surface

Successful implementation of these systems on a nanosat platform will bring the microsystem revolution to space.

Advanced four-junction solar cells promise efficiencies 50% greater than today's three-junction cells. In this development effort, Sandia is at the forefront and recently set a new mark for the highest internal quantum efficiency (> 80%) reported to date for an InGaAsN (aluminum gallium arsenide nitride) solar cell.

propagation modes, which enhance the absorption near the front surface and thereby reduce the sensitivity of the solar cell to bulk defects introduced by radiation damage. The goal is a Si solar cell with an end-of-life efficiency near 15%, which is a roughly 25% relative improvement over present commercial space Si solar cells. In this effort, we developed procedures for diffraction grating fabrication in Si, and solar cell fabrication using Si with diffractive surfaces. We validated theoretical modeling on deep subwavelength gratings and used it to design optimal gratings. Initial solar cells with diffractive surfaces have shown up to 50% improvement in near-infrared (NIR) internal quantum efficiency compared to planar-surface control cells, which is a direct confirmation of enhanced near-surface absorption using diffractive surfaces.

- *Microsystems integration.* We developed new and novel methods for the integration of nanosat electronics using wafers or slices of electronic subsystems. This multiprocess integration of electronics is also engineered to provide a substantial portion of the satellites' physical structure, thus reducing overall weight and size. The integration process developed includes the use of Sandia's unique heat-pipe technology for cooling the hot spots and transferring the heat to the outside of the satellite for transfer into deep space.

- *Advanced energy-storage system.* Batteries/storage systems are traditionally the most massive portion of a satellite bus. New Sandia battery/capacitor technologies promise significant (up to 50%) savings in both volume and weight. We developed novel methods for preparation of bulk ruthenium dioxide (RuO_2) and bulk doped RuO_2 for use in electrochemical capacitors. We prepared and submitted a patent on this process. A novel method for preparation of thin films of RuO_2 and doped RuO_2 for thin-film microelectrochemical capacitors also ensued, and we developed special inks and pastes for the air electrode of the micro zinc/air battery. In the area of microbatteries, we developed microstructures. We subsequently developed carbon (C) thin films for current collectors on Si microstructures and demonstrated a prototype lithium-ion microbattery. For on-orbit operations, we simulated a demonstration of > 1.5-year cycle-life of 18650 and 26650 lithium-ion cells in a low-Earth-orbit regime. We successfully completed launch environmental testing of 18650 lithium-ion cells with no failures.

- *Relative position/attitude determination.* To accomplish sparse aperture imaging missions, precise relative positioning and attitude determination is a paramount requirement. We

In the area of microbatteries, we developed microstructures. We subsequently developed carbon (C) thin films for current collectors on Si microstructures and demonstrated a prototype lithium-ion microbattery.

investigated the use of carrier-phase global positioning system (GPS) techniques for relative positioning of the nanosat relative to the MightySat and for attitude determination of the nanosat. GPS measurements from at least four satellites are required to calculate the relative position of the two nanosat vehicles. Measurements from at least three GPS satellites using at least three GPS antennas on the nanosat are required to calculate the attitude of the nanosat. A GPS system should produce relative position errors that are less than 2 cm and attitude information that is accurate to ~ 0.2 degree. Some development will be required to achieve a GPS system that can operate with much less than 10 watts of power.

- *Advanced miniature propulsion study.* The study examined various thruster technologies for DV (Data-V) propulsion of a 10 kg satellite to allow formation flying with a mother satellite. A liquid nitrous oxide or ammonia cold-gas system with commercial valves and regulators delivering four ~ 1 -second duration 10 mN thrusts per orbit was recommended. We also developed a computer algorithm to control the gas thruster firing to allow a nanosatellite to fly in formation with a mothersat during time-dependent drag deceleration. The algorithm produces a stable orbit behind the mothersat using only two thrusts during the second orbit.

- *Advanced system studies.* A particular National Security application of a cluster of nanosats is in sparse aperture space radar. As an advanced conceptual study, the project developed a mathematical model for computing the radiation pattern of an array of spaceborne antenna elements having radiation patterns similar to parabolic reflectors. The number, location, and orientation of the elements are arbitrary and can be specified by the user. Radiation patterns of sparse arrays are of particular interest. The model computes the vector gain (including polarization direction) and the electric field at specified field points. We implemented a mathematical model in MATLAB computer code. The user specifies geometrical and electrical characteristics of the nanosat array, and the tool produces, as output, computations of the array's power-gain pattern. Results of testing the MATLAB tool with various amplitude and phase weighting strategies for steering the array mainlobe and suppressing the array sidelobes revealed the need to investigate application-specific pattern sidelobe reduction techniques for sparse arrays.

We also developed a computer algorithm to control the gas thruster firing to allow a nanosatellite to fly in formation with a mothersat during time-dependent drag deceleration. The algorithm produces a stable orbit behind the mothersat using only two thrusts during the second orbit.

Refereed

Allerman, A. A., S. R. Kurtz, E. D. Jones, J. M. Gee, and A. Clement-Font. 1999. "The Growth of InGaAsN for High-Efficiency Solar Cells by Metalorganic Chemical Vapor Deposition." (Invited) *Proc. 195th Meeting of the Electrochemical Society* (Seattle, WA, 2–7 May).

Gee, J. M., S. H. Zaidi, and D. S. Ruby. 1999. "Advanced Silicon Space Solar Cells Using Nanotechnology." *Proc. 2nd Internat. Conf. on Integrated Micro Nanotechnology for Space Applications* (Pasadena, CA, 11–15 April).

Jones, E. D., N. A. Modine, A. A. Allerman, I. J. Fritz, S. R. Kurtz, A. F. Wright, S. T. Tozer, and X. Wei. 1999. "Optical Properties of InGaAsN: A New 1eV Bandgap Material System." *Proc. SPIE Conf., Light-Emitting Diodes: Research, Manufacturing, and Applications III* **3621** (Photonics West: Optoelectronics, San Jose, CA, 23–29 January).

Jones, E. D., N. A. Modine, A. A. Allerman, S. R. Kurtz, A. F. Wright, S. T. Tozer, and X. Wei. 1999. "Band Structure of InGaAsN Alloys and Effects of Pressure." *Phys. Rev. B* **60**: 4430–4433.

Jones, E. D., N. A. Modine, A. A. Allerman, S. R. Kurtz, A. F. Wright, S. T. Tozer, and X. Wei. 1999. "Photoluminescence Studies of InGaAsN Alloys Lattice-Matched to GaAs." (Invited) *Proc. 195th Meeting of the Electrochemical Society* (Seattle, WA, 2–7 May).

Kemme, S. A., S. H. Zaidi, and J. M. Gee. 1999. "Submicron Diffractive Gratings for Thin-Film Solar Cell Applications." *Proc. 8th Workshop on Crystalline-Silicon Photovoltaic Technology* **520-26941** (Breckenridge, CO, 9–11 August): 206–209.

Kurtz, S. R., A. A. Allerman, E. D. Jones, and C. H. Seager. 1999. "Minority Carrier Lifetimes, Defects and Solar Cells of InGaAsN, Lattice-Matched to GaAs." (Invited) *Proc. 195th Meeting of the Electrochemical Society* (Seattle, WA, 2–7 May).

Kurtz, S. R., A. A. Allerman, E. D. Jones, J. M. Gee, J. J. Banas, and B. E. Hammons. 1998. "InGaAsN Solar Cells with 1.0eV Bandgap, Lattice-Matched to GaAs." *Appl. Phys. Lett.* **74**: 729–731.

Kwon, D., R. J. Kaplar, S. A. Ringel, A. A. Allerman, S. R. Kurtz, and E. D. Jones. 1999. "Deep Levels in p- and n-Type InGaAsN for High-Efficiency Solar Cells." *Solar Energy Materials & Solar Cells* (special issue) (11th International Photovoltaic Science and Engineering Conference PVSEC-11, Hokkaido, Japan, 20–24 September).

Kwon, D., R. J. Kaplar, S. A. Ringel, A. A. Allerman, S. R. Kurtz, and E. D. Jones. 1999. "Deep Levels in p-Type InGaAsN Lattice-Matched to GaAs." *Appl. Phys. Lett.* **74**: 2830–2832.

Shul, R. J., C. G. Willison, C. T. Sullivan, S. H. Kravitz, L. Zhang, and T. E. Zipperian. 1998. "Deep High Aspect Ratio Si Etching for Advanced Packaging Technologies." *Proc. 193rd Electrochemical Society Meeting* (San Diego, CA, May).

Zaidi, S. H., J. M. Gee, D. S. Ruby, and S. R. J. Brueck. 1999. "Characterization of Si Nanostructured Surfaces." *SPIE '99* (Denver, CO, 20–23 July).

Other Communications

Allerman, A. A., S. R. Kurtz, E. D. Jones, J. M. Gee, and R. M. Sieg. 1999. "InGaAsN for High-Efficiency Solar Cells Grown by Metalorganic Chemical Vapor Deposition." Paper presented to the 41st Electronic Materials Conference, Santa Barbara, CA, 30 June–2 July.

Allerman, A. A., S. R. Kurtz, E. D. Jones, J. M. Gee, S. A. Ringel, D. Kwon, R. J. Kaplar, and J. J. Boeck. 1999. "The Growth of InGaAsN for 1.0eV Solar Cells Lattice Matched to GaAs." Paper presented to the 9th Biennial Workshop on Organometallic Vapor Phase Epitaxy, Ponte Vedra Beach, FL, 23–27 May.

Allerman, A. A., S. R. Kurtz, E. D. Jones, R. M. Sieg, and J. M. Gee. 1999. "The Growth of InGaAsN Using Dimethyldiazine by Metalorganic Vapor Deposition." Paper presented to the 11th American Conference on Crystal Growth and Epitaxy (ACCGE-11), Tucson, AZ, 1–6 August.

Haschke, G. B., R. M. Axline, and B. C. Brock. 1999. "Gain Analysis Tool for Sparse Antenna Array Using Nanosatellites—Test Report." Sandia Technical Report SAND99-2314, Sandia National Laboratories, Albuquerque, NM (September).

Jones, E. D., A. A. Allerman, S. R. Kurtz, I. J. Fritz, N. A. Modine, K. K. Bajaj, S. T. Tozer, and X. Wei. 1999. "Effective Masses for 1 and 2% Nitrogen in InGaAsN Alloys." Paper presented to the 1999 Four Corners Section Fall Meeting, Tucson, AZ, 1–2 October.

Jones, E. D., N. A. Modine, A. A. Allerman, S. R. Kurtz, A. F. Wright, S. T. Tozer, and X. Wei. 1999. "Pressure-Dependent Bandgap Energies and Masses in 1eV InGaAsN Lattice Matched to GaAs." Paper presented to the 9th Biennial Workshop on Organometallic Vapor Phase Epitaxy, Ponte Vedra Beach, FL, 23–27 May.

Jones, E. D., N. A. Modine, A. A. Allerman, S. R. Kurtz, A. F. Wright, S. T. Tozer, and X. Wei. 1999. "Pressure-Dependent Bandgap Energies and Masses in InGaAsN." Paper presented to the March Meeting of the American Physical Society, Atlanta, GA, 20–26 March.

Kurtz, S. R., A. A. Allerman, and E. D. Jones. 1999. "InGaAsN Solar Cells and Minority Carrier Properties." Paper presented to the 1999 Four Corners Section Fall Meeting, Tucson, AZ, 1–2 October.

Kurtz, S. R., A. A. Allerman, E. D. Jones, and C. H. Seager. 1999. "Minority Carrier Lifetimes and Defects in InGaAsN, Lattice-Matched to GaAs." Paper presented to the March Meeting of the American Physical Society, Atlanta, GA, 20–26 March.

Modine, N. A., E. D. Jones, A. A. Allerman, and S. R. Kurtz. 1999. "Theory of the Pressure-Dependent Band Structure of GaAsN Alloys." Paper presented to the 1999 Four Corners Section Fall Meeting, Tucson, AZ, 1–2 October.

Modine, N. A., E. D. Jones, A. F. Wright, A. A. Allerman, and S. R. Kurtz. 1999. "Ab Initio Band Structure of InGaAsN Alloys and Effects of Pressure." (Invited) Paper presented to the 195th Meeting of the Electrochemical Society, Seattle, WA, 2–7 May.

Robertson, P. J., R. J. Shul, and C. P. Tigges. 1999. "Heat Pipe Integrated Microsystems." *Proc. 2nd Internat. Conf. Integrated Micro/Nanotechnology for Space Applications (MNT99)* 1 (Pasadena, CA, 11–15 April): 336–339.

Rose, B. H. 1999. "Photovoltaic Power for the Nanosat Project." Sandia Technical Report SAND99-1503, Sandia National Laboratories, Albuquerque, NM (June).

3522060000

Information Collection (Acquisition of Information from Denied Areas)

D. D. Spencer, G. A. Thomas, R. C. Hughes, M. A. Butler, J. P. Anthes, F. T. Mendenhall, T. S. Prevender, M. W. Scott, R. D. Robinett, III, A. K. Miller

In the post-Cold War era, the intelligence community (IC) is increasingly denied access to information associated with threatening activities of foreign governments and, paradoxically, finds itself overwhelmed with data from the electronic information revolution. Sandia's broad depth of science and engineering expertise positions the laboratories to establish a unique partnering relationship with the IC in developing new technology and methods to address these many technical challenges.

We made progress on several of the missing pieces necessary to demonstrate mission capability. The main emphasis of this project is to provide and refine technologies that address sensors, sensor placement, and communication for both sensor control and data delivery.

(1) We integrated chemiresistor sensor onto a mobile robot. In this configuration, we demonstrated the feasibility of using a robot as a platform to detect chemical traces and exhausts.

(2) Another sensor program involved proposed use of a miniaturized ion mobility spectrometer (IMS) configured for either chemical or biological agent sensing. This is a tough problem, so we focused this year on the use of a larger IMS for feasibility investigation. While we believe that IMS could do biological sensing, this is difficult enough that a portable miniaturized biosensor will take considerable effort.

(3) A key technology for emplaced sensors, whether mobile or fixed, is the optimization and miniaturization of energy systems. We performed a study that investigated state-of-the-art energy sources and their applicability to sensor systems. The study included the structuring of hybrid systems that integrate a variety of energy sources, including batteries, fuel cells, photovoltaics, microgenerators, and others. We also conducted a conceptual design of a specific unattended robotic system.

(4) We looked at mobility requirements involving areas such as terrain agility, energy efficiency, rolling resistance, ground pressure, center of gravity, number of motors, and weight.

Sandia's broad depth of science and engineering expertise positions the laboratories to establish a unique partnering relationship with the IC in developing new technology and methods to address these many technical challenges.

(5) We studied capabilities for collecting data from emplaced sensors and analyzed patch versus whip antennas for line-of-sight (LOS) RF communication. One looked at accommodation of temporary loss of LOS communication; the other looked at the utility infrastructure.

3522070000

Accelerated Molecular Discovery Arrays—The Next Revolution in Biotechnology

D. S. Anex, R. Shediak, S. M. Ngola, G. B. Sartor, J. S. Schoeniger, M. J. Kelly, D. A. Chinn, D. Y. Sasaki, T. J. Shepodd

As we near the completion of the genomic sequencing era, the next revolution in biology will involve the understanding of the complex molecular interactions governed by the expression of genomic information. In collaboration with Lawrence Berkeley National Laboratory (LBNL), University of California at Berkeley (UCB), and recently, the Novartis Institute for Functional Genomics (NIFG), Sandia is developing the tools to advance this understanding through the accelerated discovery and exploitation of signal molecules that control life processes. This work extends significantly the microscale trace chemical analysis techniques currently being developed by Sandia for applications in chemical and biological defense. Not only will the discovery and identification of signal molecules have profound applications in the biomedical field, but these molecules, also referred to as bioregulators, are viewed as serious potential biological weapons. Their characterization will play an important role in our forward-looking responsibilities in emerging threats, nonproliferation, and critical infrastructures. We are developing and applying highly parallel, microfabricated arrays of chemical analysis systems known as Accelerated Molecular Discovery Arrays (AMDAs). These tools will allow the rapid isolation and identification of trace signaling biomolecules.

This project concentrated on the development of separation-based microanalytical approaches to the discovery of bioregulators (molecules that control cellular communication and regulation). Use of electrokinetic (EK) techniques allows microfluidic flow control and material handling through the application of electric fields and results in very high performance separations. We divided the separation problem into three molecular classes: protein, peptide, and small-molecule analysis. We emphasized tandem approaches, which involve continually injecting the material emerging from the first separation stage onto a second separation stage. This approach yields two-dimensional data (each axis represents the separation time for each of the separation stages). We developed laser-based strategies for the high-sensitivity online

This work extends significantly the microscale trace chemical analysis techniques currently being developed by Sandia for applications in chemical and biological defense. Not only will the discovery and identification of signal molecules have profound applications in the biomedical field, but these molecules, also referred to as bioregulators, are viewed as serious potential biological weapons.

detection of fluorescently tagged test analytes after the tandem separation.

We designated leading strategies for tandem separations: isoelectric focusing (IEF) followed by sodium dodecyl sulfate-capillary gel electrophoresis (SDS-CGE) for proteins and reversed-phase (RP) capillary electrochromatography (CEC) followed by capillary electrophoresis (CE) for peptides. For the proteins, the IEF step was demonstrated on-chip. In a joint effort, we successfully migrated SDS-CGE to an on-chip format and tested it on fluorescently labeled protein test samples. This work resulted in accelerated publication of the results in the scientific literature and a disclosure of technical advance (TA).

For the peptide separations test set, NIFG developed dye tagging, which is under way. RP-CEC stationary phases are under development for the first dimension. The CE for the second dimension simply requires an open channel.

Materials for on-chip analysis are needed not only for separation media, but also for flow restrictors, EK pumps, and salt bridges. The materials development efforts resulted in two technical advances (TAs) and one patent application.

The materials development focused on advances that will lead to high-performance, chip-based analyses. A key point is that materials should be easily introduced into channels on chips. We developed microporous materials that are self-pumping as cast (reagents remaining in the pores after polymerization can be removed electrokinetically). We demonstrated a number of microporous materials that serve as separation media (mostly RP), EK pumps, salt bridges, and flow restrictors in freestanding capillaries. We are also developing photo-definable materials that will allow the placement of materials of different function in different regions of an on-chip fluidic network. We demonstrated high-quality separations in photo-initiated monolithic polymers in freestanding capillaries for small molecules and peptides. To provide additional separation materials with a diversity of selectivity, we designed a few strategies to prepare molecularly imprinted materials with selective affinity for specific amino acids and small peptides.

We included electrochemical detection for evaluation of its applicability to biological compounds and implementation in a chip-based format. We made and tested advances in coupling electrodes to freestanding capillaries and on-chip electrode design with explosive compounds. We also tested hybrid

design with on-chip separation and external electrode in collaboration with New Mexico State University.

We fabricated prototype glass-separation chips. All of the operations for making these chips are now available locally, and a standard protocol has been developed. These operations include chip layout and design, rapid mask procurement and fabrication, photolithographic patterning, wet chemical etching, automated access port drilling, electrode deposition, and wafer bonding.

Refereed

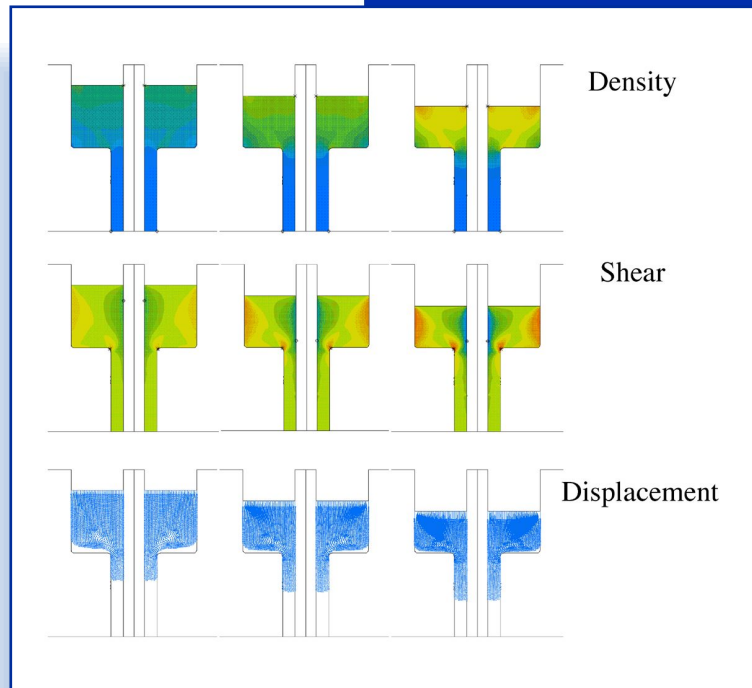
Yao, S., D. S. Anex, W. B. Caldwell, D. W. Arnold, K. B. Smith, and P. G. Schultz. 1999. "SDS Capillary Gel Electrophoresis of Proteins in Microfabricated Channels." *Proc. National Academy of Sciences* **95**(10) (11 May): 5372–5377.

We fabricated prototype glass-separation chips. All of the operations for making these chips are now available locally, and a standard protocol has been developed.

CORPORATE OBJECTIVES

The Corporate Objectives investment area addresses sophisticated research and development narrowly targeted on the goals of Sandia National Laboratories' strategic business and management units. The focus for these investments is primarily applied rather than basic research.

The Corporate Objectives (CO) investment area researches novel concepts and technologies directed to the specific needs of the Laboratories' program areas. The Nuclear Weapons CO focuses on innovative ideas relevant to meet future weapons' requirements. The Nonproliferation and Material Control CO explores advanced technologies for improving the physical security of weapons and special nuclear materials. The Energy and Critical Infrastructure CO focuses on researching technologies that enhance the safety, security, and reliability of the nation's critical infrastructures, and the Emerging Threats CO investigates technologies and concepts enabling high-impact responses to emerging national security threats. The Science and Technology (S&T) CO explores novel areas situated at the interfaces between disciplines (for example, but not limited to, physics and biology) with the potential for significant future scientific and technological impact. The Partnerships CO engages in opportunities that (1) pursue long-term strategic partnerships with industry, (2) create strategic relationships with universities, (3) collaborate with other government laboratories, and (4) develop strategic international collaborations.



The "Real-Time Design of Improved Powder Pressing Dies Using Finite-Element Method Modeling" project is exploring the characterization of an expanded powder compaction model. A user-friendly software tool is being developed that incorporates unprecedented flexibility for designing powder press tooling and pressing processes faster and more economically. An advanced model has the potential to significantly impact the design and manufacture of ceramic components with improved performance and reliability characteristics for weapons systems applications.



3530140000

Microcode Evaluation

J. W. Walkup, E. I. Cole, Jr., T. J. Drummond, T. H. Desiena, G. L. Smithberger, R. P. Fleming

Many microprocessors are microprogrammed—the base chip implements in silicon (Si) a much simpler machine than the programmer sees, and the more complex operations are implemented as small programs (microcode). There are processors that allow their microcode to be changed in the field as the processor runs, changing the way the processor executes its instructions. It is possible for an adversary to exploit this field upgrade capability to change the characteristics of the chip. Sandia evaluated the level of effort and knowledge that would be required to do this.

We selected a central processor unit (CPU), bought the appropriate in-circuit emulator (ICE) equipment, investigated the microcode download techniques, and have a tool to perform the download at will rather than simply upon power-up. The tool will also identify the processor and can modify the microcode being downloaded to test the effects of individual bits being modified.

We characterized and compared various microcode download packages and can isolate interesting sections of the data. We used a brute force technique to bypass the checking done by the processor. We can load a modified microcode patch and the processor accepts it. This patch causes the processor to lock up almost immediately.

We also deprocessed and looked at the Si die of the CPU to gain in an attempt to understand how the microcode download works. This was not fruitful because of the extensive metallization on the front of the die. Backside imaging proved to be very difficult because of the heat generated by the processor and the very small feature size.

We were unsuccessful in creating a microcode of our own.

It is possible for an adversary to exploit this field upgrade capability to change the characteristics of the chip. Sandia evaluated the level of effort and knowledge that would be required to do this.

3530150000

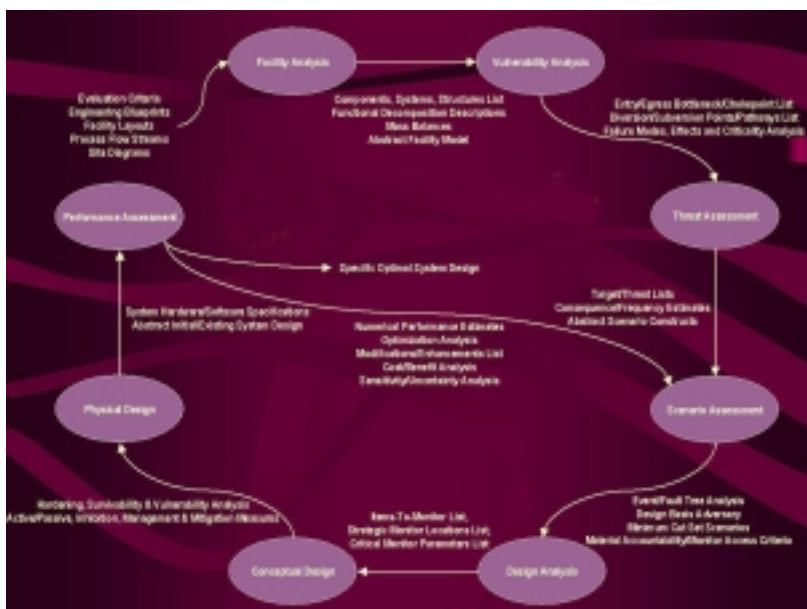
Model-Based Design and Analysis of Remote Access Monitoring Systems

S. M. Deland, J. D. Smith

Unattended monitoring systems are sensor-based systems for remotely monitoring the status of high-value assets and processes, particularly with respect to international nuclear material safeguards, nonproliferation, and transparency. Depending on the application, the purpose of the monitoring system may include detecting intrusion into a secured area, verifying that known processes are occurring as expected, and detecting diversion of nuclear material. The data collected by these monitoring systems come from a wide variety of sensors including breakbeams, radiation detectors, and video cameras.

The selection and placement of sensors in an unattended monitoring system are critical in determining how well the system meets the monitoring objectives for a given application. Designing such systems is difficult because of the range of technologies involved, mismatches between the data that current sensors can supply and the information that is needed, and the need to detect small discrepancies and anomalies that may be indicative of illicit activities. This project developed a methodology for the design of unattended monitoring systems, focusing on the selection of appropriate sensing technologies to meet unattended monitoring system requirements. The key to developing such a methodology is to abstract out the key features of facilities, processes, and sensors into a concise

Implementation of this design methodology will ensure that the unattended monitoring system will provide appropriate answers to those critical questions imposed by specific agreements or regulations.



Overview of analysis methodology for remote access monitoring systems.

model that can be manipulated mathematically. The methodology is quantitative in nature and can be used to optimize the monitoring system design against a set of established evaluation criteria. The methodology provides a basis for the development of automated tools to assist with the design of monitoring regimes and with the analysis of acquired data; such tools will be a great benefit to the international safeguards community and a significant enhancement to Sandia initiatives that use remote monitoring technology.

As an initial step in our research, we reviewed methodologies in related fields. These included physical protection methodology (PPM), a methodology for assessing physical security systems, and probabilistic risk assessment (PRA), a methodology used for assessing risk. Both methodologies are closely related and offered insights into the development of calculable models of facilities and processes, the establishment of measures of effectiveness for quantifying performance assessments, the identification of vulnerabilities or weak links in a system, and the use of an iterative approach for correcting any such weaknesses. Both make use of mathematical modeling concepts such as graphs and fault trees for quantitative analysis.

Our research focused on how to adapt these methodologies to the design of unattended monitoring systems. Once we defined the monitoring system objectives, our methodology included eight major analyses:

(1) *Facility analysis.* This analysis includes identifying major structures, systems, and components in a facility; describing each element's function; aggregating functionally related or physically common elements; and arranging them in a hierarchical structure.

(2) *Vulnerability analysis.* This analysis lists the possible failure modes of each element, assesses the impact of loss of each element, and ranks the elements in importance to the function of the facility and monitoring system. This analysis is referred to as a FMECA (Failure Modes, Effects, and Criticality Analysis) in PRA.

(3) *Threat assessment.* In this analysis, the designer identifies and characterizes possible threats and possible targets. Characteristics include capabilities of the threat, desirability of the targets, and the ease with which targets could be acquired.

(4) *Scenario assessment.* In this analysis, the designer develops scenarios for defeat of the monitoring regime based

The methodology provides a basis for the development of automated tools to assist with the design of monitoring regimes and with the analysis of acquired data; such tools will be a great benefit to the international safeguards community and a significant enhancement to Sandia initiatives that use remote monitoring technology.

on the previous analyses. The likelihood of the scenarios is assessed using fault trees.

(5) *Design analysis*. This analysis included identifying key monitoring locations and needed monitoring technologies based on the design analysis.

(6) *Conceptual design*. In this analysis, the designer selects types of sensors and general locations to be used in the monitoring system.

(7) *Physical design*. In this analysis, the designer selects specific sensors and locations.

(8) *Performance assessment*. In this analysis, the designer assesses overall performance of the monitoring system against all of the scenarios developed in the scenario assessment phase.

Implementation of this design methodology will ensure that the unattended monitoring system will provide appropriate answers to those critical questions imposed by specific agreements or regulations.

We included our results on methodology development in a larger paper on design methodology presented at the Institute of Nuclear Materials Management Annual Meeting and also incorporated them into training courses on monitoring system design given by the Cooperative Monitoring Center at Sandia.

In addition to the development of the Unattended Monitoring System Design Methodology, we prototyped a software tool for application of the methodology. We based the tool on a multi-objective optimization tool, MPATHav, originally developed for transportation risk assessment applications. The tool calculates the overall system performance based on a user-defined function for combining performance against individual monitoring objectives.

Other Communications

Drayer, D., S. M. DeLand, C. D. Harmon, J. C. Matter, R. L. Martinez, J. D. Smith, and P. E. Ebel. 1999. "Unattended Monitoring System Design Methodology." *Proc. Institute of Nuclear Materials Management, 40th Annual Meeting*, accepted.

Implementation of this design methodology will ensure that the unattended monitoring system will provide appropriate answers to those critical questions imposed by specific agreements or regulations.

3530160000

Microwave Imaging Through Walls

T. S. Prevender, D. E. Wahl, D. A. Yocky, P. A. Thompson

The intent of this project was to investigate the possibility of imaging through walls using a microwave source of energy. In particular Sandia was interested in using synthetic aperture radar (SAR) processing techniques to sharpen any images formed. We performed a set of preliminary experiments wherein the objects to be imaged consisted of conducting cylinders of different diameters. The wall in this case was made up of sheet rock separated by wooden studs. We used a bistatic radar to collect the data. Applying SAR processing techniques to the data resulted in very appreciable focusing. The next set of experiments will attempt to image complex targets consisting of office furniture located on the far side of a more complex wall.

We performed a set of experiments using a microwave emitter and collector operating in a bistatic configuration. The wall used in these experiments consisted of two half-inch-thick four-foot-by-eight-foot sections of sheet rock separated by two-inch-by-four-inch wooden studs. The imaged objects were sections of metal pipe one, two, and four inches in diameter. The microwave source produced energy pulses that penetrated the wall, were reflected from the metal pipes, and were detected by an antenna located next to the source. We accomplished range resolution by time tagging each microwave pulse and achieved cross-range resolution by applying SAR processing techniques. We collected the data at one-inch horizontal spacing for a length of eight feet. The raw data consisting of the amplitude of the reflected energy versus range showed no evidence of the metal pipes. However, when the data were processed coherently, the pipes became easily discernible and the differences in their diameters could be detected.

The intent of this project was to investigate the possibility of imaging through walls using a microwave source of energy. In particular Sandia was interested in using synthetic aperture radar (SAR) processing techniques to sharpen any images formed.

3530170000

Research of the Utility of Polarimetric Sensing

G. S. Phipps

The science of measuring the polarization state of light is called polarimetry. There are two types of polarimeters: (1) those that actively irradiate an object with light of known polarization, and (2) those that passively record radiation emitted and/or reflected by objects. Polarimeters in the thermal infrared (midwave infrared [MWIR]) are just becoming available, and accuracy and calibration issues are yet to be determined experimentally. The polarization effects of the instrument that measures light must be fully known, as well as the intervening atmosphere or media. In each case, a Müeller matrix can be used to describe instrumental and other effects. In addition, the polarimeter must be able to determine all Stokes parameters of the radiation at the instrument's entrance pupil. Such a polarimeter is known as a complete polarimeter. The subject of this report is the construction of and experiments with a complete imaging polarimeter.

Polarimeters can be also divided into two classes: (1) time-sequential or (2) snapshot. The time-sequential polarimeter measures Stokes parameters by employing one or more rotating polarization elements. A snapshot polarimeter measures Stokes parameters by aperture or amplitude division. All parameters are measured simultaneously. The extension of polarimetry from the visible to the MWIR and LWIR has been limited by the lack of IR polarizers and retarders. Also, in analogy to spectral imaging, the relatively recent availability of large-format MWIR imaging arrays is enabling an exploration of polarization's value in target and anomaly detection.

We constructed an MWIR complete imaging polarimeter consisting of a fixed wire-grid polarizer and rotating form-birefringent retarder. We optimized the retardance and the orientation angles of the retarder to minimize the sensitivity of the instrument to noise in the measurements. The optimal retardance was found to be 132° rather than the typical 90° . We found variations of $\pm 20^\circ$ in retardance with wavelength and angle of incidence to be tolerable. We found the optimal retarder-orientation angles to be $\{51.7^\circ, 15.2^\circ, -15.1^\circ, -51.7^\circ\}$. The complete imaging polarimeter utilized a liquid-nitrogen-cooled PtSi (platinum silicon) camera. The fixed wire-grid

...in analogy to spectral imaging, the relatively recent availability of large-format MWIR imaging arrays is enabling an exploration of polarization's value in target and anomaly detection.

polarizer was located at the cold stop inside the camera dewar. The complete imaging polarimeter was operated in the 4.42–5 mm spectral range.

We performed a series of imaging experiments using as targets a surface of water, an automobile, and an aircraft. The maximum degree of polarization recorded in these measurements was 49%. We measured this value in the case of the automobile and associated it with the hood of the vehicle. In the case of the aircraft, we observed the maximum degree of polarization associated with the windshield surface. The maximum degree of polarization was 16%. Further analysis of the polarization measurements revealed that in all three cases the magnitude of circular polarization was comparable to the noise in the calculated Stokes-vector components.

3530180000

Real-Time Image Analysis Using Field-Programmable Gate Arrays

K. J. Jefferson, J. C. Wehlburg, A. R. Baeza

Performance and target discrimination requirements for the next-generation remote sensing systems are driving designs toward ever higher dimensions, both spatial and spectral. Although the mission payoffs for increased dimensionality are significant, the bandwidth required for communication of the data quickly becomes unmanageable. In addition, the transformation of data into knowledge, a real-time requirement, demands tremendously increased speed in data processing. For many types of algorithms, sequential batch processing on general-purpose processors is the current choice for mode of operation, but with the real-time processing requirement, other processing methods such as adaptive and parallel processing on custom hardware must be considered. The purpose of this project is to demonstrate a real-time image-processing capability in a reconfigurable system of field-programmable gate arrays (FPGAs). Advantages of such a system are increased data processing throughput and the ability to modify the hardware configuration to implement a new algorithm. The projected usefulness of the image-processing system is in real-time ground data processing with an eye toward onboard processing as packaging and radiation-hardening issues are addressed.

We are implementing two algorithms that have application to space-collected imagery. The first algorithm allows multiple frames from a staring sensor to be integrated into a single super-resolution image by using information gained by subpixel shifts (microscan) between frames. This algorithm requires as input a sequence of images of the same scene (as from a staring sensor). It then uses the frame-to-frame sensor motion, which appears in the sequence as a linear transformation of the image, to estimate a higher-resolution image. The technique not only allows us to eliminate much of the noise, but also takes advantage of the residual motion by allowing it to give us new information about the scene. For the current demonstration, we used 16 lower-resolution input frames (32 X 32) to produce a single 128 X 128 enhanced image.

The processor was designed in FPGAs as a synchronous, pipelined structure using VHDL (programming language) and core functions. The controller is a set of state machines. The

The projected usefulness of the image-processing system is in real-time ground data processing with an eye toward onboard processing as packaging and radiation-hardening issues are addressed.

datapath includes data buffers, address generators, and data processing.

For the microscan algorithm, we have calculated the frames rate that can be directly supported based on input image size and resolution enhancement. Additional parallelization (requiring additional FPGA resources) can be used to increase the frame rate.

Improvements in small-target detection and geo-location using these hardware-based algorithms have been quantified and are substantial.

Refereed

Jefferson, K. J., A. R. Baeza, and J. C. Wehlburg.
1999. "Real-Time Image Processing Using Reconfigurable Logic." Paper presented to SPIE AeroSense, Orlando, FL, 15 April.

3531340000

Poco Switch Tubes

G. E. Boettcher

Sandia has two major objectives for this project. (1) We will explore the feasibility of developing a miniature 100 V dc laser-triggered poco sphytron, size 3.25 mm OD (outer dimension) x 1.9 mm H. (2) We will explore the use of graphite electrodes in poco sphytron design for possible advantages over metal electrodes; namely, more concise tolerancing of anode and cathode electrodes versus deep drawn metal electrodes, and in obtaining some diamond-line carbon erosion deposits instead of metal-film depositions that are highly conductive and detrimental to the tubes' short life.

(1) We eliminated the 6 mil molybdenum (Mo) trigger wire with nail head in the new poco sphytron designs. First experiments were with copper (Cu) wires to replace the Mo wire. We inserted the Cu wire into the 60 mil length ceramic probe and cut it approximately 2–3 mils longer than the probe at both ends. We then used tweezers to flatten the Cu ends into the ceramic probe. We brazed this flattened end on the rear side of the trigger probe to the tube's trigger disc. The braze was successful and eliminated the costly 8 mil hole previously required with the Mo wire design; however, upon brazing at ~ 1050°C, grain elongation in approximately 25% of the samples attempted caused Cu lead separation inside the trigger probe. We resolved this problem by using annealed nickel (Ni) wire, which has significantly less grain grown at our 1050°C braze temperature.

(2) We accomplished satisfactory tube design in both ceramic and sapphire envelope materials using Nicoro (35% Au, 62% Cu, 3% Ni alloy) braze material, niobium (Nb) interface material, and not metallization on the envelope surface to be joined. Sapphire has proven to be the material of choice for small tubes since it is less costly, is more particle-free due to its polished surface, and provides visual access. Elimination of the metallization process on both materials is both a cost savings and an environmental, health, and safety advantage.

Elimination of the metallization process on both materials is both a cost savings and an environmental, health, and safety advantage.

3531350000

Chemiresistors Based on Metal-Loaded Polymers for Solvent Spill Detection

R. C. Hughes

Sandia discovered that small, planar microsensors for solvents can be fabricated by mixing common, commercial polymers with metal powders, like graphite. Thin films of these composites can be deposited on interdigitated electrodes on an insulating substrate. An example of such a film is fabricated from polyisobutylene mixed with 40% by weight of carbon powder. The resistance of such a film appears to be dominated by percolation of charge through the conducting carbon particles. The resistance depends on the number of such contacts and thus on the volume fraction of the carbon particles. Vapors of some solvents can cause the polymer to swell and thus decrease the volume fraction of conducting particles. The electrical resistance thus increases with increasing solvent vapor pressure. We are using these findings to study this phenomenon in this new project. We are particularly interested in the reproducibility of the sensor signals, as well as long-term drift in the base (dry) resistance. Temperature dependence of the signals is also important to understand the thermodynamics of the polymer swelling. We wish to understand the role of entropy and heat of mixing of the solvent vapors in the sensor output. It may turn out that different polymers will have a sufficiently different response to various vapors that we can use arrays of sensors to identify an unknown vapor by pattern recognition (PR).

We are investigating matrices for the field-structured sensor. Ideally, it would be a polymer that is solid at room temperature, but one that can be melted nondestructively at a fairly low temperature so that we can move particles around and then refreeze them in the presence of a field (magnetic or electric). We may have found the ideal system: polyethylene glycols. These polymers can be purchased in several molecular weights. For example, PEG68 has a molecular weight of 6800 and is solid at 20°C but melts to a viscous, clear liquid at 62°C. At 90°C it is quite fluid, but not decomposing. We constructed sensors on planar electrodes using two different transduction principles. (1) Doping the films with the salt LiClO₄ ion conductivity can be measured even in a completely dry film. (2) Loading the film with about 30% by weight of carbon powder. These films have dc conductivity through the touching

Sandia discovered that small, planar microsensors for solvents can be fabricated by mixing common, commercial polymers with metal powders, like graphite.

chains of carbon particles, and they increase in resistance when the film swells. We placed both sensors in an oven in cells in which the vapors on the films could be controlled. When both films were dry, we measured them as they passed through the melting transition and on up to 90°C. They both survived the cycling. The carbon-loaded film showed a very large increase in resistance in passing through the melting transition, but maintained percolation throughout the temperature cycle. The ion-containing film actually showed a saturation in the ion conductivity with no sharp transition. Surface tension apparently held the sensors on the electrodes during the liquid phase. The reversibility means that we can replace the carbon particles with magnetic ones and observe ordering in the liquid phase and freeze in the new order by lowering the temperature in the presence of a field.

3531360000

Advance Neutron-Tube Design and Producibility

J. P. Brainard

This project has two goals: (1) to develop doped insulators to replace a difficult coating process now used to reduce wall charging in neutron tubes, and (2) to use new techniques to produce a more reproducible ion source for neutron tubes. For the first goal, Sandia will build several new insulators into tubes and test them for high-voltage hold-off. In the second goal, we are looking at how processes affect the stress and strain of thin films on substrates. Thin films are an integral part of the ion source.

(1) Replace a difficult high-voltage insulator coating process with a doped insulator. We fabricated the insulators, which are in queue waiting to be built into tubes so that we can test their performance.

(2) Improve neutron-tube ion-source reproducibility. To improve the understanding of the roles of film growth, hydride formation, and process parameters on producibility problems, we directed this project to develop capabilities to measure film properties during film growth.

This work involved the design and implementation of a long-distance optical microscope and camera system to monitor crack nucleation and growth in metal hydride thin films. The system probes film morphology during all stages of processing, including metal deposition, heating, hydride formation, and cooldown. Using transparent substrate (sapphire) cracks in metal, we view films optically to qualitatively determine the onset of crack formation and the spatially resolved crack pattern.

Sandia will build several new insulators into tubes and test them for high-voltage hold-off... we are looking at how processes affect the stress and strain of thin films on substrates. Thin films are an integral part of the ion source.

3531370000

Surface Hardening by Nanoparticle Precipitation and Atomic Clustering in Ni(Al,O)

S. M. Myers, Jr.

This project explores strengthening of the near-surface of nickel (Ni) by dense dispersions of hard oxide particles and atomic clusters in the nanometer-size range. These dispersions are formed by ion implantation and thermal diffusion of oxygen (O) and aluminum (Al) into Ni in conjunction with heat treatments to manipulate particle size. Sandia quantified mechanical properties by nanoindentation coupled with finite-element modeling (FEM), and characterized microstructures by transmission electron microscopy (TEM). Theoretical considerations suggest that the extremely small sizes and separations of the hard particles in such metal matrices may give rise to new highs of strength with retention of ductility. Specific objectives of the project are (1) to probe and understand the limits of strength that can be reached at the extremes of small particle size and high particle density, and (2) to extend such hardening to the technologically important iron-nickel (Fe-Ni) class of materials, and in particular to Ni because of its anticipated use in defense-related microelectromechanical systems (MEMS).

The previously demonstrated strength of 5 GPa for Ni implanted with O and Al was understood on the basis of microstructural characterization by TEM. We observed the average size of the Al-oxide (AlO) particles to be 1.5 nm, and when this was incorporated together with the particle volume fraction into dispersion-hardening theory, the predicted strength agreed quantitatively with the experimental result. In further experiments, we formed NiO particles within Ni by implanting O alone, and varied the size of these particles from 2 to 15 nm by heat treatment. The resultant strengths, as determined by micromechanical testing, again accorded quantitatively with dispersion-hardening theory, and confirmed the predicted inverse proportionality between strength and particle size. We also determined Young's modulus in these experiments. This elastic modulus increased only slightly from untreated Ni, consistent with predictions but in marked contrast to the two-order-of-magnitude increase in yield strength.

Thus, for the first time, the extreme strengthening of metals predicted to result from dispersions of nanometer-size hard particles has been experimentally demonstrated.

Sandia quantified mechanical properties by nanoindentation coupled with finite-element modeling (FEM), and characterized microstructures by transmission electron microscopy (TEM). Theoretical considerations suggest that the extremely small sizes and separations of the hard particles in such metal matrices may give rise to new highs of strength with retention of ductility.

3531380000

Dynamical Properties of Polymers; Computational Modeling

J. G. Curro

The Polymer Reference Interaction Site Model (PRISM) theory has been extremely successful in modeling the equilibrium structure and physical properties of bulk, amorphous polymers. In this investigation, Sandia will attempt to also use PRISM theory to extract information regarding nonequilibrium properties. In the past, dynamical properties such as the glass transition and viscoelasticity have been correlated with the static, equilibrium structure of the polymer through the free-volume distribution. Although the free-volume concept has long been useful from a qualitative viewpoint, it has not had a precise statistical mechanical interpretation. PRISM theory has the ability not only to provide this fundamental interpretation, but also to provide a computationally tractable modeling tool to compute the free-volume distribution for polymers at the atomistic level. In this project, we would use the PRISM theory to extract the free-volume distribution of a range of polyolefin polymers to test its ability to predict glass transition temperatures, diffusion constants, and viscoelastic shift factors. Molecular dynamics (MD) will be carried out on the diffusion of small molecules in polymers and on the self-diffusion of polymers in the bulk liquid state. We will obtain the velocity autocorrelation functions and the memory functions from MD simulation and interpret them within the context of mode-coupling theory.

We performed self-consistent PRISM calculations on polyethylene, polypropylene, polyisobutylene, and polydimethyl siloxane. We found the radial distribution functions to be in good agreement with available simulations. We also found the structure factors to be in good agreement with x-ray-scattering experiments.

We computed the free-volume distribution from PRISM theory for semiflexible chains as a function of chains stiffness. We found the free-volume distribution to decrease as the stiffness of the chains increases. We found good agreement between the free-volume distribution calculated from PRISM theory and from MD simulations.

We also performed MD simulations to study the diffusion of small molecules through polymers. We studied the velocity autocorrelation function as a function of the chain stiffness of

The Polymer Reference Interaction Site Model (PRISM) theory has been extremely successful in modeling the equilibrium structure and physical properties of bulk, amorphous polymers. In this investigation, Sandia will attempt to also use PRISM theory to extract information regarding nonequilibrium properties.

the polymers. We found that for freely jointed chains, the velocity autocorrelation function exhibited a power law time dependence at long times having an exponent of 1.5. For stiff polymer chains, on the other hand, the velocity autocorrelation function of the penetrant exhibits a power law behavior with an exponent of 2.5. Using this power law time dependence, it was possible to obtain the diffusion constant of the penetrant molecules much more efficiently than from traditional methods that require the simulations to be run long enough to get in the Fickian regime.

Refereed

Rottach, D. R., P. A. Tillman, J. D. McCoy, S. J. Plimpton, and J. G. Curro. 1999. "The Diffusion of Simple Penetrants in Tangent Site Polymer Melts." *J. Chem. Phys.* **111**.

3531390000

Broadening Mechanism in 2-D Excitonic and Electron Gases

E. D. Jones

This project will investigate the origins for the broadening mechanisms leading to the Gaussian photoluminescence (PL) lineshapes observed in doped and undoped quantum-well (QW) structures. All homogeneous broadening mechanisms predict a Lorentzian (lifetime) broadened lineshape while inhomogeneous effects lead to Gaussian lineshapes. Experimentally, we observe Gaussian PL lineshapes for all samples, ranging from nearly free exciton (undoped) systems to doped structures exhibiting band-to-band transitions at high magnetic fields. The latter result is surprising because it is generally believed that electron screening in doped systems will smooth out the effects of varying internal electric fields arising from QW fluctuations.

This project will consider the effects of artificially (or controlled) induced fluctuations. We will generate fluctuations due to varying QW widths by growing self-aligned islands of indium gallium arsenide (InGaAs) alloys in InGaAs single-strained-layer QW structures or by placing InAs quantum dots on the GaAs QWs in GaAs/AlGaAs systems. We can thus study the effect of randomness by also growing non-aligned (random) islands or quantum dots. We will do the same kinds of studies for the doping layer thickness for modulation-doped QWs. We can also make the PL lineshape contribution from deformation potential fluctuations viz-a-viz the electron-phonon interactions by deliberately growing InGaAs alloy-clusters formed by low-temperature growth.

We discovered that we can use the alloy fluctuation-induced broadening mechanisms for InGaAsN to measure carrier mass. Consequently, we could measure the carrier masses in InGaAsN as a function of pressure, up to 120 kbar. This represents a totally new method for carrier mass measurement, and these results compare favorably with the magnetoluminescence technique under the same pressure conditions.

Because of this feat, we are planning new experiments on AlGaAs, AlGaAsN, InGaAsN, and other alloy systems to enable us to make a mass measurement. For these alloy systems, i.e., those with compositions giving rise to a gamma-X crossing, it is impossible to make a mass measurement by the standard techniques, e.g., magneto-transport, cyclotron

This represents a totally new method for carrier mass measurement, and these results compare favorably with the magnetoluminescence technique under the same pressure conditions.

resonance, etc. The initial experiments will concentrate on double heterostructures of AlAs/AlGaAs (barrier/alloy) with varying Al concentrations, varying between 10% and 40% Al. We will apply hydrostatic pressure using a newly developed helium (He) pressure cell, thereby ensuring hydrostatic pressure. At a pressure of about 40 kbar, the gamma and X bands will cross, and because of gamma-X mixing, the mass will be pressure dependent. This pressure dependent mass will manifest itself in the full-width-at-half-maximum linewidth of the PL spectrum.

Refereed

Jones, E. D., K. Shinohara, S. Shimomura, S. Hiyamizu, I. Krivorotov, and K. K. Bajaj. 1999. "Magneto-Excitons in (411)A and (100)-Oriented GaAs/AlGaAs Multiple Quantum Well Structures." *Proc. SPIE* **3625** (Photonics West, San Jose, CA, 25–29 January): 515–521.

3531410000

Calculation and Interpretation of the Energies that Underlie Transition-Metal Surface Structure

P. J. Feibelman

Recent advances in computer power and in algorithms for first-principles electronic-structure calculation make it possible to evaluate energy versus atomic arrangement for essentially any bonding geometry of any combination of atomic species. Sandia will use this power in a systematic effort to uncover basic laws of surface energetics. Using state-of-the-art electronic-structure methods, we will determine the energies and geometries of fundamental atomic configurations at transition-metal surfaces to a well-defined level of numerical convergence. The results will serve as a standard, systematic foundation for the discovery and explanation of trends in adatom and vacancy formation energetics, diffusion mechanisms, vibration spectra, molecular-fragment stability, surface stress effects, work functions, etc. They will also provide a reference by which to judge the range of accuracy of the basic physical approximations used to represent the effects of electron exchange and correlation, that is, the local density and generalized gradient approximations.

We discovered that to within ~ 10%, the hopping-self-diffusion barrier calculated by means of the generalized gradient approximation for an unreconstructed fcc(100) metal surface equals one-sixth the bulk cohesive energy of the corresponding metal. This simple rule holds for aluminum (Al), rhodium (Rh), iridium (Ir), nickel (Ni), palladium (Pd), platinum (Pt), copper (Cu), silver (Ag) and gold (Au), and serves as a standard by which to judge whether a measured diffusion barrier is unusual. Thus, surveying measurements available for fcc(100) metal surfaces, the clearest exception to the "law" relating barrier height and bulk bonding is self-diffusion on Cu(100), for which the measured barrier is substantially lower than expected; the case of Ni(100) also warrants further exploration. Understanding what makes surface self-diffusion appear unusually facile on Cu(100), and possibly on Ni(100), is a problem of considerable interest.

We also computed the energies required to dissociate self-adsorbed dimers on Cu, Ag, and Au(100) surfaces to see whether they also scale with cohesive strength. Surprisingly, they do not. The separation energy for Cu on Cu(100) is 50%

Sandia will uncover basic laws of surface energetics....The results will serve as a standard, systematic foundation for the discovery and explanation of trends in adatom and vacancy formation energetics, diffusion mechanisms, vibration spectra, molecular-fragment stability, surface stress effects, work functions, etc.

greater than the value for Ag, compared to a cohesive energy ratio of 1.16, while that for Au is a bit less than for Ag, even though Au is more cohesive than Cu. At this point, we cannot account for this peculiar variation of computed separation energies.

Refereed

Feibelman, P. J. 1999. "Scaling of Hopping Self-Diffusion Barriers on fcc(100) Surfaces with Bulk Bond Energies." *Surf. Sci.* **423** (10 March): 169–174.

Feibelman, P. J. 1999. "Systematics of Self-Diffusion on fcc(100) Surfaces." Paper presented to the March APS Meeting, Atlanta, GA, 26 March.

3531420000

Interfacial Reactions in Ceramic Systems

R. E. Loehman

Improved functionality in advanced materials is frequently achieved by designing multimaterial structures that take advantage of the distinctive properties of each constituent. There are many examples of such heterostructures that incorporate ceramics, including familiar fiber- and particle-reinforced composites and, less obviously, cermets and multilayer structures used in packaging of hybrid microcircuits. Ceramic interfaces are an inherent feature of these composite materials. Understanding the reactions that determine their structures and properties is critical to developing practical processing methods and achieving the best performance.

This work addresses the general area of interfacial reactivity, microstructural evolution, and properties in ceramic systems. The first example is ceramic-metal composites made by reactive metal penetration, a process in which a solid ceramic preform is converted to a composite by reaction with a molten metal. The transformation is a net-shape process that gives a material with a microstructure of mutually interpenetrating metal and ceramic phases and excellent properties. A second example is interfaces between silicon nitride (SiN) and high-temperature joining materials. Control of compositions and interfacial reactions has allowed us to obtain joint strengths exceeding 550 MPa at 1000°C. This is the highest joint strength reported for ceramics at these temperatures. A third example is reactions of preceramic polymers to form ceramics and composites. Although preceramic polymers are finding uses in many applications, their interactions with ceramic powders and surfaces are not well understood.

We studied microstructures in the reaction interface between molten aluminum (Al) and dense mullite by transmission electron microscopy (TEM) to provide insight into mechanisms for forming ceramic-metal composites by reactive metal penetration. The reactions, which have the overall stoichiometry $3\text{Al}_6\text{Si}_2\text{O}_{13} + (8 + x)\text{Al} \Delta_{13}\text{Al}_2\text{O}_3 + x\text{Al} + {}_6\text{Si}$, were carried out at temperatures of 900°, 1100°, and 1200°C for 5 minutes and 60 minutes, and 1400°C for 15 minutes. Observed phases generally were those given in the above reaction; their proportions and interfacial

Ceramic interfaces are an inherent feature of these composite materials. Understanding the reactions that determine their structures and properties is critical to developing practical processing methods and achieving the best performance.

microstructures, however, were strongly dependent on the reaction temperature. Using previously measured reaction kinetics data, we modeled the observed temperature-dependence of the interfacial microstructure as three sequential steps, each one of which is rate limiting in a different temperature range.

We also investigated interfacial reactions and bonding of vanadium (V)-containing braze alloys on Si_3N_4 , SiC-SiC composites, alumina, and sapphire. Au-Pd-V (gold palladium vanadium) alloys wet, react, and bond to Si_3N_4 at 1270°C , giving VN and Pd_2Si and 4-pt bend strengths of 525 MPa. Wetting and reaction of Au-Pd-V alloys with SiC composites is variable and nonuniform, and the identification of products is inconclusive. Au-Ni-Mo-V (gold nickel molybdenum vanadium) alloys wet and react with alumina and sapphire at 1000°C and adhere to them when cooled. Contact angles are lower and bond strengths are higher for 94% alumina than for 99.8% alumina. Reaction zones found so far are thinner than 1 mm, and AlV_2O_4 and AlVO_3 are the only identified products. There is some evidence that bonding occurs preferentially at the glassy grain boundaries of the 94% alumina, accounting for their higher bond strengths. These results are different from earlier work on reaction mechanisms in titanium (Ti)-containing braze alloys.

Previous work on preceramic polymers showed that crystallization of Si_3N_4 from polycyclomethylsilazane is affected significantly by the presence of oxide-sintering aids, which can be incorporated either as molecular substitutions in the polymer or as oxide powder additives. We investigated the effects of temperature on the interactions between polysilazane, ceramic powders, and additives. We prepared specimens by depositing coatings of ceramic powders, polycyclomethylsilazane, and solvent on SiN coupons. The specimens were dried and then heated from 1000°C to 1750°C for 2 hours to pyrolyze the polymer and crystallize the resulting ceramic. We examined microstructures and compositions by electron analytical techniques to determine mechanisms of pyrolysis reactions and subsequent conversion to the ceramic and how they were affected by the form of the sintering aids used. The quality of the coating increased with conversion temperature up to 1600°C . Heating at 1750°C tended to promote interdiffusion of second phases between coating and substrate. Coatings were generally indistinguishable from the substrates on which they were placed, indicating excellent conversion to the ceramic.

Refereed

Loehman, R. E. 1998. "Interfaces in Composites, Joining, and Ceramic Coatings." Paper presented to IMA '98, Osaka,, Japan, 10 September.

Loehman, R. E., P. Lu, S. M. Johnson, and Y. Blum. 1998. "Preceramic Polymer Coatings on Silicon Nitride." Paper presented to the Rio Grande Regional Materials Symposium, Albuquerque, NM, November.

Loehman, R. E., S. M. Johnson, and Y. Blum. 1999. "Compositional and Structural Studies of the Conversion of Preceramic Polymers to Silicon Nitride." Paper presented to the Annual Meeting, American Ceramic Society, Indianapolis, IN, May.

3531430000

Direct Fabrication of Multifunctional Nanocomposites Via Supramolecular Self-Assembly

C. J. Brinker, Y. Lu

The ability to efficiently organize molecular components at the nanometer scale will greatly influence the future of advanced materials in applications for electronics, catalysis, magnetism, sensors, and mechanical design. This stems from the fact that interplay of structure, organization, and dynamics at the molecular level are all vital in determining a functional response. Based on this premise, Sandia successfully developed an efficient, continuous process to form ordered nanocomposite thin films and particles via evaporation-induced self-assembly. Thin films are prepared by spin- or dip-coating a homogeneous sol containing alcohol, silica precursors, organic monomers, initiators, and surfactant (at an initial concentration $[c_0]$ below the critical micelle concentration $[cmc]$). Evaporation of the alcohol induces the formation of micellar structures that co-organize with silica to form cubic, hexagonal, or lamellar mesophases. The organic monomers and initiators are solvated within the hydrophobic micellar interiors. Subsequent photo or thermal polymerization and washing results in a silica/polymer thin-film nanocomposite. The process can be extended to particles with ordered (vesicular) structures via aerosol processing of related sols.

We combined EISA with rapid prototyping techniques like pen-lithography, ink-jet printing (IJP), and dip-coating on microcontact-printed substrates to form hierarchically organized structures in seconds. In addition, by co-condensation of tetrafunctional silanes ($\text{Si}(\text{OR})_4$) with trifunctional organosilanes ($(\text{RO})_3\text{SiR}$) or by inclusion of organic additives, we selectively derivatized the silica framework with functional R ligands or molecules. The resulting materials exhibit form and function on multiple length scales: on the molecular scale, functional organic moieties are positioned on pore surfaces; on the mesoscale, monosized pores are organized into 1-D, 2-D, or 3-D networks, providing size-selective accessibility from the gas or liquid phase, and on the macroscale, 2-D arrays and fluidic or photonic systems may be defined.

Sandia successfully developed an efficient, continuous process to form ordered nanocomposite thin films and particles via evaporation-induced self-assembly.

For ink we use homogeneous solutions of tetraethylorthosilicate (TEOS), ethanol, water, surfactant, acid, and (optionally) organosilanes and other organic ingredients. As the ink is metered onto the surface, preferential ethanol evaporation causes enrichment of water, surfactant, and silica, establishing a 3-D (longitudinal and radial) gradient in their respective concentrations. Where cmc is exceeded, cooperative silica/surfactant self-assembly creates micelles. Further evaporation, predominantly of water, promotes the continuous self-organization of micelles into silica/surfactant liquid crystalline mesophases.

We prepared meandering macroscopic patterns in several seconds by computer-aided design (CAD)-driven micropen lithography (MPL) of a rhodamine B-containing solution on a hydrophilic surface (hydroxylated native oxide of <100> silicon). Fluorescence microscopy confirmed the rhodamine activity, and transmission electron microscopy (TEM) revealed the ordered pore structure characteristic of a cubic thin-film mesophase. The MPL linewidth can vary from micrometers to millimeters. It depends on such factors as pen dimension, wetting characteristics, evaporation rate, capillary number ($Ca = \text{ink viscosity} \times \text{substrate speed} / \text{surface tension}$), and ratio of the rates of ink supply and withdrawal (inlet velocity/substrate velocity). We demonstrated the effect of wetting by performing MPL on substrates pre-patterned with hydrophobic, hydrophilic, or mixed self-assembled monolayers (SAMs). Generally, linewidths are reduced by increasing the contact angle and by reducing the inlet/substrate velocity ratio. The conditions providing the minimum stable linewidth are bounded by a regime of capillary instability—we anticipate that this instability could be exploited to create periodic arrays of dots.

Finally, we can create patterned nanostructures by combining EISA with a variety of aerosol-processing schemes. The IJP process dispenses the ink (prepared as for MPL) as monosized, spherical aerosol droplets. Upon impaction the droplets adopt a new shape that balances surface and interfacial energies. Accompanying evaporation creates within each droplet a gradient in surfactant concentration that drives radially directed silica/surfactant self-assembly inward from the liquid-vapor interface. The greater resolution achieved compared to standard ink and our ability to selectively functionalize the ink suggests applications in display technologies.

The conditions providing the minimum stable linewidth are bounded by a regime of capillary instability—we anticipate that this instability could be exploited to create periodic arrays of dots.

Refereed

Brinker, C. J., Y. Lu, A. Sellinger, and H. Fan. 1999. "Evaporation-Induced Self-Assembly: Nanostructures Made Easy." *Advanced Materials* **11** (May): 579–585.

Sellinger, A., P. M. Weiss, A. Nguyen, Y. Lu, R. A. Assink, W. Gong, and C. J. Brinker. 1998. "Continuous Self-Assembly of Organic-Inorganic Coatings that Mimic Nacre." *Nature* **394** (16 July): 256–260.

Other Communications

Fan, H., Y. Lu, and C. J. Brinker. 1999. "Rapid Prototyping of Patterned Functional Nanostructures." *Nature*, submitted.

3531440000

Raman Investigation of Phase Changes in PZT Materials

D. R. Tallant, J. M. Grazier, J. B. Aidun, D. H. Zeuch, B. A. Tuttle, J. A. Voigt, R. L. Simpson

Sandia proposes to use Raman spectroscopy to investigate phase equilibria and environmentally induced phase changes in lead zirconate titanate (PZT) 95/5, a material of interest in weapons applications because of its ferroelectric (FE) behavior. The shock-induced phase transformation of PZT 95/5 from FE to anti-ferroelectric (AFE) is the property used in weapons components. We will develop a mechanical loading apparatus and integrate it into micro-Raman spectroscopic instrumentation for the purpose of monitoring, in situ, the FE/AFE phase change in microscopic crystals within PZT ceramic samples as a function of uniaxial and/or hydrostatic stress. If successful, this project will provide a new and unique capability for obtaining molecular-level structural information from microscale areas of materials under conditions of environmental stress that significantly affect the materials performance. The information gained for PZT 95/5 will provide a more detailed picture of its FE/AFE phase behavior and will be of direct use to the PZT supply team in selecting PZT materials for weapons components. These observations of the phase behavior of PZT 95/5 will aid in the refinement of and provide validation for single-crystal continuum models of PZT.

We successfully observed *in situ*, using Raman spectroscopy, stress-induced phase changes related to the FE-to-AFE transition in PZT materials. We accomplished all the experimental goals proposed: synthesize and characterize ceramic compositions; design and fabricate load fixture; and observe, *in situ*, stress-induced FE-to-AFE phase changes by Raman spectroscopy.

The ceramic material so studied is from the PNZT ($\text{Pb}_{0.99}\text{Nb}_{0.02}[\text{Zr}_{1-Y}\text{Ti}_Y]_{0.98}\text{O}_3$) family of compositions, whose AFE phase (for ambient conditions) exists at Ti/Zr ratios < 0.04 and whose FE phase exists at Ti/Zr ratios > 0.04 . We prepared polycrystalline ceramic bars with Ti/Zr ratios of 0.02 (AFE), 0.044 (FE), and 0.047 (FE), and confirmed their phase composition by x-ray diffraction. These materials show distinct and readily recognizable differences between the Raman bands of the AFE and FE phases in the frequency region between 20

...this project will provide a new and unique capability for obtaining molecular-level structural information from microscale areas of materials under conditions of environmental stress that significantly affect the materials performance. The information gained for PZT 95/5 will provide a more detailed picture of its FE/AFE phase behavior and will be of direct use to the PZT supply team in selecting PZT materials for weapons components.

and 700 cm^{-1} . Using the microscope accessory we obtained high-quality Raman spectra with resolution at the microscopic ($\approx 1\text{ }\mu\text{m}$) scale. The microscopic resolution is similar to the sizes of the grains in the ceramic. We designed and fabricated a load-frame fixture for applying uniaxial stress to PNZT bars while performing micro-Raman spectroscopy (180° backscatter configuration). For ceramic bars approximately 1 cm square in cross-section by 2.5 cm long, this fixture applied up to 500 MPa of uniaxial stress.

Using this fixture to apply longitudinal stress while observing microscopic regions of a ceramic bar with Raman spectroscopy, we successfully observed stress-induced FE-to-AFE transitions in individual PNZT grains. We observed stress-induced FE-to-AFE transitions in microscopic grains in separate experiments on eight ceramic FE-phase bars, four with $\text{Ti}/\text{Zr} = 0.044$ and four with $\text{Ti}/\text{Zr} = 0.047$. The changes in the Raman spectra as a result of the stress-induced transitions mirror the differences between the Raman spectra of FE ($\text{Ti}/\text{Zr} > 0.04$) and AFE ($\text{Ti}/\text{Zr} = 0.02$) ceramic compositions. In a typical experiment we monitored six locations by Raman spectroscopy as we increased the applied stress in 25 MPa steps. We observed FE-to-AFE transformations above 300 MPa .

An interesting result of this investigation is that the stress-induced transformations can be very localized: at a given applied stress, one grain may transform, but another a few tens of micrometers away may not. While the final statistics are not yet available, it appears that about half the microscopic grains selected for observation by Raman spectroscopy underwent an FE-to-AFE transformation. At a few locations the FE-to-AFE transformation appeared to reverse and then go forward as we incrementally increased the stress. Perhaps this reflects release of stress as grains slip against one another. Most, but not all, of the transformed grains relaxed to the FE phase when we removed the stress.

These experiments provided what is clearly a preliminary look at the process of FE-to-AFE transformations in PNZT ceramics.

These experiments provided what is clearly a preliminary look at the process of FE-to-AFE transformations in PNZT ceramics.

3531450000

Information Extraction from Hyperspectral Images Obtained from Satellites

D. M. Haaland, C. M. Wehlburg

This research applies newly developed multivariate analysis tools to the analysis of multispectral (MS) and hyperspectral image (HSI) data generated from imaging spectrometer systems to be flown on satellites for target recognition applications. Sandia's newly developed prediction-augmented classical least squares/partial least squares (PACLS/PLS) algorithms have the potential to more efficiently extract quantitative and target recognition information from MS and HSI. The new information-extraction methods can be tested with spectral data from either Sandia's Information-Efficient Spectral Imaging Sensor (ISIS) system or from the Multispectral Thermal Imager (MTI) system. The methods are also ideally suited for reliability monitoring using newly invented outlier detection methods for the optically computed signals from Sandia's ISIS system. In addition, we can use the new PACLS/PLS algorithm to eliminate the detrimental effects of atmospheric variations in viewing angle, elevation, and atmospheric interferants such as water vapor and carbon dioxide.

We tested multivariate approaches on existing LandSat HSI of the earth. The analyses included the use of minimum noise fraction (MNF) transformation of the spectral data to minimize noise and decorrelate the spectral data. We followed this image pretreatment with a multivariate end-member analysis to estimate the pure mineral component spectra existing in the image. We found four pure mineral spectral components and compared them to library spectra. This end-member analysis will also serve as the initial estimates in a multivariate curve resolution analysis to extrapolate to better pure-component spectra. We will then use the resulting pure-component spectra with our new PACLS and PACLS/PLS algorithm to obtain more accurate composition maps from the basic images.

We also invented a method to use the ISIS for satellite imaging that allows the efficient optical computing of ISIS to be performed while retaining the sensitive outlier detection of standard multivariate methods. Thus, we can monitor and ensure the reliability of the analyses.

Sandia's newly developed prediction-augmented classical least squares/partial least squares (PACLS/PLS) algorithms have the potential to more efficiently extract quantitative and target recognition information from MS and HSI.

We also conceived of methods to use the new PACLS and PACLS/PLS algorithms to eliminate the detrimental effects of atmospheric variations in viewing angle, elevation, and atmospheric interferants such as water vapor and carbon dioxide on the identification of targets in satellite images. For example, if we measure the spectra of multiple atmospheric variations and viewing angles from space over a constant homogeneous background, then an eigenvector decomposition of these variations will yield the important atmospheric spectral shapes that must be excluded from the image analysis and target classification. Thus, our new algorithms give us the opportunity to efficiently exclude the detrimental effects of atmospheric and instrumental variations on target identification. We will test these new approaches with satellite spectral images.

...our new algorithms give us the opportunity to efficiently exclude the detrimental effects of atmospheric and instrumental variations on target identification.

3531460000

Expanding the Security Dimension of Surety

M. E. Senglaub

Sandia explored the use of a number of modern analytic technologies in the assessment of terrorist actions and to predict trends. This work focuses on Bayesian networks as a means of capturing correlations between groups, tactics, and targets. We obtained the data that we used to test the methodology by using a special parsing algorithm written in JAVA to create records in a database from information articles captured electronically. As a vulnerability assessment technique, the approach proved very useful. The technology also proved to be a valuable development medium because of the ability to integrate blocks of information into a deployed network rather than waiting to fully deploy only after all relevant information has been assembled.

We identified the capability of using Bayesian networks in risk or vulnerability assessments. Bayesian networks allow the analyst to bring together information from a number of disciplines and to explore traditional as well as new relationships of that information to assess vulnerabilities of critical assets. The simple model that we examined in this project provided an environment to explore causal relationships of variables in an effort to garner a better understanding of terrorism.

Beta distributions could be used to approximate the high-fidelity data that should reside in detailed terrorism databases. Beta distributions have a nice set of conditions that lend themselves to be used for approximating discrete state-oriented data.

Computational environments such as agent environments like ISSAC or SWarrior could be used to statistically determine the difficulties of defeating a potential target's defenses. Coupling this information with an enhanced tactical database could provide a very respectable threat awareness capability for use by security elements.

The simple model that we examined in this project provided an environment to explore causal relationships of variables in an effort to garner a better understanding of terrorism.

Refereed

Senglaub, M. E. 1999. "Expanding the Security Dimension of Surety." Sandia Technical Report SAND99-2513, Sandia National Laboratories, Albuquerque NM (October).

3531470000

Overcoming Software Brittleness: A Swarm Intelligence Approach

G. C. Osbourn, J. W. Bartholomew

Development of bug-free, high-surety, complex software is quite difficult using current tools. The brittle nature of the programming constructs in popular languages such as C/C++ is one root cause. Brittle commands force the designer to rigidly specify the minutia of tasks rather than specifying the goals or intent of the tasks. Specification of task minutia makes code hard to comprehend, which in turn encourages design errors/limitations and makes future modifications quite difficult. The Y2K (Year 2000) problem illustrates these points. This project will develop a surety computer language for stand-alone computing environments that is implemented using the swarm intelligence of autonomous agents. Several novel surety capabilities should emerge from this approach:

(1) Reliability. Autonomous agents can appropriately decide when to act and when a task is complete, provide a natural means for avoiding brittle task specifications, and can overcome many hardware glitches.

(2) Safety, security. Watchdog safety and security agents can monitor other agents to prevent unauthorized or dangerous actions.

(3) An immune system. The small chunks of agent code can have an encryption scheme to enable detection and elimination of unauthorized and corrupted agents.

(4) Maintenance/upgrade. We can seamlessly implement upgrades for software (built from these language constructs) while executing the code (for applications that can not be taken offline). Work will include the design, implementation, and demonstration of a toolkit of these general-purpose language constructs.

Rather than implement a full surety language, this project focused on developing a small subset of this new language to illustrate overall feasibility. We decided to base this small subset on the language FORTH. We developed and implemented a small, interpreted language that mimics the core of the FORTH language. Using these commands, we designed a small number of software agents that illustrated some of the abilities required of a larger and full language implementation. In particular, we showed that a watchdog agent could act to protect certain memory locations from any other code (written

This project will develop a surety computer language for stand-alone computing environments that is implemented using the swarm intelligence of autonomous agents. Several novel surety capabilities should emerge from this approach.

in this same language) that was executing, without minutia specification. We also completed a plan for a program-building graphical user interface (GUI) and made substantial progress in implementing this GUI. The main idea behind this GUI is to let the user, not software, parse the program inputs by entering execution tokens directly into the tool. This prevents the need for a command line parser. This also prevents many types of incorrect language inputs, as the GUI simply will not accept illegal inputs, and completely avoids command and variable name typos. Further, the execution tokens can then be converted into readable English text that would be too difficult to parse by machine. We believe that the English-like text produced in this way is much easier to read and understand than C or C++ code.

The main idea behind this GUI is to let the user, not software, parse the program inputs by entering execution tokens directly into the tool.

3531480000

Synthesis and Applications of N-Type Diamond

R. J. Anderson, D. C. Dibble

Sandia synthesized free-standing diamond films that we doped with tantalum (Ta), tungsten (W), rhenium (Re), and osmium (Os) metals. We accomplished these novel syntheses by microwave-assisted chemical vapor deposition (CVD) using small amounts of metalorganic compounds in the feed stock. Raman spectroscopy shows that all of these films are very high quality diamond. Ta:diamond and W:diamond produce populated electronic levels in the bandgap at 1.95 eV and 1.80 eV below the conduction band minimum, respectively, and that in each case unpopulated impurity states lie approximately 0.07 eV below the conduction band minimum. The unpopulated impurity electronic level in Ta:diamond and W:diamond is populated in Re:diamond and in Os:diamond, thus creating an electronic level only 0.08 eV or less below the diamond conduction band minimum, which should therefore form n-type diamond. However, we have not yet successfully measured an electron current in these materials, perhaps because of frustrated intergranular transport in these polycrystalline materials, or because of compensation by the surface p-type damage layer always present in diamond grown by CVD.

Although diamond, like silicon (Si) and germanium (Ge), is a tetrahedrally bonded group-IV semiconductor, there is no electronics technology based on diamond as an active material. Similarly, the negative electron affinity (NEA) of the hydrogen (H)-terminated diamond surface suggests that diamond should be the ultimate cold-cathode source, yet there is also no technology based on this property. In each case, development is disabled by the lack of a demonstrated, dependable shallow donor to form *n*-type diamond. First, this prevents the synthesis of the *p-n* junction, the building block necessary for diamond-based active devices. Second, the field emission of electrons from the NEA surface is vitiated by the prohibitively large energy necessary to raise electrons to the conduction band from deep in the gap.

Attempts to effect shallow donor diamond based on conventional thinking have failed. However, a shallow donor level may be formed by replacing two nearest-neighbor carbon (C) atoms with an impurity having enough valence electrons to satisfy dangling bonds at the six adjacent C atoms and

Sandia synthesized free-standing diamond films that we doped with tantalum (Ta), tungsten (W), rhenium (Re), and osmium (Os) metals. We accomplished these novel syntheses by microwave-assisted chemical vapor deposition (CVD) using small amounts of metalorganic compounds in the feed stock.

additionally to populate a level near the conduction band minimum (CBM). To that end we synthesized free-standing polycrystalline diamond films containing small amounts of Ta, W, Re, and Os.

CVD of diamond by hot filament-assisted growth introduces some small amount of the filament material (typically tens to hundreds of parts per million) into the growing diamond film. However, our attempts to use this growth technique did not yield diamond of sufficient quality to measure meaningful optical and electrical properties. We then turned to microwave plasma-assisted CVD to synthesize the doped diamond. This was successful; the use of about 100 ppm concentrations of Ta ethoxide, or the carbonyls of W, Re, and Os, produced appropriately doped free-standing diamond films.

Results of spectroscopic analyses of these films are consistent with the qualitative model of bonding at the inferred impurity center. Photoluminescence (PL) and PL excitation spectra of Ta:diamond imply an occupied impurity electronic level 2.10 eV below the CBM and an empty level 0.15 eV below the CBM. Similar data from W:diamond place the corresponding states at 1.800 and 0.070 below the CBM. These data are consistent with the expectation that the six dangling bonds at the divacancy center require six valence electrons to fill the bonding shell of the defect complex. The highest occupied levels at the Ta defect (five added valence electrons) and the W defect (six added valence electrons) will be nearly isoenergetic. However, a seventh impurity valence electron would be forced into the unoccupied level near the CBM, a level that is predicted by molecular orbital theory to be a degenerate nonbonding orbital. This is consistent with infrared (IR) absorption spectra of Re:diamond (seven added valence electrons) and Os:diamond (eight added valence electrons), which show strong absorption edges at 0.080 eV. There is no detectable luminescence from Re:diamond or Os:diamond in the absence of compensating nitrogen (N). Furthermore, only Re:diamond and Os:diamond show Raman spectra with an asymmetric (Fano) phonon lineshape, similar to that observed in *n*-type Si, caused by interference between scattering from the discrete phonon excited state (0.165 eV) and from a continuum of isoenergetic electronic states above the CBM.

Spectroscopic measurements probe the electronic structure within the grains of the polycrystalline film. Electrical measurements, which rely on intergranular charge transport, have been unsuccessful so far. Even the purest CVD diamond shows *p*-type transport as grown, because of a damage layer

...the use of about 100 ppm concentrations of Ta ethoxide, or the carbonyls of W, Re, and Os, produced appropriately doped free-standing diamond films.

less than 10 nm thick at the surface. Intergranular current of our as-grown diamond is always p -type. When the Re:diamond and Os:diamond are annealed in vacuum, they become more resistive and show transient n -type current, but return to p -type current on prolonged exposure to the atmosphere. Confirmation of true n -type behavior in these materials must wait until this surface compensation and intergranular charge transport dilemma can be overcome.

3531490000

A Molecular Theory of Gatekeeper Proteins

L. J. Frink, A. G. Salinger

Predicting the behavior of ion channel proteins is important for identifying possible biological activity of drugs and toxins. Sandia is interested in predicting open channel currents through ion channel proteins using a molecular theory approach. Diffusion times are generally too long for molecular dynamics (MD) to be useful. The goals of this project were to demonstrate the feasibility and accuracy of the molecular theory approach by implementing transport equations in an existing density-functional theory (DFT) code and comparing calculations with grand canonical molecular dynamics (GCMD) simulations. Application to ion channel proteins was to follow proof-of-concept studies. The comparison of transport-DFT and GCMD was successful for a variety of simple mixtures in a variety of situations (e.g., color diffusion, diffusion in the presence of an external field and in the presence of pressure gradients). In addition, we implemented a variety of 1-D and 3-D ion channel models in the transport-DFT code.

We investigated a novel approach to modeling molecular steady-state transport for ion channel protein systems. This approach couples a molecular theory, DFT, with a diffusive (and in some cases convective) transport law to predict density and chemical potential gradients in nonequilibrium steady-state systems for several simple mixtures.

We compared the results of transport-DFT calculations explicitly with GCMD simulations for a variety of systems. We found that the two methods were in agreement for predictions of both chemical potential and density profiles given the assumption of a spatially invariant diffusion coefficient provided that the center of mass motion of the system was known. Thus, given a diffusion coefficient, both methods will yield the same flux (or ion current, in the case of ion channel proteins). To compute the flux as a function of system parameters (e.g., applied potential in ion channel experiments), we will need only a few GCMD calculations or experimental measurements to determine the bounds on diffusion coefficients. The transport-DFT approach may then be used for exploring a complete range of the parameters of interest. Given the efficiency of the transport-DFT approach, this new method may provide a powerful addition to the tools available for

The goals of this project were to demonstrate the feasibility and accuracy of the molecular theory approach by implementing transport equations in an existing density-functional theory (DFT) code and comparing calculations with grand canonical molecular dynamics (GCMD) simulations.

studying molecular steady-state transport and its effects on a variety of complex surface phenomena from capillary condensation to wetting to ion channel transport.

In addition to establishing the efficacy of the transport-DFT approach, we began applying the transport-DFT to ion channel proteins and developed a variety of 1-D and 3-D model test systems.

Refereed

Frink, L. J. D., A. Thompson, and A. G. Salinger.
1999. "Extending Molecular Theory to Steady-State
Diffusing Systems." *J. Chem. Phys.*, submitted.

3531510000

Development of Compact UV Laser Source for Climate Studies and Chemical Sensing

D. A. Kliner

Sandia is exploring the use of single-mode fiber lasers and amplifiers (originally developed for optical telecommunications) as compact, lightweight sources of tunable, narrow-bandwidth, deep-ultraviolet (UV) radiation. Such sources are required for in situ spectroscopic detection of trace species with high sensitivity and specificity in a variety of applications, including climate studies, explosives detection, and detection of chemical and biological agents.

Our main accomplishment this year was the development of a high-power, high-efficiency fiber amplifier. This amplifier exhibited, separately, 39% electrical-to-optical conversion efficiency, 89% internal optical-to-optical conversion efficiency, 3.9 W output power at 1060 nm, and 53 dB of small-signal gain. In a separate experiment, we demonstrated a new approach to obtaining linear-polarization operation of a fiber amplifier by externally applied stress-induced birefringence.

The high-efficiency fiber amplifier consisted of an 11 m piece of Yb-doped, double-clad fiber. We pumped the fiber using a v-groove side-pumping scheme developed by our collaborators at the Naval Research Laboratory (NRL). Specifically, a 0.68 NA microlens was used to focus the 975 nm output of a broad-stripe laser diode onto the facet of a v-groove cut into the inner cladding of the fiber, thereby launching 90% of the diode output power into the inner cladding. The diode had an electrical-to-optical conversion efficiency of up to 59%. The amplifier was seeded at 1060 nm in a counter-propagating geometry. With 100 mW of seed power and 4.4 W of launched pump power, the output power was 3.9 W, corresponding to a net electrical-to-optical efficiency of 36%. At an output power of 1.8 W, the electrical-to-optical efficiency was 39% (because the pump diode was more efficient at the lower current). We demonstrated wide tunability: the saturated output power was > 3.6 W between 1050 and 1110 nm.

Linear polarization is required in many applications of fiber lasers and amplifiers, including nonlinear frequency conversion. We developed a new approach to obtain linear-polarization operation of an RE-doped fiber amplifier. In this

The technique...allows single- or multiple-pass operation of the amplifier, does not increase system complexity (no additional components are inserted in the optical path), leaves the fiber ends unobstructed, introduces negligible loss, and is inexpensive to implement.

approach, the gain fiber is coiled under tension around a spool, resulting in stress-induced birefringence. The technique is general, i.e., applicable to most single-mode optical fibers (single- or double-clad), achromatic, and compatible with all standard configurations of amplifiers; it allows single- or multiple-pass operation of the amplifier, does not increase system complexity (no additional components are inserted in the optical path), leaves the fiber ends unobstructed, introduces negligible loss, and is inexpensive to implement.

These developments, which were not anticipated in our original proposal, will have a significant impact on the design and ultimate performance of a fiber-based, UV laser system. In particular, they will simplify the design, allowing a more compact, rugged system, and will permit higher UV powers to be obtained.

These developments, which were not anticipated in our original proposal, will have a significant impact on the design and ultimate performance of a fiber-based, UV laser system.

Refereed

Goldberg, L., J. P. Koplow, and D. A. V. Kliner. 1999. "High-Efficiency 3 W Side-Pumped Yb Fiber Amplifier and Laser." *Proc. Conf. on Lasers and Electro-Optics Technical Digest 1999* (Baltimore, MD, 23–28 May): 11–12.

Goldberg, L., J. P. Koplow, and D. A. V. Kliner. 1999. "Highly Efficient 4 W Yb-Doped Fiber Amplifier Pumped by a Broad-Stripe Laser Diode." *Optics Lett.* **24** (15 May): 673–675.

Koplow, J. P., L. Goldberg, R. P. Moeller, and D. A. V. Kliner. 1999. "Polarization-Maintaining, Double-Clad Fiber Amplifier Employing Externally Applied Stress-Induced Birefringence." *Optics Lett.*, submitted.

Other Communications

Kliner, D. A. V., L. Goldberg, and J. P. Koplow. 1999. "High-Efficiency, 4 W, Yb-Doped Fiber Amplifier and Polarization-Maintaining, Double-Clad, Er/Yb-Doped Fiber Amplifier." Sandia Technical Report SAND2000-8208, Sandia National Laboratories, Albuquerque, NM (October).

3531520000

Power Source Technologies for Autonomous Microsystems

G. V. Herrera, D. Ingersoll

It is recognized that the power source is an enabling technology and often the limiting one for advanced systems development. Furthermore, in spite of the fact that continued advances at the component level will invariably lead to reduced power demands, it is generally expected that the power system will continue to be the single most limiting factor in advanced systems design, development, and deployment. The primary objective of this project is to provide an assessment of the current and projected power needs for these advanced systems in the hope of identifying power system development activities that should be initiated in order to be able to meet these anticipated needs. Sandia made this assessment by conducting a series of interviews with a number of individuals involved in advanced system development, both at Sandia and at other government agencies. The individuals selected for these interviews represent a wide gamut of activities, including advanced weapon system development, robotics, micro-machines, satellites, autonomous systems, monitoring, etc.

We completed a comprehensive analysis of the power source applications of interest to Sandia and DOE and analyzed the power needs for each. We also included environmental factors that would influence the type of power source. We discovered that advanced system development is occurring in the performance range of less than 1 mW to greater than the 100 W.

Other Communications

Doughty, D., D. Ingersoll, and G. Herrera. 1999. "Power Source Technologies for Autonomous Microsystems." Internal memorandum (August).

The primary objective of this project is to provide an assessment of the current and projected power needs for these advanced systems in the hope of identifying power system development activities that should be initiated in order to be able to meet these anticipated needs.

3532280000

Advanced Radiation Sources: Rayleigh-Taylor Mitigation Via Perturbation Reduction

R. B. Spielman, S. E. Rosenthal, M. P. Desjarlais, M. R. Douglas

The understanding of Rayleigh-Taylor (RT) instabilities requires one to understand a number of fundamental issues in plasmas. These include the nature of plasma resistivity, kinetic effects, and magnetic field diffusion. Reaching a detailed understanding of all of these is not possible in the context of this project, but Sandia has made major improvements in capabilities.

The radiation magnetohydrodynamics (R-MHD) codes that we use to model z pinches use tables for the resistivity and equation-of-state (EOS) for the plasma. We used recent data to develop semi-analytic models for resistivity. This resulted in changes in the resistivity used by the codes of four to five orders of magnitude. While not perfect, these improvements are the 90% solution.

We began to address the issue of plasma kinetic effects by studying the limits of applicability of the fluid approximation and developing solutions to various forms of the Vlasov equation.

All of these physics issues together impact the diffusion of magnetic field through plasmas. This is not a simple problem! More than a quarter century ago a semi-analytic theory for diffusion was developed. There have been few advances in the field of low-density diffusion of plasmas, which is why we are looking at solutions to the Vlasov equation. But the new resistivity tables that we developed enable us to use MHD codes to solve this problem in the high-density limit.

We are using MACH2 to model the evolution of the RT instability with these new resistivity tables and are comparing these calculations with experiments.

We made major progress in understanding the underlying physics of the RT instability.

- *Plasma resistivity.* We completed work on models of plasma resistivity that covers the range of densities and temperatures that have been poorly understood in the past. The range of temperatures is from room temperature to 20+ eV. The range of densities is from solid density to as low as one millionth of solid. The model generates values of resistivity that match the well-measured room-temperature values and also merge in the high-temperature limit to the well-known

The understanding of Rayleigh-Taylor (RT) instabilities requires one to understand a number of fundamental issues in plasmas....Sandia has made major improvements in capabilities.

Spitzer resistivity. We used the model to generate large tables of resistivity values for use in MHD codes. The table formats are the same as those used for decades in the community, so our results can be (and have been) used rapidly and widely.

This model shows that we used values of resistivity as much as five orders of magnitude too high in earlier calculations. The lower resistivity results in less field diffusion, less heating, and a thinner current sheath.

- *MHD calculations.* We used the new resistivity tables to conduct a wide range of calculations of plasmas and conductors. The new values convincingly demonstrate that the lower resistivities reduce plasma heating and result in a significantly thinner sheath carrying current.

The above resulted in an increase in the impact of RT instabilities. The thinner sheath allows the faster-growing short-wavelength modes to grow. This means that small perturbations can grow rapidly during the early stages of a plasma implosion.

We are just beginning to use the new capability in the evolution of the plasma surrounding a single wire. The completion of the 3-D ALEGRA code will permit the study of the evolution of the plasma in a wire array and provide a physical basis for the perturbation levels used in the 2-D codes to date.

*We are just beginning to use the
new capability in the evolution
of the plasma surrounding a
single wire.*

Other Communications

Douglas, M. R., C. Deeney, and N. Roderick. 1999. "Investigation of Magnetic Field Effects on the Mitigation of the Magnetohydrodynamic Rayleigh-Taylor Instability in Fast Z Pinches." Paper presented to the ICOPS, Monterey, CA, June.

3532290000

Global Approaches to Infrastructural Analysis (GAIA)

D. Engi

Our country (and, in fact, the global community) is vulnerable to significant costs (in both dollars and human lives) associated with stresses arising from sources that are both manmade (e.g., war, terrorism, and political disruptions) and natural (e.g., hurricanes, tornadoes, earthquakes, droughts, and floods). There is currently a need for a comprehensive, integrated suite of information that would be of value in helping identify opportunities for technological responses to these stresses. This project is directed toward the development and deployment of a decision support system (DSS) that will provide timely, accurate, and high-impact information. The context for this information is the international arena with an emphasis on the technological aspects of responses to these stresses.

This project is motivated by Sandia's recognition that enhancing our nation's ability to manage vulnerabilities of global infrastructures is necessary to maintain our national security. We recognize the technical challenges of creating an integrated infrastructure DSS and will use a strategy consisting of architecture, process, and metrics to address these challenges. We will create an architectural framework to support the system, methods for specifying modeling and analysis and for integrating new commodities into the system, and metrics for measuring the utility of the knowledge provided. Integrating the computer modeling and simulations of diverse commodities, explicitly considering the international arena as the system, and combining the judgment of international subject matter experts are innovations now possible due to the advent of high-performance computers and the global information infrastructure.

We accomplished two major tasks and produced significant analytic results. Each was focused on exploring the science and technology of managing critical infrastructures under stress. One was for managing the ecological infrastructure and the other for managing interdependent infrastructures before, during, and after a disaster (either manmade or naturally occurring). We developed dynamic simulation models of the ecological infrastructure and of the costs and benefits of an advanced information system for managing the infrastructure.

This project is motivated by Sandia's recognition that enhancing our nation's ability to manage vulnerabilities of global infrastructures is necessary to maintain our national security.

We developed a Monte Carlo (MC) simulation of three different interdependent infrastructures subsequent to a tornado incident. We developed a dynamic simulation of a portfolio of policy options drawn from six different categories—specifically, regulations; fiscal incentives; information, education, and outreach; technology development, deployment, operations, and maintenance; intergovernmental relations; and enforcement. Results were well received and publicized by television networks in addition to the local newspapers. The experience was presented to the Federal Emergency Management Agency (FEMA) to initiate a new approach to minimizing costs (both economic and human life) to U.S. citizens through proactive mitigation of the effects of both natural and anthropogenically induced disasters.

3532310000

Capillary Elastohydrodynamics in Manufacturing Processes

P. R. Schunk

This project studies the three-way interaction between fluid flow, elastic deformation, and wetting. Sandia is developing a finite-element method (FEM) for predicting wetting of a fluid on a flexible substrate. This model requires solving two-phase coupled fluid-structural interaction problems with free boundaries. We will revise the standard formulations for applying the FEM to fluid mechanics and solid mechanics to make the solution procedures in the two phases compatible. There are several formulations for applying interfacial momentum balances and contact line forces within the FE framework; we will test these formulations to determine which are most robust and accurate. The mathematical formulation developed in this project will have direct application to capillary impregnation in deformable porous media and more general application to dynamic wetting in industrial processes such as roll coating.

We developed mathematical methods and a FE computer program to predict the deformation of planar or cylindrical elastomeric substrates during static wetting. The model predicts the deformation of an elastomeric substrate subject to force and position boundary conditions (BCs) imposed around its perimeter.

We treat the substrate as an incompressible elastomer using the Mooney-Rivlin constitutive law. The equations are posed in the Eulerian reference frame, but the mesh points currently move as material points with the solid.

There are several methods for resolving the surface tension forces exerted at the contact line on an elastic substrate. At the contact line, three line forces are exerted due to the surface free energies of the liquid-gas, liquid-solid, and solid-gas interfaces. The surface forces cause a crease, or kink, in the solid at the contact line; i.e., the normal to the solid surface is discontinuous at the contact line. Some authors suggest that the angle of the discontinuity at the contact line, or crease angle, is a physical property that depends on the three phases present and their surface free energies; this crease angle condition can be applied as a BC on the elastic deformation.

A second BC accounts for the line force exerted by the fluid-gas interface on the solid surface; this line force is treated

The mathematical formulation developed in this project will have direct application to capillary impregnation in deformable porous media and more general application to dynamic wetting in industrial processes such as roll coating.

by a formulation similar to the line force at the end of capillary surfaces in fluid mechanics. We apply a surface traction BC on the solid free surfaces that accounts for forces arising from curvature of the solid surface and the associated surface free energy; these forces are normally neglected in solid mechanics. Then, the surface traction condition is integrated by parts and results in a line integral of the surface free energy at the contact line. The line integral is replaced by the vector force exerted by surface tension in the liquid. We are testing several numerical techniques for applying this force balance at the contact line. For example, the momentum equations may or may not be rotated into surface coordinates prior to applying the BCs, or only one of the BCs may be sufficient to resolve the mechanics near the contact line.

Initial results from this model will predict the capillary rise in a slit with deformable walls. When the solid material is soft, the capillary rise can vary significantly from the predictions for a rigid slit. Future additions to the model will enable predicting dynamic wetting on elastic substrates by decoupling the mesh motion from the solid deformation. In dynamic wetting, substrate deformation can lead to a decrease in wetting speed and may be a cause of wetting hysteresis.

Refereed

Cairncross, R. A., P. R. Schunk, T. A. Baer, R. R. Rao, and P. A. Sackinger. 1999. "A Finite Element Method for Free-Surface Flows of Incompressible Fluids in Three Dimensions, Part I: Boundary-Fitted Mesh Motion." *Internat. J. Numerical Methods in Fluids* (September).

Harik, V. M., and R. A. Cairncross. 1999. "Constitutive Modeling of Interfacial Plastic Fracture." *Proc. 4th Internat. Conf. on Constitutive Laws for Engineering Materials 1* (Miami, FL, June).

3532320000

Real-Time Design of Improved Powder Pressing Dies Using Finite-Element Method Modeling

K. G. Ewsuk, D. H. Zeuch, J. G. Arguello, Jr., A. F. Fossum

Sandia is developing scientific and technological expertise in characterizing and modeling powder compaction, and compiling it into a user-friendly software package that incorporates unprecedented flexibility to design powder press tooling and pressing processes faster and more economically. This advanced computational technology, in a unique, user-friendly, software package, will provide considerable advantages in manufacturing pressed-powder compacts by mechanical and isostatic compaction, including powder compacts made of advanced ceramics and metals. With Sandia's 3-D finite-element method (FEM) computer model and our ability to develop significantly more agile and user-friendly code and platforms to complete the modeling, this project has an extremely high probability of success. The technology will contribute significantly to advanced materials and design by (1) reducing manufacturing costs, cycle time, and waste; (2) enabling more cost-effective manufacturing of specialty components and small lot sizes; (3) reducing tooling and component design, development, and prototype time; and (4) maximizing design and manufacturing flexibility/agility. A successful project will significantly impact Sandia Defense Program (DP) efforts to design and manufacture advanced ceramic components with improved performance and reliability for weapons systems, including cermets and lead zirconate titanate (PZT) voltage bars for neutron generators. Five industrial partners are potential commercial partners that are interested in developing and implementing this technology. They will serve to beta test the software package and allow us to more rapidly implement the process modeling and tool design technology developed.

We devised a unique concept to develop a user-friendly computer program to design dies for powder compaction in real time. We subsequently demonstrated the validity of this concept by developing new software to link Sandia's existing FEM, analysis, and visualization software into a user-friendly compaction code that runs on a Sun workstation under the UNIX operating system. We successfully ported the compaction code over to an IBM ThinkPad (laptop) computer

With Sandia's 3-D finite-element method (FEM) computer model and our ability to develop significantly more agile and user-friendly code and platforms to complete the modeling, this project has an extremely high probability of success. The technology will contribute significantly to advanced materials and design....

and, with the Linux operating system, used it to demonstrate 3-D compaction of a ceramic bushing fabricated by our industrial collaborators. On the laptop, the code operates at about half the speed of the Sun workstation, but it significantly enhanced our ability to demonstrate and test the software in a manufacturing environment. More recently, we identified new, affordable (\$2,500–\$4,000) desktop computers with Pentium II or III chips and the Linux operating system that allow simulations to be completed as fast as those on the original Sun workstation. Two of our partners are beta testing the software.

Within the code itself, we developed the logic to design more complex geometry and axisymmetric dies, and designed the base templates to model isostatic compaction of complex geometry parts. We completed some testing to identify bugs within the code to eliminate in subsequent versions. We also simulated the compaction of parts pressed by our industrial partner to test and validate the model. To simplify the use of the code, we also developed a graphical user interface (GUI) using Tcl/Tk (Tool Command Language/Tool Kit).

For materials parameters to input into the compaction model, we fully characterized two additional ceramic powder systems, bringing our total up to four different systems. We are also now collaborating with Penn State to characterize more materials. We designed an experimental matrix of materials to test and initiated testing to establish a database to develop intelligent technology to systematically estimate parameters for materials that have not been or can not be completely characterized. To complement this effort, we are also now collaborating with the University of New Mexico to develop a smart database to compile compaction and modeling data, and to estimate parameters for modeling. Finally, because materials parameters were not available in the literature, we procured polyurethane samples commonly used as the molds in isopressing to characterize to support our isopress modeling effort.

For materials parameters to input into the compaction model, we fully characterized two additional ceramic powder systems, bringing our total up to four different systems.

Other Communications

Arguello, J. G., A. F. Fossum, K. G. Ewsuk, and D. Zeuch. 1999. "Continuum-Based Model for Ceramic Powder Compaction." Paper presented to Fine Powder Processing '99, University Park, PA, 20–22 September.

Arguello, J. G., K. G. Ewsuk, A. F. Fossum, and D. H. Zeuch. 1999. "Development of a Software Package to Automate the Modeling of Ceramic Powder Compaction in Axisymmetric Dies." Paper presented to the 101st Annual Meeting of the American Ceramic Society, Indianapolis, IN, 25–28 April.

Ewsuk, K. G. 1999. "Controlling the Ceramic Powder Compaction Process." Paper presented to the 101st Annual Meeting of the American Ceramic Society, Indianapolis, IN, 25–28 April.

Ewsuk, K. G. 1999. "Developments in Powder Flow, Packing, and Compaction, Science and Technology at Sandia National Laboratories." Presentation at the Penn State University Particulate Materials Center Industrial Advisory Board Meeting, University Park, PA, 21 April.

Ewsuk, K. G. 1999. "Granulation and Its Influence on Flow, Packing, and Compaction." Paper presented to Fine Powder Processing '99, University Park, PA, 20–22 September.

Ewsuk, K. G. 1998. "Powder Packing and Compaction Science and Technology." Presentation to a seminar at the Rutgers University Department of Materials Science and Engineering, Piscataway, NJ, October.

Keller, J. M., J. D. French, B. Dinger, M. McDonnough, B. Gold, C. Cloutier, L. Carinci, E. Van Horn, K. Ewsuk, and B. Blumenthal. 1988. "Industry and Government Team to Improve Ceramic Manufacturing Technology." *Ceramic Bulletin* **77** (October): 6.

Zeuch, D. H., J. M. Grazier, J. G. Arguello, and K. G. Ewsuk. 1999. "Geomechanics Techniques for Characterizing Mechanical Properties of Ceramic Powders." Paper presented to the 101st Annual Meeting of the American Ceramic Society, Indianapolis, IN, 25–28 April.

3532330000

Computational Methods for Predicting the Response of Critical As-Built Infrastructure to Dynamic Loads (Architectural Surety)

R. V. Matalucci, S. W. Attaway

The goals of this project are to evaluate, verify, validate, and apply coupled existing hydrocodes and structural dynamics codes to simulate the response of federal buildings and facility systems subjected to malevolent explosive attacks and potentially to natural disasters such as hurricanes and earthquakes. Sandia will verify simulation capability with the Teraflops (Tflop) computer using Tactical Support Working Group/Defense Threat Reduction Agency (TSWG/DTRA) explosive test data from multistory, full-scale structures at White Sands Missile Range (WSMR), and small-scale tests at U.S. Army Corps of Engineers/Waterways Experiment Station (USACE/WES). We will evaluate the predictive capabilities of these coupled model simulation techniques with available building response measurements and indicate the application of this capability to the needs of several government agencies for evaluating dynamic loads (airblast, ground shock, severe winds, and ground accelerations) on structural integrity, including the response of structural materials, construction codes, and window glass and frames. We will also evaluate methodologies applicable to mitigating the effects of structural failure, window glass fracture, and flying debris on building materials and occupants.

We accomplished the following:

- (1) Developed automated input for a concrete model, which allows the user to completely describe concrete material behavior using only the unconfined strength.
- (2) Made major improvements in the concrete model to facilitate the analysis of large structural problems.
- (3) Improved the realistic steel reinforcement model for concrete structural elements.
- (4) Developed numerous PRONTO3D structural models, including a 400,000-element, 1/4-scale test structure and a 6.5-million-element model of a full-scale four-story building.
- (5) Performed uncoupled blast loading analysis of the above structures for use in validating the coupled models. This included the development of an algorithm for mapping airblast pressure time histories from hydrocode calculations to the surfaces of the PRONTO3D structural model.

The goals of this project are to evaluate, verify, validate, and apply coupled existing hydrocodes and structural dynamics codes to simulate the response of federal buildings and facility systems subjected to malevolent explosive attacks and potentially to natural disasters such as hurricanes and earthquakes.

(6) Validated the structural model against post-test data for USACE/WES 1/4-scale test structure of the four-story building DTRA test at White Sands.

(7) Validated the structural model against observations from large-scale 1000-pound blast test data from the four-story building DTRA test at White Sands.

(8) Validated the structural model against other applicable standard computational models used by other analysts in blast structural-interaction calculations.

(9) Made computational comparisons against other actual structural tests from other government agencies.

(10) Evaluated the ZAPOTEC modeling capability used for penetration impact applicable to airblast effects.

(11) Completed a series of coupled calculations to verify capability against other classical computational results.

Refereed

Attaway, S. W., K. Morrill, J. Crawford, and R. V. Matalucci. 1999. "Enhancements to PRONTO3D to Predict Structural Response from Blast." Sandia Technical Report, Sandia National Laboratories, Albuquerque, NM, in review.

3533190000

Solar-Grade Silicon

J. M. Gee, P. Ho, J. A. Van Den Avyle

The dominant material used for photovoltaic solar cells today is crystalline silicon (Si). One of the largest energy and cost components to crystalline-Si solar cells is the Si starting material. The industry uses off-grade material from electronic-grade Si production for the integrated circuit (IC) industry—which corresponds to about 10% of the total electronic-grade Si production. This source of material is not growing as rapidly as the photovoltaic industry, with the net result that the photovoltaic industry will soon become constrained by the supply of its raw material. In addition, the electronic industry goes through large business cycles that frequently cause periods of material shortages.

The photovoltaic industry can accommodate higher concentrations of impurities than the electronics industry, so it may be possible to produce Si for the photovoltaic industry with a slightly higher purity content and at much lower cost. Much of the cost in commercial electronic-grade Si production is due to use of gas-phase Si species. While gas-phase species are easily purified, they are also very costly (capital and operational costs) to handle and to decompose back into elemental Si.

Our project examined purification of Si in the liquid phase. It is more difficult to purify molten Si, but the process should be much less costly. The research included detailed thermochemical calculations, experiments conducted in a large induction furnace, and extensive interactions with industrial and other national laboratory colleagues.

We used thermochemical calculations and a review of the solar-grade literature to guide the research. The thermochemical calculations included over 700 chemical species and a wide range of temperatures, pressure, and gas ambients. The calculations were at equilibrium and did not consider kinetic limitations. The most difficult impurity to remove in Si is boron (B). B is present in high concentrations from common sources of Si, and its physical and chemical properties are similar enough to Si to make it difficult to remove. Metallurgical-grade Si is the starting material, and it contains large concentrations of B, phosphorus (P), aluminum (Al), iron (Fe), carbon (C), oxygen (O), and other metallic elements.

Our project examined purification of Si in the liquid phase. It is more difficult to purify molten Si, but the process should be much less costly.

The thermochemical calculations suggested the following:

(1) P could be removed by evaporation at high temperatures and low pressures.

(2) C could be removed in an oxidizing ambient as CO (carbon monoxide).

(3) Fe concentration could be reduced by evaporation.

(4) B could be reacted with N to form solid BN (boron nitride).

The first three observations were known from the literature, but the last item has not been described previously. It was also a surprising result in that the effect of N on molten Si should have been observed previously—N is commonly in contact with molten Si in many different industrial processes. We speculated that the N molecule (N_2) is too kinetically stable for the reaction to proceed and that a less stable N precursor might allow the B-N reaction in a Si melt to proceed. We thus conducted experiments that blew ammonia (NH_3) gas over a Si melt and chemically analyzed the resulting material.

Initial experiments were disappointing in that we did not observe significant B reductions. A possible problem with our experiment is that surface effects could prevent the N from dissolving into the Si melt.

Refereed

Gee, J. M., P. Ho, J. Van Den Avyle, and J. Stepanek. 1998. "Some Thermochemical Calculations on the Purification of Silicon Melts." *Proc. 8th Workshop on the Crystalline Silicon Solar Cell Materials and Processes 1* (Copper Mountain, CO, 17–19 August): 192–195.

Other Communications

Ho, P., and J. M. Gee. 1999. "Thermochemical Analysis for Purification of Polysilicon Melts." Sandia Technical Report SAND99-1047, Sandia National Laboratories, Albuquerque, NM (May).

3533210000

Low-Work-Function Thermionic Emission Materials

D. B. King, J. A. Ruffner, K. R. Zavadil

Thermionic diodes are two electrode devices that convert thermal energy to electrical power. The efficiency of this conversion process is critically dependent on the work function values and uniformity at the electrodes surfaces, coupled with the design of the converter. Modeling shows that a microminature converter (MTC) design could achieve efficiencies of up to 20% conversion efficiency. Microelectronic fabrication technology allows for the construction of microconverters. The remaining enabling technology is the development of low-work-function materials and processes that can be integrated into fabrication. The goal of this project is to develop low-work-function materials that demonstrate appreciable electron emission (10 amps/centimeter²) at modest operating temperatures (800°–1220°K). The candidate materials are compatible with microelectronic fabrication processes. Highly emissive cathode materials have been developed by the electron source community based on barium oxide (BaO) and scandia (Sc₂O₃). However, these emitters are macroscopic structures derived by impregnating porous tungsten (W) monolith with Ba. Scandia is either incorporated into the original W structure as part of the impregnate or as a capping layer. Sandia's goal is to develop methods for depositing highly emissive films within this class of materials that can be integrated into an MTC device. We documented a process scheme for the integration of these films into microminature diodes.

We demonstrated an ability to deposit thin-film thermionic emitters. We used radio frequency (RF) sputtering methods that can be integrated into standard integrated circuit (IC) fabrication. These films are based on BaO. We demonstrated that the practical minimum work function of 1.2 electron volts (eV) can be achieved. We showed that only a small fraction of the surface actually possesses this low work function. The existence of a variation in work function led to much smaller-than-anticipated emission current densities and rendered these films as impractical sources for energy-conversion applications at low operational voltages. We demonstrated that the most likely explanation for the under-utilization of the surface is either a limited bulk transport rate of free Ba or limited surface

Sandia's goal is to develop methods for depositing highly emissive films within this class of materials that can be integrated into an MTC device. We documented a process scheme for the integration of these films into microminature diodes.

mobility of the Ba. We discussed several strategies that should minimize these effects that represent modifications to the current fabrication process. The inclusion of porosity in these films and the use of metal capping layers over the film surface are two strategies to be used in identifying the source of poor surface utilization. We demonstrated a novel method for generating porosity in these films.

Refereed

Zavadil, K. R., J. H. Ruffner, and D. B. King. 1999. "Characterization of Sputter-Deposited Thin-Film Scandate Cathodes for Miniaturized Thermionic Converter Applications." *AIP Conf. Proc. Space Technology and Applications Internat. Forum* **458** (February) (Albuquerque, NM, 31 January): 1438–1443.

3533220000

Develop Mathematical Algorithms for the Integration of Disparate Information to Determine Critical Infrastructure Health and Status

L. A. Snyder, J. E. Stamp, K. L. Stamber, D. C. Smathers, T. J. Brown, R. G. Cox, R. D. Pollock

Sandia investigated algorithmic methods that, when applied, add credibility to the determination of the overall health of the critical infrastructures. The algorithm addresses the complexity of the critical infrastructures and their interdependencies. To determine how these interdependency issues can be algorithmically interpreted, Sandia investigated two mathematical techniques:

(1) The normalization of disparate information provided eight infrastructures. We evaluate each critical infrastructure's health based on a unique value system. An overall algorithmic method normalizes these unique values; and

(2) The weighting of that information. The importance (assigned weight) of an event in one infrastructure needs to be considered based on its effect on other parts of that infrastructure or other infrastructures. The weighting of an event might change based on its effect on the:

- infrastructure as a whole;*
- divisions within an infrastructure;*
- use of different technological applications; and/or*
- importance of the same event as seen by other infrastructures.*

We researched and developed the mathematical algorithms needed to integrate data input from different sources to produce a numerical representation of the health of the eight critical infrastructures. These data provide information that could be supplied from sources such as infrastructure operators, the intelligence community, and events impacting other infrastructures.

The mathematical algorithm research challenges were:

(1) understanding how to rank and weight data according to its importance and potential impacts;

(2) normalizing data supplied in both word form and numerical values and in different formats; and

(3) integrating the data to produce a numerical value for indicating state of health for an infrastructure and to provide input to the other infrastructures that may be impacted.

Sandia investigated algorithmic methods that, when applied, add credibility to the determination of the overall health of the critical infrastructures. The algorithm addresses the complexity of the critical infrastructures and their interdependencies.

These mathematical algorithms enabled the Fast Analysis Infrastructure Tool (FAIT) to provide a quick look at the health of our nation's critical infrastructures. FAIT is an application whose goal is to take only a few significant indicators to determine if an infrastructure event is significant to that infrastructure and can impact others. The ability to quickly input information from different sources and mathematically integrate these data into a health status is critical to helping our infrastructure customers while more inclusive modeling development is in progress.

To understand how ranked and weighted data impact an infrastructure, we consulted with industry experts to gain insight into the importance of different parameters. The parameters that we selected were event weights, confidence levels, probability that an event will occur, geological population weight, and infrastructure weighting factors.

To determine how to normalize data supplied in both word form and numerical values and in different formats, we consulted infrastructure experts who aided in determining the numerical quantification for given subjective data.

We formulated a linear algorithm to integrate the data and to produce a numerical value for indicating an infrastructure's state of health. This numerical value is also input to the other infrastructures' state-of-health calculations. The algorithm calculates the infrastructure's current health value and its influence, by percentage, on other infrastructures. Depending on the dependency of one infrastructure on another, we adjust the scaler (weighting factor) to reflect this dependency. For example, a strong relationship between two infrastructures yields a larger scaler than less dependent infrastructures.

The ability to quickly input information from different sources and mathematically integrate these data into a health status is critical to helping our infrastructure customers while more inclusive modeling development is in progress.

3533230000

SERAPHIM Propulsion Technology Design for High-Speed Rail Applications

J. B. Kelley, R. J. Kaye, B. M. Marder

Many highways in the U.S. are stretched beyond capacity, causing significant economic loss, increased regional pollution, and waste of gasoline. An ideal way to increase the capacity of these highway corridors is to build grade-separated, fixed-guideway systems within the existing rights-of-way on which high-speed transit vehicles can operate. Shifting 10% of drivers out of single-occupancy vehicles and onto transit is estimated to save 3.2 billion barrels of gasoline annually. Electric rail also produces less than 25% of unburned hydrocarbons, carbon monoxide, and nitrogen oxides per passenger mile. The Sandia-developed Segmented Rail Phased Induction Motor (SERAPHIM), a new form of linear induction motor (LIM), is an enabling technology for accomplishing this cost-effectively because it is compact, lightweight, and operates efficiently with relatively large separation gaps. A SERAPHIM motor generates thrust by pulsing alternating current through driving coils, inducing surface current in the reaction structure, and creating propulsion forces. The SERAPHIM motor overcomes shortcomings of traction motors, conventional LIMs, and synchronous induction motors. This project developed a concept design and studied system parameters and infrastructure impacts for a SERAPHIM motor aimed at a challenging set of high-speed, high-grade climbing requirements for intracity transit. We developed thrust and power versus speed curves and applied them to the test route. We modeled the electric power circuit to include the motor, switching, and stationary line power elements. Results indicate that the SERAPHIM motor is well-suited to this challenging route.

Our first task was to define a set of transportation requirements in sufficient detail to allow a point-design of the vehicle, the SERAPHIM motor, and electric power circuit. The test case for this analysis was a proposed route for intermountain transit in Colorado. The important parameters were the required passenger-carrying capacity, the average speed needed on the route, and geographic considerations such as grades, corners, maximum acceleration and deceleration profiles, speed limits dictated by traffic considerations, and

The Sandia-developed Segmented Rail Phased Induction Motor (SERAPHIM), a new form of linear induction motor (LIM), is an enabling technology for accomplishing this cost-effectively because it is compact, lightweight, and operates efficiently with relatively large separation gaps.

station locations. In particular, we used a 10-mile section with the highest grade requirement, at more than 8% grade, to establish the maximum thrust and power requirements. The Colorado Fixed Guideway Authority and the Meneran Corporation provided route data and infrastructure information. We modeled the electric power circuit to include the motor and roadbed coils, power switching, and stationary line power elements. We developed thrust and power versus speed curves and applied them to the test route. Results indicate that the benchmark station-to-station average speed of 70 mph (and peak speed of 150 mph) can be met with a SERAPHIM motor with thrust of 125 kN and peak electric power (including reactive power) of about 10 MW. We added power factor corrections for the 60 Hz ac line power to first order, but further optimization can reduce this maximum power load to the range of 5 MW.

Other Communications

Hopkins, T. (Meneran Corporation); J. P. Silva, S. A. Eurtotren-Monoviga, B. M. Marder, B. N. Turman, and J. B. Kelley (Sandia). 1999. "Maglift Monorail: A High-Performance, Low-Cost, and Low-Risk Solution for High-Speed Ground Transportation." Presentation to the High-Speed Ground Transportation Association Meeting, Seattle, WA, 8 June. Sandia Technical Report SAND99-1498C.

3534070000

Tomographically Measured Temporal Evolution of Hyperspectral Target Signatures

C. L. Grotbeck, J. L. Smith, T. W. Welton, C. E. Lanes, P. G. Stromberg, K. R. Lanes, J. C. Wehlburg

Spectral sensing applications are demanding simultaneous spatial, spectral, and temporal measurements. Threat signatures drive both the detection and tracking radars and the seeker hardware selections. They also establish requirements for the supporting detection, discrimination, aim point selection, and kill assessment algorithms. Sandia proposes to use a new technique, computed chromotomography, to measure the target spectral signatures at a temporal resolution of 10–100 Hz. With this approach, image information is dispersed spectrally and in time by a rotating prism. We use tomographic algorithms to reconstruct the image information from a two-dimensional focal plane array in spectral bands. We believe that transient spectral information can be extracted when the change occurs as a point source evolving in a relatively stable but spectrally cluttered background. We will develop hardware for a ground-based demonstration system. Algorithm development will be critical to reconstruct the spectral evolution of dynamic targets. The ground-based demonstration system could be used to characterize a large variety of targets, including missile, aircraft, and high explosive signatures. This effort will lead to a space-based system measuring the required signatures for targets in denied territory.

We developed the basic design concept, including the requirements for field-of-view (FOV), focal plane dimensions, number of pixels, wavelength region of interest, number of spectral bands, point spread function, dispersion angles, frame rates, prism rotation rates, number of bandpass filters, stop location relative to the prism, warm and cold optics, and beam collimation at the prism. The algorithm areas identified for additional development are as follows: mission space and conops; focal plane readout options, frame rates, decimation, and windowing; full frame versus fast transient detection and reconstruction; low signal-to-noise ratio (SNR) target detection; slowly varying dynamic targets; sensor cross-cueing; subframe mosaic reconstruction and edge effects; and line-of-sight (LOS) motion-induced uncertainties. Work to address each of these areas will continue. We showed the design

The ground-based demonstration system could be used to characterize a large variety of targets, including missile, aircraft, and high explosive signatures. This effort will lead to a space-based system measuring the required signatures for targets in denied territory.

feasibility, including initial concepts for a dual chromotomography (CT)/filter wheel system and the optical performance, to be viable. We completed the preliminary mechanical layout and developed thermal management concepts. We quantified readout rates and frame rates and completed initial prism design. We also completed penultimate optical design. Tolerance analysis shows that tolerances are very tight but not unreasonable. Remaining issues are thermal changes in glass optical index of refraction and mechanical positioning, and the detailed cryogenic and mechanism design. The CT algorithm, which demonstrates high spectral and temporal resolution of dynamic point source targets, is in development. We demonstrated the initial implementation with a dataset taken at an actual munitions field test. Work continues on issues identified during the first quarter of this year. We developed a concept for the mechanism for dual prism rotation and showed it to be feasible.

Refereed

Mooney, J., C. Grotbeck, T. Reeves, and P. Green.
1999. "Classification of Explosions from Spectral-Temporal Signatures."(U) *Proc. Information Infrared Symposia (IRIS) 2* (Secret) (May) (Meeting IRIS Specialty Group on Passive Sensors, Monterey, CA, 22-24 February): G-9.

3534080000

Gas-to-Liquid Microabsorber

K. Wally, R. F. Renzi, R. W. Crocker, S. H. Kravitz, D. J. Rader, B. C. Wu

Sandia is developing liquid analysis microsystems for detection of chemicals at trace concentrations. To broaden the utility of these systems, a low-power gas-to-liquid microabsorber is needed for portable hand-held detectors. Diffuse sources (1 ppb) require relatively large air samples to gather sufficient chemical for detection. Yet liquid analysis microsystems use the tiniest (under one microliter) of liquid samples to perform their detections. Therefore, the microabsorber must address this formidable mismatch in bounding conditions. Our microabsorber does so via a two-stage operation—preconcentration followed by absorption. Stage one, preconcentration, requires a microminiature gas-to-solid adsorber with rapid thermal desorption. Stage two, absorption, requires a microabsorber using microfluid solvent flow.

Developments for the integrated microabsorber are proceeding on two fronts, corresponding to the two-stage operation we envision for the device (i.e., gas-to-solid adsorption, followed by thermal desorption-to-liquid absorption). We developed preliminary models to estimate absorption performance and solvent evaporation loss. Our analysis using these preliminary models confirms the need for the two-stage approach if microfluid solvent is to be used.

Preliminary modeling of evaporation from the aqueous buffer solutions in open fluid microchannels suggests that at least 100–150 microns channel depth is needed to ensure that evaporation will not risk drying the microchannels. The EK fluid transport mechanism requires that the fluid circuit be primed at all times for electrical continuity between electrodes. Capillary wicking is an inadequately demonstrated mechanism to ensure continuous priming in the face of evaporation. The resulting microchannel geometry is tall and narrow.

The EK flow transport mechanism requires dielectric substrates, preferably glass. But high-aspect-ratio microchannels cannot be etched into ordinary glasses. Alternatively, Si microchannels produced by Bosch deep-etching process require very thick (1 to 5 microns) dielectric coatings to stand off the high voltages employed in EK flow. To date, all Si devices have proven inadequate. We are therefore investigating

Sandia is developing liquid analysis microsystems for detection of chemicals at trace concentrations. To broaden the utility of these systems, a low-power gas-to-liquid microabsorber is needed for portable hand-held detectors.

Foturan, a special photolithographically processable glass. We obtained samples of this glass and demonstrated microchannel etching, through-via etching, and thermal-diffusion bond sealing. Evaluation of EK performance remains to be investigated.

We completed the preliminary design of an open-channel microfluid circuit for fabrication in glass. Because we wish to minimize headspace above the microchannels to maximize the concentration of the thermal desorption gas pulse, we must take special precautions to ensure that the headspace does not fill from the microchannels due to capillary wicking. We are exploring a stepped geometry and hydrophobic coatings to suppress capillary wicking. We must investigate compatibility between the hydrophobic coatings employed on glass substrates in current biological applications and the nerve agents, nerve agent simulants, mustard agents, and mustard agent simulants.

The adsorption preconcentrator is well advanced. A microchip preconcentrator device was recently demonstrated. The Si device uses a thin, free-standing Si membrane. The membrane is coated on its front side with a microporous film of adsorbent made using sol-gel processing. The adsorbent has affinity for chemical weapons agents and their simulants. By controlling the thickness of the microporous film, we can trade adsorbent capacity versus rapidity of thermal desorption. The backside of the membrane incorporates a platinum (Pt) heater plated onto the Si membrane for rapid thermal desorption of the adsorbed sample.

We fabricated prototype preconcentrators and tested them at relatively high ppm exposure concentrations. Tests at lower concentrations are in process. Additional data are needed at the low concentration levels where we expect to operate. Standard isotherm models predict that these preconcentrators will adsorb only picograms of adsorbate at the 1 ppb exposure level. This appears just adequate performance to service the gas-to-liquid microabsorber. We may wish to enhance performance by adding more than one preconcentrator microchip for each microchannel in the microabsorber fluid circuit.

A final area of accomplishment deals with test apparatus. We completed the design of an apparatus to test microabsorber performance and began equipment procurement and assembly. The apparatus uses two Dynacalibrator gas-analyzer calibration instruments from VICI Metronics, Inc., to produce a single gas source containing two independently controllable gas sample concentrations. The outflow from the two calibrators can be

mixed to provide and produce a single source of gas. With this apparatus, we will be able to produce sample gas containing simulants of two separate chemical agents, for example, nerve gas simulant and mustard simulant, or a single simulant and interferant. By using more than one permeation device in each permeation chamber, other combinations are possible.

With this apparatus, we will be able to produce sample gas containing simulants of two separate chemical agents....

3534090000

High-Resolution Electromagnetic Imaging of Transport Pathways

G. A. Newman

Each year DOE invests billions of dollars to address nuclear-waste legacy issues, where the ability to predict the transport of waste and contaminants within the subsurface is of critical importance. It requires knowledge of transport of fluids in the vadose (unsaturated) zone, which is poorly understood. Geophysical inverse methods provide the only noninvasive approach essential for gathering information on the problem. Here we focus on electromagnetic (EM) methods to image subsurface electrical conductivity because of its sensitivity to subsurface flow properties. While these methods cannot detect contaminants on the parts-per-million (ppm) level, they have the potential to map migration pathways on the meter-length scale. Unfortunately, multidimensional conductivity imaging is a nontrivial problem; it is large-scale (millions of parameters) and nonlinear, and requires significant computational resources, including both memory and time. It is only recently that prototype solutions to the problem have become available with the arrival of massively parallel (MP) computers. While these solutions represent a significant improvement over approximate imaging methods, it is still not possible to image transport pathways at the desired meter scale. To do so requires implementation of highly robust and efficient nonlinear optimization procedures for large-scale inverse problems (Newton-Krylov and trust region methods) and fast preconditioners. If such developments are undertaken, as outlined in this project, it would constitute a critical breakthrough in our ability to image transport pathways. It would be directly applicable to DOE sites, where subsurface contaminant transport in the vadose zone is of paramount interest.

Sandia developed a fast precondition technique that accelerates the finite-difference solutions of the 3-D Maxwell's equations for geophysical modeling. The technique splits the electric field into its curl-free and divergence-free projections and allows for the construction of an inverse operator. Test examples show an order-of-magnitude speedup compared with a simple Jacobi preconditioner. Using this preconditioner we developed a low-frequency Neumann series expansion and used it to compute responses at multiple frequencies very

If such developments are undertaken, as outlined in this project, it would constitute a critical breakthrough in our ability to image transport pathways. It would be directly applicable to DOE sites, where subsurface contaminant transport in the vadose zone is of paramount interest.

efficiently. Simulations requiring responses at multiple frequencies show that the Neumann series is faster than the preconditioned solution, which must compute solutions at each discrete frequency. We also developed a Neumann series expansion in the high-frequency limit along with spectral Lanczos methods in both the high- and low-frequency cases for simulating multiple frequency responses with maximum efficiency.

Other Communications

Newman, G. A., and D. M. Day. 1999. "Computational Techniques for Accelerating Solutions of 3-D Geophysical Inverse Problems." *Proc. Copper Mountain Conference on Multi-Grid Methods 1* (Copper Mountain, CO, 11–16 April): 301.

3534110000

MPP Direct Numerical Simulation of Diesel Autoignition

J. H. Chen, A. R. Kerstein, A. H. McDaniel, B. A. Allan, R. L. Clay, A. E. Lutz, C. A. Kennedy, J. F. Grcar, D. J. Klinke, T. Echehki

Sandia will develop and exercise key massively parallel processing (MPP) simulation tools to study autoignition, diffusion flame burnout, and catalytic combustion, three important processes in diesel combustion.

Specifically, this project developed the following new software capabilities: (1) MPP scalable, portable direct numerical simulation (DNS) codes (low-Mach number and compressible formulations); (2) algorithms for integrating numerically stiff systems of ordinary differential equations due to disparate autoignition chemical time scales; (3) auto-Chemkin, an approach to efficiently compute the chemical source terms in unsteady fluids codes; (4) one-dimensional, spatially resolved turbulence simulations coupled with Chemkin, tailored to study mixing effects on autoignition; and (5) initial scoping of surface Chemkin formalisms to include reactions between interfaces or phases possessing nonuniform site densities for catalytic converters.

These new capabilities enabled several studies related to diesel combustion: (1) turbulent flame-flame interactions, (2) burnout of spherical diffusion flames created by the autoignition of fuel-rich parcels of the mixture, and (3) turbulent mixing effects on autoignition in a scalar mixing layer of fuel and preheated air. These initial studies concentrated on hydrogen/air, an important subsystem of more complex hydrocarbon chemistry. It represents a first step in a natural progression to more complex hydrocarbon chemistry representative of diesel fuels.

These initial studies concentrated on hydrogen/air, an important subsystem of more complex hydrocarbon chemistry. It represents a first step in a natural progression to more complex hydrocarbon chemistry representative of diesel fuels.

• New Simulation Capabilities

(1) MPP direct numerical simulation (DNS) codes.

Researchers from Carnegie-Mellon University (CMU) collaborated with Sandia to develop parallel, scalable, portable DNS codes. The activities in the compressible DNS project included restructuring a serial DNS code to facilitate a parallel port, developing a scalable 2-D DNS code that is portable across multiprocessor platforms supporting message-passing interface (MPI), profiling and benchmarking the code to provide scalability data, designing the communications within the code to facilitate extensions to 3-D, and parallelizing the

3-D code and validating it against test cases. In addition to the compressible DNS code, a low-Mach number code previously developed at U. Wisconsin is in the process of being made parallel. Using the MPP DNS code, we performed a suite of turbulent flame-flame interaction simulations on a CRAY T3E at CMU and analyzed the results. Owing to the stiff chemistry associated with autoignition in diesel combustion, we designed higher-order accurate integration schemes for the DNS code that allow partitioning of the governing equations into numerically stiff and nonstiff terms. Finally, we completed a scoping study to determine the modular structure of the next-generation DNS codes.

(2) Auto-CHEMKIN code for generating inline code for computing reaction rates. This also represented a collaboration between Sandia and CMU. In DNS of combustion, a large fraction of computational expense is associated with evaluating chemical source terms. Streamlining these computations is critical to performing DNS with complex hydrocarbon chemistry. The auto-CHEMKIN approach uses a precompiler to create a subroutine that evaluates the source terms associated with a given reaction mechanism. We benchmarked the auto-CHEMKIN code and determined the optimization path for CHEMKIN. We developed a robust version of the auto-code generator with an application programming interface (API) consistent with CHEMKIN and tested it with GRIMech 3.0 and an n-heptane mechanism.

(3) Materials and surface chemistry software for catalytic converters. An initial scoping study identified the need for improved numerical capabilities: (a) CHEMKIN-compatible channel flow codes, (b) CHEMKIN-compatible tools for parameter optimization and reaction path analysis, and (c) surface CHEMKIN formalisms to include reactions between interfaces or phases possessing nonuniform site densities.

- **Numerical studies related to diesel engine combustion**

(1) One-dimensional turbulence (ODT) simulations coupled with CHEMKIN. We investigated the effects of mixing on autoignition using detailed spatially resolved computations of the evolution of a turbulent scalar mixing layer using ODT and linear eddy models (LEMs). Both models were developed at Sandia and allow a simple implementation of turbulent mixing. Due to the low central processing unit (CPU) cost, a wide range of parameter space for turbulence and various chemical mechanisms ranging from hydrogen to diesel fuel surrogates may be explored. Initially, we used LEM to study autoignition in a hydrogen/air scalar mixing layer. We varied

...we completed a scoping study to determine the modular structure of the next-generation DNS codes.

the turbulence parameters over a wide range of chemical time scales ranging from nonpremixed to homogeneous ignition modes. We used scalar statistics obtained from the databases to determine the effect of mixing on ignition delay.

(2) *Transient spherical flame model.* Pollutant survival in diesel engines depends on the burnout of diffusion flames created by autoignition of fuel-rich parcels of the mixture. We modified a 1-D transient flame code to compute the burnout of a spherical diffusion flame. We obtained the initial size of the ignition kernel from hydroxyl (OH) images from experiments; the initial composition was fuel and air premixed to an equivalence ratio of four which, after ignition, created a fuel-rich product mixture that established a diffusion flame with the surrounding air mixture. We made computations using a hydrogen/air mechanism to test the software modifications.

3534120000

Electrokinetically Driven Mesoscale Actuators

P. H. Paul, D. A. Chinn

This project seeks to develop a family of novel mechanical actuators suitable for use in a wide range of micro-, meso-, and miniature-scale mechanical systems. These actuators are based on a unique Sandia technology, the electrokinetic pump (EKP). The EKP is a microscale device that converts electrical power directly to high-pressure fluid hydraulic power. Our approach involves three key steps. The first is the use of microporous materials to develop a practical EKP that properly balances pressure, flowrate, drive voltage, and current. The second is the development and implementation of means to convert hydraulic force to mechanical motion (e.g., bellows or diaphragms). The third is the development of the necessary fabrication and component integration capability that will be required to build working actuator prototypes.

EKP-driven devices fall into two broad categories: (1) high-force applications requiring high pressure at a finite flowrate; and (2) large displacement applications requiring relatively low drive pressure and high flowrates. High-pressure liquid chromatography (HPLC) is an important high-pressure application. We successfully demonstrated EKP-driven HPLC separations of proteins using a capillary-based system. We further demonstrated a chip-based EKP suitable for gradient separations. The next step is to develop a fully integrated chip-based HPLC including the EKPs, sample injector, separation column, and detection. We pursued two large displacement applications: (1) a miniature diaphragm valve, and (2) high-flowrate pumps for closed-loop heat-transfer systems. Key in this effort is the development of high-efficiency EKPs. This requires a sophisticated model of EKP performance including the details of flow in porous media, the structure of the double layer, and properties of the supporting electrolyte. We completed a series of characterization measurements to validate a full EKP model. We applied this model to determine suitable pump host material/electrolyte combinations. We evaluated new porous media, including phase-separated Vycor-like porous glasses, porous polymers, and phase-separated sol-gel-like porous glasses. We identified materials having suitable properties, fabricated appropriate large cross-section samples, and are testing them for these applications.

This project seeks to develop a family of novel mechanical actuators suitable for use in a wide range of micro-, meso-, and miniature-scale mechanical systems. These actuators are based on a unique Sandia technology, the electrokinetic pump (EKP).

We designed, built, and tested several different valve/diaphragm combinations. A major challenge in construction of a mesoscale valve is to create a diaphragm with finite displacement without having to be infinitely thin, hence brittle. We tested simple plane diaphragms and can use them for diameters greater than order 7 mm. We are developing smaller-diameter devices using a miniature regular bellows as well as a pleated diaphragm especially manufactured for this purpose. Frequency response of any actuator is a key operating characteristic. Testing of an EKP displayed a $1/f$ response at fixed-drive voltage from dc to over 20,000 Hz, falling below this response at higher frequencies. A $1/f$ response is the theoretically ideal behavior for these devices. We determined the fall-off above 20,000 Hz to be an artifact of the measuring method.

A major challenge in construction of a mesoscale valve is to create a diaphragm with finite displacement without having to be infinitely thin, hence brittle.

3534130000

Pathogen Detection Using Microseparations for BW Nonproliferation

J. S. Schoeniger, V. A. Vandernoot, D. J. Irvin, X. C. Huang, D. W. Arnold

The purpose of this project was to explore strategies for pathogen detection using microseparations with laser-induced fluorescence (LiF) detection. Sandia's approach was to use small-feature-size microfluidics to trap and lyse single bacteria, render their contents fluorescent using amine-reactive fluorogenic dyes, and separate these contents using electrophoresis to obtain a fingerprint of the organism's composition. We focused on two technical aspects of this problem that are necessary for further feasibility studies: (1) the limits of detection for fluorogenically labeled amino acids and proteins, and (2) the fabrication of sufficiently small microchannels for filtering/analyzing and lysing individual cells. We determined that amino acids derivatized by the amine-reactive fluorogenic dye naphthalene-2,3-dicarboxaldehyde (NDA) could be detected at a sensitivity of 5×10^{-11} M in 50-micron-diameter capillaries. In 20- and 10-micron capillaries, we achieved detection limits of 10^{-8} M. We also determined that glass microcapillaries are unsuited for studies of small absolute numbers of biomolecules (due to surface absorption losses). We systematically explored different polymer substrates for the fabrication of microfluidic systems and established a process for fabricating microchannels in polymer substrates. We found that cyclic polyolefin materials have the necessary molding properties under hot-embossing to make microchannels in the size range below 20 microns.

LiF detection is routinely used with capillary electrophoresis (CE) to detect molecules in the concentration range 10^{-9} M to 10^{-12} M. As few as 1000 molecules are detected in these CE/LiF experiments. This indicates that it is feasible to analyze the content of major expressed protein species in a single bacterium, if efficient means of separating and detecting these molecules can be established. We designed this project to explore the basic feasibility of trapping individual cells, lysing their contents into a microchannel, and detecting their contents using LiF. By maintaining channel dimensions under 20 microns, dilution upon breaking open a 1–2-micron cell is kept to a factor of ~ 1000 .

The purpose of this project was to explore strategies for pathogen detection using microseparations with laser-induced fluorescence (LiF) detection.

We employed the reactive fluorogenic dye naphthalene-2,3,-dicarboxaldehyde (NDA) for rendering proteins fluorescent. We established the sensitivity of LiF detection of NDA-labeled amino acids in capillaries of various diameters using a Krypton-ion laser and both photomultiplier tube (PMT) and charge-coupled device (CCD) detectors. Even with relatively large capillaries (≥ 50 -micron diameter), the violet wavelengths needed for detection of NDA produced high background signals. Background root-mean-square (RMS) was two to three orders of magnitude higher than dark current RMS in photon-counting PMT. Background increased when smaller capillaries (6–20 microns) were used, as did the difficulty of optical alignment. Analysis of the CCD image of the fluorescence demonstrated significant signal from the capillary wall, which we eliminated using confocal filtering. Dispersed luminescence studies showed additional background from (1) Raman in the water and (2) fluorescence of interference filters that block scattered light. After careful optimization of the filter choice, we established detection limits of 5×10^{-11} molar for NDA-glycine in 50-micron capillaries. In 10- and 20-micron capillaries, detection limits were in the range of 10^{-8} to 10^{-9} molar for NDA-glycine.

Small features can be fabricated in glass substrates suitable for electrokinetic flow studies, but to be useful for analysis of $\sim 10,000$ – $100,000$ total biomolecules, microchannels must be chemically coated to exclude protein adsorption. Our established processes for coating channel fabricated in glass require pressure injection of viscous coating solutions. Experience demonstrates the great difficulty of pressure-filling capillary channels with diameters below ~ 10 microns, even with water. Unfortunately, all glass/silicon (Si) microstructures must be top-sealed under high temperatures, making vapor-phase coating with organosilane surface modifiers before sealing infeasible. We therefore concluded that we presently have no means to successfully implement the micro-CE/LiF strategy proposed here in glass/silica/Si substrates.

Simply to be able to fabricate precoated microchannels, we were forced to develop means for fabricating microchannels in polymer substrates. Polymer substrates do not require high temperatures for bonding the top cover plate and therefore can be surface-treated prior to sealing on a top plate. We established criteria for polymer materials, including optical transparency, good moldability, resistance to base, acid, and organic solvents, and bonding suitability. Fortunately, optical

We established criteria for polymer materials, including optical transparency, good moldability, resistance to base, acid, and organic solvents, and bonding suitability.

grades of several aliphatic polymers have recently become available, widening the choice for evaluation.

We undertook a comparative evaluation of hot embossing properties of polycarbonate, acrylic (polymethyl methacrylate), and two grades of a new cyclic polyolefin, TOPAS. We made a nickel die for embossing by electroplating a Si master fabricated using deep reactive-ion etching (RIE). The Si-master contained various microfluidic test structures, including channels, intersections, and fields of posts. We hot-embossed the various substrate materials with the nickel die; we found the TOPAS resins to have generally better molding properties, and features down to ~ 20 microns were well reproduced in TOPAS. With improved die aspect ratios, facilitating demolding, and improved fabrication techniques, such as injection-compression molding, it appears likely that feature sizes up to an order of magnitude smaller may be possible. We showed that TOPAS resins could be plasma-treated to render them hydrophilic and have excellent solvent resistance and bondability. Based on these results, we believe that these polymer substrates can be used to fabricate microfluidic structures suitable for the analysis of single cells.

With improved die aspect ratios, facilitating demolding, and improved fabrication techniques, such as injection-compression molding, it appears likely that feature sizes up to an order of magnitude smaller may be possible.

3535220000

Assessing the Emerging Threat of Limited WMD Use

T. H. West

The U.S. is expending considerable resources on elements of a defense against domestic use of chemical and biological weapons—however, especially for biodefense, no overarching defensive architecture into which these elements would be integrated has been developed. In particular, there is a critical need to prioritize among the diverse options for preventing, protecting against, and responding to chemical and biological attacks against the U.S. To begin to address this need, Sandia developed analytical tools, called master timeline curves, that allow us to evaluate the performance of alternative defensive architectures across a range of attack scenarios. These curves integrate together information from the attack scenario with the associated medical consequences to produce a graphical depiction of the evolution of the attack's effects over time.

We developed analytical tools, called *master timeline curves*, that allow us to evaluate the performance of alternative defensive architectures across a range of attack scenarios. These curves integrate together information from the attack scenario with the associated medical consequences to produce a graphical depiction of an attack's effects over time. We used the information contained in these curves to evaluate the performance (defined as *reductions in fatalities*) of several competing defensive architectures across a range of attack scenarios. The evaluated defensive architectures consisted of combinations of personal protection, collective protection, mitigation, and medical measures. Our most important finding was the decisive importance of timely response, cued either by early medical surveillance or environmental monitoring.

This work provides a timely contribution to the ongoing national dialogue on responding to chemical and biological threats.

Sandia developed analytical tools, called master timeline curves, that allow us to evaluate the performance of alternative defensive architectures across a range of attack scenarios....This work provides a timely contribution to the ongoing national dialogue on responding to chemical and biological threats.

Other Communications

Sandia National Laboratories and Washington Institute. 1999. "Defense of Cities Against Chemical and Biological Attack." Presentation to CDC, Atlanta, GA, 26 September.

Sandia National Laboratories and Washington Institute. 1999. "Defense of Cities Against Chemical and Biological Attack." Presentation to DOE/CBNP, Livermore, CA, 30 July.

Sandia National Laboratories and Washington Institute. 1999. "Defense of Cities Against Chemical and Biological Attack." Presentation to DSP/Trac, Washington, DC, 9 November.

Sandia National Laboratories and Washington Institute. 1999. "Defense of Cities Against Chemical and Biological Attack." Presentation to Rose Gottemoeller, DOE/NN, Washington, DC, 16 November.

Sandia National Laboratories and Washington Institute. 1999. "Defense of Cities Against Chemical and Biological Attack." Presentation to USAMRIID, Ft. Detrick, MD, 28 September.

3535230000

Z-Pinch Fusion for Energy Applications

R. B. Spielman

Z pinches are the oldest fusion energy confinement system. Recent advances in the fields of pulsed-power engineering and Z-pinch physics prompt Sandia to revisit imploding Z pinches as a viable fusion configuration for energy.

Z pinches lack the diversity of ideas that have been developed over the last 30+ years in other fusion energy concepts. In addition, they lack the long engineering history of the other major fusion energy concepts.

We had a number of goals for this project. We needed to develop the idea or concept base for Z-pinch fusion energy concepts. We had to explore some of the key technical and cost issues that had prevented Z pinches from being considered seriously. Finally, we had to ensure that the official fusion community recognized that Z pinches had a role in the national fusion effort.

We had three key goals:

(1) Hold a workshop at Sandia on the topic of Z pinches for fusion energy; invite a wide-ranging group to discuss the possibilities; develop Z-pinch fusion energy concepts for further development. Approximately 20 people from national laboratories, universities, and private industry attended this workshop in April. We reviewed the status of Z pinches and explored the issues that are crucial for the development of economical fusion energy. We explored the role of Z pinches in this area and described and developed concepts. We identified a number of feasible concepts during the workshop and marked them for further study during the year. We prepared a final report.

(2) Review the literature in the area of Z pinches for fusion energy and compile all of the articles found on the topic. We conducted a comprehensive literature search, and indexed and compiled the articles.

(3) Participate in the development of national policy for inertial confinement fusion (ICF) for fusion energy. We presented technical reports describing the state of Z-pinch and ICF target research at Sandia and led the effort to write the report summarizing the relationship of ICF to the National Fusion Energy Program. A summary of the report included Z-pinch concepts developed by this project as part of the technical options for ICF energy.

Recent advances in the fields of pulsed-power engineering and Z-pinch physics prompt Sandia to revisit imploding Z pinches as a viable fusion configuration for energy.

Other Communications

Olson, C. 1999. "Inertial Fusion Energy." *Proc. Snowmass Fusion Energy Summer Study*, accepted.

Spielman, R. B. 1999. "Proceedings of the Sandia Workshop on Z-Pinches for Fusion Energy." *Proc. Sandia Workshop on Z-Pinches for Fusion Energy* **1** (10 May) (Albuquerque, NM, 27–28 April): 50.

3535240000

IFSAR Rapid Terrain Visualization and Real-Time Exploitation System

W. J. Bow, M. R. Platzbecker, J. C. Gilkey, T. D. Vargo

Rapid terrain visualization (RTV) is an advanced concepts technology demonstration whose goal is to create very high resolution digital topographic data (DTD) maps of large regions of the earth's surface. These high-resolution maps can be used to support mission planning activities and allow for more precise wargaming. We selected Sandia's interferometric synthetic aperture radar (IFSAR) as one of the platforms that will collect digital terrain elevation data (DTED) for this demonstration. As we collect DTED, we require an in-house 3-D terrain visualization capability for datasets that are extremely large and dense to assess the quality and performance of the data generated by the IFSAR system. This project provided these capabilities.

Sandia is pioneering a special type of radar, IFSAR, that we can use to create DTD maps. Sandia is participating in an RTV advanced concepts technology demonstration whose goal is to demonstrate the technology available for making DTD products. In this project, we developed a terrain visualization and exploitation system that can exploit the topographic data collected by an IFSAR. These tools allow a user to visualize the terrain and various features in its most natural human viewing mode of 3-D space with intuitive viewing and movement controls. The exploitation system utilizes state-of-the-art visualization techniques such as level-of-detail fading, slope shading, and texture overlay.

This visualization system consists of a commercial real-time 3-D graphical processing engine in a UNIX workstation and software designed to take advantage of the DTD and the additional IFSAR information content in the data. The availability of IFSAR rapid visualization and real-time 3-D exploitation will significantly enhance battlefield mapping for surveillance and targeting applications.

Advances have been made in ultra-fast graphic engines and industry standard 3-D software languages (e.g., OpenGL). This innovation will soon allow the leveraging of the commercial-off-the-shelf (COTS) market to create extremely low-cost terrain visualization workstations.

Sandia is pioneering a special type of radar, IFSAR, that we can use to create DTD maps....In this project, we developed a terrain visualization and exploitation system that can exploit the topographic data collected by an IFSAR.

We created a low-cost COTS ultra-high-resolution DTD real-time visualization tool that has applications to both IFSAR and RTV end-users for map generation, map visualization, targeting, and battle planning.

Other Communications

Bow, W. J., J. C. Gilkey, M. R. Platzbecker, and T. D. Vargo. 1999. "Real-Time Visualization of Extremely Large 3-D Terrain Datasets." Sandia Technical Report, in progress.

3535250000

Technologies for System-Level Innovations in Ballistic Missile Defense

M. L. Lieberman, M. E. Kipp, M. D. Tucker, M. E. Tadros, M. C. Grubelich, S. H. Fischer

This investigation assessed the feasibility of two advanced warhead concepts, namely, (1) a denial warhead that combined sticky resin and materials to decontaminate chemical and biological (C/B) agents, and (2) an implosion geometry incendiary warhead. Sandia showed conclusively that sticky resin could be combined with decontaminating materials to yield a material that possessed both properties. Limited testing of the latter concept indicated that physical parameters play a significant role in determining the effectiveness of the concept. Consequently, we concluded that one concept has been deemed feasible, while the other requires further investigation.

We showed for the first time that sticky resin materials can be combined with materials used for the decontamination of C/B agents. Such formulations exhibit apparent stability and miscibility. They offer an alternative warhead concept for attacking facilities that contain C/B agents because they create temporary denial while mitigating the risk of contamination from the agents. Preliminary analysis suggests that such a warhead could be adapted to the BLU-109 penetrator in such a manner that the weight and center of gravity would be essentially unchanged. A limited comparison of incendiary warheads utilizing imploding and exploding geometries did not yield a conclusive evaluation. Additional calculations and experiments are needed to more fully assess the relative benefits of the alternative geometries. Hydrocode calculations proved to be a useful tool and provided reasonable predictions of shrapnel velocity and particle size. The calculations also served to assess the effects of scaling from a full-size weapon configuration to the reduced test size.

We showed for the first time that sticky resin materials can be combined with materials used for the decontamination of C/B agents. Such formulations exhibit apparent stability and miscibility.

3535260000

Novel Collective Protection System for Decon of CBW Agents and Purification of Aircraft and Other Closed Environments

M. E. Tadros

Sandia developed a novel method for decontamination of air containing chemical or biological (C/B) agents. The method is based on hollow fiber membrane modules for effective capture and detoxification of gases and aerosols of C/B agents. We developed a liquid decontamination solution for circulation around the outer surfaces of the fiber while contaminated air circulates through the lumina of the fibers. The liquid does not penetrate the fiber due to capillary pressure forces. We carried out experiments with Celgard polypropylene membrane contactor (Liqui-Cel Extra-flow 2.5x8-X40). This module has an effective surface area of 1.4 m². We demonstrated effective decontamination for 2-chloroethyl ethylsulfide (simulant for mustard gas) and diethyl chlorophosphate (simulant for sarin and soman).

This method is applicable to rapid cleanup of aircraft atmosphere and other closed environments.

(1) We completed a survey of current technologies that could be employed for air decontamination in building and semiclosed environments. Charcoals and Fuller's Earth materials are still the materials of choice as adsorbents for individual (masks) and collective protection (filters for shelters, vehicles, and buildings). These materials act as sorbents and do not detoxify the contaminant. They exhibit limited-use duration and remain as a potential source of secondary emission. These systems are designed primarily for mitigation of chemical agents and have limited applicability to biological agents.

(2) We completed setup of a continuous circulating system with the hollow fiber module and gas chromatographic analysis system.

(3) We demonstrated effective decontamination of air polluted with the mustard gas simulant 2-chloroethyl ethylsulfide. The air stream contained about 4×10^4 g/m³, and the flow rate through the membrane module was 50 ml/min. Similarly, we effectively decontaminated air contaminated with diethyl chlorophosphate (simulant for sarin and soman).

Sandia developed a novel method for decontamination of air containing chemical or biological (C/B) agents....based on hollow fiber membrane modules for effective capture and detoxification of gases and aerosols of C/B agents.

3535270000

Z-Backlighter Technologies*S. M. Cameron, T. R. Lockner, T. S. Luk, D. E. Bliss*

Plasmas created by intense ultra-fast lasers interacting with solid targets have received considerable attention as bright x-ray sources for backlighting pinch or capsule implosions and for nondestructive radiographic imaging of weapons components. These diagnostic applications require precise spatial and temporal resolution for gated acquisition of high-contrast images without penumbral blurring or scattering noise. Peak source spectral brightness in the multi-kilovolt (> 10 keV) photon energy regime is needed to overcome background self-emission in such environments and to penetrate typical opacities and compressed areal densities. Because the laser drive deposits its energy impulsively over a short scalelength of near solid-density material on a subpicosecond timescale exhibiting negligible hydrodynamics, the resulting x-ray emission burst will be characterized by nonthermal distributions and extreme gradients of temperature and electron density, which are ideal for producing the prerequisite conditions. Recently, a fundamentally new regime of self-focused electromagnetic (EM) propagation has been observed for high-intensity terawatt lasers in plasma that arises from the combined action of relativistic and charge-displacement nonlinearities. As a consequence of the unprecedented power compression inherent to this channeling mechanism, excited matter combining concentrated energy density with well-ordered spatial gain structure can be created in the trapped focusing state, which would not be accessible with conventional excitation methods. The resulting laser-driven excited states do not obey uncorrelated single-electron coupling rules, but instead exhibit augmented long-range collective coupling interactions through spatially ordered coherent multi-electron motions within the channel interior. These new physical processes can enhance radiative coupling to classically forbidden inner-shell states, thereby enabling the dynamic production of so-called hollow atoms with inverted electronic configurations and core electron vacancies optimal for rapid x-ray recombination, x-ray amplification, and favorable stimulated emission rates. The enhanced inner-shell selective EM coupling can be exploited for efficient x-ray lasing and radiation yields when applied over refractively compensated gain scalelengths, such as the self-focused

Peak source spectral brightness in the multi-kilovolt (> 10 keV) photon energy regime is needed to overcome background self-emission in such environments and to penetrate typical opacities and compressed areal densities.

channel, to create a revolutionary advance in coherent backlighter technology.

In collaboration with the University of Illinois–Chicago, we used a self-focused femtosecond ultraviolet (UV) terawatt-class laser with a focused irradiance of 10^{18} W/cm² to produce L-shell x-ray emission from high-Z targets. We acquired spectra using an imaging crystal spectrometer (von Hamos) with an optimized filter package, and integrated x-ray radiation yields in the filtered energy ranges were measured with a calibrated photo cathode device (PCD). Single-shot integrated yields in L-shell gold (10–14 keV) exceeded our predicted value, and the observed spectrum, although occurring generally in the expected spectral region of neon (Ne)-like gold (Au) transitions, exhibited a predominant asymmetrical broadband feature (~ 700 eV) superimposed on bremsstrahlung continuum and line emission. Such a characteristic nonthermal emission signature arises from core-excited ionic-state configurations and is direct spectroscopic evidence of a hollow-atom excitation mechanism in which the energetic laser field collectively drives correlated electron motion to produce anomalous coupling. To our knowledge, this is the first reported measurement of gold L-shell emission from a laser-produced plasma and is the direct result of the unique interaction conditions, which can be produced with high-intensity short-pulse lasers. The achievable spectral radiances scaled to an existing hybrid Nd:glass laser deployed on the Z accelerator using our experimentally measured conversion efficiency (~ 1%) above 10 keV would facilitate an efficient, ultra-bright, hard x-ray backlighting source capable of opacity penetration of pinch/capsule implosions with compressed areal densities ~ 1–10. We also observed strong EM transients and coherent far-infrared emission at terahertz frequencies as the result of space-charge fields generated at the focus of the optical pulse due to the large transverse pondermotive force. As part of the experimental campaign, we also used the picosecond x-ray bursts to directly measure the impulse response of instrumented PCDs. In parallel with experiments, modeling efforts are ongoing toward spectroscopic analysis and stability/optimization criteria for the channeling mechanism.

To our knowledge, this is the first reported measurement of gold L-shell emission from a laser-produced plasma and is the direct result of the unique interaction conditions, which can be produced with high-intensity short-pulse lasers.

3535280000

Ultra-Intense Femtosecond Laser Interactions with Applications to High-Field Physics, Enhanced Electromagnetic Coupling in Materials, and X-Ray Generation

S. M. Cameron, T. R. Lockner, M. T. Buttram, T. S. Luk

Realization of laboratory-scale femtosecond terawatt lasers with focusable irradiances approaching 10^{20} W/cm² allows the creation of novel high-field interaction conditions for the production and regularization of many energetic processes, including x-ray and electromagnetic pulse (EMP) generation, optical fission, and gradient-wakefield particle acceleration. In this exceptional regime, rapid ionization of heavy atoms by field emission occurs during a fraction of a laser cycle, and the transient pulse amplitude reaches a substantial fraction of the atomic Coulomb field, thereby significantly altering the shape of the electron binding potential. The presence of a high-intensity laser distribution in the resulting dense plasma will modify basic constitutive properties from the basic fluid description, instead producing nonlocal currents and internal energy equilibria essentially controlled by the electron quiver velocity in the external driving field. Tunneling or cascade ionization processes induced by the combination of peak intensity with short interaction time and abrupt temporal development profile will have profound consequences for efficient rectification of ultra-wideband microwave transients, recombination x-ray lasers, enhanced collective scattering and anomalously strong atomic coupling, and evolution of nonsteady-state dielectric responses to penetrating fields. The strong dependence of electron-ion collision frequency on quiver motion will contribute to the nonlinear refractive index and enhanced dynamical EM transparency in absorptive/dispersive material systems. Channeled propagation of intense ultra-short laser pulses produced by refractive self-guiding in the relativistic self-focusing limit will establish a new class of nonlinear optical experiments with achievable power densities approaching 10^{19} W/cm³ and energy transfer (deposition) rates ~ 1 – 10 W per atom over controllable physical interaction lengths. As a consequence of the unprecedented power compression inherent to the channeling mechanism, a new unexplored class of strongly nonequilibrium-excited matter combining concentrated energy density with well-ordered spatial gain structure can be created embodying conditions

Tunneling or cascade ionization processes induced by the combination of peak intensity with short interaction time and abrupt temporal development profile will have profound consequences for efficient rectification of ultra-wideband microwave transients, recombination x-ray lasers, enhanced collective scattering and anomalously strong atomic coupling, and evolution of nonsteady-state dielectric responses to penetrating fields....

conductive to laser-driven collective excitation of energetic electronic ensembles and x-ray amplification.

In collaboration with the University of Illinois–Chicago, we used a relativistically self-focused ultraviolet (UV) femto-second terawatt laser (600 mJ/200 fs) with focusable intensity exceeding 10^{19} W/cm² along the propagation channel to excite the x-ray spectrum of coated gold targets and free-standing tantalum (Ta) foils in the 10–20 keV energy range. We observed anomalously high x-ray conversion efficiencies approaching 5% and attributed them to an enhanced power compression mechanism involving short-pulse collective coupling and electron bunching in the self-channeling process. We measured a large system-generated electromagnetic transient (SGEMP) with estimated field strength exceeding 10 KeV/m near the laser channel impact and correlated it with bremsstrahlung x-ray emission and hot electron production in the laser-material interaction. We measured hollow atom spectra of Xe(L) ~ 4 keV clusters suitable for x-ray amplification (inner-shell population inversion) and with potential for transient recombination lasing, and they exhibited strong directional anisotropy preferentially along the channel axis. Theoretical analysis of the experimental data suggests that the time-front of the intense propagating UV pulse in the channel was sufficiently abrupt to generate a collective excitation on a timescale shorter than that required for photoionized electron wavefront spreading and dephasing due to scattering. Comparative experiments with redder excitation wavelengths showed a pronounced reduction in coupling efficiency and an absence of inner-shell spectral features consistent with the longer optical period for interaction. We derived new modeling results for the transverse stability of the relativistic channeling process that demonstrated that an impressed longitudinal plasma-density gradient can produce robustness to azimuthal perturbations, including transverse spatial variations in the incident laser beam.

Refereed

Borisov, A. B., S. M. Cameron, T. S. Luk, T. Nelson, W. A. Schroeder, J. W. Longworth, Y. Dai, K. Boyer, and C. K. Rhodes. 1999. "Bifurcation of Plasma Channels Undergoing Propagation of Intense Ultraviolet Pulses with the Relativistic/Charge-Displacement Mechanism." *Internat. Conf. Electromagnetics in Advanced Applications–Litografia Geda* (Torino, Italy, September): 15.

Borisov, A. B., S. M. Cameron, Y. Dai, J. Davis, T. Nelson, W. A. Schroeder, J. W. Longworth, K. Boyer, and C. K. Rhodes. 1999. "Dynamics of Optimized Stable Channel Formation of Intense Laser Pulses with the Relativistic/Charge-Displacement Mechanism." *J. Phys. B: At. Mol. Opt. Phys.* **32** (6 May): 3511–3525.

3537190000

Design of a Prototypical Snoopy Coprocessor for DynaMICs Software Fault Monitoring with Integrity Constraints

L. J. Dalton

Computers are omnipresent in our society, and the reliability of these systems cannot always be guaranteed by traditional verification and validation (V&V) methods. A complementary approach to improving the reliability involves the use of runtime software-monitoring approaches that employ integrity constraints to define correct program behavior. Sandia directed this work toward developing a snoopy-coprocessor system that employs coprocessor and bus-monitoring hardware to facilitate concurrent execution of application and constraint-checking code. The coprocessor executes constraint-checking code while the main processor executes the application code. This is one element of a high-level goal for defining and developing a comprehensive, knowledge-based system that complements existing V&V methods, supporting production of high-quality systems.

The snoopy-coprocessor concept is part of a high-level approach to system reliability known as Dynamic Monitoring with Integrity Constraints (DynaMICs). In particular, the snoopy-coprocessor supports the dynamic monitoring mechanism, wherein the snoopy-coprocessor monitors and observes a program running in a main processor at runtime, ensures that specified constraints are satisfied, and, in so doing, detects potential faults. When the monitor detects an integrity-constraint violation, it notifies the tracing mechanism and possibly the main processor (if program termination is specified).

The work accomplished can be divided into two complementary efforts. We directed one effort at automating the generation of monitoring code from integrity constraint and knowledge specifications. The other effort focused on completing the design of a parallel discrete-event simulation of a snoopy-coprocessor system.

• *Monitoring-code generation.* The project resulted in the formal definition of a preliminary specification language for knowledge and integrity constraints as well as definition of the data dictionary, and constraint and knowledge tables that serve as repositories. In addition, work focused on development algorithms for automatically generating monitoring code from

The project resulted in the formal definition of a preliminary specification language for knowledge and integrity constraints as well as definition of the data dictionary, and constraint and knowledge tables that serve as repositories.

the specifications and data dictionary, and path-tag tables that are created during program instrumentation.

- *Design of a discrete-event simulation of a snoopy-coprocessor system.* The principle effort of the project focused on the design of a parallel discrete-event simulation that models the snoopy-coprocessor system. The system simulation used object-oriented methodology referred to as *responsibility-driven modeling*, called Class, Responsibility, and Collaboration (CRC) for its design. We achieve parallelism by partitioning the modeled system into different logical processes. The logical processes include the snoopy-coprocessor and its constituent parts, the main processor, communications and input/output (I/O) bus, and main memory. The logical processes communicate among each other via shared memory using events, each of which includes a timestamp that indicates the time at which the event is scheduled to occur, actions to be performed, and destination. Because we implemented conservative simulation, we executed only safe events—that is, we did not plan for comprehensive simulation of faults at this level.

Refereed

Gates, A. Q., and P. J. Teller. 1999. “DynaMICs: An Automated and Independent Software Fault-Detection Approach.” *Proc. HASE '99* (IEEE International Symposium on High-Assurance Systems Engineering, Washington, DC, 17–19 November).

3537210000

Analytic Verification of Treaties, Protocols, and International Agreements

M. L. Abate, K. L. Hiebert-Dodd, J. C. Forsythe

Sandia will develop and demonstrate a cost-effective methodology for verifying compliance with critical international treaties, protocols, and agreements. Although this activity focused on the Kyoto Protocol as the case study, we developed the methodology with a broader view toward synthesizing the science of verification of treaties, protocols, and agreements.

The complexity of implementing a verification scheme associated with the Kyoto Protocol or other agreement makes evident the need for an analytic approach to verification because of the intricate issues of measurement, reporting, confirmation, and administration.

We constructed simulations that demonstrated the statistical sampling plans required to detect differences between monitored and self-reported greenhouse-gas values. We used the results of these simulations to form statistical power curves that demonstrated the effectiveness of detecting noncompliance for given instrument accuracies and differences.

We showed that use of the Intergovernmental Panel for Climate Change (IPCC) guidelines for estimating emission values is subject to variability due to the following factors in the IPCC worksheets:

- Source and consumption data,
- Default and local emissions values,
- Carbon stored values, and
- Double counting.

Other Communications

Abate, M., D. Engi, and J. C. Forsythe. 1999. "The Science of Treaty Verification." Sandia Technical Report, in progress.

Beaudry, D. 1999. "Sensitivity Analysis of Greenhouse Gases Inventory: CO₂ and the Energy Sector." Presentation to the Purdue University and Sandia National Laboratories Collaboration Seminar, Albuquerque, NM, 10 September.

Jacko, R. B., and T. M. C. Labreche. 1999. "Greenhouse Gases and the Kyoto Protocol." Presentation to the Purdue University and Sandia National Laboratories Collaboration Seminar, Albuquerque, NM, 10 September.

Sandia will develop and demonstrate a cost-effective methodology for verifying compliance with critical international treaties, protocols, and agreements.

3537220000

Fabricating Microcomponents from Silicon-Carbonitride by a Novel Microcasting Process

R. E. Loehman

The objective of this project is to develop a process for fabricating microcomponents from amorphous silicon carbonitride (SiCN), a new ceramic material that is suitable for applications in extreme corrosive and temperature environments. We achieved our primary objective in that we have been able to produce parts of 10–100-micrometer dimensions by casting the SiCN precursor into a Si mold. These specimens have an amorphous structure as confirmed by x-ray diffraction. However, the deliverable for the project was to cast larger specimens up to millimeters in size. Achieving that objective has proved more difficult because it requires developing a different lithography technique for making the molds into which the SiCN specimens can be cast. A new approach to making the molds that uses the polymer photoresist itself as the mold instead of Si was proposed. Although the results appear promising, they require further development.

In collaboration with the University of Colorado (CU), we used three methods for casting the SiCN parts, described below:

- *Casting into a Si mold.* This process proved to be reasonably successful but was limited by the dimensions of the molds that can be made by etching a Si substrate. The dimensions of those mold-cavities were limited to about 100 micrometers. There is some fraying at the surface of the casting, but this problem can be overcome by polishing the filled Si surface before pyrolysis. Although this approach can work well for very small components, it is not suitable for making specimens of the size described above.

- *Casting into cavities created in a layer of a photoresist.* In this method we deposited a layer of photoresist on a substrate (we have used several different kinds, including glass and Si) and etched the mold cavity into this layer by photolithography. UC researchers are still working to improve this technique. Although there are problems with cracking of the SiCN components due to adhesion to the photoresist or the substrate, the approach seems promising enough for further work.

The objective of this project is to develop a process for fabricating microcomponents from amorphous silicon carbonitride (SiCN), a new ceramic material that is suitable for applications in extreme corrosive and temperature environments.

- *Casting into a polyfluoroethylene well.* In this method we made a rectangular well structure by machining a piece of polyfluoroethylene. This method successfully made SiCN samples with dimensions of several millimeters, which are generally free of defects and have strengths as high as 1 GPa. The castings made by this process were cut and polished to make the samples.

3537230000

Magnetic Polysilicon MEMS Devices

T. W. Krygowski

Sandia is investigating the development of magnetically driven micromachines. In this new approach we coat the microelectromechanical systems (MEMS)–based devices with a magnetically responsive material and drive them using external, macroscopic magnets. The advantages of this approach are twofold: (1) there is no direct, visible, invasive connection between the macroscopic world and the microscopic world, and (2) the microscopic device becomes comparatively simpler to design due to the absence of energy-converting systems. In this project we will deposit a thin film of magnetic material using pulsed-laser deposition (PLD) on an existing silicon (Si)-based MEMS device, then drive the system remotely by a set of high-energy magnets. We (1) designed a system for depositing thin-film magnetic material on the Si-based MEMS devices, and (2) built the experimental setup for the metal-etching process. We are pursuing a patent that covers the new innovation.

Using the magnetic MEMS technology, we will deposit a thin-film magnetic material on an existing micromachine, then drive the machine remotely using external magnets.

- In collaboration with researchers at Florida Agricultural and Mechanical University–Florida State University (FAMU–FSU) College of Engineering, we designed a deposition system for growth of thin films of magnetic materials. The system includes a 12-cylinder vacuum chamber, a 205 l/sec turbomolecular pump, optical windows for the laser beam, and substrate heater assembly capable of 1200°C.

- We built the experimental setup for the etching processes to remove unwanted parts of the thin film. The experimental procedure and setup include:

- Photoresist will be uniformly coated on the MEMS surface with a spinning machine.
- The photoresist will be packed at 80°–100°C.
- The photoresist will be exposed to UV light through a mask with designed pattern.
- Regions of the photoresist exposed to the light will be removed when the device is placed in a developer.
- Regions of the magnetic film without photoresist will be etched away when the device is placed into an acid solution (hydrochloric acid [HCl]).

Sandia is investigating the development of magnetically driven micromachines....We are pursuing a patent that covers the new innovation.

– The photoresist will be washed out with the acetone. Once the setup for the PLD is complete, we will test the system.

We designed a PLD system to grow a thin film of magnetic material on polysilicon-based micromachines. We expect the development of this technology to revolutionize the MEMS industry since it will allow the MEMS-based devices to be much simpler to design and more compact in size than current devices.

*We expect the development of
this technology to revolutionize
the MEMS industry....*

Other Communications

Kilani, M., C. J. Chen, Y. Haik, and V. Pai. 1999.
“Rectilinear Dynamics of Magnetically Driven
Microsystems.” *Proc. 2nd Internat. Conf. on Modeling
and Simulation of Microsystems* (San Juan, PR, 19–21
April): 675–678.

3537240000

Living Tissue Engineering

R. C. Dykhuizen

Tissue engineering is an emerging field involved in the development of biological substitutes, incorporating living cells and synthetic or natural materials. These constructs are designed to foster tissue regeneration and/or remodeling for the purpose of repair, replacement, or enhancement of tissue function. However, to accomplish any of these goals, procedures for storage and transport of the product must be developed. Cryogenic procedures are identified as the most likely solution. Sandia developed a freezing model for living tissue. This model accounts for the complex cellular structure of the material and the osmotic flows that occur during the freezing process. As the liquid outside the cell freezes, pure ice forms, resulting in concentration of salts in the remaining liquid. The osmotic flows that develop extract liquid from the cell in an attempt to equalize the chemical potential. The osmotic flow continues until either the cell dehydrates, the cell internal liquid solidifies, or solutes enter the cell to equilibrate the chemical imbalance.

We developed a model of tissue freezing that can simulate many real problems of importance to tissue engineering. We incorporated this model into a computer code for simulation of arbitrary freezing schedules. We input the freezing schedules as boundary conditions (BCs) to the tissue samples that are simulated. These BCs involve time-dependent temperature (or heat fluxes) and solute concentrations (or solute fluxes). A successful freezing schedule will involve introducing a cellular protective agent (CPA) solute into the tissue. Diffusion of the CPA into the tissue will modify the freezing temperature and also induce osmotic flows that may dehydrate the cells. Some dehydration is necessary to reduce or eliminate the formation of intercellular ice. The model separately tracks two material phases (liquid and solid) and two solutes (salt and CPA) within two domains (intercellular and extracellular). Due to the small cell size and the relatively large thermal conductivity, we use a single temperature for all materials and domains at any one location. However, the solute diffusion coefficients are so small that equilibrium of the solute concentrations is not assumed. We track the diffusion of both heat and solute within the tissue sample. The solidification process results in a local heat source and a concentration of solutes within the remaining

Tissue engineering is an emerging field involved in the development of biological substitutes, incorporating living cells and synthetic or natural materials.

liquid. The model calculates the temperature, solute concentrations, and ice fractions as a function of time and position within the tissue. Also, the transient cell size can be output, for it changes due to the osmotic flows that occur during the freezing process. From these outputs, the user can determine the probability of cell survival as a function of position within the tissue. The model will allow optimization of the freezing schedule to maximize cell survival. We verified the computer model in collaboration with Georgia Tech University (GTEC). GTEC performed many simulations with the model and showed how sensitive cell survival is to small changes in the freezing schedule. The freezing of living tissue is the most complex thermal model ever developed by Sandia. It is the first such model in the country, for previously only the freezing of single cells was simulated. We believe that the experience gained in developing this model will allow development of thermal models for other complex materials of interest to Sandia. Weapon materials such as foams and explosives also undergo complex phase changes during thermal transients of interest.

The freezing of living tissue is the most complex thermal model ever developed by Sandia. It is the first such model in the country, for previously only the freezing of single cells was simulated....the experience gained in developing this model will allow development of thermal models for other complex materials of interest to Sandia. Weapon materials such as foams and explosives also undergo complex phase changes during thermal transients of interest.

3537250000

The Use of Active Fiber Composites for the Health Monitoring of Wind Turbine Blades

T. W. Simmermacher

Sandia investigated the feasibility of using active fiber composite (AFC) materials for structural health monitoring (SHM) and damage detection on wind turbine blades. AFCs are built by embedding piezoelectric fibers in an epoxy matrix, applying interdigital electrodes symmetrically on the top and bottom surfaces of the matrix, and then laminating capton sheets on the two surfaces to cover the electrodes. The AFC offers the advantages of orthotropic actuation, conformability, integration as a single ply into composite structures, and highly distributed actuation and sensing. The limitations of AFCs are high cost, additional weight, and the need for a large actuation voltage on the order of 1–2 Kvolts. For SHM, we consider the AFC to have the potential to be used as a large distributed sensor that can detect damage to the blades of operating wind turbines. To investigate this, we performed damage-detection testing and sensor development using piezoceramic (PZT) patches and an AFC patch. We also performed a new boundary effect method (BEM) for damage detection and modeling of AFCs.

We used a scanning laser doppler vibrometer sensor and AFC patch actuator to detect damage on a 24-inch by 48-inch by 0.125-inch freely suspended aluminum (Al) panel. The laser is noncontact and can measure vibration at a large number of points on a structure. We used the AFC patch to generate the vibration and the operational deflection shape pattern recognition (ODSPR) method to detect damage. We attached a concentrated mass to the panel to simulate damage and detected the damage from changes in the symmetry pattern of the ODS. We then sanded the panel to remove a paint coating and painted it with reflective paint to increase the reflectivity of the laser light. After the sanding and painting, the panel no longer had any symmetric ODS shapes; thus, sanding the thin panel changed the thickness slightly and destroyed the symmetry of the ODS. The sanding effect is similar to corrosion; thus, corrosion may be detected by changes in the ODS of a structure. We simulated damage to the panel using an added mass and detected the damage by comparing the ODS patterns in the healthy and damaged cases. This testing showed that using only 200 volts excitation, the AFC patch was able to

The AFC offers the advantages of orthotropic actuation, conformability, integration as a single ply into composite structures, and highly distributed actuation and sensing.

excite the panel and generate sufficient vibration amplitude to detect damage. The AFC patch is 2.5 by 5.25 inches, which is larger than PZT patches. The larger size helps to excite vibration on large structures. A conclusion of these experiments is that a distributed sensor can substantially reduce the complexity of the SHM system, since the number of channels as well as the associated electronics can be greatly reduced. The distributed sensor also improves sensitivity by being closer to the damage. With a piezofiber composite, it may be possible to form a long antenna-type sensor over the surface of the structural component. This will enable detection of high-frequency components of the acoustic emissions (AE) signal occurring anywhere in the structure with a single or a small number of distributed sensors. We demonstrated that the charge from the individual elements of the sensor bleeds into the remaining elements of the sensor. In effect, this is an increase in the capacitance of the sensor, which reduces the signal output. The overall locations greatly increase the signal-to-noise ratio corresponding to the high-frequency components, but the bleeding effect reduces the amplitude of the signal. Furthermore, we showed connecting the PZTs with alternating polarity to increase the output voltage of the distributed sensor. These experiments indicate that we can use poling of the AFC as a spatial filter to tune the bandwidth characteristics of the sensor. We are studying this effect using a structural elastic-AFC-electric circuit model and are using the model to optimize the distributed sensor.

We established criteria for polymer materials, including optical transparency, good moldability, resistance to base, acid, and organic solvents, and bonding suitability.

Other Communications

Ghoshal, A., M. J. Sundaresan, M. J. Schulz, and P. F. Pai. 2000. "Damage Detection in Composite Structures Using Vibration Measurements." *Proc. 6th Internat. Conference on Composites Engineering 1* (Orlando, FL, January): 10.

Sundaresan, M. J., A. Ghoshal, M. J. Schulz, and P. F. Pai. 1999. "Acoustic Emission Sensing Using Piezoceramic and Active Fiber Composite Patches." *Proc. ASNT 1999 Fall Conference 1* (Phoenix, AZ, October): 10.

3537260000

Developing/Assessing Long-Term Impact of Design Innovations

T. W. Simmermacher

This project investigates the potential innovation of an energy-producing wall component (EPW), which serves as one component of a larger system of innovations for the home relating to the envelope and building systems. The EPW is a composition of developing and extant technologies, questioning how the building façade can be controlled, manipulated, and utilized to create thermal comfort and spatial integrity within interior spaces while reducing and/or generating energy. Evaluation of the EPW is not based solely on operational performance, but the process of construction, wood-light frame–dynamic simulation model (WLF–DSM) provides answers to the “what if?” questions within the process of a project. Sandia developed two prototype home designs, representing traditional and forward-looking designs, to test the DSM and to analyze the impacts of new technologies such as the EPW on the process. Physical tests in the form of prototype components placed in the context of a test chamber constructed by Sandia and MIT, coupled with aesthetic studies through visualization tools, describe the breadth of the integrative approach.

We gathered data through trade and professional publications on construction methods and approaches. We further validated the process characterization through in-depth personal interviews with practitioners and experts in the field. We assembled an expert panel of architects, engineers, builders, and contractors as a source of validation to the progress of the research. To test the accuracy and validity of the computer-based process simulation model, we developed cost, time, and safety estimates for a specific building design. These prototype buildings were proven in previous research to accurately represent common building types and to provide a basis on which practitioners and experts can accurately evaluate the simulation results. For this research, we developed two prototype designs. The first design uses a Sears kit house (from the 1920s) to represent a large percentage of the existing built residential environment. The second design is applicable to new construction and is currently being used to assess the energy effectiveness of active solar units.

Sandia developed two prototype home designs, representing traditional and forward-looking designs, to test the DSM and to analyze the impacts of new technologies, such as the EPW, on the process.

3537270000

Composite Wire Plasma Formation and Evolution

R. B. Spielman

The detailed understanding of the formation and evolution of plasma from a rapidly heated metallic wire is a longstanding challenge in the field of plasma physics and in exploding wire engineering. This physical process is made even more complicated if the wire material is composed of a number of individual layers. It is critical to understand the essential physics in order to begin the process of modeling and prediction.

This project was intended to develop the experimental and diagnostic techniques needed to study the formation and evolution of such plasmas. These diagnostics included the possibility of optical and/or x-ray backlighting.

Sandia successfully developed both optical and x-ray backlighting diagnostics. In particular, the x-ray backlighting technique demonstrated the capability for quantitative determination of the plasma density over a wide range of densities.

This diagnostic capability enabled us to learn that the process of plasma formation comprises two separate phases. First, current is passed through a cold wire and the wire is heated ohmically. Second, the heated wire evolves gases that break down and form a plasma surrounding the wire. At this point the current commutates to the plasma, and the direct heating of the wire ceases.

This understanding opens up the possibility of improving the process by controlling the initial heating of the wire and retarding the formation of the plasma.

We investigated the effect of a 50–100 nsec current ramp reaching 0–1 kA on the state of aluminum (Al) wires. We built a pulser that produces a current pulse having a 350 nsec risetime and an amplitude of 4.5 kA.

We radiographed the Al wire explosions using the method of direct x-ray backlighting using molybdenum (Mo) wire X-pinch. We found Mo-wire X-pinch experimentally to produce submicron, bright x-ray sources in the 2.5–10 keV x-ray energy range. The effective spatial resolution in these experiments was 2–3 μm .

The experiments reported here involved 12.7 μm Al wires. The timing of the radiographs obtained of the exploding wires

Sandia successfully developed both optical and x-ray backlighting diagnostics. In particular, the x-ray backlighting technique demonstrated the capability for quantitative determination of the plasma density over a wide range of densities.

ranged from 70 to 500 nsec relative to the start of the current pulse. Radiographic data illustrated the expansion as a function of time.

In less than 100 nsec, wires driven by less than 1 kA/wire expand by a factor of up to 5X in diameter and develop a foamlike structure, which is believed to be a liquid-vapor combination. It is almost certainly the energy deposited, rather than the current, that determines the development of the wire expansion rate. Expanded vapor/plasma columns without visible structure were formed by 250 nsec at 2 kA per wire.

We estimated the density of Al in the wire cores to be $0.4 \times 10^{-2} \text{ gm/cm}^3$. We conclude that the core has not lost a significant fraction of its mass by 72 nsec because the profile of the radiographic data shows it to be opaque almost over the full diameter.

We measured the voltage and current across the test wire. As the resistance of the wires increases due to heating, a substantial resistive voltage develops across the wire. As the wires heat up, their resistivity increases. Therefore, although the voltage rises for some tens of nanoseconds, the current becomes constant, resuming its rise only when the voltage collapses as a result of plasma formation around the wires. Once a low-resistance plasma is available to carry current, the current can increase at an inductance-limited rate, and essentially none of the current will continue to flow in the high-resistance path represented by the superheated liquid-metal core.

In another test, we contaminated the Al wire with oil. Data show that the oil delays the voltage collapse, implying more energy deposition in the test wire. We observed more rapid vapor-bubble-driven expansion of the wire core for the oil-contaminated test. This implies that it is not the current at the time of the radiograph that determines the wire core expansion rate, but rather the energy deposition, which depends on the current during the first 30–50 nsec of the pulse.

We made three conclusions from our work:

(1) In the initial stage of the wire explosion, energy is deposited resistively, heating it in less than 20 nsec to the melting point and, in a few more nanoseconds, to the vaporization temperature. Since the average energy per particle is well above the equilibrium evaporation temperature of the Al, material evaporates from the surface. The resulting wire-encircling vapor will be augmented by the vapor from the breaking of bubbles that develop near the surface.

...it is not the current at the time of the radiograph that determines the wire core expansion rate, but rather the energy deposition, which depends on the current during the first 30–50 nsec of the pulse.

(2) As the bubbles develop in the dense core volume, the wire begins to expand but becomes more resistive. This leads to increasing electric fields in the vapor around the wire. Eventually, a discharge will stretch from one electrode to the other along the wire, and virtually all of the current will be carried by the plasma surrounding the expanding wire core rather than in the core itself.

(3) Because Al is a low-boiling-point metal with a low resistivity, the ohmic heating that occurs before the current switches to the coronal plasma is sufficient, at least over most of the wire length, to totally evaporate the wire. Therefore the superheated, foamlike structure gives way to a fully vaporized wire in less than 200 nsec.

Refereed

Sinars, D. B., T. A. Shelkovenko, S. A. Pikuz, J. B. Greenly, and D. A. Hammer. 1999. "Exploding Aluminum Wire Plasma Formation." *Appl. Phys. Lett.*, accepted.

3537280000

DNA Microarray Technology

G. S. Davidson

Deoxyribonucleic acid (DNA) microarray technology is rapidly establishing itself as an indispensable tool to correlate large volumes of DNA sequence data with the coordinated expression of all genes within an organism. The impact and potential of DNA microarray technology have already been demonstrated through its application to health, environmental, pharmacological, and basic biological research. Microarray technology is not readily available to many in the research community due largely to the cost of setup. Further, the pace of development of the technology means that first-generation systems will be obsolete within several years, another costly aspect of this technology. The purpose of this project is to validate and improve this process.

The tasks for this project include: (1) obtain transcriptional profiles (microarray data) from yeast cells during exit from stationary phase to be analyzed by a data-mining software package (VxInsight™) developed at Sandia; and (2) document the project.

Microarray data will be available shortly. We ordered and received all reagents and supplies and performed essential control experiments to establish the reliability of the data to be collected. For example, we completed control experiments to monitor ribonucleic acid (RNA) preparations for uniform high quality. Widespread incorporation of this particular control experiment will contribute enormously to the quality of the data generated in this project and in the greater community as well—a long-term benefit for the robustness of this technology. A second control experiment to monitor the first-strand synthesis step in generating RNAs for transcriptional microarray analysis will also contribute to the quality of data generated. With these controls firmly established, we are preparing experimental RNAs for carrying out the transcriptional microarray analysis and data mining. While these wet-lab experiments are being carried out, testing and refinement of the VxInsight™ software package is ongoing. Collaborative sessions with biologists at UNM and computer scientists at Sandia led to better interfacing with the software, which we tested with data from Stanford microarray experiments in preparation for use with our data.

The impact and potential of DNA microarray technology have already been demonstrated through its application to health, environmental, pharmacological, and basic biological research.

3537290000

Research Issues in the System Engineering Aspects of High Assurance

V. L. Winter

The objective of this project was to explore new approaches for achieving high-assurance systems engineering (HASE). Sandia first studied the unique characteristics and underlying issues of systems engineering in the context of high-assurance applications. Second, we examined existing dependability methods and identified areas not adequately covered. Finally, through a case study for a successful high-consequence system development, we identified an actual list of systems engineering steps for comparison against existing dependability methods. In addition, we evaluated the efficacy of the steps in the context of unique characteristics and underlying issues related to high-assurance systems.

We developed the following ideas in this project:

- *A life-cycle approach for the systems engineering steps of HASE.* In essence, the lifecycle is a standard waterfall technique and nothing unusual; however, we showed how to carry out stepwise refinement and assurance V&V at each lifecycle step to ensure that the desired level of assurance is maintained in the system.

- *An environmental analysis that is triggered by the required level of assurance.* We are unique in this capability because the previous approaches made *ad hoc* design decisions as to which part of the environment must be analyzed for assurance reasons and which other environmental elements did not require further analysis. Such *ad hoc* decisions led to runtime catastrophes, e.g., if one of the presumed unperturbed environmental entities did behave in an unpredictable fashion at runtime, it could lead to a failure in the high-consequence system. We proposed an approach to model the environment as a hierarchically decomposed set of components. Each environmental component is labeled as one of the three following types: (1) BLACK: well above the assurance level, i.e., does not require further analysis, (2) RED: well below the assurance level, i.e., requires thorough analysis to ensure that it satisfies the desired assurance level, and (3) ORANGE: in the borderline, i.e., component may require further assurance analysis, subject to cost and schedule availability. Creation of the RED-list and ORANGE-list is done using a search on an

We are unique in this capability because the previous approaches made ad hoc design decisions as to which part of the environment must be analyzed for assurance reasons and which other environmental elements did not require further analysis.

assurance-value ordered list of physical and environmental components.

• *Along with the environmental model, proposed a CBRE (Component-Based Reliability Estimation) approach.* The CBRE technique inputs the program dependency graph (PDG) of the software design, and after integrating the PDG with the environmental model graph (EMG), it carries out an end-to-end reliability analysis. The composite graph (PDG + EMG) is a comprehensive architecture of not only the software system, but also of the relevant environmental components.

We developed (1) an algorithm for computing the assurance level of a particular component, given the reliability or assurance of other components in the (PDG+EMG), and (2) an event-oriented analysis that allows a systems engineer to respond to a set of “what-if”-type questions. The event-analysis is particularly useful for checking out top-10 “must-happen”- or “must-not-happen”-type scenarios in the application domain.

Refereed

Winter, V. L., R. Berg, S. Bhattacharya, and B. Cukic.
1999. “High-Assurance Systems Engineering.” *J. Systems Integration*, accepted.

3537310000

Investigation of Lateral Composition Modulation in GaAsSb Short-Period Superlattices

S. R. Lee

The scope of this project was to investigate whether lateral composition modulation occurs in mixed-anion compound-semiconductor thin films.

Sandia grew and characterized separately the individual heteroepitaxial layers that comprise the short-period-superlattice (SPS) structures that are expected to result in lateral composition modulation. These samples lay the groundwork for growth of the more complex superlattice structures that will ultimately result in lateral composition modulation.

The first task was to grow thick buffer layers of GaAsSb (gallium arsenide antimony) lattice-matched to InP(001). We successfully grew GaAsSb buffer layers with a composition nominally lattice-matched to InP; work continues in an effort to improve their crystal quality and reproducibility. We subsequently grew individual III-Sb layers that will eventually be incorporated into the SPS structures. We used atomic force microscopy (AFM) to examine the surface morphology of these highly lattice-mismatched layers and found that very large, rectangular, terrace-like islands were formed upon the deposition of InSb/InAs (lattice mismatch $f=6.95\%$). Work is continuing to elucidate the initial nucleation stages of III-Sb compounds since it will have a tremendous impact on the formation of lateral composition modulation.

Our first task was to grow thick buffer layers of GaAsSb lattice-matched to InP(001). Similar to InAlAs, the lattice parameter of GaAsSb varies between $5.653 < a < 6.095 \text{ \AA}$. Therefore, we can achieve lattice-matching to InP ($a=5.869 \text{ \AA}$) by growing a GaAs(0.489)Sb(0.511) random alloy. Achieving this composition in mixed-cation alloys is as simple as fixing the ratio of the constituent fluxes. Growth of lattice-matched GaAsSb layers was much more challenging due to the more volatile nature of the anion species. We grew several samples with varying As and Sb overpressures and studied them using x-ray diffraction to monitor the out-of-plane lattice parameter. We found that the As fraction decreased with decreasing As overpressure while keeping the Sb overpressure constant, as expected.

Sandia grew and characterized separately the individual heteroepitaxial layers that comprise the short-period-superlattice (SPS) structures that are expected to result in lateral composition modulation.

Furthermore, the As fraction increased with decreasing Sb overpressure while keeping the As overpressure constant. The film's quality, as indicated by the x-ray peak intensity and breadth, deteriorated for films with relatively low Sb overpressures. We grew GaAsSb buffer layers with a composition nominally lattice-matched to InP; however, work is continuing to improve their crystal quality and reproducibility. In the meantime, it may be preferable to deposit the mixed-anion SPS structures of interest on InGaAs lattice-matched buffer layers, which are already well characterized.

Next, in collaboration with the University of Michigan we examined the morphology of the III-Sb layers that would eventually be incorporated into the mixed-anion SPS structures. For these structures, the lattice mismatch between the individual layers of the SPS's is significantly large so that 3-D islands are expected when the deposited thickness exceeds 1 nm. We can observe 3-D island formation *in situ* by Reflection High-Energy Electron Diffraction (RHEED). When we deposited InSb on InAs ($f=6.95\%$), however, the RHEED pattern did not exhibit any indication of 3-D island formation. Examination of the film after growth did reveal that 3-D islands were present. AFM images clearly show islanded morphologies. The islands are generally rectangular in shape, very large (greater than $30,000 \text{ nm}^2$), and terrace-like. The islands were not evident by RHEED because of their very large size and flat tops. By way of comparison, islands that nucleate as a result of 3 nm-thick In_{0.4}Ga_{0.6}As/GaAs ($f=3.6\%$) are nominally circular with a base diameter of 18 nm and 6 nm in height. The resulting InGaAs RHEED pattern shows distinct proof of the islanded morphology. Clearly the nucleation mechanism between InSb/InAs and InAs/GaAs is significantly different. Work is continuing to elucidate the initial nucleation stages of III-Sb compounds, since it will have a tremendous impact of the formation of lateral composition modulation.

We made a first attempt to examine the individual components of the structure that resulted in lateral composition modulation in the past. We successfully achieved GaAsSb buffer layers nominally lattice-matched to InP substrates. Also, we found the morphology of very thin InSb layers to consist of very large rectangular islands, which may be well suited for initiating lateral composition modulation in more complex structures.

*We successfully achieved
GaAsSb buffer layers nominally
lattice-matched to InP
substrates.*

3537320000

New Complexing Agent for Co(II) Analysis for CP

S. E. Klassen

Sandia will evaluate a modification to an existing ultraviolet/visible (UV/Vis) spectrophotometric method for cobalt (II) analysis of the explosive 2-(5-cyanotetrazolato) pentaammine cobalt (III) perchlorate (CP). Analysis of cobalt (II) is part of the surveillance program for devices that contain CP and is an indicator of decomposition. The current method uses a complexing agent with absorption bands that overlap with those of CP. For this project we synthesized a new complexing agent and showed it to have absorption bands that overlap less with CP, which may provide more sensitivity. In collaboration with the New Mexico Institute of Mining and Technology, we obtained linearity, reproducibility, and minimum detectable limits for the two complexing agents using cobalt (II) standards. We analyzed six different CP samples using both complexing agents with mixed results.

The current method of cobalt (II) analysis in the explosive 2-(5-cyanotetrazolato)pentaammine cobalt (III) perchlorate (CP) uses 2,2'-dipyridyl-2-pyridylhydrazone (DPPH) to complex with cobalt (II), which is formed during the initial stage of CP decomposition. The maximum absorption wavelength for the DPPH-cobalt (II) complex occurs at a wavelength where CP itself contributes absorbance, and so a CP blank must also be run and its absorbance subtracted. We investigated a new complexing agent and showed it to have less interference from CP. We synthesized the quinoline analog (DPPQH) by refluxing equimolar quantities of 2,2'-dipyridylketone with 2-hydrazinoquinoline in anhydrous ethanol with glacial acetic acid as a catalyst. We then recrystallized the product from anhydrous ethanol. Infrared analysis indicated no ketone starting material was present and was taken as evidence for complete reaction. Mass spectral analysis yielded a molecular ion consistent with the formula weight of DPPQH (325 amu [atomic mass units]).

We determined analytical parameters for DPPH and DPPQH complexes with cobalt (II) standards. The wavelengths of maximum absorbance were 498 nm and 524 nm for DPPH and DPPQH, respectively. Because of its higher maximum wavelength, DPPQH will have less interference from CP itself. Both complexing agents showed lower limits of detection of

For this project we synthesized a new complexing agent and showed it to have absorption bands that overlap less with CP, which may provide more sensitivity.

0.1 ppm of cobalt (II), and the calibration curves showed good linearity ($r^2 > 0.997$) in the standard use range of 0.1 to 0.75 ppm of cobalt (II). Absorbance readings of a DPPH complex with 0.4 ppm cobalt (II) standard reproduced within 1.2%, and a similar DPPQH complex reproduced within 1%, which shows the new complexing agent has good reproducibility.

We analyzed six samples of CP that represent different degrees of thermal decomposition in triplicate using both complexing agents. The results were mixed. In some cases the agreement was good, but in other cases the difference was as much as an order of magnitude. One complexing agent did not give a consistently higher or lower reading than the other. Results with DPPQH did give consistently lower standard deviations than DPPH, showing promise for better reproducibility than DPPH in actual use. Results should be obtained with at least nine replicates to confirm this. We also determined that DPPQH requires a longer time to form a complex with cobalt (II) than DPPH. DPPQH is a larger molecule, and steric factors may control the reaction time.

We concluded that the use of DPPQH in place of DPPH does shift the maximum wavelength of the cobalt (II) complex to a region of less interference from CP. The minimum detectable limit, linearity, and reproducibility of DPPQH is at least as good as DPPH, and the use of DPPQH shows promise. Application to actual CP samples had mixed success and requires more work to uncover the source of the inconsistency.

3537330000

Enzyme-Mediated Electrochemical Redox Polymer Microelectronic Biosensor for V- and G-Type Chemical Weapons

R. P. Janek, A. W. Flounders

A novel electrochemical transduction mechanism will exploit the natural selectivity of a bioengineered enzyme that is specific for organophosphate nerve agents used in chemical weapon (CW) systems. Nature has successfully solved the problem of surviving in complex environments by miniaturizing task-specific enzymes and communicating with those enzymes via electronic pathways. Researchers at Sandia showed that immobilized organophosphate hydrolase (OPH) in a matrix of siloxane polymers containing naphthoquinone responds to micromolar concentration levels of nerve agent. As the enzyme hydrolyzes the target molecule, the local pH of the polymer will change. The pH change will amplify an electrical signal and thus serve as the transduction mechanism. This novel biosensor will be taken to the microelectronic prototype stage by fabricating thin-film carbon (C) and/or noble metal electrodes followed by redox polymer deposition and enzyme immobilization. We will perform liquid flow cell measurements on the microelectronic device and, if successful, will conduct a vapor-phase trial. We will perform this work in collaboration with the University of California–Davis.

We created a trial chemically sensitive coating and successfully incorporated it into a new microelectronic detector platform that we designed and fabricated. We synthesized pH-rectified siloxane polymers containing quinone and viologen groups. These polymers require a nitrogen (N) inert atmosphere during synthesis.

We then immobilized the siloxane polymer system onto the surface of a thin-film chemiresistor structure consisting of interdigitated arrays of metal and C lines. We investigated several microfabrication strategies in order to create arrays out of platinum (Pt) and C. C films were radio frequency (RF) and direct current (dc) sputtered in an argon (Ar) atmosphere from a cold-pressed C cathode. The C was then patterned with an aggressive oxygen (O) plasma through a titanium (Ti) mask. The pattern transfer characteristics and integrity of the C arrays were excellent; however, the electrical conductivity of the C

Researchers at Sandia showed that immobilized organophosphate hydrolase (OPH) in a matrix of siloxane polymers containing naphthoquinone responds to micromolar concentration levels of nerve agent.

was not adequate for use in a chemiresistor sensor. We fabricated Pt arrays by sputtering Ti/Pt onto silicon nitride (SiN) surfaces followed by patterning via liftoff. This method yielded structures with two-micron linewidths. We then modified Pt microelectrode finger arrays with siloxane polymer and evaluated them for enzyme activity and organophosphate detection limits.

3537340000

Design and Optimization of VLSI Systems and Reconfigurable Hardware

R. W. Brocato

Advances in very large scale integration (VLSI) technology offer challenges in the design of high-performance digital systems. These systems often have conflicting area, performance, power, cost, and reliability requirements. To satisfy these conflicting requirements, novel designs and mathematical optimizations are typically needed. For example, mathematical optimizations in the design of parallel multipliers can reduce area and power consumption by over 35% and delay by over 15%. Similarly, novel methods for table-based function approximations reduce their area by two orders of magnitude and their delay by over 20%. Application-specific processors are typically two to three orders of magnitude faster than software solutions on general-purpose processors.

Sandia's research in reconfigurable computing focused on improving the performance, cost, and power dissipation of arithmetic units and processors for digital signal-processing applications. We emphasized evaluating the cost, performance, and power dissipation of various algorithms for high-speed arithmetic when implemented using field-programmable gate arrays (FPGAs). This research has applications in several areas, including the design of encryption and decryption hardware, automatic target recognition (ATR) systems, digital filter designs, and fast Fourier transform (FFT) hardware.

The first task involved optimizing digital filter size in a sigma-delta analog-to-digital data converter. Other tasks included optimizing component size and speed for a hardware multiplier and for a floating-point unit.

We are using the results of this research to provide significant cost and performance improvements in the components and systems designed by Sandia.

Deliverables for the project consist of hardware description language (HDL) software versions written at Sandia to the suitable various projects that they are intended for.

We performed work in the following areas:

- Mathematical optimization of finite impulse response filters in a Sandia-designed sigma-delta analog-to-digital converter chip.

- Design of optimized parallel multipliers for the Sandia secure microprocessor.

Sandia's research in reconfigurable computing focused on improving the performance, cost, and power dissipation of arithmetic units and processors for digital signal-processing applicationsThis research has applications in several areas, including the design of encryption and decryption hardware, automatic target recognition (ATR) systems, digital filter designs, and fast Fourier transform (FFT) hardware.

- Conversion of an existing floating-point unit from Lehigh University to Sandia.

We completed the following:

- Hardware design language to optimize the sigma-delta converter.
- Preliminary design of optimized parallel multipliers.
- Preliminary conversion of floating-point unit.

Refereed

Schulte, M. J., P. I. Balzola, A. Akkas, and R. W. Brocato. 1999. "Integer Multiplication with Overflow Detection or Saturation." *IEEE J. Computers*, to be submitted.

3537350000

Hydrodynamic Flow in Biosystems*A. J. Hurd*

Fast multipole methods (FMM) have recently been applied to the simulation of Stokes flows with the boundary element method (BEM). Further work led to the simulation of Stokes flow for complex, multiply connected geometries. The use of massive parallelism is imperative for the treatment of realistic problems because of the very large number of degrees of freedom (DOFs) that result from the accurate geometric description of such systems.

Stokes flow is slow hydrodynamic flow of particles. The application in mind for this work is hydrodynamic flow in biosystems, such as blood circulation. The particles in blood are complex in shape and are even deformable; BEMs have the greatest promise to address this difficult situation.

The study of low-Reynolds-number flow of linear multiphase fluids is an ideal application of the BEM. The geometry becomes very complex, even with a small number of multiply connected boundaries. In addition, the geometry continually evolves as the flow progresses, necessitating remeshing at every timestep. While this would lead to prohibitive meshing operation counts with domain methods such as the finite-element method (FEM), meshing is relatively simple with the BEM. The main reason that the BEM has not been applied to treat this type of problem is that the solution of a fully dense matrix of dimension N , where N is the number of DOFs of the system, is required. The operation count, under ideal conditions, scales as N^2 . Using highly efficient algorithms, we nevertheless analyzed some dynamic problems with conventional parallel BEM implementations.

We realized the potential to treat problems large enough to make efficient use of FMM with the advent of large, massively parallel (MP) computers. This is because even though the operation count can be reduced from N^2 to $N \log N$ for Stokes flow problems, the number of DOFs N required to achieve substantial improvements over conventional methods is on the order of several thousand.

We use a completed double-layer boundary integral formulation here. For the mobility problem, this formulation leads to well-conditioned systems of equations. In this case, the most efficient method to solve large matrices is by using an iterative solver, such as the generalized minimal residual

We realized the potential to treat problems large enough to make efficient use of FMM with the advent of large, massively parallel (MP) computers. This is because even though the operation count can be reduced from N^2 to $N \log N$ for Stokes flow problems, the number of DOFs N required to achieve substantial improvements over conventional methods is on the order of several thousand.

method (GMRES) or the biconjugate gradient method (Bi-CG). These solvers are based only on the multiplication of a trial solution vector by the matrix. The algorithm used to perform the matrix-vector operation is arbitrary.

It has been shown that by appropriately numbering and distributing cluster moment tensors between processors, it is possible to achieve near-perfect scaling, with a very simple cluster subdivision scheme and some load balancing. The use of multipole acceleration for the BEM treatment of very large problems characterized by complex and evolving geometries is therefore feasible, because very large numbers of processors can be used efficiently.

Further optimization of the scaling performance can be obtained by modifying the method with which the result of the matrix-trial solution vector multiplication is to be made available to all processors. An attractive possibility is the exploitation of the small periods of idle time that necessarily result from any load imbalance that still exists. When a processor has completed its allocated part of the matrix-vector multiplication, it sends a message indicating ready status to all other processors. The first processor that receives the message will then initiate a send-receive operation, and the partial matrix-vector results can be combined. A new ready signal is then sent out for the next available processor and so on until all partial results are compounded. Thus, by the time the last processor has completed its part of the matrix-vector operation, the complete matrix-vector result will be available, eliminating the need for the MPI _ALLGATHER operation.

While the matrix-vector multiplication is at the core of the multipole accelerated BEM, many other factors influence the performance of the algorithm. For example, preconditioners can significantly reduce the number of iterations required to obtain a solution. Other important aspects that require careful parallelization are the generation of nearfield and farfield lists, meshing, and particle position tracking. However, the scalability of the matrix-vector multiplication is essential for the feasibility of large particle-level simulations of multiphase flows using multipole accelerated BEM. The results shown here are promising.

It has been shown that by appropriately numbering and distributing cluster moment tensors between processors, it is possible to achieve near-perfect scaling, with a very simple cluster subdivision scheme and some load balancing.

Other Communications

Mammoli, A. A., and M. S. Ingber. 1999. "Hydrodynamic Flow in Biosystems Using Multipole-

Accelerated Parallel BEM." *Proc. SC '99 High-Performance Computing Conference* (Portland, OR, 13–19 November).

3537360000

IR Polarimetry and Lithographic Alignment

W. C. Sweatt, S. A. Kemme

Sandia, in collaboration with the University of Arizona (UA), is studying infrared (IR) polarimetry (4–5 microns) as a means for identifying military targets. We built an instrument that has a newly devised architecture. It gives a signal-to-noise ratio (SNR) that is a factor of two better than the canonical architecture. Tests with this instrument seem to indicate a very exciting result. It may be that natural scenes produce little or no circular polarization in the mid-IR. Thus, target identification systems using IR polarization information may, if this turns out to be true, need only to measure linear polarization components.

Extreme-ultraviolet (EUV) (13.4 nm) lithography will be printing features smaller than 100 nm soon. This requires alignment of the masks and wafers to an accuracy better than 30 nm, which will be very hard to accomplish with visible light. In this study, we hoped to show that visible alignment is possible to these accuracies, and initial studies indicate that this is feasible.

- *IR polarimetry.* We designed and built a new polarimeter architecture for use in the 4–5-micron IR band and did a little field testing with it.

In a normal polarimeter system, one determines the Stokes polarization parameters by taking intensity measurements while looking through a polarizer and quarter waveplate. Four readings are taken with the waveplate rotated to the following angles: 0, 22.5, 45, and 90 degrees. We found that a three-eighths waveplate is better, and there is also a better set of angles: –52, –15, 15, and 52 degrees. These changes improve the SNR by a factor of two.

Field tests with this improved IR imaging polarimeter show that (1) only smooth, dielectric surfaces show measurable polarization, (2) only surfaces that generally face up give a polarized signal (cold space gives a contrasting temperature), and (3) all the tests run thus far show essentially no circular polarization, even though the linear polarization components may be a large fraction of the total signal.

- *Alignment in lithography systems.* We designed a set of alignment marks to help align the mask to the wafer in a lithographic stepper. They should allow the alignment to be done with visible light to the 30 nm accuracy required for

We built an instrument that has a newly devised architecture. It gives a signal-to-noise ratio (SNR) that is a factor of two better than the canonical architecture.

advanced steppers. In addition, we had to redesign the alignment mark viewing system to allow their usage.

A beamsplitter has to be mounted just in front of the wafer so the alignment system can see the reticles. The light from the mask passes through the beamsplitter, and the light coming from the wafer is reflected off the beamsplitter. A standard half-silvered mirror beamsplitter offsets the image beam passing through it. To avoid this potential error, we chose a beamsplitter that is a mirror with holes cut through it. This element passes some of the light from the mask, undeviated, and reflects the combined image signal to the camera.

Using physical optics modeling, we found that a three-hole pattern cut through the beamsplitter gives a reasonably good image for certain mask reticles. The hole pattern in the mirror looks like a pie cut into six pieces with every other piece removed, thus leaving three holes. We found that a five-hole pattern gives a slightly sharper image, though it may be too hard to make.

We also determined that a series of concentric rings makes a very good alignment mark. We suggest a set of three closely spaced narrow rings be made on the wafer and a second set of rings be made on the mask. One of these patterns is smaller than the other so the two can nest together. Using circular reticle patterns avoids any bias introduced by the three-hole beamsplitter.

We chose a width for each of the rings and each of the spaces to be 1 micron. With excellent imagery as would be expected in a stepper, the modulation of the image is about 30%, which should be easy to see with a charge-coupled device (CCD). The outside of the larger pattern has a 30-micron diameter, which does not waste much space. The inner one would have a 15-micron outer diameter.

We are fairly confident that the 30 nm resolution will be achievable with this system.

Other Communications

Sweatt, W. C., S. A. Kemme, and G. S. Phipps (Sandia); M. R. Descour, D. S. Sabatke, and J. P. Garcia (University of Arizona). 1999. "Design of and Measurements with an Optimized Infrared Imaging Polarimeter." Paper presented to the Optical Society of America Meeting, Santa Clara, CA, 28 September.

3537370000

Shock Response of Diamond Crystals

M. D. Knudson

Sandia is investigating the shock response of single-crystal diamond up to several Mbar in pressure in a collaborative effort with the Institute for Shock Physics (ISP) at Washington State University (WSU). In particular, we are designing and performing experiments to determine (1) the usefulness of diamond as a window material for high-pressure velocity interferometry measurements, (2) up to what stress diamond remains transparent, (3) up to what stress diamond remains elastic, and (4) if a two-wave structure can be detected and analyzed. We are designing shock experiments and targets and fabricating them at ISP and plan to conduct the experiments at the gas-gun facility at Sandia.

Efforts yielded an experimental design that would produce instantaneous elastic stresses up to ~ 3.4 Mbar in [110]-oriented diamond crystals. This experimental design would utilize the two-stage light gas-gun at Sandia capable of producing projectile velocities of up to 6.5 km/sec. The principle measurement technique consisted of the VISAR (velocity interferometer system for any reflector) system in place at the Sandia gas-gun facility. The basic questions to be examined in this effort are: (1) up to what stress does diamond remain transparent (and thus up to what pressure can diamond be used as a VISAR window), (2) what is the elastic limit, and (3) can a two-wave structure be detected and analyzed.

We fabricated components for a total of five targets to determine the shock properties of single-crystal diamond and assembled them at ISP. Failure of an epoxy bond at the diamond-LiF (laser-induced fluorescence) window interface during shipment of the targets to Sandia forced a reevaluation of the target design and construction, delaying the actual performance of the experiments. Examination of the design revealed an inherent weakness at the diamond-LiF interface, due to the small size of the diamond samples (2.5–3 mm diameter, 0.25–0.5 mm thick) relative to the size of the LiF. We modified the target design to include LiF windows with a smaller diameter than the diamond samples. We have fabricated several of these small LiF windows.

Sandia is investigating the shock response of single-crystal diamond up to several Mbar in pressure....

3537390000

Dynamic Computer-Aided Design Analysis of Containment Vessels for Z-Pinch Experiments

G. E. Rochau

Recent successes on Sandia's Z facility have prompted scientists and engineers to propose the construction of an even larger facility called ZX. This facility will generate 8 MJ of x-rays to study the performance of small fusion targets with yields up to 20 MJ. The ZX facility would also be used for a variety of physics experiments, some of which might include special materials. The containment requirements for such a facility will be very strict, essentially zero release of radioactive material from each high-yield shot. Development of 3-D visualization to support studies of the dynamic response of prototype containments is proposed, in collaboration with the University of Wisconsin-Madison (UWM), to help scientists and engineers design effective containment vessels.

We made considerable progress toward coupling the finite-element models (FEMs) in ProEngineer™ version 20 with detailed stress calculations of the Sandia Z machine (using ANSYS™ 5.5). In addition, we are integrating the output from the ProEngineer™ code with the MAYA™ animation code. In collaboration with the UWM, we will develop a complete package that we will apply toward the design of target chambers as well as produce high-end visualization videos of the design options.

We purchased a Silicon Graphics™ model 320 computer platform to perform the necessary work. License agreements for ANSYS™, ProEngineer™, and MAYA™ have been put in place. We are using the Sandia-generated files of Z to demonstrate the ability to rapidly manipulate complex shapes. In addition, we modeled various local experimental fusion facilities from 2-D drawings to prepare them for the more complex job of modeling ZX. We are now integrating these models into the MAYA™ project to demonstrate the final link in the integration.

Recent successes on Sandia's Z facility have prompted scientists and engineers to propose the construction of an even larger facility called ZX.

3537410000

Investigation of Nanoscience Technologies

T. A. Michalske

In collaboration with Harvard University Sandia will conduct research in the general area of nanoscale structures, biomolecular materials, and their application in support of Sandia's MEMS technology. The expertise at Harvard is crucial in fostering these fundamentally interdisciplinary developments. Specific areas of research will include:

(1) Nanofabrication, both exploiting traditional methods (mostly from silicon [Si] technology) and developing new methods (such as stamping or optical methods).

(2) Self-assembly, both of organic and inorganic systems.

(3) The dynamic response on the nanoscale: assembly and dynamics of membranes, microfluidics.

(4) Study of the hierarchy of scales in assembly.

(5) Innovative imaging methods, in particular those based on scanning probes.

(6) Hard (engineering)/soft (biological) interfaces. These include actual physical interfaces (e.g., for manipulating cells), but also conceptual interfaces between the two disciplines.

We held a series of seminars and discussions to facilitate the sharing of new results and research directions in nanoscience. We are exploring the potential for nanotechnology in areas of national defense, energy, and environment. We are interested in the integration of nanoscience and technology with microsystems and envision miniaturized engineering systems (microsystems) that can sense, think, communicate, and act. New functions and properties that can be achieved by tailoring materials at the nanometer scale could revolutionize the ability of microsystems to incorporate a broad spectrum of integrated functions.

New functions and properties that can be achieved by tailoring materials at the nanometer scale could revolutionize the ability of microsystems to incorporate a broad spectrum of integrated functions.

3537420000

Surety Science*R. D. Skocypec*

Surety is a level of confidence that a system will perform predictably and acceptably under both expected and unexpected circumstances. It is a concept that has very broad application across our complex and increasingly vulnerable society. Sandia has had a nearly 50-year history in applying surety principles to ensure that the nation's nuclear weapons are safe, secure, and reliable. The same surety principles can also be applied in a broader sense to protect our nation's critical infrastructures such as our power systems, oil and gas pipelines, water supplies, air traffic control, banking and financial services, telecommunication systems, bridges, buildings, transportation systems, and police, fire, and medical systems.

The science of surety must address the actions of the full range of possible agents on system performance, including highly adversarial agents. Consequently, the development of the scientific underpinnings for surety requires the efforts of a cross-disciplinary blend of technical and sociological expertise.

The surety of the systems that form our infrastructures—our public and private buildings and our networks for transportation, power, water, information, and finance—is of acute concern. Large economic losses and loss of life can occur because the complexities and interdependencies of the systems make them vulnerable to design and operational errors, natural disasters, and the actions of adversarial agents. Of particular concern are threats of the use of weapons of mass destruction (WMD) by religiously or politically motivated terrorists. One response to these growing dangers is Sandia's call to develop a science of surety, which is characterized by reliability in normal environments, safety in abnormal environments, and having security and use control in malevolent environments.

A major element of what we identify as Surety Science and Engineering (SSE) should be the development of models to guide the design of systems where failure can have high consequences. We need to model the behavior of three classes of agents—providers, users, and adversarial—in a probabilistic sense. We need to model the behavior of terrorists and other adversarial agents so that we can design proper defenses into

Sandia has had a nearly 50-year history in applying surety principles to ensure that the nation's nuclear weapons are safe, secure, and reliable. The same surety principles can also be applied in a broader sense to protect our nation's critical infrastructures such as our power systems, oil and gas pipelines, water supplies, air traffic control, banking and financial services, telecommunication systems, bridges, buildings, transportation systems, and police, fire, and medical systems.

high-consequence systems to deal with their threat. The key problem for SSE is to discover how to cost-effectively design systems and networks against events that have low probability but high consequence. Thus surety embraces but extends beyond the level and nature of the issues addressed by reliability and safety science today. Moreover, surety needs to engage and influence policymaking at the highest level because a physical design or technology can never provide sufficient surety to all threats. Policy must supply the remainder.

Allowing for the actions of adversarial agents on performance requires a well-informed and systematic classification of such agents and appropriate models of the likelihood of various possible adversarial actions. Depending on the particular system, it may be necessary to account for the effects of public vandalism, actions of disaffected workers, direct and collateral damage due to profit-motivated adversarial actions, and political or religious motivations for threatened and actual damage. Given both the level of complexity and the limited knowledge base on this topic, both inputs and outputs of appropriate analyses can generally be expected to be probabilistic rather than deterministic. The most useful analyses will pay careful attention to use of appropriate measures of risk perception and will be as fully informed as practicable by experts familiar with the qualitative features of each system being studied.

The relevant questions in surety studies are similar to those studied by scientists interested in the behavior of complex, interdependent systems. The methods and tools that have proven powerful in these studies should prove useful for a wide variety of surety problems. It may even be possible to transfer results directly to surety problems. The challenge will be to identify the respective meaning of the different parameters of the physical models when applied to a given surety case study. Simple examples are explored here to illustrate the relationships.

SSE will need to augment the traditional tools of numerical analysis, computer science, and operations research with the tools of soft computation and computational and artificial intelligence. We need this combination of tools to simulate the physical, informational, and human elements arising in the different alternatives being considered as possibilities for a future high-consequence system. Computational agents exhibit a form of cognition and can be used to model the human

The key problem for SSE is to discover how to cost-effectively design systems and networks against events that have low probability but high consequence.

components and institutions. A key fundamental direction for SSE should be the improvement of these tools to provide SSE with the ability to use computational surrogates for human innovation and creativity.

Other

Cook, H. E., C. E. Singer, K. A. Dahmen, and D. E. Goldberg. 1999. "Exploring the Fundamental Basis for Surety Science and Engineering." Sandia Technical Report SAND2000-0041, Sandia National Laboratories, Albuquerque, NM (7 October).

3537430000

Stabilization of Enzymatic Molecular Recognition Materials Via Crystallization and Crosslinking

A. W. Flounders

We proposed to expand Sandia's relationship with an established, well-recognized biochemistry research laboratory to further their development of enzymes for biosensors. Enzymes offer distinct advantages over other biological molecular recognition materials (MRMs) for biosensor applications. Specifically, since enzymes catalyze a chemical reaction and produce a chemical signature not present in the initial sample, they provide an unambiguous indication of analyte capture. In addition, though enzyme-based sensors may be sensitive to fouling due to nonspecific binding, they are essentially immune to false signal due to nonspecific binding. However, key to use of enzymes as MRMs is maintaining their catalytic capability when isolated from their homeostatic cellular environment and immobilized or entrapped on a sensor platform.

We propose to investigate methods to stabilize TNT (2,4,6-trinitrotoluene)-degrading enzymes to enhance their utility as chemical sensor components. Specifically, we investigated crystallization followed by crosslinking.

We achieved successful crystallization with the organophosphate degrading enzymes (OPH); time constraints prevented investigation of the TNT-degrading enzyme. However, not only was the native OPH enzyme crystallized, but two similar genetically engineered enzymes were also crystallized.

We grew high-quality, diffractable crystals of wild-type OPH for the production of cross-linked enzyme crystals. In addition, we also produced crystals of the genetically engineered H254R and H254R/H257L enzymes. The wild-type and H254R crystals diffract to a resolution of 2.9D and 2.1D, respectively, and measure about 0.5 mm x 1 mm. We have not yet determined the diffraction quality of the H254R/H257L enzyme, and at present the crystals are very thin but quite large. All of the crystallization conditions required the presence of the substrate analogue diethyl 4-methylbenzylphosphonate. The crystallization conditions of the wild-type enzyme are 50 mM CHES, pH 9.0, 13% PEG8000, 5 mM NaN₃, and 1% diethyl 4-methylbenzylphosphonate, with a protein concentration of 11

We propose to investigate methods to stabilize TNT degrading enzymes to enhance their utility as chemical sensor components.

mg/ml. The conditions for the H254R enzyme are 100 mM CHES, pH 9.0, 10% PEG6000, 5 mM NaN₃, and 1% diethyl 4-methylbenzylphosphonate, with a protein concentration of 5.5 mg/ml. The conditions for the crystallization of the H254R/H257L enzyme are being optimized. All crystals are the Co²⁺-liganded form of the enzyme, since this form is the most active against most substrates, and eventually we hope to have this structure solved as well. Assays are currently under way to determine the activity of all the crystals using paraoxon as substrate. The wild-type crystals are very thick and hold up well in the cross-linking reaction. Initial tests with the wild-type cross-linked crystals indicate small crystals have 15% activity of the soluble enzyme while large crystals maintain approximately 50% activity of the soluble enzyme.

3537440000

Novel Biosensor Fabrication Techniques

A. W. Flounders

Most chemical sensors consist of a recognition element, which provides sensor specificity, and a transduction platform, which translates chemical presence into a measurable signal. The term biosensor describes a specific class of chemical sensors that utilize a biological component (usually a protein such as an antibody or enzyme) as the chemical recognition element. Biological components have been paired with optical, piezoelectric, and microelectronic transduction platforms. To date, all microelectronic biosensor fabrication has been a two-step process. Automated wafer-scale microelectronic fabrication is followed by dicing, packaging, and manual chip-scale biochemical processing. Chip-scale biochemical processing is tedious, difficult to reproduce, and expensive; it completely negates all economy-of-scale advantages of the semiconductor manufacturing process.

We continued investigating the compatibility of well-established semiconductor fabrication tools with biochemical components to enable wafer-scale processing of biosensors, specifically, use of a photoresist priming oven for deposition of organosilane monolayers suitable for protein attachment and the use of oxygen or ammonia plasma etchers for chemical surface modification.

We prepared silicon dioxide (SiO_2) and silicon nitride (SiN) thin films in collaboration with UC–Berkeley Microfabrication Laboratory and fabricated interdigitated microelectrode arrays on these substrates. We attempted to fabricate electrodes from thin films of sputtered carbon (C). Conductive C is of great interest as an electrode material for biosensor applications because it can be easily functionalized allowing attachment of biomolecular recognition materials. However, we were unable to achieve satisfactory C resistivity with either dc or RF (radio frequency) sputter-deposition modes. As an alternate we fabricated interdigitated microelectrode arrays from sputtered platinum (Pt), and these films were sufficiently conductive.

Chip-scale biochemical processing is tedious, difficult to reproduce, and expensive; it completely negates all economy-of-scale advantages of the semiconductor manufacturing process.

Appendix A: Project Number / Title Index

<i>Project Number</i>	<i>Title</i>	<i>Page Number</i>	<i>Project Number</i>	<i>Title</i>	<i>Page Number</i>
3502330000	Functional Materials for Microsystems: Smart Self- Assembled Photochromic Films	24	3502440000	Fundamental Aspects of Micromachine Reliability	52
3502340000	Innovative Experimental and Computational Diagnostics for Monitoring Corrosion in Weapons Environments	26	3502450000	Enabling Science and Tech- nology for Cold-Spray Direct Fabrication	55
3502350000	Self-Healing Molecular Assemblies for Control of Friction and Adhesion in MEMS	29	3502460000	Atomic-Level Studies of Surfactant-Directed Materials Growth	58
3502360000	Linking Atomistic Computa- tions with Phase-Field Modeling	31	3502470000	Intelligent Polymers for Nano- device Performance Control	62
3502370000	A Combinatorial Microlab Investigation of Critical Copper- Corrosion Mechanisms	34	3502480000	Freeforming of Ceramics and Composites from Colloidal Slurries	64
3502380000	Self-Assembled Templates for Fabricating Novel Nanoarrays and Controlling Materials Growth	37	3502490000	Quantum Dot Arrays	67
3502390000	Wetting and Spreading Dynamics of Solder and Braze Alloys	39	3502510000	Laser-Assisted Arc Welding for Aluminum Alloys	69
3502410000	Improved Materials Aging Diagnostics and Mechanisms Through 2-D Hyperspectral Imaging Methods and Algorithms	42	3502520000	Reactivity of Metal-Oxide Surfaces	70
3502420000	Microscale Shock-Wave Physics Using Photonic Driver Techniques	45	3502530000	Exploiting LENS TM Technology Through Novel Materials	73
3502430000	Molecular-to-Continuum Fracture Analysis of Thermoset Polymer/Solid Interfaces	48	3502540000	Molecular Characterization of Energetic Material Initiation	76
			3502550000	Nonvolatile Protonic Memory	78
			3504340000	Integration of Mesh Optimization with 3-D All-Hex Mesh Generation	81
			3504350000	Heterogeneous Simulation	83
			3504360000	Volumetric Video Motion Sensing for Unobtrusive Human- Computer Interactions	86

Appendix A: Project Number / Title Index

<i>Project Number</i>	<i>Title</i>	<i>Page Number</i>	<i>Project Number</i>	<i>Title</i>	<i>Page Number</i>
3504370000	Hybrid Sparse-Dense Incomplete Factorization Pre- conditioners	88	3504480000	Methodology for Characterizing Modeling and Discretization Uncertainties in Computational Simulation	112
3504380000	Big Eddy—Advanced Large- Eddy Simulation Algorithms for Complex Flow Physics and Complex Geometry	91	3504490000	Global Optimization for Engin- eering Science Problems	115
3504390000	Molecular Simulation of Reacting Systems	93	3504510000	Dynamic Simulation of Mechanical Systems with Intermittent Contacts	118
3504410000	Massively Parallel Global Climate Model for Paleoclimate Applications	95	3504520000	From Atom-Picoseconds to Centimeter-Years in Simulation and Experiment	121
3504420000	Fast and Easy Parallel I/O for Efficient Scientific Computing	97	3504530000	Emergent Behavior of Large Swarms of Intelligent Agents	123
3504430000	Novel Load-Balancing for Scal- able, Parallel Electromagnetic and Plasma Physics Simulation Software	99	3504540000	Parallel Combinatorial Optimi- zation for Scheduling Problems	125
3504440000	Massively Parallel <i>Ab Initio</i> Validation for ASCI Materials Modeling	102	3504550000	Programming Paradigms for Massively Parallel Computers	128
3504450000	Computational Methods for Coupling Microstructural and Micromechanical Materials Response Simulations	104	3504560000	Multilevel Techniques for Unstructured Grid Problems on Massively Parallel Computers	130
3504460000	Integrated Quantum/Classical Modeling of Hydrogenic Materials	108	3504570000	Scalable Tools for Massively Parallel Distributed Computing	132
3504470000	The Next Generation of Teraflop Density-Functional Electronic Structure Codes	110	3504580000	Massively Parallel Methods for Simulating the Phase-Field Model	134
			3504590000	Visual Explanation and Insight	137
			3504610000	Computational Simulations of Self-Assembling Macrosystems by Direct Fabrication of Microscopic Structures	139

Appendix A: Project Number / Title Index

<i>Project Number</i>	<i>Title</i>	<i>Page Number</i>	<i>Project Number</i>	<i>Title</i>	<i>Page Number</i>
3504620000	Gamma-Ray Bursts and the Particle Mass Scale	141	3506580000	Double Quantum-Well Long-Wavelength Optoelectronic Devices	175
3506450000	A Novel Nondestructive Silicon-on-Insulator Nonvolatile Memory	143	3506590000	The Development of Integrated Chemical Microsensors in GaAs	179
3506460000	Integration of Optoelectronics and MEMS by Free-Space Microoptics	146	3506610000	Monolithic Integration of VCSELs and Detectors for Microsystems	182
3506470000	Advanced Laser Structures for Short-Pulsed Power in Active Optical Sensor Systems	149	3506620000	AlGaIn Materials Engineering for Integrated Multifunction Systems	184
3506480000	Integration of Microsensor Technology into a Miniature Robotic Vehicle	151	3506630000	Compliant Substrates for Epitaxial Integration of Dissimilar Materials	187
3506490000	Vacuum Encapsulation of MEMS Structures	153	3506640000	Post-Processed Integrated Microsystems	188
3506510000	Massively Parallel Sensor Arrays for Volatile Organic Detection	156	3506660000	Development of Radiation-Hard Sensors for Space-Based Visible and Infrared Sensing Applications	191
3506520000	Agile Dry Etching of Compound Semiconductors for Science-Based Manufacturing Using <i>In Situ</i> Process Control	158	3506680000	Silicon Three-Dimensional Photonic Crystal and Its Applications	193
3506530000	Precision-Formed Micromagnets	161	3506690000	Monolithic Micromachined Variable Tuners for Rapid Prototyping and Optimization of Microwave Circuits	195
3506540000	Time-Resolved Ion-Beam-Induced Charge-Collection (TRIBICC) Imaging	164	3506720000	Quantum Tunneling Transistors for Practical Application	198
3506550000	Composite-Resonator Surface-Emitting Lasers	167	3506730000	Development of Magnetically Excited Flexural Plate-Wave Devices for Implementation as Physical, Chemical, and Acoustic Sensors, and as Integrated Micropumps for Sensored Systems	202
3506560000	Role of Defects in III-Nitride-Based Electronics	169			
3506570000	Ultra-Low-Power Sensors for Microtelemetry Systems	172			

Appendix A: Project Number / Title Index

Project Number	Title	Page Number	Project Number	Title	Page Number
3506740000	Novel Acoustically Driven Microoptoelectronic Devices	205	3508330000	Evolvable Hardware	234
3506750000	Photonics Integration Devices and Technologies	207	3508340000	Crack Nucleation and Growth: Combining Validated Atomistic and Continuum Modeling	236
3506760000	Stress-Free Amorphous Diamond for High-Sensitivity Microsensors with Integrated Microstructures	210	3508350000	Applied Microfluidic Physics	239
3506770000	Semiconductor Current Filament Lasers	213	3508360000	Transport and Fate Simulation of Chem/Bio Agents in Critical Infrastructures	243
3506780000	Integration of Radiation-Hard Magnetic Random Access Memory with CMOS Integrated Circuits	215	3508370000	Innovative Measurement Diagnostics for Fluid/Solid and Fluid/Fluid Interactions in Rotating Flowfields	245
3508250000	Development of <i>In Situ</i> Diagnostics for Simultaneous Measurement of Transient Gas Species and Soot in Large Fires	218	3508380000	Capturing Recrystallization of Metals with a Multiscale Material Model	247
3508260000	Micromechanical Failure Analyses for Finite-Element Polymer Modeling	221	3508390000	Nondeterministic Modeling in Engineering Science	252
3508270000	Methodology for Optimal Selection of Test and Simulation Levels for Problems Involving Computational Simulation	224	3508410000	Lagrangian Modeling of Radiative Transport	255
3508280000	A Phenomenological Model for Multicomponent Transport with Electrochemical Reactions in Concentrated Solutions	226	3508420000	High-Resolution Modeling of Multiscale Transient Phenomena in Turbulent Boundary Layers	257
3508290000	Structural Simulations Using Multiresolution Material Models	228	3508430000	Dispersive Measurements of Velocity in Heterogeneous Materials	259
3508310000	Lightning-Induced Arcing	230	3508440000	A Physically-Based Computational Method for Predicting Generalized Fracture	261
3508320000	Mechanisms of Adiabatic Shear Failure	232	3510710000	Microdiagnostic MEMS Lab-on-a-Chip	265

Appendix A: Project Number / Title Index

Project Number	Title	Page Number	Project Number	Title	Page Number
3510720000	Real-Time Error Correction Using Electromagnetic Bearing Spindles	267	3510860000	Fusion of Product and Process Data Using Real-Time Streaming Visualization	296
3510730000	Thin-Film Deposition Processes Incorporating <i>In Situ</i> Monitoring Capabilities	268	3510870000	Advanced Production Planning Models	298
3510740000	Optimization of Filled Polymer Materials	270	3512290000	Weighted-Nearest-Neighbor (WNN) Decision Making for Data Mining	301
3510750000	Solid-State Neutron Generator for Use in Nuclear Weapons	272	3512310000	Varying QoS for Fixed and Mobile Networks	303
3510760000	Finite-Element Meshing Approached as a Global Minimization Process	274	3512320000	A Real-Time Decision-Support Framework to Guide Facility Response to Abnormal Events	306
3510770000	Application of Parallel Mechanism Technology to Manufacturing	276	3512330000	Data Fusion for Chemical Sensing	308
3510780000	Investigation of the Impact of Cleaning on Adhesive Bond and the Process Implications	278	3512340000	Large-Scale Distributed Information System Modeling and Simulation	310
3510790000	Standard Cells for Microelectromechanical Systems (MEMS)	281	3512350000	High-Surety SCADA for the Critical Energy Infrastructures	313
3510810000	Laser Wire Deposition for Fully Dense Shapes	284	3512360000	Agent-Based Mediation and Cooperative Information Systems	316
3510820000	High-Throughput Dry Processes for Large-Area Devices	287	3512370000	Dynamically Self-Configurable Network Protocol	318
3510830000	Assuring High Reliability and Production Readiness in Low-Volume Manufacturing	290	3512380000	Optical Backplane/Interconnect for Super-High-Speed Communication	321
3510840000	Scripting for Video Inspection	292	3512390000	PUSH Technology Demonstration	323
3510850000	Advanced Machining Processes for Microfabrication	294	3512410000	Controlling Information: Its Flow, Fusion, and Coordination	325

Appendix A: Project Number / Title Index

Project Number	Title	Page Number	Project Number	Title	Page Number
3512420000	Mission Surety for Large-Scale Real-Time Information Systems	327	3516180000	Sparse Geophysical Networks for Monitoring Deep Targets	352
3512430000	Low-Power, Reduced-Computation, Public-Key Protocols	329	3516190000	Miniature Bioaerosol Concentrator	354
3512440000	Ten-to-One-Hundred-Gigabit/Second Network Enabling R&D	331	3516210000	Recognizing Partially Obscured Targets by Combining Multiple Data Sources Using Evidential Reasoning	356
3512450000	High-Performance Commodity Interconnects for Clustered Scientific and Engineering Computing	333	3516220000	Computational Engineering of Sensor Materials and Integration with a Novel Biological Weapon Detection System	358
3512460000	AVATAR—Navigating and Mining in Massive Data	336	3516230000	Biological Weapon Detector Using Bioaffinity Array Impedance Analysis with Chemical Amplification Through Redox Recycling	361
3512470000	Algorithm-Based Fault Tolerance on Heterogeneous Massively Parallel Computers	338	3516240000	ATR/Exploitation Utilizing Ultra-High-Resolution, Complex SAR Imaging	363
3514150000	Surface Decontamination of Bacterial Protein Toxins by RF Power	341	3516250000	Thin-Skin Deployable Mirrors for Remote Sensing Systems	365
3514160000	Intense White-Light Pulse Propagation in Air Using Self-Guided Optical Filamentation: Applications to Remote Sensing and Countermeasures	343	3516260000	Dispersible Granular Sensor (Smart Sand) for Landmine Detection Based on TNT Immunoassay	368
3514170000	Improved Backscatter X-Ray Detection for Antiterrorist Applications	346	3516270000	Characterization of Underground Facilities in an Urban Environment	371
3514180000	HPM Vulnerability Assessment and Tests	348	3516280000	Dexterous Robotic Manipulation of Hazardous Materials in Unstructured Environments	373
3516170000	Imaging of Moving Targets Using Simultaneous Synthetic Aperture Radar (SAR) and Moving Target Indicator (MTI) Radar	350			

Appendix A: Project Number / Title Index

Project Number	Title	Page Number	Project Number	Title	Page Number
3516290000	Autonomous Dynamic Soaring Platform for Distributed Mobile Sensor Arrays	376	3518230000	Advanced Geosphere Transport Simulation	414
3516310000	Miniature UV Fluorescence-Based Biological Agent Sensor	378	3520340000	Hybrid Processing of Measurable and Subjective Information in Surety Analysis	418
3516320000	Automatic Planning of Life-Cycle Assembly Processes	381	3520350000	Computer-Network Vulnerability-Analysis Method	420
3516330000	Analysis of Very Large Assemblies	384	3520360000	Approximate Public-Key Authentication with Information Hiding	423
3516340000	Enabling Human Skills with Cooperative Automation	386	3520370000	New Network Analysis Approaches to Evaluate Infrastructure Risk and Reliability	424
3516350000	Cloud to CAD	389	3520380000	Improved Tools for Identifying and Quantifying Potentially Dangerous Human Actions	426
3516360000	Ergonomics in Life-Cycle Assembly Processes	392	3520390000	Advanced Signal Processing for Thermal Flaw Detection	428
3516370000	Feature Reduction of Geometric Solid Models for Analysis Tools	395	3520410000	Production Surety and Disruption Vulnerability Analysis	431
3516380000	Electrokinetic Immunoaffinity Chemical Sensors	397	3520420000	An Optically Triggered Semiconductor Switch for Firing Systems	433
3518160000	Designed Synthesis of Controlled Degradative Materials	401	3520430000	Source Code Assurance Tool	436
3518170000	Mechanistic Models for Radionuclide Desorption from Soils	403	3520440000	System-Surety Life-Cycle Engineering	438
3518180000	Adaptive 3-D Sensing	404	3520450000	Integrated Approach to Develop Microelectromechanical System (MEMS) Reliability Tools	440
3518190000	Aqueous Organic Sensor	406	3520460000	Simulation/Optimization Tools for System-Variability Analysis	444
3518210000	Designed Ionophores for Liquid-Membrane Separation and Extraction of Metal Ions	409			
3518220000	An Electromagnetic Imaging System for Environmental Site Reconnaissance	412			

Appendix A: Project Number / Title Index

<i>Project Number</i>	<i>Title</i>	<i>Page Number</i>	<i>Project Number</i>	<i>Title</i>	<i>Page Number</i>
3520470000	A Massively Parallel Microsimulation Model of Infrastructure Interdependency	447	3530150000	Model-Based Design and Analysis of Remote Access Monitoring Systems	486
3520480000	Physical Models for Predicting the Effect of Atmospheric Corrosion on Microelectronic Reliability	450	3530160000	Microwave Imaging Through Walls	489
3520490000	Backside Localization of Open and Shorted IC (Integrated Circuit) Interconnections	453	3530170000	Research of the Utility of Polarimetric Sensing	490
3520510000	Reliability Predictions for Advanced Electronics in Smoke Environments	456	3530180000	Real-Time Image Analysis Using Field-Programmable Gate Arrays	492
3520520000	Security of Bulk Power Systems	458	3531340000	Poco Switch Tubes	494
3522010000	Science on the Microdomain	461	3531350000	Chemiresistors Based on Metal-Loaded Polymers for Solvent Spill Detection	495
3522020000	Autonomous MicroChem Laboratory (μ ChemLab)	464	3531360000	Advance Neutron-Tube Design and Producibility	497
3522030000	Cooperative, Distributed Sensing and Action Using Microminiature, Intelligent Agents	467	3531370000	Surface Hardening by Nanoparticle Precipitation and Atomic Clustering in Ni(Al,O)	498
3522040000	Engineering Complex Distributed Systems	469	3531380000	Dynamical Properties of Polymers; Computational Modeling	499
3522050000	Laser Communication Nanosatellites	473	3531390000	Broadening Mechanism in 2-D Excitonic and Electron Gases	501
3522060000	Information Collection (Acquisition of Information from Denied Areas)	479	3531410000	Calculation and Interpretation of the Energies that Underlie Transition-Metal Surface Structure	503
3522070000	Accelerated Molecular Discovery Arrays—The Next Revolution in Biotechnology	481	3531420000	Interfacial Reactions in Ceramic Systems	505
3530140000	Microcode Evaluation	485	3531430000	Direct Fabrication of Multi-functional Nanocomposites Via Supramolecular Self-Assembly	508

Appendix A: Project Number / Title Index

Project Number	Title	Page Number	Project Number	Title	Page Number
3531440000	Raman Investigation of Phase Changes in PZT Materials	511	3532330000	Computational Methods for Predicting the Response of Critical As-Built Infrastructure to Dynamic Loads (Architectural Surety)	535
3531450000	Information Extraction from Hyperspectral Images Obtained from Satellites	513	3533190000	Solar-Grade Silicon	537
3531460000	Expanding the Security Dimension of Surety	515	3533210000	Low-Work-Function Thermionic Emission Materials	539
3531470000	Overcoming Software Brittleness: A Swarm Intelligence Approach	516	3533220000	Develop Mathematical Algorithms for the Integration of Disparate Information to Determine Critical Infrastructure Health and Status	541
3531480000	Synthesis and Applications of N-Type Diamond	518	3533230000	SERAPHIM Propulsion Technology Design for High-Speed Rail Applications	543
3531490000	A Molecular Theory of Gatekeeper Proteins	521	3534070000	Tomographically Measured Temporal Evolution of Hyperspectral Target Signatures	545
3531510000	Development of Compact UV Laser Source for Climate Studies and Chemical Sensing	523	3534080000	Gas-to-Liquid Microabsorber	547
3531520000	Power Source Technologies for Autonomous Microsystems	525	3534090000	High-Resolution Electromagnetic Imaging of Transport Pathways	550
3532280000	Advanced Radiation Sources: Rayleigh-Taylor Mitigation Via Perturbation Reduction	526	3534110000	MPP Direct Numerical Simulation of Diesel Autoignition	552
3532290000	Global Approaches to Infrastructural Analysis (GAIA)	528	3534120000	Electrokinetically Driven Mesoscale Actuators	555
3532310000	Capillary Elasto-hydrodynamics in Manufacturing Processes	530	3534130000	Pathogen Detection Using Microseparations for BW Nonproliferation	557
3532320000	Real-Time Design of Improved Powder Pressing Dies Using Finite-Element Method Modeling	532	3535220000	Assessing the Emerging Threat of Limited WMD Use	560
			3535230000	Z-Pinch Fusion for Energy Applications	562

Appendix A: Project Number / Title Index

Project Number	Title	Page Number	Project Number	Title	Page Number
3535240000	IFSAR Rapid Terrain Visualization and Real-Time Exploitation System	564	3537260000	Developing/Assessing Long-Term Impact of Design Innovations	583
3535250000	Technologies for System-Level Innovations in Ballistic Missile Defense	566	3537270000	Composite Wire Plasma Formation and Evolution	584
3535260000	Novel Collective Protection System for Decon of CBW Agents and Purification of Aircraft and Other Closed Environments	567	3537280000	DNA Microarray Technology	587
3535270000	Z-Backlighter Technologies	568	3537290000	Research Issues in the System Engineering Aspects of High Assurance	588
3535280000	Ultra-Intense Femtosecond Laser Interactions with Applications to High-Field Physics, Enhanced Electromagnetic Coupling in Materials, and X-Ray Generation	570	3537310000	Investigation of Lateral Composition Modulation in GaAsSb Short-Period Superlattices	590
3537190000	Design of a Prototypical Snoopy Coprocessor for DYNAMICs Software Fault Monitoring with Integrity Constraints	572	3537320000	New Complexing Agent for Co(II) Analysis for CP	592
3537210000	Analytic Verification of Treaties, Protocols, and International Agreements	574	3537330000	Enzyme-Mediated Electrochemical Redox Polymer Microelectronic Biosensor for V- and G-Type Chemical Weapons	594
3537220000	Fabricating Microcomponents from Silicon-Carbonitride by a Novel Microcasting Process	575	3537340000	Design and Optimization of VLSI Systems and Reconfigurable Hardware	596
3537230000	Magnetic Polysilicon MEMS Devices	577	3537350000	Hydrodynamic Flow in Biosystems	598
3537240000	Living Tissue Engineering	579	3537360000	IR Polarimetry and Lithographic Alignment	600
3537250000	The Use of Active Fiber Composites for the Health Monitoring of Wind Turbine Blades	581	3537370000	Shock Response of Diamond Crystals	602
			3537390000	Dynamic Computer-Aided Design Analysis of Containment Vessels for Z-Pinch Experiments	603
			3537410000	Investigation of Nanoscience Technologies	604

Appendix A: Project Number / Title Index

<i>Project Number</i>	<i>Title</i>	<i>Page Number</i>
3537420000	Surety Science	605
3537430000	Stabilization of Enzymatic Molecular Recognition Materials Via Crystallization and Crosslinking	608
3537440000	Novel Biosensor Fabrication Techniques	610

Appendix B: Awards/Recognition List

<i>Industry Week</i> Technology of the Year	3506580000	Double Quantum-Well Long-Wavelength Optoelectronic Devices
R&D Award, <i>R&D Magazine</i>	3506680000	Silicon Three-Dimensional Photonic Crystal and Its Applications
Lockheed Martin NOVA Award		
<i>Industry Week</i> Technology of the Year		
<i>Industry Week</i> R&D Star Award		
<i>Industry Week</i> Technology of the Year	3506720000	Quantum Tunneling Transistors for Practical Application
1999 ASME Renewable Energy Conference: Best Paper Award	3510820000	High-Throughput Dry Processes for Large-Area Devices
1999 Franz Edelman Award Competition for Management Science Achievement, sponsored by INFORMS (Institute for Operations Research and the Management Sciences): Finalist	3510870000	Advanced Production Planning Models
Transportation Research Board 2000 Celebration: Best Paper	3512420000	Mission Surety for Large-Scale Real-Time Information Systems
OPNETWORK '99: Distinguished Paper Award—"A Simulation Study of the Virtual Interface Architecture"	3512450000	High-Performance Commodity Interconnects for Clustered Scientific and Engineering Computing
R&D Award, <i>R&D Magazine</i> (Previously funded project— not linked in this report)	3515170000	Development of a Portable X-Ray and Gamma-Ray Detector Instrument and Imaging Camera for Use in Radioactive and Hazardous Material Management
IT Corporation: Honor for MNAtoolbox Publication	3518170000	Mechanistic Models for Radionuclide Desorption from Soils
DOE Basic Energy Science Award: Outstanding Scientific Accomplishment in Metals and Ceramic Science	3531430000	Direct Fabrication for Multifunctional Nanocomposites Via Supramolecular Self-Assembly

Appendix C: Project Performance Measures

Project Title	Project #	Performance Statistics (Number of)											Project Qualitative Assessment		
		Refereed Publications	All Other Reports and Publications	Patent Disclosures	Patent Applications	Patents	Copyrights	Students	Post-docs	Permanent Staff Hired*	Awards	New Non-LDRD-Funded Projects†	% Milestones Completed	Goals Status**	Hypotheses Status***
Functional Materials for Microsystems: Smart Self-Assembled Photochromic Films	3502330000	2						1				100%	1	6	
Innovative Experimental and Computational Diagnostics for Monitoring Corrosion in Weapons Environments	3502340000		1									95%	1	7	
Self-Healing Molecular Assemblies for Control of Friction and Adhesion in MEMS	3502350000	3	1					1				90%	2	7	
Linking Atomistic Computations with Phase-Field Modeling	3502360000	5	1					1				90%	2	6	
A Combinatorial Microlab Investigation of Critical Copper-Corrosion Mechanisms	3502370000	1	3									85%	2	7	
Self-Assembled Templates for Fabricating Novel Nanoarrays and Controlling Materials Growth	3502380000	2					1			1		85%	1	7	
Wetting and Spreading Dynamics of Solder and Braze Alloys	3502390000		1					1				90%	2	7	
Improved Materials Aging Diagnostics and Mechanisms Through 2-D Hyperspectral Imaging Methods and Algorithms	3502410000		4		2			2				100%	1	7	
Microscale Shock-Wave Physics Using Photonic Driver Techniques	3502420000		1									90%	2	7	
Molecular-to-Continuum Fracture Analysis of Thermoset Polymer/Solid Interfaces	3502430000	1	6				2	1				100%	2	7	
Fundamental Aspects of Micromachine Reliability	3502440000	11	5	1	3				1			75%	2	8	
Enabling Science and Technology for Cold-Spray Direct Fabrication	3502450000	2	5	1	1		1	1		8		95%	2	7	
Atomic-Level Studies of Surfactant-Directed Materials Growth	3502460000	8	11									90%	2	7	
Intelligent Polymers for Nanodevice Performance Control	3502470000		1				1	1		1		80%	2	8	
Freeforming of Ceramics and Composites from Colloidal Slurries	3502480000	3	4	1	1	1	3	1		1	2	65%	4	6	
Quantum Dot Arrays	3502490000						1					100%	2	6	
Laser-Assisted Arc Welding for Aluminum Alloys	3502510000		1		1		2			1		80%	2	7	
Reactivity of Metal-Oxide Surfaces	3502520000	8		1			1					90%	2	7	

Appendix C: Project Performance Measures

Project Title	Project #	Performance Statistics (Number of)											Project Qualitative Assessment		
		Refereed Publications	All Other Reports and Publications	Patent Disclosures	Patent Applications	Patents	Copyrights	Students	Post-docs	Permanent Staff Hired*	Awards	New Non-LDRD-Funded Projects†	% Milestones Completed	Goals Status**	Hypotheses Status***
Exploiting LENS Technology Through Novel Materials	3502530000	1	3						1				100%	1	7
Molecular Characterization of Energetic Material Initiation	3502540000	1											85%	2	7
Nonvolatile Protonic Memory	3502550000										1		75%	2	7
Integration of Mesh Optimization with 3-D All-Hex Mesh Generation	3504340000		1										50%	3	10
Heterogeneous Simulation	3504350000		1	1				1		1	1		100%	2	6
Volumetric Video Motion Sensing for Unobtrusive Human-Computer Interactions	3504360000		1					3			2		100%	1	6
Hybrid Sparse-Dense Incomplete Factorization Preconditioners	3504370000		1										95%	2	7
Big Eddy—Advanced Large-Eddy Simulation Algorithms for Complex Flow Physics and Complex Geometry	3504380000		1						1				100%	1	7
Molecular Simulation of Reacting Systems	3504390000										2		75%	4	7
Massively Parallel Global Climate Model for Paleoclimate Applications	3504410000	1						3					80%	2	7
Fast and Easy Parallel I/O for Efficient Scientific Computing	3504420000	1											40%	3	8
Novel Load-Balancing for Scalable, Parallel Electromagnetic and Plasma Physics Simulation Software	3504430000		1										90%	2	6
Massively Parallel <i>Ab Initio</i> Validation for ASCI Materials Modeling	3504440000	2							2				100%	1	6
Computational Methods for Coupling Microstructural and Micromechanical Materials Response Simulations	3504450000	16	3						2				90%	1	8
Integrated Quantum/Classical Modeling of Hydrogenic Materials	3504460000	2							2				90%	2	7
The Next Generation of Teraflop Density-Functional Electronic Structure Codes	3504470000	2											90%	1	6
Methodology for Characterizing Modeling and Discretization Uncertainties in Computational Simulation	3504480000	3	3										60%	3	7
Global Optimization for Engineering Science Problems	3504490000	4	1						1	1			80%	2	8

Appendix C: Project Performance Measures

Project Title	Project #	Performance Statistics (Number of)										Project Qualitative Assessment		
		Refereed Publications	All Other Reports and Publications	Patent Disclosures	Patent Applications	Patents	Copyrights	Students	Post-docs	Permanent Staff Hired*	Awards	New Non-LDRD-Funded Projects†	% Milestones Completed	Goals Status**
Dynamic Simulation of Mechanical Systems with Intermittent Contacts	3504510000	3					1		1			100%	1	6
From Atom-Picoseconds to Centimeter-Years in Simulation and Experiment	3504520000	10	1				1	2	1			90%	1	6
Emergent Behavior of Large Swarms of Intelligent Agents	3504530000	1		1							1	100%	1	7
Parallel Combinatorial Optimization for Scheduling Problems	3504540000	1										60%	3	7
Programming Paradigms for Massively Parallel Computers	3504550000		1									85%	1	7
Multilevel Techniques for Unstructured Grid Problems on Massively Parallel Computers	3504560000	2	1									95%	2	6
Scalable Tools for Massively Parallel Distributed Computing	3504570000	2										100%	1	6
Massively Parallel Methods for Simulating the Phase-Field Model	3504580000	3	1					1				100%	1	7
Visual Explanation and Insight	3504590000	3	1	2	2	1	2	1			4	90%	2	7
Computational Simulations of Self-Assembling Macrosystems by Direct Fabrication of Microscopic Structured Materials	3504610000		1									100%	1	6
Gamma-Ray Bursts and the Particle Mass Scale	3504620000											100%	1	7
A Novel Nondestructive Silicon-on-Insulator Nonvolatile Memory	3506450000		1	2	2							90%	3	6
Integration of Optoelectronics and MEMS by Free-Space Microoptics	3506460000		1	2			1	1			1	80%	3	6
Advanced Laser Structures for Short-Pulsed Power in Active Optical Sensor Systems	3506470000	2			1							85%	2	7
Integration of Microsensor Technology into a Miniature Robotic Vehicle	3506480000	1					1					90%	2	6
Vacuum Encapsulation of MEMS Structures	3506490000			1		2						100%	1	6
Massively Parallel Sensor Arrays for Volatile Organic Detection	3506510000	2										95%	1	8
Agile Dry Etching of Compound Semiconductors for Science-Based Manufacturing Using <i>In Situ</i> Process Control	3506520000	4										100%	1	7

Appendix C: Project Performance Measures

Project Title	Project #	Performance Statistics (Number of)											Project Qualitative Assessment		
		Refereed Publications	All Other Reports and Publications	Patent Disclosures	Patent Applications	Patents	Copyrights	Students	Post-docs	Permanent Staff Hired*	Awards	New Non-LDRD-Funded Projects†	% Milestones Completed	Goals Status**	Hypotheses Status***
Precision-Formed Micromagnets	3506530000		5	2	1			2					100%	1	6
Time-Resolved Ion-Beam-Induced Charge-Collection (TRIBICC) Imaging	3506540000	2											85%	2	7
Composite-Resonator Surface-Emitting Lasers	3506550000	2						1					90%	2	6
Role of Defects in III-Nitride-Based Electronics	3506560000	5											90%	1	8
Ultra-Low-Power Sensors for Microtelemetry Systems	3506570000	5					1	1			1	90%	2	6	
Double Quantum-Well Long-Wavelength Optoelectronic Devices	3506580000	4	4		1			2		1	1	50%	3	8	
The Development of Integrated Chemical Microsensors in GaAs	3506590000	4			1							100%	1	6	
Monolithic Integration of VCSELs and Detectors for Microsystems	3506610000	5						1			3	100%	1	7	
AlGaIn Materials Engineering for Integrated Multifunction Systems	3506620000	10	1									85%	2	8	
Compliant Substrates for Epitaxial Integration of Dissimilar Materials	3506630000	1										15%	3	7	
Post-Processed Integrated Microsystems	3506640000	2	3									70%	3	7	
Development of Radiation-Hard Sensors for Space-Based Visible and Infrared Sensing Applications	3506660000										1	50%	2	7	
Silicon Three-Dimensional Photonic Crystal and Its Applications	3506680000	3			6					3		100%	1	6	
Monolithic Micromachined Variable Tuners for Rapid Prototyping and Optimization of Microwave Circuits	3506690000										1	98%	1	7	
Quantum Tunneling Transistors for Practical Application	3506720000	6	6		2	1		1	1		1	75%	3	7	
Development of Magnetically Excited Flexural Plate-Wave Devices for Implementation as Physical, Chemical, and Acoustic Sensors, and as Integrated Micropumps for Sensored Systems	3506730000	1	3					1				90%	2	8	
Novel Acoustically Driven Microoptoelectronic Devices	3506740000											75%	3	7	

Appendix C: Project Performance Measures

Project Title	Project #	Performance Statistics (Number of)											Project Qualitative Assessment		
		Refereed Publications	All Other Reports and Publications	Patent Disclosures	Patent Applications	Patents	Copyrights	Students	Post-docs	Permanent Staff Hired*	Awards	New Non-LDRD-Funded Projects†	% Milestones Completed	Goals Status**	Hypotheses Status***
Photonics Integration Devices and Technologies	3506750000	2		2					1				90%	2	7
Stress-Free Amorphous Diamond for High-Sensitivity Microsensors with Integrated Microstructures	3506760000	5			1			1	1			1	100%	1	7
Semiconductor Current Filament Lasers	3506770000	1	4	1				1					90%	1	6
Integration of Radiation-Hard Magnetic Random Access Memory with CMOS Integrated Circuits	3506780000		1										100%	1	6
Development of <i>In Situ</i> Diagnostics for Simultaneous Measurement of Transient Gas Species and Soot in Large Fires	3508250000		2						1				95%	1	7
Micromechanical Failure Analyses for Finite-Element Polymer Modeling	3508260000		1										90%	2	7
Methodology for Optimal Selection of Test and Simulation Levels for Problems Involving Computational Simulation	3508270000	1	1									1	100%	1	7
A Phenomenological Model for Multicomponent Transport with Electrochemical Reactions in Concentrated Solutions	3508280000		3										90%	2	6
Structural Simulations Using Multiresolution Material Models	3508290000	2											85%	2	7
Lightning-Induced Arcing	3508310000											3	75%	2	7
Mechanisms of Adiabatic Shear Failure	3508320000								1				90%	2	7
Evolvable Hardware	3508330000												100%	1	6
Crack Nucleation and Growth: Combining Validated Atomistic and Continuum Modeling	3508340000	5							1			1	80%	2	7
Applied Microfluidic Physics	3508350000	5	6	1									100%	1	7
Transport and Fate Simulation of Chem/Bio Agents in Critical Infrastructures	3508360000												50%	3	8
Innovative Measurement Diagnostics for Fluid/Solid and Fluid/Fluid Interactions in Rotating Flowfields	3508370000		1							1			35%	4	7
Capturing Recrystallization of Metals with a Multiscale Material Model	3508380000	8	27					1	2			1	75%	2	7
Nondeterministic Modeling in Engineering Science	3508390000	5	6										95%	1	6

Appendix C: Project Performance Measures

Project Title	Project #	Performance Statistics (Number of)											Project Qualitative Assessment		
		Refereed Publications	All Other Reports and Publications	Patent Disclosures	Patent Applications	Patents	Copyrights	Students	Post-docs	Permanent Staff Hired*	Awards	New Non-LDRD-Funded Projects†	% Milestones Completed	Goals Status**	Hypotheses Status***
Lagrangian Modeling of Radiative Transport	3508410000	4										1	90%	2	6
High-Resolution Modeling of Multiscale Transient Phenomena in Turbulent Boundary Layers	3508420000	1						2					90%	1	7
Dispersive Measurements of Velocity in Heterogeneous Materials	3508430000	1											100%	1	6
A Physically-Based Computational Method for Predicting Generalized Fracture	3508440000	3						2	1		1	80%	2	7	
Microdiagnostic MEMS Lab-on-a-Chip	3510710000	4	1		1		2					100%	1	6	
Real-Time Error Correction Using Electromagnetic Bearing Spindles	3510720000						1					100%	1	7	
Thin-Film Deposition Processes Incorporating <i>In Situ</i> Monitoring Capabilities	3510730000						1					95%	1	6	
Optimization of Filled Polymer Materials	3510740000						1					100%	1	7	
Solid-State Neutron Generator for Use in Nuclear Weapons	3510750000						1	1				90%	2	7	
Finite-Element Meshing Approached as a Global Minimization Process	3510760000	1	1				1	2				80%	3	7	
Application of Parallel Mechanism Technology to Manufacturing	3510770000	1	1	3		1	2	1		1	2	90%	1	6	
Investigation of the Impact of Cleaning on Adhesive Bond and the Process Implications	3510780000	9					2	1				100%	1	6	
Standard Cells for Microelectromechanical Systems (MEMS)	3510790000	5	1	12	3	1	3	1	1	1		95%	1	6	
Laser Wire Deposition for Fully Dense Shapes	3510810000	1	2				1	1	1			100%	2	6	
High-Throughput Dry Processes for Large-Area Devices	3510820000		2	1	1	1				1		80%	2	7	
Assuring High Reliability and Production Readiness in Low-Volume Manufacturing	3510830000	1	2									90%	2	6	
Scripting for Video Inspection	3510840000										1	100%	1	7	
Advanced Machining Processes for Microfabrication	3510850000	1					3					90%	2	7	

Appendix C: Project Performance Measures

Project Title	Project #	Performance Statistics (Number of)										Project Qualitative Assessment			
		Refereed Publications	All Other Reports and Publications	Patent Disclosures	Patent Applications	Patents	Copyrights	Students	Post-docs	Permanent Staff Hired*	Awards	New Non-LDRD-Funded Projects†	% Milestones Completed	Goals Status**	Hypotheses Status***
Fusion of Product and Process Data Using Real-Time Streaming Visualization	3510860000												90%	2	7
Advanced Production Planning Models	3510870000	2	1	1			1	2		1	1	100%	1	7	
Weighted-Nearest-Neighbor (WNN) Decision Making for Data Mining	3512290000						5					100%	1	6	
Varying QoS for Fixed and Mobile Networks	3512310000										3	100%	2	7	
A Real-Time Decision-Support Framework to Guide Facility Response to Abnormal Events	3512320000	1	2	1							1	90%	2	7	
Data Fusion for Chemical Sensing	3512330000		2									95%	1	6	
Large-Scale Distributed Information System Modeling and Simulation	3512340000	1										100%	1	7	
High-Surety SCADA for the Critical Energy Infrastructures	3512350000								1			100%	1	7	
Agent-Based Mediation and Cooperative Information Systems	3512360000		1	2			3					90%	2	7	
Dynamically Self-Configurable Network Protocol	3512370000											100%	1	7	
Optical Backplane/Interconnect for Super-High-Speed Communication	3512380000						1					95%	1	7	
PUSH Technology Demonstration	3512390000											40%	3	7	
Controlling Information: Its Flow, Fusion, and Coordination	3512410000		2				1					100%	1	6	
Mission Surety for Large-Scale Real-Time Information Systems	3512420000	2	1							3		100%	1	7	
Low-Power, Reduced-Computation, Public-Key Protocols	3512430000											95%	2	7	
Ten-to-One-Hundred-Gigabit/Second Network Enabling R&D	3512440000		1	3			1					90%	2	8	
High-Performance Commodity Interconnects for Clustered Scientific and Engineering Computing	3512450000	1								1		100%	1	6	
AVATAR—Navigating and Mining in Massive Data	3512460000	3	3				2	3				85%	2	7	

Appendix C: Project Performance Measures

Project Title	Project #	Performance Statistics (Number of)											Project Qualitative Assessment		
		Refereed Publications	All Other Reports and Publications	Patent Disclosures	Patent Applications	Patents	Copyrights	Students	Post-docs	Permanent Staff Hired*	Awards	New Non-LDRD-Funded Projects†	% Milestones Completed	Goals Status**	Hypotheses Status***
Algorithm-Based Fault Tolerance on Heterogeneous Massively Parallel Computers	3512470000	2	2					5					95%	2	7
Surface Decontamination of Bacterial Protein Toxins by RF Power	3514150000			1									100%	1	7
Intense White-Light Pulse Propagation in Air Using Self-Guided Optical Filamentation: Applications to Remote Sensing and Countermeasures	3514160000	2						1		2		3	95%	2	6
Improved Backscatter X-Ray Detection for Antiterrorist Applications	3514170000												80%	3	7
HPM Vulnerability Assessment and Tests	3514180000		1									1	100%	1	6
Imaging of Moving Targets Using Simultaneous Synthetic Aperture Radar (SAR) and Moving Target Indicator (MTI) Radar	3516170000												99%	2	6
Sparse Geophysical Networks for Monitoring Deep Targets	3516180000	1											100%	1	7
Miniature Bioaerosol Concentrator	3516190000			2	2			1		1			70%	3	7
Recognizing Partially Obscured Targets by Combining Multiple Data Sources Using Evidential Reasoning	3516210000		2									1	90%	2	7
Computational Engineering of Sensor Materials and Integration with a Novel Biological Weapon Detection System	3516220000		1					1					90%	2	6
Biological Weapon Detector Using Bioaffinity Array Impedance Analysis with Chemical Amplification Through Redox Recycling	3516230000			1	1			1					85%	2	8
ATR/Exploitation Utilizing Ultra-High-Resolution, Complex SAR Imaging	3516240000											2	95%	2	7
Thin-Skin Deployable Mirrors for Remote Sensing Systems	3516250000	2	3	1				1		4			100%	1	7
Dispersible Granular Sensor (Smart Sand) for Landmine Detection Based on TNT Immunoassay	3516260000	2	7	1				2	2			3	90%	2	7
Characterization of Underground Facilities in an Urban Environment	3516270000		1										90%	2	7
Dexterous Robotic Manipulation of Hazardous Materials in Unstructured Environments	3516280000	1								1			75%	3	7
Autonomous Dynamic Soaring Platform for Distributed Mobile Sensor Arrays	3516290000				1								80%	2	7

Appendix C: Project Performance Measures

Project Title	Project #	Performance Statistics (Number of)											Project Qualitative Assessment		
		Refereed Publications	All Other Reports and Publications	Patent Disclosures	Patent Applications	Patents	Copyrights	Students	Post-docs	Permanent Staff Hired*	Awards	New Non-LDRD-Funded Projects†	% Milestones Completed	Goals Status**	Hypotheses Status***
Miniature UV Fluorescence-Based Biological Agent Sensor	3516310000				1								85%	2	7
Automatic Planning of Life-Cycle Assembly Processes	3516320000	4	3				1						98%	1	8
Analysis of Very Large Assemblies	3516330000	3					1						100%	1	8
Enabling Human Skills with Cooperative Automation	3516340000						1						100%	1	7
Cloud to CAD	3516350000		1				3						75%	2	6
Ergonomics in Life-Cycle Assembly Processes	3516360000	2	2				1						95%	2	8
Feature Reduction of Geometric Solid Models for Analysis Tools	3516370000		1										90%	2	6
Electrokinetic Immunoaffinity Chemical Sensors	3516380000	1		1	1		1						80%	2	8
Designed Synthesis of Controlled Degradative Materials	3518160000			2			1	1			1		85%	2	7
Mechanistic Models for Radionuclide Desorption from Soils	3518170000	2								1	1		100%	1	6
Adaptive 3-D Sensing	3518180000										1		100%	1	8
Aqueous Organic Sensor	3518190000	1	1				1	1	1				100%	1	6
Designed Ionophores for Liquid-Membrane Separation and Extraction of Metal Ions	3518210000	5					1	1					80%	4	8
An Electromagnetic Imaging System for Environmental Site Reconnaissance	3518220000	2											100%	1	8
Advanced Geosphere Transport Simulation	3518230000		6								2		90%	2	7
Hybrid Processing of Measurable and Subjective Information in Surety Analysis	3520340000	1		1									100%	1	7
Computer-Network Vulnerability-Analysis Method	3520350000	1		1	1		1				1		75%	2	7
Approximate Public-Key Authentication with Information Hiding	3520360000												100%	1	7

Appendix C: Project Performance Measures

Project Title	Project #	Performance Statistics (Number of)											Project Qualitative Assessment		
		Refereed Publications	All Other Reports and Publications	Patent Disclosures	Patent Applications	Patents	Copyrights	Students	Post-docs	Permanent Staff Hired*	Awards	New Non-LDRD-Funded Projects†	% Milestones Completed	Goals Status**	Hypotheses Status***
New Network Analysis Approaches to Evaluate Infrastructure Risk and Reliability	3520370000		1					1				1	80%	2	8
Improved Tools for Identifying and Quantifying Potentially Dangerous Human Actions	3520380000												90%	1	7
Advanced Signal Processing for Thermal Flaw Detection	3520390000												95%	2	6
Production Surety and Disruption Vulnerability Analysis	3520410000			1									100%	1	7
An Optically Triggered Semiconductor Switch for Firing Systems	3520420000	2	1	1	1								100%	1	7
Source Code Assurance Tool	3520430000		1									1	75%	3	7
System Surety Life-Cycle Engineering	3520440000		1										95%	2	7
Integrated Approach to Develop Microelectromechanical System (MEMS) Reliability Tools	3520450000	1	13	2	1		1	1	1			1	100%	1	7
Simulation/Optimization Tools for System-Variability Analysis	3520460000	1						2					100%	1	6
A Massively Parallel Microsimulation Model of Infrastructure Interdependency	3520470000		1									2	75%	2	7
Physical Models for Predicting the Effect of Atmospheric Corrosion on Microelectronic Reliability	3520480000	1	3					2					80%	2	8
Backside Localization of Open and Shorted IC (Integrated Circuit) Interconnections	3520490000	2	1										100%	1	6
Reliability Predictions for Advanced Electronics in Smoke Environments	3520510000	1	3					3				3	80%	3	8
Security of Bulk Power Systems	3520520000	2											100%	1	7
Science on the Microdomain	3522010000	4	3	14				6	5	1			90%	2	7
Autonomous MicroChem Laboratory (μ ChemLab)	3522020000	2	9	8	14	1		6	5	2		4	95%	2	6
Cooperative, Distributed Sensing and Action Using Microminiature, Intelligent Agents	3522030000	4					1	4					80%	1	6
Engineering Complex Distributed Systems	3522040000	10	4	4	1		1						75%	2	7

Appendix C: Project Performance Measures

Project Title	Project #	Performance Statistics (Number of)											Project Qualitative Assessment		
		Refereed Publications	All Other Reports and Publications	Patent Disclosures	Patent Applications	Patents	Copyrights	Students	Post-docs	Permanent Staff Hired*	Awards	New Non-LDRD-Funded Projects†	% Milestones Completed	Goals Status**	Hypotheses Status***
Laser Communication Nanosatellites	3522050000	12	13	4	1							10	90%	2	7
Information Collection (Acquisition of Information from Denied Areas)	3522060000								1		4	85%	2	6	
Accelerated Molecular Discovery Arrays—The Next Revolution in Biotechnology	3522070000	1		3	1			6	2			90%	1	7	
Microcode Evaluation	3530140000											50%	3	10	
Model-Based Design and Analysis of Remote Access Monitoring Systems	3530150000		1									65%	3	7	
Microwave Imaging Through Walls	3530160000				1							40%	3	7	
Research of the Utility of Polarimetric Sensing	3530170000	1						1	1			100%	2	7	
Real-Time Image Analysis Using Field-Programmable Gate Arrays	3530180000	1						1	1			75%	2	6	
Poco Switch Tubes	3531340000			1								66%	2	6	
Chemiresistors Based on Metal-Loaded Polymers for Solvent Spill Detection	3531350000			1	1			1				50%	3	7	
Advance Neutron-Tube Design and Producibility	3531360000											70%	4	8	
Surface Hardening by Nanoparticle Precipitation and Atomic Clustering in Ni(Al ₂ O ₃)	3531370000											100%	1	7	
Dynamical Properties of Polymers: Computational Modeling	3531380000	1										95%	1	7	
Broadening Mechanism in 2-D Excitonic and Electron Gases	3531390000	1										100%	2	9	
Calculation and Interpretation of the Energies that Underlie Transition-Metal Surface Structure	3531410000	2										75%	3	7	
Interfacial Reactions in Ceramic Systems	3531420000	3										85%	1	7	
Direct Fabrication of Multifunctional Nanocomposites Via Supramolecular Self-Assembly	3531430000	2	1	4				3	2	1	1	85%	1	6	
Raman Investigation of Phase Changes in PZT Materials	3531440000										1	100%	1	6	

Appendix C: Project Performance Measures

Project Title	Project #	Performance Statistics (Number of)										Project Qualitative Assessment		
		Refereed Publications	All Other Reports and Publications	Patent Disclosures	Patent Applications	Patents	Copyrights	Students	Post-docs	Permanent Staff Hired*	Awards	New Non-LDRD-Funded Projects†	% Milestones Completed	Goals Status**
Information Extraction from Hyperspectral Images Obtained from Satellites	3531450000			1					1			80%	2	8
Expanding the Security Dimension of Surety	3531460000	1										75%	2	8
Overcoming Software Brittleness: A Swarm Intelligence Approach	3531470000											95%	2	7
Synthesis and Applications of N-Type Diamond	3531480000											75%	3	8
A Molecular Theory of Gatekeeper Proteins	3531490000	1									1	70%	3	6
Development of Compact UV Laser Source for Climate Studies and Chemical Sensing	3531510000	3	1	1								80%	3	7
Power Source Technologies for Autonomous Microsystems	3531520000		1									100%	2	8
Advanced Radiation Sources: Rayleigh-Taylor Mitigation Via Perturbation Reduction	3532280000		1									90%	2	8
Global Approaches to Infrastructural Analysis (GAIA)	3532290000											100%	1	6
Capillary Elasto-hydrodynamics in Manufacturing Processes	3532310000	2						1				75%	2	7
Real-Time Design of Improved Powder Pressing Dies Using Finite-Element Method Modeling	3532320000		8									70%	3	7
Computational Methods for Predicting the Response of Critical As-Built Infrastructure to Dynamic Loads (Architectural Surety)	3532330000	1										95%	2	6
Solar-Grade Silicon	3533190000	1	1									100%	3	10
Low-Work-Function Thermionic Emission Materials	3533210000	1		1	1						1	100%	2	7
Develop Mathematical Algorithms for the Integration of Disparate Information to Determine Critical Infrastructure Health and Status	3533220000										1	100%	1	6
SERAPHIM Propulsion Technology Design for High-Speed Rail Applications	3533230000		1	2	1						1	100%	1	6
Tomographically Measured Temporal Evolution of Hyperspectral Target Signatures	3534070000	1									1	80%	2	7

Appendix C: Project Performance Measures

Project Title	Project #	Performance Statistics (Number of)										Project Qualitative Assessment		
		Refereed Publications	All Other Reports and Publications	Patent Disclosures	Patent Applications	Patents	Copyrights	Students	Post-docs	Permanent Staff Hired*	Awards	New Non-LDRD-Funded Projects†	% Milestones Completed	Goals Status**
Gas-to-Liquid Microabsorber	3534080000							1		1	1	70%	4	7
High-Resolution Electromagnetic Imaging of Transport Pathways	3534090000		1						1			60%	3	7
MPP Direct Numerical Simulation of Diesel Autoignition	3534110000							1				100%	1	6
Electrokinetically Driven Mesoscale Actuators	3534120000			2	3	1		1			1	100%	1	6
Pathogen Detection Using Microseparations for BW Nonproliferation	3534130000							1				50%	4	7
Assessing the Emerging Threat of Limited WMD Use	3535220000		5								1	100%	1	7
Z-Pinch Fusion for Energy Applications	3535230000		2									100%	1	8
IFSAR Rapid Terrain Visualization and Real-Time Exploitation System	3535240000		1									100%	1	7
Technologies for System-Level Innovations in Ballistic Missile Defense	3535250000											100%	1	8
Novel Collective Protection System for Decon of CBW Agents and Purification of Aircraft and Other Closed Environments	3535260000								1			100%	1	6
Z-Backlighter Technologies	3535270000						1		1			95%	2	6
Ultra-Intense Femtosecond Laser Interactions with Applications to High-Field Physics, Enhanced Electromagnetic Coupling in Materials, and X-Ray Generation	3535280000	2						2	1	1		95%	2	6
Design of a Prototypical Snoopy Coprocessor for DynaMICS Software Fault Monitoring with Integrity Constraints	3537190000	1						2				100%	1	7
Analytic Verification of Treaties, Protocols, and International Agreements	3537210000		3					2				90%	2	7
Fabricating Microcomponents from Silicon-Carbonitride by a Novel Microcasting Process	3537220000							1				63%	3	7
Magnetic Polysilicon MEMS Devices	3537230000		1		1			2				20%	3	7
Living Tissue Engineering	3537240000											100%	1	7
The Use of Active Fiber Composites for the Health Monitoring of Wind Turbine Blades	3537250000		2					2				96%	2	7

Appendix C: Project Performance Measures

Project Title	Project #	Performance Statistics (Number of)										Project Qualitative Assessment			
		Refereed Publications	All Other Reports and Publications	Patent Disclosures	Patent Applications	Patents	Copyrights	Students	Post-docs	Permanent Staff Hired*	Awards	New Non-LDRD-Funded Projects†	% Milestones Completed	Goals Status**	Hypotheses Status***
Developing/Assessing Long-Term Impact of Design Innovations	3537260000						1					100%	2	7	
Composite Wire Plasma Formation and Evolution	3537270000	1										100%	2	9	
DNA Microarray Technology	3537280000			1			1	2				100%	2	7	
Research Issues in the System Engineering Aspects of High Assurance	3537290000	1					2					100%	1	7	
Investigation of Lateral Composition Modulation in GaAsSb Short-Period Superlattices	3537310000											75%	4	7	
New Complexing Agent for Co(II) Analysis for CP	3537320000						2					90%	2	7	
Enzyme-Mediated Electrochemical Redox Polymer Microelectronic Biosensor for V- and G-Type Chemical Weapons	3537330000						1					100%	1	6	
Design and Optimization of VLSI Systems and Reconfigurable Hardware	3537340000	1					2		1			100%	1	7	
Hydrodynamic Flow in Biosystems	3537350000		1				1					100%	2	6	
IR Polarimetry and Lithographic Alignment	3537360000		1				2					100%	1	9	
Shock Response of Diamond Crystals	3537370000											90%	2	7	
Dynamic Computer-Aided Design Analysis of Containment Vessels for Z-Pinch Experiments	3537390000						3					85%	3	7	
Investigation of Nanoscience Technologies	3537410000											90%	2	7	
Surety Science	3537420000		1									100%	1	6	
Stabilization of Enzymatic Molecular Recognition Materials Via Crystallization and Crosslinking	3537430000											50%	3	7	
Novel Biosensor Fabrication Techniques	3537440000											50%	3	7	
		342	284	104	64	10	15	145	79	30	16	102			

Appendix C: Project Performance Measures

Project Title	Project #	Performance Statistics (Number of)										Project Qualitative Assessment			
		Refereed Publications	All Other Reports and Publications	Patent Disclosures	Patent Applications	Patents	Copyrights	Students	Post-docs	Permanent Staff Hired*	Awards	New Non-LDRD-Funded Projects†	% Milestones Completed	Goals Status**	Hypotheses Status***

† Identification of new non-LDRD-funded projects is now completed in the fiscal year following the annual report.

* Permanent Staff Hired. Laboratories operate under manpower cap. There are no increases in permanent staff.

** Goals Status

- 1 - Goals Met
- 2 - Goals Substantially Met
- 3 - Goals Partially Modified
- 4 - Goals Substantially Modified
- 5 - Goals Not Met
- 11 - Project Terminated

***Hypothesis Status

- 6 - Hypotheses Proved
- 7 - Hypotheses Remains Unchanged
- 8 - Hypotheses Modified
- 9 - Hypotheses Redefined
- 10 - Hypotheses Disproved
- 11 - Project Terminated

Appendix D: DOE Critical Technologies

Pg #	Title	Project #	Science of Complex Systems	Modeling & Simulation of Complex Systems	High-Performance Computing	Nuclear Weapons Predictive Capability (Classified)	Safety Assessments & Engineering	Use Control & Verification	Nonproliferation & Verification	Dynamic Testing in Severe Environments	High-Energy-Density Materials	Laser Technology	Pulsed Power and Accelerators	Microelectronics and Photonics	Nuclear Materials	Engineered Materials	Flexible Manufacturing	Environmentally Conscious Manufacturing	Intelligent Machines and Robotics	Waste Management	Other
70	Reactivity of Metal-Oxide Surfaces	3502520000		•												•					
73	Exploiting LENS Technology Through Novel Materials	3502530000										•				•	•	•			
76	Molecular Characterization of Energetic Material Initiation	3502540000		•						•		•									
78	Nonvolatile Protonic Memory	3502550000						•						•							
81	Integration of Mesh Optimization with 3-D All-Hex Mesh Generation	3504340000		•	•	•	•				•		•	•		•	•				
83	Heterogeneous Simulation	3504350000		•	•														•		
86	Volumetric Video Motion Sensing for Unobtrusive Human-Computer Interactions	3504360000	•	•	•		•	•	•						•				•		
88	Hybrid Sparse-Dense Incomplete Factorization Preconditioners	3504370000			•																
91	Big Eddy—Advanced Large-Eddy Simulation Algorithms for Complex Flow Physics and Complex Geometry	3504380000		•	•		•						•								
93	Molecular Simulation of Reacting Systems	3504390000		•	•	•									•	•	•				
95	Massively Parallel Global Climate Model for Paleoclimate Applications	3504410000		•	•																
97	Fast and Easy Parallel I/O for Efficient Scientific Computing	3504420000		•	•												•				
99	Novel Load-Balancing for Scalable, Parallel Electromagnetic and Plasma Physics Simulation Software	3504430000	•	•	•	•		•					•	•		•					
102	Massively Parallel <i>Ab Initio</i> Validation for ASCI Materials Modeling	3504440000			•						•					•					
104	Computational Methods for Coupling Microstructural and Micromechanical Materials Response Simulations	3504450000	•	•	•											•					
108	Integrated Quantum/Classical Modeling of Hydrogenic Materials	3504460000		•	•											•					
110	The Next Generation of Teraflop Density-Functional Electronic Structure Codes	3504470000		•	•									•		•					

Appendix D: DOE Critical Technologies

Pg #	Title	Project #	Science of Complex Systems	Modeling & Simulation of Complex Systems	High-Performance Computing	Nuclear Weapons Predictive Capability (Classified)	Safety Assessments & Engineering	Use Control & Verification	Nonproliferation & Verification	Dynamic Testing in Severe Environments	High-Energy-Density Materials	Laser Technology	Pulsed Power and Accelerators	Microelectronics and Photonics	Nuclear Materials	Engineered Materials	Flexible Manufacturing	Environmentally Conscious Manufacturing	Intelligent Machines and Robotics	Waste Management	Other
112	Methodology for Characterizing Modeling and Discretization Uncertainties in Computational Simulation	3504480000	•	•	•		•												•		
115	Global Optimization for Engineering Science Problems	3504490000			•		•		•				•				•		•	•	•
118	Dynamic Simulation of Mechanical Systems with Intermittent Contacts	3504510000		•													•		•		
121	From Atom-Picoseconds to Centimeter-Years in Simulation and Experiment	3504520000		•	•											•					
123	Emergent Behavior of Large Swarms of Intelligent Agents	3504530000		•	•														•		
125	Parallel Combinatorial Optimization for Scheduling Problems	3504540000		•	•																
128	Programming Paradigms for Massively Parallel Computers	3504550000			•																
130	Multilevel Techniques for Unstructured Grid Problems on Massively Parallel Computers	3504560000			•																
132	Scalable Tools for Massively Parallel Distributed Computing	3504570000			•																
134	Massively Parallel Methods for Simulating the Phase-Field Model	3504580000	•	•	•											•					
137	Visual Explanation and Insight	3504590000	•	•	•																
139	Computational Simulations of Self-Assembling Macrosystems by Direct Fabrication of Microscopic Structures	3504610000			•											•					
141	Gamma-Ray Bursts and the Particle Mass Scale	3504620000			•																
143	A Novel Nondestructive Silicon-on-Insulator Nonvolatile Memory	3506450000			•									•							
146	Integration of Optoelectronics and MEMS by Free-Space Microoptics	3506460000						•	•			•		•							
149	Advanced Laser Structures for Short-Pulsed Power in Active Optical Sensor Systems	3506470000						•	•			•		•							
151	Integration of Microsensor Technology into a Miniature Robotic Vehicle	3506480000	•	•					•			•		•					•		

Appendix D: DOE Critical Technologies

Pg #	Title	Project #	Science of Complex Systems	Modeling & Simulation of Complex Systems	High-Performance Computing	Nuclear Weapons Predictive Capability (Classified)	Safety Assessments & Engineering	Use Control & Verification	Nonproliferation & Verification	Dynamic Testing in Severe Environments	High-Energy-Density Materials	Laser Technology	Pulsed Power and Accelerators	Microelectronics and Photonics	Nuclear Materials	Engineered Materials	Flexible Manufacturing	Environmentally Conscious Manufacturing	Intelligent Machines and Robotics	Waste Management	Other
153	Vacuum Encapsulation of MEMS Structures	3506490000					•	•	•				•		•				•		
156	Massively Parallel Sensor Arrays for Volatile Organic Detection	3506510000											•								
158	Agile Dry Etching of Compound Semiconductors for Science-Based Manufacturing Using <i>In Situ</i> Process Control	3506520000	•									•		•		•					
161	Precision-Formed Micromagnets	3506530000												•		•					
164	Time-Resolved Ion-Beam-Induced Charge-Collection (TRIBICC) Imaging	3506540000	•											•							
167	Composite-Resonator Surface-Emitting Lasers	3506550000										•		•						•	
169	Role of Defects in III-Nitride-Based Electronics	3506560000												•		•					
172	Ultra-Low-Power Sensors for Microtelemetry Systems	3506570000							•					•		•		•	•		
175	Double Quantum-Well Long-Wavelength Optoelectronic Devices	3506580000										•		•							
179	The Development of Integrated Chemical Microsensors in GaAs	3506590000							•					•				•	•	•	
182	Monolithic Integration of VCSELs and Detectors for Microsystems	3506610000										•		•					•		
184	AlGaIn Materials Engineering for Integrated Multifunction Systems	3506620000												•		•					
187	Compliant Substrates for Epitaxial Integration of Dissimilar Materials	3506630000												•							
188	Post-Processed Integrated Microsystems	3506640000							•					•			•		•		
191	Development of Radiation-Hard Sensors for Space-Based Visible and Infrared Sensing Applications	3506660000							•					•							
193	Silicon Three-Dimensional Photonic Crystal and Its Applications	3506680000										•		•							
195	Monolithic Micromachined Variable Tuners for Rapid Prototyping and Optimization of Microwave Circuits	3506690000							•					•					•		

Appendix D: DOE Critical Technologies

Pg #	Title	Project #	Science of Complex Systems	Modeling & Simulation of Complex Systems	High-Performance Computing	Nuclear Weapons Predictive Capability (Classified)	Safety Assessments & Engineering	Use Control & Verification	Nonproliferation & Verification	Dynamic Testing in Severe Environments	High-Energy-Density Materials	Laser Technology	Pulsed Power and Accelerators	Microelectronics and Photonics	Nuclear Materials	Engineered Materials	Flexible Manufacturing	Environmentally Conscious Manufacturing	Intelligent Machines and Robotics	Waste Management	Other
198	Quantum Tunneling Transistors for Practical Application	3506720000												•							
202	Development of Magnetically Excited Flexural Plate-Wave Devices for Implementation as Physical, Chemical, and Acoustic Sensors, and as Integrated Micropumps for Sensored Systems	3506730000							•					•					•		
205	Novel Acoustically Driven Microoptoelectronic Devices	3506740000	•									•		•							
207	Photonics Integration Devices and Technologies	3506750000		•				•				•		•					•		
210	Stress-Free Amorphous Diamond for High-Sensitivity Microsensors with Integrated Microstructures	3506760000												•							
213	Semiconductor Current Filament Lasers	3506770000										•	•	•		•	•	•			
215	Integration of Radiation-Hard Magnetic Random Access Memory with CMOS Integrated Circuits	3506780000												•							
218	Development of <i>In Situ</i> Diagnostics for Simultaneous Measurement of Transient Gas Species and Soot in Large Fires	3508250000	•	•			•					•		•		•					
221	Micromechanical Failure Analyses for Finite-Element Polymer Modeling	3508260000		•						•				•		•	•				
224	Methodology for Optimal Selection of Test and Simulation Levels for Problems Involving Computational Simulation	3508270000	•	•		•	•			•											•
226	A Phenomenological Model for Multicomponent Transport with Electrochemical Reactions in Concentrated Solutions	3508280000		•																	
228	Structural Simulations Using Multiresolution Material Models	3508290000		•	•	•	•									•					
230	Lightning-Induced Arcing	3508310000		•			•														
232	Mechanisms of Adiabatic Shear Failure	3508320000		•						•						•		•			
234	Evolvable Hardware	3508330000	•	•	•			•						•			•		•		
236	Crack Nucleation and Growth: Combining Validated Atomistic and Continuum Modeling	3508340000	•	•			•									•					
239	Applied Microfluidic Physics	3508350000	•	•				•								•					

Appendix D: DOE Critical Technologies

Pg #	Title	Project #	Science of Complex Systems	Modeling & Simulation of Complex Systems	High-Performance Computing	Nuclear Weapons Predictive Capability (Classified)	Safety Assessments & Engineering	Use Control & Verification	Nonproliferation & Verification	Dynamic Testing in Severe Environments	High-Energy-Density Materials	Laser Technology	Pulsed Power and Accelerators	Microelectronics and Photonics	Nuclear Materials	Engineered Materials	Flexible Manufacturing	Environmentally Conscious Manufacturing	Intelligent Machines and Robotics	Waste Management	Other
243	Transport and Fate Simulation of Chem/Bio Agents in Critical Infrastructures	3508360000		•	•																
245	Innovative Measurement Diagnostics for Fluid/Solid and Fluid/Fluid Interactions in Rotating Flowfields	3508370000	•	•		•				•		•		•							•
247	Capturing Recrystallization of Metals with a Multiscale Material Model	3508380000		•		•	•										•				
252	Nondeterministic Modeling in Engineering Science	3508390000		•		•	•										•				
255	Lagrangian Modeling of Radiative Transport	3508410000	•	•	•		•														
257	High-Resolution Modeling of Multiscale Transient Phenomena in Turbulent Boundary Layers	3508420000		•																	•
259	Dispersive Measurements of Velocity in Heterogeneous Materials	3508430000	•	•	•							•									
261	A Physically-Based Computational Method for Predicting Generalized Fracture	3508440000	•	•	•		•									•					
265	Microdiagnostic MEMS Lab-on-a-Chip	3510710000	•	•	•	•	•	•	•	•		•	•	•	•	•	•	•	•	•	•
267	Real-Time Error Correction Using Electromagnetic Bearing Spindles	3510720000	•	•													•				
268	Thin-Film Deposition Processes Incorporating <i>In Situ</i> Monitoring Capabilities	3510730000											•		•	•					
270	Optimization of Filled Polymer Materials	3510740000	•	•						•			•		•	•					
272	Solid-State Neutron Generator for Use in Nuclear Weapons	3510750000												•	•						
274	Finite-Element Meshing Approached as a Global Minimization Process	3510760000		•																	
276	Application of Parallel Mechanism Technology to Manufacturing	3510770000		•													•		•		
278	Investigation of the Impact of Cleaning on Adhesive Bond and the Process Implications	3510780000	•	•									•		•	•	•				
281	Standard Cells for Microelectromechanical Systems (MEMS)	3510790000	•				•	•					•		•	•		•			

Appendix D: DOE Critical Technologies

Pg #	Title	Project #	Science of Complex Systems	Modeling & Simulation of Complex Systems	High-Performance Computing	Nuclear Weapons Predictive Capability (Classified)	Safety Assessments & Engineering	Use Control & Verification	Nonproliferation & Verification	Dynamic Testing in Severe Environments	High-Energy-Density Materials	Laser Technology	Pulsed Power and Accelerators	Microelectronics and Photonics	Nuclear Materials	Engineered Materials	Flexible Manufacturing	Environmentally Conscious Manufacturing	Intelligent Machines and Robotics	Waste Management	Other
363	ATR / Exploitation Utilizing Ultra-High-Resolution, Complex SAR Imaging	3516240000							•												•
365	Thin-Skin Deployable Mirrors for Remote Sensing Systems	3516250000		•					•												
368	Dispersible Granular Sensor (Smart Sand) for Landmine Detection Based on TNT Immunoassay	3516260000							•												•
371	Characterization of Underground Facilities in an Urban Environment	3516270000	•	•					•												
373	Dexterous Robotic Manipulation of Hazardous Materials in Unstructured Environments	3516280000													•				•	•	
376	Autonomous Dynamic Soaring Platform for Distributed Mobile Sensor Arrays	3516290000	•	•	•														•		
378	Miniature UV Fluorescence-Based Biological Agent Sensor	3516310000							•			•		•							
381	Automatic Planning of Life-Cycle Assembly Processes	3516320000		•														•	•		
384	Analysis of Very Large Assemblies	3516330000																•	•		
386	Enabling Human Skills with Cooperative Automation	3516340000		•														•	•	•	
389	Cloud to CAD	3516350000	•	•	•				•										•		
392	Ergonomics in Life-Cycle Assembly Processes	3516360000		•														•	•		
395	Feature Reduction of Geometric Solid Models for Analysis Tools	3516370000		•														•	•		
397	Electrokinetic Immunoaffinity Chemical Sensors	3516380000							•									•			
401	Designed Synthesis of Controlled Degradative Materials	3518160000						•										•			
403	Mechanistic Models for Radionuclide Desorption from Soils	3518170000													•	•					•
404	Adaptive 3-D Sensing	3518180000					•	•	•						•			•	•		

Appendix D: DOE Critical Technologies

Pg #	Title	Project #	Science of Complex Systems	Modeling & Simulation of Complex Systems	High-Performance Computing	Nuclear Weapons Predictive Capability (Classified)	Safety Assessments & Engineering	Use Control & Verification	Nonproliferation & Verification	Dynamic Testing in Severe Environments	High-Energy-Density Materials	Laser Technology	Pulsed Power and Accelerators	Microelectronics and Photonics	Nuclear Materials	Engineered Materials	Flexible Manufacturing	Environmentally Conscious Manufacturing	Intelligent Machines and Robotics	Waste Management	Other
566	Technologies for System-Level Innovations in Ballistic Missile Defense	3535250000							•	•											
567	Novel Collective Protection System for Decon of CBW Agents and Purification of Aircraft and Other Closed Environments	3535260000							•												•
568	Z-Backlighter Technologies	3535270000										•	•								
570	Ultra-Intense Femtosecond Laser Interactions with Applications to High-Field Physics, Enhanced Electromagnetic Coupling in Materials, and X-Ray Generation	3535280000										•		•							
572	Design of a Prototypical Snoopy Coprocessor for DynaMICs Software Fault Monitoring with Integrity Constraints	3537190000			•					•											
574	Analytic Verification of Treaties, Protocols, and International Agreements	3537210000		•					•												
575	Fabricating Microcomponents from Silicon-Carbonitride by a Novel Microcasting Process	3537220000														•	•		•		
577	Magnetic Polysilicon MEMS Devices	3537230000						•						•		•	•		•		
579	Living Tissue Engineering	3537240000	•	•	•																
581	The Use of Active Fiber Composites for the Health Monitoring of Wind Turbine Blades	3537250000					•									•					
583	Developing/Assessing Long-Term Impact of Design Innovations	3537260000		•	•	•									•	•					
584	Composite Wire Plasma Formation and Evolution	3537270000		•							•		•								
587	DNA Microarray Technology	3537280000														•			•		
588	Research Issues in the System Engineering Aspects of High Assurance	3537290000	•																		
590	Investigation of Lateral Composition Modulation in GaAsSb Short-Period Superlattices	3537310000										•		•							
592	New Complexing Agent for Co(II) Analysis for CP	3537320000					•									•					
594	Enzyme-Mediated Electrochemical Redox Polymer Microelectronic Biosensor for V- and G-Type Chemical Weapons	3537330000							•					•		•					

Appendix D: DOE Critical Technologies

Pg #	Title	Project #	Science of Complex Systems	Modeling & Simulation of Complex Systems	High-Performance Computing	Nuclear Weapons Predictive Capability (Classified)	Safety Assessments & Engineering	Use Control & Verification	Nonproliferation & Verification	Dynamic Testing in Severe Environments	High-Energy-Density Materials	Laser Technology	Pulsed Power and Accelerators	Microelectronics and Photonics	Nuclear Materials	Engineered Materials	Flexible Manufacturing	Environmentally Conscious Manufacturing	Intelligent Machines and Robotics	Waste Management	Other
596	Design and Optimization of VLSI Systems and Reconfigurable Hardware	3537340000		•	•									•							
598	Hydrodynamic Flow in Biosystems	3537350000	•	•	•																
600	IR Polarimetry and Lithographic Alignment	3537360000							•					•							
602	Shock Response of Diamond Crystals	3537370000								•	•		•			•					
603	Dynamic Computer-Aided Design Analysis of Containment Vessels for Z-Pinch Experiments	3537390000		•			•			•			•		•	•					
604	Investigation of Nanoscience Technologies	3537410000									•					•					
605	Surety Science	3537420000	•	•			•														
608	Stabilization of Enzymatic Molecular Recognition Materials Via Crystallization and Crosslinking	3537430000							•					•							
610	Novel Biosensor Fabrication Techniques	3537440000							•					•							

Appendix E: Major National Programs

Pg #	Title	Project #	Waste Management	Energy Efficiency	Renewable Energy	ES&H	Environmental Restoration	Fossil Energy	Radioactive-Waste Management	Economic Impact	Energy Research	Intelligence & National Security	Nuclear Energy	Science Education & Technical Information	Defense Programs	Department of Defense (DoD)	Other Federal Agencies*	Other (Industry, Consortia,...)**	Other Federal Agencies* Other (Industry, Consortia...)**
24	Functional Materials for Microsystems: Smart Self-Assembled Photochromic Films	3502330000													•				
26	Innovative Experimental and Computational Diagnostics for Monitoring Corrosion in Weapons Environments	3502340000													•				
29	Self-Healing Molecular Assemblies for Control of Friction and Adhesion in MEMS	3502350000								•					•	•	•	**Industry	
31	Linking Atomistic Computations with Phase-Field Modeling	3502360000									•				•				
34	A Combinatorial Microlab Investigation of Critical Copper-Corrosion Mechanisms	3502370000								•	•			•	•				
37	Self-Assembled Templates for Fabricating Novel Nanoarrays and Controlling Materials Growth	3502380000		•							•				•				
39	Wetting and Spreading Dynamics of Solder and Braze Alloys	3502390000									•				•				
42	Improved Materials Aging Diagnostics and Mechanisms Through 2-D Hyperspectral Imaging Methods and Algorithms	3502410000					•			•		•			•				
45	Microscale Shock-Wave Physics Using Photonic Driver Techniques	3502420000													•	•			
48	Molecular-to-Continuum Fracture Analysis of Thermoset Polymer/Solid Interfaces	3502430000													•	•			
52	Fundamental Aspects of Micromachine Reliability	3502440000									•								
55	Enabling Science and Technology for Cold-Spray Direct Fabrication	3502450000	•	•		•	•	•		•	•				•	•			
58	Atomic-Level Studies of Surfactant-Directed Materials Growth	3502460000									•								
62	Intelligent Polymers for Nanodevice Performance Control	3502470000										•			•				
64	Freeforming of Ceramics and Composites from Colloidal Slurries	3502480000													•	•	•	**Advanced Manufacturing	
67	Quantum Dot Arrays	3502490000						•			•								
69	Laser-Assisted Arc Welding for Aluminum Alloys	3502510000							•		•				•	•	•	**Industry Consortia	

Appendix E: Major National Programs

Pg #	Title	Project #	Waste Management	Energy Efficiency	Renewable Energy	ES&H	Environmental Restoration	Fossil Energy	Radioactive-Waste Management	Economic Impact	Energy Research	Intelligence & National Security	Nuclear Energy	Science Education & Technical Information	Defense Programs	Department of Defense (DoD)	Other Federal Agencies*	Other (Industry, Consortia,...)**	Other Federal Agencies* Other (Industry, Consortia...)**
70	Reactivity of Metal-Oxide Surfaces	3502520000	•					•		•									
73	Exploiting LENS Technology Through Novel Materials	3502530000								•					•	•			
76	Molecular Characterization of Energetic Material Initiation	3502540000														•			
78	Nonvolatile Protonic Memory	3502550000													•	•	•	•	**Texas Instruments, Intel, Motorola, Sharp
81	Integration of Mesh Optimization with 3-D All-Hex Mesh Generation	3504340000	•						•	•	•		•		•	•			
83	Heterogeneous Simulation	3504350000										•		•	•	•			
86	Volumetric Video Motion Sensing for Unobtrusive Human-Computer Interactions	3504360000								•		•	•	•	•	•	•	•	*DOE/OSS, FBI, **Entertainment
88	Hybrid Sparse-Dense Incomplete Factorization Preconditioners	3504370000													•				
91	Big Eddy—Advanced Large-Eddy Simulation Algorithms for Complex Flow Physics and Complex Geometry	3504380000	•					•			•				•	•	•		*NASA
93	Molecular Simulation of Reacting Systems	3504390000													•				
95	Massively Parallel Global Climate Model for Paleoclimate Applications	3504410000								•	•								
97	Fast and Easy Parallel I/O for Efficient Scientific Computing	3504420000									•				•	•			
99	Novel Load-Balancing for Scalable, Parallel Electromagnetic and Plasma Physics Simulation Software	3504430000													•	•	•	•	*FAA, **Microelectronics, Automotive, Portable Communications, Biomedical
102	Massively Parallel <i>Ab Initio</i> Validation for ASCI Materials Modeling	3504440000													•				
104	Computational Methods for Coupling Microstructural and Micromechanical Materials Response Simulations	3504450000													•				
108	Integrated Quantum/Classical Modeling of Hydrogenic Materials	3504460000	•								•				•				

Appendix E: Major National Programs

Pg #	Title	Project #	Waste Management	Energy Efficiency	Renewable Energy	ES&H	Environmental Restoration	Fossil Energy	Radioactive-Waste Management	Economic Impact	Energy Research	Intelligence & National Security	Nuclear Energy	Science Education & Technical Information	Defense Programs	Department of Defense (DoD)	Other Federal Agencies*	Other (Industry, Consortia,...)**	Other Federal Agencies* Other (Industry, Consortia...)**
110	The Next Generation of Teraflop Density-Functional Electronic Structure Codes	3504470000													•				
112	Methodology for Characterizing Modeling and Discretization Uncertainties in Computational Simulation	3504480000									•			•	•	•		•	**CRADAS w/Goodyear, etc.
115	Global Optimization for Engineering Science Problems	3504490000	•								•	•				•		•	**Industry
118	Dynamic Simulation of Mechanical Systems with Intermittent Contacts	3504510000												•	•	•		•	**Industry
121	From Atom-Picoseconds to Centimeter-Years in Simulation and Experiment	3504520000									•				•				
123	Emergent Behavior of Large Swarms of Intelligent Agents	3504530000										•			•				
125	Parallel Combinatorial Optimization for Scheduling Problems	3504540000													•				
128	Programming Paradigms for Massively Parallel Computers	3504550000									•					•		•	**Industry
130	Multilevel Techniques for Unstructured Grid Problems on Massively Parallel Computers	3504560000													•				
132	Scalable Tools for Massively Parallel Distributed Computing	3504570000									•				•				
134	Massively Parallel Methods for Simulating the Phase-Field Model	3504580000													•		•		*DOE
137	Visual Explanation and Insight	3504590000				•				•	•	•			•	•			
139	Computational Simulations of Self-Assembling Macrosystems by Direct Fabrication of Microscopic Structures	3504610000													•				
141	Gamma-Ray Bursts and the Particle Mass Scale	3504620000									•				•	•			
143	A Novel Nondestructive Silicon-on-Insulator Nonvolatile Memory	3506450000										•			•	•		•	**Industry
146	Integration of Optoelectronics and MEMS by Free-Space Microoptics	3506460000										•			•	•			
149	Advanced Laser Structures for Short-Pulsed Power in Active Optical Sensor Systems	3506470000										•			•				

Appendix E: Major National Programs

Pg #	Title	Project #	Waste Management	Energy Efficiency	Renewable Energy	ES&H	Environmental Restoration	Fossil Energy	Radioactive-Waste Management	Economic Impact	Energy Research	Intelligence & National Security	Nuclear Energy	Science Education & Technical Information	Defense Programs	Department of Defense (DoD)	Other Federal Agencies*	Other (Industry, Consortia,...)**	Other Federal Agencies* Other (Industry, Consortia...)**
195	Monolithic Micromachined Variable Tuners for Rapid Prototyping and Optimization of Microwave Circuits	3506690000								•	•				•	•			
198	Quantum Tunneling Transistors for Practical Application	3506720000									•								
202	Development of Magnetically Excited Flexural Plate-Wave Devices for Implementation as Physical, Chemical, and Acoustic Sensors, and as Integrated Micropumps for Sensored Systems	3506730000					•					•			•				
205	Novel Acoustically Driven Microoptoelectronic Devices	3506740000									•	•			•	•			
207	Photonics Integration Devices and Technologies	3506750000										•			•	•			
210	Stress-Free Amorphous Diamond for High-Sensitivity Microsensors with Integrated Microstructures	3506760000													•				
213	Semiconductor Current Filament Lasers	3506770000		•				•							•	•			
215	Integration of Radiation-Hard Magnetic Random Access Memory with CMOS Integrated Circuits	3506780000										•			•	•			
218	Development of <i>In Situ</i> Diagnostics for Simultaneous Measurement of Transient Gas Species and Soot in Large Fires	3508250000		•	•			•			•				•	•	•		*DOC/NIST, EPA
221	Micromechanical Failure Analyses for Finite-Element Polymer Modeling	3508260000													•	•	•		**Industry
224	Methodology for Optimal Selection of Test and Simulation Levels for Problems Involving Computational Simulation	3508270000	•				•								•	•			
226	A Phenomenological Model for Multicomponent Transport with Electrochemical Reactions in Concentrated Solutions	3508280000									•				•	•	•		**Industry
228	Structural Simulations Using Multiresolution Material Models	3508290000													•	•	•		**Industry
230	Lightning-Induced Arcing	3508310000													•	•			
232	Mechanisms of Adiabatic Shear Failure	3508320000													•	•			

Appendix E: Major National Programs

Pg #	Title	Project #	Waste Management	Energy Efficiency	Renewable Energy	ES&H	Environmental Restoration	Fossil Energy	Radioactive-Waste Management	Economic Impact	Energy Research	Intelligence & National Security	Nuclear Energy	Science Education & Technical Information	Defense Programs	Department of Defense (DoD)	Other Federal Agencies*	Other (Industry, Consortia,...)**	Other Federal Agencies* Other (Industry, Consortia...)**
234	Evolvable Hardware	3508330000								•	•				•	•			
236	Crack Nucleation and Growth: Combining Validated Atomistic and Continuum Modeling	3508340000								•					•	•			
239	Applied Microfluidic Physics	3508350000					•				•				•	•			
243	Transport and Fate Simulation of Chem/Bio Agents in Critical Infrastructures	3508360000				•						•							
245	Innovative Measurement Diagnostics for Fluid/Solid and Fluid/Fluid Interactions in Rotating Flowfields	3508370000													•	•			
247	Capturing Recrystallization of Metals with a Multiscale Material Model	3508380000								•					•	•			
252	Nondeterministic Modeling in Engineering Science	3508390000						•			•				•	•			
255	Lagrangian Modeling of Radiative Transport	3508410000													•	•	•	•	*FAA, NASA, **Insurance, Petrochemical
257	High-Resolution Modeling of Multiscale Transient Phenomena in Turbulent Boundary Layers	3508420000	•	•	•		•	•	•	•			•		•	•			
259	Dispersive Measurements of Velocity in Heterogeneous Materials	3508430000												•	•	•			
261	A Physically-Based Computational Method for Predicting Generalized Fracture	3508440000		•				•		•	•		•	•	•	•			
265	Microdiagnostic MEMS Lab-on-a-Chip	3510710000	•	•	•	•	•	•	•	•	•	•	•	•	•	•			
267	Real-Time Error Correction Using Electromagnetic Bearing Spindles	3510720000								•					•	•			
268	Thin-Film Deposition Processes Incorporating <i>In Situ</i> Monitoring Capabilities	3510730000													•				
270	Optimization of Filled Polymer Materials	3510740000													•	•	•	**Industry	
272	Solid-State Neutron Generator for Use in Nuclear Weapons	3510750000													•				
274	Finite-Element Meshing Approached as a Global Minimization Process	3510760000													•	•	•	**Industry	
276	Application of Parallel Mechanism Technology to Manufacturing	3510770000													•	•	•	**NIST, **Manufacturing	

Appendix E: Major National Programs

Pg #	Title	Project #	Waste Management	Energy Efficiency	Renewable Energy	ES&H	Environmental Restoration	Fossil Energy	Radioactive-Waste Management	Economic Impact	Energy Research	Intelligence & National Security	Nuclear Energy	Science Education & Technical Information	Defense Programs	Department of Defense (DoD)	Other Federal Agencies*	Other (Industry, Consortia,...)**	Other Federal Agencies* Other (Industry, Consortia...)**
278	Investigation of the Impact of Cleaning on Adhesive Bond and the Process Implications	3510780000													•	•		•	**Industry
281	Standard Cells for Microelectromechanical Systems (MEMS)	3510790000		•	•					•	•			•	•	•			
284	Laser-Wire Deposition for Fully Dense Shapes	3510810000								•					•	•	•	•	*Production Agencies (ASKCD), KAPL **LENS CRADA (industry)
287	High-Throughput Dry Processes for Large-Area Devices	3510820000		•							•							•	**Semiconductor industry
290	Assuring High Reliability and Production Readiness in Low-Volume Manufacturing	3510830000													•	•			
292	Scripting for Video Inspection	3510840000								•					•				
294	Advanced Machining Processes for Microfabrication	3510850000												•	•	•		•	**Industry
296	Fusion of Product and Process Data Using Real-Time Streaming Visualization	3510860000													•		•		*NIST
298	Advanced Production Planning Models	3510870000													•				
301	Weighted-Nearest-Neighbor (WNN) Decision Making for Data Mining	3512290000								•	•	•			•	•	•		*DOE Office of Safeguards & Security
303	Varying QoS for Fixed and Mobile Networks	3512310000								•					•				
306	A Real-Time Decision-Support Framework to Guide Facility Response to Abnormal Events	3512320000					•					•			•	•	•		*DARPA, FAA, State Department, FEMA, GSA
308	Data Fusion for Chemical Sensing	3512330000				•	•					•							
310	Large-Scale Distributed Information System Modeling and Simulation	3512340000										•			•				
313	High-Surety SCADA for the Critical Energy Infrastructures	3512350000		•	•			•		•	•	•							
316	Agent-Based Mediation and Cooperative Information Systems	3512360000									•	•			•				
318	Dynamically Self-Configurable Network Protocol	3512370000										•			•	•			

Appendix E: Major National Programs

Pg #	Title	Project #	Waste Management	Energy Efficiency	Renewable Energy	ES&H	Environmental Restoration	Fossil Energy	Radioactive-Waste Management	Economic Impact	Energy Research	Intelligence & National Security	Nuclear Energy	Science Education & Technical Information	Defense Programs	Department of Defense (DoD)	Other Federal Agencies*	Other (Industry, Consortia,...)**	Other Federal Agencies* Other (Industry, Consortia...)**
321	Optical Backplane/Interconnect for Super-High-Speed Communication	3512380000								•	•				•	•	•		*NSA, CIA
323	PUSH Technology Demonstration	3512390000								•	•			•	•	•			
325	Controlling Information: Its Flow, Fusion, and Coordination	3512410000									•				•	•			
327	Mission Surety for Large-Scale Real-Time Information Systems	3512420000									•					•			
329	Low-Power, Reduced-Computation, Public-Key Protocols	3512430000	•								•	•			•	•			
331	Ten-to-One-Hundred-Gigabit/Second Network Enabling R&D	3512440000													•				
333	High-Performance Commodity Interconnects for Clustered Scientific and Engineering Computing	3512450000													•	•			
336	AVATAR—Navigating and Mining in Massive Data	3512460000													•				
338	Algorithm-Based Fault Tolerance on Heterogeneous Massively Parallel Computers	3512470000								•									
341	Surface Decontamination of Bacterial Protein Toxins by RF Power	3514150000									•					•	•		*FEMA
343	Intense White-Light Pulse Propagation in Air Using Self-Guided Optical Filamentation: Applications to Remote Sensing and Countermeasures	3514160000									•				•	•			
346	Improved Backscatter X-Ray Detection for Antiterrorist Applications	3514170000									•				•				
348	HPM Vulnerability Assessment and Tests	3514180000													•	•	•		*Intelligence Agencies
350	Imaging of Moving Targets Using Simultaneous Synthetic Aperture Radar (SAR) and Moving Target Indicator (MTI) Radar	3516170000								•	•				•	•			
352	Sparse Geophysical Networks for Monitoring Deep Targets	3516180000									•					•			
354	Miniature Bioaerosol Concentrator	3516190000									•				•	•			
356	Recognizing Partially Obscured Targets by Combining Multiple Data Sources Using Evidential Reasoning	3516210000									•				•	•			

Appendix E: Major National Programs

Pg #	Title	Project #	Waste Management	Energy Efficiency	Renewable Energy	ES&H	Environmental Restoration	Fossil Energy	Radioactive-Waste Management	Economic Impact	Energy Research	Intelligence & National Security	Nuclear Energy	Science Education & Technical Information	Defense Programs	Department of Defense (DoD)	Other Federal Agencies*	Other (Industry, Consortia,...)**	Other Federal Agencies* Other (Industry, Consortia...)**
358	Computational Engineering of Sensor Materials and Integration with a Novel Biological Weapon Detection System	3516220000										•			•	•			
361	Biological Weapon Detector Using Bioaffinity Array Impedance Analysis with Chemical Amplification Through Redox Recycling	3516230000										•			•	•			
363	ATR / Exploitation Utilizing Ultra-High-Resolution, Complex SAR Imaging	3516240000										•				•			
365	Thin-Skin Deployable Mirrors for Remote Sensing Systems	3516250000										•							
368	Dispersible Granular Sensor (Smart Sand) for Landmine Detection Based on TNT Immunoassay	3516260000										•				•			
371	Characterization of Underground Facilities in an Urban Environment	3516270000										•				•			
373	Dexterous Robotic Manipulation of Hazardous Materials in Unstructured Environments	3516280000	•				•		•			•			•	•	•		*FBI
376	Autonomous Dynamic Soaring Platform for Distributed Mobile Sensor Arrays	3516290000					•					•				•			
378	Miniature UV Fluorescence-Based Biological Agent Sensor	3516310000					•					•			•	•			
381	Automatic Planning of Life-Cycle Assembly Processes	3516320000								•					•				
384	Analysis of Very Large Assemblies	3516330000								•					•				
386	Enabling Human Skills with Cooperative Automation	3516340000	•				•									•		•	**Manufacturing Industry
389	Cloud to CAD	3516350000										•			•	•			
392	Ergonomics in Life-Cycle Assembly Processes	3516360000								•					•				
395	Feature Reduction of Geometric Solid Models for Analysis Tools	3516370000								•					•				
397	Electrokinetic Immunoaffinity Chemical Sensors	3516380000					•					•				•			
401	Designed Synthesis of Controlled Degradative Materials	3518160000										•			•				

Appendix E: Major National Programs

Pg #	Title	Project #	Waste Management	Energy Efficiency	Renewable Energy	ES&H	Environmental Restoration	Fossil Energy	Radioactive-Waste Management	Economic Impact	Energy Research	Intelligence & National Security	Nuclear Energy	Science Education & Technical Information	Defense Programs	Department of Defense (DoD)	Other Federal Agencies*	Other (Industry, Consortia,...)**	Other Federal Agencies* Other (Industry, Consortia...)**
403	Mechanistic Models for Radionuclide Desorption from Soils	3518170000	•				•		•										
404	Adaptive 3-D Sensing	3518180000				•	•			•	•	•		•	•	•			
406	Aqueous Organic Sensor	3518190000	•			•	•										•		*EPA
409	Designed Ionophores for Liquid-Membrane Separation and Extraction of Metal Ions	3518210000	•																
412	An Electromagnetic Imaging System for Environmental Site Reconnaissance	3518220000				•	•		•	•					•	•			
414	Advanced Geosphere Transport Simulation	3518230000	•				•	•	•	•	•								
418	Hybrid Processing of Measurable and Subjective Information in Surety Analysis	3520340000												•	•	•	•	•	*FAA, NASA, **System modeling for reliability, risk
420	Computer-Network Vulnerability-Analysis Method	3520350000										•					•		*NSA, CIA
423	Approximate Public-Key Authentication with Information Hiding	3520360000										•			•				
424	New Network Analysis Approaches to Evaluate Infrastructure Risk and Reliability	3520370000								•		•				•	•		*Council on Critical Infrastructure
426	Improved Tools for Identifying and Quantifying Potentially Dangerous Human Actions	3520380000														•	•	•	*FAA, NASA, **Commercial airlines
428	Advanced Signal Processing for Thermal Flaw Detection	3520390000			•	•					•	•	•		•	•	•	•	*FAA, FEMA, **Transportation industry
431	Production Surety and Disruption Vulnerability Analysis	3520410000													•				
433	An Optically Triggered Semiconductor Switch for Firing Systems	3520420000													•	•			
436	Source Code Assurance Tool	3520430000										•			•	•	•		*NRC, FAA, FDA, NIST
438	System-Surety Life-Cycle Engineering	3520440000						•		•	•	•	•	•	•	•			
440	Integrated Approach to Develop Microelectromechanical System (MEMS) Reliability Tools	3520450000							•		•			•	•				

Appendix E: Major National Programs

Pg #	Title	Project #	Waste Management	Energy Efficiency	Renewable Energy	ES&H	Environmental Restoration	Fossil Energy	Radioactive-Waste Management	Economic Impact	Energy Research	Intelligence & National Security	Nuclear Energy	Science Education & Technical Information	Defense Programs	Department of Defense (DoD)	Other Federal Agencies*	Other (Industry, Consortia,...)**	Other Federal Agencies* Other (Industry, Consortia...)**
444	Simulation/Optimization Tools for System-Variability Analysis	3520460000													•			•	**Electrical Simulation Software Vendors
447	A Massively Parallel Microsimulation Model of Infrastructure Interdependency	3520470000								•	•							•	**Infrastructure Industries
450	Physical Models for Predicting the Effect of Atmospheric Corrosion on Microelectronic Reliability	3520480000								•					•	•			
453	Backside Localization of Open and Shorted IC (Integrated Circuit) Interconnections	3520490000								•					•	•		•	**Microelectronics Industry
456	Reliability Predictions for Advanced Electronics in Smoke Environments	3520510000				•							•					•	*USNRC, **Telecommunications
458	Security of Bulk Power Systems	3520520000									•	•						•	*FBI, CIA, NERC, NRC
461	Science on the Microdomain	3522010000	•			•	•				•	•						•	
464	Autonomous MicroChem Laboratory (µChemLab)	3522020000	•	•		•	•	•	•	•	•	•		•	•	•	•	•	*FBI, DEA, DOT, DOJ, **Industry
467	Cooperative, Distributed Sensing and Action Using Microminiature, Intelligent Agents	3522030000	•				•	•			•				•				
469	Engineering Complex Distributed Systems	3522040000									•	•			•	•			
473	Laser Communication Nanosatellites	3522050000		•						•	•	•			•	•			
479	Information Collection (Acquisition of Information from Denied Areas)	3522060000										•			•	•	•		*OGA
481	Accelerated Molecular Discovery Arrays—The Next Revolution in Biotechnology	3522070000										•				•	•	•	*NIH, **Biotechnology and Health Care Industries
485	Microcode Evaluation	3530140000										•							
486	Model-Based Design and Analysis of Remote Access Monitoring Systems	3530150000										•			•	•			
489	Microwave Imaging Through Walls	3530160000										•							
490	Research of the Utility of Polarimetric Sensing	3530170000										•			•	•			

Appendix E: Major National Programs

Pg #	Title	Project #	Waste Management	Energy Efficiency	Renewable Energy	ES&H	Environmental Restoration	Fossil Energy	Radioactive-Waste Management	Economic Impact	Energy Research	Intelligence & National Security	Nuclear Energy	Science Education & Technical Information	Defense Programs	Department of Defense (DoD)	Other Federal Agencies*	Other (Industry, Consortia,...)**	Other Federal Agencies* Other (Industry, Consortia...)**
492	Real-Time Image Analysis Using Field-Programmable Gate Arrays	3530180000										•			•	•			
494	Poco Switch Tubes	3531340000													•				
495	Chemiresistors Based on Metal-Loaded Polymers for Solvent Spill Detection	3531350000				•	•				•				•	•			
497	Advance Neutron-Tube Design and Producibility	3531360000													•				
498	Surface Hardening by Nanoparticle Precipitation and Atomic Clustering in Ni(Al ₂ O ₃)	3531370000	•							•	•				•				
499	Dynamical Properties of Polymers: Computational Modeling	3531380000									•				•	•			
501	Broadening Mechanism in 2-D Excitonic and Electron Gases	3531390000	•								•				•	•			
503	Calculation and Interpretation of the Energies that Underlie Transition-Metal Surface Structure	3531410000										•							
505	Interfacial Reactions in Ceramic Systems	3531420000			•		•			•	•				•				
508	Direct Fabrication of Multifunctional Nanocomposites Via Supramolecular Self-Assembly	3531430000									•				•	•			
511	Raman Investigation of Phase Changes in PZT Materials	3531440000													•				
513	Information Extraction from Hyperspectral Images Obtained from Satellites	3531450000	•				•			•	•	•		•	•	•			
515	Expanding the Security Dimension of Surety	3531460000										•			•	•			
516	Overcoming Software Brittleness: A Swarm Intelligence Approach	3531470000								•	•				•	•			
518	Synthesis and Applications of N-Type Diamond	3531480000					•			•	•				•				
521	A Molecular Theory of Gatekeeper Proteins	3531490000										•			•		•	**Medicine (NIH)	
523	Development of Compact UV Laser Source for Climate Studies and Chemical Sensing	3531510000									•						•	*NACA, EPA	
525	Power Source Technologies for Autonomous Microsystems	3531520000								•	•				•	•	•	*3-letter agencies	

Appendix E: Major National Programs

Pg #	Title	Project #	Waste Management	Energy Efficiency	Renewable Energy	ES&H	Environmental Restoration	Fossil Energy	Radioactive-Waste Management	Economic Impact	Energy Research	Intelligence & National Security	Nuclear Energy	Science Education & Technical Information	Defense Programs	Department of Defense (DoD)	Other Federal Agencies*	Other (Industry, Consortia,...)**	Other Federal Agencies* Other (Industry, Consortia...)**
526	Advanced Radiation Sources: Rayleigh-Taylor Mitigation Via Perturbation Reduction	3532280000													•				
528	Global Approaches to Infrastructural Analysis (GAIA)	3532290000		•	•			•		•	•		•			•			
530	Capillary Elasto-hydrodynamics in Manufacturing Processes	3532310000								•	•	•			•	•			
532	Real-Time Design of Improved Powder Pressing Dies Using Finite-Element Method Modeling	3532320000								•					•	•			**Association of American Ceramic Component Manufacturers Consortium I
535	Computational Methods for Predicting the Response of Critical As-Built Infrastructure to Dynamic Loads (Architectural Surety)	3532330000												•	•	•	•		*DOS, GSA
537	Solar-Grade Silicon	3533190000			•						•							•	**Photovoltaics Industry
539	Low-Work-Function Thermionic Emission Materials	3533210000		•							•				•				
541	Develop Mathematical Algorithms for the Integration of Disparate Information to Determine Critical Infrastructure Health and Status	3533220000								•		•						•	*DoD, FEMA, DOC, Electric Power, Telco
543	SERAPHIM Propulsion Technology Design for High-Speed Rail Applications	3533230000		•														•	*Federal Railroad Administration, **Industry
545	Tomographically Measured Temporal Evolution of Hyperspectral Target Signatures	3534070000										•			•	•			
547	Gas-to-Liquid Microabsorber	3534080000										•			•	•			
550	High-Resolution Electromagnetic Imaging of Transport Pathways	3534090000					•		•		•								
552	MPP Direct Numerical Simulation of Diesel Autoignition	3534110000		•							•				•				
555	Electrokinetically Driven Mesoscale Actuators	3534120000								•		•			•	•			
557	Pathogen Detection Using Microseparations for BW Nonproliferation	3534130000										•				•			
560	Assessing the Emerging Threat of Limited WMD Use	3535220000										•							

Appendix E: Major National Programs

Pg #	Title	Project #	Waste Management	Energy Efficiency	Renewable Energy	ES&H	Environmental Restoration	Fossil Energy	Radioactive-Waste Management	Economic Impact	Energy Research	Intelligence & National Security	Nuclear Energy	Science Education & Technical Information	Defense Programs	Department of Defense (DoD)	Other Federal Agencies*	Other (Industry, Consortia,...)**	Other Federal Agencies* Other (Industry, Consortia...)**
562	Z-Pinch Fusion for Energy Applications	3535230000									•		•		•				
564	IFSAR Rapid Terrain Visualization and Real-Time Exploitation System	3535240000										•			•	•			
566	Technologies for System-Level Innovations in Ballistic Missile Defense	3535250000														•			
567	Novel Collective Protection System for Decon of CBW Agents and Purification of Aircraft and Other Closed Environments	3535260000										•				•			
568	Z-Backlighter Technologies	3535270000									•	•			•	•			
570	Ultra-Intense Femtosecond Laser Interactions with Applications to High-Field Physics, Enhanced Electromagnetic Coupling in Materials, and X-Ray Generation	3535280000										•			•	•			
572	Design of a Prototypical Snoopy Coprocessor for DynaMICs Software Fault Monitoring with Integrity Constraints	3537190000											•		•	•			
574	Analytic Verification of Treaties, Protocols, and International Agreements	3537210000										•							
575	Fabricating Microcomponents from Silicon-Carbonitride by a Novel Microcasting Process	3537220000								•	•			•	•				
577	Magnetic Polysilicon MEMS Devices	3537230000								•		•			•	•			
579	Living Tissue Engineering	3537240000		•										•	•				
581	The Use of Active Fiber Composites for the Health Monitoring of Wind Turbine Blades	3537250000			•														
583	Developing/Assessing Long-Term Impact of Design Innovations	3537260000												•	•	•		•	**Architectural Surety
584	Composite Wire Plasma Formation and Evolution	3537270000													•				
587	DNA Microarray Technology	3537280000														•			
588	Research Issues in the System Engineering Aspects of High Assurance	3537290000								•	•			•	•	•			

Appendix E: Major National Programs

Pg #	Title	Project #	Waste Management	Energy Efficiency	Renewable Energy	ES&H	Environmental Restoration	Fossil Energy	Radioactive-Waste Management	Economic Impact	Energy Research	Intelligence & National Security	Nuclear Energy	Science Education & Technical Information	Defense Programs	Department of Defense (DoD)	Other Federal Agencies*	Other (Industry, Consortia,...)**	Other Federal Agencies* Other (Industry, Consortia...)**
590	Investigation of Lateral Composition Modulation in GaAsSb Short-Period Superlattices	3537310000		•							•			•					
592	New Complexing Agent for Co(II) Analysis for CP	3537320000													•			•	**Collaboration with a university
594	Enzyme-Mediated Electrochemical Redox Polymer Microelectronic Biosensor for V- and G-Type Chemical Weapons	3537330000					•				•				•				
596	Design and Optimization of VLSI Systems and Reconfigurable Hardware	3537340000									•				•	•			
598	Hydrodynamic Flow in Biosystems	3537350000							•		•			•	•			•	**Medical industry
600	IR Polarimetry and Lithographic Alignment	3537360000								•					•				
602	Shock Response of Diamond Crystals	3537370000									•				•				
603	Dynamic Computer-Aided Design Analysis of Containment Vessels for Z-Pinch Experiments	3537390000									•		•		•				
604	Investigation of Nanoscience Technologies	3537410000									•			•					
605	Surety Science	3537420000										•			•	•	•	•	*FAA, NASA, **Commercial airlines
608	Stabilization of Enzymatic Molecular Recognition Materials Via Crystallization and Crosslinking	3537430000									•				•				
610	Novel Biosensor Fabrication Techniques	3537440000									•				•				

Appendix F: Dual-Benefit Areas and Single-Use Categories

Pg #	Title	Project #	Aeronautics	Applied Molecular Biology	Ceramics	Composites	Computer Simulation and Modeling	Data Storage and Peripherals	Electronics and Photonics	Energy	Flexible Computer-Integrated Manufacturing	High-Definition Imaging and Displays	High-Performance Computing and Networking	High-Performance Metals and Alloys	Intelligent Processing Equipment	Material Synthesis and Processing	Medical Technology	Micro- and Nanofabrication	Micro- and Optoelectronics	Photonic Materials	Pollution Minimization, Remediation, and Waste Mgt.	Sensors and Signal Processing	Software	Surface Transportation Technologies	Systems Management Technologies	Defense-Related (mostly or purely)	Dual-Use (defense and non-defense-related)	Non-Defense-Related (mostly or purely)
62	Intelligent Polymers for Nanodevice Performance Control	3502470000													•						•				•			
64	Freeforming of Ceramics and Composites from Colloidal Slurries	3502480000			•	•					•				•	•											•	
67	Quantum Dot Arrays	3502490000								•					•			•		•							•	
69	Laser-Assisted Arc Welding for Aluminum Alloys	3502510000	•			•					•			•													•	
70	Reactivity of Metal-Oxide Surfaces	3502520000			•		•			•				•	•												•	
73	Exploiting LENS Technology Through Novel Materials	3502530000					•				•			•	•												•	
76	Molecular Characterization of Energetic Material Initiation	3502540000								•					•											•		
78	Nonvolatile Protonic Memory	3502550000						•										•									•	
81	Integration of Mesh Optimization with 3-D All-Hex Mesh Generation	3504340000	•		•	•	•		•	•	•		•	•	•	•	•	•	•	•				•			•	
83	Heterogeneous Simulation	3504350000					•				•		•		•							•	•		•		•	
86	Volumetric Video Motion Sensing for Unobtrusive Human-Computer Interactions	3504360000					•					•	•	•	•	•						•	•				•	
88	Hybrid Sparse-Dense Incomplete Factorization Preconditioners	3504370000											•										•				•	
91	Big Eddy—Advanced Large-Eddy Simulation Algorithms for Complex Flow Physics and Complex Geometry	3504380000	•				•			•		•									•						•	
93	Molecular Simulation of Reacting Systems	3504390000					•						•		•											•		
95	Massively Parallel Global Climate Model for Paleoclimate Applications	3504410000					•					•															•	
97	Fast and Easy Parallel I/O for Efficient Scientific Computing	3504420000					•			•		•										•					•	

Appendix F: Dual-Benefit Areas and Single-Use Categories

Pg #	Title	Project #	Aeronautics	Applied Molecular Biology	Ceramics	Composites	Computer Simulation and Modeling	Data Storage and Peripherals	Electronics and Photonics	Energy	Flexible Computer-Integrated Manufacturing	High-Definition Imaging and Displays	High-Performance Computing and Networking	High-Performance Metals and Alloys	Intelligent Processing Equipment	Material Synthesis and Processing	Medical Technology	Micro- and Nanofabrication	Micro- and Optoelectronics	Photonic Materials	Pollution Minimization, Remediation, and Waste Mgt.	Sensors and Signal Processing	Software	Surface Transportation Technologies	Systems Management Technologies	Defense-Related (mostly or purely)	Dual-Use (defense and non-defense-related)	Non-Defense-Related (mostly or purely)
202	Development of Magnetically Excited Flexural Plate-Wave Devices for Implementation as Physical, Chemical, and Acoustic Sensors, and as Integrated Micropumps for Sensored Systems	3506730000							•						•			•			•							•
205	Novel Acoustically Driven Microoptoelectronic Devices	3506740000					•		•								•	•	•	•		•						•
207	Photonics Integration Devices and Technologies	3506750000							•				•					•	•	•								•
210	Stress-Free Amorphous Diamond for High-Sensitivity Microsensors with Integrated Microstructures	3506760000							•									•	•			•						•
213	Semiconductor Current Filament Lasers	3506770000	•						•	•				•	•		•	•	•	•		•						•
215	Integration of Radiation-Hard Magnetic Random Access Memory with CMOS Integrated Circuits	3506780000							•									•	•	•						•		
218	Development of <i>In Situ</i> Diagnostics for Simultaneous Measurement of Transient Gas Species and Soot in Large Fires	3508250000					•			•											•	•			•			•
221	Micromechanical Failure Analyses for Finite-Element Polymer Modeling	3508260000	•			•			•		•					•												•
224	Methodology for Optimal Selection of Test and Simulation Levels for Problems Involving Computational Simulation	3508270000					•														•							•
226	A Phenomenological Model for Multicomponent Transport with Electrochemical Reactions in Concentrated Solutions	3508280000					•			•						•												•
228	Structural Simulations Using Multiresolution Material Models	3508290000			•	•	•									•												•
230	Lightning-Induced Arcing	3508310000					•																			•		

Appendix F: Dual-Benefit Areas and Single-Use Categories

Pg #	Title	Project #	Aeronautics	Applied Molecular Biology	Ceramics	Composites	Computer Simulation and Modeling	Data Storage and Peripherals	Electronics and Photonics	Energy	Flexible Computer-Integrated Manufacturing	High-Definition Imaging and Displays	High-Performance Computing and Networking	High-Performance Metals and Alloys	Intelligent Processing Equipment	Material Synthesis and Processing	Medical Technology	Micro- and Nanofabrication	Micro- and Optoelectronics	Photonic Materials	Pollution Minimization, Remediation, and Waste Mgt.	Sensors and Signal Processing	Software	Surface Transportation Technologies	Systems Management Technologies	Defense-Related (mostly or purely)	Dual-Use (defense and non-defense-related)	Non-Defense-Related (mostly or purely)
306	A Real-Time Decision-Support Framework to Guide Facility Response to Abnormal Events	3512320000					•						•								•	•	•		•		•	
308	Data Fusion for Chemical Sensing	3512330000		•			•															•					•	
310	Large-Scale Distributed Information System Modeling and Simulation	3512340000					•	•			•		•		•								•				•	
313	High-Surety SCADA for the Critical Energy Infrastructures	3512350000					•			•			•										•				•	
316	Agent-Based Mediation and Cooperative Information Systems	3512360000					•				•		•		•							•	•				•	
318	Dynamically Self-Configurable Network Protocol	3512370000																				•					•	
321	Optical Backplane/Interconnect for Super-High-Speed Communication	3512380000	•						•				•					•	•								•	
323	PUSH Technology Demonstration	3512390000					•	•					•		•								•				•	
325	Controlling Information: Its Flow, Fusion, and Coordination	3512410000					•						•		•							•					•	
327	Mission Surety for Large-Scale Real-Time Information Systems	3512420000					•						•									•	•				•	
329	Low-Power, Reduced-Computation, Public-Key Protocols	3512430000									•				•							•			•		•	
331	Ten-to-One-Hundred-Gigabit/Second Network Enabling R&D	3512440000					•		•				•														•	
333	High-Performance Commodity Interconnects for Clustered Scientific and Engineering Computing	3512450000					•	•			•		•														•	
336	AVATAR—Navigating and Mining in Massive Data	3512460000					•						•									•					•	
338	Algorithm-Based Fault Tolerance on Heterogeneous Massively Parallel Computers	3512470000					•	•			•		•		•							•	•			•		

Appendix F: Dual-Benefit Areas and Single-Use Categories

Pg #	Title	Project #	Aeronautics	Applied Molecular Biology	Ceramics	Composites	Computer Simulation and Modeling	Data Storage and Peripherals	Electronics and Photonics	Energy	Flexible Computer-Integrated Manufacturing	High-Definition Imaging and Displays	High-Performance Computing and Networking	High-Performance Metals and Alloys	Intelligent Processing Equipment	Material Synthesis and Processing	Medical Technology	Micro- and Nanofabrication	Micro- and Optoelectronics	Photonic Materials	Pollution Minimization, Remediation, and Waste Mgt.	Sensors and Signal Processing	Software	Surface Transportation Technologies	Systems Management Technologies	Defense-Related (mostly or purely)	Dual-Use (defense and non-defense-related)	Non-Defense-Related (mostly or purely)
341	Surface Decontamination of Bacterial Protein Toxins by RF Power	3514150000		•													•											•
343	Intense White-Light Pulse Propagation in Air Using Self-Guided Optical Filamentation: Applications to Remote Sensing and Countermeasures	3514160000							•										•	•		•				•		
346	Improved Backscatter X-Ray Detection for Antiterrorist Applications	3514170000							•			•							•	•		•					•	
348	HPM Vulnerability Assessment and Tests	3514180000							•										•	•		•				•		
350	Imaging of Moving Targets Using Simultaneous Synthetic Aperture Radar (SAR) and Moving Target Indicator (MTI) Radar	3516170000													•							•			•	•		
352	Sparse Geophysical Networks for Monitoring Deep Targets	3516180000					•								•							•				•		
354	Miniature Bioaerosol Concentrator	3516190000															•					•				•		
356	Recognizing Partially Obscured Targets by Combining Multiple Data Sources Using Evidential Reasoning	3516210000													•		•					•				•		
358	Computational Engineering of Sensor Materials and Integration with a Novel Biological Weapon Detection System	3516220000					•															•	•				•	
361	Biological Weapon Detector Using Bioaffinity Array Impedance Analysis with Chemical Amplification Through Redox Recycling	3516230000		•					•								•	•	•			•				•		
363	ATR / Exploitation Utilizing Ultra-High-Resolution, Complex SAR Imaging	3516240000																				•				•		

Appendix F: Dual-Benefit Areas and Single-Use Categories

Pg #	Title	Project #	Aeronautics	Applied Molecular Biology	Ceramics	Composites	Computer Simulation and Modeling	Data Storage and Peripherals	Electronics and Photonics	Energy	Flexible Computer-Integrated Manufacturing	High-Definition Imaging and Displays	High-Performance Computing and Networking	High-Performance Metals and Alloys	Intelligent Processing Equipment	Material Synthesis and Processing	Medical Technology	Micro- and Nanofabrication	Micro- and Optoelectronics	Photonic Materials	Pollution Minimization, Remediation, and Waste Mgt.	Sensors and Signal Processing	Software	Surface Transportation Technologies	Systems Management Technologies	Defense-Related (mostly or purely)	Dual-Use (defense and non-defense-related)	Non-Defense-Related (mostly or purely)
365	Thin-Skin Deployable Mirrors for Remote Sensing Systems	3516250000																	•	•		•					•	
368	Dispersible Granular Sensor (Smart Sand) for Landmine Detection Based on TNT Immunoassay	3516260000														•						•				•		
371	Characterization of Underground Facilities in an Urban Environment	3516270000																				•				•		
373	Dexterous Robotic Manipulation of Hazardous Materials in Unstructured Environments	3516280000													•							•	•				•	
376	Autonomous Dynamic Soaring Platform for Distributed Mobile Sensor Arrays	3516290000	•				•															•	•				•	
378	Miniature UV Fluorescence-Based Biological Agent Sensor	3516310000						•								•		•				•					•	
381	Automatic Planning of Life-Cycle Assembly Processes	3516320000					•																				•	
384	Analysis of Very Large Assemblies	3516330000					•																				•	
386	Enabling Human Skills with Cooperative Automation	3516340000					•				•				•							•	•				•	
389	Cloud to CAD	3516350000	•				•				•	•	•									•	•				•	
392	Ergonomics in Life-Cycle Assembly Processes	3516360000					•																				•	
395	Feature Reduction of Geometric Solid Models for Analysis Tools	3516370000					•																				•	
397	Electrokinetic Immunoaffinity Chemical Sensors	3516380000	•														•					•					•	
401	Designed Synthesis of Controlled Degradative Materials	3518160000				•										•						•					•	
403	Mechanistic Models for Radionuclide Desorption from Soils	3518170000								•												•					•	
404	Adaptive 3-D Sensing	3518180000					•			•			•		•							•	•	•			•	

Appendix F: Dual-Benefit Areas and Single-Use Categories

Pg #	Title	Project #	Aeronautics	Applied Molecular Biology	Ceramics	Composites	Computer Simulation and Modeling	Data Storage and Peripherals	Electronics and Photonics	Energy	Flexible Computer-Integrated Manufacturing	High-Definition Imaging and Displays	High-Performance Computing and Networking	High-Performance Metals and Alloys	Intelligent Processing Equipment	Material Synthesis and Processing	Medical Technology	Micro- and Nanofabrication	Micro- and Optoelectronics	Photonic Materials	Pollution Minimization, Remediation, and Waste Mgt.	Sensors and Signal Processing	Software	Surface Transportation Technologies	Systems Management Technologies	Defense-Related (mostly or purely)	Dual-Use (defense and non-defense-related)	Non-Defense-Related (mostly or purely)
406	Aqueous Organic Sensor	3518190000																			•	•					•	
409	Designed Ionophores for Liquid-Membrane Separation and Extraction of Metal Ions	3518210000					•																				•	
412	An Electromagnetic Imaging System for Environmental Site Reconnaissance	3518220000							•										•			•					•	
414	Advanced Geosphere Transport Simulation	3518230000					•		•	•			•									•					•	
418	Hybrid Processing of Measurable and Subjective Information in Surety Analysis	3520340000	•				•																•		•		•	
420	Computer-Network Vulnerability-Analysis Method	3520350000					•																		•		•	
423	Approximate Public-Key Authentication with Information Hiding	3520360000													•								•				•	
424	New Network Analysis Approaches to Evaluate Infrastructure Risk and Reliability	3520370000					•					•	•											•	•		•	
426	Improved Tools for Identifying and Quantifying Potentially Dangerous Human Actions	3520380000	•							•																	•	
428	Advanced Signal Processing for Thermal Flaw Detection	3520390000	•		•	•				•	•											•		•			•	
431	Production Surety and Disruption Vulnerability Analysis	3520410000					•					•	•											•			•	
433	An Optically Triggered Semiconductor Switch for Firing Systems	3520420000							•										•			•				•		
436	Source Code Assurance Tool	3520430000																					•				•	
438	System-Surety Life-Cycle Engineering	3520440000					•			•	•					•						•		•		•	•	

Appendix F: Dual-Benefit Areas and Single-Use Categories

Pg #	Title	Project #	Aeronautics	Applied Molecular Biology	Ceramics	Composites	Computer Simulation and Modeling	Data Storage and Peripherals	Electronics and Photonics	Energy	Flexible Computer-Integrated Manufacturing	High-Definition Imaging and Displays	High-Performance Computing and Networking	High-Performance Metals and Alloys	Intelligent Processing Equipment	Material Synthesis and Processing	Medical Technology	Micro- and Nanofabrication	Micro- and Optoelectronics	Photonic Materials	Pollution Minimization, Remediation, and Waste Mgt.	Sensors and Signal Processing	Software	Surface Transportation Technologies	Systems Management Technologies	Defense-Related (mostly or purely)	Dual-Use (defense and non-defense-related)	Non-Defense-Related (mostly or purely)
440	Integrated Approach to Develop Microelectromechanical System (MEMS) Reliability Tools	3520450000					•	•	•									•	•							•		
444	Simulation/Optimization Tools for System-Variability Analysis	3520460000					•	•				•											•			•		
447	A Massively Parallel Microsimulation Model of Infrastructure Interdependency	3520470000					•		•			•																•
450	Physical Models for Predicting the Effect of Atmospheric Corrosion on Microelectronic Reliability	3520480000							•										•							•		
453	Backside Localization of Open and Shorted IC (Integrated Circuit) Interconnections	3520490000							•								•										•	
456	Reliability Predictions for Advanced Electronics in Smoke Environments	3520510000							•																		•	
458	Security of Bulk Power Systems	3520520000					•		•			•															•	
461	Science on the Microdomain	3522010000															•	•									•	
464	Autonomous MicroChem Laboratory (μChemLab)	3522020000		•				•	•						•	•	•	•	•	•	•	•	•				•	
467	Cooperative, Distributed Sensing and Action Using Microminiature, Intelligent Agents	3522030000					•								•						•	•	•		•		•	
469	Engineering Complex Distributed Systems	3522040000					•				•	•			•			•				•	•				•	
473	Laser Communication Nanosatellites	3522050000					•	•	•	•	•		•	•	•	•	•	•	•	•	•	•	•		•		•	
479	Information Collection (Acquisition of Information from Denied Areas)	3522060000					•	•	•			•				•		•	•			•	•		•		•	
481	Accelerated Molecular Discovery Arrays—The Next Revolution in Biotechnology	3522070000		•											•	•	•					•					•	
485	Microcode Evaluation	3530140000													•								•				•	

Appendix F: Dual-Benefit Areas and Single-Use Categories

Pg #	Title	Project #	Aeronautics	Applied Molecular Biology	Ceramics	Composites	Computer Simulation and Modeling	Data Storage and Peripherals	Electronics and Photonics	Energy	Flexible Computer-Integrated Manufacturing	High-Definition Imaging and Displays	High-Performance Computing and Networking	High-Performance Metals and Alloys	Intelligent Processing Equipment	Material Synthesis and Processing	Medical Technology	Micro- and Nanofabrication	Micro- and Optoelectronics	Photonic Materials	Pollution Minimization, Remediation, and Waste Mgt.	Sensors and Signal Processing	Software	Surface Transportation Technologies	Systems Management Technologies	Defense-Related (mostly or purely)	Dual-Use (defense and non-defense-related)	Non-Defense-Related (mostly or purely)
486	Model-Based Design and Analysis of Remote Access Monitoring Systems	3530150000													•							•	•				•	
489	Microwave Imaging Through Walls	3530160000										•										•					•	
490	Research of the Utility of Polarimetric Sensing	3530170000																				•					•	
492	Real-Time Image Analysis Using Field-Programmable Gate Arrays	3530180000										•			•							•					•	
494	Poco Switch Tubes	3531340000																									•	
495	Chemiresistors Based on Metal-Loaded Polymers for Solvent Spill Detection	3531350000				•			•						•			•	•		•	•					•	
497	Advance Neutron-Tube Design and Producibility	3531360000			•										•											•		
498	Surface Hardening by Nanoparticle Precipitation and Atomic Clustering in Ni(Al ₂ O ₃)	3531370000												•	•			•									•	
499	Dynamical Properties of Polymers: Computational Modeling	3531380000	•				•			•																	•	
501	Broadening Mechanism in 2-D Excitonic and Electron Gases	3531390000					•	•	•									•	•		•							•
503	Calculation and Interpretation of the Energies that Underlie Transition-Metal Surface Structure	3531410000		•																							•	
505	Interfacial Reactions in Ceramic Systems	3531420000			•	•				•					•									•			•	
508	Direct Fabrication of Multifunctional Nanocomposites Via Supramolecular Self-Assembly	3531430000			•	•			•						•			•		•							•	
511	Raman Investigation of Phase Changes in PZT Materials	3531440000			•		•																			•		
513	Information Extraction from Hyperspectral Images Obtained from Satellites	3531450000					•	•	•						•	•	•	•	•	•	•	•	•				•	

Appendix F: Dual-Benefit Areas and Single-Use Categories

Pg #	Title	Project #	Aeronautics	Applied Molecular Biology	Ceramics	Composites	Computer Simulation and Modeling	Data Storage and Peripherals	Electronics and Photonics	Energy	Flexible Computer-Integrated Manufacturing	High-Definition Imaging and Displays	High-Performance Computing and Networking	High-Performance Metals and Alloys	Intelligent Processing Equipment	Material Synthesis and Processing	Medical Technology	Micro- and Nanofabrication	Micro- and Optoelectronics	Photonic Materials	Pollution Minimization, Remediation, and Waste Mgt.	Sensors and Signal Processing	Software	Surface Transportation Technologies	Systems Management Technologies	Defense-Related (mostly or purely)	Dual-Use (defense and non-defense-related)	Non-Defense-Related (mostly or purely)
515	Expanding the Security Dimension of Surety	3531460000					•																			•		
516	Overcoming Software Brittleness: A Swarm Intelligence Approach	3531470000					•	•	•						•							•	•				•	
518	Synthesis and Applications of N-Type Diamond	3531480000							•	•						•						•					•	
521	A Molecular Theory of Gatekeeper Proteins	3531490000		•			•										•										•	
523	Development of Compact UV Laser Source for Climate Studies and Chemical Sensing	3531510000							•	•												•	•				•	
525	Power Source Technologies for Autonomous Microsystems	3531520000	•						•					•	•		•					•					•	
526	Advanced Radiation Sources: Rayleigh-Taylor Mitigation Via Perturbation Reduction	3532280000					•															•					•	
528	Global Approaches to Infrastructural Analysis (GAIA)	3532290000					•																					•
530	Capillary Elastohydrodynamics in Manufacturing Processes	3532310000			•	•	•	•	•	•	•	•				•	•	•	•			•	•				•	
532	Real-Time Design of Improved Powder Pressing Dies Using Finite-Element Method Modeling	3532320000			•		•				•		•	•		•							•				•	
535	Computational Methods for Predicting the Response of Critical As-Built Infrastructure to Dynamic Loads (Architectural Surety)	3532330000					•						•														•	
537	Solar-Grade Silicon	3533190000								•				•														•
539	Low-Work-Function Thermionic Emission Materials	3533210000			•				•	•							•										•	
541	Develop Mathematical Algorithms for the Integration of Disparate Information to Determine Critical Infrastructure Health and Status	3533220000					•			•													•	•		•		

Appendix F: Dual-Benefit Areas and Single-Use Categories

Pg #	Title	Project #	Aeronautics	Applied Molecular Biology	Ceramics	Composites	Computer Simulation and Modeling	Data Storage and Peripherals	Electronics and Photonics	Energy	Flexible Computer-Integrated Manufacturing	High-Definition Imaging and Displays	High-Performance Computing and Networking	High-Performance Metals and Alloys	Intelligent Processing Equipment	Material Synthesis and Processing	Medical Technology	Micro- and Nanofabrication	Micro- and Optoelectronics	Photonic Materials	Pollution Minimization, Remediation, and Waste Mgt.	Sensors and Signal Processing	Software	Surface Transportation Technologies	Systems Management Technologies	Defense-Related (mostly or purely)	Dual-Use (defense and non-defense-related)	Non-Defense-Related (mostly or purely)
570	Ultra-Intense Femtosecond Laser Interactions with Applications to High-Field Physics, Enhanced Electromagnetic Coupling in Materials, and X-Ray Generation	3535280000							•										•	•						•		
572	Design of a Prototypical Snoopy Coprocessor for DynaMICs Software Fault Monitoring with Integrity Constraints	3537190000	•												•		•								•		•	
574	Analytic Verification of Treaties, Protocols, and International Agreements	3537210000					•															•					•	
575	Fabricating Microcomponents from Silicon-Carbonitride by a Novel Microcasting Process	3537220000			•					•					•	•	•	•				•					•	
577	Magnetic Polysilicon MEMS Devices	3537230000				•			•						•			•	•			•					•	
579	Living Tissue Engineering	3537240000	•				•			•													•				•	
581	The Use of Active Fiber Composites for the Health Monitoring of Wind Turbine Blades	3537250000				•																•					•	
583	Developing/Assessing Long-Term Impact of Design Innovations	3537260000					•															•			•		•	
584	Composite Wire Plasma Formation and Evolution	3537270000					•																			•		
587	DNA Microarray Technology	3537280000					•	•									•						•				•	
588	Research Issues in the System Engineering Aspects of High Assurance	3537290000	•				•	•					•				•	•					•				•	
590	Investigation of Lateral Composition Modulation in GaAsSb Short-Period Superlattices	3537310000						•	•	•						•		•	•	•							•	
592	New Complexing Agent for Co(II) Analysis for CP	3537320000																								•		

Appendix F: Dual-Benefit Areas and Single-Use Categories

Pg #	Title	Project #	Aeronautics	Applied Molecular Biology	Ceramics	Composites	Computer Simulation and Modeling	Data Storage and Peripherals	Electronics and Photonics	Energy	Flexible Computer-Integrated Manufacturing	High-Definition Imaging and Displays	High-Performance Computing and Networking	High-Performance Metals and Alloys	Intelligent Processing Equipment	Material Synthesis and Processing	Medical Technology	Micro- and Nanofabrication	Micro- and Optoelectronics	Photonic Materials	Pollution Minimization, Remediation, and Waste Mgt.	Sensors and Signal Processing	Software	Surface Transportation Technologies	Systems Management Technologies	Defense-Related (mostly or purely)	Dual-Use (defense and non-defense-related)	Non-Defense-Related (mostly or purely)
594	Enzyme-Mediated Electrochemical Redox Polymer Microelectronic Biosensor for V- and G-Type Chemical Weapons	3537330000							•							•	•				•					•		
596	Design and Optimization of VLSI Systems and Reconfigurable Hardware	3537340000					•	•										•								•		
598	Hydrodynamic Flow in Biosystems	3537350000	•	•	•	•						•			•													•
600	IR Polarimetry and Lithographic Alignment	3537360000						•										•			•					•		
602	Shock Response of Diamond Crystals	3537370000							•																	•		
603	Dynamic Computer-Aided Design Analysis of Containment Vessels for Z-Pinch Experiments	3537390000					•		•	•																•		
604	Investigation of Nanoscience Technologies	3537410000						•			•																•	
605	Surety Science	3537420000	•				•		•			•										•	•	•		•		
608	Stabilization of Enzymatic Molecular Recognition Materials Via Crystallization and Crosslinking	3537430000		•				•								•	•									•		
610	Novel Biosensor Fabrication Techniques	3537440000		•				•								•	•									•		

Author and Title Index

A B C D E F G H I J K L M N O P Q R S T U V W X Y Z
A

- Abate, M. L.
Analytic Verification of Treaties, Protocols, 574
- Abnormal, 306
- Accelerate, 481
- Accelerated Strategic Computing Initiative, 102
- Access, 486
- Acoustic
Microoptical Devices, 205
Sensors, 202
- Actuator, 555
- Adams, D. P.
Advanced Machining for Microfabrication, 294
Monitoring Thin-Film Deposition, 268
- Adaptive, 404
- Adaptive Visualization Aid for Touring and Recovery, 336
- Adhesive, 278
- Adiabatic, 232
- Adkins, D. R.
Flexural Plate-Wave Devices in Sensors, 202
- Adolf, D. B.
Finite-Element Polymer Modeling, 221
Structural Simulations Using Material Models, 228
- Agent
Bio/Chem, 243
Cooperative Information Systems, 316
Intelligent, 123
- Aging, 42
- Aidun, J. B.
Phase Changes in PZT Materials, 511
- Air, 343
- Aircraft, 567
- Algorithm
Fault Tolerance, 338
Infrastructure Status, 541
Large-Eddy Simulation, 91
Materials Aging Diagnostics, 42
- Alignment, 600
- Allan, B. A.
MPP Numerical Simulation of Diesel Autoignition, 552
- Allen, J. J.
Standard Cells for MEMS, 281
- Allendorf, S. W.
Transient Gas Species and Soot in Large Fires, 218
- Allerman, A. A.
Composite-Resonator Surface-Emitting Lasers, 167
Integration of Optoelectronics and MEMS, 146
Laser Communication Nanosatellites, 473
Photonics Integration Devices and Technologies, 207
Short-Pulsed Power in Active Optical Sensors, 149
VCSELs and Detectors for Microsystems, 182
- Alloy
Arc Welding, 69
Wetting and Spreading Dynamics, 39
- Aluminum, 69
- Alvin, K. F.
Modeling Uncertainties in Simulation, 112
Simulation Levels for Computational Simulation, 224
- Amatucci, V. A.
Fluid/Solid and Fluid/Fluid Interactions, 245
- Ames, A. L.
Cloud to CAD, 389
- Amplification, 361
- Anderson, D. J.
Reliability of Electronics in Smoke Environments, 456
- Anderson, R. A.
Lightning-Induced Arcing, 230
Nonvolatile Protonic Memory, 78
Quantum Dot Arrays, 67
- Anderson, R. J.
Cooperative Automation, 386
Ergonomics in Life-Cycle Assembly, 392
Robotic Manipulation of Hazardous Materials, 373
Synthesis and Applications of N-Type Diamond, 518
- Anex, D. S.
Accelerated Molecular Discovery Arrays, 481
Data Fusion for Chemical Sensing, 308
Electrokinetic Immunoaffinity Chemical Sensors, 397
- Anthes, J. P.
Information Collection, 479
- Antolak, A. J.
Applied Microfluidic Physics, 239
- Aperture, 350
- Aqueous, 406
- Arc
Lightning-Induced, 230
Welding, 69
- Architectural (Surety), 535
- Arguello, J. G., Jr.
Design of Powder Pressing Dies Using Modeling, 532
- Armistead, D. J.
Fluid/Solid and Fluid/Fluid Interactions, 245
- Armstrong, R. C.
High-Performance Commodity Interconnects, 333
Scalable Tools for Distributed Computing, 132
- Arnold, D. W.
Applied Microfluidic Physics, 239
Autonomous MicroChem Laboratory, 464
Pathogen Detection Using Microseparations, 557
- Array
Accelerated Molecular Discovery, 481
Biological Weapon Detector, 361
DNA, 587
Field-Programmable Gate, 492
Mobile Sensors, 376
Nano, 37
Quantum Dot, 67
Volatile Organic Detection, 156
- As-Built, 535

Author and Title Index

- Asbill, R. E.
Integration of Optoelectronics and MEMS, 146
- ASCII
see Accelerated Strategic Computing Initiative
- Ashbaugh, D. M.
Signal Processing for Thermal Flaw Detection, 428
- Ashby, C. I. H.
Diamond for High-Sensitivity Microsensors, 210
Dry Etching for Manufacturing, 158
High-Throughput Dry Processes, 287
- Ashley, C. S.
Smart Sand for Landmine Detection, 368
- Assurance
Low-Volume Manufacturing, 290
Source Code, 436
System Engineering, 588
- Asta, M. D.
Atomistic Computations with Phase-Field Modeling, 31
- Atomic
Surface Hardening, 498
Surfactant-Directed Materials Growth, 58
- Atomistic
Crack Nucleation and Modeling, 236
Phase-Field Modeling, 31
- Attaway, S. W.
Architectural Surety, 535
- Aurand, J. F.
TRIBICC Imaging, 164
- Authentication, 423
- Autoignition, 552
- Automation
Cooperation, 386
Life-Cycle Assembly, 381
- Autonomous
MicroChem Lab, 464
Microsystems, 525
Mobile Sensors, 376
- AVATAR
see Adaptive Visualization Aid for Touring & Recovery
- B**
- Baca, A. G.
Imaging for Environmental Site Reconnaissance, 412
Integrated Chemical Microsensors in GaAs, 179
Micromachined Tuners for Microwave Circuits, 195
Optically Triggered Switch for Firing Systems, 433
Role of Defects in III-Nitride-Based Electronics, 169
Semiconductor Current Filament Lasers, 213
- Backplane, 321
- Backscatter, 346
- Backside, 453
- Bacon, L. D.
HPM Vulnerability Assessment and Tests, 348
- Baer, M. R.
Dispersive Measurements of Velocity, 259
- Baer, T. A.
Freeforming of Ceramics from Colloidal Slurries, 64
- Baeza, A. R.
Real-Time Image Analysis, 492
- Bailey, C. G.
Autonomous MicroChem Laboratory, 464
- Baldwin, J. M.
Fusion of Data Using Real-Time Visualization, 296
- Ballistic, 566
- Bammann, D. J.
Recrystallization of Metals with Material Models, 247
- Barbour, J. C.
Critical Copper-Corrosion Mechanisms, 34
Monitoring Corrosion in Weapons Environments, 26
- Barnes, S. M.
Standard Cells for MEMS, 281
- Barney, P. S.
Real-Time Error Correction Using Spindles, 267
- Bartel, L. C.
Sparse Geophysical Networks, 352
- Bartelt, M. C.
Crack Nucleation and Growth Modeling, 236
- Bartelt, N. C.
Self-Assembled Templates for Materials Growth, 37
Surfactant-Directed Materials Growth, 58
- Bartholomew, J. W.
Overcoming Software Brittleness, 516
Sensor Arrays for Volatile Organic Detection, 156
- Barton, D. C.
Microsimulation Model of Infrastructure, 447
- Barton, D. L.
Backside Localization of IC Interconnections, 453
- Bartram, M. E.
Self-Assembled Templates for Materials Growth, 37
- Battaile, C. C.
Materials Response Simulations, 104
Monitoring Corrosion in Weapons Environments, 26
- Beaver, C. L.
Public-Key Authentication, 423
Reduced-Computation Public-Key Protocols, 329
- Benavides, G. L.
Advanced Machining for Microfabrication, 294
Parallel Mechanism Technology to Manufacturing, 276
- Bennett, R. S.
Radiation-Hard Random Access Memory, 215
- Benson, D. A.
Backside Localization of IC Interconnections, 453
- Bentley, A. E.
SCADA for the Critical Energy Infrastructures, 313
- Beresh, S. J.
Fluid/Solid and Fluid/Fluid Interactions, 245
- Berg, T. M.
Controlling Information Flow and Fusion, 325
Data Fusion for Chemical Sensing, 308
- Berry, N. M.
Data Fusion for Chemical Sensing, 308
- Bespalko, S. J.
Surety for Real-Time Information Systems, 327

Author and Title Index

- Bieg, L. F.
Parallel Mechanism Technology to Manufacturing, 276
- Billau, R. F.
Simulation/Optimization Tools, 444
- Billington, R. A.
Agent-Based Mediation, 316
Engineering Complex Distributed Systems, 469
- Bioaerosol, 354
- Bioaffinity, 361
- Biological
Bioaffinity Array, 361
Decontamination Systems, 567
Fluorescence-Based Sensor, 378
Pathogen Detection, 557
Sensor Material for Weapon Detection, 358
- Biosensor
Chemical Weapons, 594
Novel Fabrication, 610
- Biosystems, 598
- Bitsie, F.
Microdiagnostic MEMS Lab-on-a-Chip, 265
- Blade (turbine), 581
- Blair, D. S.
Aqueous Organic Sensor, 406
- Blake, R. J.
Deployable Mirrors for Remote Sensing, 365
- Bliss, D. E.
Intense White-Light Pulse Propagation in Air, 343
Z-Backlighter Technologies, 568
- Boebert, W. E.
PUSH Technology Demonstration, 323
- Boettcher, G. E.
Poco Switch Tubes, 494
- Bogdan, C. W.
Reliability of Electronics in Smoke Environments, 456
- Bond, 278
- Borns, D. J.
Models for Radionuclide Desorption from Soils, 403
- Boslough, M. B.
Distributed Mobile Sensor Arrays, 376
Global Climate Model for Paleoclimate Applications, 95
- Bow, W. J.
IFSAR Rapid Terrain Visualization, 564
Ultra-High-Resolution Complex SAR Imaging, 363
- Boyack, K. W.
Visual Explanation and Insight, 137
- Brady, P. V.
Models for Radionuclide Desorption from Soils, 403
- Brainard, J. P.
Advance Neutron-Tube Design and Producibility, 497
Monitoring Thin-Film Deposition, 268
- Braithwaite, J. W.
Corrosion of Microelectronic Reliability, 450
Critical Copper-Corrosion Mechanisms, 34
- Brandt, L. D.
Guided Facility Response to Abnormal Events, 306
- Braze, 39
- Breiland, W. G.
Critical Copper-Corrosion Mechanisms, 34
Dry Etching for Manufacturing, 158
- Brenkosh, J. P.
High-Performance Commodity Interconnects, 333
Varying QoS for Fixed and Mobile Networks, 303
- Briggs, R. D.
VCSELs and Detectors for Microsystems, 182
- Brightwell, R. B.
Programming Paradigms for Parallel Computers, 128
- Brinker, C. J.
Fabrication Via Supramolecular Self-Assembly, 508
Self-Assembled Templates for Materials Growth, 37
Smart Sand for Landmine Detection, 368
Smart Self-Assembled Photochromic Films, 24
- Brittle, 516
- Brocato, R. W.
Design and Optimization of VLSI Systems, 596
- Brock, B. C.
Laser Communication Nanosatellites, 473
- Brockmann, J. E.
Enabling Cold-Spray Direct Fabrication, 55
Guided Facility Response to Abnormal Events, 306
Reliability of Electronics in Smoke Environments, 456
Simulation of Chem/Bio Agents in Infrastructures, 243
- Brooks, J. A.
LENSTM Technology and Novel Materials, 73
- Brown, F. A.
Develop MEMS Reliability Tools, 440
- Brown, R. G.
Automatic Planning of Life-Cycle Assembly, 381
Analysis of Very Large Assemblies, 384
- Brown, T. J.
Determining Critical Infrastructure Status, 541
- Brozik, S. M.
Biological Weapon Detector, 361
- Bruskas, L. A.
Dry Etching for Manufacturing, 158
- Bryan, J. R.
Microsensors in Miniature Robotic Vehicles, 151
- Buchheit, T. E.
Laser Wire Deposition for Fully Dense Shapes, 284
Materials Response Simulations, 104
- Burg, M. S.
Standard Cells for MEMS, 281
- Burns, A. R.
Smart Self-Assembled Photochromic Films, 24
- Burst, 141
- Buss, R. J.
High-Throughput Dry Processes, 287
- Butler, M. A.
Information Collection, 479
- Butler, P. C.
Security of Bulk Power Systems, 458
- Buttram, M. T.
Laser Interactions for Electromagnetic Coupling, 570

Author and Title Index

- Buttz, J. H.
 Distributed Sensing Using Intelligent Agents, 467
- BW
see Biological (Weapon)
- Byrne, R. H.
 Microsensor in Miniature Robotic Vehicle, 151
- C**
- CAD
see Computer-Aided Design
- Calton, T. L.
 Analysis of Very Large Assemblies, 384
 Automatic Planning of Life-Cycle Assembly, 381
 Ergonomics in Life-Cycle Assembly, 392
- Cameron, S. M.
 Intense White-Light Pulse Propagation in Air, 343
 Laser Interactions for Electromagnetic Coupling, 570
 Z-Backlighter Technologies, 568
- Campbell, D. V.
 Radiation-Hard Sensors for Space-Based Sensing, 191
- Campbell, J. E.
 Simulation/Optimization Tools, 444
- Campbell, P. L.
 Source Code Assurance Tool, 436
- Capillary, 530
- Carlson, J. J.
 Adaptive 3-D Sensing, 404
 Ergonomics in Life-Cycle Assembly, 392
 Scripting for Video Inspection, 292
 Video Sensing for Human-Computer Interactions, 86
 WNN Decision Making for Data Mining, 301
- Carlson, R. E.
 SCADA for the Critical Energy Infrastructures, 313
- Carpick, R. W.
 Self-Healing Molecular Assemblies in MEMS, 29
 Smart Self-Assembled Photochromic Films, 24
- Carr, M. J.
 Intelligent Polymers for Nanodevice Control, 62
 Synthesis of Controlled Degradative Materials, 401
- Carr, R. D.
 Optimization for Scheduling Problems, 125
- Casalnuovo, S. A.
 Acoustically Driven Microoptoelectronics, 205
 AlGa_N Materials Engineering, 184
 Integrated Chemical Microsensors in GaAs, 179
 Post-Processed Integrated Microsystems, 188
- CBW
see Biological (Biological/Chemical Weapons)
- Celina, M. C.
 Aging Diagnostics Through Hyperspectral Imaging, 42
- Ceramic
 Freeforming, 64
 Interfacial Reactions, 505
- Cernosek, R. W.
 Monitoring Corrosion in Weapons Environments, 26
- Cesarano, J., III
 Freeforming of Ceramics from Colloidal Slurries, 64
 Simulations of Self-Assembling Macrosystems, 139
- Chakerian, S. Y.
 Computer-Network Vulnerability-Analysis, 420
- Chambers, R. S.
 Finite-Element Polymer Modeling, 221
 Structural Simulations Using Material Models, 228
- Chambers, W. B.
 Autonomous MicroChem Laboratory, 464
- Chanchani, R.
 Flexural Plate-Wave Devices in Sensors, 202
- Chem/Bio
see Biological
- Chemiresistors, 495
- Chen, H. Y.
 High-Performance Commodity Interconnects, 333
 Super-High-Speed Communication, 321
- Chen, J. H.
 MPP Numerical Simulation of Diesel Autoignition, 552
- Chen, K. S.
 Model for Multicomponent Transport, 226
- Chen, P. C.
 Fast and Easy Parallel I/O, 97
- Chhabildas, L. C.
 Dispersive Measurements of Velocity, 259
- Chinn, D. A.
 Accelerated Molecular Discovery Arrays, 481
 Electrokinetically Driven Mesoscale Actuators, 555
- Choquette, K. D.
 Composite-Resonator Surface-Emitting Lasers, 167
 VCSELs and Detectors for Microsystems, 182
- Chow, W. W.
 Composite-Resonator Surface-Emitting Lasers, 167
 Photonics Integration Devices and Technologies, 207
 Semiconductor Current Filament Lasers, 213
 Short-Pulsed Power in Active Optical Sensors, 149
- Christenson, T. R.
 Post-Processed Integrated Microsystems, 188
 Precision-Formed Micromagnets, 161
- Chu, D. D.
 Biological Weapon Detector, 361
 Ultra-Low-Power Sensors for Microtelemetry, 172
- Circuit
 Backside Localization, 453
 Microwave, 195
 Radiation-Hard, 215
- Claassen, J. P.
 Characterization of Underground Facilities, 371
 Sparse Geophysical Networks, 352
- Clark, D. F.
 Solid-State Neutron Generator in Nuclear Weapons, 272
- Clay, R. L.
 MPP Numerical Simulation of Diesel Autoignition, 552
- Cleaning, 278

Author and Title Index

- Climate
 Model, 95
 Study, 523
- Cloer, B. K.
 LDRD Program Overview, 13
- Cloud, 389
- Cluster
 Computing, 333
 Surface Hardening, 498
- Coats, R. S.
 Novel Load-Balancing for Simulation Software, 99
- Code
 Assurance Tool, 436
 Electronic Structure, 110
 Microcode, 485
- Cole, E. I., Jr.
 Backside Localization of IC Interconnections, 453
 Microcode Evaluation, 485
- Collective, 567
- Collins, E. W.
 High Reliability in Low-Volume Manufacturing, 290
 Simulation/Optimization Tools, 444
- Colloidal, 64
- Commodity, 333
- Communication
 High-Speed, 321
 Nanosatellites, 473
- Compact, 523
- Composite
 Active Fiber, 581
 Freeforming, 64
 Nanocomposite, 508
 Surface-Emitting Lasers, 167
 Wire Plasma, 584
- Computer
 Architectural Surety, 535
 BW Detection System, 358
 Commodity Interconnects, 333
 Containment Vessels, 603
 Distributed, 132
 Fault Tolerance, 338
 Network Vulnerability, 420
 Parallel I/O, 97
 Predicting Fracture, 261
 Programming Paradigms, 128
 Public-Key Protocols, 329
 Unstructured Grid Problems, 130
 Video Motion Sensing, 86
 see also: Model
 see also: Simulation
- Computer-Aided Design, 389
- Computer Sciences, 80–141**
- Concentrator, 354
- Containment, 603
- Cooper, J. A.
 Processing of Information in Surety Analysis, 418
- Cooperative
 Automation, 386
 Distributed Sensing, 467
 Information Systems, 316
- Coprocessor, 572
- Cordaro, J. T.
 Imaging of Moving Targets Using SAR and MTI, 350
- Corporate Objectives, 484–610**
- Corrosion
 Copper, 34
 Microelectronics, 450
 Monitoring, 26
- Coupling, 570
- Cox, R. G.
 Determining Critical Infrastructure Status, 541
 Network Analysis for Infrastructure Reliability, 424
- Crack, 236
- Craft, R. L.
 Source Code Assurance Tool, 436
- Crawford, M. H.
 AlGa_N Materials Engineering, 184
 Role of Defects in III-Nitride-Based Electronics, 169
 Smart Self-Assembled Photochromic Films, 24
 Science on the Microdomain, 461
 UV Fluorescence Biological Agent Sensor, 378
- Crocker, R. W.
 Gas-to-Liquid Microabsorber, 547
- Crosslink, 608
- Crowder, S. V.
 High Reliability in Low-Volume Manufacturing, 290
- Crowell, J. A.
 Computational Method for Predicting Fracture, 261
- Crystal
 Diamond, 602
 Metals, 247
 Molecular Recognition Materials, 608
 Photonic, 193
- Cummings, E. B.
 Applied Microfluidic Physics, 239
- Curro, J. G.
 Integrated Modeling of Hydrogenic Materials, 108
 Modeling Dynamical Properties of Polymers, 499
 Optimization of Filled Polymer Materials, 270
 Synthesis of Controlled Degradative Materials, 401
 The Impact of Cleaning on Adhesive Bond, 278
- D**
- Daily, M. R.
 Flexural Plate-Wave Devices in Sensors, 202
- Dalton, L. J.
 Snoopy Coprocessor for Software Fault Monitoring, 572
- Dandini, V. J.
 Identifying Potentially Dangerous Human Actions, 426
- Data Mining
 AVATAR, 336
 WNN, 301

Author and Title Index

- Davidson, G. S.
 DNA Microarray Technology, 587
 Evolvable Hardware, 234
- Dawson, D. B.
 Mechanisms of Adiabatic Shear Failure, 232
- Dean, L. B.
 Dynamically Self-Configurable Network Protocol, 318
 Laser Communication Nanosatellites, 473
 Super-High-Speed Communication, 321
 Ten-to-One-Hundred-Gigabit/Second Networking, 331
- de Boer, M. P.
 Diamond for High-Sensitivity Microsensors, 210
 Fundamental Aspects of Micromachine Reliability, 52
 Microdiagnostic MEMS Lab-on-a-Chip, 265
 Standard Cells for MEMS, 281
- Decontamination
 Bacterial Toxins, 341
 Closed Environments, 567
- Defects, 169
- Defense, 566
- Degradative, 401
- Deland, S. M.
 Model-Based Design of Remote Access Monitoring, 486
- Denham, H. B.
 Freeforming of Ceramics from Colloidal Slurries, 64
- Density, 110
- Deoxyribonucleic Acid, 587
- Deployable, 365
- Deposition
 Laser Wire, 284
 Thin-Film, 268
- De Sapio, V.
 Fusion of Data Using Real-Time Visualization, 296
 Parallel Mechanism Technology to Manufacturing, 276
- Desiena, T. H.
 Microcode Evaluation, 485
- Design
 Containment Vessels, 603
 Degradative Materials, 401
 Innovations, 583
 Ionophores, 409
 Monitoring Systems, 486
 Neutron-Tube, 497
 Powder Pressing Dies, 532
 SERAPHIM, 543
 Snoopy Coprocessor, 572
 VLSI, 596
- Desjardin, P. E.
 Lagrangian Modeling of Radiative Transport, 255
- Desjarlais, M. P.
 Radiation Sources: Rayleigh-Taylor Mitigation, 526
- Desorption, 403
- Detect
 Backscatter X-Ray, 346
 Bioaffinity Array for BW, 361
 Landmine, 368
 Microsystems, 182
- Novel Biological Weapon, 358
- Pathogen, 557
- Solvent Spill, 495
- Thermal Flaw, 428
- Volatile Organic, 156
- Diagnostic
 Corrosion, 26
 Lab-on-a-Chip, 265
 Large Fires, 218
 Materials Aging, 42
 Rotating Flowfields, 245
- Diamond
 Microsensors, 210
 N-Type, 518
 Shock Response, 602
- Dibble, D. C.
 Synthesis and Applications of N-Type Diamond, 518
- Diegert, C. F.
 Video Sensing for Human-Computer Interactions, 86
- Diegert, K. V.
 Modeling Uncertainties in Simulation, 112
- Dies, 532
- Diesel, 552
- Dike, J. J.
 Mechanisms of Adiabatic Shear Failure, 232
- Dillinger, J. D.
 Varying QoS for Fixed and Mobile Networks, 303
- Directed Energy, 340–348**
- Dison, H. L.
 Surety for Real-Time Information Systems, 327
- Dispersive
 Smart Sand, 368
 Velocity, 259
- Distributed
 Complex Systems, 469
 Computing, 132
 Information Systems, 310
 Intelligent Agents, 467
 Mobile Sensors, 376
- DNA
see Deoxyribonucleic Acid
- Dodd, P. E.
 TRIBICC Imaging, 164
- Dohner, J. L.
 Flexural Plate-Wave Devices in Sensors, 202
- Dohrmann, C. R.
 Finite-Element Meshing as Global Minimization, 274
- Douglas, M. R.
 Radiation Sources: Rayleigh-Taylor Mitigation, 526
- Draelos, T. J.
 Engineering Complex Distributed Systems, 469
 Public-Key Authentication, 423
 Reduced-Computation Public-Key Protocols, 329
- Draper, B. L.
 Nondestructive Nonvolatile Memory, 143
 Nonvolatile Protonic Memory, 78

Author and Title Index

- Drewien, C. A.
Aging Diagnostics Through Hyperspectral Imaging, 42
- Drummond, T. J.
Microcode Evaluation, 485
Role of Defects in III-Nitride-Based Electronics, 169
- Dugger, M. T.
Develop MEMS Reliability Tools, 440
Self-Healing Molecular Assemblies in MEMS, 29
- Dunlap, S. K.
Radiation-Hard Sensors for Space-Based Sensing, 191
- Dykhuizen, R. C.
Enabling Cold-Spray Direct Fabrication, 55
Living Tissue Engineering, 579
- E**
- Eaton, W. P.
Develop MEMS Reliability Tools, 440
- Echekki, T.
Modeling of Multiscale Transient Phenomena, 257
MPP Numerical Simulation of Diesel Autoignition, 552
- Edwards, D. M.
Guided Facility Response to Abnormal Events, 306
- Elastohydrodynamics, 530
- Elbring, G. J.
Characterization of Underground Facilities, 371
Sparse Geophysical Networks, 352
- Electrochemical
Microelectronic Biosensor, 594
Multicomponent Transport, 226
- Electrokinetic
Chemical Sensors, 397
Mesoscale Actuators, 555
- Electromagnetic
Bearing Spindles, 267
Imaging System, 412
Laser, 570
Simulation Software, 99
Transport Pathways, 550
- Electron, 501
- Electronic
Defects, 169
Smoke Environments, 456
Structure Codes, 110
see also: Microelectronic
see also: Optoelectronic
- Electronics & Photonics, 142–216**
- Ellis, D. E.
Computer-Network Vulnerability-Analysis, 420
- Emergent
Behavior, 123
Threat, 560
- Emerson, J. A.
Optimization of Filled Polymer Materials, 270
The Impact of Cleaning on Adhesive Bond, 278
- Emission, 539
- Encapsulation, 153
- Energy, 562
see also: **Directed Energy**
- Engi, D.
Global Approaches to Infrastructural Analysis, 528
- Ensz, M. T.
Freeforming of Ceramics from Colloidal Slurries, 64
Laser Wire Deposition for Fully Dense Shapes, 284
- Environmental Sciences, 400–416**
- Enzyme
Biosensor, 594
Recognition Materials, 608
- Epitaxial, 187
- Ergonomics, 392
- Escapule, W. R.
Fluid/Solid and Fluid/Fluid Interactions, 245
- Espinoza, J.
Dynamically Self-Configurable Network Protocol, 318
Source Code Assurance Tool, 436
- Etching, 158
- Evans, G. H.
Model for Multicomponent Transport, 226
- Ewsuk, K. G.
Design of Powder Pressing Dies Using Modeling, 532
- Excitonic, 501
- F**
- Fabricate
Advanced Machining, 294
Biosensor, 610
Cold-Spray, 55
Macrosystems, 139
Microcasting, 575
Nanoarrays, 37
Nanocomposites, 508
- Failure
Polymer Modeling, 221
Adiabatic Shear, 232
- Fan, D.
Atomistic Computations with Phase-Field Modeling, 31
Simulating the Phase-Field Model, 134
- Fang, H. E.
Materials Response Simulations, 104
- Farino, A. J.
Vacuum Encapsulation of MEMS Structures, 153
- Farnsworth, A. V., Jr.
Microscale Shock-Wave Physics, 45
- Faucett, D. L.
Characterization of Underground Facilities, 371
- Fault
Tolerance, 338
Monitoring, 572
- Feddema, J. T.
Distributed Sensing Using Intelligent Agents, 467
Scripting for Video Inspection, 292

Author and Title Index

- Feibelman, P. J.
Energies of Transition-Metal Surface Structure, 503
Self-Assembled Templates for Materials Growth, 37
Surfactant-Directed Materials Growth, 58
- Femtosecond, 570
- Fiber, 581
- Field, R. V., Jr.
Nondeterministic Modeling, 252
- Filament, 213
- Film, 24
see also: Thin-Film
- Finite-Element
Global Minimization, 274
Polymer Modeling, 221
Powder Pressing, 532
- Fire, 218
- Firing, 433
- Fischer, A. J.
Composite-Resonator Surface-Emitting Lasers, 167
- Fischer, S. H.
System-Level Innovations in Missile Defense, 566
- Flaw, 428
- Fleetwood, D. M.
Nondestructive Nonvolatile Memory, 143
Nonvolatile Protonic Memory, 78
- Fleming, J. G.
AlGaN Materials Engineering, 184
Silicon Three-Dimensional Photonic Crystal, 193
Vacuum Encapsulation of MEMS Structures, 153
- Fleming, R. P.
Microcode Evaluation, 485
- Flexural, 202
- Flores, R. S.
TRIBICC Imaging, 164
- Floro, J. A.
Compliant Substrates for Epitaxial Integration, 187
Monitoring Thin-Film Deposition, 268
Surfactant-Directed Materials Growth, 58
- Flounders, A. W.
Biological Weapon Detector, 361
Enzyme-Mediated Polymer Biosensor, 594
Integrated Chemical Microsensors in GaAs, 179
Novel Biosensor Fabrication Techniques, 610
Stabilization of Molecular Recognition Materials, 608
- Flow
Big Eddy, 91
Fields, 245
Hydrodynamic, 598
Information, 325
- Fluid
see Flow
see Microfluidic
- Fluorescence, 378
- Foiles, S. M.
Crack Nucleation and Growth Modeling, 236
Recrystallization of Metals with Material Models, 247
- Follstaedt, D. M.
AlGaN Materials Engineering, 184
Compliant Substrates for Epitaxial Integration, 187
Role of Defects in III-Nitride-Based Electronics, 169
- Forester, J. A.
Identifying Potentially Dangerous Human Actions, 426
- Forsythe, J. C.
Analytic Verification of Treaties, Protocols, 574
- Fossum, A. F.
Design of Powder Pressing Dies Using Modeling, 532
- Foulk, J. W., III
Computational Method for Predicting Fracture, 261
- Fracture
Predicting, 261
Thermoset Interfaces, 48
- Freeform, 64
- Free-Space, 146
- Friedmann, T. A.
Diamond for High-Sensitivity Microsensors, 210
- Frink, L. J. D.
A Molecular Theory of Gatekeeper Proteins, 521
- Frye-Mason, G. C.
Autonomous MicroChem Laboratory, 464
Integrated Chemical Microsensors in GaAs, 179
- Fuerschbach, P. W.
Laser-Assisted Arc Welding, 69
- Fusion, 562
- Fye, R. M.
Integrated Modeling of Hydrogenic Materials, 108
Simulating the Phase-Field Model, 134
- G**
- Galambos, P. C.
Standard Cells for MEMS, 281
- Gamma-Ray, 141
- Garbin, H. D.
Characterization of Underground Facilities, 371
Sparse Geophysical Networks, 352
- Gardner, J. T.
PUSH Technology Demonstration, 323
- Garino, T. J.
Precision-Formed Micromagnets, 161
- Gas
Excitonic, 501
Fires, 218
Microabsorber, 547
- Gate, 492
- Gatekeeper, 521
- Gee, J. M.
Solar-Grade Silicon, 537
- Geib, K. M.
Composite-Resonator Surface-Emitting Lasers, 167
VCSELs and Detectors for Microsystems, 182
- Gelbard, F.
Guided Facility Response to Abnormal Events, 306
Simulation of Chem/Bio Agents in Infrastructures, 243

Author and Title Index

- Geometric, 395
Geophysical, 352
Geosphere, 414
Gigabit, 331
Gilkey, J. C.
 IFSAR Rapid Terrain Visualization, 564
Gilmore, D. L.
 Enabling Cold-Spray Direct Fabrication, 55
Gladwell, T. S.
 Cooperative Automation, 386
 Ergonomics in Life-Cycle Assembly, 392
 Robotic Manipulation of Hazardous Materials, 373
Glass, M. W.
 Simulation of Chem/Bio Agents in Infrastructures, 243
Glass, S. J.
 Materials Response Simulations, 104
Goeke, R. S.
 Monitoring Thin-Film Deposition, 268
Goldsby, M. E.
 Distributed Information System Modeling, 310
 Fault Tolerance on Massively Parallel Computers, 338
Goldsmith, S. Y.
 Agent-Based Mediation, 316
 Engineering Complex Distributed Systems, 469
 System-Surety Life-Cycle Engineering, 438
Gonzales, R. A.
 Reduced-Computation Public-Key Protocols, 329
Goods, S. H.
 Mechanisms of Adiabatic Shear Failure, 232
Gottlieb, E. J.
 Distributed Sensing Using Intelligent Agents, 467
 Heterogeneous Simulation, 83
Granfield, R. J.
 SCADA for the Critical Energy Infrastructures, 313
Gray, P. C.
 Gamma-Ray Bursts and the Particle Mass Scale, 141
 Optimization for Engineering Science Problems, 115
Grazier, J. M.
 Phase Changes in PZT Materials, 511
Grcar, J. F.
 MPP Numerical Simulation of Diesel Autoignition, 552
Gregory, D. L.
 Develop MEMS Reliability Tools, 440
Grest, G. S.
 Dynamics of Solder and Braze Alloys, 39
Grid, 130
Griffith, M. L.
 Laser Wire Deposition for Fully Dense Shapes, 284
 LENSTM Technology and Novel Materials, 73
Griffiths, S. K.
 Applied Microfluidic Physics, 239
Gritz, L. A.
 Lagrangian Modeling of Radiative Transport, 255
 Reliability of Electronics in Smoke Environments, 456
 Transient Gas Species and Soot in Large Fires, 218
Grotbeck, C. L.
 Evolution of Hyperspectral Target Signatures, 545
Grubelich, M. C.
 System-Level Innovations in Missile Defense, 566
G-Type, 594
Guess, T. R.
 Finite-Element Polymer Modeling, 221
 Synthesis of Controlled Degradative Materials, 401
Guided, 343
Guilinger, T. R.
 Global Climate Model for Paleoclimate Applications, 95
H
Haaland, D. M.
 Aging Diagnostics Through Hyperspectral Imaging, 42
 Hyperspectral Images Obtained from Satellites, 513
Hadgu, T.
 Advanced Geosphere Transport Simulation, 414
Hadley, G. R.
 Short-Pulsed Power in Active Optical Sensors, 149
Hamilton, J. C.
 Atom-Picoseconds to Centimeter-Years, 121
 Crack Nucleation and Growth Modeling, 236
 Surfactant-Directed Materials Growth, 58
Hamilton, V. A.
 Public-Key Authentication, 423
 Reduced-Computation Public-Key Protocols, 329
Han, J.
 AlGaN Materials Engineering, 184
 Role of Defects in III-Nitride-Based Electronics, 169
Hance, B. G.
 Smart Sand for Landmine Detection, 368
Hansche, B. D.
 Signal Processing for Thermal Flaw Detection, 428
Harden, 498
Harff, N. E.
 Quantum Tunneling Transistors, 198
Hargis, P. J., Jr.
 UV Fluorescence Biological Agent Sensor, 378
Harmony, D. W.
 Ultra-High-Resolution Complex SAR Imaging, 363
Harrington, J. J.
 Dynamically Self-Configurable Network Protocol, 318
Harris, D. L.
 Microsimulation Model of Infrastructure, 447
Hart, W. E.
 Advanced Production Planning Models, 298
 Optimization for Engineering Science Problems, 115
 Optimization for Scheduling Problems, 125
 Production Surety and Disruption Vulnerability, 431
Haschke, G. B.
 Laser Communication Nanosatellites, 473
Haynes, R. A.
 Fast and Easy Parallel I/O, 97
Hayward, D. R.
 Microsensors in Miniature Robotic Vehicles, 151
Headley, T. J.
 LENSTM Technology and Novel Materials, 73

Author and Title Index

- Hebner, G. A.
 High-Throughput Dry Processes, 287
- Heller, E. J.
 Autonomous MicroChem Laboratory, 464
 Integrated Chemical Microsensors in GaAs, 179
 Microsensors in Miniature Robotic Vehicles, 151
- Hendrickson, B. A.
 Visual Explanation and Insight, 137
- Henfling, J. F.
 Fluid/Solid and Fluid/Fluid Interactions, 245
- Henson, T. D.
 Deployable Mirrors for Remote Sensing, 365
- Heroux, M. A.
 Incomplete Factorization Preconditioners, 88
- Herrera, G. V.
 Power Sources for Autonomous Microsystems, 525
- Herrington, P. B.
 Flexural Plate-Wave Devices in Sensors, 202
- Hiebert-Dodd, K. L.
 Analytic Verification of Treaties, Protocols, 574
- Hietala, S. L.
 Integrated Chemical Microsensors in GaAs, 179
 Micromachined Tuners for Microwave Circuits, 195
- Hietala, V. M.
 Acoustically Driven Microoptoelectronics, 205
 Integrated Chemical Microsensors in GaAs, 179
 Quantum Tunneling Transistors, 198
- Hillaire, R. G.
 Controlling Information Flow and Fusion, 325
 Data Fusion for Chemical Sensing, 308
 Fusion of Data Using Real-Time Visualization, 296
- Hilton, N. R.
 Solid-State Neutron Generator in Nuclear Weapons, 272
- Hinckley, M. K.
 Radiation-Hard Sensors for Space-Based Sensing, 191
- Hjalmarson, H. P.
 Lightning-Induced Arcing, 230
 Optically Triggered Switch for Firing Systems, 433
 Semiconductor Current Filament Lasers, 213
- Ho, P.
 Solar-Grade Silicon, 537
- Hollowell, J. A.
 Imaging of Moving Targets Using SAR and MTI, 350
- Holm, E. A.
 Materials Response Simulations, 104
 Recrystallization of Metals with Material Models, 247
- Holswade, S. C.
 Optically Triggered Switch for Firing Systems, 433
- Hopkins, P. L.
 Advanced Geosphere Transport Simulation, 414
- Horstemeyer, M. F.
 Atom-Picoseconds to Centimeter-Years, 121
- Hosking, F. M.
 Atomistic Computations with Phase-Field Modeling, 31
 Dynamics of Solder and Braze Alloys, 39
 Integration of Optoelectronics and MEMS, 146
- Houf, W. G.
 Model for Multicomponent Transport, 226
- Hough, P. D.
 Fault Tolerance on Massively Parallel Computers, 338
- Houston, J. E.
 Crack Nucleation and Growth Modeling, 236
- Hoyt, J. J.
 Atomistic Computations with Phase-Field Modeling, 31
 HPM, 348
- Hu, T. C.
 High-Performance Commodity Interconnects, 333
- Huang, X. C.
 Pathogen Detection Using Microseparations, 557
- Hubbard, G. L.
 Transient Gas Species and Soot in Large Fires, 218
- Hudson, T. B.
 Programming Paradigms for Parallel Computers, 128
- Hughes, D. A.
 Mechanisms of Adiabatic Shear Failure, 232
 Recrystallization of Metals with Material Models, 247
- Hughes, R. C.
 Biological Weapon Detector, 361
 Chemiresistors for Solvent Spill Detection, 495
 Information Collection, 479
 Ultra-Low-Power Sensors for Microtelemetry, 172
- Human
 Cooperative Automation, 386
 Danger, 426
 Video Motion Sensing, 86
- Hunter, K. O.
 Optimization for Engineering Science Problems, 115
- Hunter, T.
 Nuclear Weapons Program, 15
- Hurd, A. J.
 Hydrodynamic Flow in Biosystems, 598
 Simulations of Self-Assembling Macrosystems, 139
- Hurtado, J. E.
 Distributed Sensing Using Intelligent Agents, 467
 Emergent Behavior of Intelligent Agents, 123
- Hutchinson, R. L.
 Varying QoS for Fixed and Mobile Networks, 303
- Hux, G. A.
 Electrokinetic Immunoaffinity Chemical Sensors, 397
- Hwang, R. Q.
 Crack Nucleation and Growth Modeling, 236
 Dynamics of Solder and Braze Alloys, 39
 Reactivity of Metal-Oxide Surfaces, 70
 Self-Assembled Templates for Materials Growth, 37
- Hydrodynamic, 598
 see also: Elasto-hydrodynamics
- Hydrogenic, 108
- Hyperspectral
 Materials Aging, 42
 Satellites, 513
 Target Signatures, 545

Author and Title Index

I

I/O

see Input/Output

IC (Integrated Circuit)

see Integrated Circuit

IFSAR

see Interferometric Synthetic Aperture Radar

Image

Analysis, 492

Satellite, 513

Imaging

Environmental, 412

Hyperspectral, 42

Microwave, 489

Moving Targets, 350

SAR, 363

Transport Pathways, 550

TRIBICC, 164

Immunoaffinity, 397

Immunoassay, 368

Impedance, 361

Information

Collection, 479

Controlling, 325

Cooperative, 316

Critical Infrastructure, 541

Distributed, 310

Extraction, 513

Mission Surety, 327

Public-Key, 423

Surety Analysis, 418

Information Systems & Technology, 300–339

Infrared, 600

Infrastructure

Chem/Bio, 243

GAIA, 528

Microsimulation, 447

Risk and Reliability, 424

SCADA, 313

Status, 541

see also: Architectural (Surety)

Ingersoll, D.

Laser Communication Nanosatellites, 473

Power Sources for Autonomous Microsystems, 525

Initiation, 76

Insight, 137

Interferometric Synthetic Aperture Radar, 564

Input/Output, 97

Inspection, 292

Integrated Circuit, 453

Intelligence, 516

Intelligent

Agent Behavior, 123

Microminiature Agents, 467

Polymers, 62

Software Brittleness, 516

see also: **Sensing & Intelligent Controls**

Interconnects

Backplane, 321

Backside Localization, 453

Commodity, 333

Interface, 48

Interfacial, 505

Interferometric Synthetic Aperture Radar, 564

Intermittent, 118

International, 574

Ionophores, 409

IR

see Infrared

Irvin, D. J.

Pathogen Detection Using Microseparations, 557

Irwin, L. W.

Develop MEMS Reliability Tools, 440

Istrail, S.

Novel Biological Weapon Detection System, 358

Simulations of Self-Assembling Macrosystems, 139

J

Jakowatz, C. V., Jr.

Imaging of Moving Targets Using SAR and MTI, 350

Jamison, G. M.

Intelligent Polymers for Nanodevice Control, 62

Janek, R. P.

Biological Weapon Detector, 361

Enzyme-Mediated Polymer Biosensor, 594

Janssen, C. L.

Validation for ASCI Materials Modeling, 102

Jefferson, K. J.

Real-Time Image Analysis, 492

Jennison, D. R.

Dynamics of Solder and Braze Alloys, 39

Quantum Dot Arrays, 67

Reactivity of Metal-Oxide Surfaces, 70

Jensen, B. D.

Standard Cells for MEMS, 281

Jensen, K. M.

Scripting for Video Inspection, 292

Jessing, J. R.

Radiation-Hard Random Access Memory, 215

Johnsen, H. A.

Transient Gas Species and Soot in Large Fires, 218

Johnson, A. J.

High Reliability in Low-Volume Manufacturing, 290

Johnson, D. J.

Laser Communication Nanosatellites, 473

Johnson, D. K.

Visual Explanation and Insight, 137

Johnson, M. M.

Distributed Information System Modeling, 310

Johnston, A. M.

SCADA for the Critical Energy Infrastructures, 313

Author and Title Index

- Jones, D. A.
Advanced Production Planning Models, 298
Optimization for Scheduling Problems, 125
Production Surety and Disruption Vulnerability, 431
- Jones, E. D.
Acoustically Driven Microoptoelectronics, 205
Broadening Mechanism in Electron Gases, 501
- Jones, J. S.
Evolvable Hardware, 234
- Jorgenson, R. E.
Lightning-Induced Arcing, 230
- Jung, J.
Finite-Element Meshing as Global Minimization, 274
- K**
- Kalb, J. L.
Fluid/Solid and Fluid/Fluid Interactions, 245
- Kasunic, K. J.
Aqueous Organic Sensor, 406
Photonics Integration Devices and Technologies, 207
- Kaufman, S. G.
Robotic Manipulation of Hazardous Materials, 373
- Kay, R. R.
Radiation-Hard Sensors for Space-Based Sensing, 191
- Kaye, R. J.
SERAPHIM Propulsion for Rail Applications, 543
- Kegelmeyer, W. P.
AVATAR—Navigating in Massive Data, 336
- Kelley, J. B.
SERAPHIM Propulsion for Rail Applications, 543
- Kellogg, G. L.
Dynamics of Solder and Braze Alloys, 39
Surfactant-Directed Materials Growth, 58
- Kelly, M. J.
Accelerated Molecular Discovery Arrays, 481
Aqueous Organic Sensor, 406
- Kemme, S. A.
Aqueous Organic Sensor, 406
IR Polarimetry and Lithographic Alignment, 600
- Kennedy, C. A.
MPP Numerical Simulation of Diesel Autoignition, 552
- Kent, M. S.
Fracture Analysis of Polymer/Solid Interfaces, 48
- Kerstein, A. R.
Eddy Simulation Algorithms, 91
Modeling of Multiscale Transient Phenomena, 257
MPP Numerical Simulation of Diesel Autoignition, 552
- Key, S. W.
Structural Simulations Using Material Models, 228
- Kim, T. J.
Laser Communication Nanosatellites, 473
- King, B. H.
Freeforming of Ceramics from Colloidal Slurries, 64
- King, C.
Parallel Mechanism Technology to Manufacturing, 276
- King, D. B.
Thermionic Emission Materials, 539
- Kipp, M. E.
System-Level Innovations in Missile Defense, 566
- Kjeldgaard, E. A.
Optimization for Scheduling Problems, 125
- Klarer, P. R.
Distributed Sensing Using Intelligent Agents, 467
- Klassen, S. E.
New Complexing Agent for Co(II) Analysis for CP, 592
- Klein, P. A.
Computational Method for Predicting Fracture, 261
Crack Nucleation and Growth Modeling, 236
- Klem, J. F.
Compliant Substrates for Epitaxial Integration, 187
- Kliner, D. A.
Development of Compact UV Laser Source, 523
- Klinke, D. J.
MPP Numerical Simulation of Diesel Autoignition, 552
- Knapp, J. A.
Fundamental Aspects of Micromachine Reliability, 52
- Knorovsky, G. A.
Materials Response Simulations, 104
- Knudson, M. D.
Dispersive Measurements of Velocity, 259
Shock Response of Diamond Crystals, 602
- Knupp, M. P.
Mesh Optimization and 3-D Mesh Generation, 81
- Koch, M. W.
Recognizing Partially Obscured Targets, 356
- Koehler, F. W.
Aging Diagnostics Through Hyperspectral Imaging, 42
- Koller, M. H.
Visual Explanation and Insight, 137
- Kottenstette, R.
Autonomous MicroChem Laboratory, 464
- Kozlowski, D. M.
Parallel Mechanism Technology to Manufacturing, 276
Robotic Manipulation of Hazardous Materials, 373
- Kravitz, S. H.
Autonomous MicroChem Laboratory, 464
Biological Weapon Detector, 361
Gas-to-Liquid Microabsorber, 547
Miniature Bioaerosol Concentrator, 354
Post-Processed Integrated Microsystems, 188
- Krygowski, T. W.
Magnetic Polysilicon MEMS Devices, 577
- Kurtz, S. R.
Double Quantum-Well Optoelectronics, 175
- Kurz, K. L.
Solid-State Neutron Generator in Nuclear Weapons, 272
- L**
- Ladd, M. D.
Characterization of Underground Facilities, 371
Sparse Geophysical Networks, 352
- LaFarge, R. A.
Simulation of Systems with Intermittent Contacts, 118
- Lagrangian, 255

Author and Title Index

- Laguna, G. A.
 Analysis of Very Large Assemblies, 384
 Automatic Planning of Life-Cycle Assembly, 381
- Landmine, 368
- Lanes, C. E.
 Evolution of Hyperspectral Target Signatures, 545
- Lanes, K. R.
 Evolution of Hyperspectral Target Signatures, 545
- Larson, R. S.
 Model for Multicomponent Transport, 226
- Laser
 Arc Welding, 69
 Compact UV, 523
 Composite Resonator, 167
 Current Filament, 213
 Femtosecond, 570
 Nanosatellites, 473
 Optical Sensor, 149
 Wire Deposition, 284
- Lauffer, J. P.
 Real-Time Error Correction Using Spindles, 267
- LaVan, D. A.
 Diamond for High-Sensitivity Microsensors, 210
 Materials Response Simulations, 104
- Lawton, C. R.
 Advanced Production Planning Models, 298
 Production Surety and Disruption Vulnerability, 431
- Lee, S. R.
 AlGaN Materials Engineering, 184
 Compliant Substrates for Epitaxial Integration, 187
 Investigation of Lateral Composition Modulation, 590
 Role of Defects in III-Nitride-Based Electronics, 169
- Lehoucq, L. J.
 Controlling Information Flow and Fusion, 325
- Leininger, M. L.
 Validation for ASCI Materials Modeling, 102
- LENS™, 73
- Leonard, C. M., Jr.
 Fusion of Data Using Real-Time Visualization, 296
- Leung, K.
 Density-Functional Electronic Structure Codes, 110
- Leung, V. J.
 Finite-Element Meshing as Global Minimization, 274
- Lewis, C. L.
 Distributed Sensing Using Intelligent Agents, 467
 Simulation of Systems with Intermittent Contacts, 118
- Lewis, P. R.
 Autonomous MicroChem Laboratory, 464
- Lieberman, M. L.
 System-Level Innovations in Missile Defense, 566
- Life-Cycle
 Automatic Planning, 381
 Ergonomics, 392
 System Surety, 438
- Lightning, 230
- Lin, S. Y.
 Double Quantum-Well Optoelectronics, 175
 Photonics Integration Devices and Technologies, 207
 Silicon Three-Dimensional Photonic Crystal, 193
- Lindgren, E. R.
 Models for Radionuclide Desorption from Soils, 403
- Link, H. E.
 Agent-Based Mediation, 316
 Engineering Complex Distributed Systems, 469
- Lippert, R. A.
 Density-Functional Electronic Structure Codes, 110
- Liquid-Membrane, 409
- List, G. F.
 Advanced Production Planning Models, 298
 Production Surety and Disruption Vulnerability, 431
- Lithographic, 600
- Little, C. Q.
 Adaptive 3-D Sensing, 404
 Cloud to CAD, 389
 Ergonomics in Life-Cycle Assembly, 392
- Living, 579
- Lo, C. S.
 Finite-Element Polymer Modeling, 221
- Loads, 535
- Load-Balancing, 99
- Localization, 453
- Lockner, T. R.
 Intense White-Light Pulse Propagation in Air, 343
 Laser Interactions for Electromagnetic Coupling, 570
 Z-Backlighter Technologies, 568
- Lockwood, G. J.
 Improved Backscatter X-Ray Detection, 346
- Loehman, R. E.
 A Novel Microcasting Process, 575
 Interfacial Reactions in Ceramic Systems, 505
- Lopez, E. P.
 The Impact of Cleaning on Adhesive Bond, 278
- Loubriel, G. M.
 HPM Vulnerability Assessment and Tests, 348
 Imaging for Environmental Site Reconnaissance, 412
 Optically Triggered Switch for Firing Systems, 433
- Loucks, C. S.
 Robotic Manipulation of Hazardous Materials, 373
- Loy, D. A.
 Intelligent Polymers for Nanodevice Control, 62
 Synthesis of Controlled Degradative Materials, 401
- Lu, Y.
 Fabrication Via Supramolecular Self-Assembly, 508
- Ludowise, P. D.
 Transient Gas Species and Soot in Large Fires, 218
- Luk, T. S.
 Intense White-Light Pulse Propagation in Air, 343
 Laser Interactions for Electromagnetic Coupling, 570
 Z-Backlighter Technologies, 568
- Lund, J. C.
 Solid-State Neutron Generator in Nuclear Weapons, 272

Author and Title Index

- Lutz, A. E.
MPP Numerical Simulation of Diesel Autoignition, 552
- Lyo, S. K.
Double Quantum-Well Optoelectronics, 175
Quantum Tunneling Transistors, 198
Silicon Three-Dimensional Photonic Crystal, 193
- M**
- Machining, 294
- Macrosystems, 139
- Magnet
MEMS, 577
RAM, 215
Sensor, 202
see also: Electromagnetic
see also: Micromagnet
- Manufacturing and Process Sciences, 264**
- Mar, A.
Optically Triggered Switch for Firing Systems, 433
Semiconductor Current Filament Lasers, 213
Short-Pulsed Power in Active Optical Sensors, 149
- Marder, B. M.
SERAPHIM Propulsion for Rail Applications, 543
- Marron, L. C.
Distributed Mobile Sensor Arrays, 376
- Martin, J. E.
Quantum Dot Arrays, 67
- Martin, J. W.
Deployable Mirrors for Remote Sensing, 365
- Martin, L. E.
Aging Diagnostics Through Hyperspectral Imaging, 42
- Martin, M. F.
High Reliability in Low-Volume Manufacturing, 290
- Martin, S. J.
AlGaIn Materials Engineering, 184
- Martinez, J. L.
Neutron Generator Program, 21
- Martinez, M. J.
Advanced Geosphere Transport Simulation, 414
- Marx, K. D.
Simulation/Optimization Tools, 444
- Massively Parallel Processing, 552
- Masters, N.
Microdiagnostic MEMS Lab-on-a-Chip, 265
- Matalucci, R. V.
Architectural Surety, 535
- Materials Science & Technology, 23-79**
- Mayer, T. K.
Distributed Sensing Using Intelligent Agents, 467
- Mayer, T. M.
Fundamental Aspects of Micromachine Reliability, 52
Self-Healing Molecular Assemblies in MEMS, 29
- McDaniel, A. H.
MPP Numerical Simulation of Diesel Autoignition, 552
- McDonald, T. S.
Characterization of Underground Facilities, 371
- Mediation, 316
- Melgaard, D. K.
Aging Diagnostics Through Hyperspectral Imaging, 42
- Melius, C. F.
Validation for ASCI Materials Modeling, 102
- Memory
Nonvolatile, 143
Radiation-Hard, 215
- MEMS
see Microelectromechanical Systems
- Mendenhall, F. T.
Information Collection, 479
- Merewether, K. O.
Lightning-Induced Arcing, 230
- Mesh, 81
- Mesoscale, 555
- Metal
Ionophores, 409
Surface Structure, 503
- Metal-Loaded, 495
- Metal-Oxide, 70
- Michael, J. R.
Corrosion of Microelectronic Reliability, 450
- Michalske, T. A.
Investigation of Nanoscience Technologies, 604
Science on the Microdomain, 461
- Michalski, J. T.
Varying QoS for Fixed and Mobile Networks, 303
- Microabsorber, 547
- Microarray, 587
- Microcasting, 575
- MicroChem, 464
- Microcode, 485
- Microcomponent, 575
- Microdomain, 461
- Microelectromechanical Systems
Friction, 29
Magnetic, 577
Microdiagnostic, 265
Microoptics, 146
Reliability, 52
- Microelectronic
Biosensor, 594
Corrosion, 450
- Microfabrication, 294
- Microfluidic, 239
- Micromachine
see Microelectromechanical Systems
- Micromachined, 195
- Micromagnet, 161
- Microminiature, 467
- Microoptics, 146
- Microscale, 45
- Microsensor
Chemical, 179
Diamond, 210
- Microseparation, 557
- Microsimulation, 447

Author and Title Index

- Microsystems
 Polychromatic Films, 24
 Post-Processed, 188
 Power Source, 525
 VCSELs, 182
- Microtelemetry, 172
- Microwave
 Circuits, 195
 Imaging, 489
- Miller, A. K.
 Information Collection, 479
- Miller, D. P.
 Identifying Potentially Dangerous Human Actions, 426
- Miller, G. J., Jr.
 Solid-State Neutron Generator in Nuclear Weapons, 272
- Miller, J. C.
 Characterization of Energetic Material Initiation, 26
- Miller, J. E.
 Ionophores for Liquid-Membrane Separation, 409
- Miller, M. M.
 High-Performance Commodity Interconnects, 333
- Miller, P. A.
 High-Throughput Dry Processes, 287
- Miller, R. D.
 Reduced-Computation Public-Key Protocols, 329
- Mine
 see Landmine
- Miniature
 Bioaerosol Concentrator, 354
 Fluorescence Sensor, 378
 Intelligent Agents, 467
 Robotic Vehicle, 151
 see also: Microminiature
- Mining
 see Data Mining
- Mirrors, 365
- Missert, N. A.
 AlGaN Materials Engineering, 184
 Critical Copper-Corrosion Mechanisms, 34
 Monitoring Corrosion in Weapons Environments, 26
 Self-Assembled Templates for Materials Growth, 37
- Missile, 566
- Mitchell, E. A.
 Analysis of Very Large Assemblies, 384
 Automatic Planning of Life-Cycle Assembly, 381
 Robotic Manipulation of Hazardous Materials, 373
- Mitchell, S. A.
 Mesh Optimization and 3-D Mesh Generation, 81
- Mitigation, 526
- Mix, L. P., Jr.
 Novel Load-Balancing for Simulation Software, 99
- Mobile
 Network, 303
 Sensor, 376
- Model
 ASCI Materials, 102
 Atmospheric Corrosion, 450
 Climate, 95
 Computational Simulation, 112
 Crack Nucleation, 236
 Distributed Information, 310
 Finite-Element Polymers, 221
 Geometric Solids, 395
 Hydrogenic Materials, 108
 Infrastructure, 447
 Lagrangian, 255
 Metal Recrystallization, 247
 Monitoring Systems, 486
 Multicomponent Transport, 226
 Nondeterministic, 252
 Phase-Field, 31
 Polymer Dynamics, 499
 Powder Pressing, 532
 Production Planning, 298
 Simulating Phase-Field, 134
 Soil, 403
 Structural Simulation, 228
 Turbulent Boundary Layers, 257
- Modeling & Engineering Simulation, 217–263**
- Modine, N. A.
 Atom-Picoseconds to Centimeter-Years, 121
 Density-Functional Electronic Structure Codes, 110
- Modulation, 590
- Moen, C. D.
 Unstructured Grid Problems, 130
- Molecular
 Assemblies, 29
 Discovery Arrays, 481
 Energetic Materials, 76
 Gatekeeper Proteins, 521
 Interfaces, 48
 Reacting System, 93
 Recognition, 608
- Monitoring
 Remote, 486
 Snoopy Coprocessor, 572
 Targets, 352
 Thin-Film, 268
 Turbine Blades, 581
 Weapons, 26
- Montague, S.
 Vacuum Encapsulation of MEMS Structures, 153
- Montry, G.
 Novel Load-Balancing for Simulation Software, 99
- Morales, A. M.
 Solid-State Neutron Generator in Nuclear Weapons, 272
 UV Fluorescence Biological Agent Sensor, 378
- Morissette, S. L.
 Freeforming of Ceramics from Colloidal Slurries, 64

Author and Title Index

- Moya, M. M.
 Recognizing Partially Obscured Targets, 356
Moving Target Indicator, 350
MPP
 see Massively Parallel Processing
MTI
 see Moving Target Indicator
Multifunction
 Materials Engineering, 184
 Nanocomposites, 508
Murata, K. K.
 Guided Facility Response to Abnormal Events, 306
 Simulation of Chem/Bio Agents in Infrastructures, 243
Murphy-Dye, B. D.
 Agent-Based Mediation, 316
 Engineering Complex Distributed Systems, 469
Murray, J. R.
 Nondestructive Nonvolatile Memory, 143
Myers, D. R.
 Radiation-Hard Random Access Memory, 215
Myers, S. M., Jr.
 Role of Defects in III-Nitride-Based Electronics, 169
 Surface Hardening by Nanoparticle Precipitation, 498
- N**
Nagasubramanian, G.
 Distributed Sensing Using Intelligent Agents, 467
Nanoarrays, 37
Nanocomposite, 508
Nanodevice, 62
Nanoparticle, 498
Nanosatellite, 473
Nanoscience, 604
Nation, B. M.
 Engineering Complex Distributed Systems, 469
Neilsen, M. K.
 Materials Response Simulations, 104
Neiser, R. A., Jr.
 Enabling Cold-Spray Direct Fabrication, 55
Nelson, C. L.
 WNN Decision Making for Data Mining, 301
Nelson, J. S.
 Critical Copper-Corrosion Mechanisms, 34
Network
 Geophysical, 352
 Gigabit, 331
 Infrastructure Evaluation, 424
 Mobile, 303
 Protocol, 318
 Vulnerability, 420
Neutron Generator, 272
Neutron-Tube, 497
Nevers, J. A.
 VCSELs and Detectors for Microsystems, 182
Newman, G. A.
 Electromagnetic Imaging of Transport Pathways, 550
- Neyer, D. W.
 Electrokinetic Immunoaffinity Chemical Sensors, 397
Ngola, S. M.
 Accelerated Molecular Discovery Arrays, 481
Nicolette, V. F.
 Reliability of Electronics in Smoke Environments, 456
Nielsen, I. M.
 Validation for ASCI Materials Modeling, 102
Nilsen, V.
 Modeling of Multiscale Transient Phenomena, 257
Nilson, R. H.
 Applied Microfluidic Physics, 239
Nissen, M. R.
 Ultra-High-Resolution Complex SAR Imaging, 363
Noble, D. R.
 Model for Multicomponent Transport, 226
Nondestructive, 143
Nondeterministic, 252
Nonproliferation, 557
Nonvolatile
 Nondestructive Memory, 143
 Protonic Memory, 78
Nowlen, S. P.
 Reliability of Electronics in Smoke Environments, 456
Nuclear Weapons, 272
Nucleation, 236
- O**
Oberkampf, W. L.
 Modeling Uncertainties in Simulation, 112
Obscured, 356
O'Malley, M. W.
 Semiconductor Current Filament Lasers, 213
Oppel, F. J., III
 Heterogeneous Simulation, 83
Optical
 Backplane/Interconnect, 321
 Filamentation, 343
 Firing Systems, 433
 Sensor, 149
Optoelectronic, 146
Osborn, G. C.
 Overcoming Software Brittleness, 516
 Science on the Microdomain, 461
Ottesen, D. K.
 Transient Gas Species and Soot in Large Fires, 218
- P**
Paez, T. L.
 Nondeterministic Modeling, 252
 Signal Processing for Thermal Flaw Detection, 428
Paleoclimate, 95
Particle, 141
Pasik, M. F.
 Novel Load-Balancing for Simulation Software, 99
Pathogen, 557

Author and Title Index

- Pathway, 550
 Paul, P. H.
 Electrokinetically Driven Mesoscale Actuators, 555
 Peace, G. L.
 Imaging for Environmental Site Reconnaissance, 412
 Perturbation, 526
 Peters, R. R.
 Automatic Planning of Life-Cycle Assembly, 381
 Ergonomics in Life-Cycle Assembly, 392
 Peterson, D. W.
 Corrosion of Microelectronic Reliability, 450
 Phase-Field
 Atomistic Computations, 31
 Simulating, 134
 Phillips, C. A.
 Advanced Production Planning Models, 298
 Computer-Network Vulnerability-Analysis, 420
 Network Analysis for Infrastructure Reliability, 424
 Optimization for Scheduling Problems, 125
 Production Surety and Disruption Vulnerability, 431
 Phillips, L. R.
 Agent-Based Mediation, 316
 Engineering Complex Distributed Systems, 469
 Phipps, G. S.
 Research of the Utility of Polarimetric Sensing, 490
 Photochromic, 24
 Photonic
 Integration Devices, 207
 Shock-Wave Physics, 45
 Silicon Crystal, 193
 see also: Electronics & Photonics
 Pierson, L. G.
 Super-High-Speed Communication, 321
 Ten-to-One-Hundred-Gigabit/Second Networking, 331
 Plantenga, T.
 Distributed Information System Modeling, 310
 Plasma
 Simulation, 99
 Wire, 584
 Plate-Wave, 202
 Platzbecker, M. R.
 IFSAR Rapid Terrain Visualization, 564
 Plimpton, S. J.
 Density-Functional Electronic Structure Codes, 110
 Novel Load-Balancing for Simulation Software, 99
 Programming Paradigms for Parallel Computers, 128
 Simulating the Phase-Field Model, 134
 Plymale, D. L.
 Parallel Mechanism Technology to Manufacturing, 276
 Poco, 494
 Polarimetric, 490
 Polarimetry, 600
 Pollock, R. D.
 Determining Critical Infrastructure Status, 541
 Polymer
 Biosensor, 594
 Dynamical Properties, 499
 Filled Materials, 270
 Intelligent, 62
 Metal-Loaded, 495
 Modeling, 221
 Thermoset, 48
 Polysilicon, 577
 Post-Processed, 188
 Potter, K. S.
 UV Fluorescence Biological Agent Sensor, 378
 Powder, 532
 Power
 Laser, 149
 Microsystems, 525
 Microtelemetry, 172
 Public-Key, 329
 RF, 341
 Security, 458
 Precipitation, 498
 Prevender, T. S.
 Information Collection, 479
 Microwave Imaging Through Walls, 489
 Production
 Low-Volume Manufacturing, 290
 Modeling, 298
 Vulnerability, 431
 Programmable, 492
 Programming, 128
 Propagation, 343
 Propulsion, 543
 Protection, 567
 Proteins, 521
 Protocol
 Network, 318
 Public-Key, 329
 Treaties, 574
 Protonic, 78
 Provencio, P. P.
 Quantum Dot Arrays, 67
 Pryor, R. J.
 Distributed Mobile Sensor Arrays, 376
 Emergent Behavior of Intelligent Agents, 123
 Microsimulation Model of Infrastructure, 447
 Public-Key
 Authentication, 423
 Protocols, 329
 Pulsed Power, 149
 Purification, 567
 PUSH Technology, 323
 Puskar, J. D.
 LENSTM Technology and Novel Materials, 73

Author and Title Index

Q

QoS

see Quality of Service

Quality of Service, 303

Quantum

Dot Arrays, 67

Hydrogenic Materials, 108

Optoelectronics, 175

Tunneling Transistors, 198

R

Radar, 350

Rader, D. J.

Gas-to-Liquid Microabsorber, 547

Miniature Bioaerosol Concentrator, 354

Radiation

RAM, 215

Sensors, 191

Rayleigh-Taylor Mitigation, 526

Radiative, 255

Radio Frequency, 341

Radionuclide, 403

Rail, 543

Rakestraw, D. J.

Autonomous MicroChem Laboratory, 464

Science on the Microdomain, 461

Raman, 511

Rao, R. R.

Incomplete Factorization Preconditioners, 88

Rayleigh-Taylor, 526

Reactivity, 70

Real-Time

Decision-Support, 306

Error Correction, 267

IFSAR, 564

Image Analysis, 492

Information Systems, 327

Powder Pressing, 532

Streaming Visualization, 296

Reconfigurable, 596

Reconnaissance, 412

Recrystallization, 247

see also: Crystal

Recycle, 361

Red-Horse, J. R.

Nondeterministic Modeling, 252

Redmond, J. M.

Fundamental Aspects of Micromachine Reliability, 52

Real-Time Error Correction Using Spindles, 267

Deployable Mirrors for Remote Sensing, 365

Redox

Biological Weapons Detector, 361

Polymer Biosensor, 594

Reduction

Geometric Solids, 395

Perturbation, 526

Reedy, E. D., Jr.

Finite-Element Polymer Modeling, 221

Fracture Analysis of Polymer/Solid Interfaces, 48

The Impact of Cleaning on Adhesive Bond, 278

Reeves, P. C.

Advanced Geosphere Transport Simulation, 414

Reliability

Corrosion, 450

Infrastructure, 424

Manufacturing, 290

MEMS Tools, 440

Micromachine, 52

Smoke, 456

Remote Sensing

Design, 486

Mirrors, 365

Optical Filamentation, 343

Renlund, A. M.

Characterization of Energetic Material Initiation, 76

Reno, J. L.

Double Quantum-Well Optoelectronics, 175

Integrated Chemical Microsensors in GaAs, 179

Quantum Tunneling Transistors, 198

Renzi, R. F.

Gas-to-Liquid Microabsorber, 547

Miniature Bioaerosol Concentrator, 354

Response

Architectural Surety, 535

Diamond Crystals, 602

Facility, 306

Materials, 104

Reyes, D. N.

Standard Cells for MEMS, 281

RF

see Radio Frequency

Ricco, A. J.

Sensor Arrays for Volatile Organic Detection, 156

Rieb, D. A.

PUSH Technology Demonstration, 323

Rieger, D. J.

High-Throughput Dry Processes, 287

Integration of Optoelectronics and MEMS, 146

Rienstra, J. L.

Radiation-Hard Sensors for Space-Based Sensing, 191

Riesen, R. E.

Programming Paradigms for Parallel Computers, 128

Riley, D. J.

Novel Load-Balancing for Simulation Software, 99

Rinehart, L. F.

HPM Vulnerability Assessment and Tests, 348

Rintoul, M. D.

Materials Response Simulations, 104

Simulating the Phase-Field Model, 134

Rivera, J. J.

Scripting for Video Inspection, 292

Author and Title Index

- Robertson, P. J.
 Laser Communication Nanosatellites, 473
 Super-High-Speed Communication, 321
 Ten-to-One-Hundred-Gigabit/Second Networking, 331
- Robinett, R. D., III
 Information Collection, 479
- Robino, C. V.
 LENS™ Technology and Novel Materials, 73
- Robinson, A. C.
 Unstructured Grid Problems, 130
- Robinson, D. G.
 Corrosion of Microelectronic Reliability, 450
 Network Analysis for Infrastructure Reliability, 424
 Nondeterministic Modeling, 252
 Security of Bulk Power Systems, 458
- Robotic
 Hazardous Materials, 373
 Microsensor, 151
- Rochau, G. E.
 CAD Analysis of Containment Vessels, 603
- Rodgers, M. S.
 Integration of Optoelectronics and MEMS, 146
 Standard Cells for MEMS, 281
- Roe, D. C.
 Novel Biological Weapon Detection System, 358
 Data Fusion for Chemical Sensing, 308
- Romero, A. M.
 Solid-State Neutron Generator in Nuclear Weapons, 272
- Romero, J. A.
 Monitoring Thin-Film Deposition, 268
- Romero, V. J.
 Nondeterministic Modeling, 252
 Simulation Levels for Computational Simulation, 224
- Romig, A.
 Science and Technology Program, 18
- Rosenthal, S. E.
 Radiation Sources: Rayleigh-Taylor Mitigation, 526
- Ross, J. R.
 Transient Gas Species and Soot in Large Fires, 218
- Ruby, D. S.
 High-Throughput Dry Processes, 287
- Ruffner, J. A.
 Thermionic Emission Materials, 539
 Reactivity of Metal-Oxide Surfaces, 70
- Rutherford, B. M.
 Modeling Uncertainties in Simulation, 112
 Simulation Levels for Computational Simulation, 224
- Ryba, G. N.
 Autonomous MicroChem Laboratory, 464
- S**
- Salazar, J. S.
 Recognizing Partially Obscured Targets, 356
- Salinger, A. G.
 A Molecular Theory of Gatekeeper Proteins, 521
- Sands, D. N.
 Fast and Easy Parallel I/O, 97
- Santangelo, P. J.
 Transient Gas Species and Soot in Large Fires, 218
- SAR
 see Synthetic Aperture Radar
- Sarfaty, R. A.
 System Surety Life-Cycle Engineering, 438
- Sartor, G. B.
 Accelerated Molecular Discovery Arrays, 481
- Sasaki, D. Y.
 Accelerated Molecular Discovery Arrays, 481
 Self-Healing Molecular Assemblies in MEMS, 29
 Smart Self-Assembled Photochromic Films, 24
- Satellites
 Hyperspectral Images, 513
 Nano, 473
- Sault, A. G.
 Nonvolatile Protonic Memory, 78
 Reactivity of Metal-Oxide Surfaces, 70
- Saunders, R. S.
 Intelligent Polymers for Nanodevice Control, 62
 Synthesis of Controlled Degradative Materials, 401
- SCADA
 see Supervisory Control and Data Acquisition
- Scalable
 Distributed Computing, 132
 Simulation Software, 99
- Scheduling, 125
- Schimmel, B. D.
 Optimization for Engineering Science Problems, 115
- Schmid, A. K.
 Crack Nucleation and Growth Modeling, 236
 Self-Assembled Templates for Materials Growth, 37
- Schmidt, R. C.
 Eddy Simulation Algorithms, 91
 Modeling of Multiscale Transient Phenomena, 257
 Simulation of Chem/Bio Agents in Infrastructures, 243
- Schmitt, D. J.
 Adaptive 3-D Sensing, 404
 Cooperative Automation, 386
 Ergonomics in Life-Cycle Assembly, 392
 Parallel Mechanism Technology to Manufacturing, 276
 Scripting for Video Inspection, 292
- Schoeneman, J. L.
 Laser Communication Nanosatellites, 473
- Schoeniger, J. S.
 Novel Biological Weapon Detection System, 358
 Accelerated Molecular Discovery Arrays, 481
 Biological Weapon Detector, 361
 Electrokinetic Immunoaffinity Chemical Sensors, 397
 Pathogen Detection Using Microseparations, 557
 Smart Sand for Landmine Detection, 368
- Schoenwald, D. A.
 Microsimulation Model of Infrastructure, 447

Author and Title Index

- Schroder, K. L.
UV Fluorescence Biological Agent Sensor, 378
- Schroepfel, R. C.
Engineering Complex Distributed Systems, 469
Public-Key Authentication, 423
- Schubert, W. K.
Diamond for High-Sensitivity Microsensors, 210
Flexural Plate-Wave Devices in Sensors, 202
Post-Processed Integrated Microsystems, 188
- Schunk, P. R.
Capillary Elastohydrodynamics in Manufacturing, 530
Incomplete Factorization Preconditioners, 88
Unstructured Grid Problems, 130
- Schuster, G. R.
Micromachined Tuners for Microwave Circuits, 195
- Schwank, J. R.
Nondestructive Nonvolatile Memory, 143
- Scott, H. L.
Public-Key Authentication, 423
- Scott, M. W.
Information Collection, 479
- Scott, S. H.
Synthesis of Controlled Degradative Materials, 401
- Scripting, 292
- Seager, C. H.
Nonvolatile Protonic Memory, 78
Role of Defects in III-Nitride-Based Electronics, 169
- Sears, M. P.
Density-Functional Electronic Structure Codes, 110
Programming Paradigms for Parallel Computers, 128
- Security
Power Systems, 458
Surety, 515
- Segmented Rail Phased Induction Motor, 543
- Seidel, D. B.
Novel Load-Balancing for Simulation Software, 99
- Self-Assembly
Macrosystems, 139
Nanoarrays, 37
Nanocomposites, 508
Photochromic Films, 24
- Self-Configurable, 318
- Self-Healing, 29
- Selph, M. M.
Improved Backscatter X-Ray Detection, 346
- Semiconductor
Dry Etching, 158
Filament Lasers, 213
Firing Systems, 433
- Senglaub, M. E.
Expanding the Security Dimension of Surety, 515
- Sensing & Intelligent Controls, 349–399**
- Sensor
3-D, 404
Biological Weapon, 358
Climate Studies, 523
Data Fusion for Chemical, 308
Flexural Plate-Wave, 202
Fluorescence, 378
Immunoaffinity, 397
Intelligent Agents, 467
Laser Structures, 149
Microtelemetry, 172
Mirrors, 365
Motion, 86
Organic, 406
Polarimetric, 490
Radiation-Hard, 191
Remote, 343
Smart Sand, 368
see also: Array
see also: Biosensor
see also: Microsensor
- Separation
Ionophores, 409
Pathogen, 557
- SERAPHIM
see Segmented Rail Phased Induction Motor
- Setchell, R. E.
Microscale Shock-Wave Physics, 45
- Sexton, F. W.
TRIBICC Imaging, 164
- Shaddix, C. R.
Reliability of Electronics in Smoke Environments, 456
Transient Gas Species and Soot in Large Fires, 218
- Shadid, J. N.
Incomplete Factorization Preconditioners, 88
Unstructured Grid Problems, 130
- Shaneyfelt, M. R.
Nondestructive Nonvolatile Memory, 143
Nonvolatile Protonic Memory, 78
- Shapes, 284
- Shear, 232
- Shediac, R.
Accelerated Molecular Discovery Arrays, 481
Data Fusion for Chemical Sensing, 308
- Shelnutt, J. A.
Intelligent Polymers for Nanodevice Control, 62
Ionophores for Liquid-Membrane Separation, 409
Nonvolatile Protonic Memory, 78
- Shepodd, T. J.
Accelerated Molecular Discovery Arrays, 481
- Shinn, N. D.
Dynamics of Solder and Braze Alloys, 39

Author and Title Index

- Shock
 Diamond Crystals, 602
 Physics, 45
- Shokair, I. R.
 Controlling Information Flow and Fusion, 325
 Data Fusion for Chemical Sensing, 308
- Shul, R. J.
 AlGa_N Materials Engineering, 184
 Diamond for High-Sensitivity Microsensors, 210
 Flexural Plate-Wave Devices in Sensors, 202
 Post-Processed Integrated Microsystems, 188
 Role of Defects in III-Nitride-Based Electronics, 169
- Sicking, C. W.
 Characterization of Underground Facilities, 371
 Sparse Geophysical Networks, 352
- Siegel, M. D.
 Models for Radionuclide Desorption from Soils, 403
- Signal, 428
- Signatures, 545
- Sikorski, R. J.
 Simulation/Optimization Tools, 444
- Silicon
 Magnetic, 577
 Microcasting, 575
 Nonvolatile Memory, 143
 Photonic Crystal, 193
 Solar-Grade, 537
- Simmacher, T. W.
 Active Fiber Composites for Monitoring, 581
 Long-Term Impact of Design Innovations, 583
- Simmons, J. A.
 Double Quantum-Well Optoelectronics, 175
 Quantum Tunneling Transistors, 198
- Simpson, R. L.
 Phase Changes in PZT Materials, 511
- Simulation
 Atom-Picoseconds, 121
 Big Eddy, 91
 Chem/Bio Agents, 243
 Diesel Autoignition, 552
 Distributed Information, 310
 Geosphere Transport, 414
 Heterogeneous, 83
 Infrastructure Interdependency, 447
 Materials Response, 104
 Mechanical Systems, 118
 Plasma Physics, 99
 Reacting Systems, 93
 Self-Assembling Macrosystems, 139
 Structural, 228
 System Variability, 444
 Test Levels, 224
 Uncertainties, 112
 see also: Modeling & Engineering Simulation
- Sinclair, M. B.
 Microdiagnostic MEMS Lab-on-a-Chip, 265
- Singh, A. K.
 Electrokinetic Immunoaffinity Chemical Sensors, 397
 Smart Sand for Landmine Detection, 368
- Skocypec, R. D.
 Surety Science, 605
- Sleepe, G. E.
 Characterization of Underground Facilities, 371
 Sparse Geophysical Networks, 352
- Sloan, L. R.
 Micromachined Tuners for Microwave Circuits, 195
- Slurries, 64
- Small, D. E.
 Adaptive 3-D Sensing, 404
 Ergonomics in Life-Cycle Assembly, 392
 Video Sensing for Human-Computer Interactions, 86
- Smart
 Photochromic Films, 24
 Sand, 368
- Smathers, D. C.
 Determining Critical Infrastructure Status, 541
- Smay, J. E.
 Freeforming of Ceramics from Colloidal Slurries, 64
- Smith, J. D.
 Model-Based Design of Remote Access Monitoring, 486
- Smith, J. L.
 Evolution of Hyperspectral Target Signatures, 545
- Smith, M. F.
 Enabling Cold-Spray Direct Fabrication, 55
- Smith, N. F.
 Develop MEMS Reliability Tools, 440
 Microdiagnostic MEMS Lab-on-a-Chip, 265
- Smith, P. M.
 Nondestructive Nonvolatile Memory, 143
- Smith, T. M.
 Eddy Simulation Algorithms, 91
- Smithberger, G. L.
 Microcode Evaluation, 485
- Smoke, 456
- Sniegowski, J. J.
 Fundamental Aspects of Micromachine Reliability, 52
 Vacuum Encapsulation of MEMS Structures, 153
- Snoopy, 572
- Snyder, L. A.
 Determining Critical Infrastructure Status, 541
- Software
 Brittleness, 516
 Plasma Physics, 99
 Snoopy Coprocessor, 572
- Soil, 403
- Solar, 537
- Solder, 39
- Solvent, 495
- Soot, 218
- Sorensen, N. R.
 Corrosion of Microelectronic Reliability, 450

Author and Title Index

- Space
 Sensors, 191
see also: Free-Space
- Spahn, O. B.
 Integration of Optoelectronics and MEMS, 146
 Photonics Integration Devices and Technologies, 207
 Radiation-Hard Random Access Memory, 215
- Spencer, D. D.
 Information Collection, 479
- Spielman, R. B.
 Composite Wire Plasma Formation and Evolution, 584
 Radiation Sources: Rayleigh-Taylor Mitigation, 526
 Z-Pinch Fusion for Energy Applications, 562
- Spill, 495
- Spindle, 267
- Spires, S. V.
 Agent-Based Mediation, 316
 Engineering Complex Distributed Systems, 469
- Spletzer, B. L.
 Distributed Mobile Sensor Arrays, 376
 Distributed Sensing Using Intelligent Agents, 467
 Emergent Behavior of Intelligent Agents, 123
- Spooner, J. T.
 High Reliability in Low-Volume Manufacturing, 290
- Spray, 55
- Springer, C.
 Data Fusion for Chemical Sensing, 308
- Stabilization, 608
- Stamber, K. L.
 Determining Critical Infrastructure Status, 541
 Microsimulation Model of Infrastructure, 447
- Stamp, J. E.
 Determining Critical Infrastructure Status, 541
 SCADA for the Critical Energy Infrastructures, 313
- Stans, L.
 High-Performance Commodity Interconnects, 333
- Staple, B. D.
 Vacuum Encapsulation of MEMS Structures, 153
- Stechel, E. B.
 Density-Functional Electronic Structure Codes, 110
- Stevens, M. J.
 Fracture Analysis of Polymer/Solid Interfaces, 48
 Self-Healing Molecular Assemblies in MEMS, 29
- Stokes, R. N.
 High-Throughput Dry Processes, 287
- Strickland, J. H.
 Lagrangian Modeling of Radiative Transport, 255
- Stromberg, P. G.
 Evolution of Hyperspectral Target Signatures, 545
- Structural
 Codes, 110
 Laser, 149
 MEMS, 153
 Microscopic, 139
 Transition-Metal, 503
see also: Infrastructure
- Stuecker, J. N.
 Freeforming of Ceramics from Colloidal Slurries, 64
- Sturtevant, J. E.
 Fast and Easy Parallel I/O, 97
- Subia, S. R.
 Simulation of Chem/Bio Agents in Infrastructures, 243
- Substrate, 187
- Sullivan, C. T.
 Laser Communication Nanosatellites, 473
 Photonics Integration Devices and Technologies, 207
 Super-High-Speed Communication, 321
 VCSELs and Detectors for Microsystems, 182
- Sullivan, J. P.
 Critical Copper-Corrosion Mechanisms, 34
 Diamond for High-Sensitivity Microsensors, 210
- Superlattice, 590
- Supervisory Control and Data Acquisition, 313
- Supramolecular, 508
- Surety
 Architectural, 535
 Hybrid Processing, 418
 Information Systems, 327
 Life-Cycle, 438
 Production, 431
 SCADA, 313
 Security, 515
 Science, 605
- Surety Sciences, 417–459**
- Surface
 Decontamination, 341
 Hardening, 498
- Surface-Emitting, 167
- Surfactant, 58
- Swarm
 Intelligent Agents, 123
 Software Brittleness, 516
- Swartzentruber, B. S.
 Reactivity of Metal-Oxide Surfaces, 70
 Surfactant-Directed Materials Growth, 58
- Sweatt, W. C.
 Aqueous Organic Sensor, 406
 IR Polarimetry and Lithographic Alignment, 600
 Laser Communication Nanosatellites, 473
- Sweet, J. N.
 Corrosion of Microelectronic Reliability, 450
- Swiler, L. P.
 Computer-Network Vulnerability-Analysis, 420
- Switch
 Firing Systems, 433
 Poco, 494
- Synthesis
 Degradative Materials, 401
 Diamond, 518
- Synthetic Aperture Radar
 Moving Target, 350
 ATR, 363
 IFSAR, 564

Author and Title Index

- T**
- Tadros, M. E.
 Protection System for Decon of CBW Agents, 567
 System-Level Innovations in Missile Defense, 566
- Tallant, D. R.
 Phase Changes in PZT Materials, 511
- Tamashiro, R. S.
 Engineering Complex Distributed Systems, 469
- Tanaka, T. J.
 Reliability of Electronics in Smoke Environments, 456
- Tangyunyong, P.
 Backside Localization of IC Interconnections, 453
- Tanner, D. M.
 Develop MEMS Reliability Tools, 440
- Tappan, A. S.
 Characterization of Energetic Material Initiation, 76
- Target
 Deep, 352
 Hyperspectral Signatures, 545
 Moving, 350
 Obscured, 356
- Tarman, T. D.
 High-Performance Commodity Interconnects, 333
 Super-High-Speed Communication, 321
 Ten-to-One-Hundred-Gigabit/Second Networking, 331
 Varying QoS for Fixed and Mobile Networks, 303
- Tauscher, J. A.
 WNN Decision Making for Data Mining, 301
- Template, 37
- Temporal, 545
- Terrain, 564
- Thai, T. Q.
 PUSH Technology Demonstration, 323
- Theory, 521
- Thermal, 428
- Thermionic, 539
- Thin-Film, 268
- Thin-Skin, 365
- Thomas, E. V.
 Aging Diagnostics Through Hyperspectral Imaging, 42
 Public-Key Authentication, 423
 Reduced-Computation Public-Key Protocols, 329
- Thomas, G. A.
 Information Collection, 479
- Thompson, A. P.
 Molecular Simulation of Reacting Systems, 93
 Atom-Picoseconds to Centimeter-Years, 121
- Thompson, P. A.
 Microwave Imaging Through Walls, 489
- Threat, 560
- Three-Dimensional
 Adaptive Sensing, 404
 Mesh Optimization and Generation, 81
- Tigges, C. P.
 Flexural Plate-Wave Devices in Sensors, 202
 Micromachined Tuners for Microwave Circuits, 195
- Tikare, V.
 Atomistic Computations with Phase-Field Modeling, 31
 Laser Wire Deposition for Fully Dense Shapes, 284
 Simulating the Phase-Field Model, 134
 Simulations of Self-Assembling Macrosystems, 139
- Time-Resolved Ion-Beam-Induced Charge Connection, 164
- Tissue, 579
- Tomographic, 545
- Tong, C. H.
 Validation for ASCI Materials Modeling, 102
- Toth, R. P.
 Surface Decontamination of Toxins by RF Power, 341
- Toxin, 341
- Trahan, M. W.
 Optimization for Engineering Science Problems, 115
- Transient
 Large Fires, 218
 Turbulent Boundary Layers, 257
- Transistor, 198
- Transport
 Chem/Bio Agents, 243
 Concentrated Solutions, 226
 Geosphere, 414
 Imaging, 550
 Radiative, 255
- Treaty, 574
- TRIBICC
see Time-Resolved Ion-Beam-Induced Charge Connection
- Trinkle, J. C.
 Ergonomics in Life-Cycle Assembly, 392
- Trott, W. M.
 Dispersive Measurements of Velocity, 259
 Microscale Shock-Wave Physics, 45
- Trucano, T. G.
 Simulation Levels for Computational Simulation, 224
- Tsang, R. P.
 Varying QoS for Fixed and Mobile Networks, 303
- Tsao, J. Y.
 Compliant Substrates for Epitaxial Integration, 187
- Tube
 Neutron, 497
 Poco, 494
- Tucker, M. D.
 System-Level Innovations in Missile Defense, 566
- Tuminaro, R. S.
 Unstructured Grid Problems, 130
- Tuner, 195
- Tunneling, 198
- Turbine, 581
- Turnquist, M. A.
 Advanced Production Planning Models, 298
 Production Surety and Disruption Vulnerability, 431
- Tuttle, B. A.
 Phase Changes in PZT Materials, 511

Author and Title Index

- Two-Dimensional
Broadening Mechanism in Gases, 501
Material Aging Diagnostics, 42
- U**
- Ulibarri, T. A.
Synthesis of Controlled Degradative Materials, 401
- Ultraviolet
Laser, 523
Miniature Sensor, 378
- Underground, 371
- Urbina, A.
Signal Processing for Thermal Flaw Detection, 428
- UV
see Ultraviolet
- V**
- Vacuum, 153
- Validation, 102
- Valley, M. T.
Signal Processing for Thermal Flaw Detection, 428
- Van Den Avyle, J. A.
Solar-Grade Silicon, 537
- Vandernoot, V. A.
Electrokinetic Immunoaffinity Chemical Sensors, 397
Pathogen Detection Using Microseparations, 557
- Van Leeuwen, B. P.
Computer-Network Vulnerability-Analysis, 420
Dynamically Self-Configurable Network Protocol, 318
- Van Swol, F. B.
Integrated Modeling of Hydrogenic Materials, 108
Molecular Simulation of Reacting Systems, 93
Optimization of Filled Polymer Materials, 270
Smart Self-Assembled Photochromic Films, 24
- Vargo, T. D.
IFSAR Rapid Terrain Visualization, 564
- Vawter, G. A.
Dry Etching for Manufacturing, 158
Photonics Integration Devices and Technologies, 207
Semiconductor Current Filament Lasers, 213
Short-Pulsed Power in Active Optical Sensors, 149
- VCSEL
see Vertical-Cavity Surface-Emitting Laser
- Vedula, V. R.
Materials Response Simulations, 104
- Vehicle, 151
- Velocity, 259
- Venturini, E. L.
Precision-Formed Micromagnets, 161
- Verification, 574
- Vertical-Cavity Surface-Emitting Laser, 182
- Very Large Scale Integration, 596
- Vessel, 603
- Video
Inspection, 292
Motion Sensing, 86
- Visual, 137
- Visualization
Streaming, 296
IFSAR, 564
- VLSI
see Very Large Scale Integration
- Voigt, J. A.
Phase Changes in PZT Materials, 511
- Volatile, 156
see also: Nonvolatile
- Volponi, J. V.
Electrokinetic Immunoaffinity Chemical Sensors, 397
- Voth, T. E.
Eddy Simulation Algorithms, 91
- V-Type, 594
- Vulnerability
HPM, 348
Network, 420
Production, 431
- W**
- Wagner, J. S.
Optimization for Engineering Science Problems, 115
- Wahl, D. E.
Microwave Imaging Through Walls, 489
- Walkup, J. W.
Microcode Evaluation, 485
- Wall, F. D.
Monitoring Corrosion in Weapons Environments, 26
- Walls, 489
- Wally, K.
Biological Weapon Detector, 361
Gas-to-Liquid Microabsorber, 547
Miniature Bioaerosol Concentrator, 354
- Walraven, J. A.
Develop MEMS Reliability Tools, 444
- Walsh, D. S.
TRIBICC Imaging, 164
- Walsh, E. J.
Fault Tolerance on Massively Parallel Computers, 338
- Wampler, B. L.
Acoustically Driven Microoptoelectronics, 205
- Warne, L. K.
Lightning-Induced Arcing, 230
- Warren, M. E.
Integration of Optoelectronics and MEMS, 146
Science on the Microdomain, 461
- Warren, W. L.
Nondestructive Nonvolatile Memory, 143
- Watterberg, P. A.
Feature Reduction of Geometric Solid Models, 395
- Wave
Optoelectronics, 146
Photonic Driver, 45
Sensors, 202

Author and Title Index

- Weapon
 Bioaffinity Array, 361
 Biological Detection, 358
 Chemical Detection, 594
 Corrosion, 26
 Nuclear, 272
 WMD, 560
- Weber, T. M.
 Distributed Sensing Using Intelligent Agents, 467
- Wehlburg, C. M.
 Aging Diagnostics Through Hyperspectral Imaging, 42
 Hyperspectral Images Obtained from Satellites, 513
- Wehlburg, J. C.
 Evolution of Hyperspectral Target Signatures, 545
 Improved Backscatter X-Ray Detection, 346
 Real-Time Image Analysis, 492
 Deployable Mirrors for Remote Sensing, 365
- Weighted-Nearest-Neighbor, 301
- Welding, 69
- Wellman, G. W.
 Materials Response Simulations, 104
- Welton, T. W.
 Evolution of Hyperspectral Target Signatures, 545
- Wendt, J. R.
 Double Quantum-Well Optoelectronics, 175
 Integration of Optoelectronics and MEMS, 146
 Photonics Integration Devices and Technologies, 207
 Quantum Tunneling Transistors, 198
 Ultra-Low-Power Sensors for Microtelemetry, 172
- Wessendorf, K. O.
 Microsensors in Miniature Robotic Vehicles, 151
 Post-Processed Integrated Microsystems, 188
- West, T. H.
 Emerging Threat of Limited WMD Use, 560
- Wheeler, D. R.
 Intelligent Polymers for Nanodevice Control, 62
 Synthesis of Controlled Degradative Materials, 401
- White, R. L.
 Acoustically Driven Microoptoelectronics, 205
- Whitehead, D. W.
 Identifying Potentially Dangerous Human Actions, 426
- Wilcoxon, J. P.
 Quantum Dot Arrays, 67
- Williams, A. B.
 Unstructured Grid Problems, 130
- Wilson, C. W.
 Scripting for Video Inspection, 292
- Wimmer, S. A.
 Computational Method for Predicting Fracture, 261
- Wind, 581
- Winter, V. L.
 System Engineering Aspects of High Assurance, 588
- Wire
 Laser Deposition, 284
 Plasma Formation, 584
- Witkowski, W. R.
 Finite-Element Meshing as Global Minimization, 274
- Witzke, E. L.
 Super-High-Speed Communication, 321
 Ten-to-One-Hundred-Gigabit/Second Networking, 331
- Wix, S. D.
 Simulation/Optimization Tools, 444
- WMD
 see Weapons (of Mass Destruction)
- WNN
 see Weighted-Nearest-Neighbor
- Wong, C. C.
 Science on the Microdomain, 461
- Woods, T. E.
 PUSH Technology Demonstration, 323
- Woodworth, J. R.
 Dry Etching for Manufacturing, 158
- Wright, A. F.
 Density-Functional Electronic Structure Codes, 110
 Role of Defects in III-Nitride-Based Electronics, 169
- Wu, B. C.
 Gas-to-Liquid Microabsorber, 547
- Wu, J.
 Autonomous MicroChem Laboratory, 464
- Wunsch, S. E.
 Modeling of Multiscale Transient Phenomena, 257
- Wyckoff, P. S.
 High-Performance Commodity Interconnects, 333
- Wylie, B. N.
 Visual Explanation and Insight, 137
- Wyss, G. D.
 Network Analysis for Infrastructure Reliability, 424
- X**
- Xavier, P. G.
 Cloud to CAD, 389
 Distributed Sensing Using Intelligent Agents, 467
 Heterogeneous Simulation, 83
- X-Ray
 Backscatter, 346
 Laser, 570
- Y**
- Yang, P.
 Advanced Machining for Microfabrication, 294
 High-Throughput Dry Processes, 287
- Yarberry, V. R.
 Standard Cells for MEMS, 281
- Yee, A. A.
 Sparse Geophysical Networks, 352
- Yelton, W. G.
 Sensor Arrays for Volatile Organic Detection, 156
- Yocky, D. A.
 Microwave Imaging Through Walls, 489
 Recognizing Partially Obscured Targets, 356
- Yoshimura, A. S.
 Distributed Information System Modeling, 310
- Yost, F. G.
 Dynamics of Solder and Braze Alloys, 39

Author and Title Index

Young, W. F.
Dynamically Self-Configurable Network Protocol, 318

Z

Zak, B. D.
Global Climate Model for Paleoclimate Applications, 95

Zavadil, K. R.
Critical Copper-Corrosion Mechanisms, 34
Thermionic Emission Materials, 59
Self-Assembled Templates for Materials Growth, 37

Z-Backlighter, 568

Zeuch, D. H.
Design of Powder Pressing Dies Using Modeling, 532
Phase Changes in PZT Materials, 511

Zimmerer, D. J.
Evolvable Hardware, 234

Z-Pinch
Containment Vessels, 603
Energy Applications, 562

Zutavern, F. J.
Semiconductor Current Filament Lasers, 213
Short-Pulsed Power in Active Optical Sensors, 149

End of Document